Yasunori Nakamura *Editor*

Starch

Metabolism and Structure

Springer

Starch

Yasunori Nakamura
Editor

Starch

Metabolism and Structure

Springer

Editor
Yasunori Nakamura
Faculty of Bioresource Sciences
Akita Prefectural University
Akita, Japan

ISBN 978-4-431-55494-3 ISBN 978-4-431-55495-0 (eBook)
DOI 10.1007/978-4-431-55495-0

Library of Congress Control Number: 2015938096

Springer Tokyo Heidelberg New York Dordrecht London

Printed on acid-free paper

Springer Japan KK is part of Springer Science+Business Media (www.springer.com)

Preface

Rapid progress of research in recent years on the biosynthesis, degradation, and structure of starch produced in photosynthetic and non-photosynthetic tissues from a variety of plant species and in algae, including land plants and green algae (Chloroplastida), red algae (Rhodophyceae), and cyanobacteria, lead us to understand the whole scope of the specific metabolic systems in plants. At the same time we must revise our earlier concept of starch-related metabolism by dealing with the newly revealed dynamism of regulation of starch biosynthesis.

Genome analysis indicates that higher plants have evolved two different starch biosynthetic processes in photosynthetic and non-photosynthetic tissues by differentiation of key enzymes for starch biosynthesis, i.e., starch synthase, starch branching enzyme, and starch debranching enzyme, into multiple isozymes having specific catalytic properties. Concomitantly, plants have refined the fine structure of amylopectin, the major component of starch, so that it can be densely packed into the semi-crystalline granules having distinct size and morphology depending on plant species and tissues.

Numerous past investigations vigorously and comprehensively performed worldwide by biochemical, genetic, and molecular approaches especially since the early 1990s have established a concrete basis for contributions of individual isozymes to the fine structure of amylopectin and amylose and for their expression patterns altered by various tissues and their developmental stages. However, despite these invaluable fundamental results, at present we cannot help feeling that for a better understanding of the dynamic aspects of regulatory mechanisms for starch biosynthesis and its degradation, novel concepts should be established regarding the functional interactions between enzymes and between the enzyme(s) and glucans/dextrins. Also, we should formulate new concepts regarding the multiple functions of individual enzymes, responding to changing physiological and environmental conditions.

Detailed comparative analysis of the chain-length distribution of amylopectin from various plant sources has provided new insights into the basic skeleton of the

distinct amylopectin fine structure. Although amylopectin has long been believed to be composed of the unit structure referred to as the cluster, which includes the amorphous lamellae and the crystalline lamellae with a total size of about 9 nm universally found among the plant kingdom, Bertoft and his colleagues recently proposed an alternative model of the amylopectin structure referred to as the "backbone model" (see Chap. 1). The features of the backbone model are, first, that the construction and direction of chain-elongation (and possibly the biogenesis as well) of the cluster-linking chains (B2- and B3-chains) are distinct from the cluster chains (A- and B1-chains), while in the traditional "cluster model" the natures of both chains are not necessarily distinguished with the exception of their chain-lengths. Second, the backbone model has proposed a novel notion that the building blocks are actually the structural units constituting the individual cluster, whereas no such structural units are assumed in the cluster model. However, due to methodological limitations, the actual, exact fine structure of amylopectin remains unproven.

The fact that plants can synthesize starch granules efficiently and at a high rate and accumulate them with a specific gravity of about 1.6 (Rundle et al. 1994. J Am Chem Soc 66:130–134) at the huge amounts inside plastids inclines us to conceive that the synthesis of starch granules makes it possible for plants to survive on land. To approach the secret and miracle of their capacities, we must always pay attention to the relationship between each biochemical event during starch metabolism and the structure of glucans intervening in the enzyme actions and contributions. In this book, novel findings of the fine structures of amylopectin (Chap. 1) and amylose (Chap. 2) and the crystalline structure of starch granules (Chap. 3) are introduced and their significance is concisely explained.

We can expect that during the coming decade basic and applied studies will focus on the mechanism for dynamic features of enzyme–enzyme and enzyme–glucan interactions although these attempts will provide us with quite new findings, and each interaction must be significantly involved in the regulation of starch biosynthesis and degradation. In this book, each chapter describes the present status of our understanding of the related topics and mostly includes future perspectives. Many chapters also explain the advantages and limitations of the modern methodologies used. Thus, we believe that the book is of great use for young scientists and students who are engaged in or majoring in the starch science fields including basic science, biotechnology, and applied science such as applications for food and bioplastics to learn the whole scope of starch metabolism and its structure.

Finally, I, as an editor of the book, express my deep and sincere gratitude to all the chapter authors for their great contributions by sharing the aim of publishing a good, updated reference book for all scientists who are interested in starch science. I especially thank Professor Martin Steup for discussing the content of the book and reviewing many manuscripts.

Akita, Japan Yasunori Nakamura

Contents

Part I
Structure

Chapter 1
Fine Structure of Amylopectin

Eric Bertoft

Abstract Starch granules consist of two major polyglucans, namely, branched amylopectin and essentially linear amylose. In all nonmutant starches, amylopectin is the major component and is responsible for the internal structure of starch granules, which is the native, semicrystalline form of starch. The granules, irrespective of the plant source, consist of granular rings of alternating amorphous and semicrystalline polymers. On a smaller scale, blocklets as well as crystalline and amorphous lamellae have been identified. Amylopectin is generally accepted as the contributor to the lamellar structure, but the nature of blocklets is only beginning to be resolved. Amylopectin consists of numerous chains of glucosyl units that are divided into short and long chains. These chains are organized as clusters that have been isolated by using endo-acting enzymes, and the fine structure of the clusters have been investigated. The clusters consist of still smaller, tightly branched units known as building blocks. The organization of the clusters and building blocks in the macromolecular structure of amylopectin is to date uncertain, and two schools exist at present suggesting that amylopectin either has a treelike branched cluster structure or a building block backbone structure. The structural features of amylopectin and the two models presently in debate are discussed in this chapter.

Keywords Amylopectin structure • Cluster structure • Building blocks • Starch granules • Amylopectin models

Amylopectin is generally the major component of starch and constitutes 65–85 % of the matter in the starch granules (Table 1.1) (Fredriksson et al. 1998; Gérard et al. 2001; Hoover 2001). However, in some mutant plants, the amylopectin content is much higher – it can even reach 100 % – and the sample is then known as "waxy starch." Some mutant plants possess high-amylose starches with low amylopectin content. In these starches,the morphology of the granules is often

E. Bertoft (✉)
Department of Food Science and Nutrition, University of Minnesota, St Paul, MN, USA
e-mail: eric.bertoft@abo.fi

Y. Nakamura (ed.), *Starch*, DOI 10.1007/978-4-431-55495-0_1

Table 1.1 Crystalline structure and amylose content of some starch granules

Starch source	References	Allomorph	Relative crys-tallinity (%)	Lamellar repeat distance (nm)	Crystalline lamella thickness (nm)	Amylose content (%)
Barley	[a]	A	23.3			28.3
	[b]			8.9		
	[c]				4.9	
Wheat	[d]	A	24.0			33.2
	[e]	A	32	9.9		37.0
	[b]			9.0	4.3	
Waxy maize	[a]	A	31.4			0
	[c]				4.2	
	[f]			8.8		
	[e]	A	47	10.3		1.0
Rice	[a]	A	29.1			19.5
	[g]				4.1–4.6	12.8–24.2
	[h]	A	37.1			13.2
	[b]			8.7		
Sweet potato	[h]	A	34.4			19.8
Tapioca	[a]	A	29.9			17.6
	[h]	A	35.8			17.9
	[e]	A	32	9.8		29.8
	[b]			9.1		
Potato	[a]	B	26.4			17.9
	[h]	B	29.8			18.0
	[e]	B	43	9.0		14.0
	[i]	B		8.8	5.5	

[a]Bertoft et al. (2008)
[b]Jenkins et al. (1993)
[c]Genkina et al. (2007)
[d]Kalinga et al. (2013)
[e]Vermeylen et al. (2004)
[f]Jenkins and Donald (1995)
[g]Koroteeva et al. (2007b)
[h]Srichuwong et al. (2005b)
[i]Kozlov et al. (2007a)

defect with a lot of elongated granules (Banks and Greenwood 1973; Tester et al. 2004; Kubo et al. 2010; Jane et al. 1994; Glaring et al. 2006). The granules in waxy plants, however, are indistinguishable from those of normal amylose-containing granules (Fuwa et al. 1978; Jane et al. 1994; Song and Jane 2000). This shows that amylopectin is the principal component that contributes to the structure of starch granules.

1.1 Internal Architecture of the Starch Granule

Although starch granules from diverse plants have a large range of different sizes and shapes (Jane et al. 1994), their inner architecture appears remarkably similar. The ubiquitous structures within starch granules are granular rings, blocklets, and lamellae, which can be observed with different techniques, because they represent structural levels ranging from micrometers down to the nanometer scale.

1.1.1 Granular Rings

Granular rings are also known as "growth rings." The rings have been known as long as the starch granules – they were described already in the early 18th century by Leeuwenhoek, who developed a more practical version of the light microscope (Seetharaman and Bertoft 2012a). They appear as alternating light and dark rings with an approximate thickness of a few hundred to several hundred nanometers. The rings tend to be thicker in the interior part of the granule and become thinner toward the periphery (Pilling and Smith 2003; Wikman et al. 2014). By a limited treatment of cracked granules with amylase, the rings become more clear and appear thinner and more numerous by scanning electron microscopy (Fulton et al. 2002).

Although the granular rings are well known, the reason for their existence and their exact nature is still unclear. It was suggested already in the 19th century that the rings are laid down periodically as a result of the day and night (diurnal) cycle (Fritzsche 1834; Meyer 1895). Indeed, starch granules from barley and wheat grown in constant light were shown to lack rings (Sande-Bakhuizen 1926; Buttrose 1960, 1962). However, potato starch granules retained rings when grown under similar conditions, which suggest that yet unknown mechanisms regulate the formation of the rings (Buttrose 1962; Pilling and Smith 2003). The fact that treatment in diluted acid results in higher relative crystallinity in the remaining starch granules (Sterling 1960; Muhr et al. 1984; Vermeylen et al. 2004; Utrilla-Coello et al. 2014) suggests that amorphous areas are eroded by the acid, which in turn suggests that the granules consist of alternating amorphous and crystalline rings. Because amylose is considered to exist mostly in the amorphous state in the granules, it has been generally assumed that the amorphous rings mostly consist of amylose (Atkin et al. 1999). However, the fact that granular rings exist in both amylose-containing and waxy starches shows that amylopectin also participates in the amorphous rings.

The crystalline rings are often called semicrystalline because, as we shall see, they are not completely crystalline. Amylopectin is thought to be the major component in these rings, but amylose is probably also a part of them (Koroteeva et al. 2007a; Kozlov et al. 2007b). It should be noted, however, that the semicrystalline rings were named as crystalline by Gallant et al. (1997) and the amorphous rings were named "semi-amorphous," although the reason for these labels remained

unclear. In the work of Tang et al. (2006), the semicrystalline rings were considered "hard shells" and the amorphous were called "soft shells." Thus, the view of the nature of the granular rings remains a matter of debate in the literature.

1.1.2 Blocklet Structure

Small, birefringent units inside starch granules around one micrometer in size were observed in the 1930s and called blocklets or "Blöckchen" by the German scientists Hanson and Katz (1934a, b). They treated starch granules in diluted acid before the granules were allowed to swell in a calcium nitrate solution and described blocklets as ordered in both radial and tangential directions when observed in an ordinary light microscope. Later, these structures seem to have been forgotten, but they were redescribed by Gallant et al. in 1997. Blocklets are now observed by atomic force microscopy (AFM) of native or acid-treated granules, and, therefore, it cannot be taken for granted that these blocklets are the same as the "Blöckchen" described by Hanson and Katz in 1934. Nevertheless, blocklets were observed as protrusions on the surface of starch granules. The sizes of these blocklets on potato starch granules range between 50 and 300 nm according to Baldwin et al. (1998) or are around 30 nm according to Szymonska et al. (2003). On granules from sweet potato, maize, rice, and wheat, the blocklets were reported to have similar sizes of approximately 20–40 nm (Ohtani et al. 2000). However, Dang and Copeland (2003) reported that blocklets in rice are 100 nm wide and 400 nm long and suggested that they span a whole growth ring. Blocklets were also observed on the surface of granules isolated from wheat at different stages of the development of the kernel endosperm. It was found that blocklets on the surface of granules from early developmental stages are larger and have more fuzzy contours than at later stages and at maturity (Waduge et al. 2013).

Gallant et al. (1997) suggested a general model for the blocklet structure of starch granules. According to these authors, blocklets fill up the whole interior of the granule. Large blocklets build up the semicrystalline rings (or "crystalline" rings according to the terminology by Gallant et al.), whereas smaller blocklets build up the amorphous ("semi-amorphous") rings. Chauhan and Seetharaman (2013) studied blocklets in acid-treated (and subsequently dried) potato starch granules and confirmed the model by Gallant et al. Baker et al. (2001) found that native maize granules have blocks 400–500 nm in size that span the whole growth ring. Similar structures were reported by Atkin et al. (1998). After acid treatment, smaller blocklets 10–30 nm in size were observed within the rings (Baker et al. 2001). Chauhan and Seetharaman (2013) reported that blocklets fused together when acid-treated granules were exposed to water vapor during the observation by AFM. This indicates that the blocklet is a flexible structure that is readily observed in the dry state and takes up water under humid conditions.

Tang et al. (2006) have also proposed a model for the blocklet structure in starch granules. In their view, there exist perfect and defect (less perfect) blocklets.

The former mainly build up "hard shells" (corresponding to semicrystalline rings), and the latter are found in "soft shells" (corresponding to amorphous rings).

As blocklets so far have not been isolated from starch granules, the exact composition of a blocklet is not known. Whether the composition of the blocklets, or the structure of their molecular components, is similar or different in the alternating granular rings is so far only a matter of speculation. Dang and Copeland (2003) assumed that the blocklets consist of amylopectin and calculated that the blocklet dimensions suggests that they contain about 280 clusters of amylopectin side chains. Ridout et al. (2003, 2006) also assumed that the blocklets largely consist of amylopectin and that they are embedded in an amorphous matrix that mainly consists of amylose. This matrix, they found, swells and gives rise to the amorphous granular rings, which appear bright and soft. The dark, semicrystalline rings arise because they contain defects that do not swell, which results in a discontinuation of the swelled areas.

1.1.3 Lamellar Structure

A lamellar repeat distance of approximately 10 nm in starch granules was first reported by Sterling in 1962 using small-angle X-ray diffractometry. This was ascribed to alternating crystalline and amorphous lamellae in the semicrystalline granular rings (Cameron and Donald 1992). Later, Jenkins et al. (1993) refined the calculations to be around 9 nm and reported that this is a ubiquitous repeat distance for practically all types of starch (Table 1.1). Moreover, Jenkins and Donald (1995) found that the distance is similar irrespective of the amylose content in the granules: In waxy starch granules, the amorphous lamellae tend to be thicker and the crystalline lamellae thinner, whereas in high-amylose granules, the situation is the opposite, but the general average repeat distance remains roughly the same.

The responsible molecular component for the lamellar organization is amylopectin. The crystalline lamella is built up by double helices of short, external chains of amylopectin with an average 11–15 glucose residues (Manners 1989; Bertoft et al. 2008). Theses double helices crystallize into either a so-called A-type allomorph (typical in cereal starches) or a B-type allomorph (common in root and tuber starches) (Imberty et al. 1991), details of which are described in Chap. 3. Essentially, the A-type crystal exhibits a monoclinic unit cell involving six double helices and only little water (Imberty et al. 1988; Popov et al. 2009), whereas the B-type crystal is hexagonal, also involving six double helices, but with a central cavity filled with water (Imberty and Pérez 1988). The strands of the double helix are left handed and consist of six glucose residues per turn and a pitch of 2.1 nm. The length of the double helices corresponds approximately to the experimentally estimated thickness of the crystalline lamellae, i.e., 4.0–6.5 nm, depending on the type of starch (Table 1.1) (Kiseleva et al. 2005; Genkina et al. 2007; Koroteeva et al. 2007a; Kozlov et al. 2007a).

The amorphous lamella is situated directly adjacent to the crystalline lamella, and several of these lamellae units form "stacks" in the semicrystalline ring (Cameron and Donald 1992). The average number of repeat units appears to depend on the sample, but is in the order of 15–25 (Daniels and Donald 2003). The amorphous lamella consists of the internal part of the amylopectin molecule with most, or at least plenty, of the branches in amylopectin (French 1972). This part of the amylopectin molecule cannot, therefore, crystallize, but its structure is believed to be of importance for the crystallization of the double helices (O'Sullivan and Pérez 1999; Vamadevan et al. 2013). In comparison to the detailed knowledge of the structure and organization of the double helices in the crystalline lamella, the structure of the amorphous lamella is only poorly known. The details, however, begin to emerge, as we will see later on.

The involvement of amylose in the lamellar structure is also not well known to date and is a matter of debate. It appears, however, that amylose is a part of the structure and possibly interferes with the crystalline arrangement of the double helices of amylopectin (Koroteeva et al. 2007a; Kozlov et al. 2007b). The amylose may be intertangled with the internal chains of amylopectin in the amorphous lamella, and it might also extend into the crystalline lamella, or even through several layers of lamellae. Yuryev and coworkers have suggested that the amylose involvement depends not only on the amount of amylose in the starch but also on the specific plant species (Koroteeva et al. 2007a; Kozlov et al. 2007a, b).

The relation between the lamellar organization and the blocklet structure of the granular rings is to date only a matter of speculation. Possibly, the lamellae build up the blocklets in the semicrystalline rings. It is interesting to notice that the lamellae are only observed in wetted starch samples, but not in dry granules. This was explained on the basis of a side-chain liquid-crystalline model of branched polymers (Waigh et al. 2000b), in which the amorphous chain segments of the amylopectin are connected to the double helices and act as spacer arms: In the dry state (the so-called nematic stage), the double helices are disorganized, whereas in the wet stage (the smectic stage), the spacer arms move the double helices and align them into the observed crystalline lamellar distance. Apparently, this coincides with the swelling of the blocklets and might contribute to the appearance of the lamellae (Bertoft and Seetharaman 2012). Tang et al. (2006) suggested that the lamellar structure is found in blocklets in both semicrystalline and amorphous rings, but the structure of the blocklets is more defect in the latter rings.

1.2 Amylopectin: The Major Starch Component

Amylopectin consists of numerous short chains of α-(1,4)-linked D-glucose residues. The chains are interlinked through their reducing end side by α-(1,6)-linkages. Together the chains form a very large macromolecule with an average molecular weight (M_w) in the order of 10^7–10^8 (Aberle et al. 1994; Millard et al. 1997; Buléon et al. 1998a), and thereby the size is about one or two order of

magnitude larger than the almost linear amylose molecules (Aberle et al. 1994; Buléon et al. 1998a). Exact M_w values are, however, difficult to achieve, because the molecules are prone to aggregate in solution and to breakdown due to harsh dissolving methods, resulting in too high or too low estimations, respectively. The number-average value (M_n) is considerably smaller than M_w (McIntyre et al. 2013). The polydispersity index (M_w/M_n) is therefore large (Erlander and French 1956; Stacy and Foster 1957).

Each macromolecule has as many nonreducing ends as there are chains, but only a single glucose residue that has a free reducing end group. Takeda et al. (2003) labeled this group with the fluorescent dye 2-aminopyridine. By size-exclusion chromatography (SEC) of labeled samples, these authors showed that the amylopectin component from a range of diverse starches in fact consists of three size fractions: The largest amylopectin molecules have a number-average degree of polymerization (DP_n) of 13,400–26,500 depending on the plant species. Intermediate-sized amylopectins have DP_n 4400–8400 and the smallest molecules have DP_n 700–2100. Large amylopectin molecules were the most abundant in all starches they studied.

As in the starch granule, there exist several structural levels within the amylopectin macromolecule, namely, the unit chains, larger clusters of the chains, and the ultimate small, branched units of chains known as building blocks. Each of these levels is discussed in more detail below.

1.2.1 Unit Chains of Amylopectin

The chains in amylopectin have been divided into a range of different types by different authors. Unfortunately, the meaning of the different divisions and nomenclatures is not always apparent and has resulted in a lot of confusion and misunderstanding in the literature throughout the later decennia. Indeed, a correct understanding of the terminology is essential for a meaningful interpretation of the structure of the macromolecule. The terminology of the chains is therefore outlined in detail below.

1.2.1.1 Major Chain Categories

Already in 1952, Peat et al. (1952b) suggested a basic – and very useful – nomenclature of chains in amylopectin, which focuses on the mode of participation in the molecular structure. They realized that, based on the then generally accepted model of the structure, which had been proposed by Meyer and Bernfeld (1940), some chains carry other chains, whereas some chains do not. The latter chains were called A-chains, whereas the former chains were named B-chains. In addition, they suggested that the sole chain that carries the free reducing end group, but otherwise is similar to the B-chains, should be called C-chain. This practical nomenclature

was soon accepted by the research community. Moreover, the model by Meyer and Bernfeld (1940) implied two other principle types of chain segments: external and internal. External chains are considered as segments that extend from the outermost branch to the nonreducing end of the chain, whereas all other segments are internal. It follows that A-chains are completely external and each B-chain (and the C-chain) has one external chain segment, whereas the rest of the chain is internal.

In order to make use of this nomenclature, it is necessary to have experimental tools that distinguish the chains from each other, so that they can be identified and quantified. The first tools in this direction were based on the specific action of starch-degrading (amylolytic) enzymes. The methods were developed simultaneously with the discovery of the enzymes in the 1940s and 1950s. Thus, the enzymes phosphorylase (from rabbit liver) (Hestrin 1949; Illingworth et al. 1952) and β-amylase (from sweet potato and soybean) (Hestrin 1949; Peat et al. 1952a) were found to be so-called exo-acting enzymes, i.e., they hydrolyze the chains in amylopectin (and in amylose) from the nonreducing end until they approach the most exterior branch point, which possesses a barrier that the enzymes cannot bypass. The resulting, resistant molecule is called a limit dextrin (LD) and contains the entire internal part of the original amylopectin macromolecule together with shorter external chain stubs that the enzymes leave in front of the outermost branch points (Fig. 1.1). The relative extent of hydrolysis of the amylopectin molecule by phosphorylase or β-amylase is known as the φ- and β-limit value, respectively (Hestrin 1949; Walker and Whelan 1960b). Phosphorylase and β-amylase have also been used in sequence, which results in a so-called φ,β-LD (Hestrin 1949; Lii and Lineback 1977). Either of the limit values can be used for the estimation of the average external chain length (ECL) (Bertoft 1989; Manners 1989) and is summarized for some different samples in Table 1.2. It should be noted that ECL is only an average value, and the actual size distribution of the external chains is to date still unknown. Nevertheless,

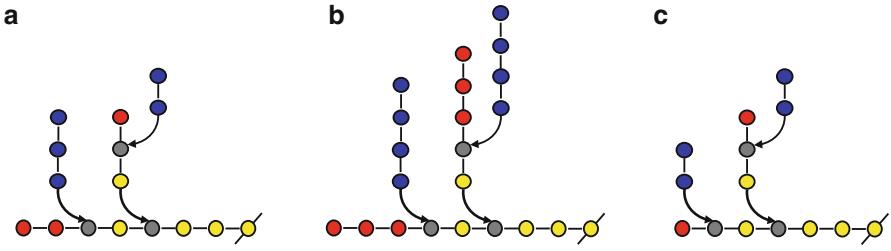

Fig. 1.1 Principal structure of limit dextrins: (**a**) β-LD, in which A-chains remain as two or three glucose residues and the external chain stubs of B-chains have one or two residues; (**b**) φ-LD, in which all A-chains have four residues and all external B-chain stubs have three residues; (**c**) φ,β-LD, in which all A-chains have two residues and all external B-chain stubs have one residue. *Blue circles* symbolize A-chains, *red circles* external B-chains, *gray circles* are glucose residues involved in a branch linkage (*arrows*), and *yellow circles* are residues in internal segments of B-chains. Note that the chain segment that carries the reducing end (/) is regarded as an internal segment

Table 1.2 Structural parameters of amylopectin from diverse plants[a]

Starch source	References	Structure type	CL	ECL	ICL	TICL	S:L	A:B
Barley	[b]	1	17.5	11.2	5.3	12.3	19.4	1.0
Wheat	[c]	1–2	17.7	12.3	4.4	12.7	16.2	1.4
	[d]		18				12.9	
Waxy maize	[b]	2	18.1	11.9	5.1	12.0	13.5	0.9
Rice	[b]	2	17.8	11.7	4.9	12.3	11.5	1.1
	[d]		18				10.8	
Sweet potato	[e]	2–3	19.6	12.8	5.8	14.0	10.1	1.1
	[d]		20				8.9	
Tapioca	[b]	3	18.8	12.4	5.3	14.6	11.0	1.3
Potato	[b]	4	23.1	14.1	8.0	19.9	6.3	1.2
	[d]		22				6.5	

[a]Structural type is based on the internal unit chain distribution of amylopectin; *CL* chain length, *ECL* external chain length, *ICL* internal chain length (between branches), *TICL* total internal chain length (the whole internal B-chain length), S:L ratio of short to long chains, A:B ratio of A- to B-chains
[b]Bertoft et al. (2008)
[c]Kalinga et al. (2013)
[d]Hanashiro et al. (2002)
[e]Zhu et al. (2011a)

ECL corresponds rather well to the reported thickness of the crystalline lamellae in starch granules (Table 1.1) (Kiseleva et al. 2005; Genkina et al. 2007; Koroteeva et al. 2007a; Kozlov et al. 2007a).

Internal chain segments are defined as the segments between the branches in amylopectin (Fig. 1.1). Just like for the external chains, there exists no method that can clarify the size distribution of these segments, but the average internal chain length (ICL) can be estimated when the average chain length (CL) and ECL is known (Bertoft 1989; Manners 1989). ICL is much shorter that ECL and some examples are shown in Table 1.2.

In addition to ECL and ICL, the limit dextrins can be used to estimate the relative number of A- and B-chains, if the LDs are debranched using specific enzymes that attack the α-(1,6)-linkages (isoamylase and pullulanase). Pioneering experiments with such enzymes were conducted in the 1950s (Hobson et al. 1951; Peat et al. 1952b), and the enzymes became commercially available a decade later. The method is based on the fact that the different exo-acting enzymes leave external chain stubs with specific lengths in the resistant dextrins. Phosphorylase, which removes glucose from the external chains (producing glucose 1-phosphate), hydrolyzes A-chains until four glucose residues remain, whereas the external segments of the B-chains become three residues long (Bertoft 1989). Therefore, chains with a degree of polymerization (DP) of 4 correspond to A-chains. The remaining B-chains in the φ-LD are all longer than DP 4, as illustrated in Fig. 1.1. β-Amylase produces maltose from the nonreducing ends, i.e., it removes two glucose residues simultaneously. If the enzyme is added to a φ-LD, it removes one maltose from each external chain stub

(whereby the number of maltose molecules produced corresponds to the number of chains in the molecule), and in the resulting φ,β-LD, all A-chains correspond to maltosyl chain stubs (Bertoft 1989). When β-amylase is used alone, without prior phosphorolysis, the A-chains remain as either maltosyl or maltotriosyl chain stubs depending whether the original external chain had an even or odd number of residues (Fig. 1.1). The external B-chain stub is DP 1 or 2 (Summer and French 1956). Because β-LDs are comparatively easy to prepare, they have been more frequently used in structural studies. However, as in the example shown in Fig. 1.1, some B-chains of the β-LD have DP 3, i.e., they are of the same length as half of the A-chains. This might interfere with the estimation of A-chains when using β-LDs, albeit in most cases the number of B-chains with DP 3 in β-LDs is very low. The number-based ratio of A:B-chains in some plants is listed in Table 1.2. In most plants, especially several with A-type allomorph crystallinity, the ratio is close to 1.0, albeit wheat appears to be an exception with a comparatively high ratio, whereas B-type crystalline starches tend to have somewhat higher ratio (Bertoft et al. 2008).

1.2.1.2 Unit Chain Distribution

The invention of gel-permeation chromatography made it possible to separate molecules by size and contributed to a much better understanding of the structure of amylopectin. The first size distribution of the chains in amylopectin was published by Lee et al. in 1968. Gunja-Smith et al. (1970) showed for the first time that amylopectin and glycogen have different structures, because glycogen has a unimodal size distribution of only short chains, whereas amylopectin has a bimodal distribution. Therefore, two additional groups of major chains are distinguished in amylopectin, namely, short (S) and long (L) chains (Fig. 1.2). S-chains constitute the major group and have size distributions from DP 6 up to approximately DP 36 in most samples and a peak DP around 11–15, which depends on the sample (Koizumi et al. 1991; Srichuwong et al. 2005b; Vermeylen et al. 2004; Bertoft et al. 2008). L-chains possess normally a peak, or sometimes only a shoulder, around DP 43–50 (Fredriksson et al. 1998; Hanashiro et al. 2002; Bertoft et al. 2008). The number of L-chains is much smaller than S-chains, and the ratio of S:L-chains is quite different in starches from different plants (Table 1.2). Typically, A-type crystalline starches – especially cereal starches – have a high ratio between 10:1 and 22:1, whereas B-type crystalline samples have ratios between 6:1 and 8:1 due to a comparatively high amount of L-chains (Biliaderis et al. 1981a; Hanashiro et al. 2002; Bertoft et al. 2008). This results in longer average chain lengths (CL) of the whole unit chain population, and it was shown that the B-type allomorph crystalline is accompanied by longer CL than the A-type (Hizukuri 1985).

Hizukuri (1986) found that amylopectin preparations from several samples possess polymodal size distributions of unit chains, i.e., the L-chains consist of at least two, maybe three, groups of chains. Moreover, the peak of S-chains possessed a shoulder approximately at DP 15–19, which suggested that S-chains also consist of at least two subgroups of chains. From the classical model by Meyer and Bernfeld

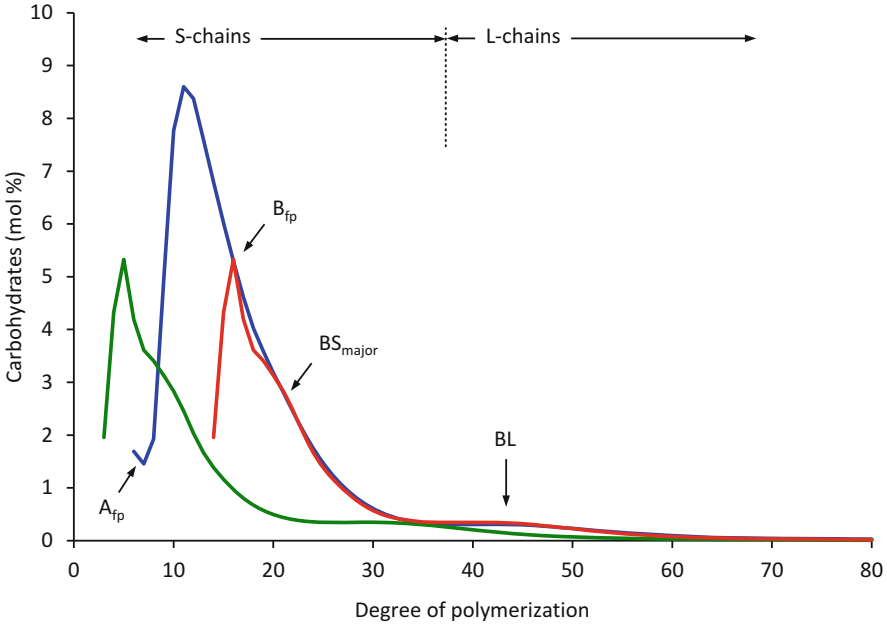

Fig. 1.2 Molar-based unit chain profile of amylopectin from finger millet (*blue line*) and its internal unit chain profile of the B-chains obtained from the φ,β-LD (*green line*). A reconstruction of the position of the internal chain profile (*red line*) was made by adding the average ECL to each of the B-chains of the φ,β-LD. Different chain categories are shown based on the unit chain profile of the amylopectin (A_{fp}-, S- and L-chains) and the reconstructed B-chain profile (Bfp-, BS_{major}, and BL-chains, of which BL-chains correspond to L-chains) (Courtesy of G. A. Annor, University of Guelph, Canada)

(1940), A-chains can generally be supposed to be shorter than B-chains. This led Hizukuri (1986) to suggest that the S-chains consist of A-chains with DP 6–15 and short B-chains, which he named B1-chains, with DP 15–36. The L-chains were all considered as B-chains and were subdivided into B2-chains (with a peak DP around 38–45), B3-chains (peak DP 62–74), and B4-chains (peak DP not clearly distinguished at DP > 80). He also suggested that the subgroups of long B-chains are involved in the interconnection of clusters of chains, details of which are discussed in Sect. 1.3.1. It is of importance to notice, however, that there is no experimental method to date that can measure the actual size distribution of A-chains. In fact, indications of the existence of long A-chains have been found in few samples, albeit in extremely small quantities (Bertoft 2004b; Bertoft et al. 2008).

Hanashiro et al. (1996) used high-performance anion-exchange chromatography (HPAEC), which gives a very high resolution of chains up to approximately DP 60. They found indications of a certain periodicity of DP 12 when they compared the unit chain distributions of amylopectin from several different plant species. They suggested that the shortest chains of fraction fa, which had DP 6–12, were the A-chains, whereas fractions fb_1 (DP 13–24), fb_2 (DP 25–36), and fb_3 (DP > 36)

corresponded to the B1-, B2-, and B3-chains, respectively. Thereby they suggested that the size ranges were shorter than earlier given by Hizukuri (1986) for the same subcategories of chains. This issue will be discussed in more detail later on. It should be noted already here, however, that the ratio of A:B-chains calculated based on this division becomes far lower than the actual A:B-chain ratio that can be measured based on debranching of limit dextrins, because fraction fa includes, in fact, only a fraction of all A-chains in amylopectin (Bertoft et al. 2008).

In addition to unit chains with DP up to the order of 100, some amylopectin samples have been shown to contain very long chains, also named "extra long" or "superlong" chains (Hanashiro et al. 2005; Inouchi et al. 2006). These chains have DP corresponding to several hundred glucose residues and are therefore of the same length as typical amylose chains. Indeed, these chains are apparently synthesized by the same enzyme as amylose, namely, granule-bound starch synthase I (GBSSI), and the chains do not exist in amylopectin from waxy samples (Aoki et al. 2006; Hanashiro et al. 2008). Very long chains have been found in comparatively large amount especially in *Indica* varieties of rice (Takeda et al. 1987), but they were detected in small amounts also in *Japonica* rice and in several other samples, e.g., cassava, sweet potato, potato, maize, and wheat (Charoenkul et al. 2006; Hanashiro et al. 2005; Noda et al. 2005; Shibanuma et al. 1994; Takeda et al. 1988; Laohaphatanaleart et al. 2009; Zhu et al. 2013). It appears that these very long chains mostly are a type of B-chains with longer or shorter external segments (Hanashiro et al. 2005; Laohaphatanaleart et al. 2009).

The size distribution of the C-chain was investigated by Hanashiro et al. (2002), who debranched amylopectin that had been labeled with 2-aminopyridine. The fluorescent C-chains were analyzed by SEC in amylopectin preparations from several different plant species, and it was shown that in most cases the C-chain possesses an almost unimodal size distribution from DP ~10 to DP ~ 100 and a peak DP around 38–43. In yam starch, however, the peak was at DP 49, and in high-amylose maize, it was as high as DP 80. Several samples also possessed a shoulder around DP 21–25. As there is only one C-chain in each amylopectin molecule, the broad size distribution shows that the size of the C-chain is very different in the individual molecules.

1.2.1.3 Internal Unit Chains and Structural Types of Amylopectin

The size distribution of the internal chains in amylopectin, which are part of the B-chains as discussed above, has been studied by debranching limit dextrins (Akai et al. 1971; Atwell et al. 1980; Biliaderis et al. 1981a; Klucinec and Thompson 2002; Lee et al. 1968; MacGregor and Morgan 1984; Mercier 1973; Robin 1981; Shi and Seib 1995). Yao et al. (2004) and Xia and Thompson (2006) debranched the β-LDs of normal and mutant maize amylopectin and found that the short B-chains possessed two size categories with peaks at DP 5 and DP 8 or 9. These chain categories were named B1a- and B1b-chains, respectively (Yao et al. 2004). Bertoft et al. (2008) analyzed the φ,β-LDs of amylopectin from a range of different plants

and found that these chain categories were, in fact, common for all samples. Because the size distribution profile of the shortest chains with DP 3–7 (and the peak at DP 5 or 6) appeared to be specific for a particular plant, they suggested the name "fingerprint" B-chains (B_{fp}-chains), whereas the major part of the short B-chains with DP 8–23 was called BS_{major}-chains. The long internal B-chains with DP > 23 (BL-chains) corresponded apparently to the same categories of B2- and B3-chains as found in the whole amylopectin (Fig. 1.2).

Bertoft et al. (2008) divided the starch samples into four different structural types based on the internal unit chain profile of their amylopectin component. Long chains in type 1 amylopectins are typically not clearly distinguished from the short BS-chains, i.e., a groove in the chromatogram between BS- and BL-chains does not exist because the size distribution of the short chains is broad and overlap largely with the long chains. Further, the number of BL-chains is low, which results in a high ratio of BS:BL-chains (approximately 7.3–9.4). Type 1 amylopectin was found in several cereals, such as barley, oat, and rye, which all possess the A-type allomorph crystallinity. The structural type of these starches was therefore labeled "A:1" to denote the allomorph type of the granule and the structural type of the amylopectin, respectively. Type 2 amylopectins were found in both A- and C-type allomorph starches (the C allomorph is a mixture of A- and B-type crystals in the same granule (Buléon et al. 1998b)). To this structural type belong, e.g., maize, rice, and finger millet ("A:2") as well as kudzu and sago palm starch ("C:2"). (Finger millet is shown as an example in Fig. 1.2). In type 2 amylopectins, BS-chains are distinguished from BL-chains by a groove in the chromatograms at approximately DP 23 (because the size distribution of BS-chains is narrower compared to type 1), and BL-chains are more numerous than in type 1 amylopectins; the ratio of BS:BL-chains is approximately 4.4–6.8. B_{fp}-chains in both type 1 and type 2 amylopectins tend to appear as a clearly distinguishable peak in the internal chain profile. In some cereals, notably maize and rice, the B_{fp}-chains amount as much as about 20 % of all chains by number in the amylopectin, whereby they are as common as the major internal chain type (BS_{major}-chains).

Structural type 3 of amylopectin possesses somewhat more BL-chains than type 2, but notably less of B_{fp}-chains, so that these chains typically only possess a shoulder in the chromatograms instead of a clear peak as in type 2 (Bertoft et al. 2008). The BS:BL-chain ratio is 3.7–4.7. Examples of type 3 structure are arrowroot ("C:3") and tapioca starch ("A:3"). Type 4 amylopectins, finally, includes all B-type allomorph starches ("B:4"), such as potato and canna starch. This structural type is characteristic of a high content of BL-chains; especially B3-chains are found in larger number than in the other types. The ratio of BS:BL-chains is therefore low, around 2.3–3.0.

It should be noted that the division between the four types of amylopectin structures cannot be taken as absolute. The division was based on a collection of seventeen starches from diverse plant species (Bertoft et al. 2008), and some structural characteristics in other samples may overlap between the types. Indeed, Zhu et al. (2011a) found that amylopectin in sweet potatoes has a structure that is intermediate to types 2 and 3, and the structure of wheat amylopectin appears to be

intermediate between types 1 and 2 (Kalinga et al. 2013). Nevertheless, the results so far suggest a common, systematic division of the structure of amylopectins that is ubiquitous among plants with a normal starch anabolism. Amylopectin from mutant plants, in which one or more enzymes involved in the synthesis of starch are absent or inactive, might not fall into either of these structural types.

The internal B-chains are shorter than the original B-chains in the whole amylopectin (Yun and Matheson 1993; Klucinec and Thompson 2002; Bertoft et al. 2008; Zhu et al. 2011a), because the external segment is removed. Therefore, their original lengths are not exactly known. However, if it is assumed that the length of the external segments generally corresponds to the average ECL of the amylopectin (into which also the A-chains are included), one can theoretically reconstruct the original length of the B-chains by adding a segment to each B-chain that corresponds to ECL. This theoretical operation has been done for several samples, and it is generally found that the reconstructed profile of the B-chains fits rather well with the original unit chain profile at DP approximately ≥ 18 (Fig. 1.2) (Bertoft et al. 2008; Laohaphatanaleart et al. 2009; Zhu et al. 2011a). This suggests that in most cases the actual length of the external segment of the B-chains corresponds to ECL and that the majority of chains at DP ≥ 18 are B-chains in the amylopectin. In types 3 and 4 amylopectins, the reconstructions suggest that the peaks of the BS_{major}-chains and B_{fp}-chains correspond to a shoulder at DP 18–21 in the unit chain profiles of the whole amylopectins. In type 1 and 2 amylopectins, the BS_{major}-chains seem to correspond to DP 18 or 19 in the original chain profile (Bertoft et al. 2008). Especially in type 1 amylopectins, a clear shoulder is apparent at this position, whereas a weak shoulder at approximately DP 14 corresponds to the reconstructed position of the B_{fp}-chains. It was suggested that chains in the original amylopectin with approximate DP < 18 are mixtures of short B-chains (mostly B_{fp}-chains) and the A-chains (Bertoft et al. 2008).

Källman et al. (2013) analyzed the size distribution of the internal C-chain in barley. Like the size distribution of the C-chain in whole amylopectins (Hanashiro et al. 2002; Takeda et al. 2003), the internal C-chain distribution was unimodal with a peak around DP 30 (Källman et al. 2013). As the C-chain in whole amylopectin has peak DP ~40, this suggests that the length of the external segment of the C-chain is similar to that of the B-chains.

1.2.2 Clustered Arrangement of the Chains

The unit chains in amylopectin were originally suggested to be arranged as clusters by Nikuni in 1969. Soon thereafter, French (1972) and Robin et al. (1974) came to similar conclusions. A major contributor to these conclusions was the fact that the unit chain distribution shows that amylopectin consists of both long and short chains, of which the latter apparently are the clustered chains, whereas the former can be assumed to interconnect the clusters. Therefore, it appears that the ratio of S:L-chains in amylopectin is a measure of the size of clusters in the form of

the number of chains (NC) that at average is included in the clusters. Because A-type allomorph crystalline starches generally have higher S:L-chain ratio, their clusters are expected to be larger than in B-type allomorphs. Takeda et al. (2003) calculated the NC of clusters on this basis, and when also considering the average DP_n of amylopectin based on estimations of 2-aminopyridine-labeled samples, they concluded that up to 120 and 111 clusters build up the large amylopectin macromolecules in normal maize and rice, respectively (A-type allomorphs), but the small amylopectin molecules have only 5.0 and 4.2 clusters in these two starches, respectively. Large amylopectin molecules in potato (B-type allomorphs) have 117 clusters, whereas the small molecules consist of 15 clusters.

1.2.2.1 Isolation of Clusters

In order to perform a direct study of the structure of clusters in amylopectin, these structural units have to be isolated, which needs catalytic tools that break the long internal chains expected to be found between the clusters. Such tools are, unfortunately, difficult to find, and to date only a limited number of endo-acting enzymes have been used for this purpose. Bender et al. in 1982 hydrolyzed potato and maize amylopectin with cyclodextrin glycosyltransferase of *Klebsiella pneumoniae*. This enzyme form cyclodextrins by attack on the external chains of amylopectin, but it also attacks longer internal chain segments, whereby branched dextrins are released. These branched dextrins were further subjected to β-amylase digestion, and the remaining β-LDs were suggested to represent the clusters of the amylopectin. Bender et al. (1982) found that the size of the β-LDs of the clusters ranged between DP 40 and 140 and at average the clusters in potato were only slightly smaller (DP 75) than in maize (DP 80). The clusters from potato had longer B-chains (CL 17.8) than in maize (CL 14.1), and the degree of branching (DB) was 9.2–11.3 %, whereas maize clusters were more tightly packed with DB 12–14 %. The ratio of A:B-chains was slightly higher in maize clusters (1.22) than in potato clusters (1.06).

Finch and Sebesta (1992) used a maltotetraose-forming amylase from *Pseudomonas stutzeri* to isolate branched limit dextrins from the β-LDs of wheat and potato amylopectin. They suggested that the branched products corresponded to the units of clusters, which in wheat had a relative molecular mass of ∼7600 (corresponding to DP ∼47) and in potato ∼23,000 (DP ∼142). Thus, the size they found for the clusters in potato was nearly double compared to the value reported by Bender et al. (1982), who used cyclodextrin glycosyltransferase for the isolation. This suggests that the result is strongly dependent on the type of enzyme used in the investigation, because different enzymes apparently have different modes of action toward amylopectin. Interestingly, however, the results from both investigations showed that the structure of the amylopectin was a major factor that influenced on the results, because otherwise the results with a particular enzyme should have been similar regardless of the source of the amylopectin. Endo-acting enzymes have therefore an important potential to be used as tools for studying the structure of amylopectin.

An enzyme that has been much used by Bertoft and coworkers, and in a more systematic way, is the α-amylase of *Bacillus amyloliquefaciens* (known as the liquefying enzyme from *B. subtilis* in older literature). This enzyme was shown to have the most specific endo-catalytic action in comparison with several other α-amylases (Bijttebier et al. 2010; Goesaert et al. 2010). The enzyme has nine or ten subsites distributed unevenly around the catalytic site, so that three subsites are situated at the site where the reducing end side of the substrate binds and six subsites at the nonreducing side (Robyt and French 1963; Thoma et al. 1970). This specific structure results in a preferential production of maltohexaose from the nonreducing ends of amylopectin. Simultaneously with this action, the enzyme also performs endo-attack at internal chains (Robyt and French 1963; Bertoft 1989). Long internal chains are effectively attacked because all nine subsites on the enzyme become filled with the glucose residues in the chain (Robyt and French 1963). If the chain segment between branches is shorter than nine residues, the reaction rate slows down markedly, because all subsites cannot interact with the chain. Bertoft and coworkers have used this phenomenon to isolate clusters from a range of different starches by stopping the reaction at the time when the rate of hydrolysis slows down (Bertoft 1986, 1991, 2007b; Bertoft et al. 2011b; Bertoft et al. 1999; Bertoft et al. 2012a; Gérard et al. 2000; Kong et al. 2009; Laohaphatanaleart et al. 2010; Wikman et al. 2011; Zhu et al. 2011c). A consequence of using the enzyme from *B. amyloliquefaciens* is that a cluster will be defined as a group of chains in which the internal chain segments are shorter than nine residues (Bertoft 2007a).

The DP range of clusters in the form of φ,β-LDs obtained with the α-amylase from *B. amyloliquefaciens* and analyzed by GPC is generally broad: from approximately DP 10–15 up to 660–850 (Bertoft et al. 2012a). Average DP of clusters in different size fractions in potato ranged from 31 to 55 (Bertoft 2007b), which was smaller than the previously reported values by Bender et al. (1982) and Finch and Sebesta (1992). However, in comparison with the reported average size (DP 75) of clusters in waxy maize by Bender et al. (1982), the value obtained with *B. amyloliquefaciens* α-amylase was rather similar (DP 70.2). Wheat was reported to have clusters of average DP 82.4 (Kalinga et al. 2014), which is much higher than the value found by Finch and Sebesta (1992).

The average sizes of clusters isolated from different sources with the α-amylase from *B. amyloliquefaciens* are listed in Table 1.3. Interestingly, Bertoft et al. (2012a) found that the sizes generally follow the structural types of the amylopectins (discussed above in Sect. 1.2.1.3). Thus, clusters from types 1 and 2 amylopectin are larger than those from types 3 and 4. Also the average number of chains (NC) in the clusters in types 1 and 2 are larger than in type 4, whereas NC is intermediate in type 3. The degree of branches (DB) is around 15 % in types 1 and 2 and lower in types 3 and 4, which corresponds fairly well with the reported values for maize and potato, respectively, by Bender et al. (1982). Further, the average chain length (CL) is short in type 1–3 amylopectins and high in type 4. Moreover, ICL follows the same pattern (Table 1.3). As the division of amylopectin structural types is based on the internal unit chain profiles, it follows that the internal structure of amylopectin reflects the size and structure of the cluster units.

Table 1.3 Cluster structure of amylopectin from selected starches[a, b]

Starch source	Allomorph: amylopectin structure type[c]	NC	DP	DB	CL	ICL
Rye	A:1	11.5	70.1	15.0	6.1	4.0
Wheat[d]	A:1–2	14.2	82.4	16.0	5.8	3.6
Waxy maize	A:2	11.6	70.2	15.2	6.0	4.0
Rice	A:2	11.1	65.8	15.3	5.9	3.9
Arrowroot	C:3	9.2	56.3	14.6	6.1	4.2
Canna	B:4	8.2	56.3	12.7	6.9	5.2

[a]Values adapted from Bertoft et al. (2012a)
[b]*NC* number of chains per cluster, *DP* degree of polymerization, *DB* degree of branching, *CL* chain length, *ICL* internal chain length
[c]Crystalline structure of granule: amylopectin structural type
[d]Adapted from Kalinga et al. (2014)

1.2.2.2 Unit Chains in Clusters

The unit chain profile of clusters isolated with the α-amylase from *B. amyloliquefaciens* typically possesses less long chains than the original amylopectin, which shows that the long chains were cut by the enzyme (Bertoft 2007b; Bertoft and Koch 2000; Bertoft et al. 2011b; Gérard et al. 2000; Kalinga et al. 2014; Kong et al. 2009; Laohaphatanaleart et al. 2010; Zhu et al. 2011c). This suggests that the long chains are involved in the interconnection of the clusters. However, some long chains also remain in the isolated clusters, especially in clusters from amylopectins of structural type 4, but in smaller amounts also from the other structural types (Bertoft et al. 2012a). The profile of the short chains is mainly similar to the profile of S-chains in the amylopectin, which shows that the short chains build up the clusters in accordance with the cluster hypothesis (Bertoft et al. 2012a).

Many short chains in the isolated clusters are identical to those in the original macromolecule, albeit they are not experimentally distinguished from the new chains that are produced by the α-amylase by hydrolysis of the longer chains in amylopectin. As a result of the enzyme activity, new types of chains are found in the isolated clusters (Bertoft et al. 2012a). Notably, chains with DP around 18–27 were typically formed from all samples analyzed so far. The majority of the new C-chains of the isolated clusters were found to correspond to this DP range (Källman et al. 2013), which is expected because each cleavage of a longer B-chain by the α-amylase results in a new chain with a reducing end. The length of these new chains corresponds to the position of the groove in the chromatograms between S- and L-chains in amylopectin, and these chains are especially prominent in clusters from type 4 amylopectins (Bertoft 2007b; Bertoft et al. 2012a). In addition, isolated clusters from all types of starches have highly increased content of chains with DP 3 (Bertoft et al. 2012a). This suggests that there exists a certain conserved interconnection mode of the clusters in all types of starches that gives rise to this type of chains (Bertoft and Koch 2000).

Because the isolated clusters apparently contain new categories of chains, a new nomenclature for chains in these clusters was suggested, in which their names are assigned lowercase letters instead of the capital letters as for amylopectin (Bertoft et al. 2012a). Thus, a- and b-chains in isolated clusters correspond to A- and B-chains in amylopectin, but the size ranges are different. In φ,β-LDs of clusters, the majority of the a-chains correspond to maltosyl stubs. Several a-chains are maltotriosyl stubs, however, which depend on the fact that a small number of very short a-chains already are produced by the α-amylase and these are not attacked by either phosphorylase or β-amylase (Bertoft 2007b). These a-chains cannot be distinguished from the shortest b-chains with the same length. b0-chains have DP 4–6 and correspond largely to the internal B_{fp}-chains in amylopectin, but a lot of b0-chains, like all b-chains, are produced as a result of the action of the α-amylase (Bertoft et al. 2012a). b1-chains have a DP range of 7–18, b2-chains 19–27, and b3-chains DP ≥ 28. A detailed discussion of the involvement of these b-chain categories in the cluster structure is found in Sect. 1.3.2.2.

1.2.3 Building Blocks

The smallest, branched unit in amylopectin is the building block. These units are in practice limit dextrins that are produced by α-amylase (Bertoft et al. 1999; Zhu et al. 2011b). The composition of building blocks in amylopectin therefore depends on the mode of action of the enzyme, and different α-amylases might give rise to different compositions as a result of the distribution and number of subsites in the enzymes (Bijttebier et al. 2010; Derde et al. 2012). The structure of α-LDs of several α-amylases has been described in detail (Bines and Whelan 1960; Hall and Manners 1978; Hughes et al. 1963; Walker and Whelan 1960a). From the viewpoint of the structure of amylopectin, the works of Umeki and Yamamoto (1972a, b, 1975a, b) on the α-LDs formed by the saccharifying and liquefying α-amylases of *B. subtilis* (the latter being identical to the α-amylase of *B. amyloliquefacens*) are of special interest. They described the structure of singly and multiply branched limit dextrins from waxy rice in great detail and found that, by far, the most prominent dextrins are only singly branched. In LDs with three or more chains, they found that the branches are separated by one or two glucose residues (i.e., ICL is 1 or 2) and that branches never appear next to each other in amylopectin (Umeki and Yamamoto 1975a).

Later, Bertoft et al. (1999) also investigated the limit dextrins produced from isolated clusters of a waxy rice sample by the α-amylase of *B. amyloliquefaciens* and called them building blocks. This is thus the same enzyme as used for the isolation of clusters, but the reaction continues at a very slow rate and ultimately reaches a limit (Zhu et al. 2011b). In order to speed up the reaction rate, the isolated clusters are in practice treated with a 100- or 200-fold amount of the enzyme. The DP range of the branched building blocks is about 5–45 (Bertoft 2007a; Bertoft et al. 2012a; Bertoft et al. 2011a; Bertoft et al. 2010; Kalinga et al. 2014; Kong et al. 2009; Zhu et al. 2011b). The largest blocks correspond thereby to the smallest clusters in size – however, building blocks are much more densely branched than clusters: ICL

in building blocks is only 1–3. Branched building blocks have been size fractionated quantitatively by GPC and debranched (Bertoft 2007a; Bertoft et al. 2012b; Bertoft et al. 2011a; Bertoft et al. 2010). It was found that the smallest building blocks with DP 5–9 generally are singly branched, i.e., they consist of two chains and were named group 2 building blocks. Group 3 building blocks have three chains and cover generally the DP range 10–14, whereas group 4, with four chains, have DP 15–19 (Fig. 1.3). Group 5 building blocks consist of a more complicated mixture of α-LDs with between five and seven chains and DP approximately 20–35, whereas, finally, group 6 have DP > 35 and at average 10–12 chains. The same groups of building blocks appear to be universal among all starches, and, moreover, in all samples analyzed so far, group 2 building blocks are most abundant (they constitute roughly 50 % of all blocks by number), whereas group 3 is the second most abundant (25–30 %). Group 4 typically constitutes ∼10 % of the blocks, and groups 5 and 6 are found in only small amounts (Bertoft et al. 2012b). This surprising fact suggests a rather conservative architectural design of the amylopectin molecule throughout the plant kingdom.

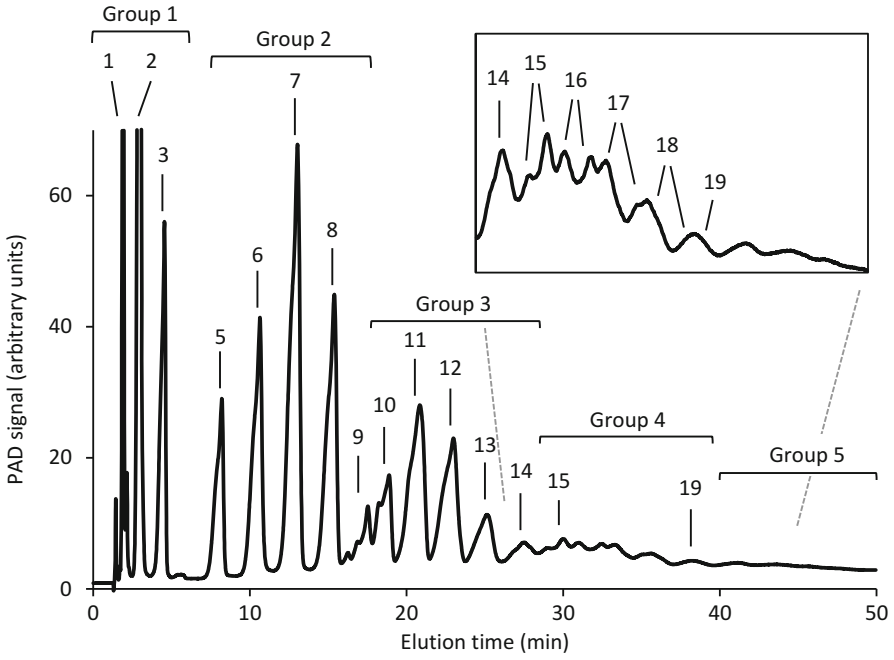

Fig. 1.3 Composition of building blocks in amylopectin from oat starch as obtained by high-performance anion-exchange chromatography with pulsed amperometric detection (HPAEC-PAD). Groups of building blocks are highlighted and numbers indicate DP. Dextrins with DP 1–3 (group 1) are glucose, maltose, and maltotriose, respectively, and come from interblock segments. Inset shows an enlargement of the complex pattern of blocks belonging to group 4. Building blocks in groups 5 or larger cannot be distinguished as peaks by this chromatographic technique

The reducing end in isolated clusters from barley was labeled with 2-aminopyridine, after which the composition of fluorescence-labeled building blocks was analyzed (Källman et al. 2013). It was found that the size distribution of labeled blocks was practically identical to the distribution of all building blocks (labeled and nonlabeled blocks). This suggests that any of the structural types of blocks can be situated at the reducing end side of the clusters with equal probability and that the organization or sequence of building blocks within a cluster apparently is random.

The degree of branching (DB) in building blocks is high, and it increases typically with the size of the blocks (Bertoft et al. 2012b). Thus, in group 2 building blocks, DB is around 14–15 %, and in group 6 DB is 19–22 %. The average CL is generally short and increases slightly from DP ∼3.6 in group 2 to DP ∼4.4 in group 6. It follows that the size distribution of the chains is narrow: chains in group 2 building blocks have DP between 2 and 7 and the major chain has DP 5. The size distribution broadens with the size of the blocks, and generally the peak position is at DP 5–7. Building blocks in group 6 tend to possess a smaller, second peak at DP 8, and it was suggested that these very large blocks might represent "immature" building blocks with a longer chain interconnecting two smaller blocks, on which one or two chains are connected (Bertoft et al. 2012b). Hypothetically, these chains would normally be "trimmed" by debranching enzymes during starch biosynthesis. "Trimming" of amylopectin chains during biosynthesis is necessary in order to form normal amylopectin (Ball et al. 1996).

The ratio of A:B-chains in building blocks is very difficult to measure exactly because the chains are very short and there exists a considerable overlap of A- and B-chains at DP 3. Nevertheless, a ratio of chains with DP 2 to chains with DP ≥ 4 can be considered as reflecting the true ratio of A:B-chains. Interestingly, building blocks from cereals tend to have a lower apparent A:B ratio than blocks from other sources like roots, tubers, and trunks (Bertoft et al. 2012b). This suggests differences in the fine structure of the building blocks. In cereals, the blocks appear to have a more preferred so-called Haworth conformation of the chains, whereas the other starches have a more preferred Staudinger conformation (Fig. 1.4). In the extreme Haworth conformation, the ratio of A:B-chains reaches zero (Haworth et al. 1937),

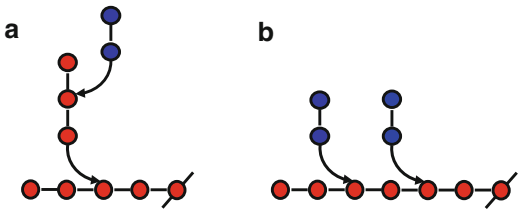

Fig. 1.4 Principal structure of a small building block with three chains with (**a**) Haworth conformation and (**b**) Staudinger conformation. *Blue circles* symbolize A-chains and *red circles* B-chains. In (**a**) the ratio of A:B-chains is 0.5 and for a very large molecule the ratio approaches zero. In (**b**) the ratio of A:B-chains is 2.0 and for a very large molecule the ratio approaches infinity

Table 1.4 Structural features of clusters from selected amylopectin samples[a, b]

Starch source	Allomorph: amylopectin structure type[c]	NC_{ap}	NC_{cltr}	LC	IB-CL	NBbl
Rye	A:1	17.2	11.5	0.5	5.9	5.5
Wheat[d]	A:1–2	17.2	14.2	0.4	6.4	6.3
Waxy maize	A:2	14.5	11.6	0.5	6.2	5.2
Rice	A:2	12.5	11.1	0.5	6.5	4.2
Arrowroot	C:3	10.4	9.2	0.8	6.7	4.1
Canna	B:4	8.1	8.2	1.2	7.6	3.7

[a]Values adapted from Bertoft et al. (2012a)
[b]NC_{ap} Expected number of chains per cluster based on the ratio of S:L-chains in amylopectin, NC_{cltr} number of chains in isolated clusters, *LC* average number of long chains (b2- and b3-chains) in isolated clusters, *IB-CL* interblock chain length, *NBbl* average number of building blocks in isolated clusters
[c]Crystalline structure of granule: amylopectin structural type
[d]Adapted from Kalinga et al. (2014)

and in the Staudinger conformation, the ratio reaches infinity (Staudinger and Husemann 1937) in a polysaccharide. Such conformational differences might have – as yet unknown – influences on starch properties and functionality.

Simultaneously with the branched building blocks, the α-amylase of *B. amyloliquefaciens* also produces short, linear dextrins with DP 1–6 ("group 1" blocks) from isolated clusters (Bertoft 2007a). If treated with β-amylase, these dextrins are shortened into DP 1–3 and are then better separated from the branched building blocks with DP ≥ 5 (Fig. 1.3) (Bertoft et al. 2011a). The linear dextrins origin from the chain segments between the building blocks in the clusters and can be used to estimate the average interblock chain length (IB-CL) when the number of branched building blocks in the isolated cluster is known (Bertoft 2007a; Kong et al. 2009; Bertoft et al. 2010). IB-CL apparently correlates with the four structural types of amylopectin (discussed in Sect. 1.2.1.3). Type 1 amylopectins have the shortest IB-CL of approximately DP 5.5–5.9, whereas type 4 has the longest segments of DP 7–8, and types 2 and 3 have intermediate IB-CL (Table 1.4) (Bertoft et al. 2012a). It was shown that IB-CL correlates positively with the onset temperature of gelatinization of starch granules (Vamadevan et al. 2013), which suggests that IB-CL is of general importance for the structural architecture of the granules and their functionality.

1.3 Models of the Semicrystalline Structure of Amylopectin

All since the nature of the linkages between the anhydroglucose units in starch was confirmed in the 1920s and 1930s (Seetharaman and Bertoft 2012a), structural models of the macromolecules have been proposed. The earliest models by Haworth et al. and Staudinger and Husemann, both published in 1937, were aimed to describe the "starch molecule." Soon after, Meyer et al. (1940) isolated the two

major components from starch and realized that only amylopectin was branched. Subsequently, Meyer and Bernfeld (1940) proposed a structure for this component, in which the branches were randomly outspread and the ratio of A:B-chains was one. Later works confirmed largely the ratio (Peat et al. 1952b; Larner et al. 1952) and the model became generally accepted. This model was attempted to account for both glycogen and amylopectin, but when it was realized that these two molecules are different, new models were suggested based on the unit chain profile of amylopectin (Gunja-Smith et al. 1970) and on the action pattern of starch branching enzyme (Borovsky et al. 1979). In our time, the cluster model, which was suggested more than four decades ago (Nikuni 1969; French 1972; Robin et al. 1974), has become largely accepted. However, all researchers today do not entirely agree with the cluster model, and it is a fact that it has never been proved definitely. Alternatives exist therefore, and both the cluster concept and the present alternatives are discussed below. A comprehensive review of the alternative backbone concept is available for the interested reader (Bertoft 2013).

1.3.1 The Cluster Model

1.3.1.1 Origin of the Cluster Concept

The cluster concept of the structure of amylopectin is the outcome of several findings that were summarized by Finch and Sebesta (1992) as (a) the isolation of multiply branched oligosaccharides (i.e., multiply branched building blocks), which represents about 35 % of the branches in amylopectin and in which ICL is only one glucosyl unit, (b) the formation of acid-resistant amylodextrins by acid hydrolysis of starch granules, (c) the existence of discrete size groups of chains (i.e., short and long chains), (d) the formation of macrodextrins (i.e., the clusters) by partial hydrolysis with cyclodextrin glycosyltransferase or α-amylase, and (e) the existence of discrete periodicities in the granules (i.e., the lamellae). Indeed, it is interesting to notice that prior to these findings, it was generally believed that the principal component that gives rise to the crystallinity of starch granules is amylose rather than amylopectin. This was due to the fact that the first helical structure that was characterized was the complex between amylose and iodine, and similar helical structures were found to be present in the granules (Seetharaman and Bertoft 2012b).

The view slowly changed starting with the finding of the lamellar repeat distance by Sterling in 1962, because the lamellae are comparatively short compared to the long chains of amylose. Kainuma and French (1972) isolated so-called Nägeli amylodextrins from potato by treating the starch granules at room temperature in 16 % H_2SO_4 for 90 days. They found that the Nägeli amylodextrins retained the sharp B-type X-ray pattern typical for potato starch even in the dry state if they were admixed with a noncrystalline filler. They argued that water is not required to maintain the helical geometry of the molecular chains and suggested that the

chains form a stable double helix with parallel strands. Each strand contains 6 glucose units per turn with a pitch of 21 Å (2.1 nm) (Kainuma and French 1972). This structure was later essentially confirmed (Imberty and Pérez 1988), and it was shown that also A-crystalline starches have similar double helices (Imberty et al. 1987, 1988). Watanabe and French (1980) analyzed the molecular structure of Nägeli amylodextrins and found that they exist of essentially three fractions with DP ∼12, ∼25, and ∼35, respectively. The smallest amylodextrins are linear chains without branches, the intermediate-sized dextrins consist of two such chains in a double helical conformation and are interconnected with a branch, whereas the larger dextrins have three or more chains and branches. Later, Imberty and Pérez (1989), using molecular modeling techniques, showed that the branch point is not a hinder for double helical formation, but likely it stabilizes the structure. Numerous investigations on the molecular structure of Nägeli amylodextrins and so-called lintner dextrins (which are essentially the same, but the granules are treated with HCl instead of H_2SO_4) have later confirmed these structures (Biliaderis et al. 1981b; Umeki and Kainuma 1981; Srichuwong et al. 2005a; Wikman et al. 2014; Jane et al. 1997; Kitahara et al. 1997; McPherson and Jane 1999; Robin et al. 1974; Bertoft 2004a). The length of the chains in these acid-resistant parts of the granules corresponds rather well to the average external chain length in amylopectin as well as to the estimated thickness of the crystalline lamellae in the granules. It appears that most of the branches are clustered into the amorphous lamellae and removed by the acid.

Thus, today it is generally agreed that amylopectin is the principal component of the lamellar structure in starch granules. The majority of the branches, which do not crystallize, participate in the internal parts of the amylopectin in the amorphous lamellae. The external chains crystallize as double helices in the crystalline lamellae and are oriented perpendicular to the surface of the granules, which forms the basis for the birefringence pattern of the granules seen in plane-polarized light as a "Maltese cross"(French 1972).

1.3.1.2 Organization of Cluster Units

The radial orientation of the short chains in amylopectin suggests that the macromolecule is oriented in the granule with the nonreducing ends toward the surface and the sole reducing end toward the center of the granule (known as the hilum). In the first cluster models suggested by Nikuni (1969) and French (1972), the amylopectin molecule was therefore oriented in this way. Robin et al. (1974), who studied the structure of acid-treated granules (lintners), suggested that the clusters are highly organized in this orientation, so that the external chains collectively form the crystalline lamellae and the clustered branches forms the amorphous lamellae. Robin et al. (1974) suggested that the S-chains (which they collectively named as "A-chains" and thereby did not apply the original nomenclature of Peat et al. (1952b); see above Sect. 1.2.1.1) form the clusters and the L-chains (which they named as "B-chains") interconnect the clusters.

Hizukuri (1986), who found a periodicity in chain length of about DP 27–28, took the concept of Robin et al. further and suggested that B2-chains extend over two crystalline lamellae and interconnect two clusters, whereas B3-chains extend over three crystalline lamellae and therefore are involved in the interconnection of three clusters. The same principle can be extended to B4-chains, etc. This elegant model would thus fit into the lamellar repeat structure when the pitch of the double helix is 2.1 nm and includes six glucosyl units (Fig. 1.5). However, the internal chain segments in the amorphous lamella do not form double helices. Furthermore, later results have shown that, in order to organize the double helices in parallel fashion and as either A- or B-type crystals, the spacer arms that connects to the double helices have to be bended considerably even into almost perpendicular directions (O'Sullivan and Pérez 1999). It is also important to note that Hanashiro et al. (1996) found another periodicity in chain length of only 12 glucosyl units, and it remains unknown how this periodicity corroborates with the model or the lamellar repeat distance.

Thompson (2000) highlighted that the model of Robin et al. from 1974 included different modes of interconnection of the cluster units. Some long B-chains in the model extend from the amorphous part of clusters in one lamella through the crystalline lamella and into the next pair of lamellae (and correspond largely to the B2-chain function in Hizukuri's model). Other long B-chains extend from the nonreducing end side of clusters into the next level of lamellae, in which case the length of the external chain in that cluster is very short. If such short external segments exist is not known, however. Finally, in a third mode of interconnection, the clusters are interconnected through chains in a single amorphous lamella, i.e., the amorphous parts of the clusters are interconnected with internal chain segments that apparently form a kind of backbone.

1.3.2 The Building Block Backbone Concept

1.3.2.1 Structural Features of Clusters

The cluster concept rests on indirect evidences for the existence of clusters. As was outlined in Sect. 1.2.2.1, attempts to isolate clusters have been done by using endo-acting enzymes, of which the α-amylase of *B. amyloliquefaciens* has been mostly used. It is clear that long chains in amylopectin are cleaved in order to produce these clusters. Further, the isolated clusters are more densely branched than the macromolecule itself, and they consist to a large extent of short chains. Some critical structural features of these clusters are, however, not entirely compatible with the cluster model (Bertoft et al. 2012a). Whereas the cluster model predicts that the number of chains (NC) should correspond to the ratio of S:L-chains in amylopectin plus approximately one chain (because a shorter segment of the L-chains remains in the isolated cluster), the NC of the isolated clusters is in many cases lower than the predicted value (Table 1.4). This is especially the case with

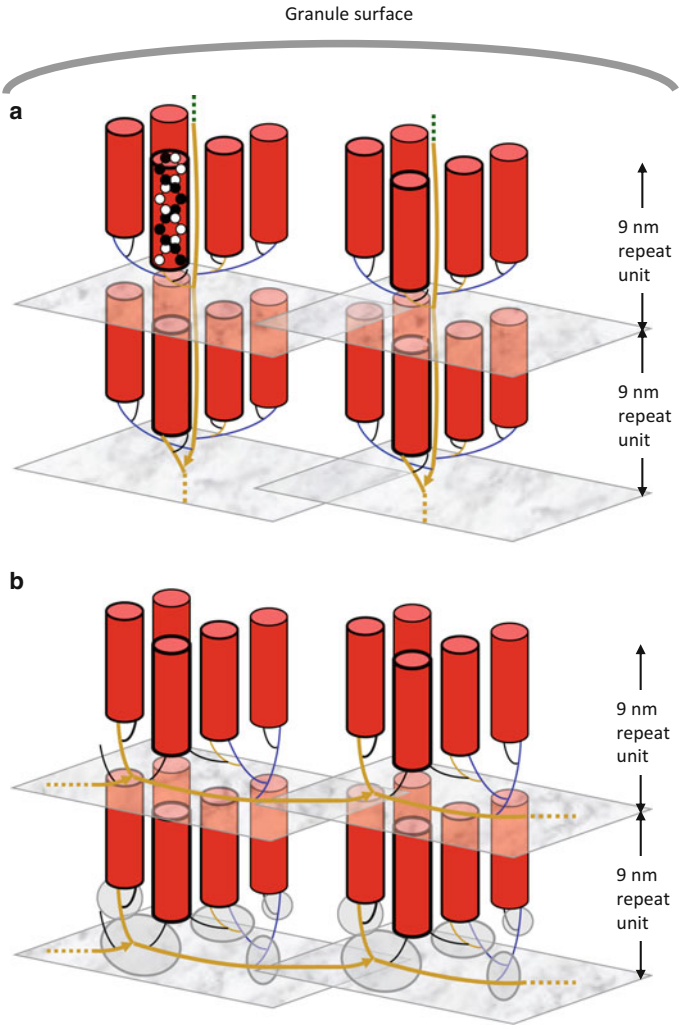

Fig. 1.5 Schematic drawings of amylopectin molecules forming the alternating crystalline and amorphous lamellae (9 nm repeat distance) in a starch granule according to (**a**) the cluster model based on Robin et al. (1974) and Hizukuri (1986) or (**b**) the building block backbone model based on Bertoft et al. (2010). In both cases, the short chains, which form double helices (symbolized as cylinders with one double helix as example) and crystallize, have their nonreducing ends toward the granule surface, but in (**a**) the macromolecules are lined up side-by-side and the long chains penetrate two or several repeat units, whereas in (**b**) the molecules are layered on top of each other and the long chains form the backbone within each amorphous lamella. Long B-chains are symbolized as thick *yellow lines*, BS_{major}-chains as thin *blue lines*, B_{fp}-chains as thin *yellow lines*, and A-chains as thin *black lines*. Building block areas are encircled in the lower layer in (**b**). The "glass plates" do not exist but are the artist's addition to highlight areas of clusters and the border between the repeat units

samples from amylopectin of structural type 1, which suggests that in these samples also short chains are involved in cluster interconnection. Also samples of type 2 tend to have clusters with lower NC – however, amylopectin from sago starch is, so far, an exception and have clusters with higher NC (Bertoft et al. 2012a). Only clusters isolated from type 4 amylopectins appear to have NC that fairly well corresponds to the expected value based on S:L-chains in the amylopectin (Table 1.4).

Another structural feature of the isolated clusters, which does not support the cluster model, is that some long b2- and b3-chains (i.e., chains with lengths that correspond to the internal BL-chains in the LD of amylopectin) remain in the cluster preparations (Bertoft et al. 2012a). The number of these chains varies. Isolated clusters from type 1 amylopectins have generally few long b-chains: at average only 0.5 chains (suggesting that only every second cluster possesses the chain). Clusters from type 2 and type 3 amylopectins have more long b-chains, and in clusters from type 4, the number of these chains is even slightly more than one, which suggests that in practice every isolated cluster has the chain (Table 1.4).

A reason to the fact that these long chains remain in the cluster preparations could simply be that the hydrolytic reaction was terminated too early. Indeed, if the reaction is allowed to proceed – which it will, but at a considerably lower rate (Zhu et al. 2011c) – the long chains disappear (and ultimately building blocks are formed) (Zhu et al. 2011b). However, this results in dextrins with less chains than in the isolated clusters, and, therefore, they correspond even less to the ratio of S:L-chains in the amylopectin. Indeed, the slow continuous hydrolysis of isolated clusters suggests that they do not contain longer internal chain segments that the α-amylase of *B. amyloliquefaciens* readily attacks (i.e., segments with ICL ≥9), and thereby the long b3-chains appear to consist of only shorter internal chain segments.

1.3.2.2 Organization of Building Blocks

As we have seen, the isolated clusters consist of still smaller and more densely branched units of building blocks. As the constitution of groups of building blocks is rather similar, though not identical, in isolated clusters from different plants species, the number of building blocks in clusters is mainly directly related to the size of the cluster (Table 1.4). Typically, small clusters, like those from structural type 4 amylopectins, contain 3–4 building blocks (Bertoft 2007a; Bertoft et al. 2012a). The comparatively large clusters found in type 1 amylopectins have typically 5–6 building blocks at average (Bertoft et al. 2012a). Very large clusters in barley (NC 18.3) were found to be build up by approximately 8 blocks (Bertoft et al. 2011a).

Bertoft et al. (2012a) found that the new chains formed when clusters are isolated generally can be divided into the distinct groups of b0-, b1-, b2-, and b3-chains already discussed above (Sect. 1.2.2.2). They suggested that these chains have specific roles in the organization of the building blocks in the clusters (Fig. 1.6). b0-chains, which are very short with DP 4–6, are of the same length as the majority of b-chains in building blocks (Bertoft et al. 2012b). It appears, therefore, that these chains are entirely included inside the building blocks and that they do not

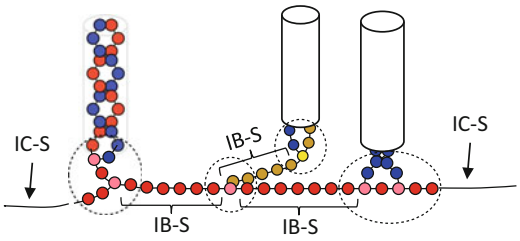

Fig. 1.6 Schematic drawing showing the building block structure of a cluster. Double helices (symbolized as cylinders with one double helix as example) are formed by the external chain segments and are removed when clusters are isolated experimentally. Building block areas are encircled. *Blue* symbols are glucose residues in a-chains, *yellow* in b1-chains, and *red* in b2-chains (or b3-chains). Residues involved in branch linkages are shown in light colors. The interblock segments (IB-S) are shown and intercluster segments (IC-S) are indicated as *dotted lines*

include any interblock segments. b0-chains are formed in large amounts when clusters are isolated together with chains of DP 3, which are mixtures of a- and b-chains (Bertoft et al. 2012a). b1-chains with DP 7–18 may include one interblock segment with DP 5–8 and parts of short-chain segments with DP 2–7 that are included in one or two adjacent building blocks. Thus, this type of chain presumably interconnects two building blocks (Fig. 1.6). The length of b2-chains (DP 19–27) suggests a length in the order of an additional interblock segment and an additional internal block segment, together approximately 12 glucosyl units. These chains, therefore, possibly contain two interblock segments and interconnect three building blocks. Finally, b3-chains appear to correspond to the addition of still a couple of these segments, whereby they would include three interblock segments. This suggests that there exists a periodicity of chain length inside the isolated cluster that roughly corresponds to DP ∼12 (Bertoft et al. 2012a). Interestingly, this is the same periodicity that Hanashiro et al. (1996) found by comparing different amylopectins, and possibly, therefore, their periodicity in chain length stems from a universal principle of the organization of building blocks in amylopectin.

The proposed structural involvement of the unit chains in the organization of the building blocks has consequences for the molecular architecture, or conformation, of the clusters. The fact that long b2- and b3-chains are rather rare in the cluster (Table 1.4) suggests a structure where these long chains form a backbone in the cluster, along which the building blocks are outspread (Fig. 1.6). The more frequently occurring b1-chains might constitute branches connecting building blocks to the backbone of the cluster.

1.3.2.3 The Backbone

A backbone concept of amylopectin structure is old: Already the structure proposed by Staudinger and Husemann in 1937 is a backbone consisting of a long chain, onto

which several short branches are attached. Later, other structures with a backbone concept were proposed, but with the difference that the backbone not necessarily consists of a single chain, but is build up from several chains that cooperatively form a backbone-like structure (Babor et al. 1968; Borovsky et al. 1979; Matheson and Caldwell 2008; Bertoft 2004b; Bertoft et al. 2010). Waigh and coworkers (2000a, b) highlighted that a backbone, onto which spacer arms connect the double helices, is compatible with a chiral side-chain liquid-crystalline model of the structure and explains to a large part the properties of amylopectin in the starch granule. The backbone, together with the spacer arms, forms the amorphous part of the macromolecule, whereas the double helices, just like in the traditional cluster model, form the crystalline lamellae.

The isolated clusters, as outlined above, apparently also have a backbone type of structure. It is easy to imagine that these clusters combine through their backbone chains and ultimately form the macromolecule (Fig. 1.5). Segments that interlink the clusters are presumably longer than those interconnecting the blocks. In a few instances, the average intercluster chain length (IC-CL) has, in fact, been estimated: In cassava IC-CL was between 10.5 and 12.3 (Laohaphatanaleart et al. 2010), in sweet potato 9.5 and 10.7 (Zhu et al. 2011c), in amaranth 10.7 and 13.8 (Kong et al. 2009), and in barley 9.5 and 14.3 (Bertoft et al. 2011a). It is noted that, in essence, there is no functional difference between the intercluster segment and the interblock segment, because they are both – in practice – interconnecting building blocks (Fig. 1.5). The only difference is that IC-CL is somewhat longer than IB-CL. The apparent intercluster involvement of the former segment is a result of the number of subsites on the α-amylase that was used for the isolation of clusters, which results in an initial effective hydrolysis of internal chain segments with $\geq$9 glucosyl residues. As a consequence, the concept of clusters becomes artificial, and the remaining actual structural units in amylopectin become the building blocks. In this context, it is very interesting to notice that Thurn and Burchard already in 1985 calculated that the clusters in amylopectin at average contain 3.22 branches (or 4.22 chains), an estimation that is not far from the average found experimentally for the building blocks in most clusters (NC 2.8–3.5) (Bertoft et al. 2012a). Thus, the building blocks are possibly identical to the "clusters" of Thurn and Burchard.

Another interesting detail, which concerns the building block backbone concept, is the fact that Hanashiro et al. (1996) only found a periodicity in chain length below DP 37 in amylopectin. This possibly suggests that the shorter chains (corresponding to b1- and probably some of the b2-chains in clusters) are mainly involved in the branches of the backbone where more defined IB-CL would affect their size distribution. In contrast, the longer chains are involved in the actual backbone, because along the backbone, a larger variability in IB-CL and IC-CL is probably found, which will diminish any periodicity in chain length. Indeed, the size distribution of the C-chain (Hanashiro et al. 2002; Källman et al. 2013) does not indicate any special chain length categories, but implies a more continuous size distribution. This suggests that the C-chain in amylopectin, as well as in the clusters, originates from the backbone (Källman et al. 2013).

An interesting detail in the backbone concept (Matheson and Caldwell 2008; Bertoft et al. 2010; Waigh et al. 2000b) is that the short chains of the amylopectin are essentially extending perpendicular to the long chains in the backbone. In the starch granules, this result is a formation of the lamellar repeat distance by amylopectin molecules positioned layer by layer on each other rather than being molecules that extend through the layers (Fig. 1.5) (Bertoft 2013). This structure is perfectly in agreement with the results of acid treatment of granules, which removes the amorphous layers and leaves the resistant crystalline layers intact. The crystalline layers have been isolated in the form of nanocrystals with dimensions that suggest they are composed of hundreds of double helices (Putaux et al. 2003). As single clusters only contain the order of 3–8 double helices, it implies that a crystalline lamella is a cooperative structure, to which building blocks from several clusters and probably amylopectin molecules contribute (Pérez and Bertoft 2010). Furthermore, it is clear that the products of acid-treated starch granules cannot distinguish between the backbone model and the more traditional cluster model (albeit they form one of the bases for the cluster concept), because the result is identical with both concepts (Bertoft 2004b).

1.3.2.4 The "Rubber Band" Principle

The structures of amylopectins from the four structural types possess some interesting features. Certain systematic changes in the structural parameters are noted when going from type 1, through type 2 and 3, to type 4 amylopectin (Tables 1.2–1.4): (a) The size of the clusters become smaller and they contain fewer building blocks, (b) the number of long b2- and b3-chains increases, (c) the external chain length increases, (d) the internal chain length between branches increases, and (e) the length of the interblock segments increases. However, there is no particular trend for the hydrolysis limit value, which is in the order of 52–60 % depending on the amylopectin sample and which enzyme is used (β-amylase alone or in combination with phosphorylase) (Bertoft 2004b; Bertoft et al. 2008). This is so because when ECL is higher, also ICL increases and the relative proportions of the external part (roughly 60 %) and the internal part (∼40 %) are about the same regardless of the source of the amylopectin. This universal feature likens the properties of a rubber band (Wikman et al. 2011), in which all parts elongate simultaneously when it becomes stretched.

This "rubber band" principle is compatible with the backbone concept (Bertoft et al. 2012a). Type 1 amylopectins have comparatively short internal (and external) chains. Also IB-CL is short and overall there exist rather few segments that correspond to IC-CL. This results in large clusters with many building blocks. Because the clusters contain very few long b-chains, many of the building blocks are probably situated outside the backbone and are connected to it through the numerous short b1-chains. Instead, type 4 amylopectins have long internal (and external) chains and IB-CL is long. Therefore, there are also many internal chains that function as intercluster segments, which result in small clusters. These clusters

contain typically more long b-chains, which suggest that most of the rather few building blocks are aligned along the backbone and more rarely connected to side chains (Bertoft et al. 2012a).

It should be noted that this systematic structural architecture of amylopectin was shown to exist among several normal starch samples and is probably valid throughout the plant kingdom (Bertoft et al. 2012a). However, the "rubber band" principle might not be applicable to starches from mutant plants, in which one or more of the naturally existing starch-synthesizing enzymes are absent or inactive. Indeed, amylopectin from barley possessing the *amo1* mutation, which gives rise to a defect starch synthase III enzyme, was shown to be an exception from the "rubber band" principle (Bertoft et al. 2011b). The amylopectin in the mutant possessed an increased φ,β-limit value compared to the wild-type, and this was due to shorter ICL, whereas ECL remained the same as in the wild-type.

1.3.3 The Superhelical Structure

Oostergetel and van Bruggen (1993) used electron optical tomography and cryo-electron diffraction to study the semicrystalline structure of potato starch granules after mild acid hydrolysis. They observed more or less continuous left-handed helical segments with a diameter of approximately 18 nm and a pitch of 10 nm. They suggested that these segments consist of the crystalline layers that form a continuous network of left-handed superhelices packed in a tetragonal array. The amylopectin molecules lie side-by-side and the whole superhelical arrangement is a cooperative super-structure, in which the neighboring superhelices are shifted relative to each other by half the helical pitch.

The model was later refined by Waigh et al. (1999), who used small-angle X-ray microfocus scattering. They described the superhelix as being composed of "pie-shaped" lamellar motifs that are attached to a distorted helical lattice. The amylopectin double helices build up the lamellar motifs, and the branches of amylopectin are found between the crystalline lamellae forming continuous helical amorphous lamellae. The pitch of the superhelix corresponds to the lamellar repeat distance of 9 nm. The physical basis of the helical lamellae (as opposed to flat lamellae) was proposed to be a product of a chiral side-chain liquid-crystalline structure of amylopectin and the presence of a chiral bending force. Inside the superhelix is a central hole with a diameter of 8 nm and unknown content, but it was assumed that it has the same density as the amorphous lamellae.

Literature concerning the superhelical structure is very limited (Waigh et al. 1999; Oostergetel and van Bruggen 1993). Oostergetel and van Bruggen (1993) based their model on the traditional cluster concept, whereas Waigh et al. (2000b) clearly suggested that it involves a backbone structure of amylopectin. With the former structure, the superhelix would be composed of a number of amylopectin molecules in parallel direction. With a backbone concept, however, it would be possible (although not necessary) that the superhelix consists of only a single

amylopectin molecule (Bertoft 2004b). The relationship between the superhelix and the other macrostructures inside starch granules is unknown to date. In particular, its connection with the blocklet structure is intriguing. Baker et al. (2001) found small blocklets in acid-treated maize starch granules with dimensions approximately 10–30 nm and noted the similarity in size with the proposed superhelix.

1.4 Conclusions

The principal component responsible for the semicrystalline structure of starch granules is amylopectin. This very large, branched molecule consists of short- and long-unit chains that are combined with α-(1,6)-linkages. Two major models presently describe the arrangement of the unit chains to form the final architecture of the macromolecule. In the more traditional cluster concept, the branches form clusters and the number of chains in the clusters is reflected in the ratio of S:L-chains in amylopectin, because the model suggests that the long chains interconnect clusters. With this model, the whole macromolecule penetrates stacks of amorphous and crystalline lamellae in the starch granules, i.e., the direction of the molecules is radial in the granule. In the newer, backbone concept, the principal, branched structural units are the building blocks, which are considerably smaller than clusters and can be experimentally isolated. In this model, the building blocks are situated along a backbone that consists to a large part, but not necessarily only, the long chains. Some building blocks can be connected to the backbone through shorter side chains. With this model, tangentially oriented amylopectin molecules form layers upon each other, which results in the semicrystalline lamellar stacks in the granules. The short chains, which crystallize, are oriented radially, however, and give rise to the birefringent property of the granules. Unfortunately, so far there is no particular experiment that definitely discriminates between the two models, and both models are also compatible with the superhelical concept of amylopectin structure.

References

Aberle T, Burchard W, Vorwerg W et al (1994) Conformational contributions of amylose and amylopectin to the structural properties of starches from various sources. Starch-Starke 46:329–335

Akai H, Yokobayashi K, Misaki A et al (1971) Structural analysis of amylopectin using Pseudomonas isoamylase. Biochim Biophys Acta 252:427–431

Aoki N, Umemeto T, Yoshida S et al (2006) Genetic analysis of long chain synthesis in rice amylopectin. Euphytica 151:225–234

Atkin NJ, Abeysekera RM, Cheng SL et al (1998) An experimentally-based predictive model for the separation of amylopectin subunits during starch gelatinization. Carbohydr Polym 36:173–192

Atkin NJ, Cheng SL, Abeysekera RM et al (1999) Localisation of amylose and amylopectin in starch granules using enzyme-gold labelling. Starch-Starke 51:163–172

Atwell WA, Hoseney RC, Lineback DR (1980) Debranching of wheat amylopectin. Cereal Chem 57:12–16
Babor K, Kalác V, Tihlárik K (1968) Structure of amylopectin (I). Preparation and structure of α-amylase macrodextrin. Chem Zvesti 22:321–326
Baker AA, Miles MJ, Helbert W (2001) Internal structure of the starch granule revealed by AFM. Carbohydr Res 330:249–256
Baldwin PM, Adler J, Davies MC et al (1998) High resolution imaging of starch granule surfaces by atomic force microscopy. J Cereal Sci 27:255–265
Ball S, Guan H-P, James M et al (1996) From glycogen to amylopectin: a model for the biogenesis of the plant starch granule. Cell 86:349–352
Banks W, Greenwood CT (1973) Molecular properties of the starch components and their relation to the structure of the granule. Ann NY Acad Sci 210:17–33
Bender H, Siebert R, Stadler-Szöke A (1982) Can cyclodextrin glycosyl transferase be useful for the investigation of the fine structure of amylopectins?: characterisation of highly branched clusters isolated from digests with potato and maize starches. Carbohydr Res 110:245–259
Bertoft E (1986) Hydrolysis of amylopectin by the alpha-amylase of *B. subtilis*. Carbohydr Res 149:379–387
Bertoft E (1989) Partial characterisation of amylopectin alpha-dextrins. Carbohydr Res 189:181–193
Bertoft E (1991) Investigation of the fine structure of alpha-dextrins derived from amylopectin and their relation to the structure of waxy-maize starch. Carbohydr Res 212:229–244
Bertoft E (2004a) Lintnerisation of two amylose-free starches of A- and B-crystalline types, respectively. Starch-Starke 56:167–180
Bertoft E (2004b) On the nature of categories of chains in amylopectin and their connection to the super helix model. Carbohydr Polym 57:211–224
Bertoft E (2007a) Composition of building blocks in clusters from potato amylopectin. Carbohydr Polym 70:123–136
Bertoft E (2007b) Composition of clusters and their arrangement in potato amylopectin. Carbohydr Polym 68:433–446
Bertoft E (2013) On the building block and backbone concepts of amylopectin structure. Cereal Chem 90:294–311
Bertoft E, Koch K (2000) Composition of chains in waxy-rice starch and its structural units. Carbohydr Polym 41:121–132
Bertoft E, Seetharaman K (2012) Starch structure. In: Tetlow I (ed) Starch: origins, structure and metabolism. Society of Experimental Biology, London, pp 1–27
Bertoft E, Zhu Q, Andtfolk H et al (1999) Structural heterogeneity in waxy-rice starch. Carbohydr Polym 38:349–359
Bertoft E, Piyachomkwan K, Chatakanonda P et al (2008) Internal unit chain composition in amylopectins. Carbohydr Polym 74:527–543
Bertoft E, Laohaphatanaleart K, Piyachomkwan K et al (2010) The fine structure of cassava amylopectin. Part 2. Building block structure of clusters. Int J Biol Macromol 47:325–335
Bertoft E, Källman A, Koch K et al (2011a) The building block structure of barley amylopectin. Int J Biol Macromol 49:900–909
Bertoft E, Källman A, Koch K et al (2011b) The cluster structure of barley amylopectins of different genetic backgrounds. Int J Biol Macromol 49:441–453
Bertoft E, Koch K, Åman P (2012a) Building block organisation of clusters in amylopectin of different structural types. Int J Biol Macromol 50:1212–1223
Bertoft E, Koch K, Åman P (2012b) Structure of building blocks in amylopectins. Carbohydr Res 361:105–113
Bijttebier A, Goesaert H, Delcour JA (2010) Hydrolysis of amylopectin by amylolytic enzymes: structural analysis of the residual amylopectin population. Carbohydr Res 345:235–242
Biliaderis CG, Grant DR, Vose JR (1981a) Structural characterization of legume starches. I. Studies on amylose, amylopectin, and beta-limit dextrins. Cereal Chem 58:496–502

Biliaderis CG, Grant DR, Vose JR (1981b) Structural characterization of legume starches. II. Studies on acid-treated starches. Cereal Chem 58:502–507

Bines BJ, Whelan WJ (1960) The mechanism of carbohydrase action. 6. Structure of a salivary α-amylase limit dextrin from amylopectin. Biochem J 76:253–257

Borovsky D, Smith EE, Whelan WJ et al (1979) The mechanism of Q-enzyme action and its influence on the structure of amylopectin. Arch Biochem Biophys 198:627–631

Buléon A, Colonna P, Planchot V et al (1998a) Starch granules: structure and biosynthesis. Int J Biol Macromol 23:85–112

Buléon A, Gérard C, Riekel C et al (1998b) Details of the crystalline ultrastructure of C-starch granules revealed by synchrotron microfocus mapping. Macromolecules 31:6605–6610

Buttrose MS (1960) Submicroscopic development and structure of starch granules in cereal endosperm. J Ultrastr Res 4:231–257

Buttrose MS (1962) The influence of environment on the shell structure of starch granules. J Cell Biol 14:159–167

Cameron RE, Donald AM (1992) A small-angle X-ray scattering study of the annealing and gelatinization of starch. Polymer 33:2628–2635

Charoenkul N, Uttapap D, Pathipanawat W et al (2006) Simultaneous determination of amylose content & unit chain distribution of amylopectins of cassava starches by fluorescent labeling/HPSEC. Carbohydr Polym 65:102–108

Chauhan F, Seetharaman K (2013) On the organization of chains in amylopectin. Starch-Starke 65:191–199

Dang JMC, Copeland L (2003) Imaging rice grains using atomic force microscopy. J Cereal Sci 37:165–170

Daniels DR, Donald AM (2003) An improved model for analyzing the small angle X-ray scattering of starch granules. Biopolymers 69:165–175

Derde LJ, Gomand SV, Courtin CM et al (2012) Hydrolysis of β-limit dextrins by α-amylases from porcine pancreas, *Bacillus subtilis, Pseudomonas saccharophila* and *Bacillus stearothermophilus*. Food Hydrocol 26:231–239

Erlander S, French D (1956) A statistical model for amylopectin and glycogen. The condensation of A-R-$B_{f\text{-}1}$ units. J Polym Sci Part A 20:7–28

Finch P, Sebesta DW (1992) The amylase of *Pseudomonas stutzeri* as a probe of the structure of amylopectin. Carbohydr Res 227:c1–c4

Fredriksson H, Silverio J, Andersson R et al (1998) The influence of amylose and amylopectin characteristics on gelatinization and retrogradation properties of different starches. Carbohydr Polym 35:119–134

French D (1972) Fine structure of starch and its relationship to the organization of starch granules. J Jpn Soc Starch Sci 19:8–25

Fritzsche J (1834) Ueber das Amylum. Ann Phys Chem 32:129–160

Fulton DC, Edwards A, Pilling E et al (2002) Role of granule-bound starch synthase in determination of amylopectin structure and starch granule morphology in potato. J Biol Chem 277:10834–10841

Fuwa H, Sugimoto Y, Tanaka M et al (1978) Susceptibility of various starch granules to amylases as seen by scanning electron microscope. Starch-Starke 30:186–191

Gallant DJ, Bouchet B, Baldwin PM (1997) Microscopy of starch: evidence of a new level of granule organization. Carbohydr Polym 32:177–191

Genkina NK, Wikman J, Bertoft E et al (2007) Effects of structural imperfection on gelatinization characteristics of amylopectin starches with A- and B-type crystallinity. Biomacromolecules 8:2329–2335

Gérard C, Planchot V, Colonna P et al (2000) Relationship between branching density and crystalline structure of A- and B-type maize mutant starches. Carbohydr Res 326:130–144

Gérard C, Barron C, Colonna P et al (2001) Amylose determination in genetically modified starches. Carbohydr Polym 44:19–27

Glaring MA, Koch CB, Blennow A (2006) Genotype-specific spatial distribution of starch molecules in the starch granule: a combined CLSM and SEM approach. Biomacromolecules 7:2310–2320

Goesaert H, Bijttebier A, Delcour JA (2010) Hydrolysis of amylopectin by amylolytic enzymes: level of inner chain attack as an important analytical differentiation criterion. Carbohydr Res 345:397–401

Gunja-Smith Z, Marshall JJ, Mercier C et al (1970) A revision of the Meyer-Bernfeld model of glycogen and amylopectin. FEBS Lett 12:101–104

Hall RS, Manners DJ (1978) The action of malted-barley alpha-amylase on amylopectin. Carbohydr Res 66:295–297

Hanashiro I, J-i A, Hizukuri S (1996) A periodic distribution of chain length of amylopectin as revealed by high-performance anion-exchange chromatography. Carbohydr Res 283:151–159

Hanashiro I, Tagawa M, Shibahara S et al (2002) Examination of molar-based distribution of A, B and C chains of amylopectin by fluorescent labeling with 2-aminopyridine. Carbohydr Res 337:1211–1215

Hanashiro I, Matsugasako J-i, Egashira T et al (2005) Structural characterization of long unit-chains of amylopectin. J Appl Glycosci 52:233–237

Hanashiro I, Itoh K, Kuratomi Y et al (2008) Granule-bound starch synthase I is responsible for biosynthesis of extra-long unit chains of amylopectin in rice. Plant Cell Phys 49:925–933

Hanson EA, Katz JR (1934a) Abhandlungen zur physikalischen Chemie der Stärke und der Brotbereitung. XVII. Über Versuche die gewachsene Struktur des Stärkekorns mikroskopisch sichtbar zu machen besonders an lintnerisierter Stärke. Z physikal Chem abt 168:339–352

Hanson EA, Katz JR (1934b) Abhandlungen zur physikalischen Chemie der Stärke und der Brotbereitung. XVIII. Weitere Versuche die gewachsene Struktur des Stärkekorns mikroskopisch sichtbar zu machen. Z physikal Chem abt 169:135–142

Haworth WN, Hirst EL, Isherwood FA (1937) Polysaccharides. Part XXIII. Determination of the chain length of glycogen. J Chem Soc Chem Commun:577–581

Hestrin S (1949) Action pattern of crystalline muscle phosphorylase. J Biol Chem 179:943–955

Hizukuri S (1985) Relationship between the distribution of the chain length of amylopectin and the crystalline structure of starch granules. Carbohydr Res 141:295–306

Hizukuri S (1986) Polymodal distribution of the chain lengths of amylopectins, and its significance. Carbohydr Res 147:342–347

Hobson PN, Whelan WJ, Peat S (1951) The enzymic synthesis and degradation of starch. Part XIV. R-enzyme. J Chem Soc:1451–1459

Hoover R (2001) Composition, molecular structure, and physicochemical properties of tuber and root starches: a review. Carbohydr Polym 45:253–267

Hughes RC, Smith EE, Whelan WJ (1963) Structure of a pentasaccharide α-limit dextrin formed from amylopectin by *Bacillus subtilis* α-amylase. Biochem J 88:63P–64P

Illingworth B, Larner J, Cori GT (1952) Structure of glycogens and amylopectins. I. Enzymatic determination of chain length. J Biol Chem 199:631–640

Imberty A, Pérez S (1988) A revisit to the three-dimensional structure of B-type starch. Biopolymers 27:1205–1221

Imberty A, Pérez S (1989) Conformational analysis and molecular modelling of the branching point of amylopectin. Int J Biol Macromol 11:177–185

Imberty A, Chanzy H, Pérez S et al (1987) New three-dimensional structure for A-type starch. Macromolecules 20:2634–2636

Imberty A, Chanzy H, Pérez S et al (1988) The double-helical nature of the crystalline part of A-starch. J Mol Biol 201:365–378

Imberty A, Buléon A, Tran V et al (1991) Recent advances in knowledge of starch structure. Starch-Starke 43:375–384

Inouchi N, Horibata T, Nakamura Y et al (2006) Structural and physicochemical characteristics of endosperm starches of rice cultivars recently bred in Japan. In: Yuryev V, Tomasik P, Bertoft E (eds) Starch: achievements in understanding of structure and functionality. Nova Science Publishers, Inc., New York, pp 65–85

Jane J-l, Kasemsuwan T, Leas S et al (1994) Anthology of starch granule morphology by scanning electron microscopy. Starch-Starke 46:121–129
Jane J-l, Wong K-s, McPherson AE (1997) Branch-structure difference in starches of A- and B-type X-ray patterns revealed by their Naegeli dextrins. Carbohydr Res 300:219–227
Jenkins PJ, Donald AM (1995) The influence of amylose on starch granule structure. Int J Biol Macromol 17:315–321
Jenkins PJ, Cameron RE, Donald AM (1993) A universal feature in the structure of starch granules from different botanical sources. Starch-Starke 45:417–420
Kainuma K, French D (1972) Naegeli amylodextrin and its relationship to starch granule structure. II. Role of water in crystallization of B-starch. Biopolymers 11:2241–2250
Kalinga D, Waduge R, Bertoft E et al (2013) On the differences in granular architecture and starch structure between pericarp and endosperm wheat starches. Starch-Starke 65:791–800
Kalinga DN, Bertoft E, Tetlow I et al (2014) Structure of clusters and building blocks in amylopectin from developing wheat endosperm. Carbohydr Polym 112:325–333
Källman A, Bertoft E, Koch K et al (2013) On the interconnection of clusters and building blocks in barley amylopectin. Int J Biol Macromol 55:75–82
Kiseleva VI, Krivandin AV, Fornal J et al (2005) Annealing of normal and mutant wheat starches. LM, SEM, DSC, and SAXS studies. Carbohydr Res 340:75–83
Kitahara K, Eitoku E, Suganuma T et al (1997) Some properties of branched and linear dextrins from Nägeli amylodextrin. Carbohydr Polym 33:187–194
Klucinec JD, Thompson DB (2002) Structure of amylopectins from *ae*-containing maize starches. Cereal Chem 79:19–23
Koizumi K, Fukuda M, Hizukuri S (1991) Estimation of the distributions of chain length of amylopectins by high-performance liquid chromatography with pulsed amperometric detection. J Chromatogr 585:233–238
Kong X, Corke H, Bertoft E (2009) Fine structure characterization of amylopectins from grain amaranth starch. Carbohydr Res 344:1701–1708
Koroteeva DA, Kiseleva VI, Krivandin AV et al (2007a) Structural and thermodynamic properties of rice starches with different genetic background. Part 2. Defectiveness of different supramolecular structures in starch granules. Int J Biol Macromol 41:534–547
Koroteeva DA, Kiseleva VA, Sriroth K et al (2007b) Structural and thermodynamic properties of rice starches with different genetic background. Part 1. Differentiation of amylopectin and amylose defects. Int J Biol Macromol 41:391–403
Kozlov SS, Blennow A, Krivandin AV et al (2007a) Structural and thermodynamic properties of starches extracted from GBSS and GWD suppressed potato lines. Int J Biol Macromol 40:449–460
Kozlov SS, Krivandin AV, Shatalova OV et al (2007b) Structure of starches extracted from near-isogenic wheat lines. Part II. Molecular organization of amylopectin clusters. J Therm Anal Cal 87:575–584
Kubo A, Akdogan G, Nakaya M et al (2010) Structure, physical, and digestive properties of starch from *wx ae* double-mutant rice. J Agric Food Chem 58:4463–4469
Laohaphatanaleart K, Piyachomkwan K, Sriroth K et al (2009) A study of the internal structure in cassava and rice amylopectin. Starch-Starke 61:557–569
Laohaphatanaleart K, Piyachomkwan K, Sriroth K et al (2010) The fine structure of cassava amylopectin. Part 1. Organization of clusters. Int J Biol Macromol 47:317–324
Larner J, Illingworth B, Cori GT et al (1952) Structure of glycogens and amylopectins. II. Analysis by stepwise enzymatic degradation. J Biol Chem 199:641–651
Lee EYC, Mercier C, Whelan WJ (1968) A method for the investigation of the fine structure of amylopectin. Arch Biochem Biophys 125:1028–1030
Lii C-Y, Lineback DR (1977) Characterization and comparison of cereal starches. Cereal Chem 54:138–149
MacGregor AW, Morgan JE (1984) Structure of amylopectins isolated from large and small starch granules of normal and waxy barley. Cereal Chem 61:222–228

Manners DJ (1989) Recent developments in our understanding of amylopectin structure. Carbohydr Polym 11:87–112
Matheson NK, Caldwell RA (2008) Modeling of α(1–4) chain arrangements in α(1–4)(1–6) glucans: the action and outcome of β-amylase and *Pseudomonas stutzeri* amylase on an α(1–4)(1–6) glucan model. Carbohydr Polym 72:625–637
McIntyre AP, Mukerjea R, Robyt JF (2013) Reducing values: dinitrosalicylate gives over-oxidation and invalid results whereas copper bicinchoninate gives no over-oxidation and valid results. Carbohydr Res 380:118–123
McPherson AE, Jane J (1999) Comparison of waxy potato with other root and tuber starches. Carbohydr Polym 40:57–70
Mercier C (1973) The fine structure of corn starches of various amylose-percentage: waxy, normal and amylomaize. Starch-Starke 25:78–83
Meyer A (1895) Untersuchungen über die Stärkekörner. Gustav Fischer, Jena
Meyer KH, Bernfeld P (1940) Recherches sur l'amidon V. L'amylopectine. Helv Chim Acta 23:875–885
Meyer KH, Brentano W, Bernfeld P (1940) Recherches sur l'amidon II. Sur la nonhomogénéité de l'amidon. Helv Chim Acta 23:845–853
Millard MM, Dintzis FR, Willett JL et al (1997) Light-scattering molecular weights and intrinsic viscosities of processed waxy maize starches in 90 % dimethyl sulfoxide and H_2O. Cereal Chem 74:687–691
Muhr AH, Blanshard JMV, Bates DR (1984) The effect of lintnerisation on wheat and potato starch granules. Carbohydr Polym 4:399–425
Nikuni Z (1969) Starch and cooking (in Japanese). Sci Cook 2:6–14
Noda T, Takigawa S, Matsuura-Endo C et al (2005) Physicochemical properties and amylopectin structures of large, small, and extremely small potato starch granules. Carbohydr Polym 60:245–251
O'Sullivan AC, Pérez S (1999) The relationship between internal chain length of amylopectin and crystallinity in starch. Biopolymers 50:381–390
Ohtani T, Yoshino T, Hagiwara S et al (2000) High-resolution imaging of starch granule structure using atomic force microscopy. Starch-Starke 52:150–153
Oostergetel GT, van Bruggen EFJ (1993) The crystalline domains in potato starch granules are arranged in a helical fashion. Carbohydr Polym 21:7–12
Peat S, Pirt SJ, Whelan WJ (1952a) Enzymic synthesis and degradation of starch. Part XV. β-Amylase and the constitution of amylose. J Chem Soc:705–713
Peat S, Whelan WJ, Thomas GJ (1952b) Evidence of multiple branching in waxy maize starch. J Chem Soc:4546–4548
Pérez S, Bertoft E (2010) The molecular structures of starch components and their contribution to the architecture of starch granules: a comprehensive review. Starch-Starke 62:389–420
Pilling E, Smith AM (2003) Growth ring formation in the starch granules of potato tubers. Plant Physiol 132:365–371
Popov D, Buléon A, Burghammer M et al (2009) Crystal structure of A-amylose: a revisit from synchrotron microdiffraction analysis of single crystals. Macromolecules 42:1167–1174
Putaux J-L, Molina-Boisseau S, Momaur T et al (2003) Platelet nanocrystals resulting from the disruption of waxy maize starch granules by acid hydrolysis. Biomacromolecules 4:1198–1202
Ridout MJ, Parker ML, Hedley CL et al (2003) Atomic force microscopy of pea starch granules: granule architecture of wild-type parent, *r* and *rb* single mutants, and the *rrb* double mutant. Carbohydr Res 338:2135–2147
Ridout MJ, Parker ML, Hedley CL et al (2006) Atomic force microscopy of pea starch: granule architecture of the *rug3-a, rug4-b, rug5-a* and *lam-c* mutants. Carbohydr Polym 65:64–74
Robin JP (1981) Study of β-limit dextrins from various native starches. Interpretation in term of amylopectin structure. Sci Aliments 1:551–567
Robin JP, Mercier C, Charbonnière R et al (1974) Lintnerized starches. Gel filtration and enzymatic studies of insoluble residues from prolonged acid treatment of potato starch. Cereal Chem 51:389–406

Robyt J, French D (1963) Action pattern and specificity of an amylase from *Bacillus subtilis*. Arch Biochem Biophys 100:451–467
Sande-Bakhuizen HLvd (1926) The structure of starch grains from wheat grown under constant conditions. Proc Soc Exp Biol Med 24:302–305
Seetharaman K, Bertoft E (2012a) Perspectives on the history of research on starch. Part I: on the linkages in starch. Starch-Starke 64:677–681
Seetharaman K, Bertoft E (2012b) Perspectives on the history of research on starch. Part IV: on the visualization of granular architecture. Starch-Starke 64:929–934
Shi Y-C, Seib PA (1995) Fine structure of maize starches from four *wx*-containing genotypes of the W64A inbred line in relation to gelatinization and retrogradation. Carbohydr Polym 26:141–147
Shibanuma K, Takeda Y, Hizukuri S et al (1994) Molecular structures of some wheat starches. Carbohydr Polym 25:111–116
Song Y, Jane J (2000) Characterization of barley starches of waxy, normal, and high amylose varieties. Carbohydr Polym 41:365–377
Srichuwong S, Isono N, Mishima T et al (2005a) Structure of lintnerized starch is related to X-ray diffraction pattern and susceptibility to acid and enzyme hydrolysis of starch granules. Int J Biol Macromol 37:115–121
Srichuwong S, Sunarti TC, Mishima T et al (2005b) Starches from different botanical sources I: contribution of amylopectin fine structure to thermal properties and enzyme digestibility. Carbohydr Polym 60:529–538
Stacy CJ, Foster JF (1957) Molecular weight heterogeneity in starch amylopectins. J Polym Sci Part A 25:39–50
Staudinger H, Husemann E (1937) Über hochpolymere Verbindungen. 150. Mitteilung. Über die Konstitution der Stärke. Liebigs Ann Chem 527:195–236
Sterling C (1960) Crystallinity of potato starch. Starch-Starke 12:182–185
Sterling C (1962) A low angle spacing in starch. J Polym Sci 56:S10–S12
Summer R, French D (1956) Action of β-amylase on branched oligosaccharides. J Biol Chem 222:469–477
Szymonska J, Krok F, Komorowska-Czepirska E et al (2003) Modification of granular potato starch by multiple deep-freezing and thawing. Carbohydr Polym 52:1–10
Takeda Y, Hizukuri S, Juliano BO (1987) Structures of rice amylopectins with low and high affinities for iodine. Carbohydr Res 168:79–88
Takeda Y, Shitaozono T, Hizukuri S (1988) Molecular structure of corn starch. Starch-Starke 40:51–54
Takeda Y, Shibahara S, Hanashiro I (2003) Examination of the structure of amylopectin molecules by fluorescent labeling. Carbohydr Res 338:471–475
Tang H, Mitsunaga T, Kawamura Y (2006) Molecular arrangement in blocklets and starch granules architecture. Carbohydr Polym 63:555–560
Tester RF, Karkalas J, Qi X (2004) Starch–composition, fine structure and architecture. J Cereal Sci 39:151–165
Thoma JA, Brothers C, Spradlin J (1970) Subsite mapping of enzymes. Studies on *Bacillus subtilis* amylase. Biochemistry 9:1768–1775
Thompson DB (2000) On the non-random nature of amylopectin branching. Carbohydr Polym 43:223–239
Thurn A, Burchard W (1985) Heterogeneity in branching of amylopectin. Carbohydr Polym 5:441–460
Umeki K, Kainuma K (1981) Fine structure of nägeli amylodextrin obtained by acid treatment of defatted waxy-maize starch – structural evidence to support the double-helix hypothesis. Carbohydr Res 96:143–159
Umeki K, Yamamoto T (1972a) Enzymatic determination of structure of singly branched hexaose dextrins formed by liquefying α-amylase of *Bacillus subtilis*. J Biochem 72:101–109
Umeki K, Yamamoto T (1972b) Structures of branched dextrins produced by saccharifying α-amylase of *Bacillus subtilis*. J Biochem 72:1219–1226

Umeki K, Yamamoto T (1975a) Structures of multi-branched dextrins produced by saccharifying α-amylase from starch. J Biochem 78:897–903
Umeki K, Yamamoto T (1975b) Structures of singly branched heptaoses produced by bacterial liquefying α-amylase. J Biochem 78:889–896
Utrilla-Coello RG, Hernández-Jaimes C, Carillo-Navas H et al (2014) Acid hydrolysis of native corn starch: morphology, crystallinity, rheological and thermal properties. Carbohydr Polym 103:596–602
Vamadevan V, Bertoft E, Seetharaman K (2013) On the importance of organization of glucan chains on thermal properties of starch. Carbohydr Polym 92:1653–1659
Vermeylen R, Goderis B, Reynaers H et al (2004) Amylopectin molecular structure reflected in macromolecular organization of granular starch. Biomacromolecules 5:1775–1786
Waduge RN, Xu S, Bertoft E et al (2013) Exploring the surface morphology of developing wheat starch granules by using atomic force microscopy. Starch-Starke 65:398–409
Waigh TA, Donald AM, Heidelbach F et al (1999) Analysis of the native structure of starch granules with small angle X-ray microfocusing scattering. Biopolymers 49:91–105
Waigh TA, Gidley MJ, Komanshek BU et al (2000a) The phase transformations in starch during gelatinisation: a liquid crystalline approach. Carbohydr Res 328:165–176
Waigh TA, Kato KL, Donald AM et al (2000b) Side-chain liquid-crystalline model for starch. Starch-Starke 52:450–460
Walker GJ, Whelan WJ (1960a) The mechanism of carbohydrase action. 7. Stages in the salivary α-amylolysis of amylose, amylopectin and glycogen. Biochem J 76:257–263
Walker GJ, Whelan WJ (1960b) The mechanism of carbohydrase action. 8. Structures of the muscle-phosphorylase limit dextrins of glycogen and amylopectin. Biochem J 76:264–268
Watanabe T, French D (1980) Structural features of naegeli amylodextrin as indicated by enzymic degradation. Carbohydr Res 84:115–123
Wikman J, Larsen FH, Motawia MS et al (2011) Phosphate esters in amylopectin clusters of potato tuber starch. Int J Biol Macromol 48:639–649
Wikman J, Blennow A, Buléon A et al (2014) Influence of amylopectin structure and degree of phosphorylation on the molecular composition of potato starch lintners. Biopolymers 101:257–271
Xia H, Thompson DB (2006) Debranching of β-dextrins to explore branching patterns of amylopectins from three maize genotypes. Cereal Chemi 83:668–676
Yao Y, Thompson DB, Guiltinan MJ (2004) Maize starch-branching enzyme isoforms and amylopectin structure. In the absence of starch-branching enzyme IIb, the further absence of starch-branching enzyme Ia leads to increased branching. Plant Physiol 136:3515–3523
Yun S-H, Matheson NK (1993) Structures of the amylopectins of waxy, normal, amylose-extender, and wx:ae genotypes and of the phytoglycogen of maize. Carbohydr Res 243:307–321
Zhu F, Corke H, Bertoft E (2011a) Amylopectin internal molecular structure in relation to physical properties of sweetpotato starch. Carbohydr Polym 84:907–918
Zhu F, Corke H, Åman P et al (2011b) Structures of building blocks in clusters of sweetpotato amylopectin. Carbohydr Res 346:2913–2925
Zhu F, Corke H, Åman P et al (2011c) Structures of clusters in sweetpotato amylopectin. Carbohydr Res 346:1112–1121
Zhu F, Bertoft E, Källman A et al (2013) Molecular structure of starches from maize mutants deficient in starch synthase III. J Agric Food Chem 61:9899–9907

Chapter 2
Fine Structure of Amylose

Isao Hanashiro

Abstract Amylose is usually the second most abundant component of starch, accounting for typically 20–30 % of its weight. In contrast to the more abundant, highly branched amylopectin, amylose is generally recognized as a linear or slightly branched molecule, both of which are present in amylose prepared from native starch. The structure of amylose can be described in terms of its size and branching. The size of amylose differs depending on the source of the starch, with average degree of polymerization in the range of ∼1,000 to ∼5,000. The branching of amylose can be characterized as a whole, or for the branched components by several structural indices, including its β-amylolysis limit (70–90 %), average chain length (200–500), number of chains per molecule (5–20, for the branched molecules), and molar fraction of branched molecule (0.2–0.5). Debranching of amylose with isoamylase and/or pullulanase is incomplete (up to ∼80 %), but still the size distribution of the debranched product can be informative. The main chain of the debranched product is comparable in size to the native amylose. A small number of long side chains are present with a chain length of from several hundred to a similar length as the main chain. The vast majority of the side chains on a molar basis are short chains, which have a chain-length distribution similar to that of amylopectin. The side chains are not arranged in a cluster fashion, which is a common fundamental structural characteristic of amylopectin.

Keywords Amylose • Branch • Cluster • Heterogeneity • Main chain • Side chain • Structure

2.1 Fractionation of Amylose from Starch Granules

The term “amylose” has been used since Meyer et al. recognized the linear nature of a glucan fraction obtained from starch by aqueous leaching (Meyer et al. 1940b, c). The linear nature confers unique properties on amylose, among which is the ability to form complexes with iodine. The formation of the iodine–amylose

I. Hanashiro (✉)
Department of Biochemical Science and Technology, Faculty of Agriculture, Kagoshima University, Kagoshima 890-0065, Japan
e-mail: ihanashi@chem.agri.kagoshima-u.ac.jp

Y. Nakamura (ed.), *Starch*, DOI 10.1007/978-4-431-55495-0_2

complex provides the means to determine the amylose content in starch granules by colorimetric (McCready and Hassid 1943; Juliano et al. 2012), potentiometric (Bates et al. 1943), or amperometric methods (Larson et al. 1953; Takeda et al. 1987a). Because of the availability of these rapid quantitative methods, amylose content has become recognized as a major determinant of the functional properties of starch, including its gelatinization and retrogradation (Tester and Morrison 1990; Fredriksson et al. 1998; Jane et al. 1999; Sasaki et al. 2000). Generally, "normal" starches contain 20–30 % (by weight) of amylose, although the content varies by the botanical as well as varietal sources of starch. In "waxy" starches, amylose is present from nearly zero to only a few percent, while in "high-amylose" starches, the amylose content can be up to 80–90 % (Cheetham and Tao 1998; Shi et al. 1998). Amylose content also varies within the same starch sample according to the size of the starch granule, with larger granules having higher amylose content (Morrison and Gadan 1987; Jane and Shen 1993; Takeda et al. 1999), as a result of the increased deposit of amylose towards the periphery of the granules (Morrison and Gadan 1987; Jane and Shen 1993; Pan and Jane 2000). Amylose is thought to be synthesized within the matrix of the starch granule that is formed by the synthesis and organization of amylopectin (Tatge et al. 1999) and is deposited in both of the semi-crystalline and amorphous regions of starch granules by interspersion among the clusters of amylopectin (Jane et al. 1992; Kasemsuwan and Jane 1994).

There are many experimental methods found in the literature for fractionation of amylose from starch. They can be divided into the following four groups based on their underlying separation principles: (1) aqueous leaching (hot-water extraction) of amylose (Meyer et al. 1940a, b; Banks et al. 1959; Greenwood and Thomson 1962; Hizukuri 1991), (2) precipitation of an insoluble complex of amylose with complexing agents (Schoch 1945; Lansky et al. 1949; Bourne et al. 1948; Banks and Greenwood 1967b; Adkins and Greenwood 1969; Takeda et al. 1986a), (3) gel-permeation chromatography, and (4) separation of soluble amylose from an insoluble complex of amylopectin with a lectin, concanavalin A (Matheson and Welsh 1988; Matheson 1996). Each method has advantages and disadvantages in terms of its requirement for starch, the yield and/or purity of amylose, and throughput. Ultimately, the benefits of each parameter must be considered, and a fractionation method must be chosen to suit the needs of each experiment. In general, the first and second methods require and yield samples in the order of grams and take a few to several weeks to be performed. The third and fourth methods require less samples and are suitable for high-throughput analysis, but because of their low yields, multifaceted analysis on the structural and functional properties of amylose is difficult. With aqueous leaching, the yield and composition of leached materials are dependent on the extraction temperature and the gelatinization temperature of the starch to be extracted. The higher the extraction temperature, the higher the yield of the leached materials and the content of the branched components in the materials including branched molecules of amylose and amylopectin (Banks et al. 1959; Greenwood and Thomson 1962; Hizukuri 1991).

Irrespective of the method chosen, there are several conditions that need to be met for successful fractionation, i.e., obtaining a quantitative yield of amylose and

avoiding selection bias in the population of the fractionated amylose. Complete dispersion of α-glucans in starch granules before the fractionation step is a prerequisite. Prior removal of lipids (defatting) in the granules and disruption of the granular structure by dimethyl sulfoxide is known to be effective for complete dispersion (Killion and Foster 1960; Banks and Greenwood 1967b; Adkins and Greenwood 1969). Granules that are not fully gelatinized can be removed from the dispersion by ultracentrifugation; otherwise, the swollen granules would interfere with the analyses of amylose (Takeda et al. 1986a). Agents for the precipitation of amylose, for which n-butanol is widely used, should be carefully chosen because the yield and purity of the fractions can vary depending on the complexing agents used (Schoch 1945; Bourne et al. 1948; French et al. 1963). To avoid oxidation and degradation of amylose at high temperatures during the fractionation procedures, dissolved oxygen can be displaced by bubbling of inert nitrogen gas. Furthermore, when structural properties are to be examined, the fractionated amylose preparation should be free from amylopectin, and confirmation of the purity of amylose can be performed by gel-permeation chromatography with a suitable column void volume (Takeda et al. 1984).

2.2 Structural Description of Amylose

Structural characteristics of amylose molecules can be generally described by two features, their size and branched structure. They are indicated in a similar manner to that of amylopectin by using the degree of polymerization (DP) and chain length (CL) for molecular size and unit-chain length, respectively. However, it is necessary to consider that an amylose preparation obtained from starch is a mixture of linear and branched molecules. It is also important to recognize how these characteristic values are experimentally obtained (most commonly, they are either weight or molar based) and whether they describe the whole component (fraction) or a specific fraction. For amylose, the average values, especially those related to branching, are less informative because of the preponderance of linear molecules and the variable ratio of linear and branched molecules.

2.2.1 Size of Amylose

As with other natural polysaccharides, amylose is polydisperse with respect to its molecular size; the size of the glucan is indicated by its molecular weight or more frequently by its degree of polymerization (DP). Because of the polydispersity, the molecular weight or DP values are generally expressed as average values and can be either weight or molar based (denoted by subscript *w* for weight or *n* for number, respectively, as in DP_w or DP_n), depending on the principle of the detection method used. For example, determination of the reducing residues by methods with high sensitivity, such as a modified Park–Johnson method (Hizukuri et al. 1981) or a

bicinchoninic acid method using a microtiter plate format (Utsumi et al. 2009), gives a number-average value, while a light scattering technique gives a weight-average value (Miles et al. 1985). The average size of amylose reported to date differs depending on the botanical as well as varietal sources, with a range in DP_n from ∼1,000 to ∼5,000 (Table 2.1). Cereal amyloses are generally smaller than amyloses of root and tuber starches, and branched amylose molecules are thought to be generally larger than linear molecules from the same amylose preparation (Takeda et al. 1989a, 1992a; Hizukuri et al. 1989).

In addition to average values, the size distribution of amylose is measured by gel-permeation chromatography (GPC) or high-performance size-exclusion chromatography in combination with a weight- and/or a molar-based detection method. Generally, amylose shows mono-modal size distribution on a weight basis (Hizukuri and Takagi 1984) and mono- or multi- (bi- or tri-)modal size distribution on a molar basis (Hanashiro and Takeda 1998). On a molar basis, small amyloses with DPs less than 1,000 were predominant (50–75 %) in amyloses from maize, wheat, barley, and rice, while amyloses with DPs over 1,000 were predominant (75–90 %) in potato and sweet potato (Hanashiro and Takeda 1998). Apparent DP distribution can be expressed by the DP values of the elution positions at which 10 and 90 % amylose, either by weight or by mole, was eluted. On a molar basis, the apparent DP distribution was 200–300 at 90 % and 2,000–4,000 at 10 % for the cereal amyloses and 440–7,900 for the sweet potato and 970–9,800 for the potato amylose (Hanashiro and Takeda 1998). On a weight basis, the apparent DP distribution is generally from 200 to 20,000 with some exceptions (Hizukuri and Takagi 1984; Takeda et al. 1986a).

2.2.2 The Branched Nature of Amylose

2.2.2.1 Evidence for the Presence of Branches in Amylose

After Meyer et al. (1940b, c) reported the isolation of the linear glucan fraction from native starch, chemical and enzymatic approaches were used to further study the molecular structure of amylose. Failure of β-amylase to degrade amylose completely (Peat et al. 1949, 1952) and the increased β-amylolysis limit of amylose by the cooperative action of β-amylase and debranching enzyme (Kjølberg and Manners 1963; Banks and Greenwood 1966) suggested the presence of α-(1,6)-linkages in the amylose. Disagreements between the DP_n determined by the osmotic pressure measurement and by determination of the non-reducing terminal residues by periodate oxidation and the fact that the latter method gives lower DP_n values confirmed the presence of α-(1,6)-branches (Potter and Hassid 1948a, b, 1951). Banks and Greenwood (1967a) proposed the presence of long side chains from the viscosity–molecular weight relationship of subfractions from potato amylose having a β-amylolysis limit of 100 % or less (60–80 %). From the differences in size distributions examined by gel-permeation chromatography and the limiting viscosity numbers of amyloses with or without debranching with isoamylase, it was

Table 2.1 Structural properties of amyloses from different botanical sources

Source	AM[a]	DP_n	CL_n	NC	β-AL	MF_B	NC_B	Reference
Rice (*japonica*)								
Sasanishiki	20.6	1,110	320	3.5	81	0.31	9.0	Takeda et al. (1986a, 1987a)
Unknown	20.3	1,100	260	4.2	77	0.43	8.5	Takeda et al. (1986a, 1987a)
Nipponbare	–	860	360	2.4	–	0.26	6.4	Hanashiro et al. (2013)
Nipponbare	18.2	1,060	260	4.1	–	0.34	10.1	Hanashiro et al. (2011)
ΔSSI	23.6	1,240	210	6.0	–	0.37	14.5	Hanashiro et al. (2011)
ΔSSIIIa	15.5	1,120	170	6.7	–	0.42	14.6	Hanashiro et al. (2011)
Rice (*indica*)								
IR64	18.3	1,020	450	2.3	87	0.25	6.1	Takeda et al. (1989a)
IR32	18.5	1,040	250	4.2	73	0.49	7.5	Takeda et al. (1986a, 1987a)
IR36	17.0	920	370	2.5	84	0.32	5.7	Takeda et al. (1986a, 1987a)
IR42	15.5	980	230	4.3	76	0.38	9.7	Takeda et al. (1986a, 1987a)
Wheat								
Chihoku	22.6	830	135	6.2	79	0.44	12.9	Shibanuma et al. (1994)
Norin-61	23.7	980	150	6.5	83	0.29	20.2	Shibanuma et al. (1994)
Western white	27.4	1,570	260	6.2	85	0.26	20.7	Shibanuma et al. (1994)
Rosella	23.9	1,500	300	5.0	85	0.63	7.3	Shibanuma et al. (1996)
Egret	24.6	1,200	270	4.4	86	0.38	10.0	Shibanuma et al. (1996)
Barley								
Sumiremochi	11.4	1,560	460	3.4	77	0.26	10.4	Yoshimoto et al. (2002)
CDC Dawn	25.4	1,220	330	3.7	79	0.21	13.8	Yoshimoto et al. (2002)
Glacier	23.2	940	530	1.8	74	0.17	5.7	Yoshimoto et al. (2000)
HA Glacier N	33.4	1,080	450	2.4	73	0.15	10.3	Yoshimoto et al. (2000)
HA Glacier A	37.4	950	350	2.7	70	0.20	9.5	Yoshimoto et al. (2000)
Maize								
White dent	–	960	305	3.1	84	0.48	5.4	Takeda et al. (1988)
W64A	18.5	830	340	2.4	81	–	–	Takeda and Preiss (1993)
B90 (*sugary-2*)	30.6	780	200	3.9	80	–	–	Takeda and Preiss (1993)
Adzuki	22.7	1,350	290	4.7	83	–	–	Yoshimoto et al. (2001)
Pea	24.0	820	340	2.4	90	–	–	Yoshimoto et al. (2001)
Common bean	25.5	920	290	3.2	86	–	–	Yoshimoto et al. (2001)
Sweet potato								
Minamiyutaka	17.2	4,400	335	13	72	–	–	Takeda et al. (1986b)
Koganesengan	18.9	4,100	380	11	73	–	–	Takeda et al. (1986b)
Norin-2	19.0	3,400	330	10	73	–	–	Takeda et al. (1986b)
Unknown	–	3,280	335	9.8	76	0.70	13.6	Takeda et al. (1987b)
Potato, Eniwa	–	4,920	670	7.3	80	–	–	Takeda et al. (1984)

AM amylose content, DP_n number-average degree of polymerization (by the modified Park–Johnson method), CL_n number-average chain length, *NC* average number of chains (DP_n/CL_n), *β-AL* β-amylolysis limit (%), MF_B molar fraction of branched molecules, NC_B average number of chains of branched molecules calculated as $[NC - (1 - MF_B)]/MF_B$

[a]Amylose content with consideration (subtraction) of contribution of amylopectin to the estimates

proposed that mango seed amylose had long side chains of DP of at least several hundreds (Würsch and Hood 1981) and amyloses from wrinkled and smooth peas carried one or two long side chains per molecule located near the non-reducing ends of the native amylose molecules (Colonna and Mercier 1984). Liberation of short chains (a shoulder at DP ∼45 and a peak at DP ∼15 in the chromatogram (Würsch and Hood 1981)) from the amylose preparation on isoamylolysis was observed in both of the studies, but the short chains were not considered side chains of amylose at that time. Meanwhile, Takeda et al. (1984) reported that potato amylose with ∼6 side chains per molecule had both short (DP>4) and long (DP>100) side chains. After optimizing the methods for quantitative highly sensitive determination of reducing and nonreducing residues of amylose (Hizukuri et al. 1981), Hizukuri, Takeda, and colleagues showed that branched molecules of amylose are generally present in starches of a wide range of botanical sources, and the branched molecules had 4.3–16.1 branches per molecule and accounted for 27–70 % (by mole) of amylose (Takeda et al. 1984, 1986a, 1987b). Advancement in microscopy has enabled imaging of branched amylose from pea starch at molecular level resolution by atomic force microscopy (Gunning et al. 2003), revealing the presence of a single-branched molecule with a long side chain and a multiple-branched molecule with shorter side chains. These images agree closely with the structure previously derived from the chemical and chromatographic data.

2.2.2.2 Classification of Unit Chains

Unit chains of amylose molecules can be classified into several groups in the same manner to those of amylopectin, i.e., A-, B-, and C-chains (see Sect. 1.2.1). The A- and B-chains are also referred to as side chains and the C-chain as the main chain. Occasionally, the B-chain is further classified into B1 and B2 among others according to the number of clusters in which a B-chain is involved. However, use of this method to classify the unit chains of amylopectin to amylose should be carefully considered because of the large difference in the branching degree of these glucan molecules and the different arrangement of branched side chains within a branched molecule.

The relative abundance of the C-chain in whole unit chains is very different between amylose and amylopectin. If assuming an amylopectin molecule with DP_n 10,000 and CL_n 20, the C-chain only accounts for about 0.2 % (one C-chain/500 unit chains) of the unit chains. Thus, the C-chain is practically negligible in terms of the chain-length distribution analysis for amylopectin, and the size distribution of unit chains is usually considered as the chain-length distribution of side chains without discriminating between the main and side chains. This is not the case for amylose, in which one molecule is only comprised of 5–20 chains (Table 2.1), and therefore, main chains should always be discriminated from side chains and *vice versa* for precise evaluation of branching in amylose. Application of the subclassification of B-chains, such as B1 and B2, to amylose should be done carefully because it is based on the premise that the side chains are organized in a cluster fashion and no convincing evidence to support the cluster structure in amylose has been reported.

2.2.2.3 Branches Resistant to Debranching Enzymes

All the enzymes known to be involved in the formation of glucan molecules during starch biosynthesis catalyze either the formation of α-(1,4)- or α-(1,6)-glucosidic linkages. It was also shown that hydrolysis of amylose by simultaneous or successive action of β-amylase and pullulanase, a debranching enzyme, completely converts amylose into maltose (Banks and Greenwood 1966; Mercier 1973; Takeda et al. 1987b). Therefore, all the branch linkages of amylose are considered to be α-(1,6)-linkages as in amylopectin. However, incomplete debranching of amylose has also been observed (Banks and Greenwood 1966; Mercier 1973; Hizukuri et al. 1981; Takeda et al. 1984, 1989b). Debranching with isoamylase alone yields 18–82 % debranching (Hizukuri et al. 1981; Takeda et al. 1984, 1986a), and the successive action of isoamylase and pullulanase caused an increase in the extent of debranching of potato amylose from 30 to 54 % (Hizukuri et al. 1981). Trimming the external part with β-amylase prior to debranching also resulted in increased values of the extent of debranching of rice amylose from 33 to 67 % (Hanashiro et al. 2013). These observed increases indicate that the incompleteness in debranching of amylose is due, in part, to steric hindrance. Other reasons for the incomplete debranching were suggested to be the presence of maltosyl branches and retrogradation of amylose during the debranching reaction (Mercier 1973; Hizukuri et al. 1981). It is of interest to note that such resistant linkages have also been found in extra-long chains (or also termed super-long chain (Horibata et al. 2004)) of amylopectin (Takeda et al. 1987a, 1989a; Hanashiro et al. 2005, 2009) and granule-bound starch synthase I synthesizes both amylose and the extra-long chains (Baba et al. 1987; Denyer et al. 1996; Hanashiro et al. 2008, 2009). It also should be noted that pea amylose was reported to be debranched completely with isoamylase in aqueous 40 % dimethyl sulfoxide (Colonna and Mercier 1984).

2.2.3 Characterization of the Branched Structure of Amylose

No index is sufficient by itself to fully describe the branching characteristics of amylose, and hence, several indices are required. Chain-length distribution, which is one of the most frequently examined characteristics used to describe the branched structure of amylopectin, has been infrequently documented for amylose. This issue is discussed separately in Sect. 2.3.1. Other examples of the indices used to describe the branched structure of amylose are detailed below.

β-Amylolysis limit: The value is expressed as the percentage of amylose converted to maltose on hydrolysis by β-amylase. This exo-acting enzyme degrades linear molecules completely into maltose (and a tiny amount of maltotriose, which comes from the reducing terminal of a linear molecule comprised of an odd number of glucosyl residues), but cannot bypass the α-(1,6)-branch linkages in branched molecules and consequently leaves a region of a branched molecule

interior to the first branched linkage from the non-reducing end. The resulting molecule, still with high molecular weight, is called β-amylase limit dextrin (β-LD), which is only slightly smaller on a molar-based measurement (DP_n) or even slightly larger on a weight basis (DP_w) than that of the parental amylose (Takeda et al. 1987b, 1989a; Hizukuri et al. 1989) because branched molecules are generally larger than linear molecules (Takeda et al. 1989a, 1992a; Hizukuri et al. 1989) and the smaller linear molecules are excluded upon β-amylolysis. The β-LD retains all the branches of the branched molecules in the parental amylose. Apparently, the β-amylolysis limit is affected by several factors, the ratio of linear and branched molecules in the amylose preparation, the number of side chains of the branched molecules, and the position of the outermost branch linkages.

The reported values of the β-amylolysis limit of amyloses from various botanical sources are 70–90 % (Banks and Greenwood 1967a; Takeda et al. 1987b). The β-amylolysis limit of branched molecules alone has been estimated to be ∼40 % by extrapolating from the relationship between the β-amylolysis limit and the molar fraction of the branched molecules (Hizukuri et al. 1989). The high correlation coefficient of the relationship (0.94 for seven rice varieties and 0.71 for 26 botanical sources including cereals, roots, and tubers) implies that the β-amylolysis limit is essentially determined by the molar fraction of the branched molecules (Hizukuri et al. 1989).

Ratio of linear molecules and branched molecules: Both a weight and molar ratio can be defined, and the molar ratio, also referred to as a molar fraction or expressed as mole%, is usually measured by determining the β-amylase limit dextrin that is labeled prior to β-amylolysis at its reducing terminal (Takeda et al. 1992b; Hanashiro et al. 2013). Amylose is first labeled with ^3H or a fluorescent compound, and then the labeled amylose is subjected to exhaustive hydrolysis with β-amylase, which gives rise to a mixture of labeled maltose, maltotriose, β-LD, and non-labeled maltose. The oligosaccharides and β-LD can be fractionated by various means including thorough washing of β-LD on a glass-fiber filter (Takeda et al. 1992b) or applying the enzyme digest directly to a high-performance liquid chromatograph equipped with size-exclusion columns (Hanashiro et al. 2013). After the fractionation, the molar ratio of label detected in the fractions of oligosaccharides and β-LD, which is attributable to linear and branched molecules of amylose, respectively, is determined. Knowledge of the molar ratio of the branched molecules is essential for better interpretation of other structural indices that are generally determined for a mixture of linear and branched amyloses, i.e., the number of chains per molecule and the β-amylolysis limit. The molar fraction of branched molecules (MF_B) has been reported to have a range of 0.15–0.70 with typical values of 0.2–0.5 (Table 2.1), depending on the botanical as well as varietal sources. The weight ratio cannot be directly measured because no method is known for separation of linear and branched molecules of amylose. However, an equation was proposed for estimation of the weight ratio from the molar fraction, DP_n of the branched molecules, and DP_n of whole amylose (Hizukuri et al. 1989).

Chain length: By definition, chain length (CL) is expressed as the number of glucosyl residues in a unit chain. Usually, the chain length is measured for a mixture of unit chains with different lengths in a given fraction or whole and expressed as averaged values, which could be either number-average CL (CL_n) or weight-average CL (CL_w). Experimentally, CL_n is obtained as a ratio of total glucosyl residues to non-reducing residues. Non-reducing residues are determined by the Smith degradation of glucan followed by enzymatic determination of glycerol, which only comes from the non-reducing residues by the Smith degradation (Hizukuri et al. 1981). On a molar basis, the amount of glycerol is equal to the amount of non-reducing residues and, hence, unit chains in the glucan. If complete debranching of all the branch linkages is assumed, as in the case of the debranching of amylopectin with a debranching enzyme such as *Pseudomonas* isoamylase (Harada et al. 1972) under optimized conditions, the amount of reducing residues that is determined after debranching is equivalent to that of the non-reducing residues and hence can be used in the calculation of CL_n. This is not applicable to amylose, which cannot be debranched completely by any debranching enzyme. Incomplete debranching of amylose needs to be considered when these enzymes are used in the structural analyses of amylose. This issue is discussed elsewhere in Sect. 2.2.2.3.

The CL_n of whole unit chains of amylopectin has been shown to be related to the crystalline structure (Hizukuri 1985), gelatinization, and retrogradation properties (Fredriksson et al. 1998; Jane et al. 1999) of starch granules. These relationships were recognized, in part, because of the comparably narrow CL range of amylopectin and the fact that the CL_n of amylopectin is determined by the ratio of short- and long-chain fractions, each having similar CL_n values irrespective of the botanical sources (Hizukuri 1985, 1986; Hanashiro et al. 2002). A unit-chain fraction with a CL_n of ~13 (A-chains) and ~24 (B1-chains) comprises ~50–70 % and ~20–30 % of amylopectin, respectively, on a molar basis. The sum of these short-chain fractions reaches ~80–90 % of the unit chains with the remaining ~7–16 % being the long-chain fraction (B2- and B3-chains) with a CL_n of ~50–60 (Hanashiro et al. 2002) (see Sect. 1.2.1.2 for the classification as A and B_n). The CL of the unit chains of amylose, which includes the main chains, exhibits a much broader CL range over two to three orders of magnitude. Moreover, one can imagine the presence or absence of even one short chain would greatly decrease or increase, respectively, the CL_n value. These peculiar properties of amylose unit chains reinforce why the differences in the CL of amylose should be interpreted with caution.

Number of chains: The number of chains (NC) indicates the average number of unit chains of which one molecule of amylose is composed. The NC is determined as the ratio of non-reducing to reducing residues. A linear amylose molecule contains one each of a reducing and non-reducing residue, and thus, the NC of linear amylose is always 1. For a branched amylose molecule, the NC should be >1 because of the presence of multiple side chains. Regardless of whether a molecule is linear or branched, each amylose molecule possesses one main chain

and NC minus 1 gives the number of side chains per molecule. The NC of various amyloses has a range from ∼2 to 10 (Table 2.1). The values close to 1 generally appear to result from a very low ratio of branched molecules in the examined amylose specimen, rather than the almost complete absence of side chains in the branched amylose.

Considering that the NC value is determined for a mixture of linear and branched molecules, which is a typical situation for amylose preparation from starch, such an estimated NC value does not necessarily represent the actual branching characteristics of branched molecules and needs to be interpreted with caution. Obviously, the NC value is affected by the composition of the amylose preparation used, and the higher the molar ratio of the linear component is, the closer the NC value approaches 1. Moreover, linear molecules are generally preponderant (Table 2.1), resulting in low NC values. Ideally, the NC should be determined after isolation of the branched molecules from the linear molecules, but no effective method has been developed for that purpose. Instead, the unfavorable effect of a coexisting linear molecule can be avoided either by measuring the NC of the β-LD of amylose or by calculation, in which the contribution of the reducing and non-reducing residues of linear molecules to the determination of the NC is excluded by consideration of a molar fraction of the branched molecule in the amylose preparation (Takeda et al. 1992a; Hanashiro et al. 2013). The value so obtained indicates the average number of unit chains of which one molecule of branched amylose is composed and is designated as the number of chains of the branched molecule (NC_B) for purposes of distinguishing it from the NC (Table 2.1). The values of NC_B for various amyloses are from ∼5 to 20 and are understandably higher than the corresponding values of NC and are more than an order of magnitude lower than expected for amylopectin. It is of interest that amyloses from starch synthase-deficient mutants (ΔSSI and ΔSSIIIa of rice, and B90 (SSIIa deficient) of maize) showed a higher degree of branching as indicated by the NC and NC_B with slightly increased MF_B values (Table 2.1), suggesting possible involvement of starch synthases, which are generally recognized as amylopectin-synthesizing enzymes, on the branched structure of amylose directly and/or indirectly (Hanashiro et al. 2011).

Extent of debranching: Amylose is not debranched completely by the bacterial debranching enzymes that are capable of completely debranching amylopectin. The extent of debranching is expressed as the mole percentage of branch linkages that are hydrolyzed by these enzymes, and the values can be obtained from the molar ratio of reducing residues that are released upon debranching to the non-reducing residues of the side chains of amylose. If the NC of amylose is known, measurement of the DP before and after debranching is adequate to calculate the extent of debranching (Hizukuri et al. 1981). The reported values for the extent of debranching greatly vary depending on the botanical source and are presumably attributable to the structural differences of amylose. However, the exact reason for the incomplete debranching is currently not known. These issues are discussed in Sect. 2.2.2.3.

2.3 Side Chains of Branched Amylose

As described in Sect. 2.2.3, several structural indices for depicting the branched structure of amylose are available, but they have limitations because they are experimentally obtained and hence describe an "averaged" structure. For further elucidation of the fine structure of branched molecules, the chain-length distribution of amylose can be examined. In such analyses, amylose is first subjected to enzymatic debranching and then to separation by size. An important issue in the chain-length distribution analysis of amylose is the incompleteness of debranching as described above, while other related issues inherent to amylose are described in this section.

The major difference in molar-based size distribution before and after hydrolysis of amylose with debranching enzymes is the emergence of a short-chain fraction with a DP_n ~20, indicating that these short chains are the major components of the side chains of amylose. This fraction of short chains is not detectable with weight-based methods such as the measurement of refractive index or total carbohydrate content because their amounts are small compared with the remaining unit chains of amylose, including linear molecules and the main chains of branched molecules. In addition to the short side chains, an appreciable amount of long side chains, which have sizes comparable to parental amylose, are also detected by the molar-based detection method.

2.3.1 Chain-Length Distribution

There have been a limited number of studies on the chain-length distribution of amylose, including maize (Takeda et al. 1992b), wheat (Shibanuma et al. 1994, 1996), and rice (Takeda et al. 1993; Hanashiro et al. 2013) endosperms, wrinkled and smooth peas (Colonna and Mercier 1984), tobacco leaves (Matheson 1996), and mango seed (Würsch and Hood 1981). There are several reasons that are thought to be responsible for the lack of studies. To examine the side chains of amylose, amylose first needs to be fractionated from starch and purified free from amylopectin, both of which are time-consuming processes. Another major reason seems to be the lack of appropriate analytical methods, in which the distinction between the main and side chain is essential because of the small number of unit chains in one molecule of amylose.

Discrimination of the main chain from the side chains can be achieved by a combination of reduction or labeling of reducing resides and enzymatic debranching in an appropriate sequence. Labeling of the residue is usually accomplished either by reduction with tritiated $NaBH_4$ or by introduction of an ultraviolet-absorbing or fluorescent compound *via* reductive amination. It is important to confirm that the labeling efficiency is independent of the DP of amylose under the employed labeling condition (Hanashiro and Takeda 1998; Hanashiro et al. 2002). The size

distribution of the main chain has been examined by labeling with tritiated $NaBH_4$ of the main chain, followed by debranching (Takeda et al. 1992b, 1993). Processing of amylose first by reduction of the main chain with cold $NaBH_4$, then debranching, and labeling with tritiated $NaBH_4$ allows incorporation of the radioactive label selectively to side-chain originating reducing residues (Takeda et al. 1992b, 1993). More conveniently, the size distribution of main chains and whole unit chains (i.e., main and side chains) can be separately measured first (Fig. 2.1), and then the difference between the two distributions is obtained by subtracting the former from the latter distribution. The difference so obtained should represent the side-chain distribution (Hanashiro et al. 2013). Because the main chain and side chain differ significantly in terms of their structural as well as functional properties, these are separately described below.

Main-chain distribution: Size distributions differ only slightly between amylose and its hydrolysate originating from the isoamylase-catalyzed reaction on a weight basis (Würsch and Hood 1981; Takeda et al. 1989a, 1992a; Matheson 1996) and the same applies to those on a molar basis when restricted to the DP range of the parental amylose (Fig. 2.1) (Takeda et al. 1992b, 1993; Hanashiro et al. 2013). These findings suggest that the main chains have sizes comparable to those of the parental amylose with a slight shift lower in the DP range. As described below, a comparably small number of long side chains and a large number of short side chains are released by the debranching of amylose. The latter is absent in the molar- and weight-based size distributions of amylose as well as in the weight-based size distribution of the isoamylolysate. The preponderance of short side chains is in accordance with the slight difference in hydrodynamic volumes of amylose molecules and their main chains. The long side chains are thought to affect the hydrodynamic properties of amylose (Banks and Greenwood 1967a; Würsch and Hood 1981; Colonna and Mercier 1984).

Side-chain distribution: With a tritium-labeling method in combination with gel-permeation chromatography, Takeda et al. revealed that the DP of the side chains of rice amylose was in the range of ~10–4,000 with a peak of a molar distribution at DP 21 while chains with DPs from 10 to 30 accounted for 74 % on a molar

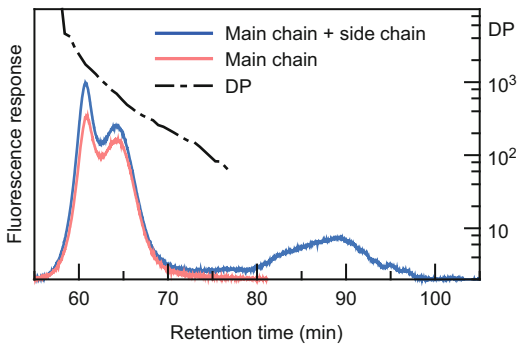

Fig. 2.1 Size distributions of debranched rice amylose that is fluorescently labeled before (main chain) or after (both main and side chain) debranching (Modified from Hanashiro et al. 2013)

basis (Takeda et al. 1993). The remaining side chains were fractionated into two fractions having a DP range of >200 and 30–200, with each fraction estimated to be 15 % and 11 %, respectively (Takeda et al. 1993). The large amount of very short chains was in agreement with the previously obtained DP_n (16–19) that was determined for side chains of rice and maize amylose after removal of long side chains as a butanol complex (Takeda et al. 1989a, 1990). Similar properties of amylose side chains were also found in maize amylose (Takeda et al. 1992b). The short side chains of amylose have received little attention in other preceding studies, in which weight-based (Colonna and Mercier 1984; Shibanuma et al. 1994) or viscometric (Banks and Greenwood 1966, 1967a; Würsch and Hood 1981) methods were adopted.

A fluorescent labeling method in combination with high-performance size-exclusion chromatography has been applied to rice amylose, and detail of the branched structure was shown by using analytical columns selected for optimal separation of short unit chains (Hanashiro et al. 2013). The size distribution of the side chains of amylose was obtained by subtraction of a profile of main chains from that of whole (both main and side) chains. The obtained side-chain distribution (Fig. 2.2) consisted of two fractions, long- and short-chain fractions, whose DP ranges were comparable to those of the original amylose molecules and similar to those of the unit chains of amylopectin molecules, respectively, and consistent with those obtained by the tritium-labeling studies (Takeda et al. 1993). The elution pattern of the short-chain fraction was similar, but not identical, to that of the amylopectin counterpart, and they were distinguishable from each other. For example, the amounts of the shortest side chains of amylopectin, such as DP 6 and 7, are generally distinctive based on their botanical sources and, hence, can be regarded as a fingerprint (Koizumi et al. 1991). The amounts of these chains were noticeably different between amylose and amylopectin. In addition, using the molar ratio of short to medium chains calculated as (A + B1):(B2 + B3) for amylopectin or (chains with length equivalent to A and B1):(chains with length equivalent to B2 and B3) for amylose, the ratio for amylose was much lower (7.96:1) than that for amylopectin (10.1–10.6:1).

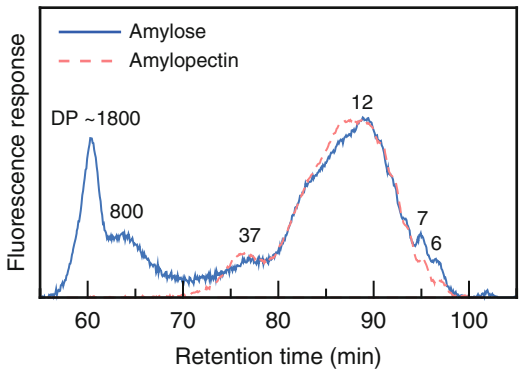

Fig. 2.2 Comparison of the size distribution of the side chains of rice amylose with the chain-length distribution of amylopectin from the same starch after correction of the detector responses to coordinate the peak height at DP 12 (Modified from Hanashiro et al. 2013)

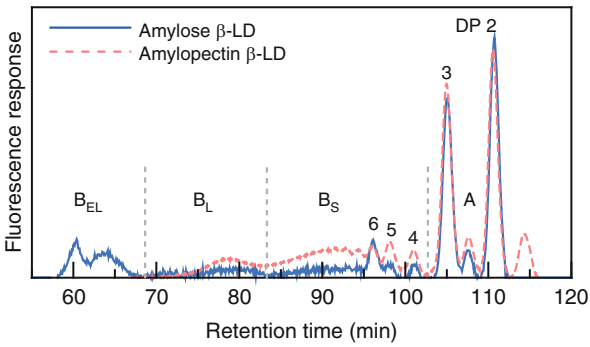

Fig. 2.3 Comparison of the size distribution of the side chains of β-LD of rice amylose with the chain-length distribution of β-LD of amylopectin from the same starch after correction of detector responses to coordinate the peak height of A-chain fraction (Modified from Hanashiro et al. 2013)

2.3.2 Arrangement of Branches Within the Amylose Molecule

It is widely accepted that the unit chains of amylopectin are arranged in a cluster fashion (Nikuni 1969; French 1972; Hizukuri 1986). Thus, it is of interest to determine whether the branches of amylose are arranged in the same fashion. Amylose and amylopectin share some similar branching features. As mentioned earlier in Sect. 2.3.1, the branches of both amylose and amylopectin are formed exclusively by α-(1,6)-linkages, and the chain-length distribution of amylopectin and the short-chain fraction of the side chains of amylose are similar to each other. Branching enzymes (BEs) are responsible for the introduction of branch linkages into the storage α-glucans. Although each BE isozyme displays different expression, function, and chain-transfer properties, the same set of BE isozymes are assumed to be acting on both amylose and amylopectin at a given stage of starch biosynthesis. Furthermore, no BE isozyme has been found to be specific for amylose synthesis unlike the amylose-specific granule-bound starch synthases. Based on these commonalities, it may be reasonable to consider that the side chains of amylose are arranged in a cluster structure as observed for amylopectin. However, experimental evidence indicates that clustered side chains in amylose are unlikely.

As observed for amylopectin (Sect. 1.2.1), the side-chain distribution of β-amylase limit dextrin (β-LD) from amylose provides important clues to the branched structure, including the molar ratio of A-chains to B-chains (A:B ratio). The models for the branched structure of starch by Haworth (1939) and Staudinger (Staudinger and Husemann 1937) can be regarded as two extreme examples, while Meyer's model (Meyer et al. 1940b) encompasses elements of these two extremes. Ideally, each of these three models gives a characteristic A:B ratio, 0, infinite, and 1, respectively. Most native amylopectins appear to have an A:B ratio close to 1.0 (an average ∼1.2) (Bertoft 2004), supporting Meyer's model as the most suitable among the three.

The A:B ratio of rice amylose has been examined by analyzing the side-chain distribution of β-LD on a molar basis (Fig. 2.3, Table 2.2). The distribution can be fractionated into extra-long B-chains (B_{EL}), long B-chains (B_L), short B-chains (B_S), and A-chains (A), where the chains of the B_S and B_L fraction have equivalent

Table 2.2 Comparison of the amount of side-chain fractions of β-LD of amylose and amylopectin

	Fraction (area %)[a]				Ratio		
β-LD	B_{EL}	B_L	B_S	A	A:B	A:B_S	$(A + B_S):(B_L + B_{EL})$
Amylose	15.1	7.1	16.0	61.8	1.6	3.9	3.5
Amylopectin	n.d.	10.0	32.7	57.3	1.3	1.8	9.0

Modified from Hanashiro et al. (2013)
n.d. not detected
[a]Fluorescence profile was divided as designated in Fig. 2.3. The fractions were designated as follows: A, A-chains; B_S, B_L, and B_{EL}, short, long, and extra-long B-chains, respectively. In the case of amylopectin, the B_S and B_L fractions can be regarded as B1 and B2 + B3 fractions, respectively. The area percentage can be regarded as a mole percentage assuming that the relative labeling efficiencies of short malto-oligosaccharides with DPs 2–5 and those of DP 6 and higher are not so significantly different. The efficiencies for the latter DP range have been shown to be constant and independent of the DP of oligosaccharides (Hanashiro et al. 2002)

length to the B1 and B2 + B3 fraction of amylopectin, respectively (Fig. 2.3). Comparisons of mole% and molar ratios of these fractions with those of amylopectin from the same starch preparation suggest that amylose has branched structure that is quite different from amylopectin. The amount of the B_S fraction of amylose is almost half of that of amylopectin, leading to the ratio of A:B_S being higher than that for amylopectin. On the contrary, the ratio of $(A + B_S):(B_L + B_{EL})$ is considerably lower in amylose. The ratio of $(A + B_S):(B_L + B_{EL})$ was reported to be 10.0:1 to 12.9:1 for cereal amylopectins including rice, maize, and wheat (Hanashiro et al. 2002). These values are supported by a clustered arrangement of 10–13 short side chains (A and B1) onto one long B-chain (B2 or B3), where a B1-chain carries 1–2 A-chain(s) and 3–4 B1-chains attached to a B2- or B3-chain. Here, it should be noted that in the above comparison, the main chains of the branched molecule were not included in the calculation of mole percentages and, hence, the molar ratios. However, the main chains account for a considerable amount in the whole unit chains as indicated by the small number of chains per amylose molecule. Thus, the ratios of A:B and $(A + B_S):(B_L + B_{EL})$ could be further lowered, taking into account the contribution of the main chains (i.e., C-chains) in the branched structure as a chain that possesses side chains, thus correcting the calculation as A:(B + C) and $(A + B_S):(B_L + B_{EL} + C)$.

Differences in the side-chain distributions of the amylose and amylopectin β-LD also reflect other aspects of the disparities in the branched structure (Hanashiro et al. 2013). A prominent peak of chains of DP 6 (Fig. 2.3) was detected in amylose, while gradual peak height changes were observed for chains with DP around 6 in amylopectin. The DP 6 chains in β-LD originate from B-chains having a span length of either 3 or 4. The span length is defined as the number of α-(1,4)-linkages that intervene between two neighboring α-(1,6)-linkages on the same chain, one is for attaching at a reducing end to another chain and one is for carrying another chain. The preference for chains with DP 6 in the β-LD of amylose implies the mechanism by which a distance between two-tiered α-(1,6)-linkages is defined is different between amylose and amylopectin. The absence of clear peaks for the

B_L and B_S fractions in amylose is another indication of the absence of a cluster structure in amylose. In the case of amylopectin, the B-chains of β-LD show a bimodal size distribution, which is primarily composed of the B_L and B_S fractions. Furthermore, the regularity of the DP range in each of the B-chain fractions of β-LD was observed as persistence of the periodicity in chain length of the parental amylopectin (Hanashiro et al. 2011). In addition, the molar percentage of the B2 + B3 fraction was relatively constant before and after β-amylolysis (Hanashiro et al. 2011). The bimodality, regularity in the DP range, and constant amount of B-chain fractions in the β-LD of amylopectin resulted from the essential features of the tandemly connected clusters of side chains in the amylopectin molecules (Nikuni 1969; French 1972; Hizukuri 1986), while the β-LD of amylose is devoid of these characteristics.

2.4 Heterogeneity in the Structure of Amylose

Structural heterogeneity is more diverse for amylose compared with that of amylopectin. It has been suggested that amylopectin molecules differ simply in size and the same branched structure is maintained among molecules with different sizes (Takeda et al. 2003). However, amylose is polydisperse in size as mentioned in Sect. 2.2.1 and, additionally, shows variations in its branched structure among the branched components.

By examining three fractions obtained by gel-permeation chromatography of maize and rice amylose, Takeda et al. (1992a) revealed that a molar fraction of the branched molecule (MF_B) and the number of chains (NC) as well as the number of chains of the branched molecule (NC_B) tended to be higher in order of increasing DP_n of the fractions and, conversely, the β-amylolysis limit became lower. These findings indicate that the branched molecules have a comparatively higher DP range than that of linear molecules and larger branched molecules have a higher number of side chains per molecule. Although the size distribution of short side chains (DP_n ~18 (Takeda et al. 1992a)) of these three fractions of amylose is not known, the clear presence of long side chains (DP_n of several hundreds to thousands) was associated only with the fraction of the highest DP_n, suggesting that the size distribution of the side chains differs according to the size of the branched molecules.

2.5 Conclusion

The structural properties of amylose greatly differ depending on the botanical source of starch. In addition, even in a given amylose preparation, a diverse range of structural heterogeneity exists in terms of the molecular size, number of side chains per molecule, and chain-length distribution. It is now considered that branched molecules are comprised of a main chain with comparable size to the native

amylose, a small amount (by mole) of long side chains with chain lengths of several hundred to similar lengths to the main chain, and a considerable amount of short side chains, which exhibit a chain-length distribution that resembles, but is distinct to that of its amylopectin counterpart. These side chains are not likely to be arranged in a cluster fashion that is commonly found in amylopectin, and the internal structure of branching in amylose is yet to be elucidated. In addition, the exact nature of the α-(1,6)-linkages that are resistant to enzymatic debranching remains to be clarified. Although our understanding of the structure–biosynthesis relationship for amylose has lagged far behind that of amylopectin, some advances in our knowledge have been obtained. Many questions still remain before we define how the structure of amylose controls the functional properties of amylose itself and/or starch and the structure of amylose is governed by genetic and biosynthetic mechanisms.

References

Adkins GK, Greenwood CT (1969) Studies on starches of high amylose-content: Part X. An improved method for the fractionation of maize and amylomaize starches by complex formation from aqueous dispersion after pretreatment with methyl sulphoxide. Carbohydr Res 11:217–224

Baba T, Yoshii M, Kainuma K (1987) Acceptor molecule of granular-bound starch synthase from sweet-potato roots. Starch-Starke 39:52–56

Banks W, Greenwood CT (1966) The fine structure of amylose: the action of pullulanase as evidence of branching. Arch Biochem Biophys 117:674–675

Banks W, Greenwood CT (1967a) Physicochemical studies on starches Part XXXII. The Incomplete β-amylolysis of amylose: a discussion of its cause and implications. Starch-Starke 19:197–206

Banks W, Greenwood CT (1967b) The fractionation of laboratory-isolated cereal starches using dimethyl sulphoxide. Starch-Starke 19:394–398

Banks W, Greenwood CT, Thomson J (1959) The properties of amylose as related to the fractionation and subfractionation of starch. Makromol Chem 31:197–213

Bates FL, French D, Rundle RE (1943) Amylose and amylopectin content of starches determined by their iodine complex formation. J Am Chem Soc 65:142–148

Bertoft E (2004) On the nature of categories of chains in amylopectin and their connection to the super helix model. Carbohydr Polym 57:211–224

Bourne EJ, Donnison GH, Haworth N et al (1948) Thymol and cyclohexanol as fractionating agents for starch. J Chem Soc 1687–1693

Cheetham NWH, Tao L (1998) Variation in crystalline type with amylose content in maize starch granules: an X-ray powder diffraction study. Carbohydr Polym 36:277–284

Colonna P, Mercier C (1984) Macromolecular structure of wrinkled- and smooth-pea starch components. Carbohydr Res 126:233–247

Denyer K, Clarke B, Hylton C et al (1996) The elongation of amylose and amylopectin chains in isolated starch granules. Plant J 10:1135–1143

Fredriksson H, Silverio J, Andersson R et al (1998) The influence of amylose and amylopectin characteristics on gelatinization and retrogradation properties of different starches. Carbohydr Polym 35:119–134

French D (1972) Fine structure of starch and its relationship to the organization of starch granules. Denpun Kagaku 19:8–25

French D, Pulley AO, Whelan WJ (1963) Starch fractionation by hydrophobic complex formation. Starch-Starke 15:349–354

Greenwood CT, Thomson J (1962) Physicochemical studies on starches. Part XXIV. The fractionation and characterization of starches of various plant origins. J Chem Soc 222–229
Gunning AP, Giardina TP, Faulds CB et al (2003) Surfactant-mediated solubilisation of amylose and visualisation by atomic force microscopy. Carbohydr Polym 51:177–182
Hanashiro I, Takeda Y (1998) Examination of number-average degree of polymerization and molar-based distribution of amylose by fluorescent labeling with 2-aminopyridine. Carbohydr Res 306:421–426
Hanashiro I, Tagawa M, Shibahara S et al (2002) Examination of molar-based distribution of A, B, and C chains of amylopectin by fluorescent labeling with 2-aminopyridine. Carbohydr Res 337:1211–1215
Hanashiro I, Matsugasako J, Egashira T et al (2005) Structural characterization of long unit-chains of amylopectin. J Appl Glycosci 52:233–237
Hanashiro I, Itoh K, Kuratomi Y et al (2008) Granule-bound starch synthase I is responsible for biosynthesis of extra-long unit chains of amylopectin in rice. Plant Cell Physiol 49:925–933
Hanashiro I, Wakayama T, Hasegawa M et al (2009) Structures of endosperm starch from a rice *wx* cultivar expressing Wx^a transgene. J Appl Glycosci 56:65–70
Hanashiro I, Higuchi T, Aihara S et al (2011) Structures of starches from rice mutants deficient in the starch synthase isozyme SSI or SSIIIa. Biomacromolecules 12:1621–1628
Hanashiro I, Sakaguchi I, Yamashita H (2013) Branched structures of rice amylose examined by differential fluorescence detection of side-chain distribution. J Appl Glycosci 60:79–85
Harada T, Misaki A, Akai H et al (1972) Characterization of *Pseudomonas* isoamylase by its actions on amylopectin and glycogen: comparison with *Aerobacter* pullulanase. Biochim Biophys Acta 268:497–505
Haworth WN (1939) The structure of cellulose and other polymers related to simple sugars. J Soc Chem Ind 58:917–925
Hizukuri S (1985) Relationship between the distribution of the chain length of amylopectin and the crystalline structure of starch granules. Carbohydr Res 141:295–306
Hizukuri S (1986) Polymodal distribution of the chain lengths of amylopectins, and its significance. Carbohydr Res 147:342–347
Hizukuri S (1991) Properties of hot-water-extractable amylose. Carbohydr Res 217:251–253
Hizukuri S, Takagi T (1984) Estimation of the distribution of molecular weight for amylose by the low-angle laser-light-scattering technique combined with high-performance gel chromatography. Carbohydr Res 134:1–10
Hizukuri S, Takeda Y, Yasuda M et al (1981) Multi-branched nature of amylose and the action of debranching enzymes. Carbohydr Res 94:205–213
Hizukuri S, Takeda Y, Maruta N et al (1989) Molecular structures of rice starch. Carbohydr Res 189:227–235
Horibata T, Nakamoto M, Fuwa H et al (2004) Structural and physicochemical characteristics of endosperm starches of rice cultivars recently bred in Japan. J Appl Glycosci 51:303–313
Jane JL, Shen JJ (1993) Internal structure of the potato starch granule revealed by chemical gelatinization. Carbohydr Res 247:279–290
Jane J, Xu A, Radosavljevic M et al (1992) Location of amylose in normal starch granules. I. Susceptibility of amylose and amylopectin to cross-linking reagents. Cereal Chem 69:405–409
Jane J, Chen YY, Lee LF et al (1999) Effects of amylopectin branch chain length and amylose content on the gelatinization and pasting properties of starch. Cereal Chem 76:629–637
Juliano BO, Tuaño APP, Monteroso DN et al (2012) Replacement of acetate with ammonium buffer to determine apparent amylose content of milled rice. Cereal Food World 57:14–19
Kasemsuwan T, Jane J (1994) Location of amylose in normal starch granules. II: Locations of phosphodiester cross-linking revealed by phosphorus-31 nuclear magnetic resonance. Cereal Chem 71:282–287
Killion PJ, Foster JF (1960) Isolation of high molecular weight amylose by dimethylsulfoxide dispersion. J Polym Sci 46:65–73
Kjølberg O, Manners DJ (1963) Studies on carbohydrate-metabolizing enzymes. 9. The action of isoamylase on amylose. Biochem J 86:258–262

Koizumi K, Fukuda M, Hizukuri S (1991) Estimation of the distributions of chain length of amylopectins by high-performance liquid chromatography with pulsed amperometric detection. J Chromatogr A 585:233–238
Lansky S, Kooi M, Schoch TJ (1949) Properties of the fractions and linear subfractions from various starches. J Am Chem Soc 71:4066–4075
Larson BL, Gilles KA, Jenness R (1953) Amperometric method for determining sorption of iodine by starch. Anal Chem 25:802–804
Matheson NK (1996) The chemical structure of amylose and amylopectin fractions of starch from tobacco leaves during development and diurnally–nocturnally. Carbohydr Res 282:247–262
Matheson NK, Welsh LA (1988) Estimation and fractionation of the essentially unbranched (amylose) and branched (amylopectin) components of starches with concanavalin A. Carbohydr Res 180:301–313
McCready RM, Hassid WZ (1943) The separation and quantitative estimation of amylose and amylopectin in potato starch. J Am Chem Soc 65:1154–1157
Mercier C (1973) The fine structure of corn starches of various amylose-percentage: waxy, normal and amylomaize. Starch-Starke 25:78–83
Meyer KH, Bernfeld P, Wolff E (1940a) Recherches sur l'amidon III. Fractionnement et purification de l'amylose de maïs naturel. Helv Chim Acta 23:854–864
Meyer KH, Brentano W, Bernfeld P (1940b) Recherches sur l'amidon II. Sur la nonhomogénéité de l'amidon. Helv Chim Acta 23:845–853
Meyer KH, Wertheim M, Bernfeld P (1940c) Recherches sur l'amidon IV. Méthylation et détermination des groupes terminaux d'amylose et d'amylopectine de maïs. Helv Chim Acta 23:865–875
Miles MJ, Morris VJ, Ring SG (1985) Gelation of amylose. Carbohydr Res 135:257–269
Morrison WR, Gadan H (1987) The amylose and lipid contents of starch granules in developing wheat endosperm. J Cereal Sci 5:263–275
Nikuni Z (1969) Denpun to chori. Chori Kagaku 2:6–14 (in Japanese)
Pan DD, Jane JL (2000) Internal structure of normal maize starch granules revealed by chemical surface gelatinization. Biomacromolecules 1:126–132
Peat S, Whelan WJ, Pirt SJ (1949) The amylolytic enzymes of soya bean. Nature 164:499–500
Peat S, Pirt SJ, Whelan WJ (1952) Enzymic synthesis and degradation of starch. Part XV. β-Amylase and the constitution of amylose. J Chem Soc 705–713
Potter AL, Hassid WZ (1948a) Starch. I. End-group determination of amylose and amylopectin by periodate oxidation. J Am Chem Soc 70:3488–3490
Potter AL, Hassid WZ (1948b) Starch. II. Molecular weights of amyloses and amylopectins from starches of various plant origins. J Am Chem Soc 70:3774–3777
Potter AL, Hassid WZ (1951) Starch. IV. The molecular constitution of amylose subfractions. J Am Chem Soc 73:593–595
Sasaki T, Yasui T, Matsuki J (2000) Effect of amylose content on gelatinization, retrogradation, and pasting properties of starches from waxy and nonwaxy wheat and their F1 seeds. Cereal Chem 77:58–63
Schoch TJ (1945) The fractionation of starch. Adv Carbohydr Chem 1:247–277
Shi YC, Capitani T, Trzasko P et al (1998) Molecular structure of a low-amylopectin starch and other high-amylose maize starches. J Cereal Sci 27:289–299
Shibanuma K, Takeda Y, Hizukuri S et al (1994) Molecular structures of some wheat starches. Carbohydr Polym 25:111–116
Shibanuma Y, Takeda Y, Hizukuri S (1996) Molecular and pasting properties of some wheat starches. Carbohydr Polym 29:253–261
Staudinger H, Husemann E (1937) Über hochpolymere Verbindungen. Über die Konstitution der Stärke. Liebigs Ann Chem 527:195–236
Takeda Y, Preiss J (1993) Structures of B90 (*sugary*) and W64A (normal) maize starches. Carbohydr Res 240:265–275
Takeda Y, Shirasaka K, Hizukuri S (1984) Examination of the purity and structure of amylose by gel-permeation chromatography. Carbohydr Res 132:83–92

Takeda Y, Hizukuri S, Juliano BO (1986a) Purification and structure of amylose from rice starch. Carbohydr Res 148:299–308
Takeda Y, Tokunaga N, Takeda C et al (1986b) Physicochemical properties of sweet potato starches. Starch-Starke 38:345–350
Takeda Y, Hizukuri S, Juliano BO (1987a) Structures of rice amylopectins with low and high affinities for iodine. Carbohydr Res 168:79–88
Takeda Y, Hizukuri S, Takeda C et al (1987b) Structures of branched molecules of amyloses of various origins, and molar fractions of branched and unbranched molecules. Carbohydr Res 165:139–145
Takeda Y, Shitaozono T, Hizukuri S (1988) Molecular structure of corn starch. Starch-Starke 40:51–54
Takeda Y, Maruta N, Hizukuri S et al (1989a) Structures of indica rice starches (IR48 and IR64) having intermediate affinities for iodine. Carbohydr Res 187:287–294
Takeda C, Takeda Y, Hizukuri S (1989b) Structure of amylomaize amylose. Cereal Chem 66:22–25
Takeda Y, Shitaozono T, Hizukuri S (1990) Structures of sub-fractions of corn amylose. Carbohydr Res 199:207–214
Takeda Y, Maruta N, Hizukuri S (1992a) Structures of amylose subfractions with different molecular sizes. Carbohydr Res 226:279–285
Takeda Y, Maruta N, Hizukuri S (1992b) Examination of the structure of amylose by tritium labelling of the reducing terminal. Carbohydr Res 227:113–120
Takeda Y, Tomooka S, Hizukuri S (1993) Structures of branched and linear molecules of rice amylose. Carbohydr Res 246:267–272
Takeda Y, Takeda C, Mizukami H et al (1999) Structures of large, medium and small starch granules of barley grain. Carbohydr Polym 38:109–114
Takeda Y, Shibahara S, Hanashiro I (2003) Examination of the structure of amylopectin molecules by fluorescent labeling. Carbohydr Res 338:471–475
Tatge H, Marshall J, Martin C et al (1999) Evidence that amylose synthesis occurs within the matrix of the starch granule in potato tubers. Plant Cell Environ 22:543–550
Tester RF, Morrison WR (1990) Swelling and gelatinization of cereal starches. I. Effects of amylopectin, amylose, and lipids. Cereal Chem 67:551–557
Utsumi Y, Yoshida M, Francisco PB Jr et al (2009) Quantitative assay method for starch branching enzyme with bicinchoninic acid by measuring the reducing terminals of glucans. J Appl Glycosci 56:215–222
Würsch P, Hood LF (1981) Structure of starch from mango seed. Starch-Starke 33:217–221
Yoshimoto Y, Tashiro J, Takenouchi T et al (2000) Molecular structure and some physicochemical properties of high-amylose barley starches. Cereal Chem 77:279–285
Yoshimoto Y, Matsuda M, Hanashiro I et al (2001) Molecular structure and pasting properties of legume starches. J Appl Glycosci 48:317–324
Yoshimoto Y, Takenouchi T, Takeda Y (2002) Molecular structure and some physicochemical properties of waxy and low-amylose barley starches. Carbohydr Polym 47:159–167

Chapter 3
Crystalline Structure in Starch

Denis Lourdin, Jean-Luc Putaux, Gabrielle Potocki-Véronèse, Chloé Chevigny, Agnès Rolland-Sabaté, and Alain Buléon

Abstract Many reviews have been published on the crystalline structure of the starch granule, addressing aspects such as birefringence, crystallinity, and structural models for A- and B-type starches. After a synthetic presentation of the general knowledge on this topic, the present review focuses on a critical description of the main techniques used to investigate the starch crystalline structure, some new data regarding crystalline lamellae, and the most recent models established for the 3D structure of crystalline domains in the granules. Structural and phase transitions occurring during hydrothermal treatments of starch are briefly presented as an introduction to a more detailed description of local order and orientation in amorphous starch materials. Recent results on the structure of amylose complexes which form by heating in the presence of guest molecules are discussed as well. Finally, results regarding the in vitro enzymatic synthesis of amylose, which self-associates into gels or particles, and in vitro enzymatic extension of glycogen external chains are described. They are evaluated as biomimetic systems for a better understanding of the mechanisms involved in starch crystallization during biosynthesis as well as in the different processes used for starch modification.

Keywords Self-association • Crystallinity • Polymorphism • Crystal structure • Single/double helix • Amylose complexing • Local order • Amorphous • Enzymatic synthesis • Amylosucrase

D. Lourdin (✉) • C. Chevigny • A. Rolland-Sabaté • A. Buléon
INRA-UR 1268 Biopolymères Interactions, Assemblages, Rue de la Géraudière, BP 71627
F-44316 Nantes cedex 3, France
e-mail: denis.lourdin@nantes.inra.fr

J.-L. Putaux
Centre de Recherches sur les Macromolécules Végétales (CERMAV), Université Grenoble Alpes, F-38000 Grenoble, France

CNRS, CERMAV, F-38000 Grenoble, France

G. Potocki-Véronèse
Institut National des Sciences Appliquées, Université de Toulouse, Toulouse, France

Institut National Polytechnique, Université Paul Sabatier, Toulouse, France

Ingénierie des Systèmes Biologiques et des Procédés, Toulouse, France

UMR5504, UMR792 Ingénierie des Systèmes Biologiques et des Procédés, Centre National de la Recherche Scientifique, Institut National de la Recherche Agronomique, Toulouse, France

Y. Nakamura (ed.), *Starch*, DOI 10.1007/978-4-431-55495-0_3

3.1 The Crystalline Structure of Native Starch

Starch is biosynthesized as semicrystalline granules whose shape and size depend on the botanical origin (Fig. 3.1a, c). The starch granule presents a hierarchical and multiscale organization with structural length scales ranging from the tenth of nanometer for the glucose monomer up to a few micrometers for the granule size. Intermediate structural levels include the crystalline and amorphous lamellae repeat distance (9–10 nm), the blocklets (30–200 nm), the growth rings (200–600 nm), and other supramolecular arrangements like superhelices (for reviews, see French 1984; Buléon et al. 1998a, b; Tang et al. 2006; Pérez and Bertoft 2010).

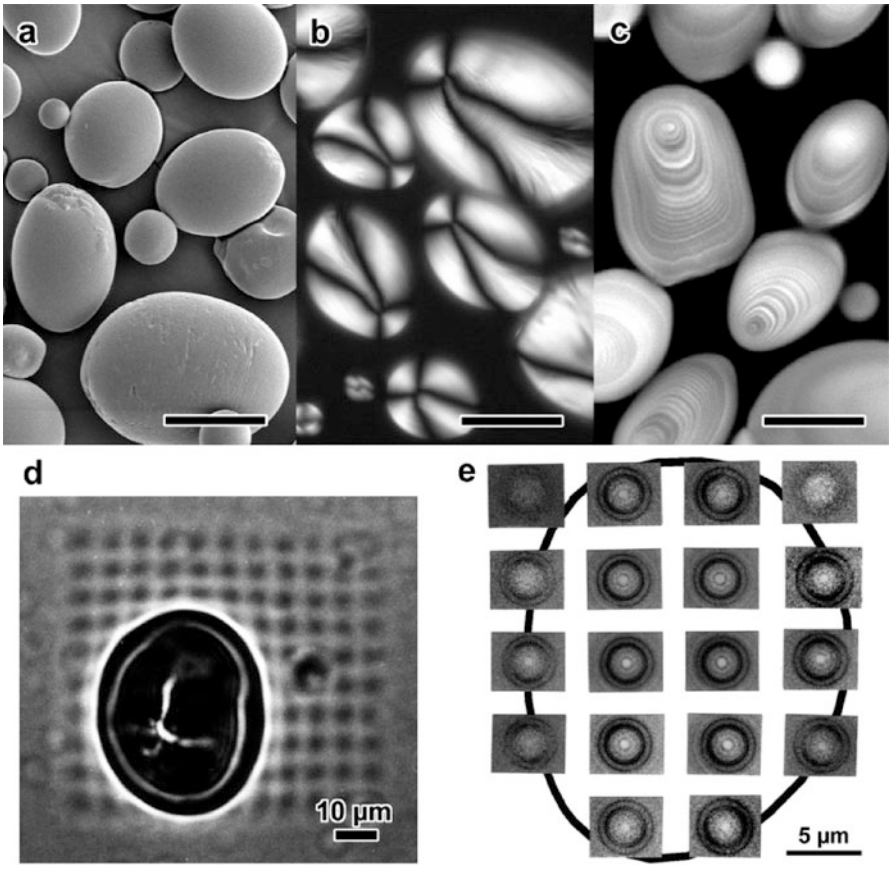

Fig. 3.1 Potato starch granules observed by scanning electron microscopy (**a**), polarized light optical microscopy (**b**), scanning confocal light microscopy (**c**). Scale bars: 20 µm (From Buléon et al. 2007 – images courtesy D. Dupeyre, CERMAV). (**d**, **e**) Synchrotron X-ray microfocus mapping of a smooth pea starch granules (From Buléon et al. 1998a, b)

3.1.1 About Chain Orientation in the Starch Granule

When starch granules are observed under polarized light, a characteristic Maltese cross (centered at the hilum) can be seen (Fig. 3.1b), which has led to consider the granules as distorted spherocrystals. The sign of birefringence is positive with respect to the spherocrystal radius (French 1984) which indicates that, theoretically, the average orientation of the polymer chains is radial. The intensity of birefringence strongly depends on the shape and orientation of the granules with respect to the light beam. Therefore, for nonspherical granules, it is more accurate to say that the orientation is perpendicular to the growth rings and to the granule surface (French 1984). This was also confirmed by solid-state light scattering of starch granules (Borch et al. 1972).

Further results on chain orientation in potato and wheat starch granules were obtained by Chanzy et al. (1990) and Helbert and Chanzy (1996), using selected area electron diffraction over 1 μm^2 on thin sections of partially hydrolyzed starch granules. However, in both studies, the diffractograms were not very well resolved because of the large amount of inelastic electron scattering inherent to this technique.

Significant improvement was achieved using synchrotron microfocus X-ray diffraction with a 1–2 μm beam. Buléon et al. (1997) (Fig. 3.1d, e) and Waigh et al. (1997) showed that the orientation of polymer chains in potato starch was very high at the periphery of the granule and perpendicular to its surface. A lower degree of orientation was found in the internal regions and at the hilum, but the interpretation was more complex since in the center of the granule, the beam averages over regions containing helices pointing forward, backward, and sideways. No specific orientation at a 1–2 μm scale was found for wheat starch granules, either at the periphery or in the center (Buléon et al. 1997), which means that the radial orientation in such granules is weak and limited to smaller domains. Nevertheless, these pioneering works also showed that it was possible to record highly oriented diffraction diagrams, very close to those stemming from recrystallized amylose fibers used to solve the three-dimensional structure of B-type amylose (Buléon et al. 1997). These results show that the corresponding models can be transposed to the crystalline domains in the starch granule.

More recently, many synchrotron microdiffraction experiments confirmed the radial chain orientation in starch granules from various botanical origins (Chanzy et al. 2006). The most recent advances of synchrotrons and the development of the ID13 microfocus beamline at ESRF (Grenoble, France) (Riekel 2000) have significantly improved the microdiffraction method which has now been applied to a number of specimens to study specific properties of individual granules, for instance, the structural changes induced by microdrop hydration (Lemke et al. 2004), high pressure (Gebhardt et al. 2007), or radiation damage propagation (Riekel et al. 2010). X-ray probes with a diameter as small as 0.5 μm are currently available, with the brilliance of the synchrotron, which allows to probe the molecular organization in individual concentric growth rings in the starch granule.

3.1.2 About Crystallinity

The inner architecture of native starch granules is characterized by "growth rings" (Fig. 3.2a, b) that correspond to concentric semicrystalline 120–400 nm-thick shells separated by amorphous regions (French 1984; Buléon et al. 1998a, b; Donald et al. 2001). The crystalline shells consist of a regular alternation of amorphous and crystalline lamellae with a repeat distance of 9–10 nm (French 1984; Cameron and Donald 1993; Jenkins et al. 1993; Cardoso and Westfahl 2010). Parallel arrays of double helices made of amylopectin short branches form crystalline lamellae (Fig. 3.2c, d). Their 5–7 nm thickness presents some variation depending on the botanical origin. Native starch granules exhibit two main allomorphic types that can be identified using X-ray scattering (Fig. 3.2g) or solid-state ^{13}C NMR spectroscopy. The A type mainly occurs in cereal starches and the B type in tubers and amylose-rich starches (Buléon et al. 1984; Zobel 1988). New morphological data on the individual crystalline lamellae of waxy maize starch granules have been reported

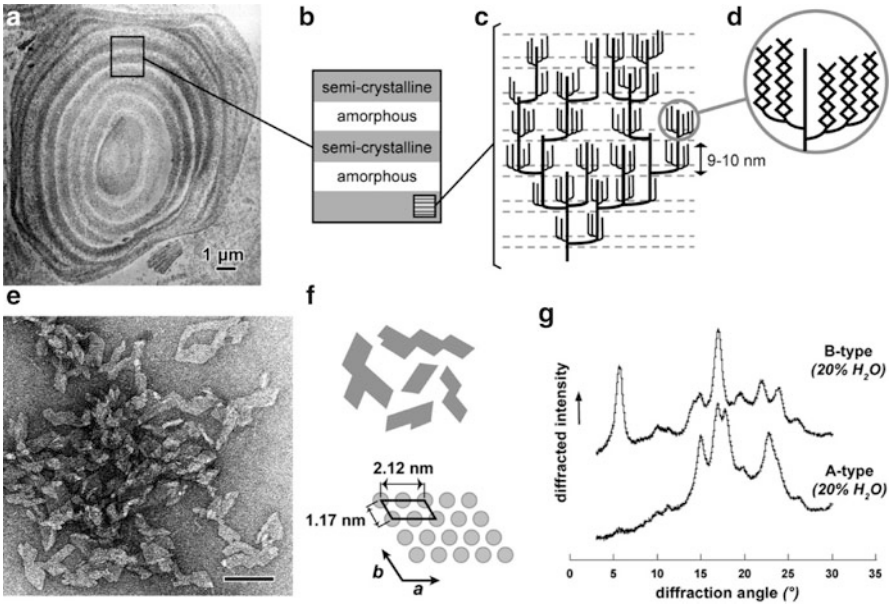

Fig. 3.2 Schematic representation of the starch granule ultrastructure from growth rings to amylopectin: (**a**) ultrathin section of a waxy maize starch granule (staining with uranyl acetate and lead citrate (TEM image courtesy I. Paintrand, CERMAV); (**b**) alternation of amorphous and semicrystalline growth rings; (**c**) clustered model of amylopectin; (**d**) detail of one cluster showing the formation of double helices from the short branches of amylopectin; (**e**) nanocrystals observed after 6 weeks of acid hydrolysis (TEM image after negative staining courtesy of H. Angellier, CERMAV – scale bar: 50 nm); (**f**) simplified drawing of the crystalline platelets and proposed molecular model in relation to the monoclinic unit cell of the A allomorph; (**g**) WAXS profiles of A- and B-type starch (From Buléon et al. 2007)

(Putaux et al. 2003). The mild hydrochloric acid hydrolysis of granules from A-type amylopectin-rich waxy maize leads to an insoluble residue consisting of polydisperse platelet nanocrystals that retain the crystalline A type of the parent granules. They form parallelepipedal blocks with a length of 20–40 nm and a width of 15–30 nm, with characteristic geometrical features such as 60–65° acute angles (Fig. 3.2e, f). Their 5–7 nm thickness is consistent with the presence of double helices made of single strands having a degree of polymerization (DP) between 15 and 18. Such crystalline lamellae could not be as clearly individualized from B-type starch, although lacy networks of acid-resistant units were obtained from low-amylose *Dianella* potato starch (Wikman et al. 2014).

The crystallinity of native starch granules varies from 15 to 45 %, depending on the starch origin, its hydration level, and the characterization method (Buléon et al. 1987; Paris et al. 1999; Zobel 1988; Gernat et al. 1993; Lemke et al. 2004; Lopez-Rubio et al. 2008). The B-starch crystallinity depends more strongly on hydration and increases with water content up to 30–33 % H_2O (dry basis), while dry potato starch does not show any clearly visible diffraction peak (Buléon et al. 1987, 1998a, b; Cleven et al. 1978). Wide-angle X-ray scattering (WAXS), solid-state ^{13}C NMR (CP-MAS), differential scanning calorimetry (DSC), and, to a lesser extent, Fourier-transform infrared spectroscopy (FTIR) are the most commonly used techniques to determine the degree of crystallinity. They are based on different physical phenomena which makes the comparison of the collected data very tricky, especially for starch. Indeed, contrary to thermoplastic samples for which the melting enthalpy is directly correlated with the crystallinity index, starch melting enthalpy cannot be used to determine crystallinity since numerous and various processes are involved during melting, including plasticization, swelling in water, competition between melting and dissolution in water, etc. Therefore, the usual relevant interpretation concerns the residual melting enthalpy which varies as the starch structure is disrupted but cannot be quantitatively correlated with the crystallinity. Moreover in case of amylose-lipid complexes, the melting of "isolated" or "amorphous" complexes is very close to that of crystalline ones since the intramolecular hydrogen bonds within the single amylose helix are much stronger than intermolecular H bonds in the crystal (Biliaderis 1992).

When using FTIR, the 1,065−870 cm^{-1} spectral region is assigned to C-O-C, C-C, and C-H stretching modes, and some peaks have been attributed to ordered (995, 1,047 cm^{-1}) or amorphous (1,022 cm^{-1}) starch (Bernazzani et al. 2000; Capron et al. 2007; Wilson et al. 1987; van Soest et al. 1995). According to Fang and coworkers (2002), the bands located at 1,023 and 1,083 cm^{-1} could be assigned to the C-O bond stretching in the C-O-C group of the anhydroglucose rings. The peak at 1,023 cm^{-1} has been shown to be typical of amorphous starch, while that at 1,049 cm^{-1} increases with increasing crystallinity. However, even when using well-defined crystalline samples, it is difficult to conclude if the FTIR signal is sensitive to short-range order or crystallinity. More recently, the technique was successfully used to determine local order in shape memory starch-based materials (Véchambre et al. 2010).

WAXS and solid-state NMR have proved to be the more reliable techniques to determine the crystallinity and the allomorphic types of starch products. WAXS signals directly stem from the crystalline regions and long-range order. Numerous methods are available to determine the crystallinity from WAXS data. Starch crystallinity was initially calculated by Sterling (1960) and Nara et al. (1978) following the methods developed by Hermans and Weidinger (1948) and Wakelin et al. (1959) for cellulose. They are based on the two-phase concept which assumes that relatively perfect crystalline domains (crystallites) are interspersed with amorphous regions. Solid-state NMR has proved to be a powerful tool to characterize some degree of molecular order such as helicity in the structure of starchy substrates (Gidley and Bociek 1985; Veregin et al. 1986; Horii et al. 1987; Morgan et al. 1995). Gidley and Bociek (1985) demonstrated that C1 and C4 glycosidic sites were more sensitive to conformational changes than the C2, C3, and C5 carbons since C1 and C4 showed higher chemical shift dispersions under various conformations of the glycosidic linkage in α(1,4) glucans. These statements have been confirmed by Veregin et al. (1987) and Gidley and Bociek (1988) who showed correlations between the C1 and C4 chemical shifts of α(1,4) glucans and their torsion angles ϕ and ψ. The multiplicity (stemming from crystallographic constraints in the crystalline regions) and the chemical shifts assigned to C1 atoms have been correlated to the glycosidic conformation and polymorphism of starch (Hewitt et al. 1986; Veregin et al. 1986; Horii et al. 1987; Paris et al. 1999) and other polysaccharides (Jarvis 1994; Isogai et al. 1989). The multiplicity of the C1 resonance is determined by space group equivalent symmetry classes (Veregin et al. 1986; Horii et al. 1987), and for starch, the C1 resonance appears as a triplet for A type and a doublet for B type. Strictly integrating these resonances, directly linked to the crystalline domains, leads to crystallinity values close to those determined by WAXS (Paris et al. 1999).

The influence of hydration on the ordering of starch chains and decrease of the spectral bandwidth was also studied (Tanner et al. 1987; Horii et al. 1987; Paris et al. 1999). The NMR data have been used to identify, and sometimes quantify, the crystalline order of native, hydrolyzed, or gelatinized starches (Willenbucher et al. 1992; Paris et al. 1999), but there is still some debate about the exact level of structure reached with this technique, i.e., the degree of helicity (molecular order) or the fraction of helices packed with respect to crystalline order (Gidley and Bociek, 1985) and the quantitative character of the measurements. While diffraction methods are the main techniques used to quantify crystallinity, shorter-range subcrystalline order can be probed by solid-state NMR spectroscopy which is sensitive to structure at the sub-nanometer level. Starch spectra are interpreted in terms of a combination of amorphous and helical conformations, irrespective of whether helices are present within crystallites or not. Thus, Lopez-Rubio and coworkers (2008) have recently proposed to jointly use WAXS and ^{13}C CP-MAS NMR spectroscopy to determine crystallinity, the amounts of single and double helices (Fig. 3.3), amorphous single and double helical components being determined from NMR spectra as described by Tan et al. (2007). In this work, the crystallinity was determined by fitting experimental WAXS curves with theoretical discrete diffraction peaks determined from the 3D structure of A or B starch and an amorphous background.

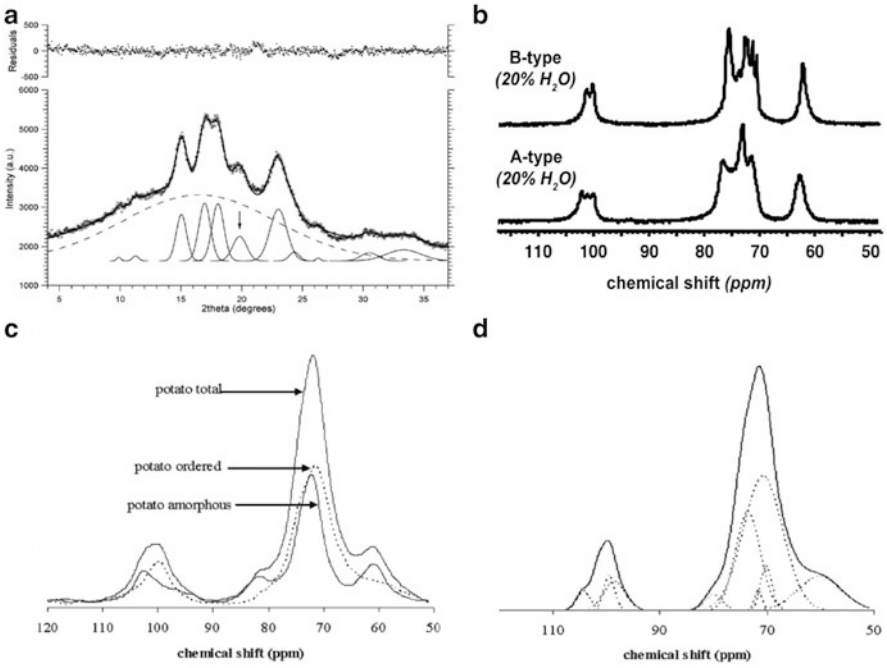

Fig. 3.3 Combined use of WAXS and ^{13}C CP-MAS NMR for the determination of helical order and crystallinity: (**a**) fit of a A-type WAXS profile using an amorphous background and discrete diffraction peaks calculated from the A-type structure (From Lopez-Rubio et al. 2008); (**b**) solid-state ^{13}C NMR spectra of A- and B-type recrystallized amylose (From Paris et al. 1999); (**c**) decomposition of the ^{13}C NMR spectrum into contributions from the amorphous and ordered phases in potato starch by subtraction at 84 ppm and (**d**) deconvolution of the ordered subspectrum for potato starch (From Lopez-Rubio et al. 2008)

3.1.3 The Three-Dimensional Models of Crystalline Domains in Starch

The low crystallinity and complex ultrastructure of the starch granule do not allow direct determination of the three-dimensional shape and distribution of the crystalline domains. Mild acid hydrolysis has widely been used to investigate the structure and properties of starch crystallites by preferential degradation of the amorphous regions (Buléon et al. 1987, 1998a, b). The extent of this preferential erosion depends on the density difference between the crystalline and the amorphous regions (Vermeylen et al. 2004). As previously mentioned, A-type nanocrystals obtained by extended mild hydrolysis of waxy maize starch granules correspond to the crystalline lamellae present in the native granule (Putaux et al. 2003) (Fig. 3.2). However, electron diffraction data could not be collected from individual platelets, because of their small lateral size and thickness.

Contrary to amylopectin which constitutes the backbone of the semicrystalline structure of starch granules, amylose can easily be crystallized from solution by cooling or addition of a precipitant. This property has been used to prepare model crystalline substrates whose diffraction data and thermal properties were analyzed to propose three-dimensional models of starch crystallites and to understand the phase transitions involved in various applications and the processing of starch (Buléon et al. 1987; Whittam et al. 1990). The resulting morphology (aggregates, precipitates, gels, single crystals, spherulites, etc. – Fig. 3.4) and allomorphic type (A, B) depend on factors such as solvent, molar mass, branching degree, concentration, or temperature (Buléon et al. 1984, 2007; Pfannemüller 1987; Gidley and Bulpin 1987). A general rule is that long chains and low recrystallization temperatures favor the B type, whereas high concentrations, high temperatures, and short chains are known to induce A-type crystallization (Buléon et al. 2007). This behavior has some similarities with the crystallization of starch during biosynthesis,

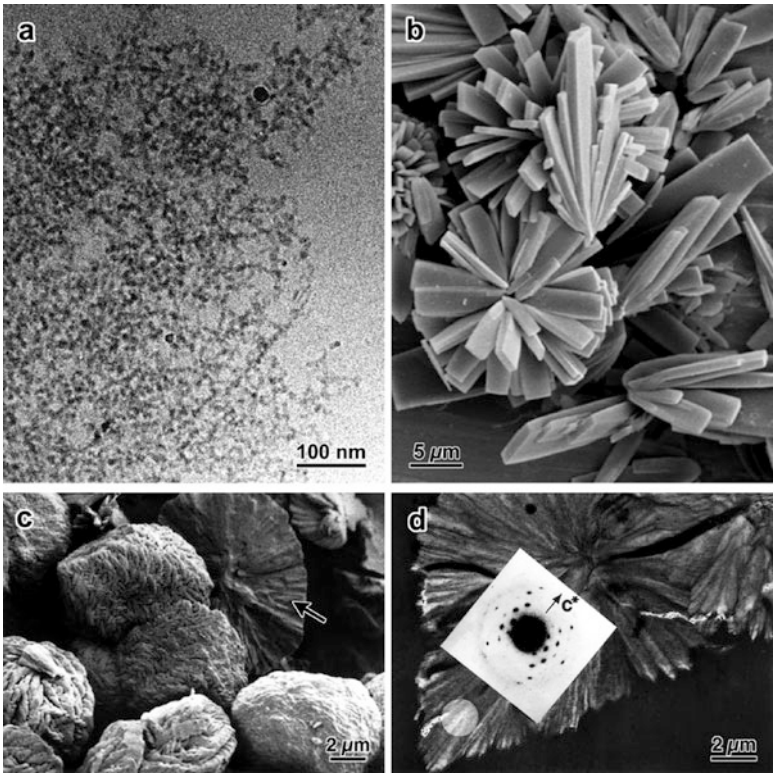

Fig. 3.4 Recrystallized amylose: (**a**) retrograded gel network from diluted long chains, (**b**) A-type crystals prepared from a narrow fraction of amylose biosynthesized in vitro (DPn = 17.4 – from Montesanti et al. 2010), (**c**) A-type spherocrystals and (d) corresponding electron diffraction pattern recorded from a ultrathin section of a spherocrystal (From Helbert et al. 1993)

since it is well known that (i) B-type starches amylopectin short chains are longer than in A type (Hizukuri 1985); (ii) A type is mostly present in cereal grains, which grow in warmer and dryer conditions than tubers starches; and (iii) an increase of temperature during the plant growth favors A type (Gérard et al. 2000).

Most molecular models proposed to describe the structure of the crystalline domains in starch granules were built using WAXS data collected from recrystallized fibers (Wu and Sarko 1978a, b; Imberty and Pérez 1988) or lamellar crystals (Imberty et al. 1988). The structural models established from A and B amylose crystals were transposed to crystalline regions of native starch, which exhibit similar but much less resolved diffraction diagrams. WAXS fiber diagrams recorded from native potato and pea starch granules using synchrotron microbeam X-ray mapping confirmed that these A- and B-type models could also be applied to describe native starch crystallites (Waigh et al. 1997; Buléon et al. 1998a, b). In these A and B structures, amylose exhibits a sixfold left-handed double helical conformation with pitches of 2.08 and 2.13 nm, respectively (Imberty et al. 1988; Imberty et al. 1988, Takahashi et al. 2004). In the A structure, these double helices are packed with the B2 space group in a monoclinic unit cell ($a = 2.124$ nm, $b = 1.172$ nm, $c = 1.069$ nm, $\gamma = 123.5°$) with four water molecules per unit cell (Imberty et al. 1988). In the B structure, double helices are packed with the $P6_1$ space group in a hexagonal unit cell ($a = b = 1.85$ nm, $c = 1.04$ nm, $\gamma = 120°$) with 36 water molecules per unit cell. The symmetry of the double helices differs in A and B structures, since the repeated unit is a maltotriosyl unit in the A form and a maltosyl unit in the B form, which is in agreement with the triplet and the doublet observed by solid-state NMR for the C1 peak for the A form and the B form, respectively (Fig. 3.3).

5–15 μm-long needlelike A-amylose single crystals have recently been prepared from dilute (0.05 % w/v) solutions of a short-chain amylose fraction ($\overline{DP}_n = 17.4$) synthesized in vitro by amylosucrase from sucrose (see Sect. 3.3). Their size and perfection allowed to collect WAXS datasets from single crystals, up to a resolution of 0.151 nm, using a microbeam of synchrotron radiation (Fig. 3.5a, b) (Popov et al. 2006, 2009). A total of 57 independent reflections were used to refine the unit cell and confirm the space group proposed by Imberty et al. (1988). However, the high resolution of the diffraction data, which was unique for a crystalline polymer, allowed to resolve important new fine details. Pockets of two intracrystalline water molecules were distributed between the double helices, resulting in helical distortions (Fig. 3.5c). In addition, a tight network of hydrogen bonds involving the primary and secondary hydroxyl groups of the glucosyl moieties stabilized the structure (Fig. 3.5d). The refinement of the new structure indicated a "parallel-down" organization of the amylose molecules within the unit cell as opposed to the previous "parallel-up" model (Imberty et al. 1988). This new feature indicates that within the crystals, the nonreducing ends of the amylose molecules are oriented toward the *c*-axis direction of the unit cell. The description of this geometry is important to correlate the crystallography of the A-type granules with their ultrastructure and mode of biosynthesis.

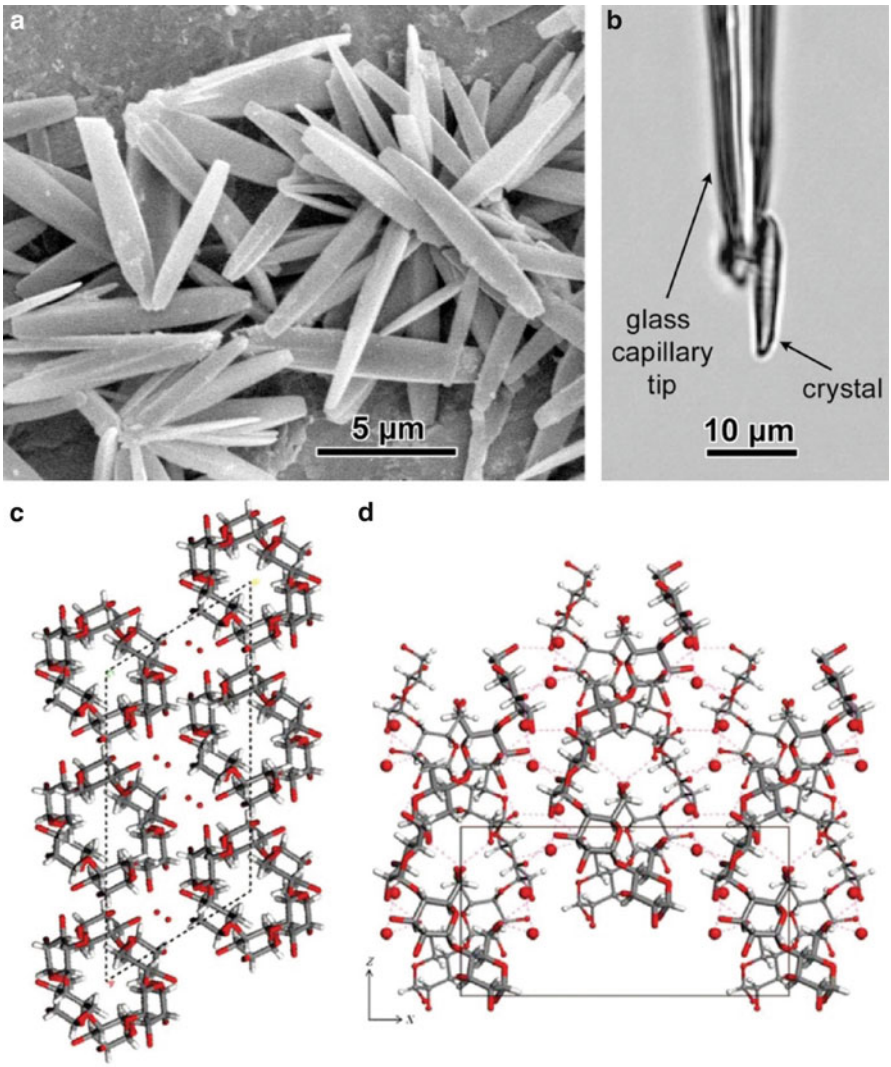

Fig. 3.5 (**a**) SEM image of A-amylose single crystals prepared by crystallizing amylose biosynthesized in vitro; (**b**) one crystal glued to a borosilicate glass capillary tip; (**c**, **d**) projections on the (*a*, *b*) and (*a*, *c*) planes of the structure determined by crystallographic analysis of the synchrotron X-ray diffraction data collected from such single crystals (From Popov et al. 2009)

The general shape of the starch nanocrystals previously mentioned and obtained by mild acid hydrolysis of waxy maize starch granules can also be described by comparison to the unit cell of the A allomorph. The base-plane projection of the nanoplatelets would be homothetic to the (*a, b*) plane of the monoclinic unit cell (Fig. 3.2f). The experimental acute angles measured from the nanocrystals (60–65°) are close to the 56.6° acute angle complementary to the γ angle of the unit cell (Fig. 3.2f) (Putaux et al. 2003; Pérez and Bertoft 2010).

3.2 Phase Transitions and Crystalline Structure of Starch

In most uses of starch, the granule is disrupted, in particular during hydrothermal treatments like extrusion, cooking, high-pressure treatments, etc. Many reviews have been published on hydrothermal treatments of starch and related phenomena such as gelatinization, melting, gelation, retrogradation, structural transition, and amylose complexing (Buléon and Colonna 2007; Colonna and Buléon 2010). Once the granule has been disrupted, the structure and properties of the resulting material are governed by the way amylose and amylopectin rearrange during cooling, which strongly depends on temperature, shear, and water content. Starch glassy materials are obtained by melting of starch in processing conditions yielding a final water content below the glass transition domain. On the contrary, as soon as a sufficient amount of water is present, amylose and amylopectin recrystallize mostly into B type. This starch retrogradation is the basis of many food uses of starch as gelling agent. During hydrothermal treatments, amylose can form semicrystalline single helical inclusion complexes with small molecules (like lipids, alcohols, flavor compounds, and various small hydrophobic molecules). The helical conformation, crystalline packing, and intra- or inter-helical inclusion depend on the complexing molecules, and these parameters govern the thermal stability of the complex and the way the guest molecule is released. Starch melting/retrogradation and starch complexing by lipids and alcohols are well documented (see, e.g., Colonna and Buléon 2010). The following section focuses, on one hand, on local order and orientation in amorphous starch, as a function of the thermomechanical history, and, on the other hand, on the most recent structures determined for amylose complexes.

3.2.1 Local Order and Orientation in Amorphous and Semicrystalline Starch Materials

Amorphous starch materials present no long-range ordering (i.e., crystallinity), but locally keep some organization and orientation which depend on the process used for the starch structure disruption and the thermomechanical history of the material. This local order can be studied by techniques such as solid-state NMR for short-range order or two-dimensional WAXS and synchrotron radiation (SR) infrared microspectroscopy for local orientation. Paris and coworkers, in the early 2000s, used ^{13}C CP-MAS solid-state NMR for the characterization of the different local-range orderings present in amorphous/semicrystalline starch, amylose, or amylopectin, prepared by different techniques like casting, freeze-drying, or 2-propanol precipitation from solution (Paris et al. 2001). All samples were amorphous except reprecipitated ones. A major part of the project consisted in providing a reliable spectral decomposition of the C1 resonance spectrum, which revealed the existence of four to five main types of α(1,4) linkages which were quantified (Paris et al. 2001). Thus, accepting the classical correlation (Gidley

and Bociek 1988) between the isotropic chemical shift and the conformational angles ($|\Phi|+|\Psi|$), a specific α(1,4) conformation was associated to each type. The conformations used for the decomposition were extracted from a refined literature analysis on NMR of α-glucans and transposed to the determination of local order within the amorphous samples studied. The bands stemming from the spectral decomposition have the following chemical shift: A (103.4−103.2 ppm), B (102.9 ppm), C (101.4−100.4 ppm), D (98.6−97.1 ppm), and E (94.5−94.4 ppm). As an example, the C1 part of the NMR spectra of casted amylose and amylopectin reprecipitated in 2-propanol, and their corresponding decomposition into four and five components, respectively, is presented in Fig. 3.6c, d. Full spectra are shown in Fig.3.6a, b for reference. A, C, D, and E peaks are present for all types of starchy materials, while the B peak is only present in 2-propanol-reprecipitated samples. The A peak is the most intense (around 50 % of total area) for all samples, except for 2-propanol-reprecipitated samples. Its chemical shift (103.3 ppm) is similar to the classical range of V-type spectra (Horii et al. 1987; Gidley and Bociek 1988) and single sixfold helical conformation. The B peak, which is only observed for 2-propanol-reprecipitated samples presenting a WAXS diagram characteristic of a mixture of amylose $V_{2\text{-propanol}}$ complex and B type, was attributed to V_H-type single helices, since at that time, amylose conformation present in amylose-2-propanol complexes was assumed to be a single sixfold helix similar to that constituting the V_H structure. Considering the new structure recently established for the $V_{2\text{-propanol}}$ crystalline complex (Nishiyama et al. 2010), this B line is more probably associated to a sevenfold single helix. The remaining conformations (C, D, E) are the most sample sensitive and subject to more variation in chemical shift. The C peak appears in the range of double helical conformation and could be associated to paracrystalline bundles stemming from uncompleted melting of starch structure or very local retrogradation. The D peak has been observed in α-cyclodextrins with twisted glycosidic linkage (Gidley and Bociek 1988) and tentatively correlated to α(1,6) linkages by Morgan et al. (1995). The chemical shift and C/D difference observed between linear (amylose) and branched (amylopectin or starch) samples suggest that D conformations are more sensitive to the presence of α(1,6) and could be closer to branching points than the C ones. E line, by far the weakest (2–8 % depending on the sample), is related to energetically unfavorable conformations such as constrained linkages.

Each type of amorphous starchy material has a specific signature with different proportions of each conformation, bringing out their thermomechanical history. Thus, the different local conformations present in amorphous amylose, amylopectin, or starch are directly related to the preparation conditions. For example, for casted samples twisted and/or constrained conformations are less present than in freeze-dried corresponding samples since chains, heated in the presence of water, may relax before complete removal of water. On contrary, during freeze-drying the conformations are frozen before removal of water, and more constrained conformations are created. More generally, E conformations are favored by more drastic methods of preparation. Rehydration and plasticization by water lead to a general decrease in line width and therefore to a more homogeneous distribution of

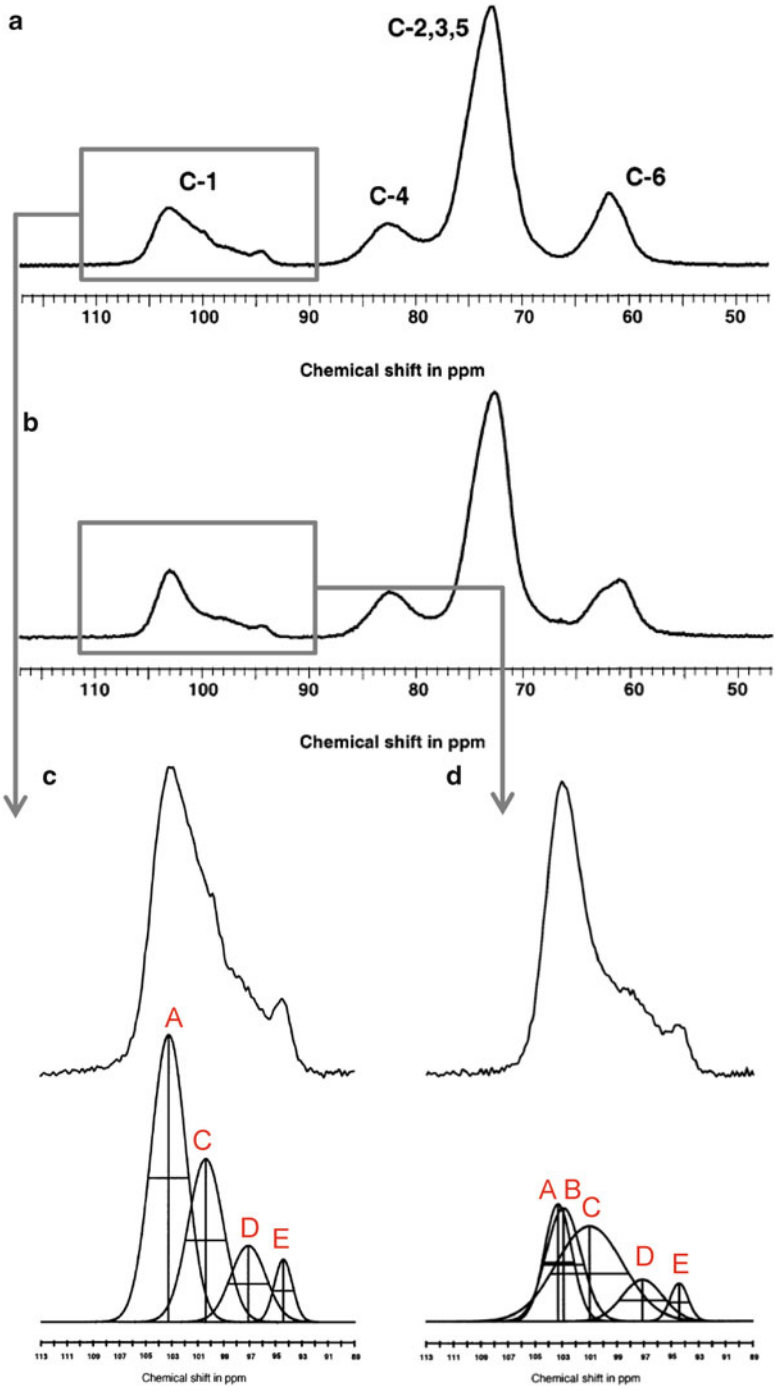

Fig. 3.6 ^{13}C CP-MAS NMR spectra of (**a**) amorphous amylose (obtained by hot casting) and (**b**) 2-propanol precipitated amylose. Enlarged C1 resonance for 2-propanol-precipitated (**c**) and casted (**d**) amylose, with corresponding deconvolution of the C1 region (From Paris et al. 2001)

conformation and show a higher sensitivity of more constrained conformations (D, E lines) and freeze-dried samples. Recently, a similar spectral decomposition was successfully performed on cross-linked starch (Thérien-Aubin et al. 2007).

The presence of a local organization in amorphous starch induces very important changes on the properties and phase transition of starch materials. An example is given by recent works showing very efficient shape memory properties of extruded starch materials (Véchambre et al. 2010). Shape memory corresponds to the ability for materials to recover their original shape after being deformed into a temporary shape. In the case of "usual" thermoplastic shape memory materials, the effect is attributed to the presence of two types of domain: one flexible and one rigid. The rigid domains determine the initial shape, while the more flexible domains become oriented in the temporary shape. This orientation remains stable in "constrained" materials, below the glass transition temperature T_g. However, at a temperature above T_g, these domains relax, which results in the recovery of the initial macroscopic shape of the unconstrained sample.

The orientation and physical cross-links and their relation with thermomechanical history have been studied in amorphous extruded starch materials. Such materials are completely transparent when observed using light microscopy, but with polarized light microscopy, constrained samples show typical and clearly visible birefringence fringes, contrary to unconstrained samples which do not present any specific birefringence. This shows that the constrained samples are anisotropic due to residual stress but that anisotropy disappears after shape recovery, due to the relaxation of residual stress. Despite strong birefringence under polarized light, no crystal melting is evidenced by DSC, and WAXS diagrams present no clear diffraction peaks but only a broad amorphous scattering band. The scattering band maximum corresponds to a repeat distance of about 0.5 nm. This is normally considered to arise from the van der Waals (VDW) contact of nonbonded atoms (VDW spacings) (Miller et al. 1984).

WAXS was used to determine the orientation within such constrained samples, usually extruded rods or thermomolded barrels, after uniaxial deformation (Véchambre et al., 2010). The WAXS diagrams were recorded in transmission mode using a two-dimensional detector from specimens lying with their long axis lying parallel to the vertical axis of the detector (Fig. 3.7a). Constrained samples exhibit periodic scattering intensity changes on the maximum of the broad amorphous scattering band, with the azimuthal angle (Fig. 3.7b). The orientation was determined by azimuthal integration between 0.680 and 0.386 nm corresponding to the amorphous scattering band. The presence of two maxima at 90 and 270° shows that orientation is parallel to the axis of deformation of the sample (Fig. 3.7c). It has been shown that orientation increases with the level of deformation. Such orientation is stable as long as moisture content keeps the sample in the glassy state (below T_g). No periodic scattered intensity was observed for the relaxed samples as for unconstrained samples.

Similar measurements revealed that the orientation decreases when the temperature of deformation increases. This decrease in orientation with increasing deformation temperature was attributed to the greater ability of chains to rapidly

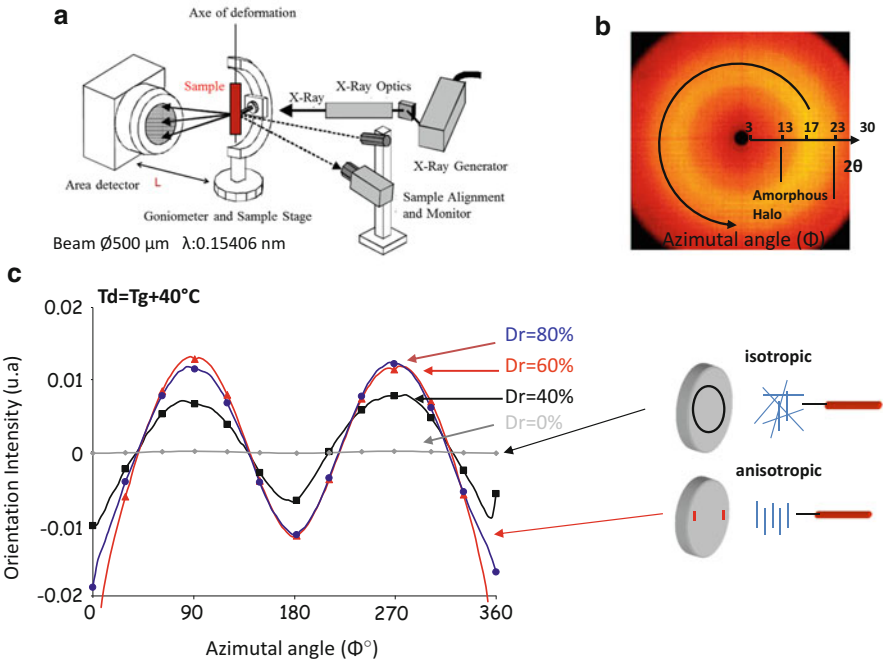

Fig. 3.7 Orientation diagrams from WAXS spectra: (**a**) WAXS setup used and positioning of the specimen, (**b**) azimuthal scan of the amorphous broad scattering from the transversal sample, (**c**) evolution of orientation as a function of the deformation rate

reorganize at higher temperatures between deformation temperature and T_g at the end of the deformation process (Véchambre et al. 2011). The recovery stress is a collateral effect of shape memory which happens when the sample is stimulated and maintained in its initial shape. It has been shown that the maximum recovery stress increases almost linearly with increasing orientation. This means that the driving force for the starch shape memory is the behavior of oriented amorphous segments that act as "entropic springs" above T_g. From these results, it is expected that amylose, to which the linear structure induces a better ability to be oriented than amylopectin, gives the higher recovery stress.

IR spectroscopy was used to look at the local orientation in constrained samples and at the chemical groups potentially involved. The intensity of the two peaks at 1,023 and 1,049 cm^{-1}, in the C-C, C-O, and C-H stretching and C-O-H bending energy range, has been widely used to determine the amount of ordered and amorphous starch, respectively (Smits et al. 1998; van Soest et al. 1995). The band at 1,153 cm^{-1} was assigned by Bernazzani and coworkers (2000) to vibrations in the environment of ordered single helices. Finally, the band at 987 cm^{-1} is very sensitive to hydration and can shift from 987 to 1,003 cm^{-1} depending on the water content. It was attributed to intramolecular hydrogen bonding of the hydroxyl group at C-6. It was also shown to develop with molecular ordering

(Sevenou et al. 2002; Capron et al. 2007). Synchrotron IR microspectroscopy, which yields higher signal-to-noise ratio, smaller recording time, and easier dichroism experiments (the synchrotron beam being naturally polarized), was applied to constrained and unconstrained samples (Véchambre et al., 2010). With this technique, spectra were collected on a surface of 12 $\mu m \times 12$ μm, and a mapping of samples of about 100 μm^2 was performed with the synchrotron IR beam parallel (PAR) or perpendicular (PER) to the axis of deformation of the sample (Fig. 3.8a). Small but significant differences, demonstrated by a statistical analysis (PCA), were observed between PAR and PER spectra contrary to unconstrained samples, which confirms the presence of a specific orientation in the constrained samples. The PCA analysis was also used to identify the main FTIR absorbance bands associate to PAR and PER spectra (Fig. 3.8b). From band attribution presented previously, molecular orientation in deformed sample is clearly related to amorphous domains. On the contrary, all the bands assigned to higher order and/or crystallinity are linked to spectra recorded in PER mode. It shows that local orientation is more present in

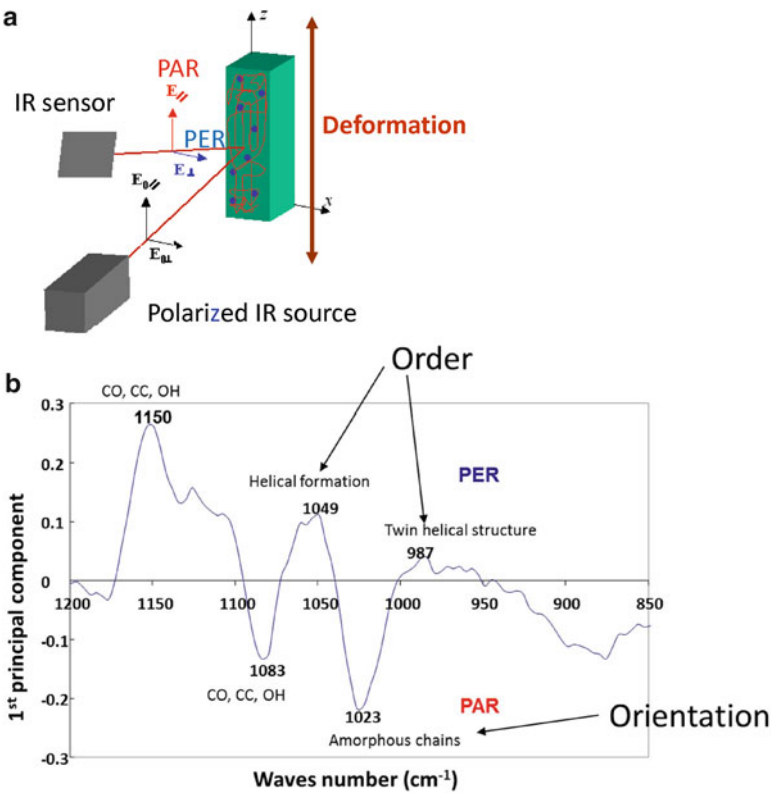

Fig. 3.8 Synchrotron infrared microspectroscopy of shape memory starch-based materials: (**a**) orientation of the specimen for dichroism experiments, (**b**) first principal component loading vector determined by the PCA and associated infrared absorptions

amorphous domains and is limited by ordered domains. The presence of bands linked to hydrogen bonds and α(1,4) linkage could evidence the presence of local order under the form of helical fragments which may be stabilized by intramolecular H bonds and play as springs during the recovery process.

3.2.2 Starch Interactions with Small Molecules and Amylose Complexing

Amylose shows the unique feature to form complexes with a large variety of molecules. When heated in the presence of starch and water, monoacyl lipids and emulsifiers as well as smaller ligands such as alcohols or flavor compounds are able to induce the formation of left-handed amylose single helices. "V amylose" is the generic term used to describe amyloses co-crystallized with such compounds. The resulting helical conformation and crystalline packing depend on the nature of the ligands and conditions for the formation of the complex. In particular, the specific interaction of amylose with lipids or aroma compounds has a strong impact on food quality (Heinemann et al. 2005; Conde-Petit et al. 2006), while the interaction between amylose and some plasticizers impacts the mechanical properties of starch-based materials. A foremost example is the use of fatty acids and monoglycerides as anti-staling agents in bread and biscuits. The incorporation of such additives in the dough induces a slower crystallization (retrogradation) of the amylopectin fraction and therefore retards the staling of bread (Morrison et al. 1993a). Experimental evidence that such complexes might be present in native starches in the amorphous state was given by Morrison et al. (1993b). In that case, amylose chains are involved in either isolated single helices or involved in crystallites too small to be resolved by WAXS.

The crystalline structure of amylose complexes was widely studied by crystallizing amylose from aqueous solutions in the presence of a large variety of small organic and inorganic molecules. Amylose forms inclusion compounds with distinct WAXS signatures that depend on the complexing agent (Takeo and Kuge 1969; Tomasik and Schilling 1998a, b; Putseys et al. 2010). Several generic families of V-amylose have been described (Buléon et al. 2007; Putaux et al. 2011a). Although the knowledge of the molecular structure is important to locate the guest molecules and understand how they are entrapped within the crystal lattice, only a small number of structures have been resolved by crystallographic approaches, and several models are still hypothetical. Besides many studies carried out on polycrystalline powders or oriented fibers (Zobel et al. 1967), electron diffraction of lamellar single crystals, in particular when performed in frozen-solvated conditions (Booy et al. 1979), combined with molecular modeling, played a crucial role in the determination of a number of structures (Yamashita et al. 1973; Helbert 1994; Brisson et al. 1991; Nishiyama et al. 2010).

The so-called V_H type, obtained when amylose is crystallized in the presence of fatty acids (Godet et al. 1993) and some alcohols (Brisson et al. 1991), is well documented. The lamellar single crystals exhibit a characteristic hexagonal shape, and the unit cell has been described by the hexagonal packing of left-handed sixfold single helices (Brisson et al. 1991). In the case of complexes formed with lipids, the aliphatic segment of the guest molecules has been shown to be located inside the helical cavity, while the polar head remained outside (Godet et al. 1993). Other sixfold helical systems have also been proposed to describe complexes formed in the presence of *n*-butanol (Rundle and Edwards 1943; Helbert and Chanzy 1994), dimethyl sulfoxide· (French and Zobel 1967), and glycerol (Hulleman et al. 1996).

Bear suggested that bulkier guest molecules should be accommodated in a larger helix with more residues per turn (Bear 1944). By comparing the volume of the unit cells of the complexes formed with *tert*-butanol and *n*-butanol, Zaslow obtained a ratio of about 7:6 in favor of the existence of a sevenfold helix for the $V_{tert\text{-butanol}}$ complex (Zaslow 1963), a conclusion supported by Yamashita and Hirai (1966). Later on, based on the electron diffraction data of $V_{2\text{-propanol}}$ single crystals, Buléon et al. (1990) proposed an alternate model: the orthorhombic unit cell would contain sixfold helices separated by a layer of guest molecules. Solving this dilemma was important as it had been observed that a large number of complexing agents (thymol, geraniol, menthone, etc.) promoted the formation of crystals exhibiting similar diffraction patterns (Helbert 1994; Nuessli et al. 2003). Recently, Nishiyama et al. (2010) refined the structure of $V_{2\text{-propanol}}$ crystals using electron diffraction data combined with conformational and packing energy analyses. They proposed an original unit cell based on sevenfold V-amylose helices whose packing was described using two regularly alternating motifs: one is nearly tetragonal and holds a cavity filled with 2-propanol and water molecules, whereas the other corresponds to four close-packed helices with only water molecules located in the inter-helical space (Fig. 3.9a–c).

An eightfold amylose single helix has been proposed to occur in the presence of three complexing molecules: 1-naphthol (Yamashita and Monobe 1971; Helbert 1994), quinoline (Helbert 1994), and salicylic acid (Oguchi et al. 1998). The helices would be organized in a tetragonal unit cell. So far, the strongest experimental evidence of an eightfold helix has been provided by Cardoso et al. (2007) who published a high-resolution transmission electron microscopy (TEM) image of the crystal lattice viewed along the helical axis and showing a repeating ring motif of 8 subunits (Fig. 3.9d-f).

Sequential washing of powdered complexes with ethanol allowed to probe intra- and inter-helical inclusions. Such approach was recently applied to the different crystalline types of amylose alcohol complexes and to aromas like linalool and menthone (Rondeau-Mouro et al. 2004; Biais et al. 2006). High-resolution magic angle spinning (HR-MAS) NMR spectra were also used to compare the chemical shifts of free and bound aroma molecules and allowed to propose hydrogen bonding schemes in amylose complexes. Moreover, free aroma was shown to be completely removed by ethanol washing. Using CP-MAS NMR and X-ray scattering experiments, it was demonstrated that the $V_{2\text{-propanol}}$ type was retained for linalool whatever the

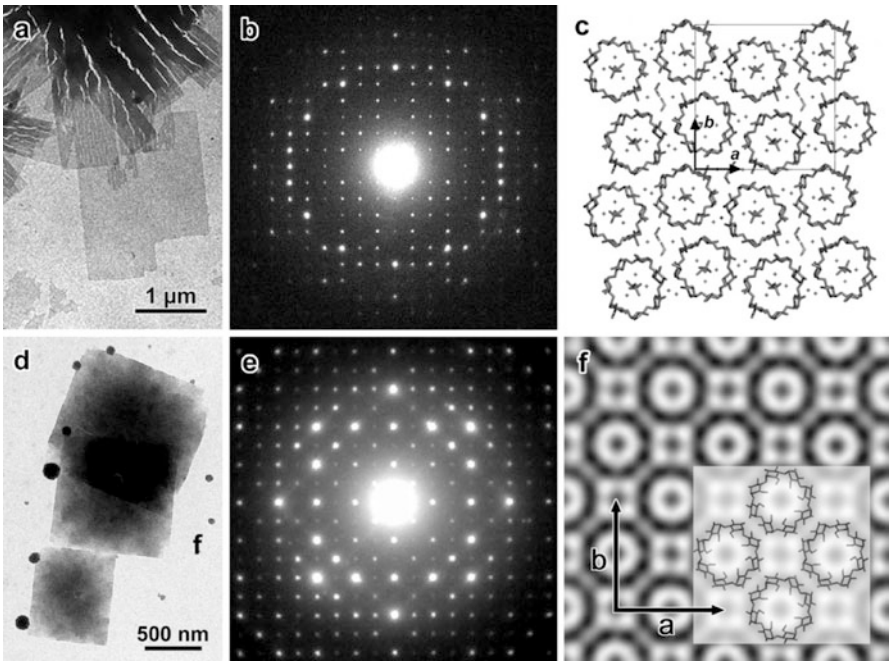

Fig. 3.9 (**a**, **d**) TEM images of amylose $V_{2\text{-propanol}}$ and $V_{1\text{-naphthol}}$ lamellar single crystals, respectively; (**b**, **e**) corresponding low temperature base-plane electron diffraction patterns recorded from frozen-wet crystals; (**c**) axial projection of the molecular model of the amylose $V_{2\text{-propanol}}$ complex. For clarity, the hydrogen atoms have been omitted. The 2-propanol guest molecules are located inside and between the sevenfold amylose single helices (From Nishiyama et al. 2010). (**f**) Averaged high-resolution TEM lattice image of the crystal structure of amylose $V_{1\text{-naphthol}}$. The projection of the network of eightfold amylose single helices has been superimposed (From Cardoso et al. 2007)

treatment used. On the contrary, it shifts toward V_H type for menthone after ethanol washing before the desorption step, reflecting the disappearance of inter-helical associations between menthone and amylose. The stability of the complex prepared with linalool shows that this ligand is more strongly linked to amylose helices. The discrepancies observed in the chemical shifts attributed to carbons C1 and C4 in CP-MAS NMR spectra of $V_{2\text{-propanol}}$ and V_H forms were attributed either to a deformation of the single helix (with possible inclusion of the ligand inside) or to the presence of the ligand between helices (only water molecules are present in the V_H form). As described above, it is now more probably related to the sixfold and sevenfold nature of amylose helices in V_H and $V_{2\text{-propanol}}$ complexes, respectively.

The formation of amylose complexes during in vitro enzymatic synthesis of amylose by phosphorylase in the presence of fatty acids or polymers like polyethers, polylactic acid, polycarbonate, or chemically modified cellulose has also been reported. This direct wrapping of amylose chains around the complexing molecule has been described as “vine-twining polymerization” (Kadokawa et al. 2002) or “parallel enzymatic polymerization system” (Kaneko et al. 2008).

3.3 In Vitro Enzymatic Synthesis of Starch Building Blocks and Biomimetic Systems

Since the complete separation of amylose and amylopectin from native starch is highly difficult, in vitro enzymatic synthesis of linear or branched α(1,4)-linked glucans has been significantly investigated during the last years, in order to mimic starch biosynthesis and, in particular, to better understand how linear chains self-associate.

3.3.1 In Vitro Synthesis of Amylose

Three classes of enzymes (glycosyltransferases, glycoside phosphorylases, and transglycosylases) are naturally able to polymerize α(1,4)-linked residues (Fig. 3.10). However, the high-yield in vitro production of amylose based on the use of Leloir glycosyltransferases (GTs) like granule-bound starch synthases (GBSS) cannot be envisaged as these enzymes use an activated sugar nucleotide donor (ADP-glucose) that is too expensive and are not active when they are not embedded in the native starch granule (Ball and Morell 2003). Thus, only glycoside phosphorylases and transglycosylases have been extensively used for in vitro amylose synthesis.

Bacterial, animal, or plant α-glucan phosphorylases (GPs), which are classified in the GT35 family because of their structural similarity with real GTs, naturally catalyze the breakdown of an α(1,4) glucosidic linkage from amylose or glycogen through a retaining mechanism, with concomitant phosphate glycosylation, to

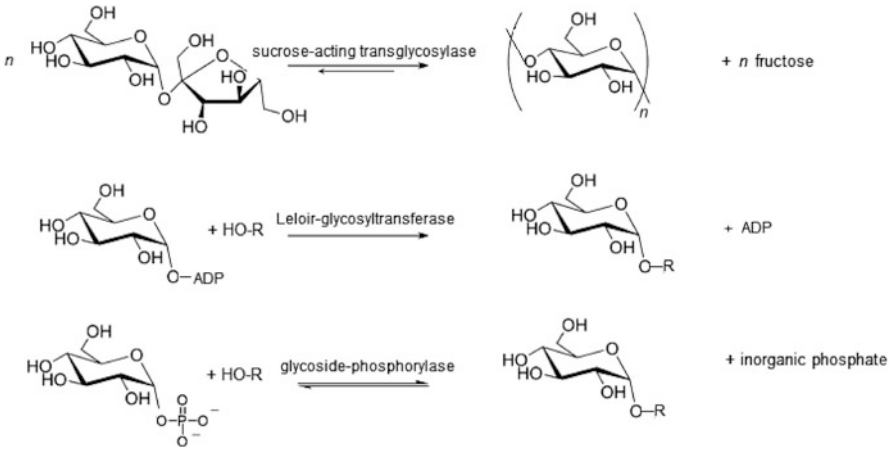

Fig. 3.10 The various enzymatic routes of α(1,4)-glycan synthesis

yield a α-D-glucose-1-phosphate (G-1-P) and a shorter α-glucan chain. These enzymes also perform reverse phosphorolysis to form a glycosidic bond between the glycosyl unit originating from the glycosyl phosphate, which acts as the sugar donor, and a carbohydrate acceptor. In this so-called synthetic reaction, the smallest glycosyl acceptor, or primer, is maltotetraose. Phosphorylase-catalyzed enzymatic polymerization is the only method used for production of amylose with low dispersity ($\overline{M}_w/\overline{M}_n < 1.2$) and with a weight-average molar mass that can be easily controlled by varying the G-1-P/primer ratio (Kadokawa 2012). However, G-1-P is too expensive for industrial synthesis of amylose, even if two-step amylose synthesis processes were developed, combining actions of phosphorylases to generate G-1-P from sucrose or cellobiose (Ohdan et al. 2006).

Bacterial amylosucrases are thus a highly attractive alternative to mimic in vitro amylose polymerization and to get knowledge on chain self-association during starch synthesis or processing. Indeed, they are the only known enzymes that catalyze, without any primer, the synthesis of an α(1,4)-linked glucan from sucrose, a cheap agroresource used as glycosyl donor, with the concomitant release of fructose. These transglycosylases, classified in family 13 of glycoside hydrolases (André et al. 2010), use a retaining non-processive mechanism to produce an amylose-like polymer of which the average chain length, dispersity, morphology, crystallinity, and chain length involved in crystals can simply be modulated by varying initial sucrose concentration and reaction time (Potocki-Véronèse et al. 2005).

The longest chains ($\overline{\mathrm{DP}}_w = 58$, $\overline{M}_w/\overline{M}_n = 3.0$) produced by *Neisseria polysaccharea* amylosucrase (NpAS) from 100 mM sucrose entangle into networks similar to those observed by TEM for amylose gels (Fig. 3.11a). These networks contain clusters of semicrystalline 10–15 nm elementary units, formed by association of molecules into parallel double helices, linked by amorphous sections containing loosely organized chains. A synchrotron SAXS study of the amylose conformation during synthesis in such conditions revealed that at an early stage of polymerization, amylose consists of a mixture of wormlike chains and double helical cylindrical structures (Roblin et al. 2013). In a second stage, individual double helices pack into clusters before crystallizing and precipitating. All the dimensions determined for wormlike chains and cylindrical conformations at different times of synthesis were in very good agreement with structural features usually observed on gels of amylose extracted from starch. Furthermore, DSC and WAXS analyses revealed that these short chains arrange into independent B-type crystalline domains, as did the samples produced from 600 mM ($\overline{\mathrm{DP}}_w = 35$, $\overline{M}_w/\overline{M}_n = 2.3$) (Fig. 3.11b). Nevertheless, in these last conditions, the chains suddenly precipitate as polycrystalline aggregates, when the limit chain length and concentration are reached during synthesis (Potocki-Véronèse et al. 2005). Remarkably, this behavior is generally also encountered for plant amylose chains, the longest ones yielding B-type networks upon retrogradation at temperatures between 4 and 30 °C, while shorter chains form polycrystalline precipitates (Buléon et al. 1984).

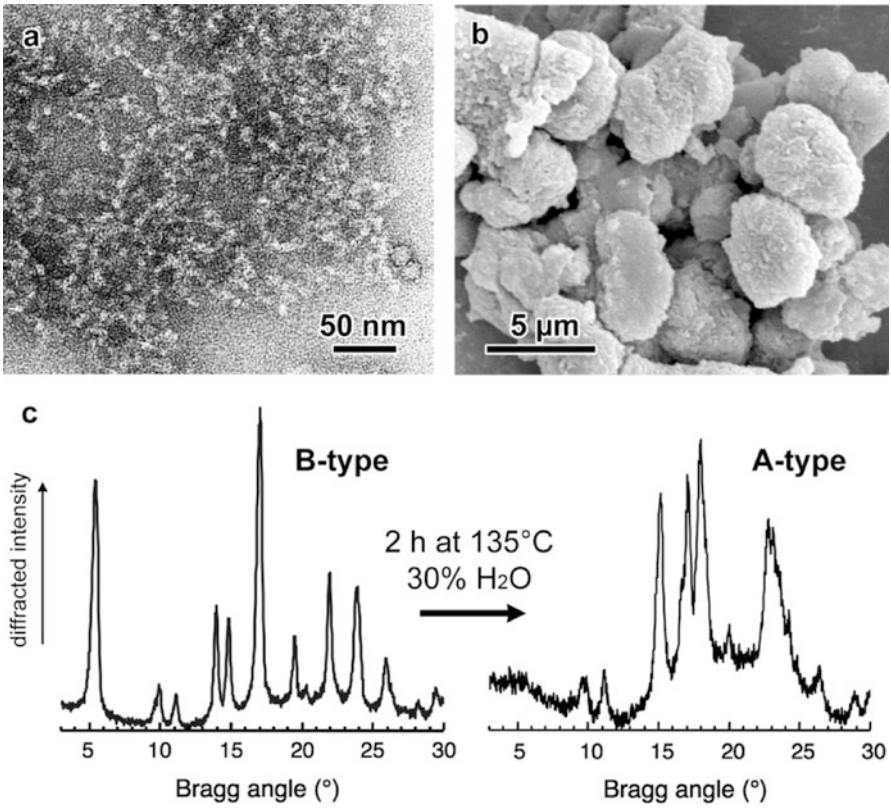

Fig. 3.11 In situ crystallization of amylose during enzymatic synthesis by amylosucrase from sucrose: (**a**) gel network (100 mM sucrose), (**b**) axialitic particles (600 mM sucrose) (From Potocki-Véronèse et al. 2005). (**c**) WAXS profiles showing the structural transition of the axialitic particles from B to A type after a heat-moisture treatment

In contrast, the crystallinity of the particles formed from the chains synthesized in vitro from 600 mM sucrose is exceptionally high (94 %) considering that they result from a self-aggregation process during enzymatic synthesis, without any optimization of the crystallization conditions (Potocki-Véronèse et al. 2005). The chain organization inside the particles is not known with precision. The analysis of the polarized optical micrographs suggests there is an axial symmetry, hence the term "axialites" used to describe the particles. Such a structure, if it is confirmed, has never been reported before for amylose, but may correspond to the axialitic organization of synthetic polymer chains (*Encyclopedia of Polymer Science* 1987). In addition, by simply heating these amylose axialites for 5 min at 90 °C, the crystallinity increases further by 30 %, without any change in their external shape. They should thus now be considered as a new standard for the determination of the relative crystallinity of starchy products (Potocki-Véronèse et al. 2005). This ability

of short chains to self-associate into a highly organized supramolecular structure is helpful for understanding the crystallization stage during starch biosynthesis. Besides amylose gelation, the behavior of these particles during hydrothermal treatments like annealing in water excess or B- to A-type transition during heat moisture treatment (Fig. 3.11c), both without any change in external morphology, is also very similar to what happens with hydrothermal treatments of starch. The exceptional crystallinity of these particles and the simplicity of the synthesis process were exploited to obtain ^{13}C-labeled amylose from 600 mM ^{13}C-sucrose and to characterize the conformation of B-type amylose by high-resolution solid-state NMR (Rondeau-Mouro et al. 2006). The assignment of the complete B-type amylose spectrum and correlations between ^{13}C-^{13}C distances and the atomic positions in the three-dimensional model obtained by low-resolution electron and X-ray diffraction of crystalline B-type fibers (Imberty and Pérez 1988) were established.

The synthesis and fractionation conditions of maltooligosaccharides and short amylose chains produced by NpAS were also optimized in order to prepare fractions with a very low dispersity ($1.003 < \overline{M}_w/\overline{M}_n < 1.01$). Several fractions, with a $\overline{DP}_w$ ranging from 10 to 40, were crystallized from dilute solutions in the presence of acetone vapors, resulting in needlelike A-type single crystals. The influence of the molecular parameters of the narrow fractions of amylose chains on the crystallization behavior and on the crystal morphology was investigated (Putaux et al. 2011b). Indeed, a $\overline{DP}_w$ of 15–19 and a low dispersity were necessary to form crystals with a 5–10 μm length, such as those shown in Fig. 3.4b (Montesanti et al. 2010). As previously mentioned in this article, the data collected by synchrotron X-ray microdiffraction from such large model single crystals (Fig. 3.5a) were successfully analyzed using classical crystallography methods, resulting in a revised structure of A amylose (Popov et al. 2009).

3.3.2 *Enzymatic Modification of Branched α(1,4)α(1,6)Glucans*

If many advances were done these last years regarding amylose chain self-association, one cannot exclude the key role played by α(1,6) branching points of amylopectin in the elaboration of the starch granule ultrastructure. A large panel of branched starchy macromolecules was synthesized in vitro either by using NpAS, GP, or amylomaltase, alone or in combination with branching and/or debranching enzymes to mimic the activities required for starch biosynthesis. NpAS was also used to modify the structure of native glycogen by elongating the external chains of the macromolecule in the presence of sucrose. In fact, glycogen is particularly efficiently glucosylated by amylosucrase, the extension rate being governed by the relative concentration of sucrose and glycogen (Putaux et al. 2006). Using different sucrose/glycogen mass ratios, original glycodendrimers

consisting of a glycogen core and a swollen amylose corona were formed within a few hours (Fig. 3.12a, c). Upon aging or drying, the amylose chains intertwined, resulting in the shrinking of the corona by the formation of crystallites and in a decrease of the particle diameter (Putaux et al. 2006). The resulting morphology depends on the initial sucrose/glycogen mass ratio. For a high ratio (around 340), the synthesized chains are long and reorganize in the form of a random organization of crystallites by a retrogradation process (Fig. 3.12b). For a low ratio (close to 1), small spikelike protrusions are seen on the surface (Fig. 3.12c). The number of glucosyl units added to glycogen external chains was estimated to be around 15. Consequently, the short chains intertwined in double helices can be expected to lie perpendicularly to the particle surface (Fig. 3.12d), like it is the case for the short branches of amylopectin in native starch granules. Such systems can thus be used to develop a biomimetic approach and reproduce in vitro the mechanisms involved in the biosynthesis of amylopectin and the structuring process of starch granules in plants. It shows that there is a close relationship between the length of the biosynthesized chains and the formation of a semicrystalline lamellar organization. Long chains may not result in the formation of lamellae, unless they are used by other biosynthetic enzymes. The

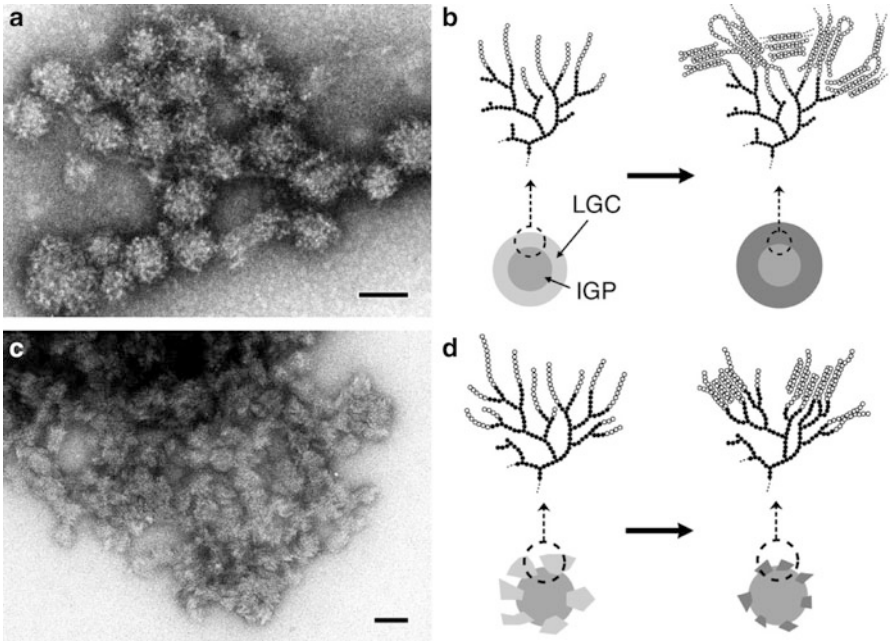

Fig. 3.12 Dendritic particles prepared by extension of glycogen external chains by amylosucrase in the presence of sucrose: (**a**, **c**) cryo-TEM images of the particles obtained with initial sucrose/glycogen weight ratios of 342 and 1, respectively; (**b**, **d**) schematic representation of the growth and subsequent crystallization of the corona of neosynthesized linear glucan chains (LGC) around the initial glycogen particle (IGP) (From Putaux et al. 2006)

influence of a debranching activity may also be studied by adding isoamylase to check the potential role of debranching enzymes during biosynthesis in amylopectin formation/crystallization.

Hyperbranched alpha-glucans have been recently produced by jointly using amylosucrase and a branching enzyme (Grimaud et al. 2013) or phosphorylase and a branching enzyme (Ciric and Loos 2013). This is another approach of amylopectin biosynthesis, but without the use of debranching enzyme, the branching rate remains higher than that of amylopectin and the average chain length too low to properly mimic the typical arborescent branching pattern observed in amylopectin (Rolland-Sabaté et al. 2014). Thus, strictly, to date, amylopectin has never been biosynthesized in vitro or at least mimicked, whatever the enzymatic cocktails used. Two methods have been reported, described as "SP-GP-BE" (based on the use of sucrose phosphorylase (SP), α-glucan phosphorylase (GP), and branching enzyme (BE)) with sucrose and maltotetraose as substrates (Ohdan et al. 2006; Kajiura et al. 2011) and "IAM-BE-AM," in which the branched linkages of starch were first hydrolyzed by an isoamylase (IAM) to produce short amylose chains that were assembled into spherical particles by a branching enzyme (BE) and an amylomaltase (AM) (Kajiura et al. 2008). Indeed, both methods resulted in the formation of glycogen-like molecules, rather than in a macromolecular architecture typical of amylopectin.

References

André I, Potocki-Véronèse G, Morel S, Monsan P, Remaud-Siméon M (2010) Sucrose-acting transglucosidases for biocatalysis. Top Curr Chem 294:25–48

Ball SG, Morell MK (2003) From bacterial glycogen to starch: understanding the biogenesis of the plant starch granule. Annu Rev Plant Biol 54:207–233

Bear RS (1944) Complex formation between starch and organic molecules. J Am Chem Soc 66:2122–2123

Bernazzani P, Chapados C, Delmas G (2000) Double-helical network in amylose as seen by slow calorimetry and FTIR. J Polym Sci B Polym Phys 38:1662–1677

Biais B, Le Bail P, Robert P, Pontoire B, Buléon A (2006) Structural and stoichiometric studies of complexes between aroma compounds and amylose. Polymorphic transitions and quantification in amorphous and crystalline areas. Carbohydr Polym 66:306–315

Biliaderis CG (1992) Structures and phase transitions of starch in food systems. Food Technol 46:98–109

Booy FP, Chanzy H, Sarko A (1979) Electron diffraction study of single crystals of amylose complexed with *n*-butanol. Biopolymers 18:2261–2266

Borch J, Sarko A, Marchessault RH (1972) Light scattering of starch granule. J Colloids Interface Sci 41:574–587

Brisson J, Chanzy H, Winter WT (1991) The crystal and molecular structure of V_H amylose by electron diffraction analysis. Int J Biol Macromol 13:31–39

Buléon A, Colonna P (2007) Physicochemical behaviour of starch in food applications. In: Belton P (ed) The chemical physics of food (Chapter 2). Blackwell Publishing Ltd, Oxford, pp 20–67

Buléon A, Duprat F, Booy FP, Chanzy H (1984) Single crystals of amylose with a low degree of polymerization. Carbohydr Polym 4:161–173

Buléon A, Bizot H, Delage MM, Pontoire B (1987) Comparison of X-ray diffraction patterns and sorption properties of the hydrolyzed starches of potato, wrinkled and smooth pea, broad bean and wheat. Carbohydr Polym 7:461–482

Buléon A, Delage MM, Brisson J, Chanzy H (1990) Single crystals of V amylose complexed with isopropanol and acetone. Int J Biol Macromol 12:25–33

Buléon A, Pontoire B, Riekel C, Chanzy H, Helbert W, Vuong R (1997) Crystalline ultrastructure of starch granules revealed by synchrotron radiation microdiffraction mapping. Macromolecules 30:3952–3954

Buléon A, Gérard C, Riekel C, Vuong R, Chanzy H (1998a) Details of the crystalline ultrastructure of C-starch granules revealed by synchrotron microfocus mapping. Macromolecules 31: 6605–6610

Buléon A, Colonna P, Planchot V, Ball S (1998b) Starch granules: structure and biosynthesis. Int J Biol Macromol 23:85–112

Buléon A, Véronèse G, Putaux J-L (2007) Self-association and crystallization of amylose. Aust J Chem 60:706–718

Cameron RE, Donald AM (1993) A small-angle X-ray-scattering study of the absorption of water into the starch granule. Carbohydr Res 244:225–236

Capron I, Robert P, Colonna P, Brogly M, Planchot V (2007) Starch in rubbery and glassy states by FTIR spectroscopy. Carbohydr Polym 68:249–259

Cardoso M, Westfahl H (2010) On the lamellar width distributions of starch. Carbohydr Polym 81:21–28

Cardoso MB, Putaux J-L, Nishiyama Y, Helbert W, Hÿtch M, Silveira NP, Chanzy H (2007) Single crystals of V-amylose complexed with α-naphthol. Biomacromolecules 8:1319–1326

Chanzy H, Vuong R, Jésior JC (1990) An electron diffraction study on whole granules of lintnerized potato starch. Starch/Staerke 42:377–379

Chanzy H, Putaux J-L, Dupeyre D, Davies R, Burghammer M, Montanari S, Riekel C (2006) Morphological and structural aspects of the giant starch granules from *Phajus grandifolius*. J Struct Biol 154:100–110

Ciric J, Loos K (2013) Synthesis of branched polysaccharides with tunable degree of branching. Carbohydr Polym 93:31–37

Cleven R, van den Berg C, van der Plas L (1978) Crystal structure of hydrated potato starch. Starch/Staerke 30:223–228

Colonna P, Buléon A (2010) Thermal transitions of starch. In: Bertolini A (ed) Starch: characterization, properties and applications (Chapter 4). CRC Press, Boca Raton, pp 71–102

Conde-Petit B, Escher F, Nuessli J (2006) Structural features of starch-flavor complexation in food model systems. Trends Food Sci Technol 17:227–235

Donald AM, Kato KL, Perry PA, Waigh TA (2001) Scattering studies of the internal structure of starch granules. Starch/Staerke 53:504–512

Encyclopedia of Polymer Science (1987) Mark HF, Bikales, NM, Overberger CG, Menges G, Kroschwitz JI (eds) vol 10. Wiley, New York, p 60

Fang JM, Fowler PA, Tomkinson J, Hill CAS (2002) The preparation and characterization of a series of chemically modified potato starches. Carbohydr Polym 47:245–252

French D (1984) Organization of starch granules. In Whistler RL, BeMiller JN, Parschall EF (eds) Starch, chemistry and technology. Academic, New York, pp 183–247

French AD, Zobel HF (1967) X-ray diffraction of oriented amylose fibers. I. Amylose dimethyl sulfoxide complex. Biopolymers 5:457–464

Gebhardt R, Hanfland M, Mezouar M, Riekel C (2007) High-pressure potato starch granule gelatinization: synchrotron radiation micro-SAXS/WAXS using a diamond anvil cell. Biomacromolecules 8:2092–2097

Gérard C, Planchot V, Colonna P, Bertoft E (2000) Relationship between branching density and crystalline structure of A- and B-type maize mutant starches. Carbohydr Res 326:130–144

Gernat C, Radosta S, Anger H, Damaschun G (1993) Crystalline parts of 3 different conformations detected in native and enzymatically degraded starches. Starch-Starke 45:309–314

Gidley MJ, Bociek SM (1985) Molecular organization in starches: a ^{13}C CP/MAS NMR study. J Am Chem Soc 107:7040–7044

Gidley MJ, Bociek SM (1988) ^{13}C CP/MAS NMR studies of amylose inclusion complexes, cyclodextrins, and the amorphous phase of starch granules: relationships between glycosidic linkage conformation and solid state ^{13}C chemical shifts. J Am Chem Soc 110:3820–3829

Gidley MJ, Bulpin PV (1987) Crystallisation of malto-oligosaccharides as models of the crystalline forms of starch: minimum chain-length requirement for the formation of double helices. Carbohydr Res 161:291–300

Godet MC, Tran V, Delage MM, Buléon A (1993) Molecular modelling of the specific interactions involved in the amylose complexation by fatty acids. Int J Biol Macromol 15:11–16

Grimaud F, Lancelon-Pin C, Rolland-Sabaté A, Roussel X, Laguerre S, Vikso-Nielsen A, Putaux J-L, Guilois S, Buléon A, D'Hulst C, Potocki-Véronèse G (2013) In vitro synthesis of hyperbranched α-glucans using a biomimetic enzymatic toolbox. Biomacromolecules 14:438–447

Heinemann C, Zinsli M, Renggli A, Escher F, Conde-Petit B (2005) Influence of amylose-flavor complexation on build-up and breakdown of starch structures in aqueous food model systems. LWT Food Sci Technol 38:885–894

Helbert W (1994) Doctoral dissertation, Joseph Fourier University of Grenoble, France

Helbert W, Chanzy H (1994) Single crystals of V amylose complexed with *n*-butanol or *n*-pentanol: structural features and properties. Int J Biol Macromol 16:207–213

Helbert W, Chanzy H (1996) The ultrastructure of starch from ultrathin sectioning in melamine resin. Starch/Staerke 48:185–188

Helbert W, Chanzy H, Planchot V, Buléon A, Colonna P (1993) Morphological and structural features of amylose spherocrystals of A-type. Int J Biol Macromol 15:183–187

Hermans PH, Weidinger A (1948) Quantitative X-ray investigations on the crystallinity of cellulose fibers. A background analysis. J Appl Phys 19:419–506

Hewitt JM, Linder M, Pérez S, Buléon A (1986) High-resolution CP-MAS ^{13}C NMR spectra of solid amylodextrins and amylose polymorphs. Carbohydr Res 154:1–13

Hizukuri S (1985) Relationship between the distribution of the chain length of amylopectin and the crystalline structure of starch granules. Carbohydr Res 141:285–306

Horii F, Yamamoto H, Hirai A, Kitamaru R (1987) Structural study of amylose polymorphs by cross-polarization-magic-angle spinning, ^{13}C-N.M.R. spectroscopy. Carbohydr Res 160:29–40

Hulleman SHD, Helbert W, Chanzy H (1996) Single crystals of V amylose complexed with glycerol. Int J Biol Macromol 18:115–122

Imberty A, Pérez S (1988) A revisit to the three-dimensional structure of B-type starch. Biopolymers 27:1205–1221

Imberty A, Chanzy H, Pérez S, Buléon A, Tran V (1988) The double-helical nature of the crystalline part of A-starch. J Mol Biol 201:365–378

Isogai A, Usuda M, Kato T, Uruy T, Atalla RH (1989) Solid state CP/MAS ^{13}C-NMR of cellulose polymorphs. Macromolecules 22:3168–3172

Jarvis MC (1994) Relationship of chemical shift to glycosidic conformation in the solid state ^{13}C NMR spectra of (1–4) linked glucose polymers and oligomers: anomeric and related effects. Carbohydr Res 259:311–318

Jenkins PJ, Cameron RE, Donald AM (1993) A universal feature in the structure of starch granules from different botanical sources. Starch/Staerke 45:417–420

Kadokawa J (2012) Preparation and applications of amylose supramolecules by means of phosphorylase-catalyzed enzymatic polymerization. Polymers 4:116–133

Kadokawa JI, Kaneko Y, Nagase SI, Takahashi T, Tagaya H (2002) Vine-twinning polymerization: amylose twines around polyether to form amylose-polyether inclusion complexes. Chem Eur J 8:3321–3326

Kajiura H, Kakutani R, Akiyama T, Takata H, Kuriki T (2008) A novel enzymatic process for glycogen production. Biocatal Biotransform 26:133–140

Kajiura H, Takata H, Akiyama T, Kakutani R, Furuyashiki T, Kojima I, Harui T, Kuriki T (2011) In vitro synthesis of glycogen: the structure, properties, and physiological function of enzymatically-synthesized glycogen. Biologia 66:387–394

Kaneko Y, Saito Y, Nakaya A, Kadokawa JI, Tagaya H (2008) Preparation of inclusion complexes composed of amylose and strongly hydrophobic polyesters in parallel enzymatic polymerization system. Macromolecules 41:5665–5670

Lemke H, Burghammer M, Flot D, Rössle M, Riekel C (2004) Structural processes during starch granule hydration by synchrotron radiation microdiffraction. Biomacromolecules 5:1316–1324

Lopez-Rubio A, Flanagan BM, Gilbert EP, Gidley MJ (2008) A novel approach for calculating starch crystallinity and its correlation with double helix content: a combined XRD and NMR study. Biopolymers 9:761–768

Miller RL, Boyer RF, Heijboer J (1984) X-ray scattering from amorphous acrylate and methacrylate polymers: evidence of local order. J Polym Sci Part B Polym Phys 22:2021–2041

Montesanti N, Véronèse G, Buléon A, Escalier PC, Kitamura S, Putaux J-L (2010) A-type crystals from dilute solutions of short amylose chains. Biomacromolecules 11:3049–3058

Morgan KR, Furneaux RH, Larsen NG (1995) Solid state NMR studies on the structure of starch granules. Carbohydr Res 276:387–399

Morrison WR, Tester RF, Snape CE, Law R, Gidley MJ (1993a) Swelling and gelatinisation of cereal starches. IV. Some effects of lipid-complexed amylose and free amylose in waxy and normal barley starches. Cereal Chem 70:385–391

Morrison W, Law R, Snape C (1993b) Evidence for inclusion complexes of lipids with V-amylose in maize, rice and oat starches. J Cereal Sci 18:107–109

Nara S, Mori A, Komiya T (1978) Study on relative crystallinity of moist potato starch. Starch/Staerke 30:111–114

Nishiyama Y, Mazeau K, Morin M, Cardoso MB, Chanzy H, Putaux J-L (2010) Molecular and crystal structure of 7-fold V amylose complexed with 2-propanol. Macromolecules 43:8628–8636

Nuessli J, Putaux J-L, Le Bail P, Buléon A (2003) Crystal structure of amylose complexes with small ligands. Int J Biol Macromol 33:227–234

Oguchi T, Yamasato H, Limmatvapirat S, Yonemochi E, Yamamoto K (1998) Structural change and complexation of strictly linear amylose induced by sealed-heating with salicylic acid. J Chem Soc Faraday Trans 94:923–927

Ohdan K, Fujii K, Yanase M, Takaha T, Kuriki T (2006) Enzymatic synthesis of amylose. Biocatal Biotransform 24:77–81

Paris M, Bizot H, Emery J, Buzaré JY, Buléon A (1999) Crystallinity and structuring role of water in native and recrystallized starches by ^{13}C CP-MAS NMR spectroscopy 1: spectral decomposition. Carbohydr Polym 39:327–339

Paris M, Bizot H, Emery J, Buzaré JY, Buléon A (2001) NMR local range investigations in amorphous starchy substrates I: structural heterogeneity probed by ^{13}C CP-MAS NM. Int J Biol Macromol 29:127–136

Pérez S, Bertoft E (2010) The molecular structures of starch components and their contribution to the architecture of starch granules: a comprehensive review. Starch/Staerke 62:389–420

Pfannemüller B (1987) Influence of chain length of short monodisperse amyloses on the formation of A- and B-type X-ray diffraction patterns. Int J Biol Macromol 9:105–108

Popov D, Burghammer M, Buléon A, Montesanti N, Putaux J-L, Riekel C (2006) A-Amylose single crystals: unit cell refinement from synchrotron radiation microdiffraction data. Macromolecules 39:3704–3706

Popov D, Buléon A, Burghammer M, Chanzy H, Montesanti N, Putaux J-L, Potocki-Véronèse G, Riekel C (2009) Crystal structure of A-amylose: a revisit from synchrotron microdiffraction analysis of single crystals. Macromolecules 42:1167–1174

Potocki-Véronèse G, Putaux J-L, Dupeyre D, Albenne C, Remaud-Simeon M, Monsan P, Buléon A (2005) Amylose synthesized in vitro by amylosucrase: morphology, structure, and properties. Biomacromolecules 6:1000–1011

Putaux J-L, Molina-Boisseau S, Momaur T, Dufresne A (2003) Platelet nanocrystals resulting from the disruption of waxy maize starch granules by acid hydrolysis. Biomacromolecules 4:1198–1202

Putaux J-L, Potocki-Véronèse G, Remaud-Simeon M, Buléon A (2006) α-D-glucan-based dendritic nanoparticles prepared by in vitro enzymatic chain extension of glycogen. Biomacromolecules 7:1720–1728

Putaux J-L, Montesanti N, Dupeyre D, Véronèse G, Buléon A (2011a) Morphology and structure of A-amylose single crystals. Polymer 52:2198–2205

Putaux J-L, Nishiyama Y, Mazeau K, Morin M, Cardoso MB, Chanzy H (2011b) Helical conformation in crystalline inclusion complexes of V-amylose: a historical perspective. Macromol Symp 303:1–9

Putseys JA, Lamberts L, Delcour JA (2010) Amylose inclusion complexes: formation, identity and physico-chemical properties. J Cereal Sci 51:238–247

Riekel C (2000) New avenues in X-ray microbeam experiments. Rep Prog Phys 63:233–235

Riekel C, Burghammer M, Davies RJ, DiCola E, Koenig C, Lemke HT, Putaux J-L, Schoeder S (2010) Raster microdiffraction with synchrotron radiation of hydrated biopolymers with nanometre step-resolution: case study of starch granules. J Synchrotron Radiat 17:743–750

Roblin P, Potocki-Véronèse G, Guieysse D, Guérin F, Axelos M, Perez J, Buléon A (2013) SAXS conformational tracking of amylose synthesized by amylosucrases. Biomacromolecules 14:232–239

Rolland-Sabaté A, Guilois S, Grimaud F, Lancelon-Pin C, Roussel X, Laguerre S, Viksø-Nielsen A, Putaux J-L, D'Hulst C, Potocki-Véronèse G, Buléon A (2014) Characterization of hyperbranched glycopolymers produced in vitro using enzymes. Anal Bioanal Chem 406:1607–1618

Rondeau-Mouro C, Le Bail P, Buléon A (2004) Structural Investigation of amylose complexes with small ligands: inter- or intra-helices associations. Int J Biol Macromol 34:309–315

Rondeau-Mouro C, Véronèse G, Buléon A (2006) High-resolution solid-state NMR of B-type amylose. Biomacromolecules 7:2455–2460

Rundle RE, Edwards FC (1943) The configuration of starch in the starch-iodine complex. IV. An X-ray diffraction investigation of butanol-precipitated amylose. J Am Chem Soc 65:2200–2203

Sevenou O, Hill S, Farhat IA, Mitchell JR (2002) Organization of the external region of the starch granule as determined by infrared microscopy. Int J Biol Macromol 31:79–85

Smits ALM, Ruhnau FC, Vliegenthart JFG, Van Soest JJG (1998) Ageing of starch based systems as observed with FT-IR and solid state NMR spectroscopy. Starch-Starke 50:478–483

Sterling C (1960) Crystallinity of potato starch. Starch/Staerke 12:182–185

Takahashi Y, Kumano T, Nishikawa S (2004) Crystal structure of B-amylose. Macromolecules 37:6827–6832

Takeo K, Kuge T (1969) Complex of starchy materials with organic compounds. Part III X-ray studies on amylose and cyclodextrin complexes. Agric Biol Chem 33:1174–1180

Tan I, Flanagan BF, Halley PJ, Whittaker A, Gidley MJ (2007) A method for estimating the nature and relative proportions of amorphous, single, and double-helical components in starch granules by ^{13}C CP/MAS NMR. Biomacromolecules 8:885–891

Tang HJ, Mitsunaga TH, Kawamura Y (2006) Molecular arrangement in blocklets and starch granule architecture. Carbohydr Polym 63:555–560

Tanner SF, Ring SG, Whittam MA, Belton PS (1987) High resolution solid state ^{13}C NMR study of some α(1–4) linked glucans: the influence of water on structure and spectra. Int J Biol Macromol 9:219–224

Thérien-Aubin H, Janvier F, Baille WE, Zhu XX, Marchessault RH (2007) Study of hydration of cross-linked high amylose starch by solid state ^{13}C NMR spectroscopy. Carbohydr Res 342:1525–1529

Tomasik P, Schilling CH (1998a) Complexes of starch with inorganic guests. Adv Carbohydr Chem Biochem 53:263–343

Tomasik P, Schilling CH (1998b) Complexes of starch with organic guests. Adv Carbohydr Chem Biochem 53:345–426

van Soest JJG, Tournois H, de Wit D, Vliegenthart JFG (1995) Short-range structure in (partially) crystalline potato starch determined with attenuated total reflectance Fourier-transform IR spectroscopy. Carbohydr Res 279:201–214

Véchambre C, Buléon A, Chaunier L, Jamme F, Lourdin D (2010) Macromolecular orientation in glassy starch materials that exhibit shape memory behavior. Macromolecules 43:9854–9858
Véchambre C, Buléon A, Chaunier L, Gauthier C, Lourdin D (2011) Understanding the mechanisms involved in shape memory starch: orientation, stress recovery and molecular mobility. Macromolecules 44:9384–9389
Veregin RP, Fyfe CA, Marchessault RH, Taylor MG (1986) Characterization of the crystalline A and B starch polymorphs and investigation of starch crystallization by high-resolution ^{13}C CP/MAS NMR. Macromolecules 19:1030–1034
Veregin RP, Fyfe CA, Marchessault RH, Taylor MG (1987) Correlation of ^{13}C chemical shifts with torsional angles from high-resolution, ^{13}C-C.P.-M.A.S. N.M.R. studies of crystalline cyclomalto-oligosaccharide complexes, and their relation to the structures of the starch polymorphs. Carbohydr Res 160:41–56
Vermeylen R, Goderis B, Reynaers H, Delcour JA (2004) Amylopectin molecular structure reflected in macromolecular organization of granular starch. Biomacromolecules 5:1775–1786
Waigh TA, Hopkinson I, Donald AM, Butler MF, Heidelbach F, Riekel C (1997) Analysis of the native structure of starch granules with X-ray microfocus diffraction. Macromolecules 30:3813–3820
Wakelin JH, Virgin HS, Crystal E (1959) Development and comparison of two X-ray methods for determining the crystallinity of cotton cellulose. J Appl Phys 30:1654–1662
Whittam MA, Noe TR, Ring SG (1990) Melting behaviour of A- and B-type starches. Int J Biol Macromol 12:359–362
Wikman J, Blennow A, Buléon A, Putaux J-L, Pérez S, Seetharaman K, Bertoft E (2014) Influence of amylopectin structure and degree of phosphorylation on the molecular composition of potato starch lintners. Biopolymers 101:257–271
Willenbucher RW, Tomka I, Muller R (1992) Thermally induced structural transitions in the starch/water system. Proceedings of the symposium on Division of Carbohydrate Chemistry and American Chemistry Society. In Bartens A (ed) Carbohydrates in industrial synthesis. Springer, Berlin, pp 93–111
Wilson RH, Kalichevsky MT, Ring SG, Belton PS (1987) A Fourier-transform infrared study of the gelation and retrogradation of waxy-maize starch. Carbohydr Res 166:162–165
Wu HC, Sarko A (1978a) The double-helical molecular structure of crystalline A-amylose. Carbohydr Res 61:27–40
Wu HC, Sarko A (1978b) The double-helical molecular structure of crystalline B-amylose. Carbohydr Res 61:7–25
Yamashita Y, Hirai N (1966) Single crystals of amylose V complexes. II. Crystals with 7_1 helical configuration. J Polym Sci Part A-2 4:161–171
Yamashita Y, Monobe K (1971) Single crystals of amylose V complexes. III. Crystals with 8_1 helical configuration. J Polym Sci Part A-2 9:1471–1481
Yamashita Y, Ryugo J, Monobe K (1973) An electron microscopic study on crystals of amylose V complexes. J Electron Microsc 22:19–26
Zaslow B (1963) Characterization of a second helical amylose modification. Biopolymers 1:165–169
Zobel HF (1988) Molecules to granules: a comprehensive starch review. Starch/Staerke 40:44–55
Zobel HF, French AD, Hinkle ME (1967) X-ray diffraction of oriented amylose fibers. II. Structure of V amyloses. Biopolymers 5:837–845

Part II
Evolution

Chapter 4
The Transition from Glycogen to Starch Metabolism in Cyanobacteria and Eukaryotes

Steven Ball, Christophe Colleoni, and Maria Cecilia Arias

Abstract α-1,4-linked glucan chains branched through α-1,6 glucosidic lineages define the most frequently found storage polysaccharides in living cells. These glucans come in two very distinct forms known as glycogen and starch. The small water-soluble glycogen particles distribute widely in Archaea, Bacteria, and heterotrophic eukaryotes, while semicrystalline solid starch seems to be restricted to photosynthetic eukaryotes. This review focusses on the so-called glycosyl-nucleotide-dependent pathway of starch and glycogen synthesis. Through comparative biochemistry of storage polysaccharide metabolism in distinct clades, we will review the evidence sustaining that starch has evolved from preexisting glycogen metabolism several times during the evolution of photosynthetic eukaryotes and cyanobacteria. This review will also describe the possible function of storage polysaccharide metabolism in establishing metabolic symbiosis during plastid endosymbiosis. We will detail the evidence sustaining that storage polysaccharide metabolism was used by three distinct organisms to establish a tripartite symbiosis that facilitated metabolic integration of free-living cyanobacteria into evolving organelles.

Keywords Starch • Amylopectin • Glucan • Amylose • Glycogen • Photosynthesis • Endosymbiosis • Chlamydia

4.1 The Comparative Biochemistry of Starch and Glycogen Metabolism in Bacteria

4.1.1 The Bacterial Eukaryote and Archeal Domains

Three distinct domains are currently recognized among living cells. A consensus is slowly being reached that defines both the Archaea and the Bacteria domains as the most ancient organizations of life on Earth. Eukaryotes are presently

S. Ball (✉) • C. Colleoni • M.C. Arias
Unité de Glycobiologie Structurale et Fonctionnelle, UMR 8576 CNRS – Université Lille 1, 59655 Villeneuve d'Ascq Cedex, France
e-mail: steven.ball@univ-lille1.fr

Y. Nakamura (ed.), *Starch*, DOI 10.1007/978-4-431-55495-0_4

thought to branch from within the Archaea as a sister to a group to the so-called TACK superphylum consisting of the Thaumarchaeota, the Aigarchaeota, the Crenarchaeota, and the Korarchaeota (Williams et al. 2012). The appearance of the first living cells and biochemical pathways will not be considered in this review. We will focus on the function, evolution, and distribution of the glycosyl-nucleotide-based pathway of glycogen synthesis which is the most widely distributed pathway in this respect but are well aware that a number of alternatives have been described, notably in bacteria, where synthesis of glycogen from maltose, trehalose,, or sucrose can operate without glycosyl-nucleotide synthesis (Chandra et al. 2011). Eukaryogenesis, the process by which the first eukaryotes have emerged from within the Archaea, is a highly controversial issue and multiple conflicting hypotheses have been proposed (Martijn and Ettema 2013). With such unknowns to relate the eukaryotic pathways of glycogen metabolism to their bacterial and archaeal relatives; deduce the implementation of this pathway during eukaryogenesis, is a speculative and perilous exercise, that we shall not attempt. On the other hand, such an approach applied to plastid endosymbiosis is today entirely feasible, as there is a large consensus on the nature of the cells involved (at minima a standard biflagellated heterotrophic phagotroph and a free-living cyanobacterium). In this review, we will compare the nature and function of the classical glycosyl-nucleotide-based pathway of storage polysaccharide metabolism in several lineages and deduce, whenever possible, the evolutionary history of this biochemical network. Figure 4.1 represents the current status of eukaryote phylogeny, with a proposed root of the tree between the Excavata and the Amoebozoa. As seen from this bird's-eye view of eukaryote diversity, glycogen is uniformly present on the so-called unikont branch (see legend of Fig. 4.1 for a definition) of the eukaryotic tree, while either α-(glycogen or starch) or β-glucan (paramylon or soluble glucans) storage polysaccharides are evidenced in the bikont branch. While Archaeplastida are uniformly α-glucan accumulators, a mix of either α- or β-glucan accumulators are evidenced in the Excavata and the polyphyletic Hacrobia group, as well as the SAR superphylum. Starch has been clearly documented in all three Archaeplastida lineages. It is also found in many alveolates and in all cryptophytes. Cryptophytes define a subgroup of the so-called Hacrobia uniting them to the haptophytes, a group presently believed to be polyphyletic (hence, they do not define a real clade anymore). Alveolates are members of the SAR (which stands for Stramenopiles, alveolates, and Rhizaria) which contain two other major groups: the Stramenopiles and Rhizaria. Both of these are β-glucan accumulators and accumulate neither glycogen nor starch (with the noticeable exception of the Blastocystis glycogen-accumulating unicellular stramenopile gut parasite (Yoshikawa et al. 2003)). It must be stressed that β-1,3-linked storage β-glucans are widely distributed in the bikont branch of the eukaryotes (Fig. 4.1, see legend for definition of bikont) and that very few reports address the biochemistry of their synthesis or mobilization (Bäumer et al. 2001; Goldemberg and Marechal 1963; Tomos and Northcote 1978; Vogel and Barber 1968). Most soluble β-glucan forms, such as laminarin, chrysolaminarin, and mycolaminarin, contain, in addition, β-1,6 branches, while the very highly crystalline paramylon found in *Euglena* (an excavate unicellular green alga) and

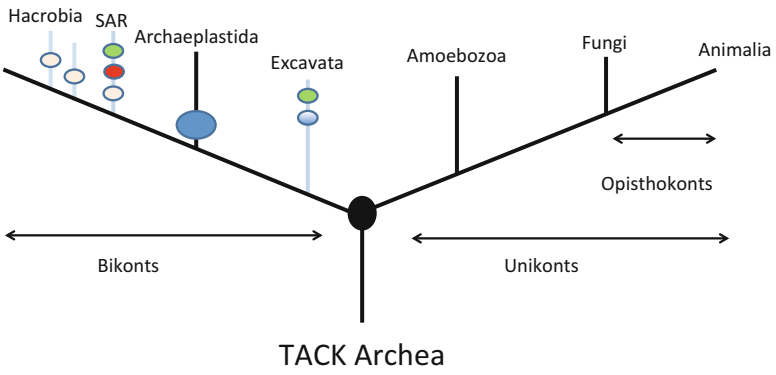

Fig. 4.1 Schematic representation of the eukaryotic domain. A simplified view of the phylogeny of eukaryotes is presented. Traditionally the eukaryotes are divided into the unikonts and bikonts which were previously thought to contain only uniflagellated cells or biflagellated cells. Although this has been brought into question, this division in two branches is kept for the sake of convenience and clarity. The tree is displayed as rooted within the Archaea (the TACK subdivision, see text). The most frequently proposed root is displayed by a *large-size black dot*, but other roots remain possible. Plastid endosymbiosis are displayed within the bikonts by oval-colored shapes. The *large-size blue-colored oval* represents the unique primary plastid endosymbiosis. The *small-size blue-colored oval* represents the Paulinella chromatophore primary endosymbiosis. All other small-size ovals display secondary endosymbioses. *Pink* represents secondary endosymbiosis of a red alga followed by fusion of the outer plastid membrane with the ER. *Red* represents secondary endosymbiosis of a red alga not followed by a fusion with the ER. *Green* represents secondary endosymbiosis of a green alga not followed by a fusion with the ER

possibly also in chlorarachniophytes (rhizarian unicellular green algae) display very high levels of crystallinity (Kiss et al. 1988). Interestingly, chlorarachniophytes are derived as *Euglena* from a β-glucan-accumulating heterotrophic phagotroph that internalized a green alga through secondary endosymbiosis. Strikingly, storage β-glucans in eukaryotes can thus be found, as is the case for α-glucans, in either water-soluble or solid crystalline form. The very few studies performed on paramylon metabolism suggest that such storage polysaccharides are synthesized from UDP-Glc by a glycosyltransferase (Bäumer et al. 2001). However, there is not one single report of a mutant, or antisense RNA or RNAi with decreased biochemical activity, associated with an alteration in β-glucan metabolism to confirm this reasonable hypothesis. To date, the sequenced genomes of all storage β-glucan-accumulating organisms have been proven to lack glycogen or starch metabolism.

As seen in Fig. 4.1, the bikont branch of the eukaryotes has experienced a number of distinct endosymbiotic events leading to acquisition of photosynthesis, eventually followed by photosynthesis loss in several clades. Bikonts have experienced one single primary endosymbiosis event and numerous secondary endosymbioses. Primary endosymbiosis of the plastid can be defined as the capture of a free-living cyanobacterium by a heterotrophic eukaryote phagotroph. There is one single major primary endosymbiosis that enabled eukaryotes to gain the ability to perform oxygenic photosynthesis. This event dated between 0.9 and 1.5 billion

years defines the founding event of the Archaeplastida clades (glaucophytes and red and green algae) (Shih and Matzke 2013; Yoon et al. 2004). All plastids in eukaryotic algae and plants are derived directly or indirectly from this event. Another much more recent primary endosymbiosis of marginal ecological impact is nevertheless known. This event involves a rhizarian cercozoan phagotroph and an α-cyanobacterium. However, to date, *Paulinella chromatophora* seems to define the sole offspring of this fairly recent, 60-million-year-old event, and no other eukaryotic alga seems to be derived from it (Bhattacharya et al. 2007; Marin et al. 2005). The Archaeplastida primary plastids have, in turn, been captured by other heterotrophic eukaryotic phagotrophs. Several events consisting of the capture of a red or a green alga have indeed been documented. These events will ultimately lead to four membrane plastids where the outermost membrane defines the phagocytosis vacuole while the second outermost membrane defines the plasma membrane of the internalized eukaryotic alga. The two innermost membranes represent the two membranes of the primary red or green plastids. Some secondary endosymbiosis-derived algae such as cryptophytes or the rhizarian chorarachniophytes still harbor nucleomorphs, which are the remnants of the red or green alga nucleus, between the 2nd and 3rd membrane, in a compartment known as the periplastidial space, that corresponds to the internalized red or green alga's former cytosol. This very complex endosymbiotic history of bikonts is further complicated by numerous instances of primary or secondary loss of photosynthesis that may be accompanied by loss of photosynthesis genes, reduction or loss of plastid DNA, and eventually plastid loss.

When approaching the evolution of storage polysaccharides metabolism in eukaryotes, it is of paramount importance to consider this endosymbiotic history for several reasons. First, this story may impact the structure of the network through acquisition of genes of endosymbiotic origin. Second, acquisition of photosynthesis may have depended chiefly on establishment of an optimal biochemical connection, at the very onset of the event. This optimal connection had to be established between two unrelated and disconnected networks. In other words, a free-living photoautotroph, internalized by phagocytosis, will not spontaneously reduce or increase supply of carbon to suit the host's demands and needs. One obvious way to overcome this would be to feed photosynthetic carbon into a host cytosolic molecular buffer that overcomes the disconnection between source and sink of carbon. Such a buffer is provided by storage compounds in the host cytosol, whose catabolism responds to the highly regulated host demands. Hence, storage lipids and polysaccharides are very high on the list of compounds that could play such a role and particular attention must be paid to evolution of their metabolism in this respect.

In this review we will show an ever-increasing amount of evidence sustaining that α-glucans have played such a molecular buffer function during primary endosymbiosis of the plastid. As far as secondary endosymbioses go, we presently have no evidence for or against such a function in establishment of the eukaryotic symbionts. A possible role of storage lipids in the early phase of the distinct symbioses remains in this respect a possibility worthy of further exploration. It must be stressed that the secondary plastids harbor distinct membrane arrangements. In most cases involving

a red alga symbiont, the first membrane which corresponds to the phagocytic vacuole membrane has fused with the ER. This in effect would place the 2nd plastid membrane called the periplastidial membrane adjacent and in contact with the ER lumen of the host. In many eukaryotes, the ER lumen contains the full suite of enzymes required for TAG biosynthesis (Beller et al. 2010). Hence, installment of a symbiotic flux, relying on export of symbiont lipids to the periplastidial membrane, would lead to TAGs budding off from the ER into the host cytosol. Such lipid bodies would offer a very convenient buffer to initiate secondary endosymbiosis and storage polysaccharides would not be per se required to trigger symbiosis. In the unique secondary endosymbiosis of a red alga that possibly generated the alveolates and in both cases of green alga secondary endosymbiosis (Euglena and chlorarachniophytes), the phagocytosis vacuole membrane did not fuse with the ER. Remarkably in all three instances, the storage polysaccharide (starch or paramylon) appears to have switched from a soluble to a solid crystalline form (although this is not entirely clear with respect to chlorarachniophytes), thereby suggesting that a sizable increase of the storage polysaccharide pool was selected in all three cases. We believe that this may suggest an essential function of storage polysaccharide metabolism in the metabolic integration of these secondary plastids. A lot more work and convincing evidence is nevertheless required before such a proposal is seriously considered.

4.1.2 Glycogen Synthesis in Bacteria

The paradigm of bacterial glycogen metabolism is defined by the ADP-Glc specific pathway, which has been abundantly studied in *E. coli* for several decades (Preiss 1984). This pathway relies on the production of ADP-Glc by ADP-Glc pyrophosphorylase, the product of the *GlgC* locus in *E. coli* which uses glucose-1-P and ATP as substrates to generate ADP-Glc and pyrophosphate. The single documented fate of this glycosyl nucleotide is to feed glycogen or starch synthesis in bacteria and Chloroplastida (green algae and plants). An additional function of ADP-Glc has been documented in cyanobacteria, where it was shown to be required for the synthesis of glucosylglycerol, an osmoprotective compound (see below). ADP-Glc is next used by a GT5 (CAZy classification glycosyltransferase family 5) glycogen synthase (GS) to generate an additional glucose bound at the nonreducing end of a growing α-1,4-glucan chain with concomitant release of ADP. Interestingly, Ugalde et al. have demonstrated that the GlgA GS of *Agrobacterium tumefaciens* is able to prime glycogen synthesis through autoglucosylation (Ugalde et al. 2003). This is important because, as we shall see below, the GT3 glycogen synthases from fungi and animals are unable to prime polysaccharide elongation and rely on the presence of glycogenin and autoglucosylating protein for this function. We presently do not know if the properties described for the *Agrobacterium* glycogen synthase apply to all other enzymes of this type in bacteria. Anyhow, no other mode of glycogen synthesis priming has been convincingly described in the bacterial

domain. The elongated glucans are then branched through branching enzyme (BE), which belongs to the GH13 group of glycosyl hydrolases (although other CAZy families have been documented in some bacteria including cyanobacteria) which is referred as the product of the *E. coli* glgB gene. BEs typically hydrolyse an α-1,4 chain and transfer a segment of chain in α-1,6 position. Catabolism is through the action of glycogen phosphorylase, the product of the glgP gene, which catalyzes orthophosphate-mediated phosphorolysis, yielding glucose-1-P from the nonreducing end of the glycogen particle. Glycogen phosphorylase typically stops digestion 4 glucose residues from any given α-1,6 branch or from any reducing end. Glycogen with short external chains of 4 glucose residues is called glycogen phosphorylase limit dextrin. These short external stubs are then released from the particle, through the action of the GlgX gene product, which directly hydrolyses the α-1,6 branch. For this reason this enzyme was named direct debranching enzyme. It is worth stressing that at least in *E. coli*, the GlgX enzyme is quite exacting and will not hydrolyze at significant rates glucans longer than 4 glucose residues (Dauvillée et al. 2005). This prevents the futile cycling of branches in the presence of BE, which transfers chains longer than 6 glucose residues. The maltotetraose released is then processed through enzymes of maltooligosaccharide metabolism, which typically include a combination of α-1,4-glucanotransferase and a specific form of phosphorylase called maltodextrin phosphorylase. The α-1,4-glucanotransferase, product of the *MALQ* (amylomaltase) gene, will hydrolyse out the reducing-end glucose from maltose and longer maltooligosaccharides and transfer the remaining oligosaccharide to other maltooligosaccharides, maltose itself being a very poor donor in this reaction (Palmer et al. 1976). The MalP gene product (maltodextrin phosphorylase) will recess back to maltotetraose all long glucans produced by amylomaltase. Some bacteria, like *E. coli*, contain two genes encoding distinct forms of phosphorylases acting selectively either on glycogen (glycogen phosphorylase) or on MOS (maltodextrin phosphorylase). Other bacteria contain a single bifunctional glucan phosphorylase. Other maltooligosaccharide-processing enzymes, such as α-glucosidase (product of the malZ gene product), act like MalP to avoid synthesis of longer MOS that would ultimately feed glycogen synthesis. In fact, in the absence of a functional MalP gene product, *E. coli* will very effectively synthesize glycogen even in the absence of functional glycogen synthase (Park et al. 2011). This suggests that an ADP-Glc-independent pathway of glycogen synthesis may be effective and functional in bacteria species feeding from MOS-rich media.

It must also be stressed that 21 % of bacterial clades investigated by Chandra et al. (2011) are able to use maltose-1-P as substrate for glycogen synthesis, through the use of α-1,4-glucan:maltose-1-phosphate maltosyltransferase, the product of the *GLGE* gene (note that GlgE is not present in *E. coli*). Over half of these clades are able to convert trehalose into maltose-1-P through the use of the product of *TRES* which converts trehalose into maltose and of Pep2 (maltokinase) which will phosphorylate maltose in the presence of ATP. This alternate pathway of glycogen synthesis is absent from *E. coli* and still relies on GlgB and the other genes described above of the classical pathway.

Finally while ADP-Glc remains, by far, the predominant glycosyl nucleotide used for glycogen synthesis in bacteria, there is one documented case of synthesis mediated through UDP-Glc in *Prevotella* (Lou et al. 1997). In this case, it must be stressed that LGTs of genes of glycogen metabolism from eukaryotic clades have been documented in related taxa (Arias et al. 2012).

The regulation of glycogen metabolism in bacteria is complex and exceedingly diverse. We will refer the reader to recent efforts addressing this topic and will make no attempts to review this (Wilson et al. 2010).

From our present knowledge of bacterial glycogen metabolism, we can confidently state that ADP-Glc pyrophosphorylase and ADP-Glc-specific GT5 GS are specific to bacterial glycogen synthesis, while debranching through a direct debranching enzyme and the ensuing coupling of the released chains to MOS metabolism is equally specific to bacteria (and in this case also to same degree to Archaea). The restricted eukaryotic distribution of such enzymes to Archaeplastida and some of their secondary endosymbiosis relatives, in face of the universal presence of the eukaryotic pathway (see below), leaves little doubt that these photosynthetic eukaryotic clades have gained the corresponding genes through lateral gene transfers from bacteria.

The classical bacterial glycogen metabolism network, as seen in *E. coli* and many other proteobacteria, is most often exceedingly simple and consists of 6–7 genes (*GLGC*, *GLGA*, *GLGB*, *GLGP*, *GLGX*, *MALQ*), depending on the specificity of the glucan phosphorylase with respect to MOS, organized in one or two operons, often in company of the *PGM* gene (phosphoglucomutase responsible for conversion of glucose-6-P to glucose-1-P) or eventually of *GLGE* (see above). In addition to this core pathway, some bacteria, including cyanobacteria, may contain additional isoforms for several steps of the network as well as additional enzymes from different CAZy families catalyzing analogous steps. This is especially true among the large-size cyanobacterial genomes which are of particular interest in this review.

4.1.3 Starch and Glycogen Biosynthesis in Cyanobacteria

In cyanobacteria and plants, oxygenic photosynthesis produces oxygen, NAD(P)H, and protons, which subsequently drive the conversion of ADP to ATP. Both NADP(H) and ATP will fuel the Calvin cycle to reduce carbon dioxide (CO_2). This primary carbon fixing reaction or carboxylase reaction is catalyzed by the ribulose-1,5 bisphosphate carboxylase/oxygenase (RuBisCO), which transfers CO_2 onto ribulose-1,5 bisphosphate producing two molecules of 3-phosphoglycerate (3-PGA). It should be stressed that this reaction is not favored in an aquatic environment since most of the CO_2 is found as bicarbonate (HCO_3^-) and carbonate (CO_3^{2-}) forms (Falkowski and Raven 2007). To circumvent this problem, cyanobacteria have evolved an extremely efficient CO_2-concentrating mechanism (i.e., active carbon transporters, carbonic anhydrases, carboxysome), which promotes the carboxylase reaction by enhancing CO_2 concentration in the vicinity of RuBisCO (for a review of this topic, see Badger and Price 2003).

Assimilated carbon is mainly stored as glycogen particles or starch granules in cyanobacteria and plants, respectively. Both homopolymers of α-D-glucose share the same α-1,4 and α-1,6 chemical linkages. Glycogen is predominately observed in most of cyanobacteria as tiny hydrosoluble particles between thylakoids membranes. Starch appears as nonaqueous semicrystalline granules in plants and several eukaryotic algae and is usually made of two α-polysaccharides: amylopectin and amylose. Until recently, starch granules were only described in Archaeplastida (plants, red alga, and glaucophytes) and other phylogenetically related organisms (Ball et al. 2011). However, Sherman's group performed the first description and partial characterization of abnormal carbohydrate granules in *Cyanothece* ATCC51142 (Schneegurt et al. 1994) but did not recognize this material as starch like. Later, a survey of storage polysaccharides in different species of cyanobacteria reported the presence of solid granules in other cyanobacterial species (Nakamura et al. 2005). Detailed characterization now indicates that such carbohydrate granules, including those of *Cyanothece* ATCC51142, are composed of a high molecular weight polysaccharide similar to amylopectin (Suzuki et al. 2013). More recently, *Cyanobacterium* sp. CLg1, a new strain isolated in the tropical North Atlantic Ocean phylogenetically related to *Crocosphaera watsonii*, accumulates starch granules made of both amylopectin and amylose (Deschamps et al. 2008a; Falcon et al. 2002). Interestingly, as in plants, the presence of amylose can be correlated to the identification of a polypeptide showing a high similarity in amino acid sequence to GBSS (granule-bound starch synthase) of plants. The latter is required for the synthesis of amylose in starch granules of various photosynthetic organisms (Delrue et al. 1992; Nelson and Rines 1962). So far, the GBSS gene is identified only in two cyanobacterial species, *Cyanobacterium* sp. CLg1 and *Crocosphaera watsonii*. Nevertheless, because GT5 ADP-Glc-specific glucan synthases are in essence prokaryotic and have never been found in eukaryotes and because archaeplastidal GBSS is related to bacterial sequences, it seems reasonable for us to propose that this type of sequence has evolved first among amylopectin-storing cyanobacteria.

Our understanding of the storage metabolism pathway in prokaryotes relies mostly on the studies in enterobacteria such as *Escherichia coli* (see preceeding paragraph for review). As pointed out earlier, the cyanobacterial storage polysaccharide network can be distinguished from that evidenced in most bacteria by an often surprisingly higher number of isoforms present at each stage of the pathway.

4.1.3.1 Biosynthesis

4.1.3.1.1 The Synthesis of ADP-Glc

In *Cyanobacteria* as in bacteria in general, ADP-Glc pyrophosphorylase (GlgC or Agp) regulates the first committed step in biosynthesis of α-glucan storage polysaccharide and for some species the synthesis of osmoprotectants. Like enterobacteria and plants, this enzyme mediates the synthesis of ADP-Glc, the sole nucleotide sugar used as substrate by the glucosyl transferase (glycogen(starch) synthase) that

belongs to the GT5 family (Cazy classication) to synthesize the α-1,4 linkages. AGPase is tightly regulated by allosteric effector defined by orthophosphate (Pi, inhibitor) and 3-phosphoglycerate (activator), which reflects the activity of the Calvin cycle. In contrast to plants, most of cyanobacteria strains possess one single glgC gene suggesting that AGPase is a homotetrameric enzyme. Nevertheless, a survey of genome sequences reveals the existence of two genes coding for glgC in *Cyanothece* ATCC51142, *Cyanothece* CCY01010, and *Acaryochloris marina* MBIC11017 (Fig. 4.2). To date, it is not clear if AGPase is active as a homotetrameric or heteromeric enzyme in these cyanobacteria. Phylogenetic analysis of the starch metabolism network of plants highlights the cyanobacterial origin of AGPase, which has evolved to maintain this cross talk with the Calvin cycle. Interestingly, the ancestral AGPase gene has been duplicated and subfunctionalized very early in the green lineage (the Chloroplastida), the small subunit considered as the catalytic part while large subunits fine tune AGPase activity. This could be correlated to starch relocalization in the chloroplast (Deschamps et al. 2008d). Because of its similarity to plant AGPase, the AGPase activity of Anabaena PCC7120 was intensively characterized by mutagenizing important amino acids responsible for allosteric effector regulation (Charng et al. 1992; Frueauf et al. 2002; Sheng and Preiss 1997).

In plants and green algae and to some extent in enterobacteria, the synthesis of ADP-Glc is exclusively committed to storage polysaccharide synthesis. Thus, mutants impaired in the synthesis of ADP-Glc grow normally in optimal growth conditions. In cyanobacteria, defects in glycogen biosynthesis lead to several physiological effects such as a decrease of photosynthesis activity, loss of viability, high salt sensitivity, and other defects (Grundel et al. 2012; Suzuki et al. 2010; Xu et al. 2013). The salt sensitivity phenotype results from a decrease of osmoprotective compounds: trehalose and glucosylglycerol (GG), which are synthesized by breaking down glycogen or by using ADP-Glc, respectively. Among the three different trehalose biosynthetic pathways reported in the literature, two are described in cyanobacteria (Wolf et al. 2003).

First, the production of trehalose from a glycogen/starch type of polysaccharide can occur through a three-step pathway: a glycogen debranching enzyme (TreX), which produces suitable maltooligosaccharides for a maltooligosyl trehalose synthase (Mts or TreY). The latter transforms the last α-1,4 linkage at the reducing end into an α-1,1 glucosidic bond. Maltooligosyl trehalose hydrolase (Mth or TreZ) will then hydrolyze the terminal trehalosyl unit of maltooligosaccharide (Higo et al. 2006). The reaction will produce trehalose and shorter maltooligosaccharides.

Second production of threhalose can occur from a starch-/glycogen-independent pathway in two steps. First trehalose phosphate synthase (TPS) will transfer the glucose residue of ADP-Glc or UDP-Glc to glucose-6-phosphate. Then trehalose-phosphate is dephosphorylated by trehalose-phosphate phosphatase (TPP). Interestingly, like TPS, cyanobacterial sucrose-phosphate synthase (SPS) is not specific with respect to the nucleotide-sugar substrate. In crude extracts of Scytonema, the specific activity of a TPS/SPS mixture is increased fivefold with ADP-Glc over that measured with UDP-Glc (Page-Sharp et al. 1999).

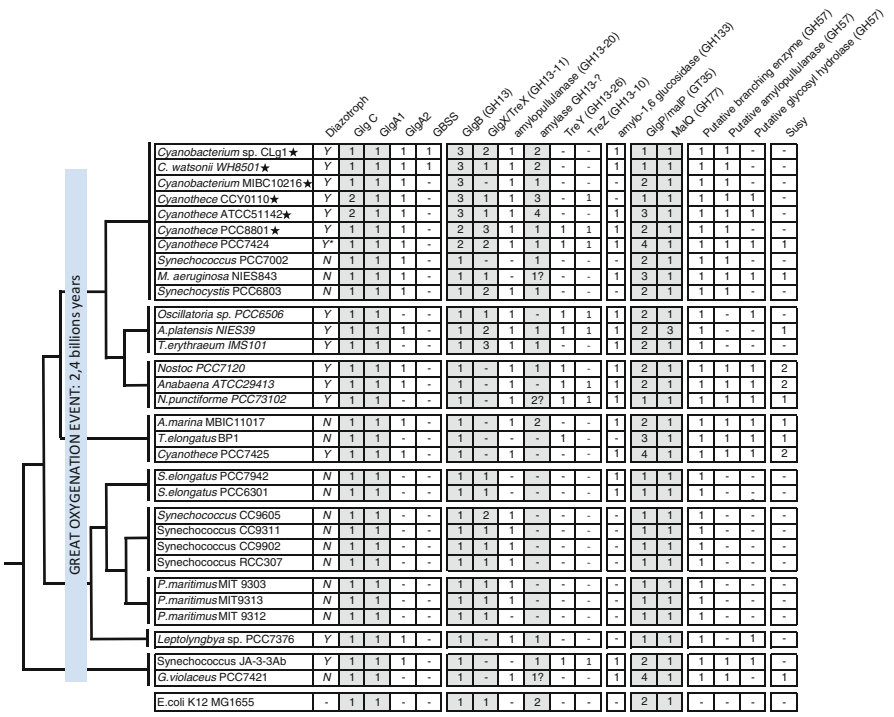

Fig. 4.2 *Black lines* depict the phylogenetic evolutionary relationship between cyanobacteria species in respect with the Great Oxygenation Event (GOE) which occurred around at 2.4 billion years ago. Representatives of each cyanobacteria clade were selected based on the availability of genome sequences. The number of enzyme isoforms found for each class of glycogen/starch and trehalose metabolism was determined using blast searches on NCBI, CyanoBase, and CAZy. Cyanobacteria strains labeled with a star were characterized to synthesize starch granules. *Y* (yes) and *N* (no) symbols reflect the ability to fix nitrogen in aerobic growth condition except for *cyanothece* PCC7424 which requires anoxic growth condition (Y*). *Escherichia coli* was used as reference for the type of isoforms found in cyanobacteria (*gray column*). Key: *BE* putative branching enzyme, *GlgC* ADP-glucose pyrophosphorylase, *GlgX/TreX* debranching enzyme, *iDBE* indirect debranching enzyme, *GlgB* branching enzyme, *GlgP/ MalP* glycogen phosphorylase/maltodextrin phosphorylase, *GlgA1/ GlgA2* glycogen synthase, *GBSS* granule-bound starch synthase, *MalQ* α-1,4-glucanotransferase, *TreY* trehalose synthase, *TreZ* trehalose hydrolase

Glucosylglycerol (GG) is the osmoprotectant compound synthesized only from ADP-Glc. GG-phosphate synthase catalyzed the first reaction using ADP-Glc and glycerol-3-phosphate. Then, a specific enzyme, GG-phosphate phosphatase will dephosphorylate GG-phosphate to produce GG. The characterization of *agp* (ADP-Glc pyrophosphorylase) mutants in *Synechocystis* PCC6803 shows clearly that in addition to the defect for glycogen biosynthesis, those mutants do not produce GG. The latter is compensated by large amount of sucrose after osmotic shock (Miao et al. 2003).

Interestingly, the presence of low amount of GG in the glgC mutant of *Synechococcus* PCC7002 suggests the existence of alternative pathway for the synthesis of ADP-Glc (Guerra et al. 2013). The first alternative source of ADP-Glc could come from sucrose synthase (Susy: EC2.4.1.13) activity. Susy activity is widespread in the plant kingdom and also found in filamentous heterocyst-forming cyanobacteria and in unicellular cyanobacteria. This enzyme catalyzes a reversible reaction in the synthesis of UDP-Glc and fructose by cleaving sucrose in the presence of UDP and vice versa. In plants, it is assumed that the major role of Susy is to supply UDP-Glc for cell wall synthesis. However, biochemical characterization of Susy of *Anabaena* PCC7119 highlighted major differences in the enzymatic properties (Porchia et al. 1999). Hence, cyanobacterial Susy activity displays a better affinity for fructose in the presence of ADP-Glc than UDP-Glc. In addition, Susy activity is sensitive to inhibition by ATP in both directions when UDP-Glc/UDP is used as the nucleotide-sugar/nucleoside substrate, while no activity was observed in the presence of adenine nucleotide. Recently, studies on the glycogen contents in mutants lacking Susy activity have shown a fourfold reduction in glycogen accompanied by an increase in ADP-Glc pyrophosphorylase activity in the knockout mutant of Susy (Curatti et al. 2008). In the presence of a nitrogen source, glycogen can be detected only in the mutant overexpressing Susy and not in the wild-type cells. Altogether, these data may suggest that Susy could contribute to the pool of ADP-Glc and consequently impact the pool of glycogen in *Anabaena*. However, a final but yet to be made convincing demonstration would consist of proving that GlgC mutants of *Anabaena* are not completely defective for glycogen accumulation.

A second theoretically possible source for ADP-Glc could consist of UDP-Glc pyrophosphorylase (GalU), which produces UDP-Glc from UTP and glucose-1-phosphate. A growing body of evidence suggests that the UGPase from *E.coli* or yeast may have some nonspecific activity toward ATP, generating ADP-Glc as an alternate product (Moran-Zorzano et al. 2007; Zea and Pohl 2004). However, the in vivo relevance of such speculations remains to be demonstrated.

4.1.3.1.2 Soluble Glycogen/Starch Synthase

Glycosyl transferases activities catalyze the α-1,4 linkages by transferring the glucose residue of ADP-Glc or UDP-Glc onto the nonreducing end of α-1,4-glucan chain. Two families of glycosyltransferase activities (GT3 and GT5) share this function among eukaryotes and prokaryotes (Coutinho and Henrissat 1999). The GT3 family is exclusively observed in the glycogen metabolism pathway of opisthokonts and of some amoebozoa and excavates, while the ADP-Glc utilizing GT5 enzymes are distributed in both prokaryotes and plants. It must be reminded that many other eukaryotic enzymes synthesize glycogen through a GT5 UDP-Glc-specific enzyme.

Another remarkable feature of glycogen synthase GT3 is their dependence on a self-autoglycosylation protein (glycogenin) to initiate glycogen synthesis (Torija et al. 2005). So far, there is no evidence of a comparable priming mechanism

in prokaryotes. However, as mentioned above, study of the *Agrobacterium* GS suggests that both priming and elongation activity are supported by this activity (Ugalde et al. 2003). Interestingly, starch synthase activities were subfunctionalized in plants for priming and elongation reactions. Thus, starch synthase III and IV are thought to be involved in polysaccharide synthesis priming, while starch synthase II and I are dedicated to the elongation of amylopectin chains (Szydlowski et al. 2009).

Except for the group of *Prochlorococcus-Synechococcus*, most of the cyanobacteria display two genes, coding for GlgA1 and GlgA2 isoforms (Fig. 4.2). Interestingly, the existence of both isoforms in the early cyanobacteria lineages might suggest that those isoforms were already present in the last cyanobacterial common ancestor. Although they were maintained through billions of years of evolution, it seems very likely that the *Prochlorococcus-Synechococcus* species, which emerged later in the evolution of cyanobacteria, have lost the GlgA2 gene during the genome reduction process. A detailed phylogenomic analysis of glycogen synthase reveals that glgA2 isoforms belong to a distinct clade composed of SSIII/SSIV starch synthase of plants and a dozen of α-proteobacteria. Interestingly, GlgA2 gene is restricted to a somewhat smaller group of bacteria (Chlamydiales, α-proteobacteria), whereas GlgA1 types of glycogen synthase are widespread among prokaryotes.

The respective functions of GlgA1 and GlgA2 activities have been recently investigated in *Synechocystis* PCC6803. Both single mutants of GlgA1 and GlgA2 produce unchanged wild-type amounts of glycogen (Grundel et al. 2012; Yoo et al. 2014). At first glance, these data suggest that there is an overlapping function of GlgA1 and GlgA2 activities. Both glycogen synthase activities are able to support both the priming and elongation reaction. However, structural characterization of the glycogen polysaccharides produced by single mutants is suggestive of different elongation properties (Yoo et al. 2014). Indeed, null *glgA2* mutants accumulate an altered glycogen structure, which contains fewer long glucans in comparison to the null *glgA1* mutant and to the wild-type reference strain. Based on the structural characterization of glycogen, the authors conclude that GlgA2 behaves as a processive enzyme while GlgA1 displays a distributive activity. Such conclusions have however not been confirmed directly by biochemical characterization of the purified enzymes.

Discovery of a GBSS gene in the genome of two cyanobacteria, *Crocosphaera watsonii* and *Cyanobacterium* sp. CLg1, defines a remarkable finding clarifying the origin of the enzyme of amylose synthesis. Phylogenetic analysis suggests a cyanobacterial origin for the GBSS found in Archaeplastida (see below). This gene gave rise by duplications to the soluble starch synthase I and II isoforms during the evolution of the Chloroplastida. GBSS has been demonstrated to define the sole enzyme required for amylose synthesis and its presence correlates perfectly with that of this starch fraction. In contrast to other starch synthase activities, this enzyme displays a unique elongation property, which consists to synthesize long glucan chains exclusively in the presence of semicrystalline polysaccharide (Maddelein et al. 1994).

4.1.3.1.3 Branching Enzyme Activity

Branching enzymes (GlgB or BE) – α-1,4-glucan: α-1,4-glucan 4-α glucosyl transferases – catalyze the formation of α-1,6 linkages in the storage polysaccharide. BE can be classified in three groups according to their enzymatic properties (e.g., preference for chain acceptors/donors) (Sawada et al. 2014). A survey of gene content in *Cyanobacteria* emphasizes the presence of two types of branching enzyme families: glycosyl hydrolase family 13 (GH13), which belongs to a large group of α-amylase family and glycosyl hydrolase family 57 (GH57) (Colleoni and Suzuki 2012). The latter is characterized by $(\beta/\alpha)_7$ barrel fold and five conserved domains important in the organization of the catalytic site (Santos et al. 2011). This family consists of diverse enzymatic activities (e.g., amylopullulanase, amylase, α-1,4-glucanotransferase, branching enzymes, and uncharacterized activities) and is restricted to Archaea and a few Eubacteria (Murakami et al. 2006; Zona et al. 2004). It is striking to observe that one putative branching enzyme GH57 gene is conserved in all cyanobacterial species, while the number of genes coding the GH13 branching enzyme varies from one to three (Fig. 4.2). Unlike the GH13 branching enzymes, the function of GH57 activities in starch or glycogen metabolism remains to be investigated. Nevertheless, a mutant of *Synechocystis* PCC6803 disrupted for its unique GH13 branching enzyme still accumulates half the wild-type amount of storage polysaccharide, while comparable mutants of yeast or *E. coli* witness a dramatic decrease or wipeout of glycogen synthesis. It seems likely that the GH57 branching enzyme is responsible for synthesis of the branches observed in the residual glycogen (Yoo et al. 2002).

The number of GH13 branching enzymes is variable among cyanobacteria. Phylogenetic analysis reveals three major classes among cyanobacteria: BE1, BE2, and BE3 (Colleoni and Suzuki 2012). The BE1 class is distributed in all cyanobacteria species, while the BE2 and BE3 classes are restricted to the order *Chroococcales*, which includes starch-synthesizing cyanobacteria. In plants, it is widely accepted that branching enzyme isoforms shape the starch granule architecture. Hence, the existence of distinct GlgB isoforms could in theory explain the structural diversity of storage polysaccharides among cyanobacteria. This reasonable assumption is apparently contradicted by the characterization of many starch-defective mutants in *Cyanobacterium* sp. Clg1 which all turned out to be defective for a GlgX-like starch debranching enzyme (Cenci et al. 2013). Had a particular BE been essential for starch rather than glycogen synthesis in this organism, mutants defective for this activity should have indeed appeared at either comparable or possibly lower but nevertheless detectable frequencies.

Characterization of branching enzyme activity is pretty scarce in the literature. A comparison of primary structure of *Synechococcus* PCC7942 reveals that the middle portion of the protein shares 62 % similarity with the *E.coli* branching enzyme, while the N-terminus displays little homology (Kiel et al. 1990). However, the N-terminus end has been reported to condition the length of the transferred glucan chain (Devillers et al. 2003). The lack of homology at the N-terminus could thus explain distinct chain-transfer patterns among branching enzymes. Recently,

branching enzyme activities of plants, yeast, human, and prokaryotes including GlgB of *Synechococcus* PCC7942 (BE1 class) have been subjected to detailed characterization. Based on transferred glucan chain preferences, data have shown that branching enzyme activities can be classified independently of their primary structure into three groups (see Sawada et al. 2014 for more details). From these studies it appears that both GlgB *E.coli* and *Synechococcus* PCC7942 belong to the group of OsBE1 (rice BEI), which introduce preferentially a new branching point on an acceptor glucan accordingly to the position of a preexisting branching point.

4.1.3.1.4 Convergent Evolution of Glucan Trimming Mechanism in Starch-Accumulating Cyanobacteria

As mentioned previously, glycogen particles define the most important type of storage polysaccharide among cyanobacteria. However, a small group of cyanobacteria belonging to the *Chroococcales* synthesize nonaqueous carbohydrate granules identified as starch granules (Fig. 4.2). A mutagenesis campaign was carried out on starch-accumulating *Cyanobacterium* sp. CLg1. Based on iodine staining of cell patches, over a hundred mutants were identified and subsequently categorized according to the ratio of soluble to insoluble polysaccharide. Among them, a dozen mutants harbor an increase in the water-soluble glycogen-like fraction and a disappearance of starch granules. This phenotype is correlated with a defect in direct debranching enzyme (DBE) activity belonging to glycosyl hydrolase family 13 (Cenci et al. 2013). Interestingly, biochemical characterization reveals that the mutants were impaired in the same type of ISA-GlgX activity as those involved in the crystallization process of starch in plants or in glycogen catabolism in *E. coli*.

The amylopectin aggregation in plants and probably in many others species relies on an isoamylase-type debranching enzyme activity (James et al. 1995; Kubo et al. 1999; Mouille et al. 1996; Wattebled et al. 2005). Like the CLg1 mutant, a defect in isoamylase activity in green algae and plants results in a substitution of starch granules by glycogen biosynthesis. Today, it is accepted that isoamylase removes selectively misplaced short glucans, which prevent amylopectin crystallization (Ball et al. 1996). Although starch-accumulating cyanobacteria predate the emergence of Archaeplastida, detailed phylogenetic studies of isoamylase enzymes failed to show the expected cyanobacterial origin of isoamylase. We can thus conclude that the cyanobacterial and plant enzymes have undergone convergent evolution to generate DBEs with similar properties. This remarkable finding suggests that there may be only one solution to generate starch from a preexisting glycogen metabolism network. We must nevertheless emphasize that some starch-accumulating cyanobacteria and the cryptophytes as well (see below) were reported to lack candidate DBE (Colleoni and Suzuki 2012; Coppin et al. 2004; Curtis et al. 2012). This raises the intriguing question of whether unidentified glucan hydrolase has evolved to ensure this function or whether combination of branching enzyme pattern could be sufficient to allow the aggregation of amylopectin (Streb et al. 2008).

4.1.3.1.5 Did the Great Oxygenation Event Trigger the Appearance of Crystalline Storage Polysaccharide in Unicellular Diazotrophic Cyanobacteria?

Cyanobacteria are one of the oldest phyla and most fascinating prokaryotes on Earth. Biomarkers (e.g., 2-methylhopanoid) and, more recently, geochemical analyses have traced back their oxygenic photosynthesis activity at least three billion years when the atmosphere was similar to anoxic environment (Crowe et al. 2013; Summons et al. 1999). It is widely accepted that the Great Oxygenation Event (GOE) occurred thanks to the release of oxygen from the splitting of water through cyanobacterial oxygenic photosynthesis 2.4 billion years ago (Kopp et al. 2005). The transition from a reductive to an oxidative environment triggered the diversification of cyanobacterial lineages and the appearance of new traits (e.g., morphology, cell size) (Blank and Sanchez-Baracaldo 2010; Latysheva et al. 2012; Sanchez-Baracaldo et al. 2014). A remarkable adaptation was achieved in nitrogen-fixing cyanobacteria. The reduction of dinitrogen to ammonium is catalyzed by an extremely oxygen-sensitive molybdenum-dependent ATP-hydrolyzing protein complex called nitrogenase (Burris 1991). Recent, phylogenetic reconstructions indicate that the last cyanobacterial common ancestor, which predates the GOE, was probably a freshwater nitrogen-fixing unicellular cyanobacterium (Larsson et al. 2011; Sanchez-Baracaldo et al. 2014). As oxygen rose, diazotrophic cyanobacteria have evolved to protect their nitrogenase activity (Bergman et al. 1997). In diazotrophic filamentous cyanobacteria, nitrogenase is localized in thick-walled specialized heterocyst cells lacking the PSII oxygen-generating complex. The large amount of energy required to fuel nitrogenase (16 ATP/N2) is supplied by neighboring cells displaying normal photosynthetic activity. Physical separation of two mutually exclusive biological processes, i.e., photosynthesis and nitrogen fixation, is possible only through the evolution of multicellularity and the ensuing cell specialization. For this reason, it was believed that nitrogen fixation could not occur in unicellular cyanobacteria. However, in 1970, two unicellular cyanobacteria strains, Gloeothece sp. and Cyanothece sp., were the first unicellular cyanobacteria described as aerobic nitrogen fixers (Singh 1973; Wyatt and Silvey 1969). In contrast to filamentous cyanobacteria that are able to fix nitrogen during the day, unicellular diazotrophic cyanobacteria perform nitrogen fixation exclusively at night. This group of unicellular cyanobacteria solved the problem by developing a temporal separation throughout circadian-clock regulation of the diurnal cycle. In the light, an accumulation of inclusion bodies is observed that disappears at night (Schneegurt et al. 1994). More recently, a survey and structural characterization of storage polysaccharide reveal that the inclusion bodies reported previously are composed of glucose residues forming semicrystalline polysaccharides similar to starch granules in plants (Deschamps et al. 2008a; Nakamura et al. 2005; Suzuki et al. 2013). This raises the question of whether the GOE was a driving force for the transition from glycogen to semicrystalline starch granules. It was noted that nitrogen fixation is engaged when the level of oxygen is low enough to allow nitrogenase

activity. To reach anoxia, unicellular aerobic nitrogen-fixing cyanobacteria exhibit high rates of dark respiration thereby consuming and decreasing O_2 levels locally in addition to ensuring the supply of the additional energy cost of N_2 fixation (Compaore and Stal 2010). Thus, unicellular diazotrophic cyanobacteria might have evolved a more efficient storage polysaccharide structure that maximizes the storage polysaccharide pool thereby allowing an efficient rate of nitrogen fixation in dark aerobic conditions. This hypothesis is reminiscent of the physiological adaptation of green algae to the anoxic production of hydrogen by hydrogenase. In that case it was indeed demonstrated that the predominant class of mutants recovered by screening for defective hydrogen production were mutants that had reverted from starch to glycogen accumulation because of a defect in isoamylase debranching enzyme activity! In addition, this assumption has been recently supported by the analysis of six Cyanothece species under various growth and incubation conditions (Bandyopadhyay et al. 2013); despite the fact that the authors did not notice that they have chosen starch- and glycogen-accumulating cyanobacteria in their experiment. It is striking for us to observe that those reported to accumulate starch as storage polysaccharide exhibit the highest rate of nitrogen fixation when compared to the glycogen-accumulating Cyanothece species in aerobic growth condition. Because we cannot of course exclude that genetic background may explain this variability in nitrogen fixation (e.g., Cyanothece PCC7525 requires anoxic condition to fix nitrogen), further analyses should be undertaken to correlate carbon limitation and specific rates of nitrogen fixation.

4.1.3.1.6 Physiological Importance of Storage Polysaccharide in Cyanobacterial Survival During Nitrogen Starvation

Glycogen biosynthesis is tightly regulated in response to different environmental cues, for instance, nitrogen starvation enhances glycogen accumulation in various bacteria species.

In non-diazotrophic cyanobacteria, limitation of the nitrogen source results in the storage of polysaccharide and a mobilization of the photosynthetic apparatus. This phenomenon named “chlorotic response” reflects a depletion of photosynthetic pigments (i.e., phycobiliprotein), which are used to supply transiently the cells in nitrogen. This nitrogen source allows protein synthesis before switching to a dormant state. Interestingly, a defect either in the ADP-Glc pyrophosphorylase or in both glycogen synthase activities results in a non-bleaching phenotype. Indeed, after a couple of days in depleted nitrogen medium, marine or freshwater cyanobacteria do not break down photosynthetic pigments and lose their viability (Grundel et al. 2012, 2013). Although the responsible signaling cascade is unknown, it is clear that the cyanobacterial survival relies on the presence of massive amounts of storage polysaccharide.

4.1.3.2 Catabolism

Photosynthetic organisms are subjected to alternating light and dark cycles. As mentioned previously, storage polysaccharide is synthesized during the day between thylakoid membranes. At night, cyanobacteria maintain their levels of ATP and NADP(H) by consuming storage polysaccharide. Several classes of catabolizing enzymes hydrolyze α-glucans into glucose and glucose-1-phosphate residues. Like in enterobacteria, glycogen phosphorylase (GlgP) and debranching enzyme (GlgX) work in synergy to cleave off the α-1,6 linkages. Glycogen phosphorylase releases directly a glucose-1-phosphate (G-1-P) from the nonreducing end of glucan chains and stops four glucose residues before the branch point. Short branched glucan are specifically cleaved off from phosphorylase limit dextrin by glycogen debranching enzyme GlgX. The number of isoforms involved in storage polysaccharide catabolism varies greatly according to the species. In cyanobacteria or *E.coli*, a defect in GlgX activity results in the accumulation of phosphorylase limit dextrin, which cannot be further metabolized (Colleoni and Suzuki 2012; Dauvillée et al. 2005). Recently, a screening for high temperature-sensitive strain of *Synechocystis* PCC6803 highlights a divergent function of both glycogen phosphorylases isoforms (Fu and Xu 2006). Surprisingly, GlgP-sll1356 is essential for growth at high temperature, whereas GlgP-sll1367 isoform is required for glycogen mobilization. Interestingly, despite the increase of GlgP-sll1356 activity in the null *glgP-sll1367* mutant, glycogen is inefficiently catabolized at night. Further investigations are required to understand the function of the GlgP-sll1356 isoform. However, we can hypothesize that sll1356 gene might encode a maltodextrin phosphorylase (MalP). This enzyme, involved in maltodextrin catabolism, predominantly acts on linear glucan oligosaccharides and is quite inefficient in its ability to digest the glycogen outer chains. Hence, like *glgP* mutants of *E.coli*, the MalP activity cannot substitute with the function of GlgP in the glycogen catabolism pathway (Alonso-Casajus et al. 2006).

Surprisingly, several cyanobacterial genomes, if complete, do not seem to encode any classical GlgX-type debranching enzymes. However, such genomes appear to contain amylopullulanase (GH13-20 and/or GH57) and amylo-1,6-glucosidase (GH133) genes (Fig. 4.2) that could supply such functions. Little is known about their role in α-glucan catabolism. Recently, amylopullulanase GH13 has been characterized from the filamentous cyanobacteria *Nostoc punctiforme* (Choi et al. 2009). In contrast to GlgX/TreX activities, this enzyme displays hydrolysis activity toward both α-1,6 and α-1,4 linkages when incubated with soluble branched polysaccharides (e.g., starch, amylopectin). The glucan chains made of 8 residues of glucose are specifically released and the resulting maltooligosaccharides are then hydrolyzed at the reducing end yielding shorter maltooligosaccharides ($G_{(n)} = G_{(n-1)} + G$). Because *N. punctiforme* does not contain any GlgX/TreX GH13 activity but harbors both maltooligosyl trehalose synthase (TreY) and maltooligosyl trehalose hydrolase (TreZ) (Fig. 4.2), it is quite possible that the GH13 amylopullulanase substitutes for the missing TreX activity, which is required to produce the suitable maltooligosaccharide for TreY. Amylo-1,6-glucosidase (GH133) shows similarity to the amino

acid sequence of the C-terminal domain of indirect debranching enzyme activity of animals and fungi. This activity could thus cleave out single α-1,6 glucose residues branched on glucan chains. So far, no biochemical characterization has ever been carried out on these cyanobacterial amylo-1,6-glucosidases. However, the characterization of the null GlgX mutant of *Synechococcus* PCC7942 brought some insights on the putative function of the amylo-1,6-glucosidase activity (Suzuki et al. 2007). Indeed, two genes encoding for candidate debranching enzyme activities, GlgX and amylo-1,6-glucosidase (GH133), have been identified in the genome of *Synechococcus* PCC7942 (Fig. 4.2). Although residual glycogen is enriched in short branched maltooligosaccharides, probably trimmed by the missing GlgX activity, the *GlgX* mutant of *Synechococcus* did not display a glycogen-excess phenotype comparable to that reported for the *E. coli* mutant (Dauvillée et al. 2005). Hence, it is entirely possible that the amylo-1,6-glucosidase may partially overlap with the GlgX activity in *Synechococcus*.

4.2 The Comparative Biochemistry of Starch and Glycogen Metabolism in Eukaryotes

A major difference between eukaryotes and bacteria is generally thought to be defined by a larger contribution in evolutionary histories of vertical inheritance and a lesser impact of horizontal gene transfer between unrelated clades. This is usually explained by the specific nature of gene sharing implied by the eukaryotic sexual cycle. The presence of a significant vertical inheritance component makes reconstitution of ancient pathways more feasible and less blurred by seemingly random gene sharing as often seen among bacteria. This in turn is required if evolutionary histories of biochemical networks are to be explained and enlightened by phylogenetic inferences. Hence, vertical inheritance usually leads to a higher level of congruence between diversification of eukaryotes and enzyme phylogenies. This assumption while still valid today must however be tempered by the presence of extensive HGTs observed as consequences of the very diverse and abundant endosymbiotic events. One may downplay the negative consequences of this type of HGT called EGT (endosymbiotic gene transfer) on the ease with which gene histories can be reconstituted. Indeed, the partners of the event are usually clearly identified and the events are also often well dated and placed within the eukaryotic tree of life. EGTs are defined as duplication of an endosymbiont gene that happens during metabolic integration of the endosymbiont followed by transfer to the host nucleus of the duplicated gene. This in turn is followed by expression and accurate localization of the gene product thereby allowing the corresponding loss of the endosymbiont gene copy. EGTs are evoked to explain the massive presence of cyanobacterial genes within the Archaeplastida (plant) nuclear genomes. At first glance this seems to only enrich gene histories without affecting our ability to reconstitute ancient pathways and recapitulate biochemical

network histories thereby enlightening gene function. Unfortunately life is indeed complicated and metabolic integration of endosymbionts does not always involve only the endosymbiont and host genomes. In fact in a majority of cases, the nuclear gene copy that replaces the endosymbiont genome's copy is not of endosymbiotic origin (and thus not a true EGT). This of course is not true for most (but not all) functions required for the maintenance and replication of the symbiont genome and for highly integrated process such as those governed by electron transport chains on evolving organelle membranes. However, for other less integrated but nevertheless numerous biological processes, the general rule concerning the origin of the gene that will replace the endosymbiont copy seems to be "whatever works!" Apart from chance (whoever gets in first!) a major factor governing the choice of a suitable source for endosymbiotic gene replacement by the nucleus could be the facility with which the product may be synthesized in the cytosol and translocated to the compartment where it will be active. What the endosymbiont does always transmit are the blueprints, the building instructions, for the novel biochemical pathways it encodes, but what the eukaryotic nucleus will choose as molecular tools to build this network is anyone's guess. In turn, this will create a lot of diversity and novelty in the constitution of the evolving organelle proteome. Fortunately for us the biochemical pathway of storage polysaccharide metabolism for most clades in eukaryotes has evolved in the eukaryotic cytosol and not in the endosymbionts from the preexisting cytosolic host glycogen metabolism pathway. As such, most of the starch metabolism enzymes are congruent with diversification of eukaryotes. This can be explained by the fact that the major pool of storage polysaccharides in all eukaryotes has always been, at least initially, exclusively cytosolic (Deschamps et al. 2008c). In the green algae and land plants, the plastidial localization of storage polysaccharides evolved after metabolic integration of the protoplastid had been partly achieved. The cryptophytes define the only case where the storage polysaccharide seems to have been maintained in the symbiont throughout the metabolic integration process of the evolving organelle. We will indeed see that in this case and in this case only, this has led to an astonishing patchwork of enzymes of distinct phylogenetic origins. Finally despite the ancient cytosolic origin of the storage polysaccharide metabolism pathways, we will see that this pathway has been indeed used to establish the first metabolic connection between endosymbiont and host at least in the case of the Archaeplastida.

4.2.1 Glycogen Metabolism in Opisthokonts

Opisthokonts define a very well-supported group uniting two major eukaryotic kingdoms (Fungi and Animalia) to a few of their unicellular ancestors; their name is derived from the presence of a unique flagellum propulsing flagellated cells from the posterior end of the cell (Cavalier-Smith et al. 2014). Glycogen metabolism in animals has been studied for nearly a century. These studies have yielded seminal contributions to our understanding of cell biology and biochemistry

in general. A review of the mass of studies that has allowed the understanding of glycogen metabolism regulation is out of the scope of this effort. Suffice it to say here that these studies have revealed the existence of glycogen itself, of cAMP, of protein kinases and phosphatases, of signal transduction, of glycosyl nucleotides themselves, and of their transferases, thereby leading to several well-deserved Nobel prizes (for review see Brautigan 2013, Wilson et al. 2010). The paradigm for opisthokont glycogen metabolism holds for both fungi and animals. It consists of glucan elongation from UDP-Glc through UDP-Glc-specific glycogen synthases, belonging to a CAZy family distinct from bacteria: the so called GT3 GS. These enzymes are notoriously unable to prime glucan elongation and require the presence of glycogenin. Glycogenin defines an autoglucosylating protein known to glucosylate selective tyrosine residues from UDP-Glc and then extend them to over 10 glucose residues (Albrecht et al. 2004). It is therefore believed that the GT3 GS uses this glucosylated primer to further extend glucans. In the absence of this primer, deregulated GT3 yeast GS is sometimes able to sustain synthesis of some glycogen in a stochastic fashion, leading to recurrent gain and losses of glycogen in the deregulated cells (Torija et al. 2005). As with bacterial glycogen synthesis (see above), the elongated glucan is branched through a GH13 glycosyl hydrolase named branching enzyme (BE). The mature glycogen particle is subjected to degradation through GT35 glycogen phosphorylase, whose basic structure and properties are analogous to the bacterial enzyme (see above). As with bacteria, the outer chains of the glycogen particle are recessed and stop 4 glucose residues from the next α-1,6 branch, generating thus glycogen phosphorylase limit dextrin. However, eukaryotes process this limit dextrin quite differently from bacteria. While bacteria directly release the short maltotetraose stubs through direct debranching enzymes, eukaryotes never produce such maltooligosaccharides. Instead, they use a bifunctional enzyme carrying two distinct catalytic domains involved first in the transfer of maltotriose from the branch to a neighboring chain within the same glycogen particle, thereby unmasking the remaining glucose at the branch, which in turn will be detached by the second α-1,6-glucosidase domain of the bifunctional debranching enzyme, which is therefore called indirect debranching enzyme (Nakayama et al. 2001). Through this mechanism, only glucose and extended glycogen chains, which define further substrates for glycogen phosphorylase, are produced. Hence, unlike bacteria or even archaea, no MOS are released by debranching, and therefore, there is no coupling to MOS catabolism in the eukaryotic cytosol. The presence of indirect DBE (iDBE) is distinctively eukaryotic, and no fusions of the two critical domains have ever been observed in prokaryotes. In addition to degradation by glycogen phosphorylase and iDBE, a hydrolytic pathway is known to operate either in lysosomes (animals) or in the fungal acid vacuole by glucoamylase or acid maltase (glucosidase). The mechanisms targeting and partitioning glycogen between the cytosol and the vacuole is an active domain of current research (for review see Wilson et al. 2010). Finally, a glucan phosphatase named laforin is known to be targeted in animals, but not in fungi, to abnormal glycogen particles in order probably to dephosphorylate them (Tagliabracci et al. 2007). The exact mode of action of laforin is presently controversial, but an

interesting possibility would be that a hypothetical glycogen kinase phosphorylates abnormal glycogen, to signal its targeting to the lysosome for degradation (Cenci et al. 2014). In the normal process of lysosome targeting and ensuing particle hydrolysis, a dephosphorylation step through this phosphatase may be mandatory. It is known that, in humans, a block at this step will have tragic consequences through the accumulation of hyperphosphorylated solid glucan bodies in the brain known as lafora bodies (Lafora and Glueck 1911). The patients suffering from the non-curable lafora disease die at a young age from epilepsy.

4.2.2 Glycogen Metabolism in Amoebozoa

Amoebozoa define a monophyletic lineage of unicellular or multicellular organisms placed among the unikonts but which in most cases define wall-less amoebal phagotrophs during their vegetative phase (for review see Glöckner and Noegel 2013). Two distinct genome sequences have been established within the monocellular amoebas: the Archamoebae (the human pathogen *Entamoeba histolytica*) and the Acanthamoebidae (*Acanthamoeba castellanii*). In addition to this, one multicellular model social amoeba genome (*Dictyostelium discoideum*) is also available among the Dictyosteliida (Glöckner and Noegel 2013). Some efforts in the 80s and 90s have been invested in dissecting glycogen metabolism in *Dictyostelium*. This has led to an in-depth biochemical characterization of the partially purified glycogen synthase activity and of two distinct glycogen phosphorylase isoforms (Rogers et al. 1992; Rutherford et al. 1992; Williamson et al. 1996). In the case of glycogen phosphorylase, the two genes encoding two distinct enzymes were selectively disrupted, and the consequences of these disruptions during the different phases of the complex Dictyostelium life cycle, were studied (Rogers et al. 1994). Disruption of Gp1 led to a 20-fold increase in the size of the glycogen pool at stationary phase in vegetative amoeba cultures. Gp2 was thought to be specifically involved in the conversion of glycogen to cellulose that occurs during sporogenesis. The gene disruption failed to demonstrate this, because of cross compensation through transcriptional and posttranslational regulation of Gp1. Interestingly, a similar function in the supply of glucose for cellulose synthesis was inferred for glycogen phosphorylase in *Acanthamoeba castellanii*. siRNA designed against Acanthamoeba's glycogen phosphorylase indeed resulted in a decrease of cyst wall assembly in this species (Lorenzo-Morales et al. 2008). A mutant defective for glycogen synthase has been selected in *Dictyostelium discoideum* (Tresse et al. 2008). In this species two glycogen synthase genes, belonging to the GT3 and GT5 families, have been reported. The candidate GT5 enzyme is fused to a truncated α-amylase domain, while the GT3 enzyme displays significant homology to the opisthokont enzyme. Disruption of the GT3 enzyme gene led to a threefold decrease of the glycogen levels, thereby suggesting that the GT5 GS ensures the synthesis of the remainder third of the glycogen pool. The mutants displayed delayed sporulation and were altered in spore stalk morphology because of abnormal autophagic cell

death of stalk cells. Glycogen synthase had been previously partly purified from wild-type cells and assumed to be of GT3 type, since at that time only one GT3 type of enzyme was thought to be present in the *D. discoideum* genome. Interestingly the laboratory of Charles Rutherford had described the presence of glucan primer-dependent and primer-independent forms, as well as that of a G6P-dependent and G6P-independent forms. The possible presence of the GT5 enzyme suggests that some of these properties may be carried specifically by either the GT5 or the GT3 forms, thereby requiring further experimentation. The gene content of the three distinct amoeba genomes is summarized in Fig. 4.3. The amoebas include all genes of the opisthokont glycogen metabolism network with the noticeable exceptions of bona fide opisthokont-like glycogenins and of laforin. The simultaneous presence of both GT3 and GT5 enzymes in *D. discoideum* and the presence of the sole GT5 enzyme in *E. histolytica* may suggest that a GT5 autoglucosylating enzyme could provide a primer for the GT3 enzyme, but this hypothesis also needs further experimentation. In addition to the opisthokont enzymes, the amoebas all contain β-amylase and the DPE2-like amylomaltase. Hence, amoebozoa contain a richer suite of glycogen metabolism enzymes than both fungi and animals. The analysis of these genomes strongly suggests that β-amylase and DPE2 that were previously thought to be plant-specific enzymes, required for starch degradation, are in fact very ancient enzymes of the eukaryotic glycogen metabolism network. β-amylase or true DPE2-like α-1,4-glucanotransferases are never found in bacteria, although some distantly related amylomaltases have been found in a few bacterial clades. We do not know however if β-amylase and DPE2 are cytosolic or lysosomal nor do we know how defects in such activities would impact glycogen content and metabolism. Because we can reasonably suspect that the opisthokonts have lost these two genes very early on, in their common ancestor, we believe that amoebozoa provides us with the paradigm of the ancient eukaryotic cytosolic glycogen metabolism network. It is most probably from such a cytosolic host network that starch metabolism evolved in Archaeplastida shortly after plastid endosymbiosis.

4.2.3 Starch Metabolism and Structure in Rhodophyceae

The red algae or Rhodophyceae (previously rhodophytes) are a large group of photosynthetic eukaryotes belonging to the super phylum Archaeplastida (Rodriguez-Ezpeleta et al. 2005). Over the past few years, phylogenetic analyses and genome sequencing have provided significant insights into the evolution of Rhodophyceae (Le Gall and Saunders 2007; Ragan et al. 1994; Yoon et al. 2006). Today it is widely accepted that Rhodophyceae define a monophyletic clade, currently composed of seven major classes: Bangiales, Florideophyceae, Porphyridiales-(1), Porphyridiales-(2), Porphyridiales-(3), Compsopogonales, and Cyanidiales. The latter consists of three genera Cyanidioschyzon, Cyanidium, and Galdieria and has received a lot of attention during the last decade. These unicellular red algae, with relatively small genomes (12 Mpb), live and thrive in particularly extreme

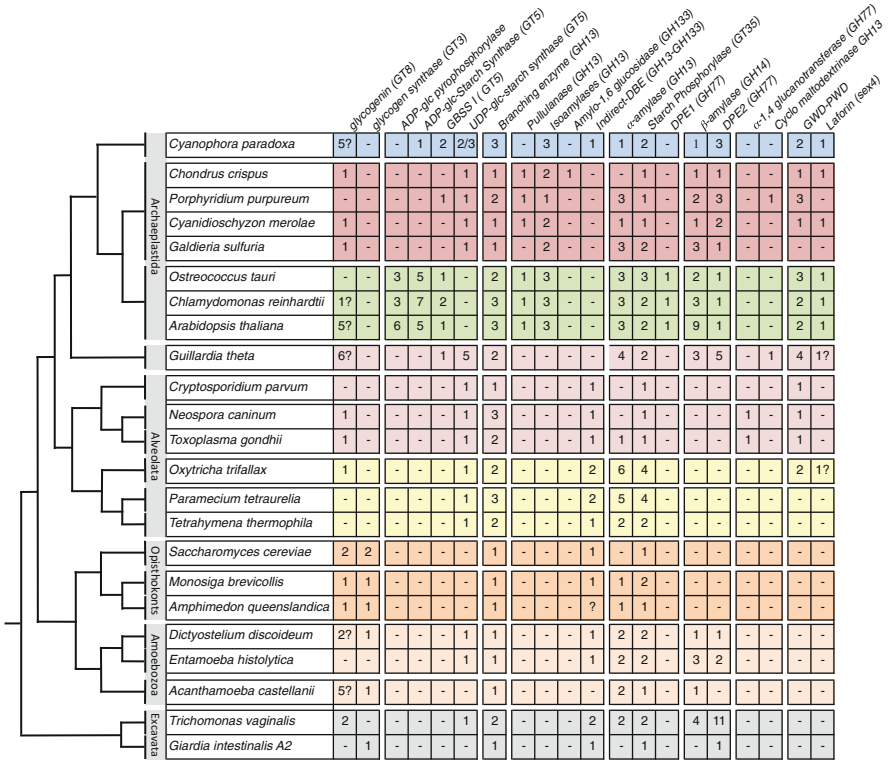

Fig. 4.3 Storage polysaccharide metabolism enzyme network in the eukaryotic domain. The number of enzyme isoforms is listed in each eukaryotic clade represented and listed according to the phylogeny of eukaryotes. Glaucophytes are represented in *blue*, Rhodophyceae in *red*, Chloroplastida in *green*, Cryptophytes in *dark purple*, apicomplexa in *light purple*, ciliates in *yellow*, opisthokonts in *pink*, amoebozoa in flesh, and excavates (metamonads) in *gray*. The number of enzyme isoforms found for each enzyme class of glycogen/starch metabolism was determined using blast searches on NCBI and CAZy

environmental conditions (pH 0.05–3; above 56 °C) unlike most eukaryotes. This remarkable adaptation required both genome reduction and extensive horizontal gene transfers (HGTs) from bacteria and archaea (Schonknecht et al. 2013). Based on phylogenetic studies, Cyanidiales are considered to be one of the most ancestral algae, which possibly diverged around 1.3 billion years ago (assuming a 1.5 billion-year-old date for plastid endosymbiosis) at the root of the Rhodophyceae (Yoon et al. 2002, 2004).

Like its green sister lineage (the Chloroplastida (previously known as "chlorophytes" or "viridiplantae" including green algae and plants), the photosynthetic carbon dioxide assimilation occurs in the plastid (i.e., rhodoplast) through the Calvin-Benson cycle. Subcellular localization of carbohydrate metabolizing enzymes of the oxidative pentose phosphate and glycolytic pathways appears to be essentially

identical with plants (Moriyama et al. 2014). Nevertheless, in contrast to the green lineage, assimilated carbon is efficiently exported to the cytosol by the triose-phosphate translocator (TPT) to promote cytosolic storage polysaccharide biosynthesis (Linka et al. 2008). Except for *Galdieria* sp. and *Cyanidium* sp. which have probably reverted from starch to glycogen synthesis (Hirabaru et al. 2010; Stadnichuk et al. 2007), most of the photosynthetic carbon is deposited in the cytosol of red alga as amylose-free starch granules called "floridean" starch (Borowitza 1978; Meeuse et al. 1960; Meeuse and Kreger 1954). Nevertheless, the absence of amylose fraction does not appear to define a universal feature of floridean starch. Extended survey of floridean starch composition highlights the presence of a significant amylose fraction in the genus Porphyridiales (McCracken and Cain 1981; Shimonaga et al. 2007). Floridean starch defines a semicrystalline polysaccharide whose crystallinity ranges from 16 to 36 % depending on red alga species (Shimonaga et al. 2008). The amylopectin of red algae contains significantly less long glucan chains (DP > 37) compared with that of plants. This CL distribution results in a semi-amylopectin structure similar to starch-accumulating cyanobacteria (Nakamura et al. 2005).

The access to four sequenced genomes within red algae, *Cyanidioschyzon merolae* (Matsuzaki et al. 2004), *Galdieria sulphuraria* (Schonknecht et al. 2013), *Porphyridium purpureum* (Bhattacharya et al. 2013), and a multicellular red alga *Chondrus crispus* (Florideophyceae) (Collen et al. 2013), have brought a complete overview of candidate genes required for the biosynthesis and breakdown of storage polysaccharides and have confirmed the UDP-Glc-based pathway in Rhodophyceae (for review Viola et al. 2001).

Compared to plants and green algae where 30–40 genes seem required, rhodophycean starch metabolism appears astonishingly simple, as less than 12 genes are required. For example, both the unicellular thermoacidophile *Cyanidioschizon merolae* and the multicellular mesophile *Chondrus crispus* contain only one starch synthase and one branching enzyme phylogenetically related to the BEI-BEII superfamily of plants. This seems sufficient to catalyze the formation of both α-1,4 and α-1,6 linkages (Sawada et al. 2014). Hence, Rhodophyceae are able to accumulate a complex semicrystalline floridean starch using a minimum set of three activities including the isoamylase-type activity responsible for the crystallinity of amylopectin.

In addition, the analysis of genome sequences clearly reveals the absence of genes encoding ADP-Glc pyrophosphorylase (AGPase) and ADP-Glc utilizing starch synthase in all red algae species. These genomic data conflict with previous biochemical characterizations, which have suggested the presence of both activities (Fredrick 1968; Nagashima et al. 1971; Sesma and Iglesias 1998; Sheath et al. 1979). This discrepancy may reflect the nonspecificity of UDP-Glc pyrophosphorylase and UDP-Glc-utilizing starch synthases of red algae toward ATP and ADP-Glc, respectively, as reported for others organisms (Deschamps et al. 2006; Moran-Zorzano et al. 2007; Zea and Pohl 2004).

The regulation of floridean starch biosynthesis is not well known in red algae. In contrast to plants, it seems unlikely that the amount of floridean starch is directly

controlled by the flux of UDP-Glc. Indeed, UDP-Glc serves as substrate for many enzymes, like trehalose-phosphate synthase, galactose-1-phosphate uridylyltransferase, or UDP-galactose-4-epimerase (Lluisma and Ragan 1998). This nucleotide sugar is involved in multiple biosynthetic pathways such as cell wall, isofloridoside, and floridoside synthesis (Pade et al. 2014). Interestingly, floridoside shares functions analogous to those of sucrose in plants: it is an osmoprotectant, potentially used to translocate carbon between cells, and represents a major soluble source of storage carbon (Ekman et al. 1991). Hence, the floridean starch pathway relies, just like that of eukaryotic glycogen metabolism, on the sole use of UDP-Glc. However, there is presently no evidence for or against the existence of posttranslational floridean starch synthase modifications (i.e., phosphorylation) analogous to those described for the opisthokont GT3 glycogen synthase.

Phylogenetic trees show that UDP-Glc starch synthases of red algae belong to the same GT5 family as those found in the Glaucophyta sister archaeplastidal lineage and also in other glycogen or starch-accumulating bikonts and amoebozoa derived or not from secondary endosymbiosis (Coppin et al. 2004). The latter is completely unrelated to the GT3 UDP-Glc glycogen synthase found in animals and fungi (Ball et al. 2011; Price et al. 2012). Only granule-bound starch synthase, the enzyme responsible for amylose synthesis within starch granules, shows a common cyanobacterial origin for all Archaeplastida (Cenci et al. 2014). Interestingly, the presence of a GT5 UDP-Glc starch synthase in red algae is correlated with the presence of a gene encoding a candidate glycogenin. However, such correlations are not universal features of other protist GT5 or GT3 glycogen (starch) synthases. It has been shown that the GT5 UDP-Glc starch synthase of *Gracilaria* sp. displays a significant glycosyl transferase activity toward amylose, whereas little or no activity was observed toward glucan chains made of 2–7 residues of glucose (Nyvall et al. 1999). Thus, it is reasonable to hypothesize that the glycogenin of *Gracilaria* sp. might prime the synthesis of longer glucan chains (>7) required for the starch synthase of *Gracilaria* sp. Nevertheless, the genome of *Porphyridium* sp. lacks glycogenin genes. So far, no biochemical characterization has been carried out to show whether this starch synthase has evolved to initiate directly the synthesis of glucan chains as reported for some glycogen synthases of prokaryotes (Ugalde et al. 2003). An alternative hypothesis would be that one of the multiple α-1,4-glucanotransferase activities (DPE2-like) may be responsible for the priming reaction.

Based on genome content, it seems that floridean starch catabolism is similar to the starch degradation pathway in green plants and algae. With the exception of the few glycogen-accumulating red algae such as *G.sulphuraria*, glucan water dikinase (GWD) or phosphoglucan water dikinase (PWD) and laforin genes are found in red alga genomes (Fig. 4.3). Laforin of red algae and glaucophytes have their glucan-binding and dikinase domains organized in a fashion similar to the animals and unlike that which is found in Chloroplastida (SEX4: phosphoglucan phosphatase). In plants, both GWD and PWD are required to initiate the first committed step in starch catabolism through the phosphorylation of semicrystalline starch granules at the C6 and C3 positions, while laforin is involved in cleaving

out the phosphate from phosphorylated glucans (Kotting et al. 2005, 2009; Yu et al. 2001). Interestingly, in both *C. merolae* and *Porphyridium* sp., the GWD activity appears sufficient to loosen the tight crystal packing of amylopectin and to allow an efficient degradation of amylopectin through actions of phosphorylases and both β-and α-amylase activities. Maltose molecules released by the β-amylase activity are probably further metabolized in the cytosol thanks to the action of DPE2. The latter defines an α-1,4-glucanotransferase which catalyzes the transfer of a glucose residue from maltose to an acceptor glucan. This disproportionation reaction allows then further actions of hydrolytic enzymes. Interestingly, some red algal species such as *Gracilaria sp*. possess an α-glucosidase activity belonging to the GH31 family localized in the rhodoplasts (Yu et al. 1999; Yu and Pedersen 1993). This enzyme defines an α-1,4-glucan lyase (EC 4.2.2.13) producing 1,5-anhydrofructose from the nonreducing ends of either long α-1,4-linked glucans or short maltooligosaccharides such as α- and β-maltose (Nyvall et al. 2000). The function of this 1,5-anhydrofructose is not clear in *Gracilaria*. It is known that 1,5-anhydrofructose is a highly reducing carbohydrate (Yu and Pedersen 1993). For this reason, Yu and collaborators have proposed that it might protect rhodoplasts against reactive oxygen species (ROS). However, the cytosolic localization of starch biosynthesis raises the question of the source of maltooligosaccharides in the rhodoplasts. To address this question, further investigations should be undertaken to prove whether maltooligosaccharides are synthesized in the rhodoplasts as proposed by Viola et al. (2001) or whether they are directly imported from the cytosol through an uncharacterized transporter.

4.2.4 Starch Metabolism and Structure in Glaucophyta

Glaucophytes represent one of the three clades that emerged from plastid endosymbiosis. Although the order of divergence of the Archaeplastida lineages remains a topic of recurrent debate, an ancient early divergence of the glaucophytes is generally favored. This correlates with many traits that are believed to be ancestral in these algae, as, for example, the presence of a muroplast with many cyanobacterial morphological features (including a peptidoglycan wall and carboxysome-like structures) (Facchinelli et al. 2013; Fathinejad et al. 2008; Pittenauer et al. 1993). *Cyanophora paradoxa*, the model glaucophyte species, defines one of the 14 biflagellated single-cell algae living in acidic freshwater ponds. Together with *Glaucocystis nostochinearum*, *Cyanophora paradoxa* is presently the only experimentally tractable organism. No sexual reproduction is known to occur in glaucophytes and only one genome sequence has been quite recently reported for *Cyanophora paradoxa* (Price et al. 2012). A haploid genome sequence of 70 Mbp is presently hypothesized for this vegetative possibly diploid species with around 28,000 putative protein-coding genes. This is two- to threefold more genes and a fivefold larger genome than those reported for unicellular or multicellular red algae. Hence, Glaucophyta may not have experienced the extent

of gene losses and genome simplification that occurred in the early diverging Rhodophyceae. In this context, one can view the exceedingly simple pathway of floridean starch synthesis in red algae as a highly derived character and the network evidenced in *Cyanophora paradoxa* as more ancestral. Remarkably, the *Cyanophora* genome contains the whole suite of genes that have been proven to be active for starch synthesis in Archaeplastida, with the only exception of ADP-Glc pyrophosphorylase. *Cyanophora* contains all the eukaryotic glycogen metabolism genes, including iDBE, as evidenced in *Dictyostelium discoideum*. The presence of bona fide indirect DBE came as complete surprise as multiple GLGX-ISA-like direct debranching enzymes are also evidenced in this genome. Some of the host-derived glycogen metabolism functions have remained simple such as α- and β-amylase and laforin, while others are present in multiple copies such as GT5 UDP-Glc starch synthases (2–3 genes), branching enzymes (3 genes), phosphorylases (2 genes), and DPE2-like amylomaltases (3 isoforms). Among the redundant enzymes we believe that multiple forms of both phosphorylases and BEs may have existed prior to plastid endodsymbiosis, as they do not present cases of more recent gene duplication followed by subfunctionalization. Hence, the multiple BE isoforms are, by no means, related to the BEI, BEII, BEIIa, and BEIIb subfunctionalizations that occurred specifically in the Chloroplastida lineage. In support of an early diversification of several enzymes in eukaryotes, we have indeed seen that glycogen phosphorylases often exist in distinct isoforms in amoebozoan genomes. On the other hand, some of the *Cyanophora* host glycogen metabolism network enzyme genes may have duplicated and subfunctionalized after plastid endosymbiosis. DPE2 amylomaltase-like genes usually present in 1 copy in glycogen metabolism networks are indeed present in multiple copies. This correlates with the presence of multiple copies of the GlgX-ISA-like DBEs. Because the eukaryotic glycogen metabolism network only contains DPE2 as an oligosaccharide-processing enzyme which is coupled to the presence of the maltose-producing β-amylase, we can hypothesize that duplication of DPE2 genes followed by subfunctionalization into enzymes with a less restrictive substrate specificity would have allowed metabolism of maltotetraose and longer glucans possibly produced by the multiple GlgX-ISA-like enzyme forms. This could also be the case when multiple DPE2s are evidenced in Rhodophyceae. These speculations are in agreement with the biochemical observation in *Cyanophora paradoxa* (Fettke et al. 2009) not only of a DPE2-like activity with high affinity to glycogen as in Chloroplastida but also of an enzyme form displaying lower affinity with respect to the glycogen acceptor. The *Cyanophora* genome also contains spectacular evidence of LGTs of chlamydial genes (see below). In phylogenetic trees there is even one of the chlamydial GlgX-ISA-like proteins that appears nested within the group of Chlamydiales, while two other copies are found together with the rhodophycean enzymes. The most spectacular finding in the analysis of the recently sequenced genome of *C. paradoxa* is no doubt the presence of a GT5 enzyme belonging to the SSIII-SSIV subgroup of ADP-Glc-utilizing archaeplastidal starch synthases (Price et al. 2012). In 2008, we speculated that the common ancestor of Archaeplastida probably contained an ADP-Glc-specific glucan synthase of the SSIII-SSIV family

(to account of the presence of such enzymes in the chloroplasts of green algae and plants) that enabled the polymerization of ADP-Glc into the cytosolic host storage polysaccharide stores (Deschamps et al. 2008b). Finding such an enzyme candidate sequence in the *Cyanophora* genome that moreover defines a common LGT from chlamydial intracellular pathogens further convinced us that Glaucophyta indeed defined the coelacanths of plastid endosymbiosis. Before the *Cyanophora paradoxa* genome had been sequenced, some biochemical investigations have been performed by Plancke et al. (2008) and by Fettke et al. (2009) with respect to the nature of the starch metabolism pathway and to its structure. Starch was shown to consist of high amylose (over 30 %) granules with an amylopectin fraction enriched in very small glucans displaying an otherwise bimodal chain-length distribution (Plancke et al. 2008). Multiple small-size cavities have been detected on the granules. These cavities too small to accommodate standard pyrenoid structures suggest that starch granules may be associated with specific cellular structures in the cytoplasm. The nature of such structures is unclear and deserves future attention. UDP-Glc-specific starch synthases had been clearly evidenced and studied as well as multiple forms of starch phosphorylases. One of the starch phosphorylase isoforms was found as a starch-bound 92 kDa protein. A bifunctional GBSS using both UDP-Glc and ADP-Glc was also found and studied (Plancke et al. 2008). However, the subsequent finding of two distinct GBSS genes in the *Cyanophora* genome may indicate that these properties may be carried differently by two distinct GBSS proteins. One important biochemical finding is that of a high mass multimeric isoamylase-like enzyme. In Chloroplastida such quaternary assemblies of isoamylase subunits are thought to be important for the insolubilization of soluble pre-amylopectin into insoluble starch (Ball et al. 1996). Although all archaeplastidal ISA-GlgX-like DBEs are derived from a single GlgX-like chlamydial ancestral protein, the diversification of chloroplastidal isoamylases into three distinct subunit enzymes is clearly posterior to redirection of the pathway to plastids. Hence, the two mutlisubunit enzymes have most probably evolved independently in Chloroplastida and Glaucophyta suggesting that such elaborate organizations are essential for efficient conversion of soluble to semicrystalline polysaccharides. The presence of a GBSS activity that displayed higher affinity (but lower activity) toward ADP-Glc correlates with a mixed inhibition of starch phosphorylase with lower concentrations of ADP-Glc when compared to UDP-Glc. These properties suggest either that these properties are fossils of a previous state when both glycosyl nucleotides possibly coexisted in the cytosol of the common Archaeplastida ancestor or that *Cyanophora paradoxa* still uses ADP-Glc today despite the absence of ADP-Glc pyrophosphorylase. In favor of the extant utilization of ADP-Glc is the finding of an SSIII-SSIV candidate sequence in the *Cyanophora* genome. Such enzymes indeed define glucan-elongating enzymes that exclusively use ADP-Glc both in cyanobacteria and Chloroplastida. All the results summarized above suggest that the glaucophyte network can be viewed as a living fossil of a very ancestral and interesting situation which has truly enlightened our vision of the evolution of starch metabolism. We believe that more experimental studies deserve to address many of the unknowns raised by these first reported genomic and biochemical studies.

4.2.5 *Starch Metabolism and Structure in Chloroplastida: Why So Complex?*

Starch metabolism in green algae has been the topic of many detailed studies and has been extensively reviewed (Ball 1998, 2002; Ball and Deschamps 2008; Busi et al. 2013). Thus, we will not further review this topic in this chapter. However, we believe that a comparison of the Chloroplastida network with those of their Glaucophyta and Rhodophyceae sister lineages remains of relevance here.

The most striking feature of the green lineage storage polysaccharide metabolism network is its very high level of functional redundance. A minimum of 30 and most often over 40 genes are thought to explain the complexity of starch metabolism in plants. Yet this astonishingly high number of isoforms has been generated from a less diverse number of ancestral genes than that which is present in extant Glaucophyta. This can be quite simply explained if one considers that storage polysaccharide metabolism was exclusively cytosolic in the common ancestors of the Archaeplastida and that all the genes of the cyanobacterial enzyme network with the exception of ADP-Glc pyrophosphorylase had already been lost from the cyanobiont genome (as is the case today for the chromatophore genome of *Paulinella chromatophora* (Nowack et al. 2008). The transfer of the starch network to the plastid was triggered by some unknown selection pressure. We have proposed that resistance to additional photooxidative stresses, generated by the evolution of the LHC antennae, adapted to high light intensities, might have generated a demand for a storage polysaccharide pool to prevent ROS synthesis or ROS-induced damage, due among others to chlorophyll biosynthesis (Deschamps et al. 2008c). Anyhow, the previous loss of storage polysaccharide metabolism genes from the cyanobiont would have considerably complicated the return of such enzymes to the plastid. Indeed, it is impossible to imagine that all the required genes from the cytosolic starch network would have simultaneously duplicated and simultaneously acquired plastid-targeting signal. Hence, it is impossible to imagine that rewiring starch metabolism to plastids could occur in one step, or only a few steps, in a way compatible with such steps being retained by natural selection. Fortunately, this complexity can be broken down into a series of manageable steps, if one envisions that the return of glucan metabolism to plastids was a very long process, encompassing two intermediate states, that may have lasted thousands or millions of years. Hence, we proposed that the evolving Chloroplastida first contained a major starch pool in the cytosol and a minor MOS pool in plastids (as may be the case for extant Florideophycidae, which have been convincingly shown to contain plastidial glucan lyase and hence must contain either glycogen or more likely MOS in the rhodoplasts) (Deschamps et al. 2008d). This may have lasted for a while, until natural selection may have favored the evolution of a larger pool of plastidial glycogen. During that time, starch was still accumulated in the cytosol. Finally, plastidial starch synthesis was favored over that of cytosolic polysaccharide synthesis. The interesting thing about these intermediate stages is that we know that the biochemical properties of enzymes that have become optimized to act either on

MOS or on glycogen or starch are quite different and exacting. Hence, to move from one stage to another, it would have been easier to duplicate a gene from the cytosolic starch metabolism network and subfunctionalize it rather than accumulate mutations within a single enzyme, to optimize it, with respect to several distinct situations. We believe that this very neatly explains the specific redundancy of the enzymes of the Chloroplastida network and have previously reviewed this topic in reasonable detail (Deschamps et al. 2008a, b, c, d). It is by this mechanism that the unique glaucophyte-like chlamydial SSIII-SSIV gene has duplicated and generated several isoforms finally yielding the SSIII and SSIV enzymes. This process also explains the generation of SSI and SSII from duplicated cytosolic GBSS gene copies, the generation of BEI and several BEIIs from the unique rhodophycean BEI-II-like enzyme, the generation of ISA2 and ISA3 from a unique ISA2-3-like cytosolic chlamydial ancestor, the generation of several BAM proteins from the unique rhodophycean gene, etc. In this process, some of the archaeplastidal enzymes appear to have resisted recruitment to the plastid. This could be due possibly to problems dealing with their targeting to plastids. Such enzymes might display a low suitability to interact with chaperones and to renature correctly in the plastid stroma. This may explain why, for instance, a DPE2-like protein was not recruited from the starch cytosolic network as an α-1,4-glucanotransferase and why, consequently, an LGT of DPE1 from a foreign proteobacterial source was favored. This may also be a reason why pullulanases are polyphyletic in Rhodophyceae and Chloroplastida. Resistance of laforin to targeting to plastids may also explain why a new gene was created with reorganized CBM and dikinase domains. Notwithstanding these exceptions, the green lineage starch metabolism network can be quite simply explained from recruitment from a subset of proteins evidenced in Glaucophyta and Rhodophyceae. In addition to DPE1, the only true novelty in the chloroplastidal starch metabolism network seems to be the MEX1 transporter (Lu and Sharkey 2006). This gene may have been created de novo during Chloroplastida evolution. On the other hand it may have been recruited by LGT from a cyanobacterial source since a single but significant case of MEX-like protein was found in these organisms (Weber, personal communication). Another striking observation in Chloroplastida as a whole is the astonishing level of conservation of isoform number and functions, from the earliest diverging picophytoplanktonic Prasinophyceae microalgal species to the highly sophisticated and comparatively much more recently diverging monocot plants. This also applies to Rhodophyceae when considering the evolutionary distance between Cyanidiales and *Florideophycideae*. In the prasinophyte *Ostreococcus tauri*, small cell size correlates with the simplification of most plant pathways, the only exception being starch metabolism. These observations suggest that unlike most of the redundancies witnessed today in land plant networks which can be attributed to the acquisition of multicellularity, starch metabolism complexity reflects a very early and specific event that occurred during evolution of the very first green cells. This complexity reflects that of the biochemical rewiring of pathways in novel cellular compartments, rather that any intrinsic complexity in the biochemistry of starch synthesis and mobilization.

4.2.6 Starch Metabolism and Structure in Cryptophytes

Cryptomonads are single-cell biflagellated protists, which live both in marine and freshwater environments. At the basis of the cryptomonad clade lies heterotrophic species belonging to the genus *Goniomonas*, with no evidence of a past phototrophic history (for review see Deane et al. 2002). These phagotrophic organisms have no plastids or starch and are not reported to contain storage polysaccharides. They are close to the so-called katablepharids, another clade of poorly described heterotrophic biflagellated phagotrophs. The cryptophytes are cryptomonads which have undergone secondary endosymbiosis with a red alga. Many cryptophyte clades are known to inhabit environments with low light and they are among those photosynthetic organisms that are able to fix carbon deep into the water column thanks, among others, to the phycobilin-containing pigments they have inherited from their red algal symbionts. Cryptophytes and chlorarachniophytes are unique among secondary endosymbiosis lineages, by the fact that the periplastidial space, which corresponds to the cytoplasm and nucleus of the alga symbiont, has not undergone the dramatic reduction evidenced in stramenopiles, haptophytes, euglenids, or alveolates. In both clades, a remnant of the nucleus of the engulfed alga, called the nucleomorph, remains with 50–200 genes located in three minichromosomes. All four genomes (nuclear, nucleomorph, plastid, and mitochondria) of the model cryptophyte species *Guillardia theta* have been sequenced (Archibald and Lane 2009; Curtis et al. 2012; Douglas et al. 2001; Douglas and Penny 1999; Grosche et al. 2014). Unlike all other secondary endosymbiosis lineages, cryptophytes accumulate starch in the periplast with no evidence for the presence of any kind of storage polysaccharide in the cytosol. Deschamps et al. (2006) and Haferkamp et al. (2006) have studied the structure biosynthesis and degradation of this periplastidial starch. The starch structure resembled that reported for *Chlamydomonas*. It contained amylose and an active GBSS that could use both ADP-Glc and UDP-Glc efficiently (Deschamps et al. 2006). The GBSS had properties analogous to the *Chlamydomonas* enzyme, but with a lower specific activity. The GBSS protein displayed a phylogeny consistent with the red alga ancestry of the plastid symbiont. It had a plastid-targeting bipartite topogenic signal, with both a typical signal and transit peptide. The transit peptide however did not start with the canonical phenylalanine thought to condition import of proteins in glaucophyte muroplasts and in Rhodophyceae rhodoplasts (Steiner et al. 2005). This phenylalanine was replaced by a serine in the GBSS sequence; as a result of that the protein, that had crossed the first two membranes, thanks to the signal peptide, was trapped into the periplastidial space (Haferkamp et al. 2006). The serine-containing transit peptide was nevertheless cleaved off. No trace of ADP-Glc pyrophosphorylase activity, protein, or gene could be found in *Guillardia* through enzyme or antibody assays or bioinformatic studies. Again consistent with the red alga ancestry of the symbiont, only UDP-Glc-specific soluble glucan synthases could be evidenced biochemically. We were thus expecting to find a gene encoding the unique characteristic GT5 multipurpose rhodophycean enzyme, upon annotating the *Guillardia theta* genome.

What we found, instead, was five distinct GT5 enzymes of an entirely different type. This type consisted of enzymes phylogenetically derived from the chloroplastidal GBSS-SSI-SSII superclade. The phylogeny rejected a red alga ancestry but was consistent with either a green alga GBSS or a green alga SSI or SSII source. Because we do not see any evidence for a green alga bona fide GBSS in *Guillardia*, we believe that SSI or SSII are the most likely sources for such enzymes. It must be remembered that SSI and SSII are, most probably, derived phylogenetically from the duplication of an ancestor green alga GBSS gene, during the reconstruction of storage polysaccharide metabolism, within the evolving green chloroplast. The soluble SSI and SSII glucan synthases in green algae and terrestrial plants clearly cannot sustain glucan synthesis on their own, because of their inability to prime polysaccharide synthesis. Furthermore, these soluble enzymes are thought to be distributive in their mode of action and to differ by their ability to yield different size classes of glucans. We would like to propose a plausible mechanism for their evolution.

After secondary endosymbiosis of the red alga symbiont, the latter encoded the unique and multipurpose GT5 rhodophycean enzyme within its nucleomorph genome. This defined a truly magical protein able to prime polysaccharide synthesis, to interact with rhodophycean BE, to produce glucans with chain-length distribution compatible with their insolubilization into amylopectin-like molecules, and to be targeted by the kinases and phosphatases that regulate storage polysaccharide metabolism in the eukaryotic cytosol. Most of these functions are taken over by four and three different specialized starch synthases, respectively, in the green lineage and glaucophytes. We have outlined previously that in Rhodophyceae, there has been and still is a selection pressure for the maintenance of small-size genomes and a low total number of genes. Once trapped within its host, the selection pressure that previously applied to the rhodophycean genome no longer held for the host nuclear genome. Why did the unique gene encoding the GT5 rhodophycean enzyme not transfer to the host nucleus? There are several possibly not mutually exclusive explanations to this difficult question. First, for some unknown reason the frequency of transfer of genes from the symbiont genome to the host nucleus may be significantly lower than the rate of transfer from other sources (viruses, transformation, phagotrophy . . .). These unknown reasons might also be those that explain the maintenance of the nucleomorph in cryptophytes. It was proposed that one possible reason would be the maintenance of the symbiont, at one or two copies per cell, which would preclude autophagy as a possible source for symbiont DNA (Curtis et al. 2012). This, at first glance, seems to be supported by the observation that plastid DNA transfer to the host nucleus can be reproduced experimentally in tobacco (Stegemann et al. 2003) which harbors several plastids per cell while it cannot be reproduced in *Chlamydomonas reinhardtii* which contains a single chloroplast (Lister et al. 2003). This is also supported by the recent observations made on insect bacterial endosymbionts (Husnik et al. 2013). In this context, those that will be transferred to the host nucleus are only those rhodophycean genes that cannot, for functional reasons, be replaced by genes from other sources. But even in that case, one cannot exclude that the actual source for the transferred rhodophycean sequence

may have been a piece of DNA coming from an organism highly related to the symbiont, present in the environment and entering the organism, through the same mechanisms as those from standard lateral gene transfers. Another reason which may have prevented LGT of the unique multifunctional GT5 rhodophycean enzyme would be the possible intrinsic inability, for this enzyme, if synthesized in the host cytosol, to follow the classical route of proteins targeted to the periplast through the bipartite topogenic signal. This route entails the ability for the protein to be taken in charge by defined chaperones, through the ER and through the periplastidial membrane, and then refold in the periplast. As far as we know, GT5 UDP-Glc-specific glucan synthases are only found in the cytosol of eukaryotes, and no genes encoding such enzymes have adapted to the targeting of their gene product in other cellular compartments. Thus, is it is entirely possible that the targeting of such an enzyme to the periplast would require several mutations in the gene sequence, further complicating its recruitment. The SSI-SSII chloroplastidial sequence offered several advantages for their recruitment in this context. The gene already carried a transit peptide and was adapted to protein targeting to plastids. It thus only needed to be fused downstream of a possible signal peptide to generate the BTP-containing protein. The enzyme had already been optimized with respect to its suitability in renaturing in foreign environments and to be taken in charge by different types of protein chaperones. In addition, being derived from GBSS, which is able to accommodate both types of nucleotide sugars in all three archaeplastidal lineages, the recruited sequence could have evolved fast into a protein able to use UDP-Glc as predominant or sole glycosyl-nucleotide substrate. Nevertheless, this change of selectivity and of environment is evidenced by the presence, in phylogenies, of a long branch supporting the *Guillardia* enzymes, within the chloroplastidal GBSSI-SSI-SSII superclade. The chloroplastidan enzyme was not able to replace, at once, all the functions played by the unique rhodophycean Swiss knife-like enzyme. We believe it initially played a minor, but significant, role by supplying different lengths of glucans to the otherwise monomodal, semi-amylopectin-like structure evidenced in floridean starch of Rhodophyceae. Because the previous selection pressures that maintained simplicity in the red alga genome were no longer operating on the secondary alga nuclear genome, natural selection favored the appearance of a green alga-like multimodal distribution of amylopectin chains and the LGT of the novel SSI-II-like synthase was selected. After selection, both genes were subfunctionalized. The chloroplastidan glucan synthase specialized, for instance, in the synthesis of a subset of chains and the rhodophycean enzyme specializing in the synthesis of chains of distinct lengths. During this process, random gene duplications occurring in the nuclear genome of the host would have sent additional forms of the chloroplastidan enzyme in the periplast, opening further opportunities for mutations, followed by subfunctionalization, to take over additional specialized functions, such as synthesis priming, interaction with branching enzyme, or synthesis of glucans of distinct lengths. The rhodophycean enzyme progressively retreated into a more and more specialized role, until the last nuclear gene duplication of the SSI-SSII-related gene covered the last specialized role of the GT5 rhodophycean

enzyme. The latter could thus now be lost from the nucleomorph genome and was definitively replaced by five separate SSI-SSII-like green genes.

In the case of Guillardia's GBSS, why was this enzyme not replaced by a green alga gene? One striking feature of periplastidial starch synthesis in cryptophytes is the physical association between starch and the pyrenoid across the two inner membranes of the secondary plastid (starch being periplastidial) that separate the starch granule from the pyrenoid surface. In green algae, starch is directly in contact with the pyrenoid in the stromal space of the chloroplast. The presence of GBSS in algae seems to correlate with a need for pyrenoidal starch synthesis (see Sect. 4.3.7). The synthesis of amylose by GBSS in red and green algae is thus adapted to metabolite concentrations which could be different because of a different cellular compartmentalization. GBSS is an enzyme of cyanobacterial origin, initially present in the cytosol of the Archaeplastida common ancestor (Deschamps et al. 2008a). A GBSS sequence was recruited in the ancestor green algae to be targeted to the chloroplast. There is thus no specific reason to suppose that the rhodophycean enzyme would not likewise be recruited by the host cell to be targeted to the secondary periplast. Hence, because of functional reasons, the red alga gene was favored over a green alga version. When we look at the branching enzyme genes in the *Guillardia theta* genome, we here again are surprised to find two distinct sequences unrelated to the single rhodophycean enzyme sequence. The rationale for the recruitment of such enzymes would be the requirement of diversification of BE activity when several distinct glucan elongation enzymes had been selected. The subfunctionalization of two single novel enzymes to suit the novel SSI-SSII starch synthases was favored over the highly selected red algal enzyme adapted to function with the rhodophycean sole glucan synthase. The two BEs are phylogenetically related to either chlorophyte sequences of rather restricted distribution (present in only a few green algae) or a group of cyanobacterial and alveolate sequences. Once again, recruitment of foreign enzymes seems either to have been favored or to have happened more rapidly. As far as phosphorylases are concerned, two sequences affiliated respectively to amoebozoa and glaucophytes and alveolates have been found in the genome. The predominance of enzymes of eukaryotic phylogeny, when looking at phosphorylases and branching enzymes, begs the question of the host status prior to secondary endosymbiosis. We know nothing about the possible accumulation of small amounts of either glycogen or β-glucans or both in the putative heterotrophic host ancestors exemplified by *Goniomonas* and katablepharids. Hence, what is presently seen as a complex set of HGTs might simplify into a vertical inheritance component, if such organisms were shown to contain glycogen metabolism genes. One must also remember that nearly all phagotrophs contain some genes of α-glucan catabolism as they need to digest α-glucan containing preys. In this respect, it is striking to note that at least one beta-amylase gene of *Guillardia theta* is phylogenetically related to a *Naegleria* enzyme. *Naegleria gruberi* is known to lack glycogen metabolism and to synthesize β-glucans. These enzymes evolved in these organisms to digest their preys. Other enzymes of starch catabolism defined by the GWD-PWD dikinases and by the DPE2 amylomaltases are found in the *Guillardia* genome. It is striking

to see that in both cases some isoforms display a clear red algal phylogeny (3 out of 5 DPE2 candidate sequences) and one PWD candidate sequence, while all others make a very convincing case for a green algal phylogenetic origin. The phylogenies are unambiguous and the aforementioned enzymes can be classified as green or red with confidence. From the preceding discussion, the cryptophyte starch metabolism network appears to be defined as a very complex patchwork of genes of distinct phylogenetic origins. A significant minority of enzymes seem to have been recruited from the symbiont rhodophyte starch metabolism network, while a majority seem to have been recruited from green algae. In addition, a significant component of eukaryotic glycogen metabolism networks is present in cryptophytes, which is unrelated to the classical archaeplastidal enzymes. Whether this defines another case of recruitment of foreign genes or whether such sequences were present in the heterotrophic ancestors of cryptophytes remains to be investigated. The most surprising discovery in the *Guillardia* genome as far as starch metabolism is concerned lies no doubt in the absence of candidate gene sequence for direct or indirect starch or glycogen debranching enzymes. Because the genome is well covered, reasonably assembled, and well annotated, it seems unlikely that such sequences would have escaped us (Curtis et al. 2012). However, a candidate direct debranching enzyme activity was evidenced biochemically but not characterized in detail. It remains possible that among the GH13 α-amylase-like sequences, some activities may, in fact, define a novel kind of debranching enzyme. *Guillardia theta* and cryptophytes may thus very well define a case where crystallization of amylopectin may not rely on previously described starch debranching enzymes.

4.2.7 Starch Metabolism and Structure in Alveolates

Alveolates define a monophyletic grouping of three major eukaryotic clades: the early diverging heterotrophic ciliates, the dinoflagellates, and the obligatory intracellular apicomplexa parasites. Alveolates are always unicellular. A majority of alveolates are heterotrophic (all ciliates, all apicomplexa, and many dinoflagellates). However, many dinoflagellates and all chromerids are considered as photosynthetic algae. There is a very complex and controversial endosymbiotic history in alveolates (Baurain et al. 2010; Cavalier-Smith 1999). The presence of a true nonphotosynthetic plastid in apicomplexa parasites and of red alga-derived photosynthetic plastids in chromerids (a clade intermediate between dinoflagellates and apicomplexa) and some dinoflagellate species (known as the peridinin plastid-harboring dinoflagellates) argues for a secondary "red" endosymbiosis at least in the common ancestor of dinoflagellates and apicomplexa (Delwiche 1999). However, if such a founding event indeed exists, the exact position of secondary endosymbiosis of a red alga remains controversial and some studies suggest that this event occurred in the common ancestor of all alveolates including the early diverging ciliates (Reyes-Prieto et al. 2008). The picture is further considerably complicated by the occurrence of several tertiary endosymbioses that occurred selectively in dinoflagellates

(tertiary endosymbiosis qualifies the capture by a eukaryotic phagotroph of a secondary endosymbiosis-derived alga). During these tertiary endosymbiosis, heterotrophic dinoflagellate phagotrophs themselves resulting most probably from secondary endosymbiosis, followed by plastid loss, or loss of photosynthesis, or both, have acquired plastids from other primary or secondary eukaryotic algae, leading to an astonishing diversity of plastids (for a review of dinoflagellate evolution, see (Wisecaver and Hackett 2011)). To further complicate the issues, both dinoflagellates and ciliates are able to transiently steal and benefit from plastids or algae ingested by phagocytosis, a phenomenon known as kleptoplasty (Serodio et al. 2014). In all alveolates, storage polysaccharides are found in the cytosol in the form of either glycogen found in majority of ciliates or of starch found in most dinoflagellates and apicomplexa. There are some exceptional cases where storage polysaccharide metabolism was lost altogether. This seems to have been the case in the malaria-causing *Plasmodium* genus and in related apicomplexa. Most other apicomplexa seem however to have retained starch metabolism in their cytosol (Coppin et al. 2004). Among ciliates, a glycogen structure was convincingly reported for *Paramecium aurelia* and *Tetrahymena* (Manners and Ryley 1952). However, paraglycogen, a polysaccharide described as amylopectin like, has been reported in more ancestral (holotrich) ciliates (Forsyth and Hirst 1953). Looking at the genome contents of *Apicomplexa*, a picture of a rather simple pathway emerges, characterized by one major GT5 UDP-Glc-specific glucan synthase candidate sequence of two to three branching enzymes of a single iDBE α-amylase, GWD, and starch phosphorylase. The starch of *Toxoplasma gondii* was shown to consist only of amylopectin, with a structure recalling the semi-amylopectin structures of cyanobacteria and Rhodophyceae, because of the monomodal type of CL distribution (Coppin et al. 2004). An enzyme preferring UDP-Glc over ADP-Glc could be evidenced in *T. gondii* extracts. Ciliates are characterized by a comparable simple synthesis pathway but with a significantly higher number of enzymes involved in glycogen catabolism. Phylogenetically speaking there are both overlaps and specificities in the distinct isoforms, when apicomplexa and ciliates are compared. For instance, ciliates have one of their branching enzymes in common with apicomplexa, but also display a ciliate-specific isoform related to Rhodophyceae and Glaucophyta, while apicomplexa also have an additional specific isoform, phylogenetically related to one of the three glaucophyte BEs. One of the distinctive features of the ciliate apicomplexa network is both the absence of direct DBE and that of β-amylase and the DPE2 amylomaltases. As far as dinoflagellates are concerned, the picture, as could be expected, seems to be much more complicated with respect to the number and diversity of enzymes, probably as a consequence of tertiary endosymbioses. In *Symbiodinium*, the dinoflagellate species living in symbiosis with corals and which, supposedly, contains the classical peridinin-containing plastids, the network detected in the partial genome sequence included direct DBEs such as pullulanases and isoamylases and β-amylases (Shoguchi et al. 2013). It is not clear though that the peridinin-containing dinoflagellate plastids define the original secondary

plastids of dinoflagellates. EST sequencing of heterotrophic dinoflagellates, such as *Crypthecodinium cohnii*, has indeed been shown to contain genes encoding proteins with plastid-targeting sequences (Sanchez-Puerta et al. 2007). Hence, it is entirely possible that dinoflagellates may have lost photosynthesis very early on and adopted the phagotrophic way of life. All known plastid-containing photosynthetic dinoflagellates may thus represent tertiary endosymbiosis events, and their biochemical network of starch metabolism must be considered under this light as suggested by Petersen et al. (2014).

Deschamps et al. (2008a, b, c, d) and Dauvillee et al. (2009) have performed a detailed study of starch synthesis and structure, in the early diverging heterotrophic dinoflagellate *Crypthecodinium cohnii*. They found a classical starch, which unlike apicomplexa, contained both amylopectin and amylose. The amylopectin displayed a polymodal CL distribution similar to cryptohyte or green alga starch (Deschamps et al. 2008b). *C. cohnii* starch was crystalline and displayed an A type of diffraction pattern like that of green algae and cryptohytes and unlike starch from *Cyanophora paradoxa* which was of the classical B type. The dinoflagellate GBSS was quite different from those found in cryptophytes, Rhodophyceae, Glaucophyta, and Chloroplastida. First, it contained a 110 kDa GBSS, twice as large as standard GBSS proteins. This was mainly due to a large extension at the N-terminus, which seems to be conserved in other dinoflagellates. This GBSS differed from all other enzymes of this type by the fact that it did not use ADP-Glc at detectable rates and therefore defined an exclusively UDP-Glc-utilizing enzyme. Zymogram analysis revealed several UDP-Glc-utilizing soluble starch synthases and a set of glycosyl hydrolases and transferases. *Crypthecodinium cohnii* had been previously described as a manageable genetic system where selection of mutants and genetic crosses are feasible (Tuttle and Loeblich 1974, 1977). Deschamps et al. (2008a, b, c, d) and Dauvillee et al. (2009) have selected mutants showing various altered starch accumulation phenotypes, by screening through iodine vapors. Mutants showing a selective defect in the UDP-Glc-specific soluble starch synthase zymogram pattern were isolated with reduced starch accumulation. The low starch phenotype co-segregated in crosses with the glucan-synthase defect. This suggests strongly that the bioinformatics-based speculations proposing a UDP-Glc pathway in the cytosol of several lineages, other than the green algae and plants, are likely to be correct. Another interesting feature of starch metabolism in *Crypthecodinium cohnii* is the timing of storage polysaccharide accumulation. In this heterotrophic dinoflagellate, starch typically accumulates in log-phase cultures, as soon as glucose is added to the medium, a situation very different from what happens in most heterotrophic bacteria and fungi, where glycogen most often accumulates at the transition between log and stationary phase. This, according to Deschamps et al. and Dauvillée et al., correlates with the phagotrophic nature of these marine organisms that have to deal with sudden bursts of reduced carbon in an otherwise oligotrophic medium (Dauvillee et al. 2009).

4.2.8 Glycogen Metabolism in Excavates

Excavates represent mostly unicellular flagellated eukaryotes harboring 2–4 flagellae and most often a conspicuous ventral feeding grove (hence the term excavates). Some amoebal forms are known, as well as a few multicellular slime molds. The excavates may not define a monophyletic group and are usually thought to have diverged close to the root of the eukaryotic tree. From the point of view of storage polysaccharides, among the two major excavate divisions, the amitochondriate metamonads and the discoba that contain discoid cristae within the mitochondria, only the former seems to accumulate glycogen as storage polysaccharide (Ladeira et al. 2005; Manners and Ryley 1955), while the latter (with organisms such as *Naegleria*, *Trypanosoma*, or *Euglena*) are reported to contain either β-glucans, such as paramylon, or mannans, or both. The metamonads have a glycogen metabolism network resembling that of Amoebozoa (see Fig. 4.3). It is most probably UDP-Glc based and contains, as in Amoebozoa, both a GT3 (found exclusively in *Giardia lamblia*) and a GT5 UDP-Glc-specific glucan synthase (found exclusively in *Trichomonas vaginalis*). Surprisingly, candidate-glycogenin-like sequences have been found associated with the *Trichomonas* network and not in the GT3 GS-containing *Giardia*. Both metamonad clades contain eukaryotic iDBE phosphorylase and BE. A DPE2-like amylomaltase candidate sequence is found in both clades, but convincing β-amylase candidate sequences usually associated with DPE2 are only found in *Trichomonas*. The corresponding enzyme sequences usually yield long branches in phylogenetic trees, complicating their positioning. Because of this and their parasitic way of life, caution must be taken with respect to the presence of possible LGTs in their storage polysaccharide enzyme networks.

4.3 The Evolution of the Starch Pathway in Archaeplastida

4.3.1 Reconstructing the Ancient Network of Starch Metabolism in Archaeplastida

If we compare the storage polysaccharide metabolism networks in Archaeplastida that are evidenced in Fig. 4.3 and if we inspect the corresponding phylogenetic trees, a picture emerges that agrees with the monophyletic nature of the Archaeplastida. There is a complete set of genes encoding the full suite of enzymes required for eukaryotic glycogen metabolism in Glaucophyta. This network resembles that evidenced in *Trichomonas* and Amoebozoa. It typically includes GT5 UDP-Glc-specific glycogen (starch) synthase, eukaryotic BEs and phosphorylase, iDBE, and unlike fungi and animals (but like excavates and Amoebozoa) DPE2 and β-amylase. In addition to this, it most probably contained the laforin phosphatase, which is not found as such in the excavates and Amoebozoa but which is present in the animal lineage. As pointed out, the Rhodophyceae display a comparable network which

however lacks the iDBE which was anyhow potentially redundant with the direct ISA-GlgX-like DBEs and was probably lost because of this. The Chloroplastida also lack the iDBE but further lack the UDP-Glc-specific GT5 glycogen synthase. All other eukaryotic enzymes, with the noticeable exception of DPE2, and one of the phosphorylase isoforms are located in plastids in the green algae and land plants, while the whole network including the storage polysaccharide is entirely cytosolic in Rhodophyceae and Glaucophyta. Glaucophyta and Chloroplastida also share GT5 SSIII-SSIV-like glucan synthases. These enzymes are of bacterial origin and in all bacteria examined to date use ADP-Glc as a substrate. In *Cyanophora*, the corresponding enzyme is most probably cytosolic, while the SSIII-IV starch synthases are plastidial in the green lineage. Also found in all three lineages is GBSS an enzyme with a cyanobacterial monophyletic origin. This enzyme is always associated to starch granules and is selectively responsible for amylose synthesis. In cyanobacteria and Archaeplastida, this starch synthase is unable to synthesize glucans as a soluble enzyme. Hence, the presence of a common single GBSS gene suggests that the last common ancestor of all Archaeplastida was a starch accumulator. This last common ancestor must thus have had the possibility not only to synthesize semicrystalline polysaccharides but also and most importantly to mobilize them. The presence of the bacterial ISA-GlgX-like direct DBEs, in all Archaeplastida, is in line with this observation, since these enzymes have been demonstrated, both in Chloroplastida and cyanobacteria, to be responsible for the aggregation of precursors of amylopectin synthesis into semicrystalline starch granules. In cyanobacteria, insoluble semi-amylopectin starch-like granules can be directly digested by starch bound phosphorylases. Eukaryotic glycogen phophorylases or β-amylases and their archaeplastidal derivatives are, however, unable to digest starch. Hence, one wonders why the cyanobacterial phosphorylase gene was not transferred to the eukaryotic nucleus for expression in the cytosol. In the last common archaeplastidal ancestor, a novel pathway of starch catabolism emerged (see Cenci et al. 2014 for detailed discussion). This made use of a preexisting pathway of glycogen phosphorylation that included an unknown glycogen kinase and the corresponding laforin phosphatase (see Sect. 4.2.1). The transition of glycogen to starch metabolism in the last common archaeplastidal ancestor was made possible by the replacement of the preexisting glycogen kinase, that was ineffective toward crystalline starch, by a novel enzyme resulting of a rather simple gene fusion (Cenci et al. 2014). This consisted of a fusion of a CBM (carbohydrate binding module) to a preexisting dikinase domain. This protein was able to drive the phosphorylation of amylopectin crystallites, thereby rendering the inaccessible hydrophobic crystals more hydrophilic and thus accessible to the eukaryotic enzymes of glycogen catabolism that were poorly adapted to deal with such structures. This gene fusion possibly generated the first glucan-phosphoglucan water dikinase, which defines the only true novelty that was made in the common ancestor of Archaeplastida (Cenci et al. 2014). Hence, the minimum number of genes that must have been contained in the last common ancestor of Archaeplastida, to explain, through vertical inheritance, the extant distribution of genes in Archaeplastida, consists of one GT5 UDP-Glc-specific glycogen (starch) synthase, one SSIII-SSIV ADP-Glc-specific glucan

synthase, one ADP-Glc pyrophosphorylase subunit, two branching enzymes, one phosphorylase, one β-amylase, two DPE2-like amylomaltase (one supplying the DPE1-like function), two ISA-GlgX (one supplying the isoamylase function), one iDBE, one GBSS, one PWD-GWD-like protein, and one laforin (Deschamps et al. 2008c). ADP-Glc pyrophosphorylase defined the only protein which we suspect to have been active in the evolving plastids. Indeed, this enzyme of cyanobacterial phylogenetic origin is tightly coupled through its substrates and allosteric effectors to the Calvin cycle. Since the Calvin cycle never left the plastid stroma, it is reasonable to assume that the enzyme remained in this compartment. We have proposed that, apart the maintenance of ADP-Glc pyrophosphorylase, most other cyanobacterial enzymes of storage polysaccharide metabolism were lost in the common Archaeplastida ancestor. This proposal is justified through several distinct observations:

1. Today in both Glaucophyta and Rhodophyceae, there are no traces of storage polysaccharides in the plastid.
2. In general a correlation has been established between the obligate intracellular nature of bacteria and the absence of storage polysaccharide metabolism (Henrissat et al. 2002). A remarkable exception to this rule is defined by the Chlamydiales intracellular pathogens. The cyanobiont would thus be expected to lose its ability to synthesize storage polysaccharides early on. This has in fact happened in the chromatophores of *Paulinella* where no traces of starch, glycogen, or glycogen metabolism genes can be found (Nowack et al. 2008), while the α-cyanobacterial free-living ancestors of chromatophores contain the full suite of cyanobacterial glycogen metabolism genes.
3. The complexity of starch metabolism in Chloroplastida can be easily explained, if the cyanobiont had lost its glycogen metabolism genes. Had the evolving cyanobacteria kept its glycogen metabolism pathway, the replacement of the cyanobiont enzymes by eukaryotic versions would not have been as systematic, nor would it have entailed such dramatic duplications and subfunctionalizations. One would have expected at least partial conservation of some cyanobacterial enzymes through HGT to the nucleus, as well as occasional replacement of cyanobacterial enzyme versions, by enzymes from other bacteria, which would be better adapted to the prokaryotic pathway of storage polysaccharide metabolism.
4. The efflux of carbon from the cyanobiont and cyanobacterial storage polysaccharide synthesis are competing processes. The early transfer of the chlamydial ATP translocator to the three archaeplastidal lineages, by HGT, argues that there was an early need for ATP in darkness in the evolving cyanobiont. Such a need would not have existed, if the latter had substantial storage polysaccharide pools.

From all these considerations, we hypothesize the presence of a cytosolic network of starch metabolism (Fig. 4.4b) in the last common ancestor of Archaeplastida with no significant pool of polysaccharides synthesized by the cyanobiont. The presence of the bacterial SSIII-SSIV glucan synthase in the cytosol of the last common ancestor suggests that this ancestor fed both ADP-Glc and UDP-Glc into starch metabolism. This implies that, to be used in the ancestor's cytosol, this bacterial specific glycosyl nucleotide synthesized by the cyanobiont must be

exported to the host cytoplasm by a suitable transporter. For this reason, we have inferred the presence of a nucleotide-sugar translocator in the inner membrane of the evolving plastid.

The evidence that we have concerning the existence of an ancient ADP-Glc translocator in the last common ancestor of the Archaeplastida comes from the phylogenetic analyses performed by Weber et al. (2006) and the functional studies reported by Colleoni et al. (2010). Indeed, Weber et al. (2006) reported that all extant carbon translocators of the major pPT family that are present on the inner membrane of plastids of Rhodophyceae and Chloroplastida can be traced back to a unique ancestral protein, which is derived from a eukaryotic (host) *n*ucleotide-*s*ugar *t*ranslocators (Weber et al. 2006). These purine sugar nucleotide transporters that include Golgi GDP-mannose translocators were demonstrated to transport ADP-Glc, as fast as their normal substrate, but with lower affinity (Colleoni et al. 2010). In addition to this, the most studied extant pPT carbon translocator (the triose-phosphate translocator) has been previously demonstrated to be able to reach the mitochondria's inner membrane when expressed in yeast without its transit peptide (Loddenkotter et al. 1993). This remarkable property if it was displayed by the ancestral protein would have greatly facilitated its recruitment at a time where protein targeting machineries to the evolving plastid had not *yet appeared*.

4.3.2 In the Beginning There Was . . . Glycogen?

The reconstruction proposed in Fig. 4.4b defines a status of storage polysaccharide metabolism compatible only with the presence of starch in the eukaryotic cytosol. This does not define the status of storage polysaccharide at the onset of plastid endosymbiosis, but rather that which characterized the last common ancestor of the three Archaeplastida clades. This last common ancestor already had common elements of the machinery targeting proteins to plastids and defined a significantly advanced stage of metabolic integration of the evolving cyanobiont. By looking at the extant diversity of heterotrophic eukaryotes, there is no evidence for the accumulation of starch in clades other than those derived from primary or secondary endosymbiosis of the plastid. Hence, at the onset of plastid endosymbiosis, we can safely assume the presence of a slightly more simple network than that displayed in Fig. 4.4b. This network yielded glycogen rather than starch in the cytosol. Hence, there was no immediate need for glucan nor phosphoglucan water dikinases, no need for GBSS which is only active when associated to starch granules, and no need for multiple forms of ISA-GlgX-like proteins. This status of storage polysaccharide is displayed in Fig. 4.4a. Nevertheless, we believe that the transition from glycogen to starch metabolism was rapidly favored because of the huge amounts of photosynthetic carbon that became available to the Archaeplastida ancestor. This transition was probably facilitated by the presence, at the onset of plastid endosymbiosis, in the cytosol of an ancestral GlgX direct DBE. This activity as discussed in this review is not a natural component of the cytosolic glycogen metabolism machinery, and its presence in the eukaryotic cytosol at the onset

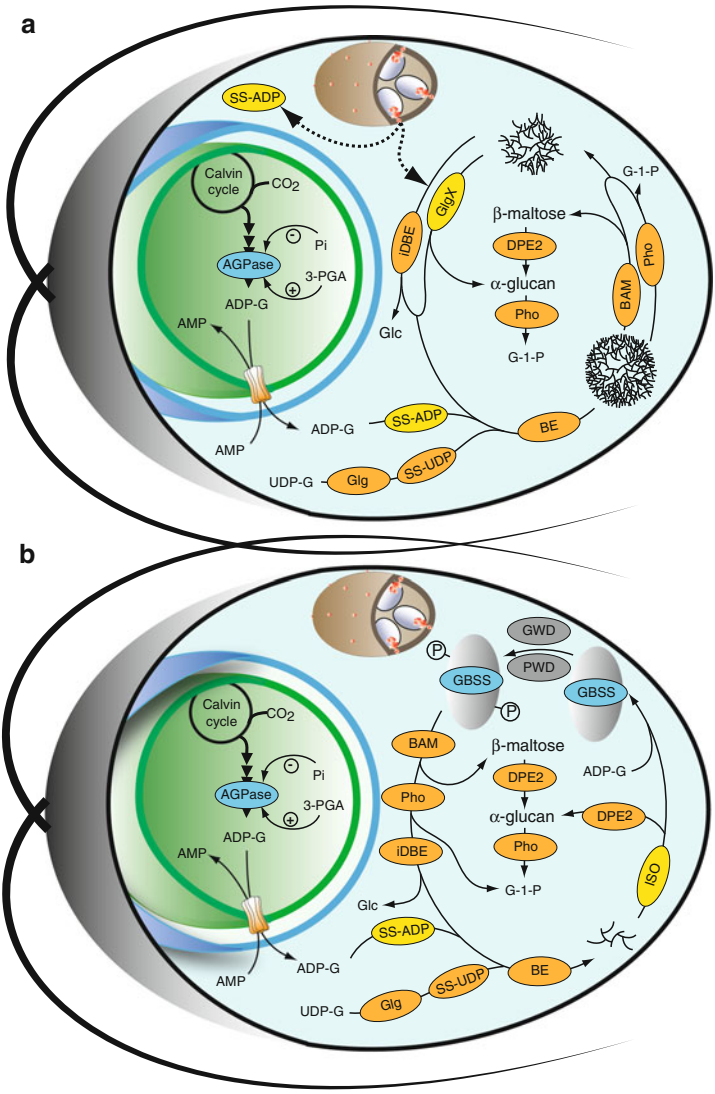

Fig. 4.4 Metabolic reconstruction of storage polysaccharide metabolism at the onset of plastid endosymbiosis (**a**) and in the last common Archaeplastida ancestor (**b**). The reconstruction was built by assuming vertical inheritance of those enzymes displaying a common phylogenetic origin and shared between the three Archaeplastida clades (Deschamps et al. 2008a). The number of enzymes was minimized according to the suspected gene duplications and subfunctionalizations which occurred selectively in Chloroplastida. ADP-glucose pyrophosphosphorylase and SSIII-SSIV (displayed as SS-ADP) are the only enzymes which are respectively found only in Chloroplastida and Glaucophyta. The reconstruction yields the network (**b**) as it was possibly operating in the last common ancestor of Archaeplastida before the three lineages diverged. This network produced starch as evidenced by the common presence of GBSS. To derive the glycogen metabolism network that was operating at the onset of endosymbiosis (**a**), we deleted those enzymes that are specific to crystalline polysaccharide metabolism (GBSS, GWD-PWD).

of plastid endosymbiosis can be deduced by the cytosolic effector nature of this protein that is phylogenetically derived from Chlamydiales intracellular pathogens. We have detailed in the preceeding paragraphs the observations that establish that GlgX proteins had been recruited prior to plastid endosymbiosis to enable some cyanobacteria to synthesize starch-like polymers in a polyphyletic fashion. Hence, this subfamily of the large GH13 family of glycosylhydrolases defines the perfect candidate to provide the switch from glycogen to starch metabolism. In a similar fashion, duplication within chlamydial symbionts of the gene encoding the GlgX chlamydial effector protein would have enabled novel effector subunits to provide the multimeric isoamylase function. Cenci et al. (2014) have shown through phylogenetic analysis that both in Glaucophyta and Rhodophyceae, the gene encoding the ISA-GlgX protein had indeed been duplicated. It is tempting to speculate that this happened, as the gene was still encoded by the chlamydial symbiont, further strengthening the interdependence of the ménage à trois (see Sect. 4.3.5 for definition) at plastidial endosymbiosis. The duplication and evolution of isoamylase, from the ancestral *GlgX* chlamydial gene, would have required the dikinase CBM fusion to optimize the mobilization of the novel form of carbohydrate stores. LGT of the cyanobacterial GBSS gene would have quickly followed, as amylose synthesis provides a convenient additional storage mechanism, in case the amylopectin synthesis machinery is overflowed by carbon. The successful EGT of the GBSS cyanobacterial gene, for expression in the host cytosol, suggests all this happened fast after the onset of plastid endosymbiosis, before all the genes from the cyanobacterial network of glycogen-starch metabolism had been lost. The invention of the glucan-phosphoglucan water dikinases offered, in addition, the possibility to integrate a novel first step of starch mobilization which replaced the direct access of

Fig. 4.4 (continued) The GWD-PWD are shaded in grey because they do not define pre-existing proteins of eukaryotic or bacterial phylogeny but rather a post-endosymbiosis gene fusion involving two domains of undefined origin (see text). Those enzymes phosphorylate starch granules by adding phosphate residues to the C6 and C3 positions of a glucosyl unit. Most of the enzymes are phylogenetically derived from the eukaryotic glycogen metabolism network (displayed in beige) which is essentially complete and operating in the host cytosol as is the case in all heterotrophic eukaryotes documented. Enzymes of cyanobacterial phylogenetic origin are displayed in blue, while those of chlamydial origin are shown in *yellow*. The host-derived NST ADP-glucose transporter (see text) is displayed in beige on the cyanobiont's inner membrane. Abbreviations are as follows: *AGPase* ADP-glucose pyrophosphorylase, *Glg* glycogenin, *SS-UDP* UDP-glucose specific GT5 glycogen(starch) synthase, *BE* branching enzyme, *BAM* β-amylase, *Pho*phosphorylase, *GlgX* GlgX-type of direct DBE (debranching enzyme), *iDBE* indirect debranching enzyme, *DPE2* amylomaltase or disproportionating enzyme (according to specificity), *Pho* glycogen or maltodextrin phosphorylase (according to specificity), *SS-ADP* SSIII-SSIV-type of ADP-glucose-specific soluble starch (glycogen) synthase, *GBSS* granule-bound starch synthase, *PWD-GWD* phosphoglucan or glucan water dikinases. Starch granules are displayed in white. Glycogen particles and oligosaccharide breakdown products are displayed in *black*. The chlamydial inclusion vesicle is displayed in *light brown* and the reticulate chlamydial bodies are shown in *gray* attached through the TTS (type three secretion system) to the inclusion vesicle membrane. Figure 4.5a displays the secretion of the chlamydial GlgX and GlgA (SS-ADP ancestor of SSIII-SSIV) effector proteins

the enzymes of glycogen catabolism to the glycogen pools (see Cenci et al. 2014 for a detailed discussion). We believe the evolving Archaeplastida capitalized on this to initiate a novel regulation of carbon breakdown that took into account the activity of the cyanobiont. In addition, this switch prevented direct access of intracellular Chlamydiales pathogens to the carbon pools, through their effector phosphorylases.

4.3.3 The Astonishing Features of the Ancient Glycogen Metabolism Network

As was pointed out in this chapter, storage polysaccharides and storage lipids define ideal buffers to circumvent all physiological problems, due to the disconnection of supply and demand for carbon, between the two unrelated partners of plastid endosymbiosis. The flux of carbon that became apparent in our first efforts of reconstruction of storage polysaccharide metabolism (Fig. 4.4a, b) convinced us that this pathway could have defined the biochemical flux through which photosynthetic carbon was exported at plastid endosymbiosis. This defines the symbiotic flux at the heart of symbiosis: the "raison d'être" of the cyanobiont-host partnership. It strokes us that the flux was optimal, at the very onset of the event. Indeed, according to Fig. 4.4a the substrate that flows out of the cyanobiont consists of ADP-Glc, which is the glycosyl-nucleotide sugar committed to storage in bacteria. Hence, the carbon that escapes the cyanobiont physically corresponds to that which was committed to storage anyhow. There is no penalty for the cyanobiont in the light, since this was committed to leave temporarily cyanobacterial metabolism. However, the loss of carbohydrate stores would have to be compensated for in darkness. There are several options here that include either the early targeting of the chlamydial ATP import protein to the cyanobiont inner membrane, or alternatively the cyanobiont could have maintained the synthesis of smaller amounts of glycogen by losing its former ability to synthesize large amounts of starch. This would have entailed the maintenance of a minimal amount of carbohydrate stores required in darkness and nevertheless the export of the large surplus of ADP-Glc. This would have further delayed the requirement for an immediate targeting of the chlamydial ATP import protein to the cyanobiont inner membrane, in the absence of the TOC machinery. In the cytosol of the host, ADP-Glc would not have interfered with any of the host's pathways since this metabolite is neither produced nor used by eukaryotes. The presence of the SSIII-SSIV glucan synthase in the host cytosol is inferred to have fed this carbon initially in the glycogen pool. The presence of this enzyme, in the cytosol, was required in the reconstruction of the ancient storage polysaccharide metabolism, to explain the presence of the SSIII-SSIV enzymes in Chloroplastida. It is this enzyme which, in the reconstruction, is responsible for establishing the biochemical link between the cyanobiont and its host. Five years after hypothesizing with such speculations the ancient presence of this activity, the corresponding enzyme sequence was found in the genome of the glaucophyte *Cyanophora paradoxa* genome sequence thereby considerably strengthening this hypothesis.

4.3.4 The Ancient Biochemical Link of Plastid Endoysmbiosis

One of the major findings of the *Cyanophora paradoxa* genome sequencing project consisted in the detection of a candidate UhpC-like transporter harboring clear-cut plastidial targeting sequences (Curtis et al. 2012). This correlated with the absence of candidate plastidial pPT transporters sequences, while several host NSTs of the eukaryotic endomembrane system were nevertheless detected. These results from bioinformatic studies were confirmed by the proteomic analysis carried on the glaucophyte plastids (the muroplast) by Facchinelli et al. (2013). In these studies the authors were surprised to find only 14 distinct candidate transporter proteins (including both thylakoid and envelope fractions), 3 of which were presumed to be of chlamydial descent (2 UhpC transporters and one ATP transporter) (Facchinelli et al. 2013). The figure of less than 14 candidate transporters, including the thylakoids, pales by comparison to the five- to tenfold higher figures reported for Rhodophyceae and Chloroplastida. Hence, it seems that the maintenance of the thick peptidoglycan layer prevented massive exploration of novel transport possibilities freezing the muroplast in an ancestral state of metabolite exchange. This at first glance agrees with the presence of the full glycolytic sequence observed in the muroplast stroma of *Cyanophora paradoxa* (Facchinelli et al. 2013). UhpC in proteobacteria has been proved to be a glucose-6-P sensor, regulating the import of hexose-P, but not a transporter (Schwoppe et al. 2003). *Chlamydia pneumoniae* UhpC was convincingly demonstrated to have lost the glucose-6-P sensor activity, upon gaining the transport properties (Schwoppe et al. 2002). This transport is in fact an exchange reaction between glucose-6-P and orthophosphate. This type of transport had been previously demonstrated to operate on purified *Cyanophora paradoxa* muroplasts (Schlichting and Bothe 1993). The UhpC gene was acquired by all three Archaeplastida clades, and displays a monophyletic origin in Archaeplastida. However, in both Rhodophyceae and Chloroplastida, the gene product is located elsewhere and not in plastids. In addition, only the *Chlorophyceae* and *Prasinophyceae* seem to have retained the gene which was apparently lost from all land plants and possibly also from the streptophyte green alga lineage.

Hence, the pressing question arises which came in first at the onset of endosymbiosis: UhpC or NST (nucleotide-sugar translocator) ? There is, as yet, no clear answer to this question, and both scenarios are equally viable. In a first scenario, NST successfully reached the inner membrane of the cyanobiont, at the onset of plastid endosymbiosis, as we initially proposed. This scenario is supported by the demonstrated ability of some members of this family of transporters to reach inner membranes of organelles in the absence of a protein-targeting machinery (Loddenkotter et al. 1993). In this scenario, the UhpC gene was transferred to the last common ancestor of Archaeplastida to fulfill a yet to be investigated function within the host but outside of the evolving plastid. The transporter was then recruited to the muroplast, from a duplicated copy that had gained a plastid-targeting sequence after divergence of the Glaucophyta from the other Archaeplastida lineages. Exchange of glucose-6-P for orthophosphate substituted for ADP-Glc export, thereby explaining

the loss of the ADP-Glc pyrophosphorylase, together with the NST gene, from the glaucophyte lineage. In a second scenario, UhpC came in first and the pPTs were acquired selectively by the Rhodophyceae and Chloroplastida lineages, from an ancient NST, after these lineages diverged from the Glaucophyta. Duplicated copies of the UhpC gene were then recruited by the common ancestor of the red and green algae to work elsewhere in the cell. If we assume that UhpC reached the inner membrane of the cyanobiont at the onset of the event, there would be no need for storage polysaccharide synthesis in the host cytosol from ADP-Glc. Yet, the existence of an SSIII-SSIV-like glucan synthase sequence in the *Cyanophora paradoxa* genome sequence clearly contradicts this conclusion. There is no need in eukaryotes for such an enzyme to sustain glycogen synthesis in the cytosol. Hence, even if the enzyme present in extant glaucophytes is likely to fulfill an important function in starch synthesis that is likely to be independent from the presence of ADP-Glc, this was clearly not the case for the ancestral gene product that was transferred from the Chlamydiales pathogens to the common ancestor of Archaeplastida. Another problem with a simplistic view of the UhpC first scenario comes from its phylogenetic origin. How could a hydrophobic transporter protein present on the membranes of Chlamydiales reach the inner membrane of the cyanobiont at the onset of plastid endosymbiosis? UhpC is not documented as an effector protein in Chlamydiales. It is very difficult to reconcile this observation with an early targeting of this transporter to the cyanobiont inner membrane. A way around this problem would be to imagine that the gene encoding this transporter had been transferred selectively to the common ancestor of Archaeplastida prior to plastid endosymbiosis to fulfill an unknown function in the heterotrophic phagotrophic ancestor of Archaeplastida. The UhpC transporter then reached the cyanobiont inner membrane, in the absence of the protein-targeting machinery. Under this hypothesis, the chlamydial phylogenetic origin of the protein is purely coincidental. This hypothesis has three major disadvantages. First it does not allow to understand why the glaucophytes should have lost the ancestral UhpC function of the heterotrophic eukaryotic ancestor while the latter should have been maintained in green and red algae. Second, it does not allow to understand what the benefits would have been for the transfer of the SSIII-SSIV glucan synthase gene for expression in the cytosol of the common Archaeplastida ancestor. Yet, this prokaryotic gene was indeed transferred and is evidenced today in the *Cyanophora* genome. Third, UhpC has not been documented to display an innate ability to reach the inner membranes of organelles. Hence, there is truly no reason to prefer this simplistic version over the comparable version of the NST first scenario. Nevertheless, we do not believe that the Chlamydiales origin of this transporter can be coincidental as this protein would have participated in the establishment of the metabolic link between the cyanobiont and its host. It is therefore very tempting to favor the UhpC first scenario, but in a fashion that explains the targeting of this protein at the onset of plastid endosymbiosis, and not in the simplistic version detailed above. In the meantime, it is presently very difficult to prefer any of the aforementioned scenarios and more information is needed. In particular, we need to know what function is fulfilled by UhpC transporters in red and green algae and what are the biochemical properties

of these transporters with respect to the targeting of organelle membranes in the absence of protein translocation machineries. We also need to further study the eukaryotic ancestors of the pPTs in more detail.

4.3.5 Two Models for a Successful "Ménage à Trois"

A growing number of phylogenetic studies demonstrate that Archaeplastida are characterized by the presence of 30–50 genes that display a common phylogenetic origin with intracellular bacterial pathogens of the order Chlamydiales (Moustafa et al. 2008). These obligatory intracellular pathogens replicate within inclusion vesicles, derived from endocytic membranes inside eukaryotic cells such as amoebas or animal cells (for review see Collingro et al. 2011). The presence of a continuous cell wall precludes infection, explaining why fungi plants and nonphagotrophic algae are immune to chlamydial infections. Nevertheless, if comparable studies are performed in the animal or fungal kingdoms, the signals decrease to 50 or 20 % respectively, of their intensity seen in Archaeplastida (Ball et al. 2013). This is especially relevant, because the fungi and animals have presently been more extensively studied and sampled than the Archaeplastida. So, how can we explain the presence of such a phylogenomic signal in clades that are immune to *Chlamydia* infections? Part of the answer came with the realization that over one-third of the LGTs, uniting Chlamydiales to Archaeplastida, were common to at least two of the three Archaeplastida lineages (Becker et al. 2008; Collingro et al. 2011; Huang and Gogarten 2007; Moustafa et al. 2008). Hence, a significant part of these LGTs can be dated back to a time where these lineages had not yet diverged. This time coincides with that of plastid endosymbiosis. Indeed, the common ancestor of Archaeplastida is not thought to have been surrounded by a continuous cell wall and is highly suspected to have been an active phagotroph, rendering it highly susceptible to chlamydial infections. While this explains the presence of chlamydial LGTs in the Archaeplastida genomes, it does not explain the selective enrichment of Archaeplastida, relatively to the animals, which unlike the latter were continuously exposed to chlamydial infections, ever since they diverged from their unicellular choanozoan-like ancestors. Several authors have explained this by hypothesizing a specific role of Chlamydiales intracellular pathogens in plastid endosymbiosis (Huang and Gogarten 2007; Becker et al. 2008; Moustafa et al. 2008; Collingro et al. 2011). In 2013, Ball et al. demonstrated that the SSIII-SSIV ancestral glucan synthase present in the cytosol of *Cyanophora paradoxa* and in the plastids of the green algae and land plants was an enzyme of chlamydial affiliation. In our reconstruction of the ancient storage polysaccharide metabolism network, we had proposed the existence of two key proteins that established, according to us, the efflux of photosynthetic carbon from the cyanobiont and its assimilation in the host glycogen pools. These are respectively the NST ADP-Glc transporter and the cytosolic ancestor of the ADP-Glc-specific SSIII-SSIV glucan synthase. To explain the presence of the SSIII-SSIV enzyme in the cytosol of the

common Archaeplastida ancestor, Ball et al. proposed that this gene in Chlamydiales encoded an effector protein that was secreted by these intracellular pathogens through the TTS (type three secretion system) in the cytosol of their host. By using a semi-in vitro TTS system in *Shigella*, Ball et al. demonstrated that genes from Parachlamydiaceae (the closest relatives to the archaeplastidal enzymes) encoding GlgC (ADP-Glc pyrophosphorylase), GlgA (ancestor of the archaeplastidal SSIII-SSIV glucan synthase), GlgX (debranching enzyme ancestor of the archaeplastidal isoamylase), and GlgP (glycogen phosphorylase) were indeed effector proteins secreted by the pathogens into their host's cytosol. From the Chlamydiales point of view, these effectors would induce cytosolic ADP-Glc synthesis and induction of glycogen synthesis at the beginning of the infection. Toward the end of the infection, the pathogen's unregulated glycogen phosphorylase would induce massive breakdown of the glycogen pool and its conversion into glucose-1-P and maltotetraose. Quite significantly, maltotetraose does not define a suitable substrate for cytosolic degradation by host enzymes. Hence, the pathogens induce formation of a metabolite, for which only they can find further use. The effector nature of the GlgA protein of *Chlamydia trachomatis* was further proven by others using an in vivo approach in a homologous system (Lu et al. 2013). If we assume that a heterotrophic phagotroph ancestor, infected by such pathogens, internalized a cyanobiont and managed to have an NST targeted to its inner membrane, then in effect, plastid endosymbiosis would have rescued the infected cell, by feeding unlimited amounts of ADP-Glc into the cytosolic glycogen pools, thanks to the presence of the pathogen's GlgA (SSIII-SSIV-like) glucan synthase. Without a single mutation in the pathogen's genome, this instantly changed the nature of the GlgA effector from potentially a virulence effector to a symbiogenic effector at the heart of one of the most important symbioses associations to have appeared on our planet. Ball et al. (2013) further outlined that plastid endosymbiosis was, in effect, a "ménage à trois," where three partners participated in a common carbon assimilation flux (Fig. 4.5a). This affords for a straightforward explanation of all observations, including the phylogenomic signal of Chlamydiales in Archaeplastida. Because, unlike the cyanobiont, the pathogen's compartment did not offer any other purpose than encoding useful genes, the chlamydial partner eventually disappeared, after it had exhausted all possibilities of evolving useful effectors to the tripartite symbiosis. Hence, the selection pressure that maintained the chlamydial compartment was the constant evolution of beneficial effectors to keep ahead of the LGT of its genes to the host nucleus. The ISA-GlgX effector, in this context, might define another example of beneficial cytosolic effector. Indeed, the switch to starch, in the common Archaeplastida ancestor, was most probably triggered by a gene duplication of GlgX. This, as we outlined above, happened fast after the onset of plastid endosymbiosis. We believe this could have happened before EGT of the ISA-GlgX effector genes to the nucleus of the host. Hence, maintenance of the pathogen would have been required for continued starch synthesis.

How does the "ménage à trois" stand in face of the UhpC first hypothesis? As we outlined above, we do not believe that the fact that UhpC defines a gene of Chlamydial phylogeny can be coincidental in the context of plastid endosymbiosis.

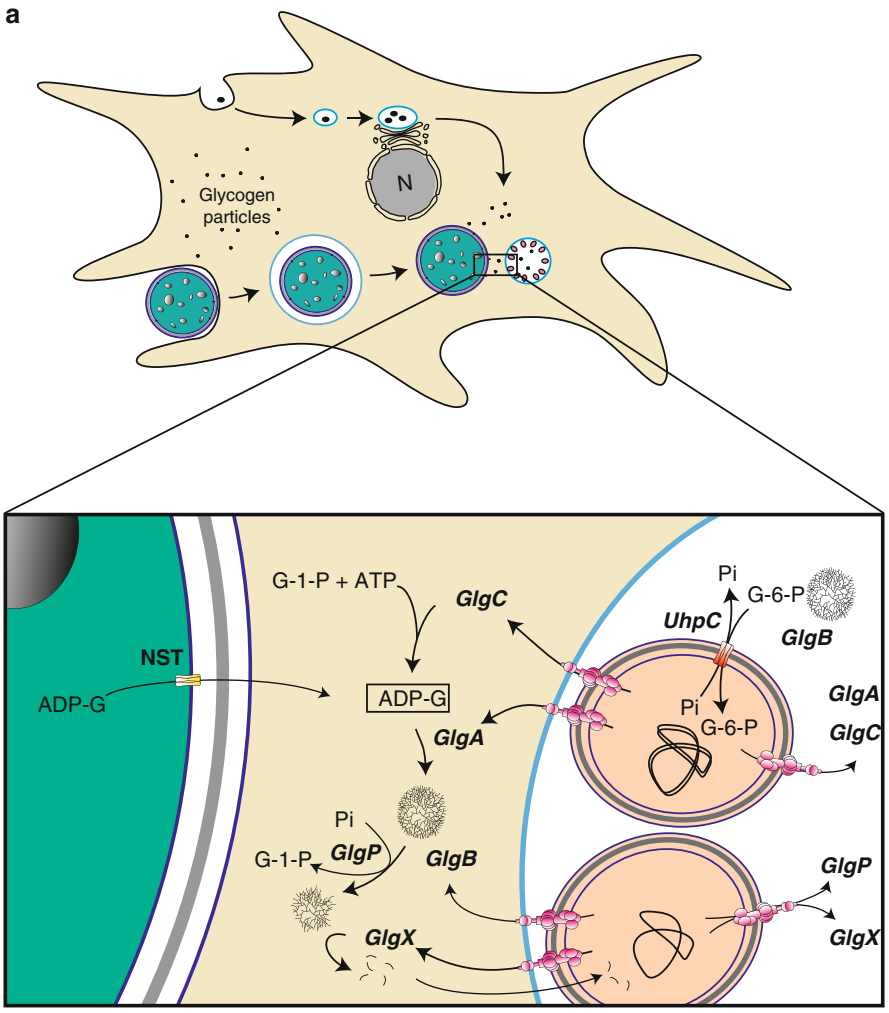

Fig. 4.5 Two alternative scenarios explaining the ménage à trois hypothesis. (**a**) The classical ménage à trois hypothesis (NST first scenario). Panel (**a**) recapitulates the scenario previously detailed in Fig. 4.4a. The large-size cyanobiont (in blue-green with starch granules displayed) is shown entering the host independently from the chlamydial pathogen (to scale) a mere *thick black dot*. A section displaying the tripartite interaction is *enlarged* and *boxed*. The chlamydial reticulate bodies are displayed attached through their syringe-like TTS (type three secretion system, displayed in *pink*) to the inclusion vesicle membrane (in *light blue*). Glycogen particles are depicted in *black* within the inclusion vesicle and in the host cytosol. Only the enzymes of chlamydial provenance are displayed and abbreviated by their gene symbols: *GlgA* glycogen synthase, *GlgB* branching enzyme, *GlgC* ADP-glucose pyrophosphorylase, *GlgP* glycogen (maltodextrin) phosphorylase, and *GlgX* GlgX-type of direct DBE. The NST (ADP-glucose transporter) transporter is highlighted on the cyanobiont membrane which was reached independently of an inexisting TIC-TOC protein import machinery. (**b**) The modified (chlamydioplast) ménage à trois (UhpC first scenario) hypothesis. The cyanobiont is shown entering together with a chlamydial elementary body.

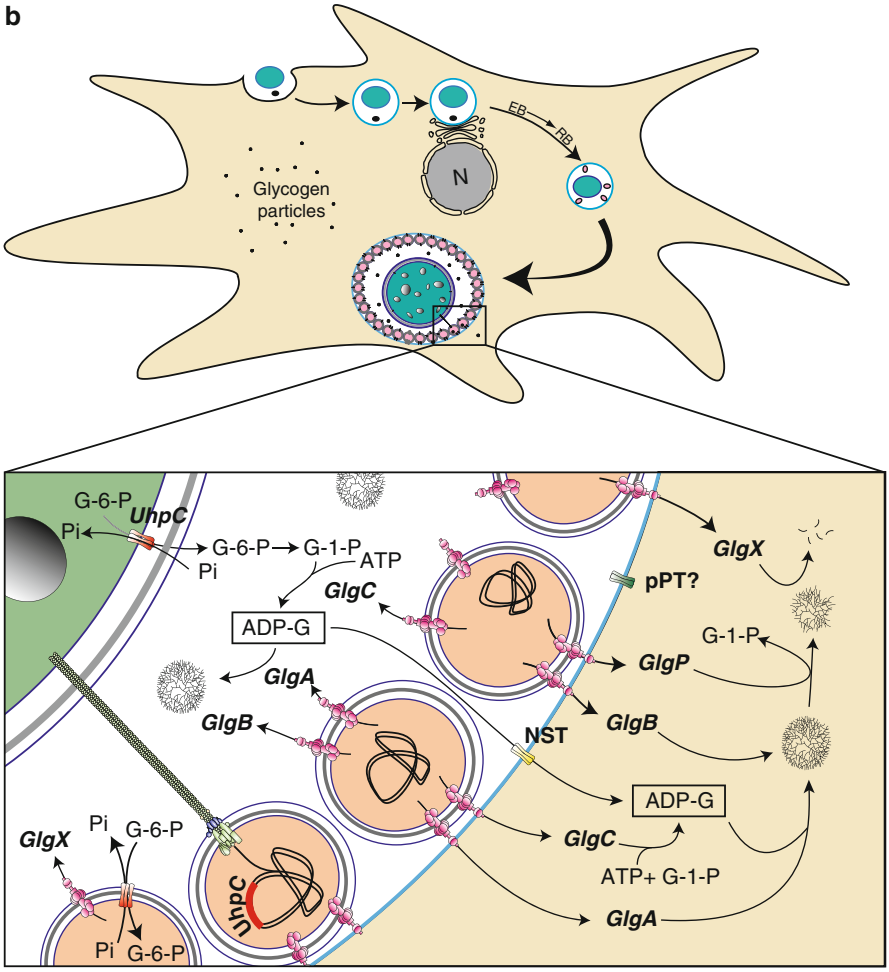

Fig. 4.5 (continued) The elementary body differentiates into reticulate bodies attached through their TTS to the modified phagocytic vacuole thereby preventing phagocytosis of the cyanobiont. The T4SS (type four secretion system displayed in *green*, *blue,* and *black*) responsible for conjugative DNA transfer transfers ad minima the UhpC and NTT (ATP import protein) chlamydial genes for expression within the cyanobiont. UhpC is displayed in red on the cyanobiont inner membrane, while NST is displayed in yellow on the inclusion vesicle. The low affinity ADP-glucose transporter (NST) will transport the overflow of carbon assimilation to the cytosol where it will be metabolized as depicted in Figs. 4.4b and 4.5a

Hence, we do not believe that UhpC had already been transferred to the host ancestor genome prior to plastid endosymbiosis. Rather, we believe that UhpC was transferred, post endosymbiosis, to the nucleus of the host. If UhpC defines the original carbon translocator, we must assume a very early targeting of this protein to the inner envelope of the cyanobiont. If we assume that UhpC was encoded by a Chlamydiales

intracellular pathogen that infected the host of plastid endosymbiosis, it is very hard to imagine that such a hydrophobic transporter could have been secreted through the TTS and targeted to the inner membrane of the cyanobiont. In order to solve this problem, Facchinelli et al. (2013) have proposed that the cyanobiont entered by phagocytosis together with the Chlamydiales pathogen (Fig. 4.5b). We know that Parachlamydiaceae which are the pathogens that are closest by sequence to the genes transferred by EGT to Archaeplastida possess a fully functional type IV secretion system (Collingro et al. 2011) that would enabled the conjugative transfer of chlamydial DNA to the cyanobiont. This would have facilitated the very early transfer of the UhpC and the NTT (ATP import protein) genes to the cyanobiont genome for expression of these hydrophobic transporter proteins on the cyanobiont inner membrane. Possibly, other useful chlamydial genes could have been transmitted in this fashion to stabilize the cyanobiont in the inclusion vesicle environment. To be able to benefit from the cyanobiont's export of glucose-6-P, there was a need for the pathogen to have a biochemical buffer between the unsynchronized supply and demand of carbon within the inclusion vesicle for similar reasons as those that we have outlined concerning cytosolic storage polysaccharide synthesis. In *Chlamydia trachomatis*, massive intravesicular glycogen accumulation has been documented to the point where iodine staining of infected tissues constitutes a diagnostic feature of infection of human tissues by *C. trachomatis*. In addition to this, we know that at least in *C. trachomatis*, the GlgA effector enzyme is secreted in the host cytosol and that glycogen synthesis is also induced in the host cytosol upon infection with Chlamydiae (Ojcius et al. 1998). Hence, it very likely that Chlamydiales can trigger glycogen synthesis and degradation in all three compartments: in the host cytosol, in the inclusion vesicle, and within the bacterial pathogens. In this context, if divisions of the pathogens within the inclusion vesicle slowed down and if the cyanobiont supplied an excess of carbon, the latter would have been redirected to the intravesicular glycogen pool. It is plain to see that the cyanobiont is enslaved by the pathogen and that the latter gets most of the photosynthate (Fig. 4.5b). Hence, the Chlamydiales are on top of the "ménage à trois." But what's in there for the eukaryotic host? Facchinelli et al. (2013) proposed that the Golgi NST was targeted as a low affinity ADP-Glc translocator to the inclusion vesicle membrane (Fig. 4.5b). This would have been very simple, as this inclusion vesicle is in continuity and derived from the host endomembrane system. Colleoni et al. have previously documented that host GDP-mannose translocators, phylogenetically related to the pPT translocators, transport ADP-Glc as efficiently as the natural GDP-mannose substrate but with lower affinity. Hence, whenever the sink of carbon toward the Chlamydiales decreased, the concentration of ADP-Glc within the inclusion vesicle would rise leading to an efflux of the nucleotide sugar toward the host cytosol. In the cytosol, the situation would be exactly the same as that detailed in the NST first scenario and the ménage à trois would have been operating in a similar fashion. The UhpC scenario detailed above (Fig. 4.5b) displays a number of very attractive features. It explains how phagocytosis aborted and how the cyanobiont benefitted from the remodeling of the phagocytosis vesicle into a stable inclusion vesicle by the Chlamydiales pathogens. The environment

offered by the inclusion vesicle is less dense than the cytosol and more similar to the external medium to which free-living cyanobacteria are better adapted. The chlamydial genes, required for carbon efflux and ATP import, would have been readily transmitted to the cyanobiont at the onset of plastid endosymbiosis. Other chlamydial genes stabilizing the cyanobiont in an intracellular environment could also have been directly transferred by conjugative transfer. We would like to refer to this stage as the "chlamydioplast" stage of plastid endosymbiosis. At this stage, the presence of the outer LPS-like polysaccharide shell, surrounding the cyanobiont, would not have prevented the transfer and expression of UhpC. The efflux of Glucose-6-P, on the other hand, would have minimized the synthesis of all polysaccharides within the cyanobiont. Because of the presence of the inclusion membrane, it is unlikely that the events that led to the appearance of the TIC-TOC protein import machinery were initiated at the chlamydioplast stage. However, this stage remains compatible with massive gene losses and conjugative transfers of chlamydial genes, in effect priming the cyanobiont for its future escape to the cytosol. It also was compatible with EGT to the nuclear genome of cyanobacterial genes for expression of the products in the host cytosol but not for their targeting back to the cyanobiont. Hence, the GBSS gene could have been transferred to the host nucleus at this stage and in the host cytosol starch would already have replaced glycogen thanks to the chlamydial GlgX effectors. We believe that the outer polysaccharide layers disappeared at this stage, thereby exposing the outer cyanobacterial membrane. Because of the efflux of glucose-6-P, we believe that the massive synthesis of cyanobacterial starch was replaced by that of minimal amount of glycogen through the loss of the genes required for starch crystallization. This would have increased the resistance to oxidative stress that would otherwise have been generated by the complete loss of cyanobacterial starch. The presence of a significant glycogen pool in the cyanobiont together with the chlamydial ATP import protein would have also allowed the loss of the cyanobacterial respiratory complexes. The presence in the TIC-TOC apparatus of a common core set of genes in the three Archaeplastida lineages suggests that the cyanobiont escaped from the chlamydioplast, very early on, before divergence of the 3 Archaeplastida lineages. This allowed the common evolution of the TIC-TOC machinery. Exposure of the cyanobiont membranes to the cytosol could have enabled the direct targeting of NST to the cyanobiont inner membrane. The fast evolution of TOC would have stabilized this targeting of the NST protein and would have facilitated EGT to the host nucleus of both chlamydial transporter genes present in the cyanobiont genome. Before divergence of the glaucophytes, the last common ancestor achieved complete loss of all glycogen metabolism genes with the exception of ADP-Glc pyrophosphorylase. Upon divergence from the Rhodophyceae and Chloroplastida, the Glaucophyta lost both the NST transporter and ADP-Glc pyrophosphorylase. On the other hand, the common ancestor of both Rhodophyceae and Chloroplastida kept the UhpC nuclear gene but redirected the gene product to other compartments. Hence, UhpC disappeared from the inner cyanobiont membrane in the common ancestor of the evolving red and green algae. The peptidoglycan layer also disappeared in this ancestor. This disappearance enabled the pyrenoid to physically interact

with cytosolic starch across the two plastidial membranes, an interaction which was previously prevented by the peptidoglycan layer. This interaction allowed the exploration of new transporter properties facilitated by the duplication of the NST gene which led to the pPT transporters. The green algae further evolved to redirect cytosolic starch metabolism to the evolving chloroplasts, while the red algae kept the pPTs but lost both the original NSTs, ADP-Glc pyrophosphorylase and the cytosolic ADP-Glc-specific SSIII-SSIV chlamydial glucan synthase.

Both "ménage à trois scenarios" detailed above are presently compatible with all recorded observations. Future studies on the NST ancestors or on the UhpC transporters are required to help us distinguish between these alternatives.

4.3.6 Polyphyletic Transitions of Glycogen to Starch Metabolism in the Eukaryote and Bacterial Domains

When we initially tackled the study of the evolution of storage polysaccharide metabolism, we had misinterpreted the phylogeny of the plant isoamylases and initially believed these enzymes to be of cyanobacterial origin (Deschamps et al. 2008a). The finding of starch-like structures in cyanobacteria initially suggested to us that there may have been one single acquisition of starch from glycogen metabolism that happened over two billion years ago in single-cell diazotrophic cyanobacteria, possibly at a time when nitrogenase became exposed to critical levels of oxygen. This would have been followed by transmission of this ability at primary plastid endosymbiosis to Archaeplastida through EGT of the required cyanobacterial isoamylase. The Archaeplastida would have in turn transmitted this ability through secondary endosymbiosis to the cryptophytes and the alveolates. This simple and attractive scenario turned out to be completely wrong! First, acquisition of starch (or semi-amylopectin) in cyanobacteria turns out to be distinctively polyphyletic. Indeed, while genetic approaches carried out in *Cyanobacterium* CLg1 demonstrated that an isoamylase-like enzyme was responsible for generating semi-amylopectin (Cenci et al. 2013), genome sequences of other starch or semi-amylopectin-accumulating clades suggest that at in some clades, GH13 direct DBEs are apparently absent. If the corresponding genomes are complete, this observation implies that, in these clades, the enzymes responsible for turning glycogen metabolism into starch are evidently different and that starch acquisition has therefore occurred several times in cyanobacteria. In addition to this, we now know that the ancestor of the plant isa1 gene is of chlamydial origin. So, not only did starch appear, possibly many times, from glycogen metabolism in cyanobacteria, but the appearance of starch metabolism in Archaeplastida was also independent of these events. From our present knowledge of starch metabolism evolution, it remains plausible that transition to starch occurred only once in the cytosol of the last common Archaeplastida ancestors. Yet, because the starch metabolism pathway was probably redirected stepwise to the chloroplast, the network went through

another sequence of glycogen to starch transition in the green algae and land plants evolving chloroplasts (Deschamps et al. 2008c). Hence, Archaeplastida experienced at minima two such transitions. In starch-storing secondary endosymbiosis lineages (cryptophytes and alveolates), the secondary eukaryotic host of endosymbiosis is generally thought to be distinct. This correlates with a distinct localization of starch and a different nature of the enzyme network. To be more specific, bona fide debranching enzyme candidate sequences are absent altogether from cryptophytes, while direct DBEs were apparently replaced by indirect DBE in alveolates (not taking into account the tertiary endosymbiosis dinoflagellate lineages). This again suggests a distinct transition in the alveolate cytosol. The cryptophytes possibly never experienced such a transition, since starch was present in the periplastidial space at the very beginning of the event. Evidently in this case the rhodophycean isoamylase-like enzyme that we highly suspect to be responsible for amylopectin crystallization was replaced by an enzyme from another CAZy subfamily. The only activity which in eukaryotes was never replaced by distinct families of enzyme sequences is defined by the glucan and phosphoglucan water dikinases. These enzyme sequences correlate 100 % with the presence of starch-like structures in eukaryotes and can be taken as a diagnostic of the presence of semicrystalline α-glucan polysaccharides. We believe that in cyanobacteria, the absence of such dikinases stems from the absence of a preexisting pathway of glycogen phosphorylation. This absence must have required coevolution and adaptation of the glycogen catabolism machinery to the presence of more hydrophobic polysaccharides. Quite significantly, in eukaryotes, the glucan dikinase genes disappear whenever a clade reverts from starch to glycogen metabolism. Going back from starch to glycogen is documented in at least two cases in Cyanidiales (*Galdieria sp.* and *Cyanidium sp*) and possibly also in ciliates, in at least one case, in alveolates (the ciliates). We believe that in cyanobacteria this would also have been frequent. Hence, we can conclude that transition of glycogen to starch metabolism and reversion to glycogen seem to have occurred frequently both in cyanobacteria and eukaryotes from distinct enzyme networks. Such transitions would have been dictated by polysaccharide structure optimization with respect to distinct types of cell physiologies.

4.3.7 Why Amylose?

Amylose (defined as chains exceeding DP100 with less than 1 % branches) does not define a universal feature of starches accumulating in both the bacterial and eukaryotic domains. However in both domains, amylose synthesis always requires the presence of GBSS (granule-bound starch synthase) an enzyme belonging to the GT5 bacterial CAZy family of glycogen(starch)synthases. We believe that the cyanobacterial origin of this enzyme is presently beyond doubt (Ball et al. 2013). The reasoning is as follows. First the GBSS-SSI-SSII supergroup of starch synthases in all organisms is monophyletic and displays only bacteria and archaea at the root of this superclade. Second the phylogeny of the GBSS subgroup places

the cyanobacterial enzymes as sisters to the Chloroplastida, glaucophytes, and Rhodophyceae and not within either the green or red algae. Had the cyanobacterial enzyme been acquired by LGT from green or red algae, the *Cyanobacterium* CLg1 and *Crocosphaera watsonii* GBSS sequences would have been expected to lie within the red or green algae possibly in a polyphyletic fashion. Hence, the GBSS phylogeny is consistent with the enzyme having evolved in cyanobacteria and been transmitted by EGT to Archaeplastida. Robust grouping of SSI-SSII enzymes of green algae with the GBSS sequences is interpreted as originating from gene duplications that happened during the process of the complex rewiring of the storage polysaccharide network to the evolving chloroplast. Outgroup rooting of the GBSS-SSI-SSII superclade displays an origin at midpoint between the GBSS and SSI-SSII subgroup. The very high bootstrap support evidenced for this node reflects more the fact that this supergroup is unquestionably monophyletic, rather than correctly positioned with respect to the general GT5 phylogenetic tree. This can be attributed to the fact that the GBSS-SSI-SSII superclade is distantly related to other GT5 starch(glycogen) synthases and that the SSI-SSII subgroup has itself substantially diverged from the GBSS subgroup. Hence, as outlined in Ball et al. (2013), we believe that the true root position of the GBSS-SSI-SSII superclade lies at the base of the cyanobacterial GBSS sequences.

Very few cyanobacteria and Rhodophyceae display the presence of amylose, while the latter is universally present in Chloroplastida and possibly also in Glaucophyta. One can speculate relatively to the benefits of amylose synthesis. A universal property of GBSS is defined by its apparent low affinity for its glycosyl-nucleotide substrates and its apparent low activity in the unbound form. The processivity of the Chloroplastida enzyme seems confirmed by those evidenced in semi-in vitro systems analyzed with *Cyanobacteria*, Glaucophyta, cryptophytes, and dinoflagellates (Deschamps et al. 2006, 2008a, b; Plancke et al. 2008). In all these systems, amylose synthesis is triggered by very high nucleotide-sugar concentrations by processive elongation. A substantial part of this synthesis escapes branching, quite simply because the polysaccharide product is sheltered within the granule and therefore escapes the action of the hydrosoluble branching enzymes. In wild-type cells, amylose accounts to up to 30 % maximum of the weight of the granule and many times less. Amylose synthesis typically acts as an overflow mechanism, when the amylopectin synthesis machinery is insufficient to deal with the rising nucleotide-sugar concentrations. This will enable amylose containing starch to incorporate an additional 10–30 % glucose within the granules. However, overflow is not the only possible function of amylose synthesis. Wattebled et al. showed that intensive de novo synthesis of amylose, in semi-in vitro systems, results in a very strong alteration of starch granule morphogenesis that is accompanied by a switch from a classical lenticular shape to a tubular fused network, probably resulting from fusion of distinct altered starch granules (Wattebled et al. 2002). Hence, GBSS affords for localized polysaccharide synthesis that triggers starch granule fusion, thereby acting as a molecular glue. If we couple this property, to the very low apparent affinity of this enzyme toward its glycosyl-nucleotide substrate, we can predict that GBSS will respond dramatically to localized substrate gradients. In

effect, localized nucleotide-sugar gradients will induce a morphogenesis response, whereupon the granules will surround the glycosyl-nucleotide source. This very conveniently explains the surrounding of the pyrenoids, which will contain most of the active RuBisCO in normal CO_2-limited conditions. It is striking to note that GBSS and amylose are present in all cases where a localized pyrenoidal starch sheet is evidenced (all green algae, cryptophytes, Porphyridiales). In other red algae, where starch is uncoupled from the pyrenoid, floridean starch appears devoid of amylose. This also appears to be the case in heterotrophic alveolates. Pyrenoids are certainly involved in the CO_2 concentration mechanism, operating in aqueous environments, where they are considered to define carboxysome-like structures devoid of carbonic anhydrase. Quite strikingly, in Glaucophyta and green algae GBSS transcription is massively induced in low CO_2 conditions. Pyrenoidal starch is not required for the CCM to operate normally but results from the generation through the pyrenoids of localized metabolite concentration gradients (Izumo et al. 2011; Villarejo et al. 1996). The correlation between pyrenoidal starch and the presence of amylose is nevertheless insufficient to account for the presence of GBSS in cyanobacteria glaucophytes and land plants which are all devoid of pyrenoids (except for the hornworts). Nevertheless, we would like to suggest that in all these cases selection for amylose-containing starches can also be explained by a combination of morphogenetic and metabolic reasons.

4.4 Conclusions

Investigating the evolution of starch metabolism has yielded a number of insights that have impacted both our understanding of the biochemistry of starch metabolism and our understanding of the metabolic integration of novel organelles.

The major conclusions that we can deduce from these approaches on our understanding of the biochemistry of starch metabolism are as follows:

1. Comparative biochemistry of starch metabolism proves that starch synthesis and degradation is not inherently more complex than those of glycogen. The presence of 30–40 genes in the green lineage that display specific and only partly redundant functions for the synthesis or degradation of starch has mislead researchers to believe that the apparent complexity of the polysaccharide structure had to be matched by an equally complex metabolic pathway. This is clearly not the case, and this complexity results more from the history of a pathway, which was redirected to plastids, at a time when the genes of storage polysaccharide metabolism had already been lost from the ancestral plastid genome. This history testifies to the apparent low costs that entail gene duplications and subfunctionalizations. The simplest networks that are sufficient to yield starch are those displayed by the red algae and the apicomplexa parasites. Presently, researchers are trying to achieve starch granule synthesis in vitro. We therefore

strongly believe that the enzymes that should be used for these approaches are those that are evidenced in the red alga or apicomplexa networks.

2. The generation of cyanobacterial mutants that overaccumulate glycogen and are defective for starch synthesis mirrors analogous results obtained in green algae and plants. The finding of a defect for an isoamylase type of direct DBE emphasizes a remarkable case of convergent evolution, where at two independent times nature has recruited a similar enzyme, from its molecular toolbox, to achieve the crystallization of amylopectin and the insolubilization of starch granules. This result strongly suggests that polysaccharide debranching may define a universal feature required to generate amylopectin from a preexisting glycogen synthesis machinery. Nevertheless, bioinformatic analysis clearly demonstrates the absence of isoamylase candidate sequences, in some starch-accumulating cryptophytes and alveolates. We believe that other CAZymes have been recruited to replace the classical DBE isoamylase function in these clades, but this, however, remains to be demonstrated. If this is the case, then the comparison of the 3D structures and organization of all these very diverse enzymes will facilitate the finding of those common features, which are responsible for amylopectin crystallization.
3. It is generally believed that GT3 glycogen synthases require glycogenin for glycogen synthesis priming, and GT5 glycogen and starch synthases do not. The study of the distribution of glycogenin among eukaryotes and its correlation to that of the GT5 and GT3 enzymes seems at first glance to invalidate this idea. Polysaccharide synthesis priming could thus define a built-in general property of glycogen synthases that could be occasionally lost in a quite unpredictable clade-specific fashion.

Our studies on the evolution of the starch metabolism pathway have also impacted our current understanding of the establishment of plastid endosymbiosis as follows:

1. The reconstruction of a hypothetical ancient storage polysaccharide network in the common ancestor of Archaeplastida suggests that cytosolic storage polysaccharides may have acted as buffers between the unsynchronized supply and demand of carbon at the onset of plastid endosymbiosis.
2. The finding that both the SSIII-SSIV ancestral enzyme and isoamylase are phylogenetically derived from chlamydial effector proteins secreted by these pathogens in the cytosol of eukaryotes provides a detailed scenario, explaining the early phases of plastid endosymbiosis.

References

Albrecht T, Haebel S, Koch A et al (2004) Yeast glycogenin (Glg2p) produced in Escherichia coli is simultaneously glucosylated at two vicinal tyrosine residues but results in a reduced bacterial glycogen accumulation. Eur J Biochem 271:3978–3989

Alonso-Casajus N, Dauvillee D, Viale AM et al (2006) Glycogen phosphorylase, the product of the glgP Gene, catalyzes glycogen breakdown by removing glucose units from the nonreducing ends in Escherichia coli. J Bacteriol 188:5266–5272

Archibald JM, Lane CE (2009) Going, going, not quite gone: nucleomorphs as a case study in nuclear genome reduction. J Hered 100:582–590

Arias MC, Danchin EG, Coutinho P et al (2012) Eukaryote to gut bacteria transfer of a glycoside hydrolase gene essential for starch breakdown in plants. Mob Genet Elem 2:81–87

Badger MR, Price GD (2003) CO2 concentrating mechanisms in cyanobacteria: molecular components, their diversity and evolution. J Exp Bot 54:609–622

Ball S (1998) Regulation of starch biosynthesis. Kluwer Academic Publishers, Dordrecht

Ball S (2002) The intricate pathway of starch biosynthesis and degradation in the monocellular alga Chlamydomonas reinhardtii. Aust J Chem 55:1–11

Ball S, Deschamps P (2008) Starch metabolism. In: Stem DB (ed) The chlamydomonas sourcebook: 2. Organellar and metabolic processes. Academic, London, pp 1–40

Ball S, Guan HP, James M et al (1996) From glycogen to amylopectin: a model for the biogenesis of the plant starch granule. Cell 86:349–352

Ball S, Colleoni C, Cenci U et al (2011) The evolution of glycogen and starch metabolism in eukaryotes gives molecular clues to understand the establishment of plastid endosymbiosis. J Exp Bot 62:1775–1801

Ball SG, Subtil A, Bhattacharya D et al (2013) Metabolic effectors secreted by bacterial pathogens: essential facilitators of plastid endosymbiosis? Plant Cell 25:7–21

Bandyopadhyay A, Elvitigala T, Liberton M et al (2013) Variations in the rhythms of respiration and nitrogen fixation in members of the unicellular diazotrophic cyanobacterial genus Cyanothece. Plant Physiol 161:1334–1346

Bäumer D, Preisfeld A, Ruppel HG (2001) Isolation and characterization of paramylon synthase from *Euglena gracilis* (Euglenophyceae). J Phycol 37:38–46

Baurain D, Brinkmann H, Petersen J et al (2010) Phylogenomic evidence for separate acquisition of plastids in cryptophytes, haptophytes, and stramenopiles. Mol Biol Evol 27:1698–1709

Becker B, Hoef-Emden K, Melkonian M (2008) Chlamydial genes shed light on the evolution of photoautotrophic eukaryotes. BMC Evol Biol 8:203

Beller M, Thiel K, Thul P et al (2010) Lipid droplets: a dynamic organelle moves into focus. FEBS Lett 584:2176–2182

Bergman B, Gallon JR, Rai AN et al (1997) N2 fixation by non-heterocystous cyanobacteria. FEMS Microbiol Rev 19:139–185

Bhattacharya D, Archibald JM, Weber AP et al (2007) How do endosymbionts become organelles? Understanding early events in plastid evolution. Bioessays 29:1239–1246

Bhattacharya D, Price DC, Chan CX et al (2013) Genome of the red alga Porphyridium purpureum. Nat Commun 4:1941

Blank CE, Sanchez-Baracaldo P (2010) Timing of morphological and ecological innovations in the cyanobacteria – a key to understanding the rise in atmospheric oxygen. Geobiology 8:1–23

Borowitza MA (1978) Plastid development and floridean starch grain formation during carposporogenesis in the coralline red alga Lithothrix aspergillum gray. Protoplasma 95:217–228

Brautigan DL (2013) Protein Ser/Thr phosphatases – the ugly ducklings of cell signalling. FEBS J 280:324–345

Burris RH (1991) Nitrogenase. J Biol Chem 266:9339–9342

Busi MV, Barchiesi J, Martin M et al (2013) Starch metabolism in green algae. Starch/Stärke 66:28–40

Cavalier-Smith T (1999) Principles of protein and lipid targeting in secondary symbiogenesis: euglenoid, dinoflagellate, and sporozoan plastid origins and the eukaryote family tree. J Eukaryot Microbiol 46:347–366

Cavalier-Smith T, Chao EE, Snell EA et al (2014) Multigene eukaryote phylogeny reveals the likely protozoan ancestors of opisthokonts (animals, fungi, choanozoans) and Amoebozoa. Mol Phylogenet Evol 81C:71–85

Cenci U, Chabi M, Ducatez M et al (2013) Convergent evolution of polysaccharide debranching defines a common mechanism for starch accumulation in cyanobacteria and plants. Plant Cell 25:3961–3975

Cenci U, Nitschke F, Steup M et al (2014) Transition from glycogen to starch metabolism in Archaeplastida. Trends Plant Sci 19:18–28

Chandra G, Chater KF, Bornemann S (2011) Unexpected and widespread connections between bacterial glycogen and trehalose metabolism. Microbiology 157:1565–1572

Charng YY, Kakefuda G, Iglesias AA et al (1992) Molecular cloning and expression of the gene encoding ADP-glucose pyrophosphorylase from the cyanobacterium Anabaena sp. strain PCC 7120. Plant Mol Biol 20:37–47

Choi JH, Lee H, Kim YW et al (2009) Characterization of a novel debranching enzyme from Nostoc punctiforme possessing a high specificity for long branched chains. Biochem Biophys Res Commun 378:224–229

Collen J, Porcel B, Carre W et al (2013) Genome structure and metabolic features in the red seaweed Chondrus crispus shed light on evolution of the Archaeplastida. Proc Natl Acad Sci U S A 110:5247–5252

Colleoni C, Suzuki E (2012) Chapter 5: Storage polysaccharide metabolism in Cyanobacteria. In: Tetlow IJ (ed) Starch: origins, structure and metabolism, vol 5, Essential reviews in experimental biology. Society for Experimental Biology, London

Colleoni C, Linka M, Deschamps P et al (2010) Phylogenetic and biochemical evidence supports the recruitment of an ADP-glucose translocator for the export of photosynthate during plastid endosymbiosis. Mol Biol Evol 27:2691–2701

Collingro A, Tischler P, Weinmaier T et al (2011) Unity in variety – the pan-genome of the Chlamydiae. Mol Biol Evol 28:3253–3270

Compaore J, Stal LJ (2010) Oxygen and the light–dark cycle of nitrogenase activity in two unicellular cyanobacteria. Environ Microbiol 12:54–62

Coppin A, Varre JS, Lienard L et al (2004) Evolution of plant-like crystalline storage polysaccharide in the protozoan parasite Toxoplasma gondii argues for a red alga ancestry. J Mol Evol 60:257–267

Coutinho PM, Henrissat B (1999) Carbohydrate-active enzymes: an integrated database approach. Royal Society of Chemistry, Cambridge

Crowe SA, Dossing LN, Beukes NJ et al (2013) Atmospheric oxygenation three billion years ago. Nature 501:535–538

Curatti L, Giarrocco LE, Cumino AC et al (2008) Sucrose synthase is involved in the conversion of sucrose to polysaccharides in filamentous nitrogen-fixing cyanobacteria. Planta 228:617–625

Curtis BA, Tanifuji G, Burki F et al (2012) Cryptophyte and chlorarachniophyte nuclear genomes reveal evolutionary mosaicism and fate of nucleomorphs. Nature 492:59–65

Dauvillée D, Kinderf IS, Li Z et al (2005) Role of the Escherichia coli glgX gene in glycogen metabolism. J Bacteriol 187:1465–1473

Dauvillee D, Deschamps P, Ral JP et al (2009) Genetic dissection of floridean starch synthesis in the cytosol of the model dinoflagellate Crypthecodinium cohnii. Proc Natl Acad Sci U S A 106:21126–21130

Deane JA, Strachan IM, Saunders GW et al (2002) Cryptomonad evolution: nuclear 18S rDNA phylogeny versus cell morphology and pigmentation. J Phycol 38:1236–1244

Delrue B, Fontaine T, Routier F et al (1992) Waxy Chlamydomonas reinhardtii: monocellular algal mutants defective in amylose biosynthesis and granule-bound starch synthase activity accumulate a structurally modified amylopectin. J Bacteriol 174:3612–3620

Delwiche CF (1999) Tracing the thread of plastid diversity through the tapestry of life. Am Nat 154:S164–S177

Deschamps P, Haferkamp I, Dauvillée D et al (2006) Nature of the periplastidial pathway of starch synthesis in the cryptophyte Guillardia theta. Eukaryot Cell 5:954–963

Deschamps P, Colleoni C, Nakamura Y et al (2008a) Metabolic symbiosis and the birth of the plant kingdom. Mol Biol Evol 25:536–548

Deschamps P, Guillebeault D, Devassine J et al (2008b) The heterotrophic dinoflagellate Crypthecodinium cohnii defines a model genetic system to investigate cytoplasmic starch synthesis. Eukaryot Cell 7:872–880

Deschamps P, Haferkamp I, d'Hulst C et al (2008c) The relocation of starch metabolism to chloroplasts: when, why and how. Trends Plant Sci 13:574–582

Deschamps P, Moreau H, Worden AZ et al (2008d) Early gene duplication within chloroplastida and its correspondence with relocation of starch metabolism to chloroplasts. Genetics 178:2373–2387

Devillers CH, Piper ME, Ballicora MA et al (2003) Characterization of the branching patterns of glycogen branching enzyme truncated on the N-terminus. Arch Biochem Biophys 418:34–38

Douglas SE, Penny SL (1999) The plastid genome of the cryptophyte alga, Guillardia theta: complete sequence and conserved synteny groups confirm its common ancestry with red algae. J Mol Evol 48:236–244

Douglas S, Zauner S, Fraunholz M et al (2001) The highly reduced genome of an enslaved algal nucleus. Nature 410:1091–1096

Ekman P, Yu S, Pedersén M (1991) Effects of altered salinity, darkness and algal nutrient status on floridoside and starch content, alpha-galactosidase activity and agar yield of cultivated *Gracilaria sordida*. Br Phycol J 26:123–131

Facchinelli F, Pribil M, Oster U et al (2013) Proteomic analysis of the Cyanophora paradoxa muroplast provides clues on early events in plastid endosymbiosis. Planta 237:637–651

Falcon LI, Cipriano F, Chistoserdov AY et al (2002) Diversity of diazotrophic unicellular cyanobacteria in the tropical North Atlantic Ocean. Appl Environ Microbiol 68:5760–5764

Falkowski P, Raven JA (2007) Aquatic photosynthesis. Princeton University Press, Princeton

Fathinejad S, Steiner JM, Reipert S et al (2008) A carboxysomal carbon-concentrating mechanism in the cyanelles of the 'coelacanth' of the algal world, Cyanophora paradoxa? Physiol Plant 133:27–32

Fettke J, Hejazi M, Smirnova J et al (2009) Eukaryotic starch degradation: integration of plastidial and cytosolic pathways. J Exp Bot 60:2907–2922

Forsyth G, Hirst EL, Oxford AE (1953) Protozoal polysaccharides. Structure of a polysaccharide produced by Cycloposthium. J Chem Soc 2030–2033

Fredrick JF (1968) Biochemical evolution of glucosyl transferase isozymes in algae. Ann N Y Acad Sci 151:413–423

Frueauf JB, Ballicora MA, Preiss J (2002) Alteration of inhibitor selectivity by site-directed mutagenesis of Arg(294) in the ADP-glucose pyrophosphorylase from Anabaena PCC 7120. Arch Biochem Biophys 400:208–214

Fu J, Xu X (2006) The functional divergence of two glgP homologues in Synechocystis sp. PCC 6803. FEMS Microbiol Lett 260:201–209

Glöckner G, Noegel A (2013) Comparative genomics in the Amoebozoa clade. Biol Rev 88:215–225

Goldemberg SH, Marechal LR (1963) Biosynthesis of paramylon in Euglena gracilis. Biochim Biophys Acta 71:743–744

Grosche C, Hempel F, Bolte K et al (2014) The periplastidal compartment: a naturally minimized eukaryotic cytoplasm. Curr Opin Microbiol 22C:88–93

Grundel M, Scheunemann R, Lockau W et al (2012) Impaired glycogen synthesis causes metabolic overflow reactions and affects stress responses in the Cyanobacterium Synechocystis sp. PCC 6803. Microbiology 158:3032–3043

Guerra LT, Xu Y, Bennette N et al (2013) Natural osmolytes are much less effective substrates than glycogen for catabolic energy production in the marine cyanobacterium Synechococcus sp. strain PCC 7002. J Biotechnol 166:65–75

Haferkamp I, Deschamps P, Ast M et al (2006) Molecular and biochemical analysis of periplastidial starch metabolism in the cryptophyte Guillardia theta. Eukaryot Cell 5:964–971

Henrissat B, Deleury E, Coutinho PM (2002) Glycogen metabolism loss: a common marker of parasitic behaviour in bacteria? Trends Genet 18:437–440

Higo A, Katoh H, Ohmori K et al (2006) The role of a gene cluster for trehalose metabolism in dehydration tolerance of the filamentous cyanobacterium Anabaena sp. PCC 7120. Microbiology 152:979–987

Hirabaru C, Izumo A, Fujiwara S et al (2010) The primitive rhodophyte Cyanidioschyzon merolae contains a semiamylopectin-type, but not an amylose-type, alpha-glucan. Plant Cell Physiol 51:682–693

Huang J, Gogarten JP (2007) Did an ancient chlamydial endosymbiosis facilitate the establishment of primary plastids? Genome Biol 8:R99

Husnik F, Nikoh N, Koga R et al (2013) Horizontal gene transfer from diverse bacteria to an insect genome enables a tripartite nested mealybug symbiosis. Cell 153:1567–1578

Izumo A, Fujiwara S, Sakurai T et al (2011) Effects of granule-bound starch synthase I-defective mutation on the morphology and structure of pyrenoidal starch in Chlamydomonas. Plant Sci 180:238–245

James MG, Robertson DS, Myers AM (1995) Characterization of the maize gene sugary1, a determinant of starch composition in kernels. Plant Cell 7:417–429

Kiel JA, Boels JM, Beldman G et al (1990) Nucleotide sequence of the Synechococcus sp. PCC7942 branching enzyme gene (glgB): expression in Bacillus subtilis. Gene 89:77–84

Kiss JK, Roberts EM, Brown RM et al (1988) X-ray and dissolution studies of paramylon storage granules from Euglena. Protoplasma 146:150–156

Kopp RE, Kirschvink JL, Hilburn IA et al (2005) The Paleoproterozoic snowball Earth: a climate disaster triggered by the evolution of oxygenic photosynthesis. Proc Natl Acad Sci U S A 102:11131–11136

Kotting O, Pusch K, Tiessen A et al (2005) Identification of a novel enzyme required for starch metabolism in Arabidopsis leaves. The phosphoglucan, water dikinase. Plant Physiol 137:242–252

Kotting O, Santelia D, Edner C et al (2009) STARCH-EXCESS4 is a laforin-like Phosphoglucan phosphatase required for starch degradation in Arabidopsis thaliana. Plant Cell 21:334–346

Kubo A, Fujita N, Harada K et al (1999) The starch-debranching enzymes isoamylase and pullulanase are both involved in amylopectin biosynthesis in rice endosperm. Plant Physiol 121:399–410

Ladeira RB, Freitas MA, Silva EF et al (2005) Glycogen as a carbohydrate energy reserve in trophozoites of Giardia lamblia. Parasitol Res 96:418–421

Lafora GR, Glueck B (1911) Beitrag zur histopathologie der myoklonischen epilepsie. Z Gesamte Neurol Psychiatr 6:1–14

Larsson J, Nylander JA, Bergman B (2011) Genome fluctuations in cyanobacteria reflect evolutionary, developmental and adaptive traits. BMC Evol Biol 11:187

Latysheva N, Junker VL, Palmer WJ et al (2012) The evolution of nitrogen fixation in cyanobacteria. Bioinformatics 28:603–606

Le Gall L, Saunders GW (2007) A nuclear phylogeny of the Florideophyceae (Rhodophyta) inferred from combined EF2, small subunit and large subunit ribosomal DNA: establishing the new red algal subclass Corallinophycidae. Mol Phylogenet Evol 43:1118–1130

Linka M, Jamai A, Weber AP (2008) Functional characterization of the plastidic phosphate translocator gene family from the thermo-acidophilic red alga Galdieria sulphuraria reveals specific adaptations of primary carbon partitioning in green plants and red algae. Plant Physiol 148:1487–1496

Lister DL, Bateman JM, Purton S et al (2003) DNA transfer from chloroplast to nucleus is much rarer in Chlamydomonas than in tobacco. Gene 316:33–38

Lluisma AO, Ragan MA (1998) Characterization of a galactose-1-phosphate uridylyltransferase gene from the marine red alga Gracilaria gracilis. Curr Genet 34:112–119

Loddenkotter B, Kammerer B, Fischer K et al (1993) Expression of the functional mature chloroplast triose phosphate translocator in yeast internal membranes and purification of the histidine-tagged protein by a single metal-affinity chromatography step. Proc Natl Acad Sci U S A 90:2155–2159

Lorenzo-Morales J, Kliescikova J, Martinez-Carretero E et al (2008) Glycogen phosphorylase in Acanthamoeba spp.: determining the role of the enzyme during the encystment process using RNA interference. Eukaryot Cell 7:509–517

Lou J, Dawson KA, Strobel HJ (1997) Glycogen biosynthesis via UDP-glucose in the ruminal bacterium Prevotella bryantii B1(4). Appl Environ Microbiol 63:4355–4359

Lu Y, Sharkey TD (2006) The importance of maltose in transitory starch breakdown. Plant Cell Environ 29:353–366

Lu C, Lei L, Peng B et al (2013) Chlamydia trachomatis GlgA is secreted into host cell cytoplasm. PLoS One 8:e68764

Maddelein ML, Libessart N, Bellanger F et al (1994) Toward an understanding of the biogenesis of the starch granule. Determination of granule-bound and soluble starch synthase functions in amylopectin synthesis. J Biol Chem 269:25150–25157

Manners DJ, Ryley JF (1952) Studies on the metabolism of the Protozoa. II. The glycogen of the ciliate Tetrahymena pyriformis (Glaucoma piriformis). Biochem J 52:480–482

Manners DJ, Ryley JF (1955) Studies on the metabolism of the protozoa. 6. The glycogens of the parasitic flagellates Trichomonas foetus and Trichomonas gallinae. Biochem J 59:369–372

Marin B, Nowack EC, Melkonian M (2005) A plastid in the making: evidence for a second primary endosymbiosis. Protist 156:425–432

Martijn J, Ettema TJ (2013) From archaeon to eukaryote: the evolutionary dark ages of the eukaryotic cell. Biochem Soc Trans 41:451–457

Matsuzaki M, Misumi O, Shin IT et al (2004) Genome sequence of the ultrasmall unicellular red alga Cyanidioschyzon merolae 10D. Nature 428:653–657

McCracken DA, Cain JR (1981) Amylose in Floridean starch. New Phytol 88

Meeuse BJ, Kreger DR (1954) On the nature of floridean starch and Ulva starch. Biochim Biophys Acta 13:593–595

Meeuse BJ, Andries M, Wood JA (1960) Floridean starch. J Exp Bot 11:129–140

Miao X, Wu Q, Wu G et al (2003) Sucrose accumulation in salt-stressed cells of agp gene deletion-mutant in cyanobacterium Synechocystis sp PCC 6803. FEMS Microbiol Lett 218:71–77

Moran-Zorzano MT, Alonso-Casajus N, Munoz FJ et al (2007) Occurrence of more than one important source of ADPglucose linked to glycogen biosynthesis in Escherichia coli and Salmonella. FEBS Lett 581:4423–4429

Moriyama T, Sakurai K, Sekine K et al (2014) Subcellular distribution of central carbohydrate metabolism pathways in the red alga Cyanidioschyzon merolae. Planta 240:585–598

Mouille G, Maddelein ML, Libessart N et al (1996) Preamylopectin processing: a mandatory step for starch biosynthesis in plants. Plant Cell 8:1353–1366

Moustafa A, Reyes-Prieto A, Bhattacharya D (2008) Chlamydiae has contributed at least 55 genes to Plantae with predominantly plastid functions. PLoS One 3:e2205

Murakami T, Kanai T, Takata H et al (2006) A novel branching enzyme of the GH-57 family in the hyperthermophilic archaeon Thermococcus kodakaraensis KOD1. J Bacteriol 188:5915–5924

Nagashima H, Nakamura S, Nisizawa K et al (1971) Enzymatic synthesis of floridean starch in red alga Serraticardia maxima. Plant Cell Physiol 12:243–253

Nakamura Y, Takahashi J, Sakurai A et al (2005) Some Cyanobacteria synthesize semi-amylopectin type alpha-polyglucans instead of glycogen. Plant Cell Physiol 46:539–545

Nakayama A, Yamamoto K, Tabata S (2001) Identification of the catalytic residues of bifunctional glycogen debranching enzyme. J Biol Chem 276:28824–28828

Nelson OE, Rines HW (1962) The enzymatic deficiency in the waxy mutant of maize. Biochem Biophys Res Commun 9:297–300

Nowack EC, Melkonian M, Glockner G (2008) Chromatophore genome sequence of Paulinella sheds light on acquisition of photosynthesis by eukaryotes. Curr Biol 18:410–418

Nyvall P, Pelloux J, Davies HV et al (1999) Purification and characterisation of a novel starch synthase selective for uridine 5′-diphosphate glucose from the red alga Gracilaria tenuistipitata. Planta 209:143–152

Nyvall P, Pedersen M, Kenne L et al (2000) Enzyme kinetics and chemical modification of alpha-1,4-glucan lyase from Gracilariopsis sp. Phytochemistry 54:139–145

Ojcius DM, Degani H, Mispelter J et al (1998) Enhancement of ATP levels and glucose metabolism during an infection by Chlamydia. NMR studies of living cells. J Biol Chem 273:7052–7058
Pade N, Linka N, Ruth W et al (2014) Floridoside and isofloridoside are synthesized by trehalose 6-phosphate synthase-like enzymes in the red alga Galdieria sulphuraria. New Phytol. doi:10.1111/nph.13108
Page-Sharp M, Behm CA, Smith GD (1999) Involvement of the compatible solutes trehalose and sucrose in the response to salt stress of a cyanobacterial Scytonema species isolated from desert soils. Biochim Biophys Acta 1472:519–528
Palmer TN, Ryman BE, Whelan WJ (1976) The action pattern of amylomaltase from Escherichia coli. Eur J Biochem 69:105–115
Park JT, Shim JH, Tran PL et al (2011) Role of maltose enzymes in glycogen synthesis by Escherichia coli. J Bacteriol 193:2517–2526
Petersen J, Ludewig AK, Michael V et al (2014) Chromera velia, endosymbioses and the rhodoplex hypothesis – plastid evolution in cryptophytes, alveolates, stramenopiles, and haptophytes (CASH lineages). Genome Biol Evol 6:666–684
Pittenauer E, Schmid ER, Allmaier G et al (1993) Structural characterization of the cyanelle peptidoglycan of Cyanophora paradoxa by 252Cf plasma desorption mass spectrometry and fast atom bombardment/tandem mass spectrometry. Biol Mass Spectrom 22:524–536
Plancke C, Colleoni C, Deschamps P et al (2008) Pathway of cytosolic starch synthesis in the model glaucophyte Cyanophora paradoxa. Eukaryot Cell 7:247–257
Porchia AC, Curatti L, Salerno GL (1999) Sucrose metabolism in cyanobacteria: sucrose synthase from Anabaena sp. strain PCC 7119 is remarkably different from the plant enzymes with respect to substrate affinity and amino-terminal sequence. Planta 210:34–40
Preiss J (1984) Bacterial glycogen synthesis and its regulation. Annu Rev Microbiol 38:419–458
Price DC, Chan CX, Yoon HS et al (2012) Cyanophora paradoxa genome elucidates origin of photosynthesis in algae and plants. Science 335:843–847
Ragan MA, Bird CJ, Rice EL et al (1994) A molecular phylogeny of the marine red algae (Rhodophyta) based on the nuclear small-subunit rRNA gene. Proc Natl Acad Sci U S A 91:7276–7280
Reyes-Prieto A, Moustafa A, Bhattacharya D (2008) Multiple genes of apparent algal origin suggest ciliates may once have been photosynthetic. Curr Biol 18:956–962
Rodriguez-Ezpeleta N, Brinkmann H, Burey SC et al (2005) Monophyly of primary photosynthetic eukaryotes: green plants, red algae, and glaucophytes. Curr Biol 15:1325–1330
Rogers PV, Luo S, Sucic JF et al (1992) Characterization and cloning of glycogen phosphorylase 1 from Dictyostelium discoideum. Biochim Biophys Acta 1129:262–272
Rogers PV, Sucic JF, Yin Y et al (1994) Disruption of glycogen phosphorylase gene expression in Dictyostelium: evidence for altered glycogen metabolism and developmental coregulation of the gene products. Differentiation 56:1–12
Rutherford CL, Peery RB, Sucic JF et al (1992) Cloning, structural analysis, and expression of the glycogen phosphorylase-2 gene in Dictyostelium. J Biol Chem 267:2294–2302
Sanchez-Baracaldo P, Ridgwell A, Raven JA (2014) A neoproterozoic transition in the marine nitrogen cycle. Curr Biol 24:652–657
Sanchez-Puerta MV, Lippmeier JC, Apt KE et al (2007) Plastid genes in a non-photosynthetic dinoflagellate. Protist 158:105–117
Santos CR, Tonoli CC, Trindade DM et al (2011) Structural basis for branching-enzyme activity of glycoside hydrolase family 57: structure and stability studies of a novel branching enzyme from the hyperthermophilic archaeon Thermococcus kodakaraensis KOD1. Proteins 79:547–557
Sawada T, Nakamura Y, Ohdan T et al (2014) Diversity of reaction characteristics of glucan branching enzymes and the fine structure of alpha-glucan from various sources. Arch Biochem Biophys 562C:9–21
Schlichting R, Bothe H (1993) The cyanelle (Organelles of a low evolutionary scale) possess a phosphate-translocator and a glucose-carrier in Cyanophora paradoxa. Botanica Acta 106:428–434

Schneegurt MA, Sherman DM, Nayar S et al (1994) Oscillating behavior of carbohydrate granule formation and dinitrogen fixation in the cyanobacterium Cyanothece sp. strain ATCC 51142. J Bacteriol 176:1586–1597

Schonknecht G, Chen WH, Ternes CM et al (2013) Gene transfer from bacteria and archaea facilitated evolution of an extremophilic eukaryote. Science 339:1207–1210

Schwoppe C, Winkler HH, Neuhaus HE (2002) Properties of the glucose-6-phosphate transporter from Chlamydia pneumoniae (HPTcp) and the glucose-6-phosphate sensor from Escherichia coli (UhpC). J Bacteriol 184:2108–2115

Schwoppe C, Winkler HH, Neuhaus HE (2003) Connection of transport and sensing by UhpC, the sensor for external glucose-6-phosphate in Escherichia coli. Eur J Biochem 270:1450–1457

Serodio J, Cruz S, Cartaxana P et al (2014) Photophysiology of kleptoplasts: photosynthetic use of light by chloroplasts living in animal cells. Philos Trans R Soc Lond B Biol Sci 369:20130242

Sesma JI, Iglesias AA (1998) Synthesis of floridean starch in the red alga Gracilaria gracilis occurs via ADP-glucose. In: Garab G (ed) Photosynthesis: mechanisms and effects. Kluwer Academic Publishers, Dordrecht, pp 3537–3540

Sheath RG, Hellebust JA, Sawa T (1979) Floridean starch metabolism of Porphyridium purpureum Rhophyta I. Changes during ageing of batch culture. Phycologia 18:292–293

Sheng J, Preiss J (1997) Arginine294 is essential for the inhibition of Anabaena PCC 7120 ADP-glucose pyrophosphorylase by phosphate. Biochemistry 36:13077–13084

Shih PM, Matzke NJ (2013) Primary endosymbiosis events date to the later Proterozoic with cross-calibrated phylogenetic dating of duplicated ATPase proteins. Proc Natl Acad Sci U S A 110:12355–12360

Shimonaga T, Fujiwara S, Kaneko M et al (2007) Variation in storage alpha-polyglucans of red algae: amylose and semi-amylopectin types in Porphyridium and glycogen type in Cyanidium. Mar Biotechnol (NY) 9:192–202

Shimonaga T, Konishi M, Oyama Y et al (2008) Variation in storage alpha-glucans of the Porphyridiales (Rhodophyta). Plant Cell Physiol 49:103–116

Shoguchi E, Shinzato C, Kawashima T et al (2013) Draft assembly of the Symbiodinium minutum nuclear genome reveals dinoflagellate gene structure. Curr Biol 23:1399–1408

Singh PK (1973) Nitrogen fixation by the unicellular blue-green alga *Aphanothece*. Arch Mikrobiol 92:59–62

Stadnichuk IN, Semenova LR, Smirnova GP et al (2007) A highly branched storage polyglucan in the thermoacidophilic red microalga Galdieria maxima cells. Prikl Biokhim Mikrobiol 43:88–93

Stegemann S, Hartmann S, Ruf S et al (2003) High-frequency gene transfer from the chloroplast genome to the nucleus. Proc Natl Acad Sci U S A 100:8828–8833

Steiner JM, Yusa F, Pompe JA et al (2005) Homologous protein import machineries in chloroplasts and cyanelles. Plant J 44:646–652

Streb S, Delatte T, Umhang M et al (2008) Starch granule biosynthesis in Arabidopsis is abolished by removal of all debranching enzymes but restored by the subsequent removal of an endoamylase. Plant Cell 20:3448–3466

Summons RE, Jahnke LL, Hope JM et al (1999) 2-Methylhopanoids as biomarkers for cyanobacterial oxygenic photosynthesis. Nature 400:554–557

Suzuki E, Umeda K, Nihei S, Moriya K, Ohkawa H, Fujiwara S, Tsuzuki M, Nakamura Y (2007) Role of the GlgX protein in glycogen metabolism of the cyanobacterium, Synechococcus elongatus PCC 7942. Biochim Biophys Acta 1770:763–773

Suzuki E, Ohkawa H, Moriya K et al (2010) Carbohydrate metabolism in mutants of the cyanobacterium Synechococcus elongatus PCC 7942 defective in glycogen synthesis. Appl Environ Microbiol 76:3153–3159

Suzuki E, Onoda M, Colleoni C et al (2013) Physicochemical variation of cyanobacterial starch, the insoluble alpha-Glucans in cyanobacteria. Plant Cell Physiol 54:465–473

Szydlowski N, Ragel P, Raynaud S et al (2009) Starch granule initiation in Arabidopsis requires the presence of either class IV or class III starch synthases. Plant Cell 21:2443–2457

Tagliabracci VS, Turnbull J, Wang W et al (2007) Laforin is a glycogen phosphatase, deficiency of which leads to elevated phosphorylation of glycogen in vivo. Proc Natl Acad Sci U S A 104:19262–19266

Tomos AD, Northcote DH (1978) A protein-glucan intermediate during paramylon synthesis. Biochem J 174:283–290

Torija MJ, Novo M, Lemassu A et al (2005) Glycogen synthesis in the absence of glycogenin in the yeast Saccharomyces cerevisiae. FEBS Lett 579:3999–4004

Tresse E, Kosta A, Giusti C et al (2008) A UDP-glucose derivative is required for vacuolar autophagic cell death. Autophagy 4:680–691

Tuttle RC, Loeblich AR 3rd (1974) Genetic recombination in the dinoflagellate Crypthecodinium cohnii. Science 185:1061–1062

Tuttle RC, Loeblich AR 3rd (1977) N-methyl-N′-nitro-N-nitrosoguanidine and UV induced mutants of the dinoflagellate Crypthecodinium cohnii. J Protozool 24:313–316

Ugalde JE, Parodi AJ, Ugalde RA (2003) De novo synthesis of bacterial glycogen: Agrobacterium tumefaciens glycogen synthase is involved in glucan initiation and elongation. Proc Natl Acad Sci U S A 100:10659–10663

Villarejo A, Martinez F, del Pino Plumed M et al (1996) The induction of the CO2 concentrating mechanism in a starch-less mutant of Chlamydomonas reinhardtii. Physiol Plant 98:798–802

Viola R, Nyvall P, Pedersen M (2001) The unique features of starch metabolism in red algae. Proc Biol Sci 268:1417–1422

Vogel K, Barber AA (1968) Degradation of paramylon by Euglena gracilis. J Protozool 15:657–662

Wattebled F, Buleon A, Bouchet B et al (2002) Granule-bound starch synthase I. A major enzyme involved in the biogenesis of B-crystallites in starch granules. Eur J Biochem 269:3810–3820

Wattebled F, Dong Y, Dumez S et al (2005) Mutants of Arabidopsis lacking a chloroplastic isoamylase accumulate phytoglycogen and an abnormal form of amylopectin. Plant Physiol 138:184–195

Weber AP, Linka M, Bhattacharya D (2006) Single, ancient origin of a plastid metabolite translocator family in Plantae from an endomembrane-derived ancestor. Eukaryot Cell 5:609–612

Williams TA, Foster PG, Nye TM et al (2012) A congruent phylogenomic signal places eukaryotes within the Archaea. Proc Biol Sci 279:4870–4879

Williamson BD, Favis R, Brickey DA et al (1996) Isolation and characterization of glycogen synthase in Dictyostelium discoideum. Dev Genet 19:350–364

Wilson WA, Roach PJ, Montero M et al (2010) Regulation of glycogen metabolism in yeast and bacteria. FEMS Microbiol Rev 34:952–985

Wisecaver JH, Hackett JD (2011) Dinoflagellate genome evolution. Annu Rev Microbiol 65:369–387

Wolf A, Kramer R, Morbach S (2003) Three pathways for trehalose metabolism in Corynebacterium glutamicum ATCC13032 and their significance in response to osmotic stress. Mol Microbiol 49:1119–1134

Wyatt JT, Silvey JK (1969) Nitrogen fixation by gloeocapsa. Science 165:908–909

Xu Y, Guerra LT, Li Z et al (2013) Altered carbohydrate metabolism in glycogen synthase mutants of Synechococcus sp. strain PCC 7002: cell factories for soluble sugars. Metab Eng 16:56–67

Yoo SH, Spalding MH, Jane JL (2002) Characterization of cyanobacterial glycogen isolated from the wild type and from a mutant lacking of branching enzyme. Carbohydr Res 337:2195–2203

Yoo SH, Lee BH, Moon Y et al (2014) Glycogen synthase isoforms in Synechocystis sp. PCC6803: identification of different roles to produce glycogen by targeted mutagenesis. PLoS One 9:e91524

Yoon HS, Hackett JD, Pinto G et al (2002) The single, ancient origin of chromist plastids. Proc Natl Acad Sci U S A 99:15507–15512

Yoon HS, Hackett JD, Ciniglia C et al (2004) A molecular timeline for the origin of photosynthetic eukaryotes. Mol Biol Evol 21:809–818

Yoon HS, Müller KM, Stheath RG et al (2006) Defining the major lineages of red algae (Rhodophyta). J Phycol 42:482–492

Yoshikawa H, Nagashima M, Morimoto K et al (2003) Freeze-fracture and cytochemical studies on the in vitro cyst form of reptilian Blastocystis pythoni. J Eukaryot Microbiol 50:70–75

Yu S, Pedersen M (1993) Alpha-1,4-glucan lyase, a new class of starch/glycogen-degrading enzyme. II. Subcellular localization and partial amino-acid sequence. Planta 191:137–142

Yu S, Bojsen K, Svensson B et al (1999) alpha-1,4-glucan lyases producing 1,5-anhydro-D-fructose from starch and glycogen have sequence similarity to alpha-glucosidases. Biochim Biophys Acta 1433:1–15

Yu TS, Kofler H, Hausler RE et al (2001) The Arabidopsis sex1 mutant is defective in the R1 protein, a general regulator of starch degradation in plants, and not in the chloroplast hexose transporter. Plant Cell 13:1907–1918

Zea CJ, Pohl NL (2004) General assay for sugar nucleotidyltransferases using electrospray ionization mass spectrometry. Anal Biochem 328:196–202

Zona R, Chang-Pi-Hin F, O'Donohue MJ et al (2004) Bioinformatics of the glycoside hydrolase family 57 and identification of catalytic residues in amylopullulanase from Thermococcus hydrothermalis. Eur J Biochem 271:2863–2872

Part III
Metabolism

Chapter 5
Biosynthesis of Reserve Starch

Yasunori Nakamura

Abstract Plants have developed two distinct starch biosynthetic systems composed of over 30 kinds of enzymatic reaction network in photosynthetic and non-photosynthetic cells. Higher plants have also evolved a process in which cells can accumulate huge amounts of starch as granules inside the amyloplast of the reserve organs. Primarily the coordinated expression of several sets of distinct isozymes with specific enzymatic properties enables plant cells to synthesize starch with distinct fine structure and form the starch granules with specific semicrystalline structure, granular morphology, and physicochemical properties in plastids. This chapter overviews the current status of our understanding of metabolic regulation of starch biosynthesis in reserve organs by focusing on functions of individual isozymes examined by numerous in vivo and in vitro studies that have been performed to reveal how individual isozymes contribute to the synthesis of the reserve starch. The results raised the high possibility that at least some isozymes have multiple functions in starch biosynthesis under different conditions depending on the presence of various glucans and interaction/association with other enzymes. The features of starch biosynthetic process in plant tissues are also discussed with emphasis on the biochemical mechanism(s) underlying the coordinate actions among various enzymes.

Keywords Amylopectin • Amyloplast • Assimilatory starch • Chloroplast • Cluster structure • Isoamylase • Phosphorylase • Pullulanase • Reserve starch • Starch branching enzyme • Starch debranching enzyme • Starch synthase

Y. Nakamura (✉)
Faculty of Bioresource Sciences, Akita Prefectural University, Shimoshinjo-Nakano, Akita 010-0195, Japan

Akita Natural Science Laboratory, 25-44 Oiwake-Nishi, Tennoh, Katagami, Akita 010-0101, Japan
e-mail: nakayn@silver.plala.or.jp

Y. Nakamura (ed.), *Starch*, DOI 10.1007/978-4-431-55495-0_5

5.1 Introduction

Starch is stored in plastids of essentially all plant tissues and consumed as both energy and carbon source when required. During photosynthesis plants accumulate storage compounds mainly in the form of starch and sucrose from CO_2 and water. CO_2 is first incorporated into the phosphorylated intermediates in the Calvin-Benson cycle. Starch and sucrose are synthesized from fructose 6-P (F6P) and triose-P such as dihydroxyacetone-P or 3-phosphoglycerate (PGA), the Calvin-Benson cycle intermediates, in the chloroplast and cytosol, respectively. The phosphorylated intermediates are also used for the biosynthesis of other compounds such as proteins, lipids, nucleic acids, and other polysaccharides. ATP and NAD(P)H needed for these compounds including starch and sucrose are basically provided from the photophosphorylation system and the light-dependent electron transport system of photosynthesis, respectively. Thus, the balance (ratio) of inorganic phosphate (Pi)/total P (inorganic plus organic P), ATP/ADP, and NAD(P)H/NAD(P)$^+$ in each cellular compartment, such as chloroplast and cytosol, is fundamentally important to maintain high rates of photosynthesis and homeostasis of whole cells. The synthesis of starch and sucrose plays an important role in photosynthetic CO_2-fixation activity by returning Pi to the photophosphorylation system and the Calvin-Benson cycle. Since sucrose is synthesized in the cytosol, the released Pi is returned to chloroplasts by the triose-P/Pi translocator (TPT) located in the chloroplast inner envelope when carrying triose-P/PGA into the cytoplasm, as shown in Fig. 5.1a. The photosynthetic reactions must run very quickly to support all the energy-requiring physiological and biochemical events in plants under the light condition. Therefore, the carbon flow from the Calvin-Benson cycle to the starch and sucrose synthesis forms the primary metabolic process in plant cells.

As shown in Fig. 5.1c, the first step for the starch biosynthesis in green plants is the formation of ADPglucose, a glucose donor, from glucose 1-phosphate (G1P) and ATP as catalyzed by ADPglucose pyrophosphorylase (AGPase, EC 2.7.7.27) according to the following equation:

$$\text{G1P} + \text{ATP} \rightarrow \text{ADPglucose} + \text{PPi}$$

This step needs ATP and releases inorganic pyrophosphate (PPi), which is quickly decomposed into two molar equivalents of Pi by a high activity of inorganic pyrophosphatase in the stroma. Thus, the AGPase reaction actually proceeds in the ADPglucose synthetic direction, although the reaction is reversible in nature. The synthesis of starch is supported by chain elongation by transferring glucose moieties derived from ADPglucose to the nonreducing end of a glucan primer according to the equation catalyzed by starch synthase:

$$\text{ADPglucose} + \text{glucan primer } (G_n) \rightarrow \text{glucan } (G_{n+1}) + \text{ADP}$$

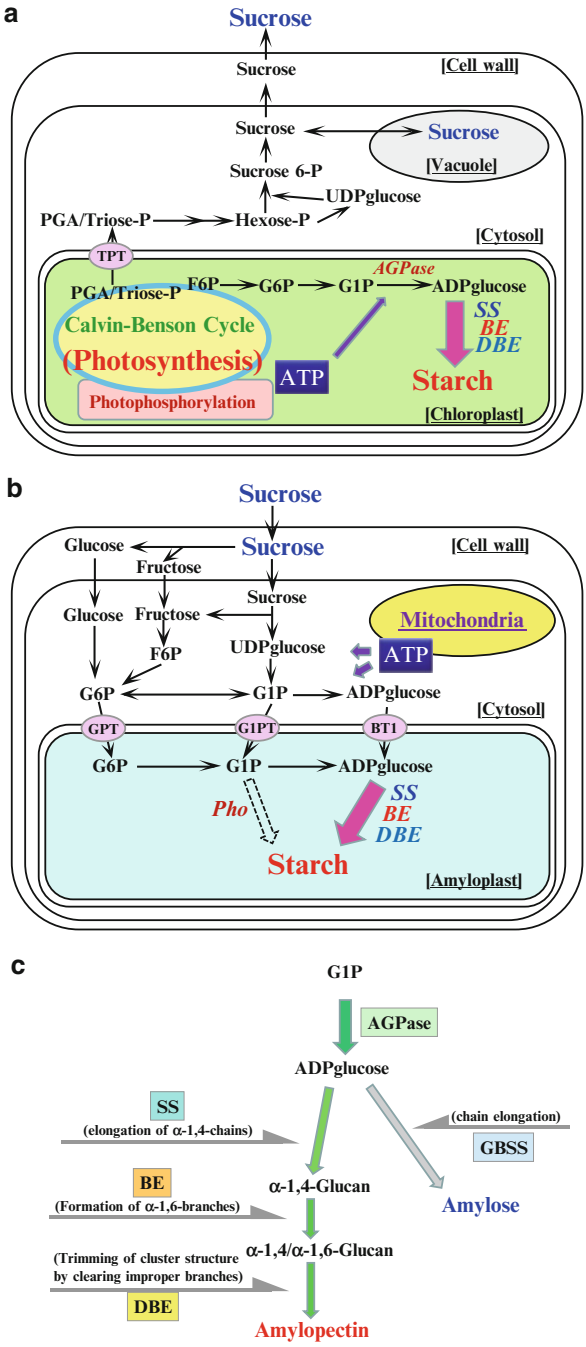

Fig. 5.1 Schematic representation of the starch biosynthetic pathway and the related metabolism in photosynthetic and non-photosynthetic tissues. (**a**) The synthesis of assimilatory starch in the leaf. (**b**) The synthesis of reserve starch in storage tissues. (**c**) The starch synthetic pathway from G1P. Abbreviations: *BT1* Brittle-1 protein (ADPglucose transporter), *TPT* triose phosphate/Pi translocator, *GPT* G6P/Pi translocator, *G1PT* putative G1P transporter (Fettke et al. 2010b)

where G_n and G_{n+1} denote glucans having number of glucose residues with n and $n+1$, respectively.

The amylopectin chains are elongated by a soluble form of starch synthase (SS, EC 2.4.1.21), whereas the amylose chain elongation is catalyzed by a starch granule-bound form of starch synthase, GBSS (Fig. 5.1c).

The α-1,6-glucosidic linkage is then introduced by starch branching enzyme (BE, EC 2.4.1.18). Finally, the fine structure of amylopectin is achieved via the trimming action (removal of unnecessary branches) of starch debranching enzymes (DBE).

In this way, amylopectin is basically synthesized by coordinate actions of three classes of enzymes, SS, BE, and DBE, whereas amylose is mainly synthesized by GBSS. However, the regulation of the starch synthesis is complex because each class of the enzymes has multiple isozymes with distinct properties.

The amylopectin and amylose molecules are densely packed into the starch granules having a high specific gravity up to 1.6 (Rundle et al. 1944), and the fine structure of amylopectin is responsible for the semicrystalline nature of starch granules. It is evident that if normal amylopectin fine structure is disturbed, the morphology and physicochemical properties of starch granules are altered or sometimes the granular structure is lost. The distinct structure of amylopectin is frequently described as "cluster structure," "bimodal chain-length distribution structure," or "asymmetric branching structure" (Hizukuri 1986; Thompson 2000; Pérez and Bertoft 2010, also see Chap. 1 in this volume). This means that the branches of amylopectin molecules are formed in at least two regions referred to as the amorphous lamella and the crystalline lamella, keeping a constant length of a single cluster (about 9 nm) in all plant sources (Jenkins et al. 1993, also see Chap. 1 in this volume) (Fig. 5.2).

Starch biosynthesis in reserve organs is characterized by a high rate of starch production from sucrose and an efficient formation of the starch granules including amylopectin and amylose. At the initial developmental stage of reserve organs, the initial starch synthetic process is critical, while during the maturing stages when starch is synthesized at the maximum rate, the primary starch biosynthetic process which can be referred to as the starch amplification process (or reproduction process) must be predominantly operating. This chapter mainly deals with the amplification process where the homogeneous glucan molecules are very rapidly reproduced to increase the starch amount, whereas the initiation process is described in Chap. 9 (also see D'Hulst and Merida 2012).

5.2 Comparison of Starch Biosynthetic Pathway Between Photosynthetic and Non-photosynthetic Tissues

Plants have developed the energy storage system in which a great amount of starch granules can be accumulated in reserve tissue. These starch granules are usually referred to as the reserve starch while those synthesized in chloroplasts

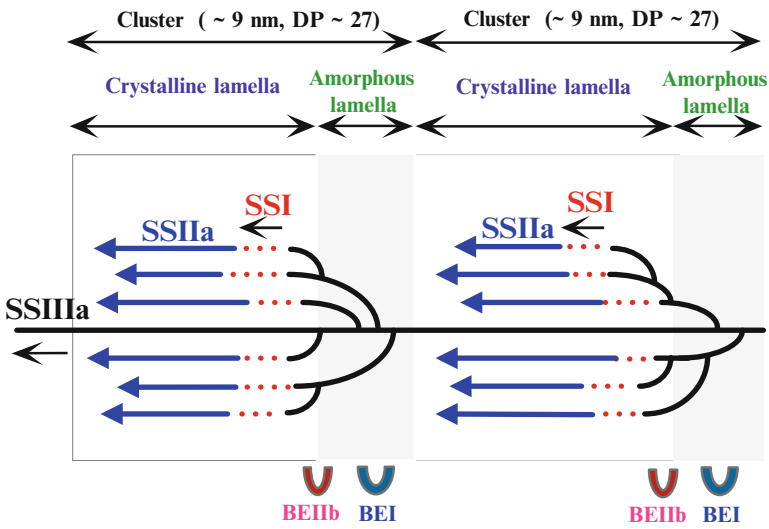

Fig. 5.2 Schematic representation of the cluster structure of amylopectin and the synthesis of cluster chains and branches in cereal endosperm via concerted elongation reactions by SSI, SSIIa, and SSIIIa isozymes and by branching reactions by BEI and BEIIb isozymes. The basic structure of amylopectin cluster composed of the repeated amorphous lamellae and the crystalline lamellae. The figure also presents the lengths of amylopectin chains determined by SS isozymes. SSI, SSIIa, and SSIIIa play distinct roles in the synthesis of very short chains, short and intermediate A- and B1-chains, and long B1- and B2-3-chains, respectively, and that branches localized in the amorphous lamellae and the crystalline lamellae and/or the interregion between both lamellae are mainly formed by BEI and BEIIb, respectively. The figure is drawn based on the results with rice plants and enzymes (Nakamura 2002, 2014)

of photosynthetic cells are called the assimilatory starch. The physiological role of both types of starch is different, i.e., the reserve starch is stored for the long period and used for the next generation while the assimilatory starch is temporarily accumulated during the day but is consumed during the following night period to support the biological activities in plant tissues. The importance of the different functions of both starches seems to be supported by the structural differences between them.

The whole metabolic pathway and events in the starch biosynthetic process as well as other related metabolic pathways in higher plants are different between assimilatory starch produced in chloroplasts (Fig. 5.1a) and reserve starch produced in amyloplasts (Fig. 5.1b). First, the pathway of the synthesis of ADPglucose, a glucose donor for starch synthesis by serving the substrate for SS and GBSS, totally differs between chloroplasts and amyloplasts. In chloroplasts, F6P, a member of the Calvin-Benson cycle, is first converted to glucose 6-P (G6P) and then to G1P by a plastidial glucose-phosphate isomerase (PGI) and phosphoglucomutase (PGM), respectively. Subsequently, G1P is metabolized to ADPglucose by AGPase (Fig. 5.1a). In amyloplasts, however, the starting metabolite for starch synthesis

is sucrose which is translocated to reserve tissues from leaves through phloem (Fig. 5.1b). Sucrose enters the cytosol via the sucrose transporter, and the first step for sucrose degradation is catalyzed by sucrose synthase to form UDPglucose and fructose. UDPglucose is then converted to G1P by UDPglucose pyrophosphorylase (UGPase). In cereals, G1P is mainly used as substrate for ADPglucose synthesizing reaction catalyzed by a cytosolic AGPase (Denyer et al. 1996; see also Chap. 11), and ADPglucose is then transported into amyloplasts via the ADPglucose transporter, sometimes referred to as the Brittle1 protein (Sullivan 1995; Shannon et al. 1998). In other reserve organs such as potato tubers and pea embryo, most of the G1P are transferred to G6P, which is imported into amyloplasts by the G6P translocator. G6P is metabolized to ADPglucose via G1P by both plastidial PGM and AGPase activities in amyloplasts. It is also possible that G1P is partially directly moved into amyloplasts by the putative G1P transporter (Fettke et al. 2010b). The translocated sucrose is also, at least partly, degraded by cellulose-bound invertase into glucose and fructose. After both compounds are transported into the cytosol by the hexose transporter, they are converted to G6P and F6P by hexokinase. F6P is converted into G6P by cytosolic PGI and, subsequently, to G1P to form ADPglucose by the actions of PGM and AGPase in the cereal cytoplasm or directly enters into amyloplasts in other species. During the early developmental stage of the cereal endosperm, it is considered that G6P moves into amyloplasts to some extent to be metabolized to ADPglucose by plastidial PGM and AGPase.

Second, the supply of ATP is different between chloroplast and amyloplast although ATP is essential for the AGPase reaction in both. In chloroplasts ATP is supplied from the photophosphorylation system functioning during photosynthesis. On the other hand, in non-photosynthetic cells, ATP is provided from the oxidative phosphorylation system operating in mitochondria during dark respiration (Fig. 5.1b). The generated ATP is provided to cytosolic AGPase in the cytoplasm or plastidial AGPase after the import into amyloplasts via the nucleoside triphosphate transporter.

Third, the types of translocators/transporters functioning in the non-photosynthetic cells are different from those in photosynthetic cells. In non-photosynthetic cells, many metabolic processes localized in different cellular compartments and organelles play distinct roles in starch synthesis. Thus, many translocators/transporters are needed to provide enzymes with metabolites and cofactors required for these actions and activities, as explained above. In contrast, chloroplasts in photosynthetic cells contain almost all of enzymes and cofactors for the whole starch biosynthetic processes. Thus, these processes can be independently operative during photosynthesis. More precisely, chloroplasts are specialized to produce two major photosynthates, starch and sucrose, and triose-P and/or PGA, the major primary CO_2-fixation products, are imported into the cytosol by the triose-P translocator (TPT) to produce sucrose in the cytosol (Fig. 5.1a). To facilitate the cytosolic sucrose synthesis, TPT transports inorganic phosphate (Pi) from cytosol into chloroplasts in exchange for triose-P and/or PGA as the counterpart. It is noted that translocators/transporters in non-photosynthetic reserve cells are different from

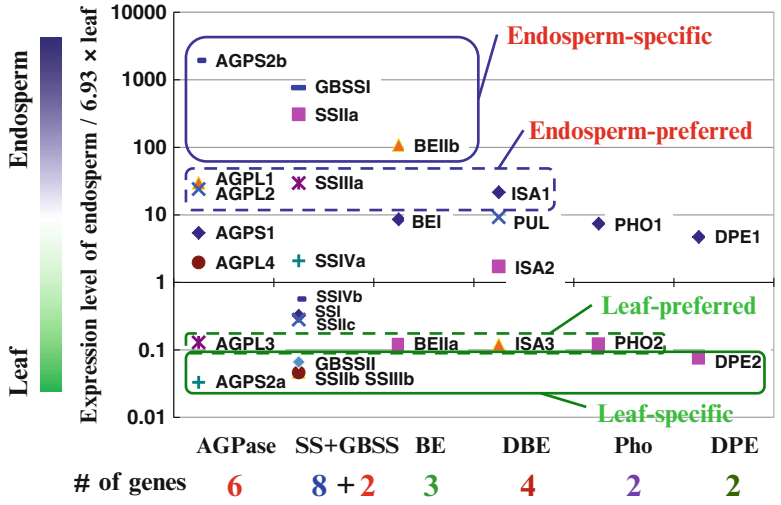

Fig. 5.3 Transcript levels of genes encoding starch metabolism in endosperm and leaf of rice (Data are from Ohdan et al. 2005)

those in photosynthetic cells and must have been developed during the process of plant evolution (Weber and Linka 2011).

Fourth, the regulatory mechanism for enzymatic actions and activities is different between reserve and assimilatory starch syntheses. In chloroplasts, starch synthesis is closely related to photosynthesis; the regulatory properties of AGPase and possibly other starch synthetic enzymes too, which are present in photosynthetic cells, are different from those in non-photosynthetic cells (see in details in Chap. 11).

Fifth, starch structure including the fine structure of amylopectin and starch granular structure differs between reserve and assimilatory starches.

Sixth, isozymes are differently expressed in both tissues, in addition to different levels of enzymatic activities between tissues (Nakamura et al. 1989). For example, some isozymes such as SSIIa, GBSSI, BEIIb, and ISA1 are almost exclusively or preferentially expressed in developing rice endosperm while others such as SSIIb, GBSSII, BEIIa, and ISA3 in the leaf (Ohdan et al. 2005), as presented in Fig. 5.3.

5.3 Functions and Properties of Enzymes Involved in the Biosynthesis of Reserve Starch

The contribution of each isozyme of starch synthetic enzymes to the synthesis of amylopectin and amylose has been investigated by using a variety of plant sources and species, purified enzyme preparations, mutants, and transformants

generated in at least the last three decades. The accumulated results provide us with the most reliable and invaluable fundamental information and materials. First, the presence and the relative activities or protein amounts of multiple isozymes and isoforms have been demonstrated. Second, their enzymatic properties such as reactivity toward various glucans including branched glucans (amylopectin and glycogen), amylose, and malto-oligosaccharides (MOS); effects of chemicals, metabolites, and temperature on activities; and association with other enzymes or starch granules have been elucidated. Third, the genes encoding each isozyme of starch synthetic enzymes were isolated, and structural features of individual proteins and their expression patterns in various tissues and the developmental stages were determined. Fourth, mutants defective in the target genes were isolated and used to characterize the functions of the genes. Fifth, the transgenic lines in which the target gene functions were modified were prepared, and various starch-related phenotypes were analyzed. The use of the transformants was of great interest to prove the function of the gene by detecting whether the mutated phenotype reverted to the wild-type one and to test the possibility of how and to what extent structural and functional properties of starch granules can be modified by bioengineering of the gene. Sixth, in vitro studies with the purified preparations of the target isozymes provided direct information on their enzymatic properties, functions, and enzymatic reaction mechanisms. Since in in vitro experiments the influences of other functionally overlapping and/or interacting isozymes can be neglected, properties of the target isozymes can be directly examined. In addition, the reaction conditions including the use of the appropriate primer/substrate glucans can be selected. Kinetic parameters and effects of cofactors on the activity can be determined. Seventh, the currently developed "omics" analyses enabled us to have the whole scope of the roles of all enzymes operating in the same tissues under various physiological conditions (Smith et al. 2004; Ohdan et al. 2005). By this approach, we can scrutinize the contribution of the target gene/enzyme to starch biosynthesis, which might fluctuate by tissue-, developmental stage-, and diurnal-specific manners. The different phenomena occurring between plant species can be also compared at the molecular level.

All these results serve as invaluable bases of most complexities and variations in various aspects of regulation of starch biosynthesis.

5.3.1 The Biosynthesis of Amylopectin

5.3.1.1 Soluble Starch Synthase (SS)

SS elongates the preexisting α-1,4-glucosidic chains of amylopectin by adding glucose moiety from ADPglucose to the nonreducing end of the chains. This reaction is the only step to increase the number of glucose residues of the starch because no change occurs in glucose amount of the starch after the BE and DBE reactions. In amylopectin molecules, the length or degree of glucose polymerization (DP) of side

chains should be strictly controlled, because otherwise double helices (Kainuma and French 1972) composed of adjacent chains having similar lengths are not uniformly arranged. How can this structure be achieved? The rate of starch biosynthesis is very rapid and the newly formed amylopectin clusters are immediately packed into the starch granules. Therefore, chain length should be controlled simultaneously as they are formed because trimming of chain length of individual chains afterward is actually impossible once they are formed. The other basic requirement for side chains of amylopectin is that their nonreducing part should be left non-branched so that the external segments are long enough to form double helices with DP $\geq$ 10 (Gidley and Bulpin 1987). During the synthesis of amylopectin side chains by SS, the chain branching reactions catalyzed by BE are restrained until the chains reach the length of DP 12, the minimal chain length required for BE reaction (Guan et al. 1997; Nakamura et al. 2010; Sawada et al. 2014), or longer. To satisfy all these requirements, plants possess multiple SS isozymes with distinct chain elongation properties for reserve starch biosynthesis.

5.3.1.1.1 Multiple SS Isozymes

Green plants have four types of SS isozymes, the SSI, SSII, SSIII, and SSIV types, while it is likely that some higher plants such as rice and potato have in addition the SSV type (see review by Fujita and Nakamura 2012). Since early 1970s, many reports have shown the occurrence of multiple SS isoforms in reserve organs and leaves of rice (Tanaka and Akazawa 1971), maize (Ozbun et al. 1971b; Tanaka and Akazawa 1971), potato (Hawker et al. 1972), and spinach (Ozbun et al. 1971a, 1972; Hawker et al. 1974), which were separated by DEAE column chromatography and distinguished from each other based on reactivities toward the glucan type and chemicals such as citrate, suggesting the involvement of coordinate actions of multiple SS isozymes in starch biosynthesis. Later, genome analysis indicated that higher plants have many *SS* genes, e.g., a total of nine genes (one *SSI*, three *SSII*, two *SSIII*, two *SSIV*, and one *SSV*) in rice plants (Hirose and Terao 2004; Ohdan et al. 2005).

5.3.1.1.2 Structures and Basic Enzymatic Properties

SS as well as GBSS belongs to the CAZy glucosyltransferase family 5 (GT5). Green plants have at least four types of SS and one type of GBSS, which are structurally and functionally distinct. These five enzymes have commonly a core sequence with an approximate size of 60 kDa and include two conserved regions referred to as the GT5 and GT1 domains which are separated by a linker region. In addition, they have the N-terminal extensions with different sizes – those of GBSS and SSIII/SSIV being the shortest and longest, respectively. The GT5 domain contains the highly conserved motif KXGGL considered to be responsible for the catalytic activity, while the N-terminal extension is likely to regulate catalytic activity, affecting bind-

ing affinity of SS for carbohydrates (Gao et al. 1998; Cao et al. 1999; Li et al. 2000; Leterrier et al. 2008; Schwarte et al. 2013).

The crystal structure of barley SSI with an omission of the N-terminal extension was revealed by Cuesta-Seijo et al. (2013), following the analysis of rice GBSSI (Momma and Fujimoto 2012). Structural similarities among plant SS were verified by the presence of the three distinct domains, i.e., the N-terminal domain, the central catalytic domain, and the C-terminal domain (Leterrier et al. 2008; Schwarte et al. 2013).

It is generally known that plant SS isozymes exhibit high activities toward various branched glucans including amylopectin and glycogen while the activities for linear MOS and amylose are very low (Edwards et al. 1999a; Damager et al. 2001; Imparl-Radosevich et al. 2003; Senoura et al. 2007; Nakamura et al. 2014). It is also well known that SSI and SSII are markedly activated by high concentrations ($\geq$0.3 M) of citrate (Ozbun et al. 1971b; Hawker et al. 1974; Boyer and Preiss 1979; Pollock and Preiss 1980; Senoura et al. 2007; Nakamura et al. 2014) (for other properties of SS, see review by Fujita and Nakamura 2012).

5.3.1.1.3 Chain Preferences of SS Isozymes

The contributions of individual SS isozymes to starch synthesis, the fine structure of amylopectin, and physicochemical properties of starch granules have been extensively examined using SS mutants and transformants generated from a number of plant species (see review by Fujita and Nakamura 2012) and by in vitro studies with purified enzyme preparations and selected glucan primers.

Although SSI accounted for about 60–70 % of the SS activity in wild-type cereal endosperm and *Arabidopsis* leaves, the single *ss1* mutation was likely to cause only a slight change in the starch-related phenotypes. It is, however, noted that amylopectin from rice *ss1* mutant lines with no or varied levels of residual SSI activities in the endosperm had consistently reduced chains of DP 8–12 and enriched chains of DP 6–7 and DP 16–19, whereas changes in the proportion of long chains of DP $\geq$ 21 were very low or unchanged (Fujita et al. 2006) (Fig. 5.4b). The similar impact of suppression of *SSI* expression on amylopectin chain profile was reported in wheat endosperm (McMaugh et al. 2014). These results suggest that SSI plays a distinct role in the synthesis of chains of DP 8–12 from A-chains of DP 6–7 and the external segments of B-chains emerging from the nearest branch point. Delvallé et al. (2005) also found that the mutation of *Arabidopsis SSI* gene markedly reduced chains of DP 8–12 but increased chains of DP 17–20. These results are consistent with the view that SSI is involved in the synthesis of short external segments of amylopectin chains.

It is well known that defective *SSII* gene function has profound effects on starch synthesis and amylopectin structure in reserve organs of many plant species. Craig et al. (1998) reported that mutations of *SSII* gene (the *rugosus5* locus) of pea dramatically reduced the amount of intermediate chains and increased the amount of short chains. Later, Edwards et al. (1999b) and Lloyd et al. (1999) extensively

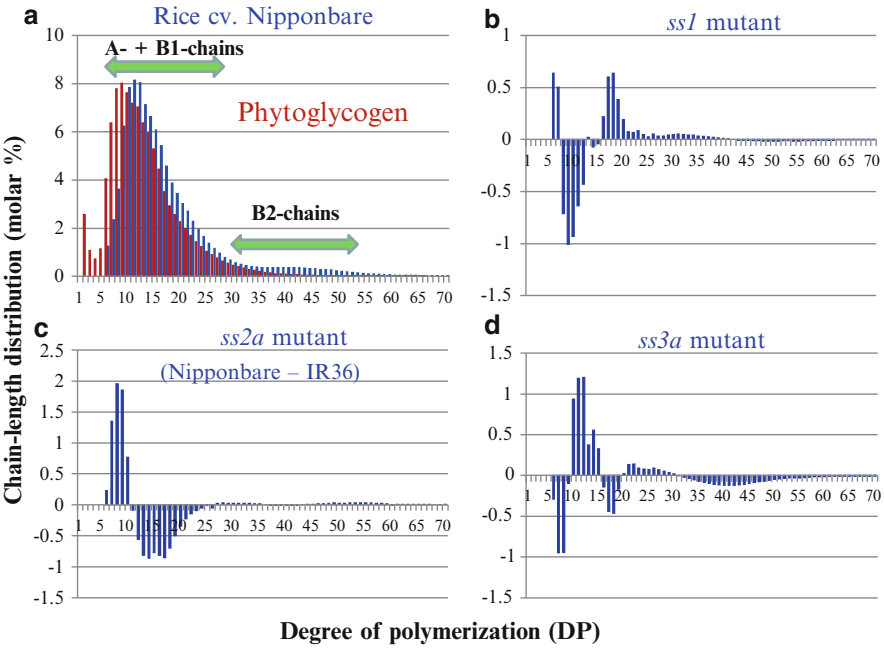

Fig. 5.4 Changes in structure of amylopectin of rice mutants defective in starch synthase (SS) isozymes. (**a**) Amylopectin in endosperm from wild-type *japonica* rice cultivar Nipponbare (*blue bars*), as compared to phytoglycogen from *sugary-1* mutant line (EM41) of rice (brown bars). (**b**) Amylopectin from *ss1* mutant (Fujita et al. 2006). (**c**) Amylopectin from *ss2a* mutant (Nakamura et al. 2005a). (**d**) Amylopectin from *ss3a* mutant (Fujita et al. 2007)

analyzed the effects of antisense inhibition of either SSII or SSIII and both activity levels in potato tubers on the amylopectin chain lengths. The consequence of SSII inhibition was distinct because short chains of DP 6–13 greatly decreased while intermediate chains of DP 15–25 markedly increased. A series of studies by Umemoto et al. (1999, 2002) and Nakamura et al. (2002, 2005a) characterized the contribution of rice SSIIa to the fine structure of amylopectin. They showed that most of *japonica*-type rice varieties had enriched chains of DP 6–10 and depleted chains of DP about 12–24, compared with typical *indica*-type varieties although no significant difference was found in the proportion of B2- and B3-chains (Umemoto et al. 1999; Nakamura et al. 2002) (Fig. 5.4c) and that the *japonica*-type varieties had an inactive mutated *ss2a* gene while the *indica*-varieties had an active *SSIIa* gene (Nakamura et al. 2005a). The same trends in chain profiles for amylopectin were observed in the *ss2a* mutants from wheat (the *sgp-1* mutant, Yamamori et al. 2000) and barley (the *sex6* mutant, Morell et al. 2003). Similar results were reported in maize *sugary-2* mutant endosperm (Takeda and Preiss 1993; Zhang et al. 2004), sweet potato cv. *Quick sweet* tuberous root (Katayama et al. 2002; Kitahara et al. 2005), and *Arabidopsis* leaf (Zhang et al. 2008). All these results support the

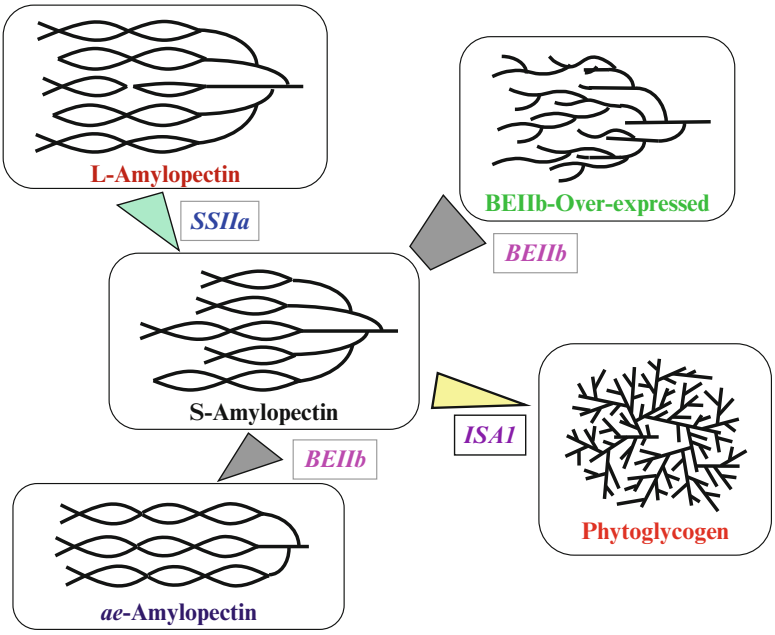

Fig. 5.5 Pattern of changes in the cluster structure of amylopectin caused by different levels of key enzymes in starch biosynthesis. The fine structure of amylopectin is altered by different levels of SSIIa, BEIIb, and ISA1 activities in rice endosperm, keeping the distinct structural pattern of the cluster depending on the individual enzyme, and this is referred to as "cluster-world" (Nakamura et al. 2009; Nakamura 2014)

conclusion that SSII(a) plays a distinct role in the synthesis of intermediate chains of amylopectin, and this role cannot be effectively supplemented by other SS isoforms (Fig. 5.5).

It is known that the *dull1* mutation of maize caused by defective *SSIIIa* gene had a modified granular morphology and physicochemical properties (Mangelsdorf 1947; Davis et al. 1955; Gao et al. 1998, see also reviews by Shannon and Garwood 1984 and Shannon et al. 2007). Fontaine et al. (1993) and Ral et al. (2006) proposed a specific role of SSIII in the synthesis of intermediate and long chains of amylopectin in *Chlamydomonas reinhardtii* based on the chain-length analysis of the *ss3* mutant, *sta-3*. Loss of SSIII in potato tuber resulted in changes in amylopectin and starch granule structure, and data suggested that SSIII is involved in the synthesis of long chains although the extent of difference in chain-length profile was too small to clearly evaluate the function of SSIII (Edwards et al. 1999b; Lloyd et al. 1999). Fujita et al. (2007) analyzed in details the amylopectin chain profiles of amylopectin in rice endosperm and found that the *ss3a* mutant had fewer chains of DP 6–9, DP 16–19, and DP 33–55 and more chains of DP 10–15 and DP 20–25 than the wild-type (Fig. 5.4d). They proposed a major role of SSIIIa in synthesizing long chains (B2- and B3-chains), judging from the observation that the increased pattern

of long chains in the *ss3a* mutant was specific and the increase of very short chains (DP 6–9) was considered to be caused by the elevated level of SSI due to the pleiotropic effect of *ss3a* mutation. Recently, Lin et al. (2012) reported the fine structure of amylopectin in the maize *dull1* mutants, similar to the rice *ss3a* mutants. The barley *ss3a* mutant (*amo1*) endosperm contained amylopectin with less short chains of DP 9–10 and more intermediate chains of DP 15–24 while no significant change was detected in long chains (Li et al. 2011).

The *ss3(a)* mutation frequently produced marked starch-related phenotypic changes such as the starch content, starch granule morphology, and the starch physicochemical properties, despite the absence of noticeable change in chain-length pattern. The results suggest that SSIII(a) plays an additional integral role in starch granule biosynthesis.

Although SSIV accounted for only a minor portion of the total SS activity, its function in starch biosynthesis was likely to be specific. Roldán et al. (2007) revealed that loss of SSIV reduced the number of starch granules per chloroplast in *Arabidopsis* leaves, suggesting that SSIV plays an essential part in the starch granule initiation. The specific role of SSIV in *Arabidopsis* was verified by further studies (Szydlowsky et al. 2009; Crumpton-Taylor et al. 2013). The observation that the *ss4/ss3* double mutants completely lost starch granules suggests that the role of SSIV can be partially supported by SSIII, possibly due to some structural and functional similarities (Szydlowsky et al. 2009; 2011). Although studies on the contribution of SSIV to the starch biosynthesis in cereal endosperm are limited, recently Toyosawa et al. (2015) found that a single mutation of the *SSIVa* or *SSIVb* gene had minor impacts on starch phenotype in rice endosperm, whereas the *ss4b/ss3a* double mutants altered the polygonal starch granules into the spherical granules, although the number of granules per amyloplast and the starch content per seed were only slightly affected. The results suggest the possibility that the impact of SSIV depends on plant species (see details in Chaps. 6, 9, and 10).

Despite numerous in vivo studies on SS, only a few in vitro studies have been reported. Commuri and Keeling (2001) examined the chain-length specificities of maize SSI and determined the relationship between dissociation constant (Kd) of SSI for the external chain length of synthesized glycogen and the SSI activity. The catalytic activity evidently decreased with the increase in the average DP values of external chains and almost dropped to zero when DP exceeds about 11, these DP values being in accord with the increase of glucan affinity. They concluded that the activity of SSI decreases with the chain length of external chains due to its very high affinity for the longer chains. Recently, Nakamura et al. (2014) directly measured the chain length of the products formed by in vitro enzymatic reactions between rice SSI, SSIIa, or SSIIIa and amylopectin. It is noted that SSI specifically elongated very short chains of DP 6 and 7 of A-chains and external segments of B-chains to mainly the length of DP 8 in these chains, although they could be further elongated by the prolonged incubation. Analysis of the SSIIa and SSIIIa reaction products was consistent with in vivo results, suggesting that SSIIa and SSIIIa preferentially synthesize intermediate chains and intermediate/long chains, respectively.

5.3.1.1.4 The Roles of SS Isozymes in Amylopectin Biosynthesis

Undoubtedly, concerted reactions of individual SS isozymes are essential for construction of the organized structure of amylopectin with uniform size and shape of unit clusters. The chain-length distribution of amylopectin in reserve starch granules forms two distinct peaks: a large short- and intermediate-chain peak and a small long-chain peak with most abundant chains of approximately DP 10–14 and DP 35–45, respectively, sharply in contrast with the pattern of phytoglycogen or glycogen lacking the second peak (Fig. 5.4a). The lengths of the former intra-cluster chains (A- and B1-chains) and those of the latter inter-cluster chains (B2- and B3-chains) must be strictly controlled, otherwise the shape of the bimodal distribution would be distorted and the ratio of the two peaks must be changed. However, it is well known that these features are primarily conserved during development of the storage organ of each plant species. The chain length in itself is the result of the SS elongation reaction. BE indirectly affects the length by introducing branched linkages, which results in the reactivation of the long external chains to SS by decreasing the length of the external segment because each SS isozyme very specifically and sensitively recognizes the length of the external segment of substrate and product chain. The most likely explanation for requirement of multiple SS isozymes for the synthesis of amylopectin is that the branched chains are elongated by coordinate reactions of SSI, SSII, and SSIII isozymes with different chain-length preferences until the lengths reach the nonreducing end of the cluster.

Past biochemical, molecular, and genetic investigations supported the almost consistent view that properties of SSI, SSII, and SSIII are specific to forming very short chains of DP up to about 10, intermediate intra-cluster A- and B1-chains of DP up to about 24, and long inter- and intra-cluster B2-/B3-chains and B1-chains, respectively, of DP longer than about 20, respectively (Fujita and Nakamura 2012) (Fig. 5.2). The features of SS reaction properties are as follows: first, activities of SS are largely dependent on the chain length of the external segment of primer chains, being sharply in contrast with those of Pho and GBSS because both of them can synthesize very long chains such as amylose and amylopectin super-long chains. Second, SS shows a high activity toward branched glucan such as amylopectin and glycogen, whereas it has a very low activity toward linear glucan or MOS. In contrast, both Pho and GBSS are similarly reactive to either linear or branched glucans.

How can SS limit the length of amylopectin chains? Although no convincing evidence is available, several possibilities can be considered. First, as described above, Commuri and Keeling (2001) reported that catalytic ability of maize SSI decreased with the increase of external chain length in the range of DP 6–14 and then exponentially dropped to DP 21, due to the increase of its affinity for the longer chains. However, it remains to be resolved whether and to what extent the properties of SSII and SSIII are influenced by chain lengths. Second, the amylopectin chain increases the hydrophobic properties in aqueous medium with the increase in the chain length, as found in linear MOS, and this might inhibit the accessibility of SS to the nonreducing end of the primer chain. Third, since SS generally shows a

higher catalytic action with branched glucans than linear glucans, as stated above, the actual substrate for SS might be the branched duplicate chains positioned in the same direction and having the similar length. As elongation of the single chain by SS progresses, the difference in chain length between adjacent chains will become larger, dramatically reducing the rate of chain elongation. All these properties might result in the cessation of further increase of the cluster size. It was found that rice SSIIa had a capacity for the synthesis of L-type amylopectin having longer A- and B1-chains in test tubes when it was incubated with S-type amylopectin having shorter cluster chains and prepared from a rice *ss2a* mutant *japonica* cultivar (Nakamura et al. 2005a) (Fig. 5.5), indicating that SSIIa is specialized to elongate intra-cluster chains by acting on short chains formed by BE reactions.

5.3.1.2 Starch Branching Enzyme (BE)

BE introduces the branch structure into α-glucan with α-1,6-glucosidic linkage by transferring the chain at its reducing end onto the acceptor chain. The transferred chain is derived from the donor chain by cleaving off its nonreducing part of the chain, and the remaining part of the chain is referred to as the residual chain (Borovsky et al. 1979) (Fig. 5.6). When BE uses an acceptor chain different from the donor chain, the reaction is referred to as the inter-chain BE reaction, whereas in the intra-chain reaction, BE utilizes the same single chain as both acceptor and donor chains. In both cases, the total number of chains increases while that of glucose residues is unchanged during the BE reaction.

Although glucose amount in the glucan during the BE reaction is unchanged, it plays an essential role in starch biosynthesis in terms of not only the glucan fine structure but also eventually in the catalytic activity of SS and the rate of starch production in plant tissues. The amylopectin cluster structure enables the macromolecule to form the semicrystalline granular structure so that plant cells can store the inert glucans for a long period. The branched structure also has numerous

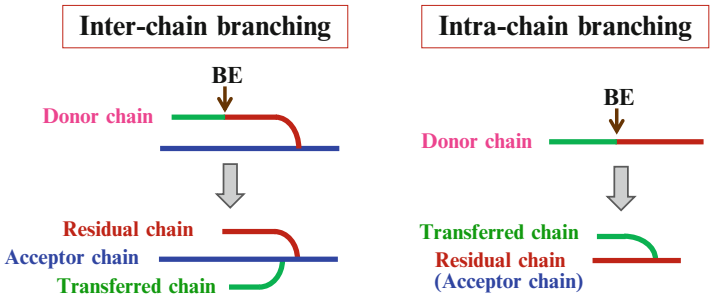

Fig. 5.6 α-Glucan branching reaction catalyzed by starch branching enzyme (BE). Note that after the BE enzymatic reaction, the number of chains increases while the number of glucose residues is unchanged either by the inter-chain or intra-chain branching reaction

chains, serving for SS reaction as acceptors at their nonreducing ends, and this supports a high rate of starch production. The formation of a branch in the middle of linear long chain also affects the functionality of the chain. Because the linear α-1,4-chain segment increases its hydrophobic nature with the increase of DP, the long non-branched chain segment becomes insensitive to SS isozymes (Commuri and Keeling 2001). Thus, the branch formation by BE results in reactivation of long chains by accepting the transferred chains because SS can again act on them at their external segments.

5.3.1.2.1 Multiple BE Isozymes

Numerous past investigations reported that green plants have two types of BE isozymes, BEI and BEII, in various species such as maize (Boyer and Preiss 1978; Dang and Boyer 1988), rice (Nakamura et al. 1992a; Yamanouchi and Nakamura 1992; Mizuno et al. 1993), wheat (Morell et al. 1997; Rahman et al. 2001), barley (Sun et al. 1998), pea (Smith 1988; Burton et al. 1995), kidney bean (Nozaki et al. 2001; Hamada et al. 2001), potato (Larsson et al. 1996), spinach (Hawker et al. 1974), popular (Han et al. 2007b), and apple (Han et al. 2007a). BEII is known to be further functionally and structurally differentiated into BEIIa and BEIIb, encoded by different genes in cereals such as rice (Yamanouchi and Nakamura 1992; Mizuno et al. 1993), maize (Guan and Preiss 1993; Fisher et al. 1996), barley (Sun et al. 1998), wheat (Morell et al. 1997), and sorghum (Mutisya et al. 2003), whereas generally no such differentiation of BEIIb-type is found in dicot plants. Generally, BEIIb is specifically or mainly expressed in cereal endosperm, playing a distinct role in determining the fine structure of amylopectin while BEIIa is ubiquitously expressed in every tissue (see reviews by Nakamura 2002, 2014; Tetlow 2012). Thus, monocots have totally three functional BE isozymes in the endosperm and two isozymes in the other tissues such as leaf. On the other hand, most dicot tissues are likely to have only two BE isozymes. Although some dicots such as *Arabidopsis* and apple have multiple BEII-type isozymes (Han et al. 2007a), their function and structure were very similar and it is unlikely that they play different roles in amylopectin biosynthesis. The location and the clustering of the α-1,6-linkages is fundamentally important to the construction of the amylopectin structure, such that the formation of branches in amylopectin molecules by coordinated actions of BE isozymes must be precisely controlled. Considering this requirement, the limited number of BE isozymes expressed in plant tissues is rather surprising compared with many SS isozymes. How can only two or three isozymes suffice such requirements? The point might be further strengthened if one considers that plant BEs must have a common origin as that of glycogen BEs from eukaryotes such as animals and fungi, but not the bacterial BE origin (Patron and Keeling 2005; Deschamps et al. 2008).

The different expressions of multiple *BE* genes were examined in various plant species during development of reserve organs. It was generally seen that in both monocots and dicots, BEII-type gene(s) was (were) expressed from the early developmental stage of the reserve organ, while BEI-type gene was highly

expressed at the latter developmental stage in both monocot seeds such as rice (Mizuno et al. 1993; Hirose and Terao 2004; Ohdan et al. 2005), maize (Gao et al. 1996), wheat (Morell et al. 1997), and barley (Sun et al. 1998) and dicot seeds such as pea (Burton et al. 1995) and kidney bean (Hamada et al. 2001). In cereal endosperm, BEIIa was found to be expressed from the very early stage, followed by a marked expression of BEIIb (Hirose and Terao 2004; Ohdan et al. 2005). The physiological significance of these expression patterns remains largely to be resolved in the future.

5.3.1.2.2 Structures and Basic Enzymatic Properties

BEs are members of the CAZy glycoside hydrolase family 13 (GH13), which is also referred to as the α-amylase family. Eukaryote BEs are further classified as subfamily 8, while almost all of bacterial BEs are members of subfamily 9 (Stam et al. 2006). Some thermophilic bacteria have other types of BEs belonging to the GH57 family (Murakami et al. 2006; Palomo et al. 2009). The GH13 BEs have three major domains, the A domain or the central (β/α)-barrel catalytic domain, the N-terminal domain, and the C-terminal domain, although the A domain sequence is highly conserved, whereas other two domains show a high variability, and this structural features were directly revealed by the X-ray crystallographic analysis of rice BEI (Noguchi et al. 2011; Chaen et al. 2012, also see review by Tetlow 2012 and many references therein).

Enzymatic properties of BEs have been elucidated. These include reactivity toward various glucans including branched glucans (amylopectin and glycogen), amylose, and malto-oligosaccharides (MOS) (Tetlow 2012); chemicals such as cyclodextrins (Vikso-Nielsen and Blennow 1998), phosphorylated metabolites (Morell et al. 1997), and citrate (Hamada et al. 2001, 2002); temperature dependence of activities (Takeda et al. 1993; Hamada et al. 2002; Ohdan et al. 2011; Sawada et al. 2013); and association with starch granules (Rahman et al. 1995; Mu-Forster et al. 1996; Hamada et al. 2001, 2002; Grimaud et al. 2008; Liu et al. 2012b; Abe et al. 2014). For other properties of BE, see review by Tetlow (2012).

5.3.1.2.3 Chain Preferences of BE Isozymes

The contributions of individual BE isozymes to the fine structure of amylopectin have been studied by analyzing changes in amylopectin structure in *be* mutants and transformants generated from a number of plant species such as maize (Hedman and Boyer 1982; Blauth et al. 2001, 2002; Yao et al. 2004, also see review by Shannon and Garwood 1984), rice (Nishi et al. 2001; Nakamura 2002; Satoh et al. 2003; Tanaka et al. 2004; Butardo et al. 2011), wheat (Regina et al. 2006; Sestili et al. 2010), barley (Regina et al. 2010; Carciofi et al. 2012), and pea (Smith 1988; Bhattacharyya et al. 1990). For other *be* mutants, see Tetlow (2012).

The impacts of these mutations were apparent when BEII-type forms were lacking while *be1* mutants showed no or only a slight morphological and starch-related phenotypic changes. One most remarkable example is the pea mutant line called *rugosus* (*r*) which was used by Mendel as his experimental material and had a shriveled seed with a reduced starch synthesis caused by a loss of BEII-type (or A-type) isozyme (Smith 1988; Bhattacharyya et al. 1990). The other well-known example is the maize *be2b* mutant referred to as the *amylose extender* (*ae*) which caused a dramatic increase in amylose content and an alteration of amylopectin structure with longer chain length, which resulted in the commercially useful functional properties of the endosperm starch being resistant to digestion and gelatinization (Shannon et al. 2007; Li et al. 2008). The results suggest the specific role of BEII in starch biosynthesis in dicot reserve organs and BEIIb in monocot seeds, and their roles cannot be significantly supported by BEI and BEI plus BEIIa, respectively. Conversely, the role of BEI can be mostly complemented by BE isozyme(s). However, attention should be paid to the observations that in wheat and barley endosperms, the impact of BEIIa deficiency was much more similar to that of BEIIb deficiency of maize and rice (Yao et al. 2004; Nishi et al. 2001; Tanaka et al. 2004; Butardo et al. 2011), whereas suppression of BEIIb expression in wheat and barley resulted only in minor changes in starch phenotypes (Regina et al. 2006; Regina et al. 2010) (see Sect. 5.5.2).

Figure 5.7b shows that loss of BEIIb activity in rice endosperm caused a marked increase in long chains of DP ≥ 35 (B2- and B3-chains) and intermediate chains of DP 15–30 (A-chains plus B1-chains) and a great decrease in short chains of DP 6–12 in amylopectin (Nishi et al. 2001). The results support the notion that BEIIb forms short chains in the middle of the cluster instead of the root of the cluster, and therefore in its absence the number of chains per cluster (the ratio of A-chains plus B1-chains/B2-chains plus B3-chains) is significantly reduced (Figs. 5.2, 5.4, and 5.7). By contrast, the *be1* mutant of rice had amylopectin with more chains of DP 6–12 and slightly less chains of DP 16–25 and DP ≥ 37 (Fig. 5.7a), suggesting that BEI plays a part in the synthesis of intermediate and long chains (Satoh et al. 2003). The situation is likely common among cereal endosperm (Yao et al. 2004; Regina et al. 2010; Butardo et al. 2011; Liu et al. 2012a), although the possibility that BEI also affects the position of branches of amylopectin in maize endosperm cannot be ruled out (Xia et al. 2011).

The contribution of each BE isozyme to the amylopectin structure has been analyzed more precisely and in details by in vitro studies. It was firstly reported that maize BEII preferentially transferred very short chains of DP 6 to about 12 with most preferred chains of DP 6 for BEIIa and DP 7 and 6 for BEIIb, while BEI formed most effectively intermediate chains of DP about 10–12 (Takeda et al. 1993; Guan et al. 1997). Subsequently, BEs from other plant sources such as rice (Mizuno et al. 2001; Nakamura et al. 2010), kidney bean (Hamada et al. 2001; Nozaki et al. 2001), potato (Rydberg et al. 2001), green alga *Chlorella* (Sawada et al. 2009), and cyanobacterium *Synechococcus* (Sawada et al. 2013, 2014) were shown to have similar chain-length preferences as maize BE isozymes (see review by Tetlow 2012) and consistent with the enzymatic properties suggested by in vivo studies.

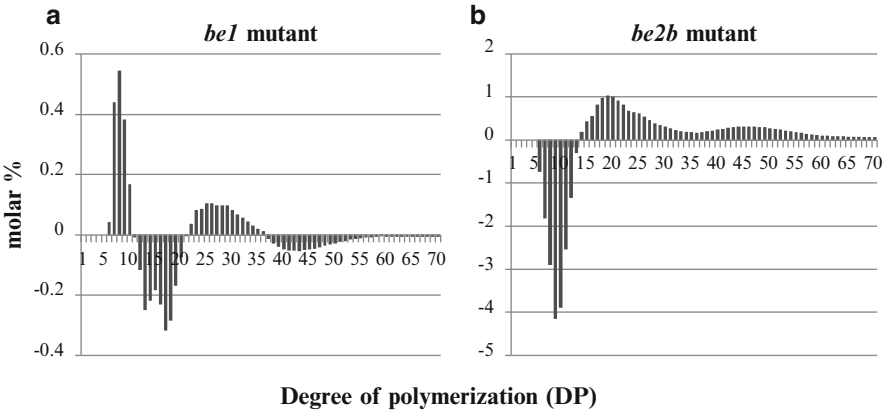

Fig. 5.7 Changes in the amylopectin structure of mutants defective in starch branching enzyme (BE) isozymes of rice. Changes in the fine structure of amylopectin in rice endosperm caused by *be1* (Satoh et al. 2003) (**a**) and *be2b* (Nishi et al. 2001) (**b**) mutations. The data shown are differences after subtraction of chain-length distribution of amylopectin of the wild-type from that of the mutant

As an example of these in vitro studies, results with three rice BE isozymes are summarized (Nakamura et al. 2010), as shown in Fig. 5.8. First, when branched glucan such as amylopectin is used as substrate, the minimum chain lengths of substrate chains and the transferred chains for BE reaction were DP 12 and 6, respectively. In contrast, the minimum chain length of amylose required for branching was about DP 48 for BEI and DP $\succ$ 100 for BEIIa and BEIIb. Second, the most preferable chain lengths for branching of amylopectin by BEI, BEIIa, and BEIIb were DP 10–12, DP 6, and DP 7 and 6, respectively. Third, BEI could attack the internal chain segments of amylopectin chains but to a lesser extent than the external chain segments, while BEIIa and BEIIb could not. These results are basically consistent with those of corresponding BE isozymes from other plant species as described above, although precise comparison with BEs from various sources is difficult because these studies used different substrate, reaction conditions, and methods for measuring chain profiles.

Recently, Sawada et al. (2013, 2014) analyzed and compared the chain preference of a total of ten BEs from various organisms including rice (OsBEI, OsBEIIa, and OsBEIIb), *Chlorella kessleri* (ChlBE), red alga *Porphyridium purpureum* (PopBE1 and PopBE2), *Synechococcus elongatus* (ScoBE), *Escherichia coli* BE (EcoBE), human (HosBE), and yeast (SacBE). It was found that EcoBE had the same enzymatic properties as OsBEI, while ScoBE and ChlBE had BEIIb-type properties. On the other hand, HosBE, SacBE, and two PopBEs exhibited the OsBEIIa-type properties. Analysis of chain-length profile of phosphorylase-limit dextrins (Φ-LD) of the BE reaction products revealed that EcoBE, ScoBE, PopBE1, and PopBE2 preferred A-chains as acceptors, while OsBEIIb used B-chains more frequently than A-chains. The preference of BE for acceptor chain seemed to reflect on the

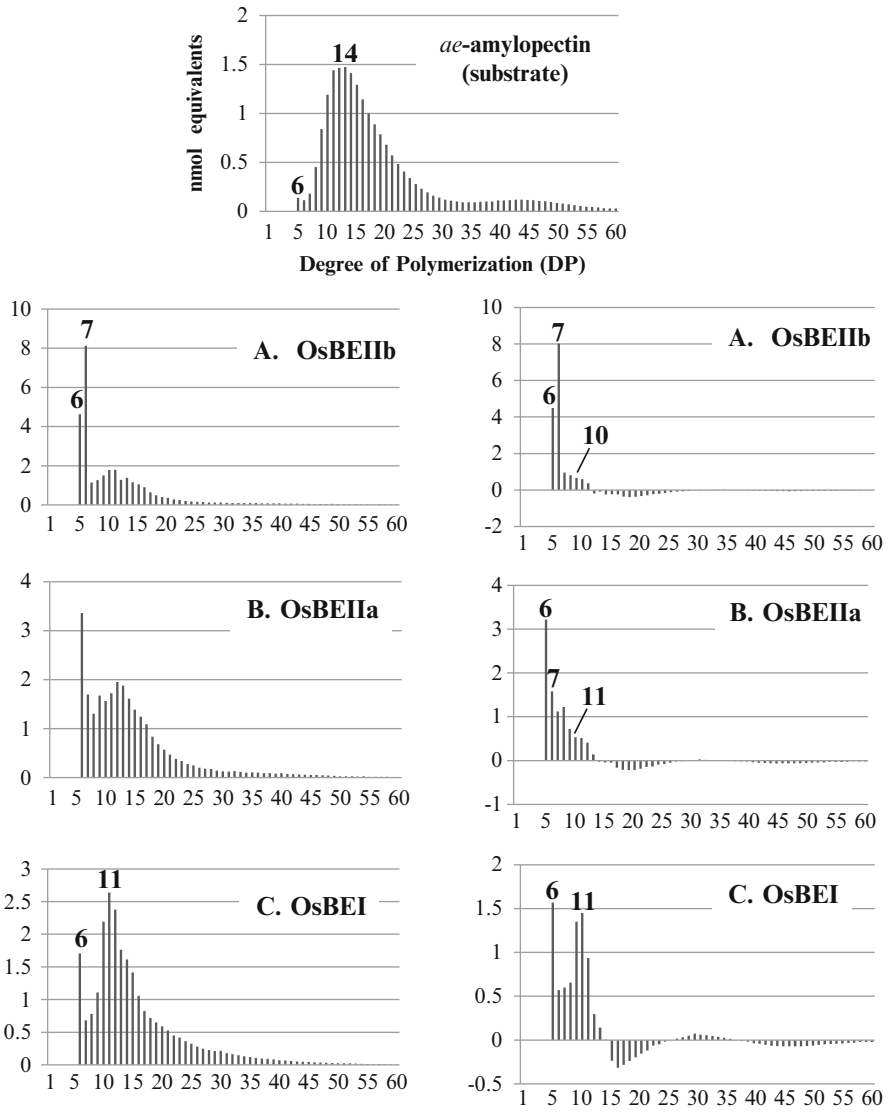

Fig. 5.8 Chain preference of starch branching enzyme (BE) isozymes analyzed by in vitro studies. The chain-length distribution of the reaction product of rice BE with *ae*-amylopectin used as substrate is shown. (**a**) The BEIIb reaction product. (**b**) The BEIIa reaction product. (**c**) The BEI reaction product (Data are from Sawada et al. 2014)

molecular structure of α-glucans in terms of the ratio of A-chains to B-chains in at least some organisms such as algae. The results showed for the first time the preference of some BEs to the acceptor chains and the location of branches.

This information provides new insights into the mechanism for the synthesis of amylopectin cluster structure.

It is stressed that features of the chain preference of BE were maintained irrespective of the glucan substrate for the in vitro BE reaction, i.e., amylopectin or amylose (Guan et al. 1997; Nakamura et al. 2010), the duration of enzymatic reaction (Guan et al. 1997; Nakamura et al. 2010), and the reaction temperature (Nakamura et al. 2010; Ohdan et al. 2011), indicating that the specific chain preference of BE isozymes is consistent regardless of the structure of glucan substrate. Thus, the specificities of individual BEs for chain length of the glucans can be applicable to their roles under any physiological conditions.

5.3.1.2.4 The Roles of BE Isozymes in Amylopectin Biosynthesis in Cereal Endosperm

The contribution of BEIIb and BEI to the fine structure of amylopectin sharply contrasts from each other, and this is basically observed in any cereal endosperm. As seen in rice endosperm as a representative example, the view is supported by the different chain-length distribution pattern of amylopectin between *be2b* and *be1* mutants (Fig. 5.7). The observation that the extent of change in chain-length profile was much higher in *be2b* mutant than *be1* mutant indicates that the function of BEIIb is specific and this cannot be complemented by other BE isozymes while that of BEI can significantly be supported by other BEs. No phenotypic change in the amylopectin structure was detected in the *be2a* mutant, suggesting that the role of BEIIa is not specific and might merely be to support BEIIb and BEI. Because leaf *be2a* mutant amylopectin had less short chains compared to long chains, BEIIa might play an important part in forming short amylopectin chains in the leaf where BEIIb is not expressed. The specific role of BEIIb in rice endosperm was supported by the results with transgenic lines in which *BEIIb* gene was introduced into the *be2b* mutant (Tanaka et al. 2004). The extent of amylopectin chain pattern alteration among transformants was depending on the expressed level of BEIIb; remarkably most of the starch was replaced by water-soluble polysaccharides (WSP) when it was highly overexpressed (Fig. 5.5; see also Sect. 5.4.3.2).

5.3.1.3 Starch Debranching Enzyme (DBE)

Plants have two types of α-glucan debranching enzymes: isoamylase (ISA, EC 3.2.1.68) and pullulanase (PUL, EC 3.2.1.41). Both ISA and PUL directly debranch the α-1,6-glucosidic linkage, differing from DBE from heterotrophic eukaryotes such as animals and yeasts which removes the branched chain by the consecutive 4-α-glucanotransferase (EC 2.4.1.25) and amylo-1,6-glucosidase (EC 3.2.1.33) reactions (see reviews by Lee and Whelan 1971 and Nakamura 1996).

5.3.1.3.1 Involvement of DBE in Amylopectin Biosynthesis

One of the most striking biochemical events in the starch biosynthesis in plants is the fact that DBE is essential for the synthesis of cluster structure of amylopectin. Although some information suggesting the involvement of DBE in amylopectin synthesis had been reported through the analysis of phytoglycogen-producing *sugary-1* mutants from maize (Pan and Nelson 1984) and rice (Nakamura et al. 1992b), direct evidence that ISA1 plays a crucial role in amylopectin biosynthesis and in its absence amylopectin is replaced by phytoglycogen devoid of cluster structure (Figs. 5.4a and 5.5) was reported by James et al. (1995) using the gene-tagging method. Since then the essential roles of DBEs in amylopectin synthesis have been verified by extensive investigations of a variety of mutants and transformants from maize (James et al. 1995; Beatty et al. 1999; Dinges et al. 2001; Dinges et al. 2003; Kubo et al. 2010; Lin et al. 2012, 2013), rice (Nakamura et al. 1996, 1997; Kubo et al. 1999, 2005; Fujita et al. 2003, 2009; Utsumi et al. 2011), potato (Hussain et al. 2003; Bustos et al. 2004), barley (Burton et al. 2002), *Arabidopsis* (Zeeman et al. 1998; Dellate et al. 2005; Wattebled et al. 2005, 2008; Streb et al. 2008; Pfister et al. 2014; Streb and Zeeman 2014), *Chlamydomonas* (Mouille et al. 1996; Colleoni et al. 1999a, 1999b; Dauvillée et al. 2000, 2001; Sim et al. 2014), and *Cyanobacterium* sp. CLg1 (Cenci et al. 2013) (also see review by Hennen-Bierwagen et al. 2012), although in this chapter experimental results with maize and rice endosperm are mainly described.

Green plants usually have four DBEs: three ISA isozymes, ISA1, ISA2, and ISA3, and one PUL (Ball et al. 2011). The essential role of ISA1 was proven by the molecular studies showing that the *sugary-1* phenotype reverted to wild-type one when normal *ISA1* gene was introduced into the *sugary-1* mutant of rice (Kubo et al. 2005; Utsumi et al. 2011) (Fig. 5.9). Biochemical studies indicated that ISA2 functioned in a form of heteromeric complex with ISA1, although ISA2 itself lacked the catalytic site as DBE due to replacement and/or deletion of essential catalytic residues conserved in ISA1 and ISA3 (Hussain et al. 2003; Bustos et al. 2004). ISA3 likely plays a part in degrading branched glucans in the leaf (Hennen-Bierwagen et al. 2012), but not in the glucan synthesis in the endosperm (Yun et al. 2011). It is interesting that both ISA1 homomer and ISA1-ISA2 heteromer were present in maize endosperm (Kubo et al. 2010) and leaf (Lin et al. 2013), rice endosperm (Utsumi and Nakamura 2006; Utsumi et al. 2011), and *Chlamydomonas* (Sim et al. 2014). In contrast, only the ISA1-ISA2 heteromer existed in potato tuber (Hussain et al. 2003) as in *Arabidopsis* leaves (Dellate et al. 2005). It was found that the ISA1 homomer, but not the heteromer, was only the functional form in rice endosperm (Utsumi et al. 2011) while in maize endosperm the homomer played a major role in amylopectin synthesis but the heteromer could also support at least partly the normal starch synthesis (Kubo et al. 2010). These differences in the ISA functional form(s) between rice and maize were supported by the results indicating that the presence of the heteromer only caused by overexpression of *ISA2* gene resulted in abnormal starch production in rice endosperm (Utsumi et al. 2011). It is noted that in the rice leaf the heteromer was the functional form for normal

a **Scanning electron micrograph of starch granules**

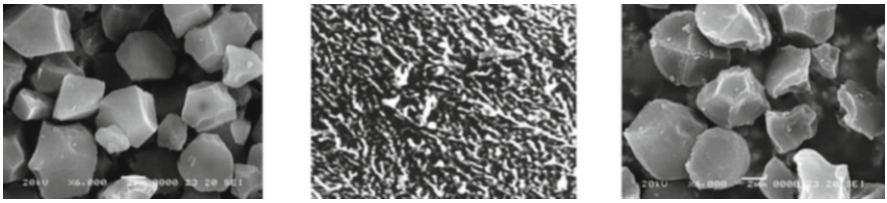

Taichung-65 (WT) | ***EM914 (sugary-1)*** | **Transformant (#914-8-1)**

b **Thermal properties of starch**

	Wt of seed (mg)	To (°C)	ΔH (J/g)	λ-max (nm)
Kinmaze (WT)	**20.7**	**55.5**	**6.46**	**575**
EM914 (*sugary-1*)	**11.1**	**ND**	**ND**	**470**
#914-8-1	**18.9**	**50.0**	**5.54**	**555**
#914-24-2	**17.4**	**44.5**	**3.94**	**560**

ND, not detectable.

Fig. 5.9 Changes in starch granular structure of mutants defective in isoamylase1 (ISA1) of rice and complementation of the mutant phenotype by introducing normal *ISA1* gene from wheat. Granular morphology (**a**) and thermal properties (**b**) of α-glucans in rice endosperms of wild-type, an *isa1* (*sugary-1*) mutant line EM914, and OsISA1 transformants (Data are from Kubo et al. 2005)

starch biosynthesis and that the heteromer was more resistant to high temperature at 40 °C than the homomer (Utsumi et al. 2011). In maize leaves, both homomer and heteromer existed (Lin et al. 2013). One likely reason for this phenomenon in rice is that the functional form of ISA should be more resistant in the leaf than in the endosperm presumably because intracellular environment due to diurnal and physiological conditions fluctuates more frequently and severely in the leaf than in the endosperm.

In the *sugary-1* mutant endosperm, the activity of PUL was concomitantly reduced in maize (Pan and Nelson 1984; Dinges et al. 2003) and rice (Nakamura et al. 1996), and the reduced level of PUL was almost related with the severity of *sugary-1* mutation or the extent of decreased ISA activity in rice endosperm (Nakamura et al. 1997), suggesting that PUL together with ISA plays a part in amylopectin biosynthesis in cereal endosperm. Later, Fujita et al. (2009) provided evidence that the role of PUL was to supplement the role of ISA when absent, but in its presence the PUL's role was only limited, if any, in developing rice

endosperm, basically consistent with previous results with maize (Beatty et al. 1999; Dinges et al. 2003) and rice endosperm (Kubo et al. 1999) endosperm.

5.3.1.3.2 Multiple DBE Isozymes, Structure, Basic Properties, and Functions

Both ISA and PUL are also members of the α-amylase family, the GH13, like BEs. The structural features of ISA (Katsuya et al. 1998; Sim et al. 2014) and PUL (Vester-Christensen et al. 2010) were revealed.

The ISA protein was first purified to homogeneity from developing endosperm of rice and shown to be in a form of ISA1 homomultimer (Fujita et al. 1999). However, Hussain et al. (2003) discovered that potato tuber had three ISA isozymes, ISA1, ISA2, and ISA3, and confirmed that the ISA1-ISA2 heteromer was responsible for the ISA activity contributing to the starch synthesis in potato tuber. The results are consistent with the previous report by Ishizaki et al. (1983) that the finally purified ISA activity preparation from potato tuber included two protein components with the same protein amount. Three distinct *ISA* genes and one *PUL* gene have been identified in all green plants so far examined (Hussain et al. 2003; Rahman et al. 2003; Deschamps et al. 2008; Hennen-Bierwagen et al. 2012).

The enzymatic properties of ISA have been examined in several sources. Utsumi and Nakamura (2006) showed that both ISA1 homomer and ISA1-ISA2 heteromer purified from developing rice endosperm had a broad chain-length preference like *Pseudomonas amyloderamosa* ISA. In contrast, the ISA from *E. coli*, which is sometimes referred to as GlgX protein and can be classified as an ISA subclass, was shown to be specific for hydrolysis of only very short chains of DP 2–4 (Dauvillée et al. 2005). Later, Takashima et al. (2007) proved that the ISA1-ISA2 heteromer purified from developing kidney bean had a broad chain-length preference, while the purified ISA3 only debranched the DP 2–4 chains. Comparative analyses by Kobayashi et al. (unpublished) also indicated that ISA-type DBE could be classified into three types, i.e., type 1, the rice ISA1 and *P. amyloderamosa* ISA that could act on any chains having various DP values; type 2, rice ISA3 and ISAs from cyanobacteria *Cyanothece* sp. ATCC51142 and *Synechococcus elongatus* PCC7942 that had the capacity for hydrolysis of short chains of DP up to about 13; and type 3, *E. coli* ISA that could only hydrolyze the DP 2–4 chains.

Information on the crystal structure of plant DBEs is available for *Chlamydomonas* ISA1 (CrISA1) (Sim et al. 2014) and barley PUL (Vester-Christensen et al. 2010). It is interesting that the homodimeric CrISA1 structure had a unique elongated structure with monomers connected end to end, and the distinct dimeric structure was commonly conserved in ISA1 homomer and ISA1-ISA2 heteromer at least in green plants (Dauvillée et al. 2000; Sim et al. 2014).

The molar mechanism as to how DBE is involved in amylopectin synthesis is not clear. This is because it is difficult to reveal the mechanism at molecular level under the present situation where nobody has succeeded to establish the reconstituted system for amylopectin biosynthesis in test tubes. Several ideas have been provided to explain why DBE is needed to synthesize the cluster structure of amylopectin.

One most likely idea is that the role of DBE is to remove the unnecessary branches which are accidentally and rarely formed at the improper position on the cluster chains by BE (Nakamura 2002). The reason for the hypothesis is that cleavage of wrongly formed branches by DBE is indispensable to the cluster structure, because, otherwise, the presence of such branches will interfere with the formation of a bundle of double helices. This topic is further discussed below (Sect. 5.4.2).

5.3.1.4 Granule-Bound Starch Synthase (GBSS)

There are a few reports indicating the involvement of GBSS in amylopectin synthesis such as *Chlamydomonas* (Delrue et al. 1992; Maddelein et al. 1994). Rice endosperm frequently had the extra-long chains of DP > 100, which is referred to as super-long chains (SLC) (Takeda et al. 1987a; Hanashiro et al. 2005). Substantial evidence was provided that GBSS was responsible for the synthesis of the long chains (Takeda et al. 1987a; Inouchi et al. 2005; Hanashiro et al. 2008). The SLC was also detected in amylopectin from many dicot and monocot plants (see Chapter 1). It is known that the amount of SLC in amylopectin greatly affected the quality of cereal starch, which was derived from changes in physicochemical properties such as the setback value measured by rapid visco analyzer (Horibata et al. 2004; Inouchi et al. 2005).

5.3.2 The Biosynthesis of Amylose

5.3.2.1 GBSS and BE

Mutants having amylose-free starch called *waxy* mutants have been isolated from many plant species (Collins and Kempton 1911; Ikeno 1914; Jacobsen et al. 1989, see reviews by Shannon and Garwood 1984 and Shannon et al. 2007), and it is evident that GBSS was responsible for the synthesis of amylose (Nelson and Rines 1962; Murata et al. 1965; Visser et al. 1991).

There are two types of GBSS referred to as GBSSI and GBSSII or GBSSIb encoded by two different genes and expressed in reserve tissues such as cereal endosperm, potato tuber, and pea embryo and other tissues such as leaf, pericarp, cereal embryo, and aleurone layers (Fujita and Taira 1998; Nakamura et al. 1998; Tomlinson et al. 1998; Dian et al. 2003). Although assimilatory starch had a lower amylose content than reserve starch (Tomlinson et al. 1997, 1998), it is unknown if this was caused by the difference in enzyme features between GBSSI and GBSSII.

Denyer et al. (1999b) showed that GBSSI from pea embryo synthesized amylose in a processive manner by adding more than one glucose residue for each enzyme-glucan primer while SSII elongated MOS in a distributive manner, by adding only one glucose residue to the primer chain during association of the enzyme-primer complex. They also found that GBSSI had a much higher affinity for amylopectin

as an effector than as a substrate, suggesting the critical feature of GBSSI for the synthesis of amylose (Denyer et al. 1999a).

It is known that some amylose molecules from a limited number of botanical sources so far analyzed had a branched structure with a less frequency of branches than amylopectin (Hizukuri et al. 1981; Takeda et al. 1987b, see also Chapter 2). Hanashiro et al. (2013) analyzed the features of branched chains in amylose molecules. Since short side chains of amylose were not highly ordered in amylose unlike in amylopectin, it is difficult at present to assess which BE isozyme is involved in the synthesis of amylose branches and what the donor chains are for providing amylose with branched chains.

5.4 Regulation and Features of the Biosynthetic Process of Reserve Starch

During their biological evolutions, green plants have developed a metabolic system in which the homogeneous structure of amylopectin molecules having the semicrystalline properties are efficiently reproduced at a high rate and immediately stored in the form of granule inside plastids. However, the fine structure of amylopectin changes in response to different expression levels of key isozymes involved in amylopectin synthesis, keeping a distinct pattern of change depending on each isozyme (Fig. 5.5), as described above. Thus, under a fixed physiological condition, the distinct amylopectin fine structure is basically determined by the balance between chain elongation reaction catalyzed by SS and chain branching reaction by BE, whereas DBE merely removes the improper branches to trim the cluster structure. How can only two kinds of reactions determine the skeleton of the highly organized cluster structure? One possible scenario is that plants have evolved the way by refining several combinations of interactions between different classes of starch synthetic enzymes and the same class of isozymes. How do plants coordinate the distinct and overlapping functions of individual isozymes during the synthesis of amylopectin?

5.4.1 Functional Interactions Between Multiple Enzymes

So far examined, no isoforms of SS, BE, and DBE show the sigmoidal curve in their activity changes in response to varied substrate and/or cofactor concentrations, a typical behavior for the regulatory enzymes like AGPase (see Chap. 11). Instead, their catalytic activities are controlled in a different way, and their activities greatly vary depending on the types of glucans such as amylopectin, amylose, maltodextrins, and MOS. More actually, reaction products formed by some enzymes affect the actions of other enzymes by providing suitable substrates for their catalysis. One of such examples is the observation that the length of branched chains

formed by rice BEIIb was almost exclusively DP 7 or 6 (Nakamura et al. 2010) and the major substrate chains for rice SSI and its product were chains of DP 6–7 and DP 8, respectively (Nakamura et al. 2014). The DP 8 chain could then be elongated to form the intermediate intra-cluster chains by SSIIa (Nakamura et al. 2005a). The results suggest the close functional interactions among BEIIb, SSI, and SSIIa during amylopectin biosynthesis in rice endosperm and that these interactions between other combinations of enzymes play important roles in amylopectin biosynthesis in reserve tissues.

A number of results provided evidences for several kinds of physical association between enzymes while other results showed that some enzymes catalytically interacted with other enzymes/isozymes during the synthesis of amylopectin.

5.4.1.1 Catalytic Interactions

Recently, Nakamura et al. (2012, 2014) presented evidence that rice SSI and plastidial phosphorylase (Pho1, EC 2.4.1.1) could synthesize glucans in the absence of added glucan primer when either BE isozyme was present (see Chap. 9 in details). These SSI-BE and Pho1-BE interactions were established by stimulating mutual catalytic activities and increasing affinities for substrate glucans of the counterpart enzymes. The results might be some examples of the close catalytic interactions among some different enzymes in starch-synthesizing tissues. It is stressed that these interactions were realized in the presence of branched glucans or dextrins (Nakamura et al. 2012).

5.4.1.2 Protein-Protein Interactions

Tetlow et al. (2004, 2008) showed the protein-protein complex among starch synthetic enzymes in amyloplasts of developing wheat endosperm. It is noteworthy that the protein phosphorylation accelerated the formation of the protein multimer composed of BEIIb, BEI, and Pho1 as well as the BEIIb catalytic activity. The different combinations of starch synthetic enzyme complexes were also verified in developing maize endosperm, and the protein phosphorylation was likely to stimulate the functional roles of the enzymes in starch biosynthesis (Hennen-Bierwagen et al. 2008, 2009; Liu et al. 2012a, b, also see review by Emes and Tetlow 2012). These results strongly suggest that the heteromeric protein complexes are essentially involved in starch biosynthesis, and this topic is described in details in Chap. 8.

5.4.2 Models for the Starch Biosynthetic Process

During the course of evaluation of key enzymes, several models for explaining the functions of these enzymes have been proposed.

Ball et al. (1996) proposed a model by incorporating the newly established specific role of DBE (see Sect. 5.3.1.3) in the amylopectin synthesis by trimming the shape of its cluster structure, and therefore this model is referred to as "the glucan-trimming model" (Fig. 5.10a). They claim that the basic frame of amylopectin is constructed by combined actions of SS for chain elongation and BE for chain branching. Excess branches formed during BE reactions should be instantly cleared off by the action of DBE (mainly ISA), because otherwise these irregularly formed branches prevent the glucan crystallization.

Myers et al. (2000) stressed a concept that the crystallization process plays a distinct role during the biogenesis of amylopectin crystal (Fig. 5.10b). During the crystallization process, the removal of pre-amylopectin from the aqueous phase by DBE reaction is needed to make the mature amylopectin inaccessible to further enzymatic modification. This model explains the involvement of nonenzymatic chemical (or spontaneous) behavior of glucan chains after modification by various enzymes in the normal amylopectin biosynthetic process.

Nakamura (2002) proposed a newer model named "the two-step branching and improper branch clearing model" to explain the contribution of each isozyme during amylopectin biosynthesis in cereal endosperm (Fig. 5.10d), although his model was based on the biochemical analyses of SS, BE, and DBE isozymes in rice endosperm. This model emphasized that although interacting reactions between SS and BE isozymes play major roles in the synthesis of amylopectin structure, two different kinds of combinations between SS and BE isozymes play essential parts in the synthesis of normal cluster structure in cereal endosperm and that the role of ISA is to remove a few unnecessary branches that are spontaneously formed by BE reactions at the less-clustered improper positions. It is conceived that a small amount of such wrongly positioned branches is produced at regions remote from where most of the branches are correctly and densely synthesized, and these wrongly and dispersedly formed branches can be removed by ISA more easily than those normally and densely formed branches. This model hypothesizes that the first branches at the root of the cluster are mainly synthesized by BEI, eventually forming the amorphous lamellae, and the second branches are preferentially synthesized by BEIIb. As a result, most of the second branches are considered to be present at the border between the amorphous lamellae and the crystalline lamellae (Fig. 5.2). The first branched chains with the intermediate length synthesized by BEI are mainly elongated by SSIIIa and to a lesser extent by SSIIa and SSI, while the second branched chains with the short chain length formed by BEIIb are sequentially elongated by SSI and SSIIa, as described above (Sect. 5.4.1.1).

Recently, the Myers' group demonstrated a modified model that explains in more details their ideas (Hennen-Bierwagen et al. 2012) (Fig. 5.10c). They postulated equilibrium between crystalline and non-crystalline glucans and claimed that ISA1-ISA2 plays a crucial role in transferring the non-crystalline disordered glucans into the crystalline-competent glucans by eliminating some branches that hinder the spontaneous crystallization.

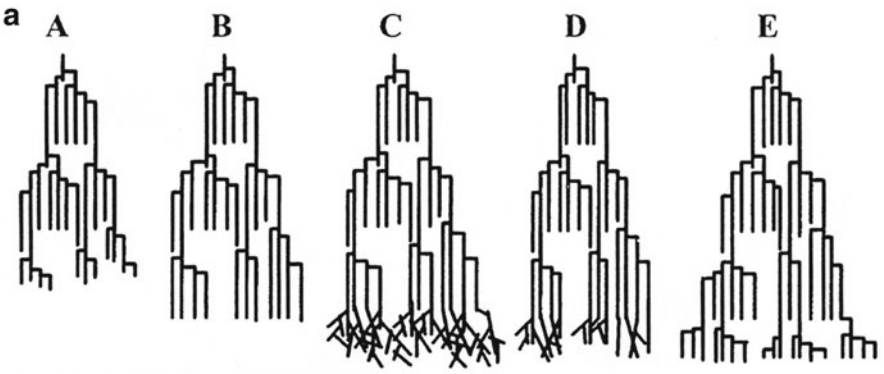

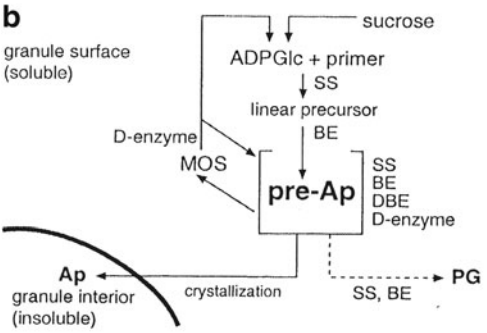

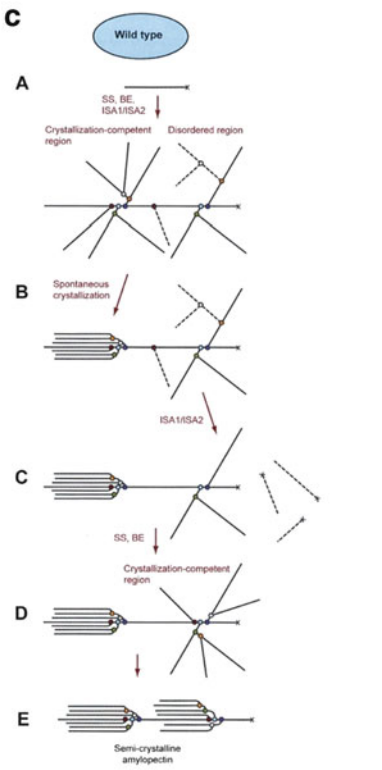

Fig. 5.10 Models for the synthesis of amylopectin. (**a**) The glucan-trimming model (Ball et al. 1996). (**b**) The glucan crystallization model (Myers et al. 2000). (**c**) The modified crystallization model (Hennen-Bierwagen et al. 2012). (**d**) The two-step branching and improper branches clearing model (Nakamura 2002) with a slight modification

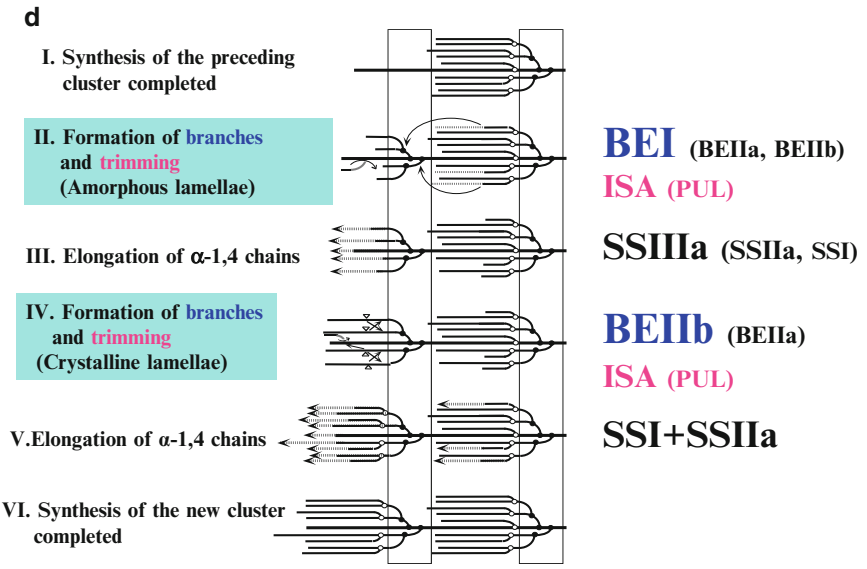

Fig. 5.10 (continued)

Until now, no consensual model applicable for many plant species and tissues has been reported yet. A new model incorporating novel experimental results and ideas is waiting to be proposed.

5.4.3 Features of the Biosynthetic Process of Reserve Starch

5.4.3.1 Starch Biosynthesis and Its Degradation

For the most part the starch synthetic process is distinctly segregated from the degradation process. Classes and/or types of enzymes involved are almost different in both processes from each other, and especially in reserve organs, the timing of operation of each process is distinctive. Nevertheless, in several aspects, both processes are considered to be closely related. There are some direct and indirect evidences for the involvement of other enzymes besides SS, BE, and DBE in the starch biosynthesis in reserve tissues. At least some hydrolase, phosphorylase (Pho), and transglucosidase-type enzymes, which have been considered to play major roles in starch degradation, are highly expressed in tissues exhibiting vigorous starch production.

In spite of the high expression levels of Pho1 in reserve tissues from many plant species in accordance with the increase in their starch production, the in vivo function of Pho1 is still a matter of controversy. The Pho1 reaction is freely reversible and Pho1 itself can catalyze either the glucan synthetic or the degradable

direction. However, the mutations at the *Pho1* locus caused a severe reduction of starch biosynthesis in *Chlamydomonas* (Dauvillée et al. 2006) and rice endosperm (Satoh et al. 2008), strongly suggesting that Pho1 is involved in starch biosynthesis. Several reports have supported this idea. First, Fettke et al. (2010a, 2012) showed that G1P was efficiently and directly incorporated into reserve starch granules in potato tuber cells, suggesting the G1P pathway functions in parallel with the authentic AGPase pathway in starch biosynthesis. Second, Hwang et al. (2010) proved that rice Pho1 could elongate MOS to be used by SS in the glucan synthetic direction even under physiological conditions of high Pi/G1P concentrations. Third, Nakamura et al. (2012) showed the catalytic interaction in glucan synthesis between rice Pho1 and BE in the omission of added glucan primer, as described above. All these results support the view that Pho1 plays a critical role in starch biosynthesis as well as starch degradation.

It was reported that plastidial disproportionating enzyme (DPE1, EC 2.4.1.25) was involved in amylopectin biosynthesis in *Chlamydomonas reinhardtii* (Colleoni et al. 1999a, 1999b; Wattebled et al. 2003), although the contradictory results that DPE1 had no direct role in starch biosynthesis in *Arabidopsis* leaves were shown (Critchley et al. 2001).

The potential involvement of the chloroplastic α-amylase (EC 3.2.1.1) in the synthesis of phytoglycogen in *Arabidopsis* leaves under the condition where all DBE activities were lacking was reported by Streb et al. (2008). The authors hypothesized that SS and BE can basically synthesize starch-type glucans while DBE is indirectly involved in the synthesis (Zeeman et al. 2010). They explained that the role of DBE is to facilitate the crystallization of glucans by removing wrongly positioned branches because otherwise the glucan-degrading enzymes such as α-amylase can easily attack these untrimmed glucans. As a result, in the absence of DBE, the glucans unusually have very short chains of DP ≤ 5, which results in the formation of WSP.

It should be taken into account that a significant amount of MOS is liberated during the process of trimming of amylopectin cluster by DBE, and this MOS should be recycled into the synthetic process. Under physiological condition, most of its glucose residue must be recovered for the biosynthetic process to maintain the high yield of starch production from sucrose. In fact, the level of MOS is usually low in in vivo conditions, although the metabolic process involved in the fate of MOS during starch synthesis has not been fully examined. Besides the four major classes of starch synthetic enzymes (AGPase, SS, BE, and DBE), several types of enzymes presumably play distinct roles in this process. Initially, MOS can be easily degraded until it becomes the length of DP4 by Pho1 to form G1P. In addition, glucose and maltose can be generated by DPE1, α-amylase, and β-amylase (EC 3.2.1.2) from MOS, and this glucose will be converted to G1P by hexokinase and PGM. G1P will be again used by AGPase to form ADPglucose which enters the starch synthetic process via the ADPglucose pathway. The role of DPE1 is specific because it disproportionates the original MOS ranging from much smaller including glucose and maltose to larger MOS, which eventually makes MOS more easily metabolized by hexokinase for glucose and Pho1 and amylases for larger MOS.

All these results lead us to a conclusion that Pho1, DPE, and amylases have dual functions in both the synthesis and degradation of starch granules under various physiological and genetic conditions.

5.4.3.2 Factors Causing Damage to the Cluster Structure

The basic cluster structure of amylopectin is highly conserved even in the mutants whose chain-length profiles are profoundly modified by lesion of any SS, BE, and DBE isozymes. So far examined, six factors are known to be able to change the reserve glucans devoid of the cluster structure, although most of these factors were already stated above (Sect. 5.3.1). First, loss of ISA activity caused phytoglycogen production instead of amylopectin. Second, overexpression of *ISA2* gene also resulted in phytoglycogen synthesis by bereaving the ISA1 homomer in rice endosperm because all the ISA1 proteins formed the ISA1-ISA2 heteromer that had no or little trimming activity for the synthesis of normal amylopectin at least in rice and maize endosperm. Third, excess of BEIIb activity inhibited the formation of organized branches and resulted in the synthesis of WSP in rice endosperm (Tanaka et al. 2004) (Fig. 5.11). Fourth, Lin et al. (2012) showed that when activities of both SSIII and ISA1 or ISA2 were defective in maize, phytoglycogen was produced in the endosperm. The close correlation between ISA and SS activities in starch/WSP accumulation was also found in *Arabidopsis* leaves (Pfister et al. 2014). Fifth, the mutation of rice *Sugary-2* gene led to WSP synthesis especially at early stage of the endosperm development (Nakagami et al. unpublished) (Fig. 5.11), although the gene was recently mapped on the rice genome position different from any *DBE* genes (Nakamura T et al. unpublished). Sixth, α-amylase removed the capacity of *Arabidopsis* for the synthesis of starch-type glucan in the leaf when its ISA activity was lost (Streb et al. 2008), as described above.

In summary, the activity of ISA is likely to be the primary factor in the prevention of phytoglycogen production. In addition, balance of activities between multiple enzymes such as between ISA1 and ISA2, SSIII and ISA, BEIIb and SS, and DBE and α-amylase might be important for the synthesis of starch-type glucans, although comprehensive and more precise biochemical analyses are needed to draw the conclusion.

5.4.3.3 Minimum Sets of Enzymes Required for Construction of the Cluster Structure

It is known that in addition to green plants, some primitive algae including cyanobacteria, grey algae, and red algae could produce starch-like granules, although their amylopectin had less organized cluster structure than higher plant amylopectin and hence it is usually referred to as semi-amylopectin (Nakamura et al. 2005b; Deschamps et al. 2008; Shimonaga et al. 2008; Sawada et al. 2014,

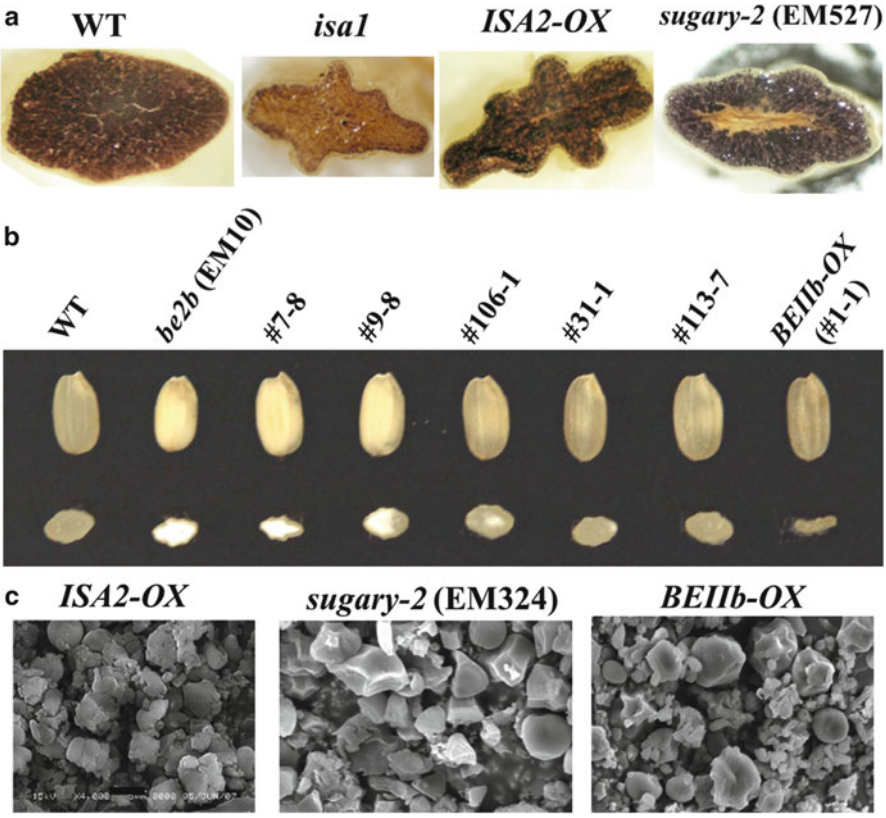

Fig. 5.11 Mutants and transformants producing water-soluble polysaccharide-(WSP)-type glucans in the rice endosperm. (**a**) Cross-section of rice kernels: wild-type (WT), a *sugary-1* (*isa1*) line, an *ISA2* overexpressed (*ISA2-OX*) line, a *sugary-2* (*isa2*) line. (**b**) Seed morphology of rice transformants with different expression levels of BEIIb in which the normal rice *BEIIb* gene was introduced into a *be2b* mutant line (EM10) (see details by Tanaka et al. 2004). Note that the *BEIIb* overexpressed line (*BEIIb-OX*, #1-1), the mature seed became shriveled due to accumulation of water-soluble polysaccharides. (**c**) Scanning electron micrographs of glucan granular morphology in endosperm of the *ISA2* overexpressed line (Utsumi et al. 2011), a *sugary-2* mutant line (Nakagami et al. unpublished), and the *BEIIb* overexpressed line (Tanaka et al. 2004) of rice (See text in details)

also see review by Colleoni and Suzuki 2012 and Chap. 4). Compared with a marked differentiation of starch synthetic enzymes into multiple isozymes in green plants, no significant differentiation in the glucan-metabolizing enzyme genes was found in the starch-synthesizing primitive algae. Some semi-amylopectin producing cyanobacteria such as *Crocosphaera watsonii* had three *SS* gene, three *BE* genes, and one *ISA* gene (Patron and Keeling 2005; Deschamps et al. 2008; Ball et al. 2011). *Cyanidioschyzon merolae* had one *SS* gene, one *BE* gene, and two *ISA* genes, and another unicellular red alga *Porphyridium purpureum* having one *SS*

gene, two *BE* genes, and one *ISA* gene (Coppin et al. 2005; Patron and Keeling 2005; Deschamps et al. 2008; Ball et al. 2011; Bhattacharya et al. 2013) could also synthesize semi-amylopectin (Hirabaru et al. 2010; Shimonaga et al. 2006, 2008). It is also known that many mutant and transformant lines prepared from higher plants having a single major SS isozyme, BE isozyme, or ISA1 out of corresponding multiple isozymes could also produce starch-like glucans (Tetlow 2012; Fujita and Nakamura 2012; Hennen-Bierwagen et al. 2012).

All these results indicate that the presence of multiple isozymes in each class of starch synthetic enzymes is not an absolute requirement for the synthesis of starch. Rather, it is likely that multiple isozymes enable plant tissues to efficiently produce starch under varying physiological and environmental conditions by giving them differentiation in capacities for production of various types of tissue- and species-specific starches with refined structural features.

5.4.3.4 Reactivity and Binding Affinity of Starch Biosynthetic Enzymes Toward Glucans

During the starch synthesis, the fine structure of glucan molecule changes in every step of consecutive reactions involved in numerous starch synthetic enzymes. How can each isozyme act correctly on the exact glucan substrate by selecting it among various structures of glucans simultaneously formed by many other enzymes? Biochemical in vitro studies showed that SS and BE recognized the length of external segments of A- and B-chains (Guan et al. 1997; Commuri and Keeling 2001; Nakamura et al. 2010, 2014; Sawada et al. 2014), although some BE isozymes such as BEI could also attack the internal segments of B2- and B3-chains to some extent (Nakamura et al. 2010; Sawada et al. 2014). It was also established that SS and BE were much more preferentially reactive toward branched glucans than linear MOS and dextrins/glucans (Nakamura et al. 2010, 2014 and many references therein), suggesting that the actual glucan substrates for SS and BE during in vivo starch synthesis are the dual parallel chains or the double helical chains, respectively, of the branched glucans/dextrins, as proposed by Borovsky et al. (1979) for BE. Recently, it was found that SSI from rice (Nakamura et al. 2014) and SS from *Arabidopsis* (Brust et al. 2014) could efficiently synthesize glucans by interacting closely with BE isozymes, possibly forming the protein complex, in the absence of added primer as found in the interaction between Pho1 and BE (Nakamura et al. 2012). It is noted that these interactions were mediated by branched glucans, but not by linear glucans (Nakamura et al. 2012; Brust et al. 2014). These results strongly suggest that at least SSI, BEs, and Pho1 can closely interact with their counterparts including many types of glucans varied under different physiological conditions.

5.5 Future Perspectives for Research on the Biosynthesis of Reserve Starch

5.5.1 Major Subjects Unresolved

Despite huge amounts of biochemical, molecular, genetic, physicochemical, and structural studies as well as theoretical analyses and proposals for long time, we have to admit that there are still a lot of important subjects related to starch biosynthesis remaining unresolved.

First, how is the cluster structure constructed, especially how the length of single cluster is made constant? Concomitant with analytical studies on the enzymatic reaction mechanisms, the minimum requirements of the glucan fine structure needed for construction of the cluster should be defined (see Chap. 1).

Second, although currently the most conventional method for determination of the fine structure of glucans is to measure their chain-length distributions by HPLC or capillary electrophoresis, the method only measures the proportion of component chains of the glucan, but neither method can give any information on the position of branches. However, it is much more important to know the localized positions of branched chains and the lengths of internal segments of chains than to simply know the chain-length distribution of the glucan.

Third, how are the protein-protein multimeric structures related to their specific functions? Further analytical data are needed to clarify the mechanism for the actions of multimeric structure and to reveal the extent of involvement of enzyme interactions in starch biosynthesis.

Fourth, in which way do the enzymes interact with glucans? Starch biosynthetic enzymes are known to closely interact with environmental glucans in different ways, and some of them such as GBSS, BEIIb, and SSI were tightly and lightly bound to starch granules at different proportions while others such as DBEs were almost exclusively soluble in the stroma compartment. However, since enzymes were usually non-covalently associated with carbohydrates, it was difficult to elucidate the mechanism on how the bindings of enzymes to glucans influenced their functions/activities. The mechanism on how the carbohydrate-binding module (CBM) present in GH13 family enzymes (Janeček et al. 2011) and SSIII (Schwarte et al. 2013) relates to their enzymatic actions awaits resolution.

Fifth, how are enzymes related with glucan granule morphology? There have been some reports showing that some enzymes were even present in specific plastid membrane spaces and compartments, e.g., SSIIIa, SSIVb, GBSSI, and ISA3 (Gámez-Arjona et al. 2011; Yun et al. 2011; Kawagoe 2013; Toyosawa et al. 2015). It is likely that they play important roles in the starch granule initiation, development, and morphology, as well as in the conventional starch biosynthetic process, although the mechanisms as to how they are involved in these events remain to be elucidated.

5.5.2 *Diversity of Regulation of Starch Biosynthesis Among Plant Species and Pleiotropic Effects*

Notably it is known that relative activities of major SS isozymes greatly differed among plant species and this affected the species-specific structural and functional features of starch (Edwards et al. 1999b; Fujita and Nakamura 2012). For example, SSI was a major component of the total SS activity in the endosperm of maize (Cao et al. 1999), rice (Fujita et al. 2006), and *Arabidopsis* leaf (Delvallé et al. 2005; Zhang et al. 2005), but not in pea embryo (Craig et al. 1998) and potato tuber (Marshall et al. 1996) where SSII and SSIII, respectively, accounted for the bulk activity of SS. The results might support the variation on the mode of amylopectin chains synthesized through concerted actions of different combinations of SS isozymes and/or other synthetic enzymes such as BE and DBE depending on the plant species and tissues.

BEII is differentiated into distinct BEIIa and BEIIb isozymes in cereals, but not in dicots. In maize and rice endosperm, the specific chain preference of BEIIb was likely to be one of the strongest determinants of starch properties, and this role could not be supplemented by BEIIa (Nishi et al. 2001; Klucinec and Thompson 2002; Yao et al. 2004; Butardo et al. 2011). In contrast, the implication of BEIIa was more significant than BEIIb in wheat and barley endosperm (Regina et al. 2005), while loss of both BEIIa and BEIIb showed much more profound effects on starch structure than that of only BEIIa (Regina et al. 2006, 2010; Sestili et al. 2010). The results suggest that in wheat and barley, the functions of BEIIa and BEIIb largely overlap, whereas in rice and maize, BEIIb has a distinct role in starch biosynthesis. It is likely that the difference in contribution of BEIIa and BEIIb was not merely due to the relative activity of BEIIa to BEIIb because in rice endosperm their activities were at the same level (Yamanouchi and Nakamura 1992) and the distinct role of BEIIb was evident even if it had lower activity levels compared to the BEIIa (Tanaka et al. 2004). In addition, the silencing of the *BEIIa* gene profoundly influenced the amylose content and starch granule morphology in wheat and barley (Regina et al. 2006, 2010), while the *be2b* mutation had a minor impact on amylose content in rice (Nishi et al. 2001; Butardo et al. 2011). Remarkably, Carciofi et al. (2012) succeeded to produce amylose-only starch in barley endosperm by silencing all the *BE* genes. The impact of BEIIb/IIa gene on amylose content in maize was more similar to wheat and barley than rice because maize *ae* starch contained high amylose content (Li et al. 2008). Starch phenotypes of *be2b* (*ae*) mutants were considerably different between maize and rice (Banks et al. 1974; Baba et al. 1982; Nishi et al. 2001; Li et al. 2008). These results indicate that BEIIb exhibited a great variation in terms of its distinct function and expression level in cereal endosperm among species.

The roles of ISAs, their presence and composition, and their contributions to starch biosynthesis were dramatically different depending on plant species and tissues (Hennen-Bierwagen et al. 2012; Facon et al. 2013). One example is that the complete loss of *ISA1* gene caused most cells to synthesize both starch-type glucans and WSP in many plant sources, while starch was completely replaced by WSP in

rice endosperm (Nakamura et al. 1997) and *Chlamydomonas* (Mouille et al. 1996), although the exact reason remains to be clarified.

Several reports showed that multiple forms of some enzymes such as SSI (Baba et al. 1993) and BEIIa (Yamanouchi and Nakamura 1992) in rice endosperm, BEI in wheat endosperm (Båga et al. 2000), and BEII from kidney bean (Hamada et al. 2002) were generated from a single gene by transcriptional or posttranscriptional regulation and/or modification. However, the physiological significances of multiple forms of the same enzymes were unclear.

There are ample evidences showing the pleiotropic effects of losses of some enzymes on the enhancement or reduction on the levels of other enzymes (Sestili et al. 2010 and references therein). These suggest the presence of some factors which integrate the expression and amounts of numerous genes and proteins involved in starch metabolism and the close interrelation via protein-protein and protein-glucan interactions. The effects were possibly caused by many reasons at various levels. Recently, the specific and complex relations were found in protein levels and presence (e.g., binding to starch granules) among SSI, SSIIIa, BEI, and BEIIb in rice endosperm using various SSI-BE (Abe et al. 2014) and SSIIIa-BE (Asai et al. 2014) double mutants (see Chap. 10 in details), although some of them might have been caused by effects on association of protein complex among them in maize endosperm reported by Liu et al. (2012a, b). The molecular mechanism and physiological significance for some pleiotropic effects will be elucidated in the future.

5.5.3 New Approaches and Techniques Required

A number of new approaches will help us to understand the regulatory mechanisms for starch biosynthesis. First, a new practical method to determine the branch position in glucan chains should be established. This would give new insights into the possible roles of enzymes in determining the distribution and location of branches in amylopectin (Xia et al. 2011). Hizukuri (1996) proposed the enzymatic method for determination of the average span length and the average number of α-1,4-linkages between the nearest branch linkages, by calculating the number of glucosyl stubs of the B-chains treated with a sequential hydrolysis by β-amylase, isoamylase, and β-amylase. Usui et al. (2009) established a method for measuring directly the α-1,6-glucosidic linkages and the α-1,4-linkages along with MOS by negative ion Q-TOF MS/MS spectrometry method. However, a new standard method to determine exactly the position of α-1,6-linkages of glucans needs to be developed.

Second, methods to establish a reconstituted system to synthesize glucans with the cluster structure by in vitro enzymatic reactions are desirable. So far, no attempts have been successful to synthesize glucans having the cluster structure by in vitro reactions, whereas it is easy to synthesize glycogen-type glucans in test tubes in the presence of SS and BE. Since the use of readily available glucans composed of a

mixture of chains with different lengths does not lead to a clear conclusion regarding characteristics of the enzyme, the choice of appropriate glucan primers with known structural features and lengths of component chains which are chemically and/or enzymatically prepared and the appropriate combination of candidate enzymes might be essentially important.

Third, factors which potentially integrate the starch biosynthetic process in plant tissues (She et al. 2010; Wang et al. 2013; Peng et al. 2014) need to be fully characterized. The use of transgenic lines carrying various types of constructs might provide important insights into the subject, because multiple candidate gene functions can be simultaneously modified by using, for example, the RNAi technology.

Acknowledgments The author thanks Dr. Perigio B. Francisco, Jr. for critical reading of the manuscript and polishing the English used in the paper. The author also thanks Dr. Takayuki Sawada for the assistance with some figures.

References

Abe N, Asai H, Yago H et al (2014) Relationships between starch synthase I and branching enzyme isozymes determined using double mutant rice lines. BMC Plant Biol 14:80

Asai H, Abe N, Matsushima R, et al. (2014) Deficiencies in both starch synthase (SS) IIIa and branching enzyme IIb lead to a significant increase in amylose in SSIIa-inactive japonica rice seeds. J Exp Bot 65:5497–5507

Baba T, Arai Y, Yamamoto T et al (1982) Some structural features of amylomaize starch. Phytochemistry 21:2291–2296

Baba T, Nishihara M, Mizuno K et al (1993) Identification, cDNA cloning, and gene expression of soluble starch synthase in rice (*Oryza sativa* L.) immature seeds. Plant Physiol 103:565–573

Båga M, Nair RB, Repellin A et al (2000) Isolation of a cDNA encoding a granule-bound 152-kilodalton starch-branching enzyme in wheat. Plant Physiol 124:253–263

Ball S, Guan H-P, James MG et al (1996) From glycogen to amylopectin: a model for the biogenesis of the plant starch granule. Cell 86:349–352

Ball S, Colleoni C, Cenci U et al (2011) The evolution of glycogen and starch metabolism in eukaryotes gives molecular clues to understand the establishment of plastid endosymbiosis. J Exp Bot 62:1775–1801

Banks W, Greenwood CT, Muir DD (1974) Studies on starches of high amylose content. Part 17. A review of current concepts. Starch 26:289–300

Beatty MK, Rahman A, Cao H et al (1999) Purification and molecular genetic characterization of ZPU1, a pullulanase-type starch-debranching enzyme from maize. Plant Physiol 119:255–265

Bhattacharya D, Price DD, Chan CX et al (2013) Genome of the red alga *Porphyridium purpureum*. Nat Commun 4:2931

Bhattacharyya MK, Smith AM, Ellis THN et al (1990) The wrinkled-seed character of pea described by Mendel is caused by a transposon-like insertion in a gene encoding starch-branching enzyme. Cell 60:115–122

Blauth SL, Yao Y, Klucinec JD et al (2001) Identification of *Mutator* insertional mutants of starch-branching enzyme 2a in corn. Plant Physiol 125:1396–1405

Blauth SL, Kim KN, Klucinec J et al (2002) Identification of *Mutator* insertional mutants of starch-branching enzyme 1 (*sbe1*) in *Zea mays* L. Plant Mol Biol 48:287–297

Borovsky D, Smith EC, Whelan WJ et al (1979) The mechanism of Q-enzyme action and its influence on the structure of amylopectin. Arch Biochem Biophys 198:627–631
Boyer CD, Preiss J (1978) Multiple forms of (1–4)-α-D-glucan, (1–4)-α-D-glucan-6-glycosyl transferase from developing *Zea mays* L. kernels. Carbohydr Res 61:321–334
Boyer CD, Preiss J (1979) Properties of citrate-stimulated starch synthesis catalyzed by starch synthase I of developing maize kernels. Plant Physiol 64:1039–1042
Brust H, Lehman T, D'Hulst C et al (2014) Analysis of the functional interaction of Arabidopsis starch synthase and branching enzyme isoforms reveals that the cooperative action of SSI and BEs results in glucans with polymodal chain length distribution similar to amylopectin. PLoS One 9:e102364
Burton R, Bewley JD, Smith AM et al (1995) Starch branching enzymes belonging to distinct enzyme families are differentially expressed during pea embryo development. Plant J 7:3–15
Burton RA, Jenner H, Carrangis L et al (2002) Starch granule initiation and growth are altered in barley mutants that lack isoamylase activity. Plant J 31:97–112
Bustos R, Fahy B, Hylton CM et al (2004) Starch granule initiation is controlled by a heteromultimeric isoamylase in potato tubers. Proc Natl Acad Sci U S A 101:2215–2220
Butardo VM, Fitzgerald MA, Bird AR et al (2011) Impact of down-regulation of *starch branching enzyme IIb* in rice by artificial microRNA- and hairpin RNA-mediated RNA silencing. J Exp Bot 62:4927–4941
Cao H, Imparl-Radosevich J, Guan H et al (1999) Identification of the soluble starch synthase activities of maize endosperm. Plant Physiol 120:205–215
Carciofi M, Blennow A, Jensen SL et al (2012) Concerted suppression of all starch branching enzyme genes in barley produces amylase-only starch granules. BMC Plant Biol 12:223
Cenci U, Chabi M, Ducatez M et al (2013) Convergent evolution of polysaccharide debranching defines a common mechanism for starch accumulation in cyanobacteria and plants. Plant Cell 25:3961–3975
Chaen K, Noguchi J, Omori T (2012) Crystal structure of the rice branching enzyme I (BEI) in complex with maltopentaose. Biochem Biophys Res Commun 424:508–511
Colleoni C, Suzuki E (2012) Storage polysaccharide metabolism in cyanobacteria. In: Tetlow I (ed) Starch: origins, structure and metabolism, vol 5, Essential reviews in experimental biology. The Society for Experimental Biology, London, pp 217–253
Colleoni C, Dauvillee D, Mouille G et al (1999a) Genetic and biochemical evidence for the involvement of α-1,4 glucanotransferases in amylopectin synthesis. Plant Physiol 120:993–1004
Colleoni C, Dauvillee D, Mouille G et al (1999b) Biochemical characterization of the *Chlamydomonas reinhardtii* α-1,4 glucanotransferase supports a direct function in amylopectin biosynthesis. Plant Physiol 120:1005–1014
Collins GN, Kempton JF (1911) Inheritance of waxy endosperm in hybrids of Chinese maize. Proc IV Int Genet Congr (Paris) 347–356
Commuri PD, Keeling PL (2001) Chain-length specificities of maize starch synthase I enzyme: studies of glucan affinity and catalytic properties. Plant J 25:475–486
Coppin A, Varre JS, Lienard L et al (2005) Evolution of plant-like crystalline storage polysaccharide in the protozoan parasite Toxoplasma gondii argues for a red alga ancestry. J Mol Evol 60:257–267
Craig J, Lloyd JR, Tomlinson K et al (1998) Mutations in the gene encoding starch synthase II profoundly alter amylopectin structure in pea embryos. Plant Cell 10:413–426
Critchley JH, Zeeman S, Takaha T et al (2001) A critical role for disproportionating enzyme in starch breakdown is revealed by a knock-out mutation in Arabidopsis. Plant J 26:89–100
Crumpton-Taylor M, Pike M, Lu K et al (2013) Starch synthase 4 is essential for coordination of starch granule formation with chloroplast division during Arabidopsis leaf expansion. New Phytol 200:1064–1075
Cuesta-Seijo JA, Nielsen MM, Marri L et al (2013) Structure of starch synthase I from barley: insight into regulatory mechanisms of starch synthase activity. Acta Crystallogr D Biol Crystallogr D69:1013–1025

D'Hulst C, Merida A (2012) Once upon a time: inception of the understanding of starch initiation in plants. In: Tetlow I (ed) Starch: origins, structure and metabolism. , vol 5, Essential reviews in experimental biology. The Society for Experimental Biology, London, pp 55–76

Damager I, Denyer K, Motawia MS et al (2001) The action of starch synthase II on 6'-α-maltotoriosyl-maltohexaose comprising the branch point amylopectin. Eur J Biochem 268:4878–4884

Dang PL, Boyer CD (1988) Maize leaf and kernel starch synthases and starch branching enzymes. Phytochemistry 27:1255–1259

Dauvillée D, Mestre V, Colleoni C et al (2000) The debranching enzyme complex missing in glycogen accumulating mutants of Chlamydomonas reinhardtii displays an isoamylase-type specificity. Plant Sci 157:145–156

Dauvillée D, Colleoni C, Mouille G et al (2001) Biochemical characterization of wild-type and mutant isoamylases of *Chlamydomonas reinhardtii* supports a function of the multimeric enzyme organization in amylopectin maturation. Plant Physiol 125:1723–1731

Dauvillée D, Kinderf IS, Li Z et al (2005) Role of the *Escherichia coli glgX* gene in glycogen metabolism. J Bacteriol 187:1465–1473

Dauvillée D, Chochois V, Steup M et al (2006) Plastidial phosphorylase is required for normal starch synthesis in *Chlamydomonas reinhardtii*. Plant J 48:274–285

Davis JH, Kramer HH, Whistler RL (1955) Expression of the gene du in the endosperm of maize. Agron J 47:232–235

Dellate T, Trevisan M, Parker ML et al (2005) Arabidopsis mutants *Atisa1* and *Atisa2* have identical phenotypes and lack the multimeric isoamylase, which influences the branch point distribution of amylopectin during starch synthesis. Plant J 41:815–830

Delrue B, Fontaine T, Routier F et al (1992) Waxy *Chlamydomonas reinhardtii*: monocellular algal mutants defective in amylose biosynthesis and granule-bound starch synthase activity accumulate a structurally modified amylopectin. J Bacteriol 174:3612–3620

Delvallé D, Dumez S, Wattebled F et al (2005) Soluble starch synthase I: a major determinant for the synthesis of amylopectin in *Arabidopsis thaliana* leaves. Plant J 43:398–412

Denyer K, Dunlap F, Thornbjørnsen T et al (1996) The major form of ADP-glucose pyrophosphorylase in maize (*Zea mays* L.) endosperm is extra-plastidial. Plant Physiol 112:779–785

Denyer K, Waite D, Edwards A et al (1999a) Interaction with amylopectin influences the ability of granule-bound starch synthase I to elongate malto-oligosaccharides. Biochem J 342:647–653

Denyer K, Waite D, Motawia S et al (1999b) Granule-bound starch synthase I in isolated starch granules elongates malto-oligosaccharides processively. Biochem J 340:183–191

Deschamps P, Colleoni C, Nakamura Y et al (2008) Metabolic symbiosis and the birth of the plant kingdom. Mol Biol Evol 25:536–548

Dian W, Jiang H, Chen Q et al (2003) Cloning and characterization of the *granule-bound starch synthase II* gene in rice: gene expression is regulated by the nitrogen level, sugar and circadian rhythm. Planta 218:261–268

Dinges JR, Colleoni C, Myers AM et al (2001) Molecular structure of three mutations at the maize *sugary1* locus and their allele-specific phenotypic effects. Plant Physiol 125:1406–1418

Dinges JR, Colleoni C, James MG et al (2003) Mutational analysis of the pullulanase-type debranching enzyme of maize indicates multiple functions in starch metabolism. Plant Cell 15:666–680

Edwards A, Borthakur A, Bornemann S et al (1999a) Specificity of starch synthase isoforms from potato. Eur J Biochem 266:724–736

Edwards A, Fulton DC, Hylton CM et al (1999b) A combined reduction in activity of starch synthases II and III of potato has novel effects on the starch of tubers. Plant J 17:251–261

Emes MJ, Tetlow IJ (2012) The role of heteromeric protein complexes in starch synthesis. In: Tetlow I (ed) Starch: origins, structure and metabolism, vol 5, Essential reviews in experimental biology. The Society for Experimental Biology, London, pp 255–278

Facon M, Lin Q, Azzaz AM et al (2013) Distinct functional properties of isoamylase-type starch debranching enzymes in monocot and dicot leaves. Plant Physiol 163:1363–1375

Fettke J, Albrecht T, Hejazi M et al (2010a) Glucose 1-phosphate is efficiently taken up by potato (*Solanum tuberosum*) tuber parenchyma cells and converted to reserve starch granules. New Phytol 185:663–675

Fettke J, Malinova I, Albrecht T et al (2010b) Glucose-1-phosphate transport into protoplasts and chloroplasts from leaves of Arabidopsis. Plant Physiol 155:1723–1734

Fettke J, Leifels L, Brust H et al (2012) Two carbon fluxes to reserve starch in potato (*Solanum tuberosum* L.) tuber cells are closely interconnected but differently modulated by temperature. J Exp Bot 63:3011–3029

Fisher DK, Gao M, Kim K (1996) Allelic analysis of the maize amylose-extender locus suggests that independent genes encode starch-branching enzymes IIa and IIb. Plant Physiol 110:611–619

Fontaine T, D-Hulst C, Maddelein ML et al (1993) Toward an understanding of the biogenesis of the starch granules. Evidence that Chlamydomonas starch synthase II controls the synthesis of intermediate size glucans of amylopectin. J Biol Chem 268:16223–16230

Fujita N, Nakamura Y (2012) Distinct and overlapping functions of starch synthase isoforms. In: Tetlow I (ed) Starch: origins, structure and metabolism, vol 5, Essential reviews in experimental biology. The Society for Experimental Biology, London, pp 115–140

Fujita N, Taira T (1998) A 56 kDa protein is a novel granule-bound starch synthase existing in the pericarps, aleurone layers, and embryos of immature seeds of diploid wheat (*Triticum monococcum* L.). Planta 207:125–132

Fujita N, Kubo A, Francisco PB Jr et al (1999) Purification, characterization, and cDNA structure of isoamylase from developing endosperm of rice. Planta 208:283–293

Fujita N, Kubo A, Suh DS et al (2003) Antisense inhibition of isoamylase alters the structure of amylopectin and the physiological properties of starch in rice endosperm. Plant Cell Physiol 44:607–618

Fujita N, Yoshida M, Asakura N et al (2006) Function and characterization of starch synthase I using mutants in rice. Plant Physiol 140:1070–1084

Fujita N, Yoshida M, Kondo T et al (2007) Characterization of SSIIIa-deficient mutants of rice: the function of SSIIIa and pleiotropic effects by SSIIIa deficiency in the rice endosperm. Plant Physiol 144:2009–2023

Fujita N, Toyosawa Y, Utsumi Y et al (2009) Characterization of pullulanase (PUL)-deficient mutants of rice (*Oryza sativa* L.) and the function of PUL on starch biosynthesis in the developing rice endosperm. J Exp Bot 60:1009–1023

Gámez-Arjona FM, Li J, Raynaud S et al (2011) Enhancing the expression of starch synthase class IV results in increased levels of both transitory and long-term storage starch. Plant Biotechnol J 9:1049–1060

Gao M, Fisher DK, Kim K et al (1996) Evolutionary conservation and expression patterns of maize starch branching enzyme I and IIb genes suggest isoform specialization. Plant Mol Biol 30:11223–11232

Gao M, Wanat J, Stinard PS et al (1998) Characterization of *dull1*, a maize gene coding for a novel starch synthase. Plant Cell 10:399–412

Gidley MJ, Bulpin PV (1987) Crystallization of malto-oligosaccharides as models of the crystalline forms of starch. Carbohydr Res 161:291–300

Grimaud F, Rogniaux H, James MG et al (2008) Proteome and phosphoproteome analysis of starch granule-associated proteins from normal maize and mutants affected in starch biosynthesis. J Exp Bot 59:3395–3406

Guan H, Preiss J (1993) Differentiation of the properties of the branching isozymes from maize (*Zea mays*). Plant Physiol 102:1269–1273

Guan H, Li P, Imparl-Radosevich J et al (1997) Comparing the properties of *Escherichia coli* branching enzyme and maize branching enzyme. Arch Biochem Biophys 342:92–98

Hamada S, Nozaki K, Ito H et al (2001) Two starch-branching-enzyme isoforms occur in different fractions of developing seeds of kidney bean. Biochem J 359:23–34

Hamada S, Ito H, Hiraga S et al (2002) Differential characteristics and subcellular localization of two starch-branching enzyme isoforms encoded by a single gene in *Phaseolus vulgaris* L. J Biol Chem 277:16538–16546

Han Y, Bendik E, Sun F et al (2007a) Genomic isolation of genes encoding starch branching enzyme II (SBEII) in apple: Towards characterization of evolutionary disparity in *SbeII* genes between monocots and eudicots. Planta 226:1265–1276

Han Y, Sun F, Rosales-Mendoza S et al (2007b) Three orthologs in rice, *Arabidopsis*, and *Populus* encoding starch branching enzymes (SBEs) are different from other *SBE* gene families in plants. Gene 401:123–130

Hanashiro I, Matsunaga J, Egashira T et al (2005) Structural characterization of long unit-chains of amylopectin. J Appl Glycosci 52:233–237

Hanashiro I, Ito K, Kuratomi Y et al (2008) Granule-bound starch synthase I is responsible for biosynthesis of extra-long unit chains of amylopectin in rice. Plant Cell Physiol 49:925–933

Hanashiro I, Sakaguchi I, Yamashita H (2013) Branched structures of rice amylose examined by differential fluorescence detection of side-chain distribution. J Appl Glycosci 60:79–85

Hawker JS, Ozbun JL, Preiss J (1972) Unprimed starch synthesis by soluble ADPglucose-starch glucosyltransferase from potato tubers. Phytochemistry 11:1287–1293

Hawker JS, Ozbun JL, Ozaki H et al (1974) Interaction of spinach leaf adenosine diphosphate glucose α-1,4-glucan α-4-glucosyl transferase and α-1,4-glucan, α-1,4-glucan-6-glucosyl transferase in synthesis of branched α-glucan. Arch Biochem Biophys 160:530–551

Hedman KD, Boyer CD (1982) Gene dosage at the *amylose-extender* locus of maize: effects on the levels of starch branching enzymes. Biochem Genet 20:483–492

Hennen-Bierwagen TA, Liu F, Marsh RS et al (2008) Starch biosynthetic enzymes from developing *Zea mays* endosperm associate in multisubunit complexes. Plant Physiol 146:1892–1908

Hennen-Bierwagen TA, Lin Q, Grimaud F et al (2009) Proteins from multiple metabolic pathways associate with starch biosynthetic enzymes in high molecular weight complexes: a model for regulation of carbon allocation in maize amyloplasts. Plant Physiol 149:1541–1559

Hennen-Bierwagen TA, James MG, Myers AM (2012) Involvement of debranching enzymes in starch biosynthesis. In: Tetlow I (ed) Starch: origins, structure and metabolism, vol 5, Essential reviews in experimental biology. The Society for Experimental Biology, London, pp 179–215

Hirabaru C, Izumo A, Fujiwara S et al (2010) The primitive rhodophyte *Cyanidioschyzon merolae* contains a semiamylopectin-type, but not an amylose-type α-glucan. Plant Cell Physiol 51:682–693

Hirose T, Terao T (2004) A comprehensive expression analysis of the starch synthase gene family in rice (*Oryza sativa* L.). Planta 220:9–16

Hizukuri S (1986) Polymodal distribution of the chain lengths of amylopectins, and its significance. Carbohydr Res 147:342–347

Hizukuri S (1996) Starch: analytical aspects. In: Eliasson AC (ed) Carbohydrates in food starch. Essential reviews in experimental biology, vol 5. Marcel Dekker Inc, New York/Basel/Hong Kong; The Society for Experimental Biology, London, pp 115–140

Hizukuri S, Takeda Y, Yasuda M et al (1981) Multi-branched nature of amylose and the action of debranching enzymes. Carbohydr Res 94:205–213

Horibata T, Nakamoto M, Fuwa H et al (2004) Structural and physicochemical characteristics of endosperm starches of rice cultivars recently bred in Japan. J Appl Glycosci 51:303–313

Hussain H, Mant A, Seale R et al (2003) Three isoforms of isoamylase contribute different catalytic properties for the debranching of potato glucans. Plant Cell 15:133–149

Hwang S, Nishi A, Satoh H et al (2010) Rice endosperm-specific plastidial α-glucan phosphorylase is important for synthesis of short-chain malto-oligosaccharides. Arch Biochem Biophys 495:82–92

Ikeno S (1914) Über die Bestäubung und die Bastardierung von Reis. Z Pflanzenzucht 2:495–503

Imparl-Radosevich JM, Gameon JR, McKean A et al (2003) Understanding catalytic properties and functions of maize starch synthase isozymes. J Appl Glycosci 50:177–182

Inouchi N, Hibiu H, Li T et al (2005) Structure and properties of endosperm starches from cultivated rice of Asia and other countries. J Appl Glycosci 52:239–246

Ishizaki Y, Taniguchi H, Maruyama Y et al (1983) Debranching enzymes of potato tubers (Solanum tuberosum L.). I. Purification and some properties of potato isoamylase. Agric Biol Chem 47:771–779

Jacobsen E, Hovenkamp-Hermelink JHM, Krijgheld HT et al (1989) Phenotypic and genotypic characterization of an amylase-free starch mutant of the potato. Euphytica 44:43–48

James MG, Robertson DS, Myers AM (1995) Characterization of the maize gene *sugary1*, a determinant of starch composition in kernels. Plant Cell 7:417–429

Janeček Š, Svensson B, MacGregor EA (2011) Structural and evolutional aspects of two families of non-catalytic domains present in starch and glycogen binding proteins from microbes, plants and animals. Enzym Microb Technol 49:429–440

Jenkins PJ, Cameron RE, Donald AM (1993) A universal feature in the starch granules from different botanical sources. Starch 45:417–420

Kainuma K, French D (1972) Naegeli amylodextrin and its relationship to starch granule structures. III Role of water in crystallization of B-starch. Biopolymers 11:2241–2250

Katayama K, Komae K, Kohyama K et al (2002) New sweet potato line having low gelatinization temperature and altered starch structure. Starch 54:51–57

Katsuya Y, Mezaki Y, Kubota M et al (1998) Three-dimensional structure of *Pseudomonas* isoamylase at 2.2 Å resolution. J Mol Biol 281:885–897

Kawagoe Y (2013) The characteristic polyhedral, sharp-edged shape of compound-type starch granules in rice endosperm is achieved via the septum-like structure of the amyloplast. J Appl Glycosci 60:29–36

Kitahara K, Fukunaga S, Katayama K et al (2005) Physicochemical properties of sweet potato starches with different gelatinization temperatures. Starch 57:473–479

Klucinec JD, Thompson DB (2002) Structure of amylopectins from *ae*-containing maize starches. Cereal Chem 79:19–23

Kubo A, Fujita N, Harada K et al (1999) The starch-debranching enzymes isoamylase and pullulanase are both involved in amylopectin biosynthesis in rice endosperm. Plant Physiol 121:399–409

Kubo A, Rahman S, Utsumi Y et al (2005) Complementation of *sugary-1* phenotype in rice endosperm with the wheat *Isoamylase1* gene supports a direct role for isoamylase1 in amylopectin biosynthesis. Plant Physiol 137:43–56

Kubo A, Colleoni C, Dinges JR et al (2010) Functions of heteromeric and homomeric isoamylase-type starch debranching enzymes in developing maize endosperm. Plant Physiol 153:956–969

Larsson CT, Hofvander P, Khoshnoodi J et al (1996) Three isoforms of starch synthase and two isoforms of branching enzyme are present in potato tuber starch. Plant Sci 117:9–16

Lee EYC, Whelan WJ (1971) Glycogen and starch debranching enzymes. In: Boyer PD (ed) The enzymes, vol 5. Academic, New York, pp 191–234

Leterrier M, Holappa L, Broglie KE et al (2008) Cloning, characterization and comparative analysis of a starch synthase IV gene in wheat: functional and evolutional implications. BMC Plant Biol 8:98

Li Z, Mouille G, Kosar-Hashemi B et al (2000) The structure and expression of the wheat starch synthase III gene: motif in the expressed gene define the lineage of the starch synthase III gene family. Plant Physiol 123:613–624

Li L, Jiang H, Campbell M, et al. (2008) Characterization of maize *amylose-extender* (*ae*) mutant starches. Part I: Relationship between resistant starch contents and molecular structures. Carbohydr Polym 74:396–404

Li Z, Li D, Du X et al (2011) The barley *amo1* locus is tightly linked to the starch synthase *IIIa* gene and negatively regulates expression of granule-bound starch synthetic genes. J Exp Bot 62:5217–5231

Lin Q, Huang B, Zhang M et al (2012) Functional interactions between starch synthase III and isoamylase-type starch-debranching enzyme in maize endosperm. Plant Physiol 158:679–692

Lin Q, Facon M, Putaux JL et al (2013) Function of isoamylase-type starch debranching enzymes ISA1 and ISA2 in the *Zea mays* leaf. New Phytol 200:1009–1021

Liu F, Ahmed Z, Lee EA et al (2012a) Allelic variants of the *amylose-extender* mutation of maize demonstrate phenotypic variation in starch structure resulting from modified protein-protein interactions. J Exp Bot 63:1167–1183

Liu F, Romanova N, Lee EA et al (2012b) Glucan affinity of starch synthase IIa determines binding of starch synthase I and starch-branching enzyme IIb to starch granules. Biochem J 448:373–387

Lloyd JR, Landschütze V, Kossman J (1999) Simultaneous antisense inhibition of two starch-synthase isoforms in potato tubers leads to accumulation of grossy modified amylopectin. Biochem J 338:515–521

Maddelein ML, Libessart N, Bellanger F et al (1994) Toward an understanding of the biogenesis of the starch granule. J Biol Chem 269:25150–25157

Mangelsdorf PC (1947) The inheritance of amylaceous sugary endosperm and its derivatives in maize. Genetics 32:448–458

Marshall J, Sidebottom C, Debet M et al (1996) Identification of the major starch synthase in the soluble fraction of potato tuber. Plant Cell 8:1121–1135

McMaugh SJ, Thistleton JL, Anschaw E et al (2014) Suppression of starch synthase I expression affects the granule morphology and granule size and fine structure of starch in wheat endosperm. J Exp Bot 65:2189–2201

Mizuno K, Kawasaki T, Shimada H et al (1993) Alteration of the structural properties of starch components by the lack of an isoform of starch branching enzyme in rice seeds. J Biol Chem 268:19084–19091

Mizuno K, Kobayashi E, Tachibana M et al (2001) Characterization of an isoform of rice starch branching enzyme, RBE4, in developing seeds. Plant Cell Physiol 42:349–357

Momma M, Fujimoto Z (2012) Interdomain disulfide bridge in the rice granule bound starch synthase I catalytic domain as elucidated by X-ray structural analysis. Biosci Biotechnol Biochem 76(8):1591–1595

Morell M, Blennow A, Kosar-Hashemi B (1997) Differential expression and properties of starch branching enzyme isoforms in developing wheat endosperm. Plant Physiol 113:201–208

Morell MK, Kosar-Hashemi B, Cmiel M et al (2003) Barley *sex6* mutants lack starch synthase IIa activity and contain a starch with novel properties. Plant J 34:173–185

Mouille G, Maddelein M-L, Libessart N et al (1996) Preamylopectin processing: a mandatory step for starch biosynthesis in plants. Plant Cell 8:1353–1366

Mu-Forster C, Huang R, Powers JR et al (1996) Physical association of starch biosynthetic enzymes with starch granules of maize endosperm. Plant Physiol 111:821–829

Murakami T, Kanai T, Takata H et al (2006) A novel branching enzyme of the GH-57 family in the hyperthermophilic archaeon Thermococcus kodakaraensis KODI. J Bacteriol 188:5915–5924

Murata T, Sugiyama T, Akazawa T (1965) Enzymic mechanism of starch synthesis in glutinous rice grains. Biochem Biophys Res Commun 18:371–376

Mutisya J, Sathish P, Sun C et al (2003) Starch branching enzymes in sorghum (*Sorghum bicolor*) and barley (*Hordeum vulgare*): Comparative analyses of enzyme structure and gene expression. J Plant Physiol 160:921–930

Myers AM, Morell MK, James MG et al (2000) Recent progress toward understanding biosynthesis of the amylopectin crystal. Plant Physiol 122:989–997

Nakamura Y (1996) Some properties of starch debranching enzymes and their possible role in amylopectin biosynthesis. Plant Sci 121:1–18

Nakamura Y (2002) Towards a better understanding of the metabolic system for amylopectin biosynthesis plants: Rice endosperm as a model tissue. Plant Cell Physiol 43:718–725

Nakamura Y (2014) Mutagenesis and transformation of starch biosynthesis of rice and the production of novel starches. In: Tomlekova N, Kozgar I, Wani R (eds) Mutagenesis: exploring novel genes and pathways. Wageningen, Wageningen Academic, pp 251–278

Nakamura Y, Yuki K, Park SY et al (1989) Carbohydrate metabolism in the developing endosperm of rice grains. Plant Cell Physiol 30:833–839

Nakamura Y, Takeichi T, Kawaguchi K et al (1992a) Purification of two forms of starch branching enzyme (Q-enzyme) from developing rice endosperm. Physiol Plant 84:329–335

Nakamura Y, Umemoto T, Takahata Y et al (1992b) Characteristics and roles of key enzymes associated with starch biosynthesis in rice endosperm. Gamma Field Symp 31:25–44
Nakamura Y, Umemoto T, Takahata Y et al (1996) Changes in structure of starch and enzyme activities affected by *sugary* mutations in developing rice endosperm. Possible role of starch debranching enzyme (R-enzyme) in amylopectin biosynthesis. Physiol Plant 97:491–498
Nakamura Y, Kubo A, Shimamune T et al (1997) Correlation between activities of starch debranching enzyme (R-enzyme or pullulanase) and α-glucan structure in endosperms of *sugary-1* mutants of rice. Plant J 12:143–153
Nakamura T, Vrinten P, Hayakawa K et al (1998) Characterization of a granule-bound starch synthase isoform found in the pericarp of wheat. Plant Physiol 118:451–459
Nakamura Y, Sakurai A, Inaba Y et al (2002) The fine structure of amylopectin in endosperm from Asian cultivated rice can be largely classified into two classes. Starch 54:117–131
Nakamura Y, Francisco PB Jr, Hosaka Y et al (2005a) Essential amino acids of starch synthase IIa differentiate amylopectin structure and starch quality between japonica and indica rice varieties. Plant Mol Biol 58:213–227
Nakamura Y, Takahashi J, Sakurai A et al (2005b) Some cyanobacteria synthesize semi-amylopectin type α-polyglucan instead of glycogen. Plant Cell Physiol 46:539–545
Nakamura Y, Fujita N, Utsumi Y et al (2009) Revealing the complex system of starch biosynthesis in higher plants using rice mutants and transformants. In: Shu Q (ed) Induced mutations in the genomics era. Food and Agriculture Organization of the United Nations, Rome, pp 165–167
Nakamura Y, Utsumi Y, Sawada T et al (2010) Characterization of the reactions of starch branching enzymes from rice endosperm. Plant Cell Physiol 51:776–794
Nakamura Y, Ono M, Utsumi Y et al (2012) Functional interaction between plastidial starch phosphorylase and starch branching enzymes from rice during the synthesis of branched maltodextrins. Plant Cell Physiol 53:869–878
Nakamura Y, Aihara S, Crofts N et al (2014) *In vitro* studies of enzymatic properties of starch synthases and interactions between starch synthase I and starch branching enzymes from rice. Plant Sci 224:1–8
Nelson OE, Rines HW (1962) The enzymatic deficiency in the waxy mutant of maize. Biochem Biophys Res Commun 9:297–300
Nishi A, Nakamura Y, Tanaka N et al (2001) Biochemical and genetic analysis of the effects of amylose-extender mutation in rice endosperm. Plant Physiol 127:459–472
Noguchi J, Chaen K, Vu NT et al (2011) Crystal structure of the branching enzyme I (BEI) from *Oryza sativa* L with implications for catalysis and substrate binding. Glycobiology 21:1108–1116
Nozaki K, Hamada S, Nakamori T et al (2001) Major isoforms of starch branching enzymes in premature seeds of kidney bean (*Phaseolus vulgaris* L.). Biosci Biotechnol Biochem 65:1141–1148
Ohdan T, Francisco PB Jr, Hosaka Y et al (2005) Expression profiling of genes involved in starch synthesis in sink and source organs of rice. J Exp Bot 56:3229–3244
Ohdan T, Sawada T, Nakamura Y (2011) Effects of temperature on starch branching enzyme properties of rice. J Appl Glycosci 58:19–26
Ozbun JL, Hawker JS, Preiss J (1971a) Multiple forms of α-1,4 glucan synthetase from spinach leaves. Biochem Biophys Res Commun 43:631–636
Ozbun JL, Hawker JS, Preiss J (1971b) Adenosine diphosphoglucose-starch glucosyl transferases from developing kernels of waxy maize. Plant Physiol 48:765–769
Ozbun JL, Hawker JS, Preiss J (1972) Soluble adenosine diphosphate glucose-arufa-1,4-glucan arufa-4-glucosyltransferases from spinach leaves. Biochem J 126:953–963
Palomo M, Kralj S, van der Maarel MJEC et al (2009) The unique branching pattern of Deinococcus glycogen branching enzymes are determined by their N-terminal domains. Appl Environ Microbiol 75:1355–1362
Pan D, Nelson NE (1984) A debranching enzyme deficiency in endosperms of *sugary-1* mutants of maize. Plant Physiol 74:324–328

Patron NJ, Keeling PJ (2005) Common evolutionary origin of starch biosynthetic enzymes in green and red algae. J Phycol 41:1131–1141

Peng C, Wang Y, Liu F et al (2014) *FLOURY ENDOSPERM6* encodes a CBM48 domain-containing protein involved in compound granule formation and starch synthesis in rice endosperm. Plant J 77:917–930

Pérez S, Bertoft E (2010) The molecular structures of starch components and their contribution to the architecture of starch granules: a comprehensive review. Starch 62:389–420

Pfister B, Lu K, Eicke S, et al (2014) Genetic evidence that chain length and branch point distributions are linked determinants of starch granule formation in Arabidopsis. Plant Physiol 165:1457–1474

Pollock C, Preiss J (1980) The citrate-stimulated starch synthase of starchy maize kernels: Purification and properties. Arch Biochem Biophys 204:578–588

Rahman S, Kosar-Hashemi B, Samuel MS et al (1995) The major proteins of wheat starch granules. Aust J Plant Physiol 22:793–803

Rahman S, Regina A, Li Z et al (2001) Comparison of starch-branching enzyme genes reveals evolutionary relationships among isoforms. Characterization of a gene for starch-branching enzyme IIa from the wheat D genome donor *Aegilops tauschii*. Plant Physiol 125:1314–1324

Rahman S, Nakamura Y, Li Z et al (2003) The *sugary*-type isoamylase gene from rice and *Aegilops tauschii*: characterization and comparison with maize and *Arabidopsis*. Genome 46:496–506

Ral JP, Colleoni C, Wattebled F et al (2006) Circadian clock regulation of starch metabolism establishes GBSSI as a major contributor to amylopectin synthesis in *Chlamydomonas reinhardtii*. Plant Physiol 142:305–317

Regina A, Kosar-Hashemi B, Li Z et al (2005) Starch branching enzyme IIb in wheat is expressed at low levels in the endosperm compared to other cereals and encoded at a non-syntenic locus. Planta 222:899–909

Regina A, Bird A, Topping D et al (2006) High-amylose wheat generated by RNA interference improves indices of large-bowel health in rats. Proc Natl Acad Sci U S A 103:3546–3551

Regina A, Kosar-Hashemi B, Ling S et al (2010) Control of starch branching in barley defined through differential RNAi suppression of starch branching enzyme IIa and IIb. J Exp Bot 61:1469–1482

Roldán L, Wattebled F, Lucas MM et al (2007) The phenotype of soluble starch synthase IV defective mutant of *Arabidopsis thaliana* suggests a novel function of elongation enzymes in the control of starch granule formation. Plant J 49:492–504

Rundle RE, Daasch L, French D (1944) The structure of the "B" modification of starch from film and fiber diffraction diagrams. J Am Chem Soc 66:130–134

Rydberg U, Andersson L, Andersson R et al (2001) Comparison of starch branching enzyme I and II from potato. Eur J Biochem 268:6140–6145

Satoh H, Nishi A, Yamashita K et al (2003) Starch-b ranching enzyme I-deficient mutation specifically affects the structure and properties of starch in rice endosperm. Plant Physiol 133:1111–1121

Satoh H, Shibahara K, Tokunaga T et al (2008) Mutation of the plastidial α-glucan phosphorylase gene in rice affects the synthesis of branched maltodextrins. Plant Cell 20:1833–1849

Sawada T, Francisco PB Jr, Aihara S et al (2009) *Chlorella* starch branching enzyme II (BEII) can complement the function of BEIIb in rice endosperm. Plant Cell Physiol 50:1062–1074

Sawada T, Nakagami T, Utsumi Y et al (2013) Characterization of starch and glycogen branching enzymes from various sources. J Appl Glycosci 60:69–78

Sawada T, Nakamura Y, Ohdan T et al (2014) Diversity of reaction characteristics of glucan branching enzymes and the fine structure of α-glucan from various sources. Arch Biochem Biophys 562:9–21

Schwarte S, Brust H, Steup M et al (2013) Intraspecific sequence variation and differential expression in starch synthase genes of Arabidopsis thaliana. BMC Res Notes 6:84

Senoura T, Isono N, Yoshikawa M et al (2007) Characterization of starch synthase I and II expressed in early developing seeds of kidney bean (*Phaseolus vulgaris* L.). Biosci Biotechnol Biochem 68:1949–1960

Sestili F, Janni M, Doherty A et al (2010) Increasing the amylose content of durum wheat through silencing of the *SBEIIa* genes. BMC Plant Biol 10:144

Shannon JC, Garwood DL (1984) Genetics and physiology of starch development. In: Whistler RL, BeMiller JN, Paschall EF (eds) Starch: chemistry and technology, 2nd edn. Academic, New York, pp 25–86

Shannon JC, Pein FM, Cao HP et al (1998) Brittle-1, an adenylate translocator, facilitates transfer of extraplastidial synthesized ADP-glucose into amyloplasts of maize endosperms. Plant Physiol 117:1235–1252

Shannon JC, Garwood DL, Boyer CD (2007) Genetics and physiology of starch development. In: BeMiller JN, Whistler RL (eds) Starch: chemistry and technology, 3rd edn. Academic, New York, pp 23–82

She K, Kusano H, Koizumi K et al (2010) A novel factor *FLOURY ENDOSPERM2* is involved in regulation of rice grain size and starch quality. Plant Cell 22:3280–3294

Shimonaga T, Fujiwara S, Kaneko M et al (2006) Variation in storage α-polyglucans of red algae: Amylose and semi-amylopectin-types in *Porphyridium* and glycogen-type in *Cyanidium*. Mar Biotechnol 9:192–202

Shimonaga T, Konishi M, Oyama Y et al (2008) Variation in storage α-glucans of the Porphyridiales (Rhodophyta). Plant Cell Physiol 49:103–116

Sim L, Beeren SR, Findinier J, et al (2014) Crystal structure of the Chlamydomonas starch debranching enzyme isoamylase ISA1 reveals insights into the mechanism of branch trimming and complex assembly. J Biol Chem 289:22991–23003

Smith AM (1988) Major differences in isoforms of starch-branching enzyme between developing embryos of round- and wrinkled-seeded peas (*Pisum sativum* L.). Planta 175:270–279

Smith SM, Fulton DC, Chia T et al (2004) Diurnal changes in the transcriptome encoding enzymes of starch metabolism provide evidence for both transcriptional and posttranscriptional regulation of starch metabolism in Arabidopsis leaves. Plant Physiol 136:2687–2699

Stam MR, Danchin EGJ, Ranchured C et al (2006) Dividing the large glycoside hydrolase family 13 into subfamilies: towards improved functional annotations of amylase-related proteins. Protein Eng Des Sel 19:555–562

Streb S, Zeeman SC (2014) Replacement of the endogenous starch debranching enzymes ISA1 and ISA2 of Arabidopsis with the rice orthologs reveals a degree of functional conservation during starch synthesis. PLoS One 9:e92174

Streb S, Delatte T, Umhang M et al (2008) Starch granule biosynthesis in Arabidopsis is abolished by removal of all debranching enzymes but restored by the subsequent removal of an endoamylase. Plant Cell 20:3448–3466

Sullivan TD (1995) The maize *brittle1* gene encodes amyloplast membrane polypeptides. Planta 196:477–484

Sun C, Sathish P, Ahlandsberg S et al (1998) The two genes encoding starch-branching enzymes IIa and IIb are differentially expressed in barley. Plant Physiol 118:37–49

Szydlowsky N, Ragel P, Raynaud S et al (2009) Starch granule initiation in *Arabidopsis* requires the presence of either class IV or class II starch synthases. Plant Cell 21:2443–2457

Szydlowsky N, Ragel P, Hennen-Bierwagen TA (2011) Integrated functions among multiple starch synthases determine both amylopectin chain length and branch linkage location in *Arabidopsis* leaf starch. J Exp Bot 62:4547–4559

Takashima Y, Senoura T, Yoshizaki T et al (2007) Differential chain-length specificities of two isoamylase-type starch debranching enzymes from developing seeds of kidney bean. Biosci Biotechnol Biochem 71:2308–2312

Takeda Y, Hizukuri S, Juliano BO (1987a) Structure of rice amylopectins with low and high affinities for iodine. Carbohydr Res 168:79–88

Takeda Y, Hizukuri S, Takeda C et al (1987b) Structures of branched molecules of amyloses of various botanical origins, and molar fractions of branched and unbranched molecules. Carbohydr Res 165:139–145

Takeda Y, Guan H, Preiss J (1993) Branching of amylose by the branching isoenzymes of maize endosperm. Carbohydr Res 240:253–263

Takeda Y, Preiss J (1993) Structures of B90 (sugary) and W64A (normal) maize starches. Carbohydr Res 240:265–275

Tanaka Y, Akazawa T (1971) Enzymic mechanism of starch synthesis in ripening rice grains VI. Isozymes of starch synthase. Plant Cell Physiol 12:493–505

Tanaka N, Fujita N, Nishi A et al (2004) The structure of starch can be manipulated by changing expression levels of starch branching enzyme IIb in rice endosperm. Plant Biotechnol J 2:507–516

Tetlow I (2012) Branching enzymes and their role in determining structural and functional properties of polyglucan. In: Tetlow I (ed) Starch: origins, structure and metabolism, vol 5, Essential reviews in experimental biology. The Society for Experimental Biology, London, pp 141–177

Tetlow IJ, Wait R, Lu Z et al (2004) Protein phosphorylation in amyloplasts regulates starch branching enzyme activity and protein-protein interactions. Plant Cell 16:694–708

Tetlow IJ, Beisel KG, Cameron S et al (2008) Analysis of protein complexes in amyloplasts reveals functional interactions among starch biosynthetic enzymes. Plant Physiol 146:1878–1891

Thompson DB (2000) On the non-random nature of amylopectin branching. Carbohydr Polym 43:223–239

Tomlinson KL, Lloyd JR, Smith AM (1997) Importance of isoforms of starch-branching enzyme in determining the structure of starch in pea leaves. Plant J 11:31–43

Tomlinson KL, Lloyd JR, Smith AM (1998) Major differences in isoform composition of starch synthase between leaves and embryos of pea (*Pisum sativum* L.). Planta 204:86–92

Toyosawa Y, Kawagoe Y, Matsushima R, et al. (2015) Deficiency of starch synthase IIIa and IVb leads to dramatic changes in starch granule morphology in rice endosperm (submitted)

Umemoto T, Nakamura Y, Satoh H et al (1999) Differences of amylopectin structure between two rice varieties in relation to the effects of temperature during grain-filling. Starch 51:58–62

Umemoto T, Yano M, Satoh H et al (2002) Mapping of a gene responsible for the difference in amylopectin structure between *japonica*-type and *indica*-type rice varieties. Theor Appl Genet 104:1–8

Usui T, Ogata M, Murata T et al (2009) Sequential analysis of α-glucooligosaccharides with α-(1–4) and α-(1–6) linkages by negative ion Q-TOF MS/MS spectrometry. J Carbohydr Chem 28:421–430

Utsumi Y, Nakamura Y (2006) Structural and enzymatic characterization of the isoamylase1 homo-oligomer and the isoamylase1-isoamylase2 hetero-oligomer from rice endosperm. Planta 225:75–87

Utsumi Y, Utsumi C, Sawada T et al (2011) Functional diversity of isoamylase oligomers: The ISA1 homo-oligomer is essential for amylopectin biosynthesis in rice endosperm. Plant Physiol 156:61–77

Vester-Christensen MB, Hachem MA, Svensson B et al (2010) Crystal structure of an essential enzyme in seed starch degradation: barley limit dextrinase in complex with cyclodextrins. J Mol Biol 403:739–750

Vikso-Nielsen A, Blennow A (1998) Isolation of starch branching enzyme I from potato using γ-cyclodextrin affinity chromatography. J Chromatogr 800:382–385

Visser RGF, Somhorst I, Kuipers GJ et al (1991) Inhibition of the expression of the gene for granule-bound starch synthase in potato by antisense constructs. Mol Gen Genet 225:289–296

Wang J, Xu H, Zhu Y et al (2013) OsbZIP58, a basic leucine zipper transcription factor, regulates starch biosynthesis in rice endosperm. J Exp Bot 64:3453–3466

Wattebled F, Ral JP, Dauvillée D et al (2003) STA11, a *Chlamydomonas reinhardtii* locus required for normal starch granule biogenesis, encodes disproportionating enzyme. Further evidence for a function of α-1,4 glucanotransferases during starch granule biosynthesis in green algae. Plant Physiol 132:137–145

Wattebled F, Dong Y, Dumez S et al (2005) Mutants of Arabidopsis lacking a chloroplastic isoamylase accumulates phytoglycogen and an abnormal form of amylopectin. Plant Physiol 138:184–195

Wattebled F, Planchot V, Dong Y et al (2008) Further evidence for the mandatory nature of polysaccharide debranching for the aggregation of semicrystalline starch and for overlapping functions of debranching enzymes in Arabidopsis leaves. Plant Physiol 148:1309–1323

Weber APM, Linka N (2011) Connecting the plastids: Transporters of the plastid envelope and their role in linking plastidial with cytosolic metabolism. Annu Rev Plant Biol 62:53–77

Xia H, Yandeau-Nelson M, Thompson DB et al (2011) Deficiency of maize starch-branching enzyme I results in altered starch fine structure, decreased digestibility and reduced coleoptiles growth during germination. BMC Plant Biol 11:95

Yamamori M, Fujita S, Hayakawa K et al (2000) Genetic elimination of a starch granule protein, SGP-1, of wheat generates an altered starch with apparent high amylose. Theor Appl Genet 101:21–29

Yamanouchi H, Nakamura Y (1992) Organ specificity of isoforms of starch branching enzyme (Q-enzyme) in rice. Plant Cell Physiol 33:985–991

Yao Y, Thompson DB, Guiltinan MJ (2004) Maize starch-branching enzyme isoforms and amylopectin structure. In the absence of starch-branching enzyme IIb, the further absence of starch-branching enzyme Ia leads to increased branching. Plant Physiol 136:3515–3523

Yun M, Umemoto T, Kawagoe Y (2011) Rice debranching enzyme isoamylase3 facilitates starch metabolism and affects plastid morphogenesis. Plant Cell Physiol 52:1068–1082

Zeeman SC, Umemoto T, Lue W et al (1998) A mutant of *Arabidopsis* lacking a chloroplastic isoamylase accumulates both starch and phytoglycogen. Plant Cell 10:1699–1711

Zeeman SC, Kossman J, Smith AM (2010) Starch: its metabolism, evolution, and biotechnological modification in plants. Annu Rev Plant Biol 61:209–234

Zhang X, Colleoni C, Ralushana V et al (2004) Molecular characterization demonstrates that the *Zea mays* gene *sugary2* codes the starch synthase isoform SSIIa. Plant Mol Biol 54:865–879

Zhang X, Myers AM, James MG (2005) Mutations affecting starch synthase III in *Arabidopsis* alter leaf starch structure and increase the rate of starch synthesis. Plant Physiol 138:663–674

Zhang X, Szydlowski N, Delvallé D et al (2008) Overlapping functions of the starch synthase SSII and SSIII in amylopectin biosynthesis in *Arabidopsis*. BMC Plant Biol 8:96–113

Chapter 6
Starch Biosynthesis in Leaves and Its Regulation

Christophe D'Hulst, Fabrice Wattebled, and Nicolas Szydlowski

Abstract Plants assimilate carbon during photosynthesis using light energy to reduce atmospheric CO_2 and to produce sugars and chemical energy (ATP). Sugars are partly incorporated directly into starch granules in leaf chloroplasts for short-term storage or are exported to non-photosynthetic organs for long-term storage. Indeed, starch accumulation in photosynthetic tissues is transient since it undergoes recurrent cycles of synthesis and degradation following day/night oscillation. Transient starch is synthesized during the day while photosynthesis is active and is degraded at night to provide carbon and energy to the plant when photosynthesis is inactive. Conversely, storage starch accumulates over long periods in storage organs such as seeds or tubers where it is degraded to sustain germination before photosynthesis becomes effective. Transient and storage starch syntheses occur in plastid stroma and involve dedicated enzymatic activities typically supported by several genetically independent isoforms. Although highly similar, both processes hold specific features regarding synthesis and regulation. In this chapter, we describe the mechanism of starch synthesis in photosynthetic tissues (mostly leaves) and its regulation. Several aspects are specifically highlighted here such as: (1) the function of starch synthases for the initiation of starch synthesis and the elongation of the amylopectin- and amylose-forming glucans, (2) the implication of branching enzymes and debranching enzymes for the formation of branch points and the control of their distribution within the polysaccharides, and (3) the regulation of the pathway in leaves especially by the circadian clock, the redox state of the cell and the influence of physiological factors, and the formation of protein-protein complexes.

Keywords Starch • Polysaccharide • Glucan • Leaf • Photosynthesis • Circadian clock • Redox regulation

C. D'Hulst (✉) • F. Wattebled
Unité de Glycobiologie Structurale et Fonctionnelle, UMR8576 CNRS, Université Lille 1, 59655 Villeneuve d'Ascq cedex, France
e-mail: christophe.dhulst@univ-lille1.fr

N. Szydlowski
Miniaturisation pour l'analyse, la synthèse et la protéomique, USR3290 CNRS, Université Lille 1, 59655 Villeneuve d'Ascq cedex, France

Y. Nakamura (ed.), *Starch*, DOI 10.1007/978-4-431-55495-0_6

6.1 Initiation of Starch Synthesis in Leaves: The Central Role of Starch Synthases

Starch biosynthesis occurs in the stroma of the chloroplast in plant photosynthetic tissues. It involves several enzymes all encoded by the nuclear genome of the plant and subsequently transferred to the plastid after translation. The first committed step of starch synthesis in plants is the synthesis of the unique precursor: ADP-glucose. This glucosyl-nucleotide is synthesized by the condensation of ATP and glucose-1-phosphate and the release of inorganic pyrophosphate (PPi). This reaction is catalyzed by the ADP-glucose pyrophosphorylase (AGPase), a heterotetrameric enzyme of the stroma. The synthesis of ADP-glucose is the rate-limiting step of starch synthesis, AGPase activity being tightly regulated at different levels (see Sect. 6.4 in this chapter for more details). Once synthesized, this nucleotide sugar will provide the building blocks (i.e., the glucose residues) for the synthesis of amylose and amylopectin molecules. The biosynthetic enzymes responsible for the elaboration of these polymers have been extensively studied, and their proposed functions in leaves will be described in Sects. 6.2 and 6.3 of this chapter. In contrast, mechanisms underlying the initial steps of the formation of a new starch granule remain unclear. However, this aspect of the metabolism is of major importance because it will determine the leaf ability to store photosynthetic products. Two distinct processes may operate at these early steps of the granule biogenesis: (1) de novo synthesis of one or several so-called primers, consisting of $\alpha(1 \rightarrow 4)$ glucans long enough to be utilized by starch synthases (the elongating enzymes responsible for the synthesis of $\alpha(1 \rightarrow 4)$ bounds of starch polymers), and (2) assembly of the amylopectin and/or amylose molecules and/or their primers (in potential association with other components such as proteins) to initiate the formation of the quaternary structure of starch (D'Hulst and Mérida 2010) (see Chap. 9 for in-depth description of these aspects).

Contrary to starch, glycogen (the storage glucan in animal, fungi, and bacteria) displays a homogenous structure, which does not require specific organization of the polymers. Nevertheless, priming is also necessary to initiate the synthesis of a new particle. This process is either performed by glycogenins in animals and fungi (Blumenfeld et al. 1983; Lomako et al. 2004) or by glycogen synthases in bacteria (Ugalde et al. 2003). In both cases, the enzyme catalyzes glucose transfer on a tyrosine residue within its own sequence (Lomako et al. 1988; Ugalde et al. 2003). This self-glucosylation step produces a primer which is subsequently elongated by glycogen synthases regardless of the nature of the organism. Although eight sequences were identified in *Arabidopsis* by homology with the mammalian enzyme (Chatterjee et al. 2005), only one of these loci encodes a protein containing a predicted chloroplast transit peptide. However, the product of this gene was later shown to localize to the Golgi apparatus, where it is involved in xylan metabolism (Mortimer et al. 2010; Rennie et al. 2012).

On the other hand, soluble starch synthases (SSs) have been proposed to be responsible for glucan priming in plant leaves (Roldán et al. 2007; Szydlowski

et al. 2009). Four SS isoforms, SS1, SS2, SS3, and SS4, are found in plant genomes. Chloroplasts of *ss4 Arabidopsis* mutants accumulate one (or two in some cases) starch granule when 5–7 granules per chloroplast are observed in wild-type plants (Roldán et al. 2007). This decrease in the number of initiation events induces the overaccumulation of ADP-glucose, which indirectly leads to photooxidative stress and altered plant growth (Ragel et al. 2013). This phenotype is unique and specifically related to the inactivation of the *SS4* locus among *SS* genes, defining the corresponding enzyme as a major contributor for starch initiation (Szydlowski et al. 2009; D'Hulst and Mérida 2010). Moreover, most leaf chloroplasts of *ss3 ss4* double mutant plants do not accumulate starch (Szydlowski et al. 2009). This observation suggests a dominant role for SS3 in the initiation of the residual granule observed in *ss4* plastids. However, the presence of residual starch in a few chloroplasts of *ss3 ss4* mutant plants (Crumpton-Taylor et al. 2013) indicates that SS1 and SS2 isoforms may also participate in the priming reaction although at less efficiency. Indeed, when the latter isoforms are inactivated in an *ss4* mutant background, some chloroplasts are also empty of starch (Szydlowski et al. 2009). Self-glucosylation experiments were performed in vitro with SS3 or SS4 recombinant proteins expressed in *E. coli* (Szydlowski et al. 2009). For both enzymes, no activity could be detected in the experimental conditions used. However, the self-glucosylation ability of starch synthases *in planta* or with the use of native proteins remains to be investigated.

Starch initiation begins during the early stages of leaf development (Crumpton-Taylor et al. 2012). Furthermore, chloroplasts of immature wild-type *Arabidopsis* leaves contain more starch granules compared to mature leaves (Crumpton-Taylor et al. 2012). However, this is not the case in *ss4* mutant plants in which the synthesis of the residual granule occurs only in mature leaves (Crumpton-Taylor et al. 2013). This suggests that two temporally distinct mechanisms may operate for starch initiation. The first, involving SS4, takes place at the early developmental stages when leaves start to expand. The second only occurs in mature leaves and involves predominantly the SS3 isoform. The question arises on whether the latter mechanism takes place in a wild-type context (i.e., when SS4 is also present) or only occurs in the *ss4* mutant background, and remains to be investigated. Indeed, although most initiation events happen during early leaf development in wild-type plants, de novo synthesis of starch at leaf maturity was also reported (Crumpton-Taylor et al. 2012). Similarly, it is difficult to predict whether SS1 and SS2 are partially redundant with SS3 for this function or if their absence would destabilize complexes comprising SS3 and consequently alter its activity (D'Hulst and Mérida 2010). Indeed, these three isoforms possess functional redundancies regarding their glucan-elongating activities in *Arabidopsis* leaves (Zhang et al. 2008; Szydlowski et al. 2011). On the other hand, although evidence is missing for their existence in leaf chloroplasts, multiprotein complexes involving the three isoforms were identified in amyloplasts of the wheat and maize endosperms (Hennen-Bierwagen et al. 2008; Tetlow et al. 2008). Systematic analysis of starch accumulation, as well as of activities and expression levels of the starch biosynthetic enzymes during leaf development, in the wild-type, and the mutant combinations including mutations at the four *SS* loci, will help to address these questions.

Many assumptions can be made regarding the initial process that leads to the three-dimensional architecture of starch. Structural information on the nature and organization of the molecules composing the hilum (the nucleus of a granule) is missing. This is due to the physicochemical properties of starch polysaccharides and limitation of the available methods. However, it is tempting to speculate that mature granule morphology is determined by the growth direction of starch polymers during granule expansion and thus derives from their orientation at the hilum. Consequently, modifications of mature granule shape would reflect alteration of the hilum composition and/or structure. *ss4* mutant granules do not display the characteristic flattened lenticular shape of *Arabidopsis* wild-type starch (Roldán et al. 2007). They appear as swollen spherical particles, resembling to most of studied storage starches from different botanical origins (Jane et al. 1994). In this mutant, the lack of SS4 may provoke hilum destabilization, leading to radial expansion of the polymers composing residual starch. Indeed, electron micrographs of *ss4* mutant starch reveal a less electron-dense zone of several tens of nm of diameter in the hilum region that is not observed in wild-type starch (Roldán et al. 2007). However, no evidence yet allows discriminating between direct or indirect involvement of SS4 in shaping this area of the granule. The variable N-terminal region of SS4 sequence contains several predicted long coiled-coil domains known to favor physical interaction between proteins (Rose and Meier 2004). Indeed, interaction of SS4 with fibrillin 1a and 1b (FBN1s) was recently reported (Gámez-Arjona et al. 2014). These proteins are located to plastoglobules (plastoglobules are proteolipidic structures associated to thylakoid membranes), suggesting that starch initiation would occur at these specific regions of the chloroplast. One could speculate that SS4, in interaction with FBN1s and other proteins and/or other classes of molecules (such as lipids of the plastoglobules), forms a nucleation center, leading to de novo initiation of a starch granule. Nevertheless, native SS4 has never yet been identified in association with starch. Moreover, fluorescence signal of AtSS4-GFP fusion proteins is only detectable in specific areas at the periphery of starch granules when expressed in chloroplasts of *Arabidopsis* leaf cells (Szydlowski et al. 2009). As mentioned above, residual starch of *ss4* mutant plants is predominantly initiated by the SS3 isoform. It is not known if this population of granules is present in wild-type *Arabidopsis* plants or if SS4 directly participates to its elaboration in a wild-type context. Further work is thus required to assess the potential implication of SS4 in the nucleation of a starch granule.

It is intriguing that SS4 is absolutely required for determining the correct number of starch granules per chloroplast. As mentioned above, plastids of mature *ss4* mutant leaves generally contain one (sometimes two) granule at the end of the light period (Roldán et al. 2007), whereas wild-type plants accumulate 5.5 ± 0.3 granules per chloroplast on average (Crumpton-Taylor et al. 2012). Individual chloroplast volume in wild-type *Arabidopsis* leaves is widely heterogeneous (Crumpton-Taylor et al. 2012). However, the number of starch granules per plastid is strongly correlated with the stromal volume of the latter (Crumpton-Taylor et al. 2012). These data indicate a tight relationship between the unit volume of stroma and the number of initiation events. Such relationship might thus be disturbed in

Arabidopsis ss4 mutant leaves since no modification of average plastid volume has been reported for the corresponding transgenic plant lines. With regard to the lack of knowledge about granule nucleation and hilum composition, it is difficult to predict the molecular basis of SS4 involvement in modulating this process. A recent study assessed the effect of an increased plastid volume (i.e., by genetically manipulating plastid division) on starch accumulation in an *ss4* mutant background (Crumpton-Taylor et al. 2013). Mutations at *ARC* loci (ARC proteins are components of the plastid division machinery) lead to decreased plastid number per mesophyll cell and strongly increased chloroplast volume (Crumpton-Taylor et al. 2013). Starch initiation was only restored in few chloroplasts of immature leaves of *arc ss4* double mutant plants (Crumpton-Taylor et al. 2013), confirming that the link between stromal volume and occurrence of granule initiation is disturbed in the absence of SS4. On the other hand, no evidence relating SS4-driven control of starch granule number to plastid division has been obtained. Addressing the latter question, as well as deciphering the underlying mechanisms, represents the next challenge in understanding starch initiation in plant leaves.

6.2 The Synthesis of Amylopectin Is Complex and Requires at Least Elongating, Branching, and Debranching Enzymes

Amylopectin is composed of glucose residues linked together by α(1 → 4) and α(1 → 6) O-glycosidic linkages (see Chap. 1 for exhaustive description of the fine structure of amylopectin). Although amylopectins from different botanical and/or organ origins share common features (notably the universal 9–10 nm periodicity of crystalline/amorphous lamellae alternation) (Jenkins et al. 1993), the crystallinity of leaf starches studied so far differs from that of other sources such as cereal or leguminous storage organs. Amylopectin double helices interact with water molecules within starch crystals, and their organization is more relaxed in the former (displaying the B allomorph) compared to the latter (displaying the A allomorph or a mix between A and B allomorphs, respectively) (Imberty et al. 1988; Buléon et al. 1998). These differences most likely account for glucan chain length distribution (Hizukuri 1985) and repartition of α-1,6 linkages within amylopectin (Jane et al. 1997; Gérard et al. 2000). It is widely accepted that determination of these features requires a core set of enzymes comprising at least α(1 → 4)-glucan α-4-glucosyltransferase (starch synthases, SSs), α(1 → 4)-glucan:α(1 → 4)-glucan-6-glucanotransferase (starch branching enzymes, BEs), α-dextrin endo-α(1 → 6)-glucosidase, and α(1 → 6)-glucanohydrolase (starch debranching enzymes, DBEs) activities. On the other hand, α(1 → 4)-glucan glucanohydrolase (α-amylase) and α(1 → 4)-glucan maltohydrolase (β-amylase) were proposed to also participate in amylopectin synthesis in plant leaves (Streb et al. 2008; Wu et al. 2014) as well as disproportionating enzymes (4-α-glucanotransferase) (Colleoni et al. 1999a, b)

and plastidial starch phosphorylase (Dauvillée et al. 2006). Understanding why amylopectin is differently shaped with regard to its organ/botanical origin relies on the determination of functions, specificities, redundancies, interactions, and regulation of these enzymes in the different systems. In addition to studies of leaf-starch metabolism in different crops of interest, the use of the model plant *Arabidopsis thaliana*, as well as of the associated biomolecular tools, allowed elucidating several of these aspects in leaves. In particular, recent research had benefited from reverse genetics and T-DNA insertion mutant collections, which have permitted rapid investigation of a gene function. Importantly, this approach allowed combining mutations at numerous loci of interest to assess redundancies and/or interactions between isoforms. In the next paragraphs we will focus on the function of SS, BE, and DBE in the synthesis of amylopectin although other enzymes may be also involved in that process.

6.2.1 Starch Synthases Involved in Amylopectin Synthesis

Similar to what is observed for glycogen metabolism, elongation of starch glucans requires $\alpha(1 \rightarrow 4)$-glucan α-4-glucosyltransferase activities. In plants, the corresponding enzymes are called starch synthases and transfer the glucose residue of ADP-glucose to the nonreducing end of an elongating glucan to build the $\alpha(1 \rightarrow 4)$ bonds. Plant genomes contain six sequences phylogenetically related to glycogen synthases, namely, *SS1*, *SS2*, *SS3*, *SS4*, *SS5*, and *GBSS1* (Deschamps et al. 2008). The granule-bound starch synthase, GBSS1, is only active when physically associated with starch (Rongine De Fekete et al. 1960). Moreover, this enzyme is responsible for amylose biosynthesis (Nelson and Rines 1962) and will be described in a dedicated section of this chapter. As stated above, SS4 is involved in starch initiation and the control of granule number per plastid (Roldán et al. 2007). However, no impact of the *ss4* mutation on amylopectin structure in plant leaves has been reported. Furthermore, there is no evidence for the involvement of SS5 in any aspect of starch metabolism. Thus, to our knowledge, only SS1, SS2, and SS3 isoforms contribute to the determination of amylopectin glucan chain length and will be highlighted in this section.

The three isoforms share a conserved C-terminal catalytic domain of about 450 amino acid residues in length that is similar to glycogen synthase sequences. Glycogen and starch synthases form part of the GT-5 (retaining glucosyl transferase) family of the CAZy (carbohydrate-active enzyme) classification (Cantarel et al. 2009) and contain two strictly conserved motifs of five amino acid residues in length. These motifs, K-X-G-G-L and X-X-G-G-L, are located to the N-terminal and C-terminal extremities of the catalytic domain, respectively (Cao et al. 1999). The former is responsible for sugar-nucleotide binding as well as being involved in the catalytic mechanism (Furukawa et al. 1990, 1993; Buschiazzo et al. 2004). On the other hand, SS3 protein sequence differs from those of SS1 and SS2, as illustrated by a longer N-terminal variable region upstream from the catalytic

domain. SS3 contains three starch-binding domains (SBDs) which favors physical interaction with starch polymers and thus contributes to its activity (Palopoli et al. 2006; Valdez et al. 2008).

SS1 isoform seems to have only little or no impact on amylopectin synthesis in storage organs of potato and barley (Kossmann et al. 1999). Indeed, no major modification of amylopectin structure was reported in the corresponding RNAi lines or mutant, respectively (Tyynelä and Schulman 1993; Kossmann et al. 1999). In potato, this may be related to very low expression levels of the corresponding gene in wild-type tubers (Kossmann et al. 1999). However, *SS1* is highly expressed in leaves of this species (Kossmann et al. 1999) but its function in this organ has not been studied so far. Similarly, *SS1* expression levels are much higher in rice leaves when compared to seeds (Hirose and Terao 2004). Nevertheless, contrary to what is observed in potato tuber, amylopectin chain length distribution is altered in the rice endosperm of the corresponding mutant (Fujita et al. 2006). *ss1 Arabidopsis* mutant plants display a comparable phenotype (Delvalle et al. 2005). Leaves of the latter accumulate starch with major structural modifications, comprising a decrease of the amylopectin/amylose ratio and alteration of the polymodal chain length distribution of amylopectin. Relative proportion of the shortest chains (DP 8 to 12) is substantially reduced in mutant amylopectin compared to the wild type (Delvalle et al. 2005). This phenotype is accompanied by an increase in the proportion of chains with a DP comprised between 12 and 23 glucose residues. Thus, this enzyme was proposed to be the determinant activity for the synthesis of the smallest chains of amylopectin molecules (Delvalle et al. 2005). Such a function *in planta* corroborates data from in vitro study of the recombinant enzyme from maize expressed in *E. coli* (Commuri and Keeling 2001). Moreover, chain length distribution analysis after β-amylolysis showed that these small glucans are the outer chains of the molecule (Delvalle et al. 2005). On the other hand, these structural modifications alter neither the starch crystallinity nor allomorph configurations (Delvalle et al. 2005).

Genomes of some plant species contain several isoforms of SS2 while others contain only a single gene encoding this enzyme. In particular, maize contains two isoforms, namely, SS2a and SS2b (Harn et al. 1998), and three isoforms are found in the rice genome, SS2-1, SS2-2, and SS2-3 (Hirose and Terao 2004; Jiang et al. 2004). Like the SS1 from potato and rice, the latter isoforms are differentially expressed in leaves and storage organs (Harn et al. 1998; Jiang et al. 2004). Indeed, maize *SS2b* or rice *SS2-2* are expressed in leaves, while maize *SS2a* or rice *SS2-3* are expressed in the endosperm (Harn et al. 1998; Jiang et al. 2004). On the other hand, rice *SS2-1* is expressed in both types of organs during the whole life cycle, whereas other isoforms are expressed at different stages of development (Jiang et al. 2004). These expression profiles may account for different functions of each isoform in starch synthesis in these species. However, all *ss2* mutants characterized so far display the same phenotype regardless of the organ considered. Modification of starch composition and structure was assessed in storage organs of pea (Craig et al. 1998), barley (Morell et al. 2003), and maize (Zhang et al. 2004), as well as in *Arabidopsis* leaves (Zhang et al. 2008). In each case the phenotype was similar

in decreasing amylopectin/amylose ratio and, in turn, starch quantity, decreasing glucans of DP between 12 and 30 while increasing the proportion of short glucans, and alteration of starch crystallinity (Craig et al. 1998; Morell et al. 2003; Zhang et al. 2004; Szydlowski et al. 2011). Thus, SS2 seems to be responsible for the synthesis of glucans of $12 < DP < 30$ regardless of the species/organ considered so far.

Two isoforms of SS3 are found in the rice genome, namely, SS3-1 and SS3-2 (Dian et al. 2005). *SS3-1* is expressed in both leaves and the endosperm at early stages of development, while the other isoform is only expressed in the endosperm (Dian et al. 2005). The function of SS3 in storage starch biosynthesis was investigated in maize (Gao et al. 1998) and potato (Abel et al. 1996) by mutagenesis and RNA interference, respectively. In addition, the phenotype of an *ss3* mutant of *Chlamydomonas* was also characterized (Fontaine et al. 1993). In each case, although phenotypes of RNAi potato lines were moderated, inactivation of *SS3* leads to similar phenotypes. The latter include a decrease in starch content and enrichment of glucans of $DP < 10$ and $DP > 40$ as well as more or less pronounced alteration of starch granule morphology (Fontaine et al. 1993; Abel et al. 1996; Gao et al. 1998). According to structural analysis of mutant starch, the function of SS3 in amylopectin synthesis in *Arabidopsis* leaves seems to be similar to its respective counterpart in storage organs, although with less impact on the chain length distribution (Zhang et al. 2005). However, contrary to the other species, starch content in *ss3* mutant *Arabidopsis* leaves is significantly higher than that of the wild-type at the end of the light period (Zhang et al. 2005). These data suggest that, in addition to its role in the synthesis of the longest glucan chains of amylopectin (i.e., with a DP comprised approximately between 10 and 40 depending on the species considered), SS3 plays some regulatory function in starch biosynthesis in leaves (Zhang et al. 2005). Indeed, the inactivation of *SS3* in *Arabidopsis* is also associated with an increase of total SS activity in leaves which may explain this phenotype (Zhang et al. 2005).

As described in the previous paragraphs, forward and reverse genetic approaches showed that SS1, SS2, and SS3 possess some specificity in leaves and preferentially elongate the shortest, medium, and longest glucans of the amylopectin molecule, respectively. However, depending on the species considered, the number of isoforms in a given species, and expression profiles of the corresponding genes in leaves or storage organs, their contribution to the synthesis of the molecule can be modulated. Other levels of complexity account for redundancies between isoforms especially between SS2 and SS3 (Zhang et al. 2008) or between SS1 and SS3 (Szydlowski et al. 2011) for the synthesis of glucans of $12 < DP < 28$ or $6 < DP < 10$, respectively, as shown by phenotypic analysis of the corresponding double mutant plants of *Arabidopsis*. In leaves of these mutants, modifications of amylopectin structure not only reflect the addition of single mutant phenotypes but are more exacerbated for the $12 < DP < 28$ and $6 < DP < 10$ populations of glucans (Zhang et al. 2008; Szydlowski et al. 2011). Moreover, β-amylolysis of amylopectins from *ss1 ss2* and *ss1 ss3* double mutant leaves suggests that SS activities not only dictate the chain length distribution but also contribute to the placement of $\alpha(1 \rightarrow 6)$ bonds within

amylopectin (Szydlowski et al. 2011). This was recently confirmed by studying mutant combinations in *Arabidopsis* including mutations at *SS* and *DBE* loci (Pfister et al. 2014) (this will be described in more details in the section dedicated to DBEs). It is finally worth noting that complexes including SSs and BEs have been identified in the wheat and maize endosperms (Grimaud et al. 2008; Tetlow et al. 2008). Although such physical interactions have yet to be reported for the leaf enzyme counterparts, functional interactions between SSs and BEs were recently studied in vitro (Brust et al. 2014). Importantly, combination of SS1 and BE activities leads to the production of branched glucans with a polymodal distribution similar to that seen for *Arabidopsis* leaf starch (Brust et al. 2014).

6.2.2 Formation of the α(1 → 6) Linkages in Starch: The Specific Function of Branching Enzymes

The enzymes responsible for the formation of α(1 → 6) bonds of amylopectin are α(1 → 4)-α-D-glucan:(1 → 4)-α-D-glucan-6-glycosyl transferases (EC 2.4.1.18), also known as starch branching enzymes (BEs or Q factor). BE activity was initially identified in potato (Haworth et al. 1944). The latter cleave an α(1 → 4) bond of a preexisting glucan chain and transfer the resulting fragment in α(1 → 6) position by an intra- or intermolecular mechanism. Plants generally contain two or three genetically independent isoforms of BE that were subdivided into two classes based on their amino acid sequences (Burton et al. 1995). Biochemical characterization of their activities indicates that BEI (or BE B) isoforms are more active on amylose and can transfer longer glucans compared to BEII (or BE A) enzymes. On the other hand, BEII isoforms are more active on amylopectin than BEIs (Guan and Preiss 1993; Takeda et al. 1993).

Both BEI and BEII are expressed in potato and pea leaves with most of the branching activity supported by BEII (Smith et al. 1990; Jobling et al. 1999). Mutation at the *rugosus* locus of pea leads to the disappearance of an A-class branching enzyme (BEII) associated with a tenfold decrease of total leaf branching enzyme activity (Smith et al. 1990; Tomlinson et al. 1997). When this mutant is cultivated under high irradiance, the rate of leaf-starch synthesis decreased by 40 % compared to the wild-type due to a reduction of the rate of photosynthesis (Smith et al. 1990). Moreover, the iodine-λ_{max} of amylopectin from *rugosus* mutant leaves and the average chain length of the molecule increased (Tomlinson et al. 1997).

The role of the other isoform, BEI, in starch metabolism has been poorly studied in dicots, and downregulation of this enzyme has only a small impact on starch metabolism (Flipse et al. 1996). Indeed, no differences in the amylopectin content or chain length distribution could be detected in tuber starch from amylose-free potato lines with reduced *BEI* expression. However, physicochemical properties of starch suspension showed differences compared to the wild-type suggesting that minor (or uncharacterized) structural modifications may occur when the expression of BEI is reduced (Flipse et al. 1996).

Monocots differ from dicots since they contain two types of BEII enzymes, namely, BEIIa and BEIIb (Dang and Boyer 1988). Both genes are tissue specific and their expression differs during seed development. After purification of BEs from maize leaves and kernels, it was suggested that BEI and BEIIa are expressed in both organs, whereas BEIIb expression is restricted to the endosperm (Dang and Boyer 1988). These results were later confirmed indicating that BEIIa and BEIIb are genetically independent and differentially expressed in leaves and endosperm (Fisher et al. 1996a, b; Gao et al. 1996, 1997). These expression patterns were corroborated in other cereals such as barley and rice where BEIIa is expressed in most plant organs (endosperm, leaf, and root) and the embryo, while BEIIb expression was limited to the endosperm (Yamanouchi and Nakamura 1992; Sun et al. 1998; Nishi et al. 2001). Since BEIIb expression is restricted to the endosperm, mutants lacking this enzyme accumulate high-amylose starch with structurally modified amylopectin in this organ (Garwood et al. 1976; Hedman and Boyer 1982), whereas they cannot be differentiated from the wild-type regarding leaf starch (Dang and Boyer 1989). In maize leaves, BEIIa is the major branching enzyme activity. Indeed in *be2a* mutant lines, the branching activity is decreased by sevenfold at the middle of the light phase. Since BEIIb is not expressed in leaves, the residual activity is most probably due to BEI, and, although BEI proteins were not detected by immunoblot, the corresponding mRNA was identified by RT-PCR (Yandeau-Nelson et al. 2011).

The influence of BEIIa activity on transitory starch metabolism was evident by the phenotype of *mutator* insertion lines lacking the corresponding enzyme. Leaves of these mutants produce amylopectin with reduced branching compared to the wild-type while kernel starch was unaffected by the mutation. Moreover, an accelerated senescence phenotype was associated with the lack of BEIIa in leaves (Blauth et al. 2001). Yandeau-Nelson et al. (2011) reported that *be2a* mutant lines accumulate wild-type amount of starch in leaves during the day but have reduced degradation rate compared to the wild-type. Indeed, only 40 % of starch is degraded at night in the mutant, while more than 80 % is degraded in the wild-type. The amount of starch remaining at the end of the day is even larger in the senescent regions of *be2a* leaves. This reduction of the degradation process is likely caused by alteration of starch granule structure and composition. Indeed, starch produced by *be2a* lines differs from wild-type starch in several aspects. Scanning electron microscopy analyses of purified starch granules revealed "lobular and fused" structures instead of the uniform discs observed in the wild-type (Yandeau-Nelson et al. 2011). This alteration of the granule shape is probably caused by a decrease in the amylopectin to amylose ratio. Moreover, structural analysis of mutant starch revealed that amylopectin is enriched in intermediate to long glucans (DP > 25) and contains fewer short glucan chains (Dinges et al. 2003).

The function of BEI in monocot leaves is unclear since *be1* null mutants of maize produce starch that are undistinguishable from that of the wild-type (Blauth et al. 2002). Among the dicots, *Arabidopsis* represents a particular case since two genes, *BE2.1* (or *BE3*) and *BE2.2* (or *BE2*), both encoding A-class branching enzymes are expressed in leaves and are involved in transient starch synthesis (Fisher et al.

1996a, b). Expression of both genes differs throughout the diurnal cycle. Indeed, *BE2.1* expression is regulated by light while that for *BE2.2* remains unaffected (Khoshnoodi et al. 1998; Smith et al. 2004). However, accumulation of transcripts of both genes is favored when glucose, fructose, and sucrose are supplied during the day (Khoshnoodi et al. 1998). Interestingly, no enzyme of the BEI family can be found in the genome of this species.

Phenotypic analysis of *Arabidopsis* mutant lines lacking either BE2 or BE3 indicates that these enzymes possess redundant functions. Indeed, each single mutant contains starch and amylose contents similar to those of the wild-type. Only modifications in the chain length distribution of amylopectin were reported: relative proportions of short chains (DP 5–8) were slightly reduced and those of intermediate chains (DP 9–15) were slightly increased. However, when mutations affecting both enzymes are combined, plants fail to accumulate starch, indicating that no other enzyme can compensate for their functions. In this double mutant, starch is substituted by high levels of α-maltose, and plants display a severe plant growth retardation as well as pale leaf phenotype (Dumez et al. 2006). All data collected so far regarding transitory starch metabolism suggest that BEIIa and BEII are the major starch-branching enzymes involved in amylopectin synthesis in monocots and dicots, respectively, whereas the potential function of BEI in leaf remains to be elucidated.

6.2.3 *Maturation of the Polysaccharide Structure: Debranching as a Mandatory Controlling Step*

The semicrystalline nature of amylopectin is a consequence of the specific distribution of $\alpha(1 \rightarrow 6)$ linkages within this polymer. Indeed, branch points are concentrated in amorphous lamellae but are extremely rare in other regions of the molecule, where linear glucans can intertwine to form crystalline double helices.

As described in Chap. 5, this organization results from the concerted action of starch synthases, branching, and debranching enzymes. In plants, debranching enzymes (DBE) are members of the GH13 (glycoside hydrolase) family of the CAZy classification. DBEs specifically cleave $\alpha(1 \rightarrow 6)$ linkages and are subdivided into two classes depending on their substrate specificity. Isoamylases (ISA) act on amylopectin and glycogen, while pullulanases (PU) (also called limit dextrinases, LDA) are active on amylopectin and pullulan (a highly branched polyglucan composed of maltotriosyl residues linked together by $\alpha(1 \rightarrow 6)$ bonds) but not on glycogen. Genes encoding debranching enzymes are well conserved throughout the Chloroplastida. All organisms studied so far contain one pullulanase- and three isoamylase-encoding genes (ISA1, ISA2, and ISA3) (Deschamps et al. 2008). PU and ISA3 are mainly involved in starch degradation and have minor role in polysaccharide synthesis. Indeed, as observed in maize or *Arabidopsis*, pullulanase null mutants accumulate normal amount of starch in photosynthetic tissues, and the structure of amylopectin is close to that of the wild-type reference.

Table 6.1 Amino acid sequence comparison of the four conserved regions of ISA1 and ISA2 proteins from *Arabidopsis* (At), maize (Zm), rice (Os), and potato (St)

Protein	GenBank access number	Region 1	Region 2	Region 3	Region 4
AtISA1	NP_181522	**DVVLNH**	**GFRFDLGS**	**AEAWD**	**FICAHDG**
ZmISA1	AAB97167	**DVVFNH**	**GFRFDLAS**	**AEAWD**	**FVCAHDG**
OsISA1	BAA29041	**DVVFNH**	**GFRFDLAS**	**AEAWD**	**FVCAHDG**
StISA1	AAN15317	**DVVFNH**	**GFRFDLAS**	**AEAWD**	**FVCAHDG**
AtISA2	NP_171830	**EVVFTH**	**GFCFINAS**	**ADCWD**	**YISRNSG**
ZmISA2	AAO17048	**EVVFTH**	**GFCFINAP**	**ADPWS**	**YVSRNSG**
OsISA2	AAT93894	**EVVFTH**	**GFCFINAP**	**ADPWS**	**HVSRNSG**
StISA2	AAN15318	**EVVFTH**	**GFVFVNAS**	**ADNWN**	**YIARNSG**

In *red* are reported the eight amino acids found in all active proteins of the α-amylases superfamily (GH13) (Hussain et al. 2003; Hennen-Bierwagen et al. 2012). ISA2 proteins lack essential amino acids required for enzyme activity in all four regions

However, pullulanase is able to participate in transient starch synthesis under certain circumstances. This function has been highlighted when mutations affecting PU and ISA1 were combined, leading to less starch and to the accumulation of more soluble polysaccharide (Dinges et al. 2003; Wattebled et al. 2005, 2008; Streb et al. 2008).

There is no doubt that ISA3 is essential for starch degradation in *Arabidopsis* leaves. Nevertheless, its involvement in starch synthesis is similar to that of pullulanase and was inferred when ISA1 and/or ISA2 proteins were also missing. Indeed, in a wild-type context, ISA3 has no obvious function in starch synthesis (Wattebled et al. 2005; Delatte et al. 2006). Since ISA3 and pullulanase do not influence starch synthesis in a wild-type context, the debranching activity involved in transient starch anabolism is mainly dependent on the presence of ISA1 and ISA2 proteins. These proteins behave very differently. In all organisms, ISA2 is not active and lacks essential catalytic amino acids (Table 6.1) conserved within the GH13 family (Hussain et al. 2003; Hennen-Bierwagen et al. 2012). In all plants, ISA2 proteins can form active hetero-oligomer complexes with ISA1. However, depending on its tissular or botanical origin, ISA1 can also be active by itself in the form of a homo-oligomer (see below).

In *Arabidopsis* leaves, the isoamylase activity involved in starch synthesis requires the presence of both ISA1 and ISA2 proteins and was called ISO1 (Wattebled et al. 2005). Mutant plants lacking ISA1 and/or ISA2 display the same phenotype including a minimal decrease of 80 % of the starch content at the end of the day (Zeeman et al. 1998; Delatte et al. 2005; Wattebled et al. 2005). In these plants, the reduction of starch content is associated with the accumulation of a highly branched soluble polysaccharide in mesophyll cells. This material resembles glycogen and was therefore called phytoglycogen. Moreover, the residual starch, mainly accumulated by epidermal and bundle sheath cells, is profoundly modified at the level of granule size and amylopectin structure (Delatte et al. 2005). Indeed, starch granules are much smaller than in the wild-type and amylopectin is enriched in very short chains (DP 3–5).

In monocots such as rice or maize, ISA1 is active in the endosperm either in complex with ISA2 or with itself as a homo-oligomer. Inactivation of ISA1 in maize, barley, or rice endosperms generates a phenotype similar to that observed in the corresponding mutant of *Arabidopsis* (James et al. 1995; Nakamura et al. 1996; Dinges et al. 2001; Burton et al. 2002). However, since ISA1 can form active homo-oligomers (i.e., without the requirement of ISA2), *isa2* mutants of maize and rice display a wild-type starch phenotype (Utsumi and Nakamura 2006; Kubo et al. 2010; Utsumi et al. 2011).

Studies were conducted in rice and maize to assess whether the homo-oligomer active form of ISA1 is a specific feature of cereal endosperms or also exists in leaves. Interestingly, in rice, only hetero-oligomers were purified from leaves, whereas both homo- and hetero-oligomers were catalytically active in the endosperm (Utsumi et al. 2011). The lack of homo-oligomers in leaves could result either from a predominant expression of *ISA2* or from the rapid degradation of the heteromeric form. Indeed, ISA1 homo-complexes are less stable than ISA1/ISA2 hetero-complexes. The former are quickly inactivated at 40 °C, while the latter remain active more than 30 min in these conditions (Utsumi et al. 2011). ISA1 homo-oligomer may also behave differently in leaf. Indeed, in maize leaves, ISA1 homo-oligomers appear as a weak and diffuse band on specific native-gel activity assays, whereas it is clearly visible as a sharp blue band when extracted from the endosperm (Lin et al. 2013). The presence of the ISA1 homo-oligomer in leaf was further confirmed by western blot. Phenotypes induced by the absence of ISA1 or ISA2 on polysaccharides were determined. Unlike *Arabidopsis*, *isa1* or *isa2* maize mutants do not accumulate phytoglycogen. However, they display severe reduction in starch content, reduced average granule size, and modification of amylopectin, similar to what is observed in *Arabidopsis*. Interestingly, these phenotypes are more pronounced in the isa1 mutant than in the isa2 mutant. The presence of tiny amounts of ISA1 homo-oligomers can partially counterbalance the lack of ISA2 but cannot restore a wild-type phenotype conversely to what occurs in the endosperm (Lin et al. 2013).

To determine if the ability of ISA1 from cereals to function as a homo-oligomer is species dependent, ISA1 from maize or rice were expressed in *isa1 isa2 Arabidopsis* double mutant plants. The *isa1 isa2* double mutant accumulates large amounts of phytoglycogen while the starch content is strongly reduced. Expression of ISA1 from maize or rice in the *isa1 isa2* mutant restores wild-type starch synthesis (Facon et al. 2013; Streb and Zeeman 2014). This result indicates that ISA1 from cereals can function without ISA2 even in a heterologous physiological context. This property is likely the consequence of evolutionary divergence between monocots and dicots (Facon et al. 2013).

Finally, three isoamylase activities were detected by zymogram in crude extracts of *Chlamydomonas reinhardtii*. Genetic studies revealed that two out of these three activities are composed by ISA1 and ISA2 proteins. The latter are assembled into hetero-oligomer, while the third activity corresponds to ISA1 homo-oligomers (Dauvillée et al. 2001a, b; Sim et al. 2014). The ISA1 homo-oligomer can sustain starch synthesis to a near wild-type level when growth conditions mimic the leaf

cell physiological context (Dauvillée et al. 2001a, b). Recently the crystal structure of the ISA1 homo-oligomer was elucidated and revealed that it is composed of two ISA1 subunits associated by their C-terminal domains (Sim et al. 2014), as previously suggested for the maize leaf enzyme (Facon et al. 2013). Sequence alignment comparison indicates that the dimeric organization of the ISA1 homo-oligomer may be conserved in all plants (Sim et al. 2014).

6.2.4 Physical and Functional Interactions

Amylopectin crystallization is a complex mechanism that is not yet completely elucidated. The involvement of isoamylases in this process is indisputable as shown by mutant analysis. Data accumulated since 20 years fully support the trimming model of amylopectin synthesis (Ball et al. 1996; Myers et al. 2000). However, other factors can also affect amylopectin crystallization. Indeed, enzymes of the starch pathway do not work independently but physically and/or functionally interact with each other. These interactions have been mostly studied in storage tissues (see Chap. 8) although the intricate interaction between enzymes of the starch pathways is also evident in leaves. For instance, in maize leaves, the absence of ISA1 or PU was shown to cause the loss of BE2a activity although the protein content is unmodified, suggesting that the activity of BE2a is altered because of posttranslational modifications (Dinges et al. 2003). In *Arabidopsis* the implication of starch synthases for controlling the distribution of $\alpha(1 \rightarrow 6)$ linkages within amylopectin has been suggested after the study of mutant lines defective for several starch synthases. Indeed, defects in both SS1 and SS2 or both SS1 and SS3, but not in the corresponding single mutants, modify amylopectin branch points distribution (Szydlowski et al. 2011). The precise reason of such modification is not yet known. However, the destabilization of protein complexes involving BEs (and consequently BEs activity) may be one explanation. More recently functional interactions between starch synthases and debranching enzymes during starch synthesis have been exemplified by the combination of mutations affecting SS1, SS2, SS3, and ISA1 in Arabidopsis (Pfister et al. 2014). It is proposed that outer chain length is controlled by starch synthases activity and is a key factor to ensure further amylopectin crystallization. It is then postulated that isoamylases are involved in the degradation of incorrectly synthesized glucans that remain water soluble when starch synthase activity is altered. However, the higher water-soluble polysaccharides content observed in *ss2- ss3- isa*-triple mutant could simply arise because of ISA activity deficiency. Moreover in maize endosperm, combination of mutations for SS3 (*du1-ref*) and ISA2 (*isa2-339*) induces higher water-soluble polysaccharides accumulation without reduction of debranching enzyme activity (Lin et al. 2012) ruling out the involvement of debranching enzymes for the removing of water-soluble polysaccharides.

6.3 Amylose Synthesis Is Controlled by a Dedicated Elongating Enzyme Located Within the Starch Granule

In addition to amylopectin, starch also contains amylose, which represents between 20 and 30 % of the average granule dry weight. Similar to amylopectin, amylose is composed of glucose residues linked together by $\alpha(1 \rightarrow 4)$ and $\beta(1 \rightarrow 6)$ O-glycosidic bonds. However, the proportion of α-1,6 linkages is smaller (less than 1 %) in the molecule of amylose compared to the moderately branched amylopectin molecule (5–6 %). The contribution of amylose to the crystallinity of starch is not yet fully understood. On one hand, amylose can form single helices in vitro (Godet et al. 1995) and some correlations between amylose contents and starch crystallinity were observed in *Chlamydomonas* (Wattebled et al. 2002) or maize (Cheetham and Tao 1998). On the other hand, one could argue that a direct effect of amylose on starch crystallinity cannot be discriminated from an indirect effect of amylose on amylopectin crystallinity *in planta*.

Studies in some species like tobacco, for example, suggested that amylose content is lower in leaf starch compared to storage starches (Matheson 1996). Furthermore, amylose polymers appeared to be on average smaller in transitory starch from leaves of this species. Nevertheless, it is difficult to generalize since leaf starch from other species can contain as much or more amylose than storage starches (BeMiller and Whistler 2009). Moreover, there is no report on variation in structure and/or content of this polymer within a broad population of leaf starches from different botanical origins.

Contrary to amylopectin glucans, amylose is biosynthesized by only one starch synthase, the GBSS. The latter is only active when it is physically associated with starch (Rongine De Fekete et al. 1960). This isoform is thus located within the starch granule *in planta* and can represent up to 95 % of the total starch-bound protein content. GBSS is a processive enzyme using ADP-glucose as a substrate and contains the catalytic amino acid residues conserved in all starch synthases (Denyer et al. 1999a, b; Edwards et al. 1999) (see above section for more details). However, studies performed with *Chlamydomonas*, potato, and pea starches showed that GBSS uses the long external glucans of amylopectin as acceptor substrates (van de Wal et al. 1998) and that malto-oligosaccharides enhance amylose synthesis (Denyer et al. 1996).

In *waxy* mutants of wheat, amylose synthesis sometimes still occurs in some organs while storage starch is free of amylose (Nakamura et al. 1998), suggesting that two isoforms of GBSS, encoded by two different loci, may be differentially expressed according to the organ considered. Indeed, wheat contains two GBBS isoforms, namely, GBSS1 and GBSS2 (Vrinten and Nakamura 2000). In this species, GBSS2 is encoded by a locus different from that encoding GBSS1. The former is expressed in leaves, while the latter is highly expressed in the endosperm (Vrinten and Nakamura 2000). Thus, GBSS2 seems to be the main enzyme responsible for amylose synthesis in wheat leaves. Conversely to wheat, *Arabidopsis* genome contains only one isoform of GBSS which is regulated both at the transcriptional and activity levels during day/night cycles (Tenorio et al. 2003).

6.4 The Regulation of Starch Synthesis and Degradation in Leaves

As described in the previous paragraphs and chapters, starch metabolism is relatively complex. It is controlled by a quite broad set of enzymes responsible for the formation and the cleavage of only two O-glycosidic linkages between glucose residues. Although the functions of many of these enzymes have been unraveled during the last two decades, the regulation of their activities has remained elusive. However, the regulation of enzyme activities is a key aspect because it strictly controls starch accumulation and degradation. Consequently it also controls carbon flux within the cell and particularly in leaves where starch metabolism is submitted to diurnal fluctuations. Indeed starch synthesis occurs during the illuminated period when photosynthesis is active. The polymer is subsequently degraded in the dark providing carbon and energy to the whole plant, sustaining its development and maintaining the carbon balance even when photosynthesis is off. Consequently, starch metabolism is highly regulated in leaves, and the storage polysaccharide appears as a regulator for plant growth and yield although it is still debating how this regulation occurs (Sulpice et al. 2009; Gibson et al. 2011). Regulation occurs at different levels including gene transcription and enzyme activities. This requires different mechanisms such as control by the circadian clock, transcriptional regulation of gene expression, redox control of protein activities, as well as posttranslational modifications, protein-protein complexes formation, and other physiological regulations.

It is now well established that both starch accumulation and degradation occur almost linearly (albeit with opposite signs) in *Arabidopsis* leaves throughout the diurnal cycle (Caspar et al. 1985; Gibon et al. 2004) and that about 95 % of starch is degraded at the end of the night (Graf and Smith 2011). However, starch accumulates to a lesser extent in plants cultivated under short-day condition. Moreover, the rate of starch degradation is negatively correlated to the length of the dark period (Lu et al. 2005). Thus, plants adjust the rate of starch degradation according to the ratio between night and day lengths and consequently to the level of starch accumulated at the end of the light period (Lu et al. 2005). Interestingly, plants immediately accommodate the rate of starch degradation after an unexpected arrival of night (Graf et al. 2010). Such adjustment avoids sugar starvation during the dark period and is under the control of the circadian clock as shown by the impairment of the rate of starch degradation in the clock-altered *cca1/lhy* mutant of *Arabidopsis* (Graf et al. 2010). Indeed, assuming that the length of the whole diurnal cycle is not modified, leaf cells can anticipate the arrival of day and night but can also rapidly adjust to changes in night length preventing carbon/sugar starvation (Graf et al. 2010). It is not clear at which level the circadian clock impacts starch degradation. The expression of starch enzymes is likely to be tuned by the clock as suggested by others (Zabawinski et al. 2001; Smith et al. 2004; Lu et al. 2005; Ral et al. 2006). However, the protein abundance of some of the starch-degrading enzymes (e.g., DPE2, PHS2, and SEX1) is not modified throughout the cycle (Lu et al. 2005)

suggesting that posttranslational regulation of enzyme activity is responsible for the control of starch degradation rather than enzyme amounts.

Although the circadian clock is probably an important regulator of starch breakdown, it is likely not the only controlling step of starch degradation in leaves. Indeed, immediate adjustment of the rate of starch degradation still occurs in the *cca1/lhy* clock mutant when unexpected early night is applied (Scialdone et al. 2013). It has been suggested that two molecules provide information on (1) the concentration of starch at end of day and (2) on the expected time of dawn. Such molecules have not yet been identified, although phosphate groups at C_6 and C_3 positions on some of the glucose residues of starch were proposed as candidates to regulate the rate of starch degradation (Scialdone et al. 2013). It is not clear whether or not the same process applies for the control of starch synthesis.

The rate of starch degradation is also compromised in the *ss4* mutant of *Arabidopsis*. As described above, SS4 is one of the major factors controlling the initiation of starch synthesis. The lack of SS4 leads to the accumulation of fewer (one, rarely two, starch granule per chloroplast) but larger starch granules in chloroplasts (Roldán et al. 2007). The rates of both starch synthesis and degradation as well as plant growth are reduced in the *ss4* mutant compared to the wild-type, although the circadian clock and the starch-degrading machinery are unaffected in this mutant (except for the activities of both starch phosphorylases PHS1 and PHS2 which are enhanced) (Roldán et al. 2007). It was suggested that the surface of the starch granules represents a key factor in controlling the rate of starch synthesis and degradation (Roldán et al. 2007; D'Hulst and Mérida 2010). Indeed, if one compares starch granules to perfect spheres (this assumption has no impact on the following rationale, although granules resemble oblate spheroids) and considering homogenous distribution of starch within these spheres, for a given volume of starch at the end of the day, the cumulated surface of six granules (the average number of granules per wild-type chloroplasts) is about 2× larger than that of a single granule. Thus, the surface accessibility for synthesis and degradation is different between the wild-type and the *ss4* mutant. Taking into account that starch content is decreased in the latter, this surface is about 1.6 times larger in the wild-type at the end of the day. This may explain the reduction in both the rates of starch synthesis and degradation as well as why starch is not fully depleted at the end of the night in the *ss4* mutant.

It is not yet clear whether the number of granules in plant leaves is unaffected throughout a day/night cycle. However, if this parameter is constant, the total starch volume and the surface available for enzymes of the degradation pathway will be lower at anticipated night arrival in a wild-type background. Moreover, based on the same postulates and data published by Lu et al. (2005), the ratio between the total granule surface after 12 h of light and 8 h of light would be 1.6. Thus, such a reduction of the granule surface may also account, even partly, for the reduced rate of starch degradation and to the immediate control of this process when the day length is unexpectedly shortened. Interestingly, *SS4* gene expression seems to be controlled by the transcription factors AtCOL (constans like) and AtIDD5 (indeterminate domain 5) (Ingkasuwan et al. 2012). In the corresponding mutants of *Arabidopsis* (i.e., *col* and *idd5*), starch granule size and number per chloroplast were

altered as well as plastid morphology (as observed by TEM on ultrathin sections of leaves). The inference of such regulation is still not understood and requires further investigation but may provide new insights in the regulation of starch granule initiation and thus starch synthesis as well as degradation control.

Regulation of starch metabolism in leaves also occurs through other mechanisms. For instance, it is suspected that enzymes of the starch pathway physically interact to form heteromultimeric complexes in plant storage organs (Hennen-Bierwagen et al. 2008; Tetlow et al. 2008; Liu et al. 2012). In some instances, their formation is conditioned by the posttranslational modification (phosphorylation) of the enzymes involved (Makhmoudova et al. 2014). However, conversely to sink organs, their formation in leaves has been poorly studied. Apart from the formation of ADP-glucose pyrophosphorylase (AGPase) (see Chap. 11 for details) and debranching enzymes (isoamylases) complexes (see Sect. 6.2.3 for details), no other protein-protein interaction has been formerly described so far in leaves. It is assumed that the control of the formation of these complexes is crucial for the tuned regulation of starch synthesis and degradation and thus plant homeostasis.

Redox control of enzymes is also one of the regulatory steps of starch metabolism in leaves. The first example described was the control of AGPase (a more complete description of AGPase activity and regulation is presented in Chap. 11), the enzyme catalyzing the synthesis of ADP-glucose. This reaction is considered as the rate-limiting step for starch synthesis. AGPase activity was shown to be regulated in photosynthetic tissues such as leaves of *A. thaliana* (Crevillen et al. 2003), barley (Kleczkowski 2000), rice (Lee et al. 2007), and maize (Huang et al. 2014) or *Chlamydomonas reinhardtii* (Ball et al. 1991). The regulation results from the ratio between concentrations of allosteric effectors such as 3-phosphoglyceric acid (3-PGA) and inorganic phosphate (Pi). AGPase activity is also modulated by the redox state of the protein as shown in potato, pea, and *Arabidopsis* leaves (Hendriks et al. 2003) and previously demonstrated in potato tubers (Ballicora et al. 2000; Tiessen et al. 2002). Indeed, AGPase is a heterotetramer composed of two small (catalytic) and two large (regulatory) subunits. In the oxidized state, the catalytic subunits of the leaf and potato tuber enzyme can form a dimer maintained by a disulfide bond between two Cys^{12} cysteine residues (Fu et al. 1998; Hädrich et al. 2012). Dimerization occurs at night and leads to a strong reduction of enzyme activity (Hendriks et al. 2003). The disulfide bond is reduced during the light period, but also in the dark when leaves are supplied with sucrose. AGPase activity is consequently increased as well as starch synthesis. Interestingly, AGPase activity is under the control of the circadian clock as demonstrated in *Chlamydomonas reinhardtii* (Zabawinski et al. 2001). Regulation by the clock applies at both gene expression and enzyme activity suggesting that the circadian clock modulates the whole starch metabolism.

The redox control of starch synthesis in leaves is not limited to the regulation of AGPase activity. Such type of regulation was also reported for several *Arabidopsis* enzymes such as: ISA1/ISA2, LDA, SS1, SS3, BE2, BAM3 (β-amylase), AMY3 (α-amylase), GWD (glucan water dikinase), and DSP4 (SEX4) (phosphoglucan

phosphatase) (Mikkelsen et al. 2005; Sokolov et al. 2006; Sparla et al. 2006; Valerio et al. 2011; Glaring et al. 2012; Seung et al. 2013; Silver et al. 2013). This suggests that the whole pathway is under redox control allowing a tight regulation of enzyme activities during the day/night cycle. For instance, AMY3 is inactive in its oxidized form (when a disulfide bond is formed between the Cys^{499} and Cys^{587} residues) and is reactivated by thioredoxins (Seung et al. 2013). Recently a plastid-localized NADPH-dependent thioredoxin reductase C (NTRC) was found to interact with AGPase in *Arabidopsis* (Michalska et al. 2009; Lepistö et al. 2013). Moreover, starch accumulation is impaired in *ntrc* mutant plants particularly when the latter are cultivated under short-day conditions. Conversely, overexpression of NTRC enhanced plant growth and biomass indicating a direct control of starch synthesis by this thioredoxin reductase (Toivola et al. 2013). Interestingly, the over expression of the plastidial thioredoxin f in tobacco increases leaf-starch accumulation by up to 700 % (Sanz-Barrio et al. 2013). However, high starch accumulation is not a consequence of AGPase redox activation as proposed earlier for *Arabidopsis* (Li et al. 2012). Indeed, it was suggested that the redox control of SS3/SS4 (starch synthases 3 and 4) is responsible for this increase of the starch content in *Arabidopsis* leaves (Li et al. 2011).

Finally, starch metabolism in *Arabidopsis* leaf is physiologically controlled by the concentration of trehalose-6-phosphate (Tre6P). Tre6P is a nonreducing disaccharide composed by two glucose residues and found at very low level in *Arabidopsis* leaves. It is synthesized from Glc-6-P and UPG-glucose by the trehalose-6-phosphate synthase (*AtTPS1*) (Avonce et al. 2004). AtTPS1 was proposed to act as a regulator for glucose signaling in *Arabidopsis*. An osmoprotectant function of trehalose was excluded because of its very low levels in plants. Indeed, Tre6P concentration in leaves increases during the day but also when the dark period is unexpectedly extended for 6 h as well as in a *pgm* starchless mutant (Lunn et al. 2006). Increased concentration of Tre6P is accompanied by a modulation of AGPase redox state in favor of the reduced active form of the enzyme. Consequently starch content is increased after 4 h of illumination (except in the *pgm* mutant) (Lunn et al. 2006). This observation confirmed previous results indicating that the redox modulation of AGPase activity is controlled by Tre6P, the concentration of which being in turn regulated by sugars (Kolbe et al. 2005). Interestingly, oscillation of sugar levels during day/night cycles acts as a metabolic feedback to the circadian clock (Haydon et al. 2013). Thus, over its function in carbon and energy storage, starch, which metabolism is controlled by the circadian clock, may also contribute to the entrainment and the robustness of the clock in photosynthetic tissues. However, the molecular mechanisms underlying this regulation are still not unraveled.

References

Abel GJW, Springer F, Willmitzer L et al (1996) Cloning and functional analysis of a cDNA encoding a novel 139 kDa starch synthase from potato (*Solanum tuberosum* L.). Plant J 10:981–991

Avonce N, Leyman B, Mascorro-Gallardo JO et al (2004) The Arabidopsis trehalose-6-P synthase AtTPS1 gene is a regulator of glucose, abscisic acid, and stress signaling. Plant Physiol 136:3649–3659

Ball S, Marianne T, Dirick L et al (1991) A Chlamydomonas reinhardtii low-starch mutant is defective for 3-phosphoglycerate activation and orthophosphate inhibition of ADP-glucose pyrophosphorylase. Planta 185:17–26

Ball S, Guan H-P, James M et al (1996) From glycogen to amylopectin: a model for the biogenesis of the plant starch granule. Cell 86:349–352

Ballicora MA, Frueauf JB, Fu Y et al (2000) Activation of the potato tuber ADP-glucose pyrophosphorylase by thioredoxin. J Biol Chem 275:1315–1320

BeMiller JN, Whistler RL (2009) Starch: chemistry and technology. Elsevier Science, New York

Blauth SL, Yao Y, Klucinec JD et al (2001) Identification of Mutator insertional mutants of starch-branching enzyme 2a in corn. Plant Physiol 125:1396–1405

Blauth SL, Kim K-N, Klucinec J et al (2002) Identification of Mutator insertional mutants of starch-branching enzyme 1 (sbe1) in *Zea mays* L. Plant Mol Biol 48:287–297

Blumenfeld ML, Whelan WJ, Krisman CR (1983) The initiation of glycogen biosynthesis in rat heart. Eur J Biochem 135:175–179

Brust H, Lehmann T, D'Hulst C et al (2014) Analysis of the functional interaction of Arabidopsis starch synthase and branching enzyme isoforms reveals that the cooperative action of SSI and BEs results in glucans with polymodal chain length distribution similar to amylopectin. PLoS ONE 9:e102364

Buléon A, Gérard C, Riekel C et al (1998) Details of the crystalline ultrastructure of C-starch granules revealed by synchrotron microfocus mapping. Macromolecules 31:6605–6610

Burton RA, Bewley JD, Smith AM et al (1995) Starch branching enzymes belonging to distinct enzyme families are differentially expressed during pea embryo development. Plant J 7:3–15

Burton RA, Jenner H, Carrangis L et al (2002) Starch granule initiation and growth are altered in barley mutants that lack isoamylase activity. Plant J 31:97–112

Buschiazzo A, Ugalde JE, Guerin ME et al (2004) Crystal structure of glycogen synthase: homologous enzymes catalyze glycogen synthesis and degradation. EMBO J 23:3196–3205

Cantarel BL, Coutinho PM, Rancurel C et al (2009) The carbohydrate-active enzymes database (CAZy): an expert resource for Glycogenomics. Nucleic Acids Res 37:D233–D238

Cao H, Imparl-Radosevich J, Guan H et al (1999) Identification of the soluble starch synthase activities of maize endosperm. Plant Physiol 120:205–216

Caspar T, Huber SC, Somerville C (1985) Alterations in growth, photosynthesis, and respiration in a starchless mutant of *Arabidopsis thaliana* (L.) deficient in chloroplast phosphoglucomutase activity. Plant Physiol 79:11–17

Chatterjee M, Berbezy P, Vyas D et al (2005) Reduced expression of a protein homologous to glycogenin leads to reduction of starch content in Arabidopsis leaves. Plant Sci 168:501–509

Cheetham NWH, Tao L (1998) Variation in crystalline type with amylose content in maize starch granules: an X-ray powder diffraction study. Carbohydr Polym 36:277–284

Colleoni C, Dauvillee D, Mouille G et al (1999a) Genetic and biochemical evidence for the involvement of alpha −1,4 glucanotransferases in amylopectin synthesis. Plant Physiol 120:993–1004

Colleoni C, Dauvillee D, Mouille G et al (1999b) Biochemical characterization of the chlamydomonas reinhardtii alpha −1,4 glucanotransferase supports a direct function in amylopectin biosynthesis. Plant Physiol 120:1005–1014

Commuri PD, Keeling PL (2001) Chain-length specificities of maize starch synthase I enzyme: studies of glucan affinity and catalytic properties. Plant J 25:475–486

Craig J, Lloyd JR, Tomlinson K et al (1998) Mutations in the gene encoding starch synthase II profoundly alter amylopectin structure in pea embryos. Plant Cell Online 10:413–426

Crevillen P, Ballicora MA, Merida A et al (2003) The different large subunit isoforms of *Arabidopsis thaliana* ADP-glucose pyrophosphorylase confer distinct kinetic and regulatory properties to the heterotetrameric enzyme. J Biol Chem 278:28508–28515

Crumpton-Taylor M, Grandison S, Png KMY et al (2012) Control of starch granule numbers in Arabidopsis chloroplasts. Plant Physiol 158:905–916

Crumpton-Taylor M, Pike M, Lu K-J et al (2013) Starch synthase 4 is essential for coordination of starch granule formation with chloroplast division during Arabidopsis leaf expansion. New Phytol 200:1064–1075

D'Hulst C, Mérida Á (2010) The priming of storage glucan synthesis from bacteria to plants: current knowledge and new developments. New Phytol 188:13–21

Dang PL, Boyer CD (1988) Maize leaf and kernel starch synthases and starch branching enzymes. Phytochemistry 27:1255–1259

Dang P, Boyer C (1989) Comparison of soluble starch synthases and branching enzymes from leaves and kernels of normal and amylose-extender maize. Biochem Genet 27:521–532

Dauvillée D, Colleoni C, Mouille G et al (2001a) Two loci control phytoglycogen production in the monocellular green alga *Chlamydomonas reinhardtii*. Plant Physiol 125:1710–1722

Dauvillée D, Colleoni C, Mouille G et al (2001b) Biochemical characterization of wild-type and mutant isoamylases of *Chlamydomonas reinhardtii* supports a function of the multimeric enzyme organization in amylopectin maturation. Plant Physiol 125:1723–1731

Dauvillée D, Chochois V, Steup M et al (2006) Plastidial phosphorylase is required for normal starch synthesis in *Chlamydomonas reinhardtii*. Plant J 48:274–285

Delatte T, Trevisan M, Parker ML et al (2005) Arabidopsis mutants *Atisa1* and *Atisa2* have identical phenotypes and lack the same multimeric isoamylase, which influences the branch point distribution of amylopectin during starch synthesis. Plant J 41:815–830

Delatte T, Umhang M, Trevisan M et al (2006) Evidence for distinct mechanisms of starch granule breakdown in plants. J Biol Chem 281:12050–12059

Delvalle D, Dumez S, Wattebled F et al (2005) Soluble starch synthase I: a major determinant for the synthesis of amylopectin in *Arabidopsis thaliana* leaves. Plant J 43:398–412

Denyer K, Clarke B, Hylton C et al (1996) The elongation of amylose and amylopectin chains in isolated starch granules. Plant J 10:1135–1143

Denyer K, Waite D, Edwards A et al (1999a) Interaction with amylopectin influences the ability of granule-bound starch synthase I to elongate malto-oligosaccharides. Biochem J 342:647–653

Denyer K, Waite D, Motawia S et al (1999b) Granule-bound starch synthase I in isolated starch granules elongates malto-oligosaccharides processively. Biochem J 340:183–191

Deschamps P, Moreau H, Worden AZ et al (2008) Early gene duplication within chloroplastida and its correspondence with relocation of starch metabolism to chloroplasts. Genetics 178:2373–2387

Dian W, Jiang H, Wu P (2005) Evolution and expression analysis of starch synthase III and IV in rice. J Exp Bot 56:623–632

Dinges JR, Colleoni C, Myers AM et al (2001) Molecular structure of three mutations at the maize sugary1 locus and their allele-specific phenotypic effects. Plant Physiol 125:1406–1418

Dinges JR, Colleoni C, James MG et al (2003) Mutational analysis of the pullulanase-type debranching enzyme of maize indicates multiple functions in starch metabolism. Plant Cell 15:666–680

Dumez S, Wattebled F, Dauvillee D et al (2006) Mutants of Arabidopsis lacking starch branching enzyme II substitute plastidial starch synthesis by cytoplasmic maltose accumulation. Plant Cell 18:2694–2709

Edwards A, Borthakur A, Bornemann S et al (1999) Specificity of starch synthase isoforms from potato. Eur J Biochem 266:724–736

Facon M, Lin Q, Azzaz AM et al (2013) Distinct functional properties of isoamylase-type starch debranching enzymes in monocot and dicot leaves. Plant Physiol 163:1363–1375

Fisher D, Gao M, Kim K-N et al (1996a) Two closely related cDNAs encoding starch branching enzyme from *Arabidopsis thaliana*. Plant Mol Biol 30:97–108

Fisher DK, Gao M, Kim KN et al (1996b) Allelic analysis of the maize amylose-extender locus suggests that independent genes encode starch-branching enzymes IIa and IIb. Plant Physiol 110:611–619

Flipse E, Suurs L, Keetels CJAM et al (1996) Introduction of sense and antisense cDNA for branching enzyme in the amylose-free potato mutant leads to physico-chemical changes in the starch. Planta 198:340–347

Fontaine T, D'Hulst C, Maddelein ML et al (1993) Toward an understanding of the biogenesis of the starch granule. Evidence that Chlamydomonas soluble starch synthase II controls the synthesis of intermediate size glucans of amylopectin. J Biol Chem 268:16223–16230

Fu Y, Ballicora MA, Leykam JF et al (1998) Mechanism of reductive activation of potato tuber ADP-glucose pyrophosphorylase. J Biol Chem 273:25045–25052

Fujita N, Yoshida M, Asakura N et al (2006) Function and characterization of starch synthase I using mutants in rice. Plant Physiol 140:1070–1084

Furukawa K, Tagaya M, Inouye M et al (1990) Identification of lysine 15 at the active site in *Escherichia coli* glycogen synthase. Conservation of Lys-X-Gly-Gly sequence in the bacterial and mammalian enzymes. J Biol Chem 265:2086–2090

Furukawa K, Tagaya M, Tanizawa K et al (1993) Role of the conserved Lys-X-Gly-Gly sequence at the ADP-glucose-binding site in *Escherichia coli* glycogen synthase. J Biol Chem 268:23837–23842

Gámez-Arjona FM, Raynaud S, Ragel P et al (2014) Starch synthase 4 is located in the thylakoid membrane and interacts with plastoglobule-associated proteins in Arabidopsis. Plant J 80(2):305–316

Gao M, Fisher D, Kim K-N et al (1996) Evolutionary conservation and expression patterns of maize starch branching enzyme I and IIb genes suggests isoform specialization. Plant Mol Biol 30:1223–1232

Gao M, Fisher DK, Kim KN et al (1997) Independent genetic control of maize starch-branching enzymes IIa and IIb (Isolation and characterization of a Sbe2a cDNA). Plant Physiol 114:69–78

Gao M, Wanat J, Stinard PS et al (1998) Characterization of dull1, a maize gene coding for a novel starch synthase. Plant Cell Online 10:399–412

Garwood DL, Shannon JC, Creech RG (1976) Starches of endosperm possessing different alleles at the amylose-extender locus in *Zea mays* L. Cereal Chem 53:355–364

Gérard C, Planchot V, Colonna P et al (2000) Relationship between branching density and crystalline structure of A- and B-type maize mutant starches. Carbohydr Res 326:130–144

Gibon Y, Bläsing OE, Palacios-Rojas N et al (2004) Adjustment of diurnal starch turnover to short days: depletion of sugar during the night leads to a temporary inhibition of carbohydrate utilization, accumulation of sugars and post-translational activation of ADP-glucose pyrophosphorylase in the following light period. Plant J 39:847–862

Gibson K, Park J-S, Nagai Y et al (2011) Exploiting leaf starch synthesis as a transient sink to elevate photosynthesis, plant productivity and yields. Plant Sci 181:275–281

Glaring MA, Skryhan K, Kötting O et al (2012) Comprehensive survey of redox sensitive starch metabolising enzymes in *Arabidopsis thaliana*. Plant Physiol Biochem 58:89–97

Godet MC, Bizot H, Buléon A (1995) Crystallization of amylose—fatty acid complexes prepared with different amylose chain lengths. Carbohydr Polym 27:47–52

Graf A, Smith AM (2011) Starch and the clock: the dark side of plant productivity. Trends Plant Sci 16:169–175

Graf A, Schlereth A, Stitt M et al (2010) Circadian control of carbohydrate availability for growth in Arabidopsis plants at night. Proc Natl Acad Sci 107:9458–9463

Grimaud F, Rogniaux H, James MG et al (2008) Proteome and phosphoproteome analysis of starch granule-associated proteins from normal maize and mutants affected in starch biosynthesis. J Exp Bot 59:3395–3406

Guan HP, Preiss J (1993) Differentiation of the properties of the branching isozymes from maize (*Zea mays*). Plant Physiol 102:1269–1273

Hädrich N, Hendriks JHM, Kötting O et al (2012) Mutagenesis of cysteine 81 prevents dimerization of the APS1 subunit of ADP-glucose pyrophosphorylase and alters diurnal starch turnover in *Arabidopsis thaliana* leaves. Plant J 70:231–242

Harn C, Knight M, Ramakrishnan A et al (1998) Isolation and characterization of the zSSIIa and zSSIIb starch synthase cDNA clones from maize endosperm. Plant Mol Biol 37:639–649

Haworth WN, Peat S, Bourne EJ (1944) Synthesis of amylopectin. Nature 154:236

Haydon MJ, Mielczarek O, Robertson FC et al (2013) Photosynthetic entrainment of the *Arabidopsis thaliana* circadian clock. Nature 502:689–692

Hedman K, Boyer C (1982) Gene dosage at the amylose-extender locus of maize: effects on the levels of starch branching enzymes. Biochem Genet 20:483–492

Hendriks JHM, Kolbe A, Gibon Y et al (2003) ADP-glucose pyrophosphorylase is activated by posttranslational redox-modification in response to light and to sugars in leaves of Arabidopsis and other plant species. Plant Physiol 133:838–849

Hennen-Bierwagen TA, Liu F, Marsh RS et al (2008) Starch biosynthetic enzymes from developing maize endosperm associate in multisubunit complexes. Plant Physiol 146:1892–1908

Hennen-Bierwagen TA, James MG, Myers AM (2012) Involvement of debranching enzymes in starch biosynthesis. In: Tetlow IJ (ed) Starch: origins, structure and metabolism, vol 5. Society for Experimental Biology, London

Hirose T, Terao T (2004) A comprehensive expression analysis of the starch synthase gene family in rice (*Oryza sativa* L.). Planta 220:9–16

Hizukuri S (1985) Relationship between the distribution of the chain length of amylopectin and the crystalline structure of starch granules. Carbohydr Res 141:295–306

Huang B, Hennen-Bierwagen TA, Myers AM (2014) Functions of multiple genes encoding ADP-glucose pyrophosphorylase subunits in maize endosperm, embryo, and leaf. Plant Physiol 164:596–611

Hussain H, Mant A, Seale R et al (2003) Three isoforms of isoamylase contribute different catalytic properties for the debranching of potato glucans. Plant Cell 15:133–149

Imberty A, Chanzy H, Pérez S et al (1988) The double-helical nature of the crystalline part of A-starch. J Mol Biol 201:365–378

Ingkasuwan P, Netrphan S, Prasitwattanaseree S et al (2012) Inferring transcriptional gene regulation network of starch metabolism in *Arabidopsis thaliana* leaves using graphical Gaussian model. BMC Syst Biol 6:100

James MG, Robertson DS, Myers AM (1995) Characterization of the maize gene sugary1, a determinant of starch composition in kernels. Plant Cell Online 7:417–429

Jane J-L, Kasemsuwan T, Leas S et al (1994) Anthology of starch granule morphology by scanning electron microscopy. Starch-Stärke 46:121–129

Jane J-L, Wong K-S, McPherson AE (1997) Branch-structure difference in starches of A- and B-type X-ray patterns revealed by their Naegeli dextrins. Carbohydr Res 300:219–227

Jenkins PJ, Cameron RE, Donald AM (1993) A universal feature in the structure of starch granules from different botanical sources. Starch-Stärke 45:417–420

Jiang H, Dian W, Liu F et al (2004) Molecular cloning and expression analysis of three genes encoding starch synthase II in rice. Planta 218:1062–1070

Jobling SA, Schwall GP, Westcott RJ et al (1999) A minor form of starch branching enzyme in potato (*Solanum tuberosum* L.) tubers has a major effect on starch structure: cloning and characterisation of multiple forms of SBE A. Plant J 18:163–171

Khoshnoodi J, Larsson CT, Larsson H et al (1998) Differential accumulation of Arabidopsis thaliana Sbe2.1 and Sbe2.2 transcripts in response to light. Plant Sci 135:183–193

Kleczkowski LA (2000) Is leaf ADP-glucose pyrophosphorylase an allosteric enzyme? Biochim Biophys Acta Gen Subj 1476:103–108

Kolbe A, Tiessen A, Schluepmann H et al (2005) Trehalose 6-phosphate regulates starch synthesis via posttranslational redox activation of ADP-glucose pyrophosphorylase. Proc Natl Acad Sci U S A 102:11118–11123

Kossmann J, Abel GJW, Springer F et al (1999) Cloning and functional analysis of a cDNA encoding a starch synthase from potato (*Solanum tuberosum* L.) that is predominantly expressed in leaf tissue. Planta 208:503–511

Kubo A, Colleoni C, Dinges JR et al (2010) Functions of heteromeric and homomeric isoamylase-type starch-debranching enzymes in developing maize endosperm. Plant Physiol 153:956–969

Lee S-K, Hwang S-K, Han M et al (2007) Identification of the ADP-glucose pyrophosphorylase isoforms essential for starch synthesis in the leaf and seed endosperm of rice (*Oryza sativa* L.). Plant Mol Biol 65:531–546

Lepistö A, Pakula E, Toivola J et al (2013) Deletion of chloroplast NADPH-dependent thioredoxin reductase results in inability to regulate starch synthesis and causes stunted growth under short-day photoperiods. J Exp Bot 64:3843–3854
Li J, Ezquer I, Bahaji A et al (2011) Microbial volatile-induced accumulation of exceptionally high levels of starch in Arabidopsis leaves is a process involving NTRC and starch synthase classes III and IV. Mol Plant-Microbe Interact 24:1165–1178
Li J, Almagro G, Muñoz FJ et al (2012) Post-translational redox modification of ADP-glucose pyrophosphorylase in response to light is not a major determinant of fine regulation of transitory starch accumulation in Arabidopsis leaves. Plant Cell Physiol 53:433–444
Lin Q, Huang B, Zhang M et al (2012) Functional interactions between starch synthase III and isoamylase-type starch-debranching enzyme in maize endosperm. Plant Physiol 158:679–692
Lin Q, Facon M, Putaux J-L et al (2013) Function of isoamylase-type starch debranching enzymes ISA1 and ISA2 in the *Zea mays* leaf. New Phytol 200:1009–1021
Liu F, Ahmed Z, Lee EA et al (2012) Allelic variants of the amylose extender mutation of maize demonstrate phenotypic variation in starch structure resulting from modified protein-protein interactions. J Exp Bot 63:1167–1183
Lomako J, Lomako WM, Whelan WJ (1988) A self-glucosylating protein is the primer for rabbit muscle glycogen biosynthesis. FASEB J 2:3097–3103
Lomako J, Lomako WM, Whelan WJ (2004) Glycogenin: the primer for mammalian and yeast glycogen synthesis. Biochim Biophys Acta Gen Subj 1673:45–55
Lu Y, Gehan JP, Sharkey TD (2005) Daylength and circadian effects on starch degradation and maltose metabolism. Plant Physiol 138:2280–2291
Lunn JE, Feil R, Hendriks JHM et al (2006) Sugar-induced increases in trehalose 6-phosphate are correlated with redox activation of ADPglucose pyrophosphorylase and higher rates of starch synthesis in *Arabidopsis thaliana*. Biochem J 397:139–148
Makhmoudova A, Williams D, Brewer D et al (2014) Identification of multiple phosphorylation sites on maize endosperm starch branching enzyme IIb, a key enzyme in amylopectin biosynthesis. J Biol Chem 289:9233–9246
Matheson NK (1996) The chemical structure of amylose and amylopectin fractions of starch from tobacco leaves during development and diurnally-nocturnally. Carbohydr Res 282:247–262
Michalska J, Zauber H, Buchanan BB et al (2009) NTRC links built-in thioredoxin to light and sucrose in regulating starch synthesis in chloroplasts and amyloplasts. Proc Natl Acad Sci 106:9908–9913
Mikkelsen R, Mutenda KE, Mant A et al (2005) a-Glucan, water dikinase (GWD): a plastidic enzyme with redox-regulated and coordinated catalytic activity and binding affinity. Proc Natl Acad Sci U S A 102:1785–1790
Morell MK, Kosar-Hashemi B, Cmiel M et al (2003) Barley sex6 mutants lack starch synthase IIa activity and contain a starch with novel properties. Plant J 34:173–185
Mortimer JC, Miles GP, Brown DM et al (2010) Absence of branches from xylan in Arabidopsis gux mutants reveals potential for simplification of lignocellulosic biomass. Proc Natl Acad Sci 107:17409–17414
Myers AM, Morell MK, James MG et al (2000) Recent progress toward understanding biosynthesis of the amylopectin crystal. Plant Physiol 122:989–998
Nakamura Y, Umemoto T, Takahata Y et al (1996) Changes in structure of starch and enzyme activities affected by *sugary* mutations in developing rice endosperm. Possible role of starch debranching enzyme (R-enzyme) in amylopectin biosynthesis. Physiol Plant 97:491–498
Nakamura T, Vrinten P, Hayakawa K et al (1998) Characterization of a granule-bound starch synthase isoform found in the pericarp of wheat. Plant Physiol 118:451–459
Nelson OE, Rines HW (1962) The enzymatic deficiency in the waxy mutant of maize. Biochem Biophys Res Commun 9:297–300
Nishi A, Nakamura Y, Tanaka N et al (2001) Biochemical and genetic analysis of the effects of amylose-extender mutation in rice endosperm. Plant Physiol 127:459–472
Palopoli N, Busi MV, Fornasari MS et al (2006) Starch-synthase III family encodes a tandem of three starch-binding domains. Protein Struct Funct Bioinf 65:27–31

Pfister B, Lu K-J, Eicke S et al (2014) Genetic evidence that chain length and branch point distributions are linked determinants of starch granule formation in Arabidopsis. Plant Physiol 165:1457–1474

Ragel P, Streb S, Feil R et al (2013) Loss of starch granule initiation has a deleterious effect on the growth of Arabidopsis plants due to an accumulation of ADP-glucose. Plant Physiol 163:75–85

Ral J-P, Colleoni C, Wattebled F et al (2006) Circadian clock regulation of starch metabolism establishes GBSSI as a major contributor to amylopectin synthesis in *Chlamydomonas reinhardtii*. Plant Physiol 142:305–317

Rennie EA, Hansen SF, Baidoo EEK et al (2012) Three members of the Arabidopsis glycosyltransferase family 8 are xylan glucuronosyltransferases. Plant Physiol 159:1408–1417

Roldán I, Wattebled F, Lucas MM et al (2007) The phenotype of soluble starch synthase IV defective mutants of *Arabidopsis thaliana* suggests a novel function of elongation enzymes in the control of starch granule formation. Plant J 49:492–504

Rongine De Fekete MA, Leloir LF, Cardini CE (1960) Mechanism of starch biosynthesis. Nature 187:918–919

Rose A, Meier I (2004) Scaffolds, levers, rods and springs: diverse cellular functions of long coiled-coil proteins. Cell Mol Life Sci CMLS 61:1996–2009

Sanz-Barrio R, Corral-Martinez P, Ancin M et al (2013) Overexpression of plastidial thioredoxin f leads to enhanced starch accumulation in tobacco leaves. Plant Biotechnol J 11:618–627

Scialdone A, Mugford ST, Feike D et al (2013) Arabidopsis plants perform arithmetic division to prevent starvation at night. eLife 2:e00669

Seung D, Thalmann M, Sparla F et al (2013) *Arabidopsis thaliana* AMY3 is a unique redox-regulated chloroplastic α-amylase. J Biol Chem 288:33620–33633

Silver DM, Silva LP, Issakidis-Bourguet E et al (2013) Insight into the redox regulation of the phosphoglucan phosphatase SEX4 involved in starch degradation. FEBS J 280:538–548

Sim L, Beeren SR, Findinier J et al (2014) Crystal structure of the Chlamydomonas starch debranching enzyme isoamylase ISA1 reveals insights into the mechanism of branch trimming and complex assembly. J Biol Chem 289(33):22991–23003

Smith A, Neuhaus HE, Stitt M (1990) The impact of decreased activity of starch-branching enzyme on photosynthetic starch synthesis in leaves of wrinkled-seeded peas. Planta 181:310–315

Smith SM, Fulton DC, Chia T et al (2004) Diurnal changes in the transcriptome encoding enzymes of starch metabolism provide evidence for both transcriptional and posttranscriptional regulation of starch metabolism in Arabidopsis leaves. Plant Physiol 136:2687–2699

Sokolov LN, Dominguez-Solis JR, Allary A-L et al (2006) A redox-regulated chloroplast protein phosphatase binds to starch diurnally and functions in its accumulation. Proc Natl Acad Sci 103:9732–9737

Sparla F, Costa A, Lo Schiavo F et al (2006) Redox regulation of a novel plastid-targeted beta-amylase of Arabidopsis. Plant Physiol 141:840–850

Streb S, Zeeman SC (2014) Replacement of the endogenous starch debranching enzymes ISA1 and ISA2 of Arabidopsis with the rice orthologs reveals a degree of functional conservation during starch synthesis. PLoS ONE 9:9

Streb S, Delatte T, Umhang M et al (2008) Starch granule biosynthesis in Arabidopsis is abolished by removal of all debranching enzymes but restored by the subsequent removal of an endoamylase. Plant Cell 20:3448–3466

Sulpice R, Pyl E-T, Ishihara H et al (2009) Starch as a major integrator in the regulation of plant growth. Proc Natl Acad Sci 106:10348–10353

Sun C, Sathish P, Ahlandsberg S et al (1998) The two genes encoding starch-branching enzymes IIa and IIb are differentially expressed in barley. Plant Physiol 118:37–49

Szydlowski N, Ragel P, Raynaud S et al (2009) Starch granule initiation in Arabidopsis requires the presence of either class IV or class III starch synthases. Plant Cell 21:2443–2457

Szydlowski N, Ragel P, Hennen-Bierwagen TA et al (2011) Integrated functions among multiple starch synthases determine both amylopectin chain length and branch linkage location in Arabidopsis leaf starch. J Exp Bot 62:4547–4559

Takeda Y, Guan H-P, Preiss J (1993) Branching of amylose by the branching isoenzymes of maize endosperm. Carbohydr Res 240:253–263

Tenorio G, Orea A, Romero J et al (2003) Oscillation of mRNA level and activity of granule-bound starch synthase I in Arabidopsis leaves during the day/night cycle. Plant Mol Biol 51:949–958

Tetlow IJ, Beisel KG, Cameron S et al (2008) Analysis of protein complexes in wheat amyloplasts reveals functional interactions among starch biosynthetic enzymes. Plant Physiol 146: 1878–1891

Tiessen A, Hendriks JHM, Stitt M et al (2002) Starch synthesis in potato tubers is regulated by post-translational redox modification of ADP-glucose pyrophosphorylase: a novel regulatory mechanism linking starch synthesis to the sucrose supply. Plant Cell 14:2191–2213

Toivola J, Nikkanen L, Dahlström KM et al (2013) Overexpression of chloroplast NADPH-dependent thioredoxin reductase in Arabidopsis enhances leaf growth and elucidates in-vivo function of reductase and thioredoxin domains. Front Plant Sci 4:389

Tomlinson KL, Lloyd JR, Smith AM (1997) Importance of isoforms of starch-branching enzyme in determining the structure of starch in pea leaves. Plant J 11:31–43

Tyynelä J, Schulman AH (1993) An analysis of soluble starch synthase isozymes from the developing grains of normal and shx cv. Bomi barley (*Hordeum vulgare*). Physiol Plant 89:835–841

Ugalde JE, Parodi AJ, Ugalde RA (2003) De novo synthesis of bacterial glycogen: agrobacterium tumefaciens glycogen synthase is involved in glucan initiation and elongation. Proc Natl Acad Sci U S A 100:10659–10663

Utsumi Y, Nakamura Y (2006) Structural and enzymatic characterization of the isoamylase1 homo-oligomer and the isoamylase1–isoamylase2 hetero-oligomer from rice endosperm. Planta 225:75–87

Utsumi Y, Utsumi C, Sawada T et al (2011) Functional diversity of isoamylase oligomers: the ISA1 homo-oligomer is essential for amylopectin biosynthesis in rice endosperm. Plant Physiol 156:61–77

Valdez HA, Busi MV, Wayllace NZ et al (2008) Role of the N-terminal starch-binding domains in the kinetic properties of starch synthase III from *Arabidopsis thaliana*. Biochemistry 47:3026–3032

Valerio C, Costa A, Marri L et al (2011) Thioredoxin-regulated β-amylase (BAM1) triggers diurnal starch degradation in guard cells, and in mesophyll cells under osmotic stress. J Exp Bot 62:545–555

van de Wal M, D'Hulst C, Vincken J-P et al (1998) Amylose is synthesized in vitro by extension of and cleavage from amylopectin. J Biol Chem 273:22232–22240

Vrinten PL, Nakamura T (2000) Wheat granule-bound starch synthase I and II are encoded by separate genes that are expressed in different tissues. Plant Physiol 122:255–264

Wattebled F, Buléon A, Bouchet B et al (2002) Granule-bound starch synthase I. A major enzyme involved in the biogenesis of B-crystallites in starch granules. Eur J Biochem 269:3810–3820

Wattebled F, Dong Y, Dumez S et al (2005) Mutants of Arabidopsis lacking a chloroplastic isoamylase accumulate phytoglycogen and an abnormal form of amylopectin. Plant Physiol 138:184–195

Wattebled F, Planchot V, Dong Y et al (2008) Further evidence for the mandatory nature of polysaccharide debranching for the aggregation of semicrystalline starch and for overlapping functions of debranching enzymes in Arabidopsis leaves. Plant Physiol 148:1309–1323

Wu AC, Ral J-P, Morell MK et al (2014) New perspectives on the role of α- and β-amylases in transient starch synthesis. PLoS ONE 9:e100498

Yamanouchi H, Nakamura Y (1992) Organ specificity of isoforms of starch branching enzyme (Q-enzyme) in rice. Plant Cell Physiol 33:985–991

Yandeau-Nelson MD, Laurens L, Shi Z et al (2011) Starch-branching enzyme IIa is required for proper diurnal cycling of starch in leaves of maize. Plant Physiol 156:479–490

Zabawinski C, Van Den Koornhuyse N, D'Hulst C et al (2001) Starchless mutants of *Chlamydomonas reinhardtii* lack the small subunit of a heterotetrameric ADP-glucose pyrophosphorylase. J Bacteriol 183:1069–1077

Zeeman SC, Umemoto T, Lue W-L et al (1998) A mutant of Arabidopsis lacking a chloroplastic isoamylase accumulates both starch and phytoglycogen. Plant Cell 10:1699–1712
Zhang X, Colleoni C, Ratushna V et al (2004) Molecular characterization demonstrates that the *Zea mays* gene *sugary2* codes for the starch synthase isoform SSIIa. Plant Mol Biol 54:865–879
Zhang X, Myers AM, James MG (2005) Mutations affecting starch synthase III in Arabidopsis alter leaf starch structure and increase the rate of starch synthesis. Plant Physiol 138:663–674
Zhang X, Szydlowski N, Delvalle D et al (2008) Overlapping functions of the starch synthases SSII and SSIII in amylopectin biosynthesis in Arabidopsis. BMC Plant Biol 8:96

Chapter 7
Starch Degradation

Julia Smirnova, Alisdair R. Fernie, and Martin Steup

Abstract Degradation of starch (and of glycogen as well) converts carbohydrates accumulated as metabolically inert storage products back into forms that are usable for various biosynthetic and catabolic routes. Starch and glycogen share their basic biochemistry, but distinct physicochemical and enzymatic differences exist. Structural (dis)similarities of hydroinsoluble starch and hydrosoluble glycogen are briefly discussed. Various types of starch-degrading enzymes and their mode of action are presented. Features frequently observed in starch-degrading enzymes, such as carbohydrate-binding modules and secondary binding sites, are discussed including kinetic implications. Approaches to identify proteins functional in vivo starch degradation and their limitations are discussed. Three types of in vivo starch degradation are distinguished: degradation of transitory starch, mobilization of reserve starch in dead tissue, and that in living cells. Most of the current biochemical knowledge of starch degradation relates to mobilisation of transitory starch. We discuss this process in the context of cellular organisation and location/distribution of starch granules within the cell. Transitory starch degradation is initiated at the granule surface and includes local transitions from a hydroinsoluble ordered to a soluble state. Transition is facilitated by iterating cycles of phosphorylating and dephosphorylating reactions that act on starch-related glucosyl residues. In the

J. Smirnova
Max-Planck-Institute of Molecular Plant Physiology, Department 1 (Willmitzer), Am Mühlenberg 1, 14476 Potsdam-Golm, Germany

Institute of Biochemistry and Biology, Department of Plant Physiology, University of Potsdam, Karl-Liebknecht-Str. 20-25, Building 20, 14476 Potsdam-Golm, Germany

Institute of Biophysics and Medical Physics of the Charité, Universitätsmedizin Berlin, Campus Berlin Mitte, 10117 Berlin, Germany

A.R. Fernie
Max-Planck-Institute of Molecular Plant Physiology, Department 1 (Willmitzer), Am Mühlenberg 1, 14476 Potsdam-Golm, Germany

M. Steup (✉)
Institute of Biochemistry and Biology, Department of Plant Physiology, University of Potsdam, Karl-Liebknecht-Str. 20-25, Building 20, 14476 Potsdam-Golm, Germany

Department of Molecular and Cellular Biology, University of Guelph, Guelph, ON, N1G 2W1 Canada
e-mail: msteup@uni-potsdam.de

Y. Nakamura (ed.), *Starch*, DOI 10.1007/978-4-431-55495-0_7

stroma, four main products are synthesised by highly interconnected paths and are then exported into the cytosol. Plastidial transporters and cytosolic downstream processes are presented which link starch degradation to biosynthetic or degradative routes all originating from the cytosol. Finally, current views on plastidial transitory starch degradation as controlled by the cytosol are discussed.

Keywords Amylose • Amylopectin • Glycogen • Carbohydrate-active enzymes • Carbohydrate-binding module (CBM) • Reserve starch • Secondary binding site (SBS) • Starch degradation • Starch modification • Transitory starch

7.1 Introduction

Higher plants often withdraw reduced carbon compounds from ongoing metabolic processes by accumulating a storage carbohydrate that is both osmotically inert and metabolically inactive. As a highly efficient form to store carbon, capacity to metabolise starch is more than a billion years old going back to the establishment of chloroplast-containing cells. By starch degradation, reduced carbon is converted back into a metabolically active state which can easily be utilised by many paths of the plant. For photoautotrophic organisms, the day–night cycle periodically causes interruptions of photosynthesis and large alterations of the intracellular carbon fluxes. It usually is associated with changes in the environmental temperature. Under natural conditions, length of light and dark periods generally varies throughout the year.

Environmental variations, such as changes in temperature, act also on heterotrophic tissues, organs, or plants which indirectly depend on the carbon fixation performed by photoautotrophic cells. They may, however, not be directly exposed to the light and dark periods. Seedlings completely rely on the degradation of storage products that have been accumulated by the mother plant until they are photosynthesis competent and the environmental conditions permit photoautotrophic growth. As starch is degraded under variable external conditions, the entire process must be precisely regulated to reliably provide reduced carbon to living cells and to prevent carbon starvation. Starch degradation is also performed by many non-plant organisms, such as bacteria or animals. Although the basic enzymology of non-plant starch degradation is similar, it deviates in several aspects from that of plants and is not considered here.

Compared to other biopolymers, chemical features of starch are simple as it is essentially built of a single monosaccharyl type, i.e. the α-D-glucosyl moiety, and contains only two types of interglucose linkages, namely α-1,4- and α-1,6-bonds. Furthermore, glucosyl residues are covalently modified with a very low frequency. Despite its chemical simplicity, the physical order of the glucosyl moieties and of the α-glucan chains within native starch is complex and has not yet been fully elaborated. To the best of our knowledge, no cell-free synthesis of starch-like particles has yet been reported.

The structural complexity of native starch is mirrored by both the complex starch-related biochemistry and the multiple control of the expression of starch-related genes, all of which are located in the nucleus. Turnover of plastidial starch is assumed to be based on a close collaboration of 30–40 (iso)enzymes directly or indirectly involved in forming or cleaving interglucose bonds (Deschamps et al. 2008), but these numbers are likely to underestimate the biochemical complexity. Heteromeric protein complexes are functional that enable the plastid to temporarily and locally combine several enzyme activities (Hussain et al. 2003; Bustos et al. 2004; Delatte et al. 2005; Kubo et al. 2010; Emes and Tetlow 2012; Sundberg et al. 2013; Sim et al. 2014; see Chap. 8 this volume). Mechanisms of forming and targeting the complexes to distinct areas of starch granules as well as their disassembly are largely unknown. Repeatedly, 14-3-3 proteins have been reported to be directly involved in the regulation of starch metabolism (for details see Denison et al. 2011), but their action is incompletely understood. Additional plastidial or extraplastidial proteins essentially lacking catalytic activity affect starch metabolism (Zeng et al. 2007; Fulton et al. 2008; Isshiki et al. 2008; Lohmeyer-Vogel et al. 2008; Li et al. 2009; Fu and Xue 2010; Yin and Xue 2012). Some starch-regulating genes encode transcription factors, such as β-amylase-like proteins (Reinhold et al. 2011; Soyk et al. 2014) and the starch biosynthesis regulator1 (RSR1) which indirectly affects starch properties by controlling the expression of genes encoding reserve starch biosynthetic enzymes (Fu and Xue 2010). Finally, some structural features of native starch may spontaneously arise due to self-organisation of α-glucan chains, but, possibly, proteins facilitate this process (Hejazi et al. 2010; Regina et al. 2012).

During the last decades, starch and starch-related biochemistry have attracted interests from a wide range of disciplines including applied sciences (see also Chaps. 10, 11, and 12 this volume), non-linear optics and molecular medicine. Novel enzymes and transporters have been discovered now considered to be essential for starch metabolism. Metabolic routes that for decades were presented in textbooks had to be refined.

Carbon fluxes towards and from starch certainly affect the carbon status of a cell. A disturbed leaf starch turnover often results in reduced size of the entire plant, and essentially all processes controlling plant growth and development are, via sugar sensing, directly or indirectly linked to starch turnover (Moghaddam and Van den Ende 2012; Sparks et al. 2013; Ruan 2014; Häusler et al. 2014; Lastdrager et al. 2014; Pfister et al. 2014; Schmitz et al. 2014). In addition, transitory starch metabolism is also closely coupled to processes previously thought to be unrelated to starch, such as polysome loading and protein biosynthesis (Pal et al. 2013).

Rates of assimilatory starch synthesis and degradation are also controlled by the circadian clock. Transitory starch degradation is carefully balanced to prevent carbon starvation but also to ensure that more than 90 % of the carbon stored is mobilised even when length of and temperature during the dark period vary (Graf et al. 2010; Graf and Smith 2011; Paparelli et al. 2013; see below).

In autotrophic and heterotrophic tissues, starch granule formation is closely linked to plastid division (Yun and Kawagoe 2010; Crumpton-Taylor et al. 2013). Under some conditions, however, starch-derived compounds destabilise

chloroplasts and, finally, lead to lysis of the entire organelle (see below). Because of these manifold interactions, it is increasingly difficult to strictly distinguish starch-related genes or gene products and those unrelated to starch.

Recently, starch metabolism has been widely accepted as an area that permits to successfully study early evolutionary processes leading to the formation of a photosynthesis-competent eukaryote. Metabolism of starch is thought to originate from that of glycogen functional in the host. Transition from glycogen to starch was, however, a multistep process and some recent algal groups appear to represent intermediate stages of this transition (Ball et al. 2011; Ball 2012; Cenci et al. 2014; see also Chap. 4 this volume).

Last, but not least, fundamental enzymatic processes leading to accumulation and mobilisation of storage carbohydrates appear to be similar in plants and animals. Mammalian mutations that cause disturbed glycogen metabolism are usually associated with several severe diseases designated as glycogen storage diseases (GSDs). Therefore, seemingly very distant areas of life sciences, i.e. molecular medicine and plant biochemistry, have started to closely interact (Gentry et al. 2007, 2013; Nitschke et al. 2013).

Several comprehensive reviews discussing various aspects of starch metabolism in plants have been published in the last years (Fettke et al. 2009; Keeling and Myers 2010; Kötting et al. 2010; Zeeman et al. 2010; Stitt and Zeeman 2012; Sonnewald and Kossmann 2013; Zhang and Wing 2013; Zhou et al. 2013; Lloyd and Kossmann 2015). Here we present some recent results, views and developments in the field of starch degradation in higher plants. Because of space limitation, the review is largely restricted to plants that perform C3 photosynthesis and utilize starch as their dominant carbon store.

7.2 (Bio)Chemical and Structural Properties of Starch and Glycogen

In the following, basic information on internal structure and morphology of native starch particles is given (see also Chaps. 1, 2, 3, and 13 this volume). We then discuss both similarities and differences in starch and glycogen, the common storage polysaccharide in most heterotrophic organisms, and briefly mention wild-type higher plants that simultaneously form starch and glycogen.

7.2.1 Starch and Glycogen Share Chemical and Functional Features but Differ in Some Physicochemical and Biochemical Properties

Starch is deposited as hydroinsoluble, highly dense particles designated as granules. The internal structure of starch particles seems to be evolutionarily conserved

(Buléon et al. 1998; Zeeman et al. 2010; Bertoft 2013). By contrast, both size (diameters ranging from 0.1 to 100 μm) and morphology of native starch vary largely, depending on plant species and organ (Jane et al. 1994; Cenci et al. 2014). In many species and/or tissues, the entire starch particle population consists of a single granule type. In other cases, such as the endosperm of wheat, barley, rye and triticale, the same cell, however, forms several granule populations (designated as A, B and C type; please note that this classification is unrelated to the starch allomorph) that differ in size, time of appearance and biochemical features (Stoddard 1999; Peng et al. 2000). Furthermore, up to several dozen small non-fusing particles (each of which is polyhedral and possesses a diameter of 3–8 μm) may form a functional unit designated as compound starch (Jane et al. 1994). As an example, the rice endosperm massively accumulates this starch type.

Given that starch structure and biochemistry actually permit an essentially unlimited particle growth, it is unexpected that in higher plants granule populations largely differ in average size and size distribution. For various reasons, cells appear to arrest granule growth at largely different biosynthetic stages (see also Huang et al. 2014; Mahlow et al. 2014). Recently described proteins, such as SSG4 and FLO6, are likely involved in defining starch particle sizes (Matsushima et al. 2014; Peng et al. 2014), but plastidial and/or cellular mechanisms are unknown that permit sensing and controlling of granular volume.

Typically, starch granules are composed of two types of polyglucan molecules designated as amylopectin and amylose. The former is dominant in terms of both quantity and relevance for the internal granule structure (see below), but amylose might stabilise structural elements formed by amylopectin (Bertoft 2013; see Chaps. 1 and 3 this volume). Amylopectin and amylose are disperse α-glucans; the average size of amylopectin usually exceeds that of amylose. Several methods are used to distinguish and/or to physically separate both polyglucan types, including the absorption spectrum of the iodine-starch complexes, gel filtration or treatment of solubilised starch with butanol-isoamyl alcohol. It is, however, uncertain whether these methods permit a reliable distinction and/or separation of the two types of α-glucans if, due to genetic reasons, starch is massively altered (Vilaplana et al. 2012).

In amylose, amylopectin and glycogen, α-1,4-interglucose bonds are the dominant interglucose linkages. They result in elongation and formation of a left-handed helical structure of α-glucans or glucan chains. Helices of at least 18 α-1,4-interlinked glucosyl residues appear to selectively react with iodine (Bailey and Whelan 1961). Because of its short helical regions, glycogen is poorly stained by iodine.

In the three α-glucan types mentioned above, branching is formed by α-1,6-interglucose bonds which account for less than 10 % of the total interglucose linkages. By each branching, the number of nonreducing end(s) per polyglucan molecule increases by one, but the single reducing terminus remains unchanged.

The term ‘amylose’ designates a heterogeneous mixture of α-glucan molecules possessing a wide range of degrees of polymerisation (DP). Based on the total number of interglucose linkages, amylose contains less α-1,6-interglucose bonds (not exceeding 1 % of the total interglucose bonds) than amylopectin or lacks

branchings completely (see also Chap. 2 this volume). In aqueous solution, amylose forms a flexible random coil including left-handed helical segments that tend to be favoured at low hydration levels. The crystalline structure of isolated amylose has been determined, but it is strongly affected by chain length distribution and other parameters (Nishiyama et al. 2010; Putaux et al. 2011; Roblin et al. 2013). In addition, non-amylose compounds, such as lipids, strongly interact with amylose (López et al. 2012). As inside the starch granule, neighbouring compounds may exert similar effects, the in vivo structure(s) of amylose remains uncertain. Amylose appears to be unevenly distributed within the granule (Pérez and Bertoft 2010; Buléon et al. 2014).

In amylopectin, approximately 5–7 % of all interglucose bonds are branchings. Due to clustering, vicinal α-glucan side chains are capable of forming parallel double helices which then are arranged in a defined physical order yielding the A-type or the B-type starch allomorph.

While the actual amylopectin structure(s) remains hypothetical, it is widely accepted that several structural features of native starch granules are determined by intra- and/or intermolecular organisation of amylopectin (for details see Pérez and Bertoft 2010; Bertoft 2013; see also Chap. 1 this volume).

In higher plants, metabolism and function of plastidial starch appear to be related to those of cytosolic glycogen which in most heterotrophic eukaryotic cells serves as storage polysaccharide. The overall branching frequency of mammalian glycogen is in a similar range as that of amylopectin (Ball et al. 2011), but branching points are more evenly distributed in glycogen than in amylopectin (Roach et al. 2012; Cenci et al. 2014). Probably interconnected with the more even distribution of branchings, two major physicochemical differences exist between starch particles and glycogen molecules: Glycogen is typically hydrosoluble but, when hydroinsoluble, is associated with severe diseases such as epilepsy (Minassian et al. 1998; Pederson et al. 2013; Gentry et al. 2013). For steric reasons glycogen is predicted to have an upper size limit (approximately 40 nm diameter; Meléndez-Hevia et al. 1993). Likewise, empirically determined diameters of glycogen (β-particles) rarely exceed 45 nm. Larger glycogen particles (α-particles) are exclusively formed by closely associated (but not covalently linked) β-particles (Ryu et al. 2009; Sullivan et al. 2014).

Eukaryotic biosynthesis of starch and glycogen largely relies on the same two reaction types, chain elongation and branching. Chains are elongated by repetitive glucosyl transfers from a donor molecule to the nonreducing end(s) of a given α-glucan forming additional α-1,4-interglucose bonds. ADP-glucose is the most common glucosyl donor for starch biosynthesis. Eukaryotic glycogen formation relies on UDP-glucose, whereas prokaryotes often use ADP-glucose. In all cases, glucosyl transfer reactions result in a strictly directional chain growth (for details see Fujita and Nakamura 2012; Roach et al. 2012) and massively alter size (DP), but the molar amounts of α-glucans remain unchanged. Formation of α-1,6-interglucose bonds causes branching of chains and does not alter molar amounts nor the total DP of α-glucans as glucan chains act both as glucanosyl donor and acceptor.

In amylopectin, clustering of branchings is essential for double-helix formation. According to the model of ‘glucan trimming’ (or of ‘preamylopectin processing’),

clustering is achieved by hydrolysing excess branches mediated by a single or several isoamylase complex(es) that selectively or preferentially act(s) during biosynthesis of amylopectin (Ball and Morell 2003; Fujita et al. 2003, 2009; Kubo et al 2005; Sim et al. 2014; see also Chap. 5 this volume). Recent studies performed with double or multiple knockout mutants from *Arabidopsis* suggest that starch granule biosynthesis requires a carefully balanced ratio of chain elongation and branching reactions. Disturbance of this balance appears to favour amylolysis of α-glucan chains and/or formation of a plastidial hydrosoluble glycogen-like polyglucan, designated as phytoglycogen (Wattebled et al. 2005). In *Arabidopsis* leaves, the amount of the latter storage carbohydrate undergoes dial fluctuations, but its turnover does not allow normal growth of the entire plant (Streb et al. 2008, 2012; Pfister et al. 2014). Glycogen, by contrast, appears to be formed without any trimming.

7.2.2 Starch and Glycogen-Like Polysaccharides Formed Within a Single Organism

Only few higher plant wild-type species, such as *Cecropia peltata* (Bischof et al. 2013) and *Ryparosa kurrangii* (Webber et al. 2007), synthesise both starch and a glycogen-like hydrosoluble α-polyglucan. Both carbohydrate stores are formed in plastids but are functionally diverse and physically separated as they reside in different cell types. Starch is the general carbon storage product of mesophyll cells. By contrast, glycogen-like α-glucans are restricted to plastids of some highly specialised organs/tissues collectively designated as food bodies. They form a heterogeneous group of multicellular systems occurring in those plants only that mutualistically interact with ants. Until now, only glycogen-like polysaccharides from *Cecropia peltata* have been characterised in more detail (Bischof et al. 2013).

Mesophyll cells of some higher plant mutants, however, form both starch and a hydrosoluble glycogen-like α-polyglucan designated as phytoglycogen. In *Arabidopsis* the two carbohydrate stores are synthesised when isoamylase isozyme 1 (ISA1) involved in preamylopectin processing is lacking (Zeeman et al. 1998; Delatte et al. 2005; Wattebled et al. 2008). This phenotypical feature points again to a similar enzymatic apparatus required for starch and glycogen metabolism.

7.2.3 Major Starch Pools in Higher Plants

Higher plants usually contain several major starch pools that are functionally divers and interconnected by whole-plant partitioning of carbohydrates (Fig. 7.1). Biosynthesis of transitory (or assimilatory) starch is locally and temporarily immediately linked to photosynthesis as it proceeds in the stroma of photosynthesising chloroplasts. In the subsequent dark phase, transitory starch is often degraded.

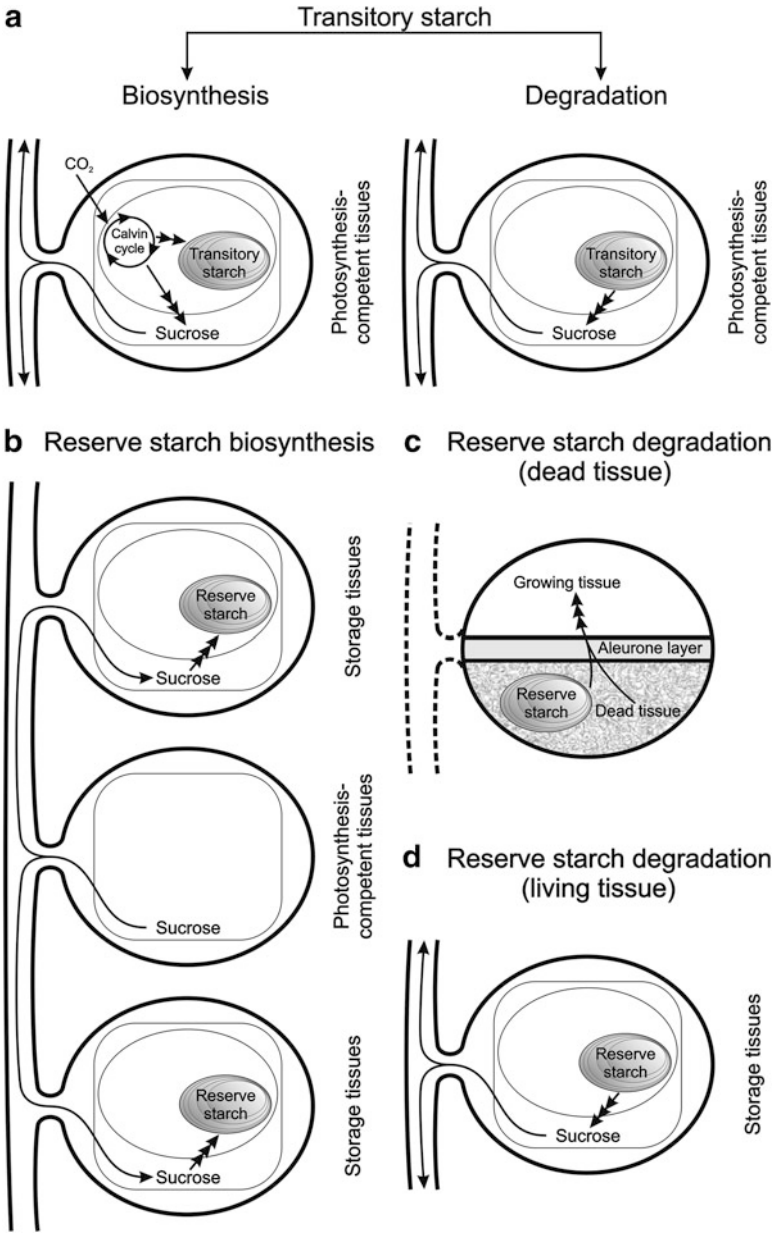

Fig. 7.1 Major starch pools in higher plants
(**a**) Transitory (synonymous with assimilatory) starch is formed by photosynthesising chloroplasts and is restricted to source organs. Biosynthesis is driven by intermediates of the Calvin cycle and occurs only during illumination. In darkness, typically most of the transitory starch is degraded and converted to transport metabolites, such as sucrose. Metabolism of assimilatory starch, therefore, consists of iterating phases of biosynthesis and degradation

Thus, leaves often perform many diel cycles of biosynthesis and degradation of transitory starch in the same organelle. Utilisation of transitory starch is essentially restricted to the individual plant that forms it. In terms of evolution, transitory starch constitutes the by far oldest starch pool (Ball et al. 2011; Facchinelli et al. 2013; Cenci et al. 2014; Nougué et al. 2014).

Another major proportion of the reduced carbon gained by photosynthesis is either temporarily stored in the vacuole or used to synthesise transport metabolites which, in many plant species, largely consist of sucrose. Transport metabolites move from mesophyll cells of source organs into the phloem and, via long distance transport, are then approaching sink organs which often massively accumulate another starch pool designated as reserve starch (Turgeon and Wolf 2009; De Schepper et al. 2013). During illumination, biosynthesis of reserve starch is mainly driven by intermediates linked to the reductive pentose phosphate cycle in source organs. During darkness, reserve starch biosynthesis relies on the nocturnal conversion of transitory starch to sucrose or to other transport metabolites. Unlike the metabolically more active transitory starch, reserve starch is often continuously formed over several weeks. The amount of reserve starch per plant frequently exceeds that of transitory starch. Reserve starch is essential for growth and development of plant seedlings during those periods of time in which photosynthetic carbon fixation is impossible. It is, however, also relevant for various non-plant uses, such as food of animals or humans and as starting material for various technological applications including energy conversion (Zeeman et al. 2010). In addition, minor starch pools largely unrelated to the central carbon metabolism exist in higher plants and as such will not be considered here.

While reserve starch is consistently synthesised in living cells of sink organs, its mobilisation separates two major subgroups as starch can be degraded in either living cells or dead tissue (Fig. 7.1). Starch metabolism differs in both subgroups. Reserve starch degradation in living cells occurs in differentiated storage organs, such as potato tubers, yam roots, cotyledons or the endosperm of many dicots, as well as in more specialised duration organs, such as the turions from Lemnaceae. In all these cases, starch is degraded over several days or weeks following transition of the organ or of parts of it from sink to source. Several cycles of biosynthesis and

Fig. 7.1 (continued) (**b**) Reserve starch formed in nongreen plastids of sink organs is continuously synthesised over an extended period of time which largely exceeds a single light period. It utilises transport metabolites derived from either Calvin cycle intermediates or from starch. Reserve starch biosynthesis often is a major determinant of the strength of the sink. In terms of quantity, reserve starch frequently exceeds that of transitory starch. Size, shape and allomorph of the reserve starch granules often differ from those of the assimilatory starch synthesised by source organs of the same plant

(**c**) Following an extended period of reserve starch biosynthesis, the starch-containing tissue may undergo apoptosis as typical for cereal seeds. Degradation products obtained by lysis of the entire tissue are imported by living cells

(**d**) Reserve starch is degraded in living cells permitting a limited number of starch synthesising and degrading phases

degradation can occur within the same tissue, although the turnover is slow and the turnover number is low as compared to assimilatory starch (see Sect. 7.4.1.2).

In the other subgroup, typically represented by the endosperm of cereal seeds, reserve starch is degraded following a period of desiccation. During this period the starch-storing tissues or organs undergo one of the various selective apoptosis programmes of higher plants. Subsequently, starch is mobilised extracellularly. Degrading enzymes have either been deposited during starch biosynthesis within the granules in a catalytically inactive state or are synthesised at the onset of starch degradation in surrounding living cells and are then exported to the dead tissue. Reserve starch mobilisation is closely associated with the enzymatic degradation of the entire starch-storing tissue including lysis of proteins and cell wall materials. Products derived from the various degradation processes are resorbed by vicinal living cells or tissues and are then recycled for further uses until the seedling reaches photosynthesis competence. In this subgroup of starch degradation, only the onset of reserve starch degradation (which is closely associated with seed germination) can be controlled and, subsequently, rates of degradation can be modulated. Another period of starch synthesis, however, cannot be initiated once desiccation occurred (see Sect. 7.4.1.1).

7.3 Current Knowledge of Starch-Degrading Pathways

During the last decades, the view on in vivo starch-degrading paths has been largely altered. In most cases progress achieved relates to transitory starch, whereas biochemical knowledge of reserve starch degradation is less advanced (Vriet et al. 2010; Tanackovic et al. 2014). In the following we discuss both advantages and limitations of the genetic approaches used and summarise the current knowledge as to how starch-degrading enzymes act under in vitro and in vivo conditions.

7.3.1 Identification of Starch-Degrading Gene Products by Using Knockout Mutants

When grown under normal conditions, mutants of higher and lower plants that are impaired in transitory starch degradation often gradually accumulate more starch than the wild-type resulting in a starch-excess phenotype. Furthermore, this phenotype is often retained following prolonged darkness. Time dependence and degree of starch excess, however, may largely vary depending on the plant species and the gene affected. The macroscopic phenotype of these mutants can qualitatively be tested by iodine staining of decolorised leaves or cells, and therefore, a large number of potentially relevant lines can be screened within a short period of time. After selecting the respective mutants, the affected gene locus is determined. In the past, this approach led to the discovery of novel starch-related proteins that

are functional inside the plastid, in the cytosol (see below) or even in the nucleus (Reinhold et al. 2011). Furthermore, novel transporters of the inner plastidial envelope membrane were identified that mediate the export of starch-derived maltose or glucose (Niittylä et al. 2004; Cho et al. 2011). In addition, bioinformatic approaches were used to search for novel genes that possess sequence similarities to identified starch-related genes or even to non-plant genes. By using these tools, genes may, however, be identified whose products have a dual or multiple function also acting in other paths, such as starch biosynthesis, or even in routes unrelated to starch metabolism. Detailed biochemical analyses, therefore, are required to fully determine the function(s) of a given gene product.

The procedures outlined above may, however, fail to detect any starch-excess phenotype when single knockout mutants can compensate the loss of function by altering carbon fluxes. For compensation, either existing paths are used or novel routes are established. In either case, the phenotype of the respective mutant will be close to or even indiscernible from that of the wild-type. In the undisturbed (i.e. wild-type) plant the gene product of interest may, however, participate in the analysed path. Similarly, contradicting phenotypical features of mutants from different plant species that are affected in essentially the same gene are ambiguous as they may reflect either species-dependent differences in the undisturbed metabolic paths or, alternatively, different abilities of compensating a loss of function (Asatsuma et al. 2005; Yu et al. 2005). Furthermore, compensating degradative paths may possess an overlapping but not identical temperature dependence as compared to the blocked route as it has been observed in starch biosynthesis (Satoh et al. 2008; Fettke et al. 2012b). If so, screening conditions may strongly affect identification of mutants. Finally, in *Arabidopsis thaliana* a single constitutive knockout of a starch-related gene can be associated with altered expression levels of more than 100 other genes, and therefore, the resulting phenotype may be caused by complex alterations of gene expression rather than by the loss of function of a single gene product (Comparat-Moss et al. 2010).

Starch metabolism (as well as that of glycogen; Wilson et al. 2010; Gentry et al. 2013) tends to be closely integrated into the entire biology of the respective cell and organ. Thus, a distinct block in starch degradation may even result in signalling processes that finally lead to disintegration of the entire chloroplast. If so, older leaves gradually loose photosynthetic capacity containing less starch and chlorophyll as compared to young leaves. Chloroplasts are disintegrated in several mutants impaired in transitory starch degradation but remain functional when essentially starch-free mutants are used as genetic background (Stettler et al. 2009; Cho et al. 2011; Malinova et al. 2014). Chloroplast disintegration appears to be related to the large group of sugar-mediated signalling effects (for review see Eveland and Jackson 2012; Ruan 2014), but neither the chemical nature of the signalling molecule(s) nor the subcellular site(s) of biosynthesis has been determined. Furthermore, it is unclear whether the various metabolic blocks all give rise to the same signal(s) or various mechanistically different but phenotypically similar cellular responses exist. In any case, chloroplast disintegration massively alters central carbon metabolism and may also significantly

affect screening procedures. Mutants containing inducible RNAi constructs may offer some advantages as compared to constitutive knockout lines (Weise et al. 2012; Martins et al. 2013).

7.3.2 How to Define 'Starch-Degrading Enzymes'?

Frequently, the term 'starch-degrading enzymes' lacks any precise definition. In a strict sense, it may designate enzymes using native starch as carbohydrate substrate, but for several reasons, this definition is not meaningful. Enzymes acting on starch granules often are capable to utilise solubilised α-glucans as well (and, possibly, even at higher rates; see below). Furthermore, structural alterations at the surface of native starch may favour local accessibility of degrading enzymes, but these processes are often not fully understood. The term 'starch' itself is ambiguous as it frequently designates both native particles and granule-derived hydrosoluble α-glucans containing both amylose and amylopectin. Finally, isolation of starch granules intends to retain in vivo structures of the particles, but minor artificial changes occurring unnoticed cannot be excluded.

For practical reasons, we use here a wider definition of 'starch-degrading enzymes'. We define plastidial and cytosolic enzymes as starch-degrading when they are likely to operate in starch-degrading paths and in vitro act on starch or on α-glucans (including glycogen and maltodextrins) that are chemically similar to starch. Most of these enzymes cleave interglucose bonds. We do, however, include those enzymes that do not act on interglucose bonds per se but are functionally related to their cleavage by other enzymes. This definition does not, however, imply that starch-like α-glucans act as in vivo substrate of the respective enzyme. Under in vivo and/or in vitro conditions, the catalytic action of a 'starch-degrading enzyme' may even lead to an increase in the DP of an α-glucan. Furthermore, 'starch-degrading enzymes' may also be involved in other processes.

7.3.3 Cleavage of Interglucose Bonds by Starch-Degrading Enzymes from Higher Plants

Interglucose bonds are cleaved by transferases that depending on the carbohydrate moiety transferred, the reaction mechanism used, the target bond cleaved and chemical features of the acceptor can be grouped into various enzyme types, each of which may be represented by several isozymes. We include enzymes mediating 'disproportionating reactions' that, within a single catalytic cycle, cleave and form interglucose linkages (Fig. 7.2).

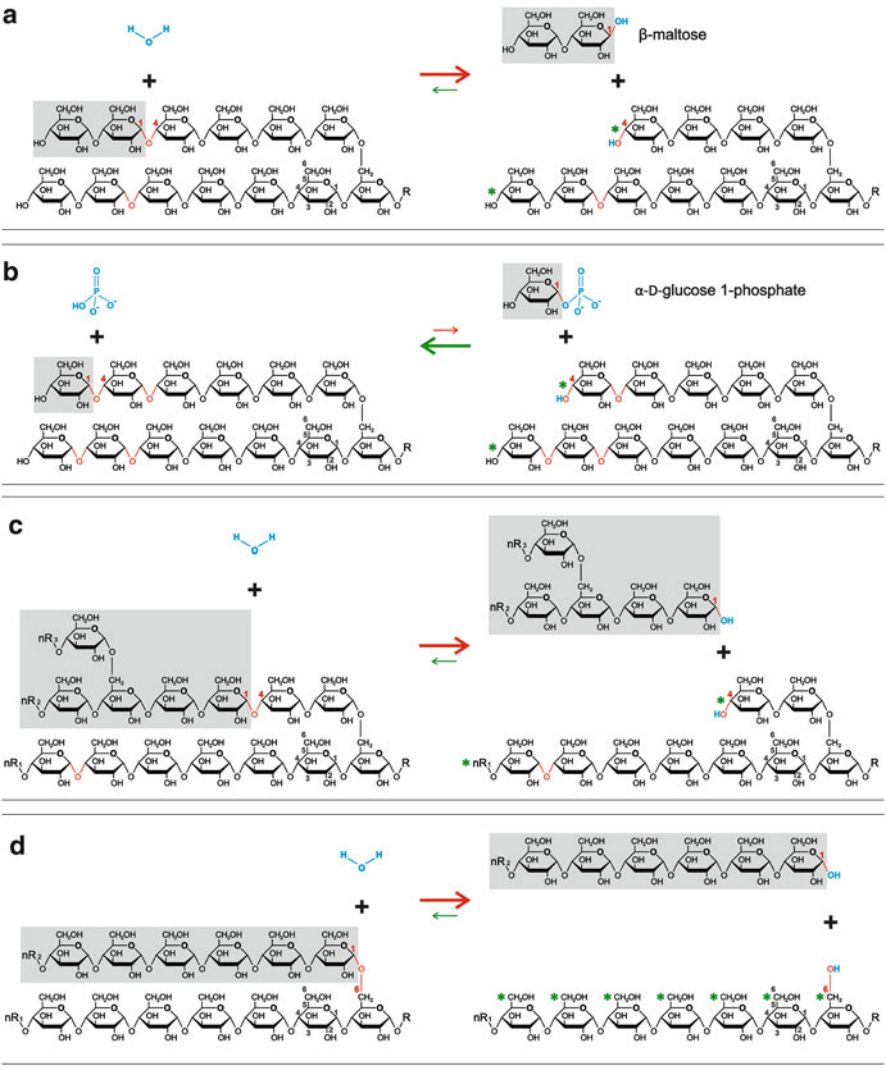

Fig. 7.2 Enzymatic actions of starch-degrading enzymes on interglucose bonds of α-glucans
For the sake of clarity, not all non-reducing ends of α-glucan chains have been labelled. (**a**) *Directed action of β-amylases*. On the *left*, an A-type (*upper row*) and a B-type (*lower row*) α-glucan chain of a branched α-glucan are shown together with a water molecule (*blue*). The A-type chain is linked to the B-type chain by a single α,1-6-interglucose bond but does not carry any further branching. Both a single β-maltosyl residue and a free β-maltose are marked in grey. An α-1,4-interglucose bond of the B chain (*lower row*) can also act as target of a hydrolytic action of β-amylases (marked in *red*). Vicinity of target bonds relative to branching point is shown randomly. Although thermodynamically favoured, hydrolytic reactions are reversible. For condensation, the nonreducing end of the A chain (*upper row* on the *left* side) and of the B chain (both marked with a *green asterisks*) potentially acts as a β-maltosyl acceptor. Carbon atoms 1 and 4 are marked in some glucosyl residues. R: glucanyl residue containing the reducing end of a chain. Directed hydrolysis is given by a *red arrow*. Condensation is indicated by a *smaller arrow* in *green*

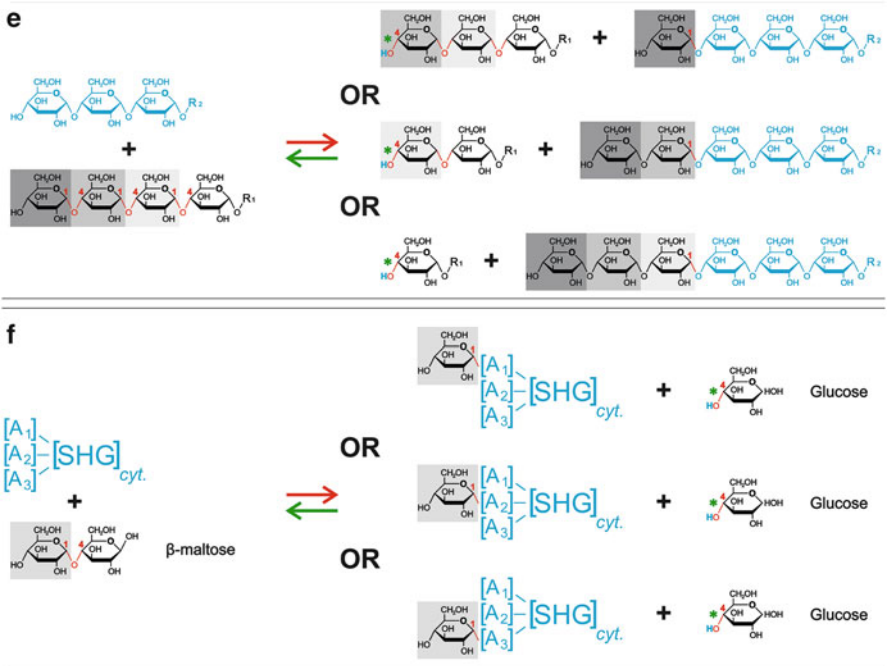

Fig. 7.2 (continued) (**b**) *Directed action of phosphorylases*. On the *left*, an A-type and a B-type chain (as in Fig. 7.2a) are shown. Orthophosphate (*left side*) and α-D-glucose 1-phosphate (*right side*) are also given. A single glucosyl transferred from the nonreducing end of the A chain to orthophosphate yielding α-D-glucose 1-phosphate is marked in *grey*. As a potential target for an enzymatic action, the terminal α-1,4-interglucose bond of the B chain is also given in *red*. Furthermore, two other interglucose bonds are labelled in *red* as potential targets for subsequent phosphorolytic actions. The phosphorolytic reaction is indicated by a *red arrow*. In the reverse reaction, the nonreducing end (*green asterisks*) of the A and the B chain acts as glucosyl acceptor. The glucan synthesising reaction is indicated by a *larger arrow* (*green*) as V_{max} exceeds that of phosphorolysis. Vicinity of the target bonds relative to the branching point is shown randomly. In some glucosyl residues, carbon atoms 1 and 4 are indicated. R: a glucanyl residue containing the reducing end

(**c**) *Non-directed action of α-amylases*. On the *left*, a branched α-glucan and a water molecule (*blue*) are shown. The α-1,4-interglucose bond to be hydrolytically cleaved (B chain; *left side middle row*) is labelled in *red* and the α-glucanyl residue to be liberated by endohydrolysis of a single α-1,4 interglucose is marked in *grey*. On the *right*, the α-glucan liberated (consisting of both an A and a B chain) is marked in *grey*. This glucan enters the pool of branched hydrosoluble α-glucans. A further interglucose bond of the B chain (*red*) is a target for another action of α-amylases. Vicinity of target bonds relative to the branching points is shown randomly. Hydrolysis is thermodynamically favoured and indicated by a *red arrow*. For the reverse reaction (condensation; *small green arrow*), a potential acceptor site for the glucanyl transfer is also marked (*Green asterisks*). In some glucosyl residues, carbon atoms 1 and 4 are labelled. R: glucanyl residue containing the reducing end (C chain). nR1, nR2 and nR3: glucanyl residues containing the nonreducing end of the C, B and A chains, respectively

7.3.3.1 Exo-hydrolases (β-Amylases)

The quantitatively most prominent exo-hydrolases acting on α-glucans are β-amylases (glycoside hydrolase family 14; GH14) which typically transfer maltosyl residues from the nonreducing end of a linear α-glucan or of an α-glucan chain to water following an inverting (i.e. single replacement) mechanism. Thereby, the anomeric carbon is converted from α- to β-configuration and β-maltose is released (Fig. 7.2a). Subsequently, the same α-glucan or glucan chain may act further as maltosyl donor until a minimum distance to either the reducing end or to a branching point is reached. Although additional reaction types have been reported for β-amylases (Hehre et al. 1979, 1986; Mikami et al. 1994; Fazedas et al. 2013), formation of β-maltose appears to be their main starch-related activity. This concurs with the starch-excess phenotype of transgenic potato plants lacking a functional plastidial β-amylase (Scheidig et al. 2002). β-Amylases completely convert linear α-glucans to maltose (plus a maltotriose if the initial DP equals $2n-1$), but branched α-glucans are incompletely degraded as exo-hydrolases cannot bypass any

Fig. 7.2 (continued) (**d**) *Direct debranching of α-glucans*. Following hydrolysis of a single α-1,6-interglucose bond, the A chain (*grey*; *left*) is released as a linear α-glucan whose free carbon atom 1 (reducing end) is in the α-configuration and the α-glucan released enters the pool of hydrosoluble α-glucans. Direct debranching is thermodynamically favoured and given as *red arrow*. Due to the reversibility of enzyme-mediated reactions, the reverse reaction cannot be excluded (*small green arrow*). For this direction, potential acceptor sites are marked (*right side* carbon atoms 6; *Green asterisks*). In some glucosyl residues, carbon atoms 1 and 6 are marked. R: glucanyl residue containing chain C and the reducing end. nR1: glucanyl residue of the B chain containing the nonreducing end. nR2: glucanyl residue of the A chain containing the nonreducing end
(**e**) *'Disproportionating reactions' as mediated by the plastidial disproportionating enzyme 1 (DPE1)*. For the DPE1-mediated reactions, two linear oligoglucans are substrates. One is donor (*left side lower row*) and the other one is acceptor (*left side upper row*; *blue*) for a transfer of a carbohydrate residue consisting of one to three glucosyl moieties. Depending on the size of the α-glucanyl residue, transferred rates of the transfer differ largely. When acting on two maltotriose molecules, the enzyme forms maltopentaose plus glucose or maltotetraose plus α-maltose. Both transfer reactions are easily reversible as indicated by two *arrows* equal in size. Due to multiple and easily reversible transfer reactions, DPE1 generates a polydisperse α-glucan mixture. Both the sum of the interglucose bonds and the total amount of glucosyl moieties distributed in the reaction mixture remain constant
(**f**) *'Disproportionating reactions' as mediated by the cytosolic disproportionating enzyme 2 (DPE2)*. A disaccharide, typically β-maltose, acts as donor (*left side lower row*) and cytosolic heteroglycans (SHG_{cyt}; *left side*; marked as *blue*) as acceptor of a glucosyl residue (marked in *grey*). Heteroglycans are branched glycans and carry several nonreducing ends as potential acceptor sites. Some details of the glucosyl transfer are still hypothetical. Three sites (A_1 to A_3) are shown but neither the number of sites nor the selecting mechanism(s) is known. The acceptor sites may be formed by terminal glucosyl and/or by other terminal sugar residues. The interglucose bond in β-maltose that is cleaved when the disaccharide acts as glucosyl donor is marked in *red*. In some glucosyl moieties, carbon atoms 1 and 4 are labelled. Several reversible transfer reactions are possible that all mediate the formation of glucosylated heteroglycans and release free glucose (*right side*). Glucosyl transfer is easily reversible as indicated by the two *arrows* equal in size. For further information, see text

branching point. Typically, plants contain a relatively high number of β-amylase isozymes that differ in kinetic features and in vivo are functionally diverse since they possess various subcellular locations (for review see Fettke et al. 2012a). As β-amylases from plants act on single helices, they prefer hydrosoluble rather than highly ordered and hydroinsoluble glucans (Edner et al. 2007; Hejazi et al. 2008).

7.3.3.2 Phosphorylases

In a functional state, phosphorylases (GH13) are oligomeric proteins selectively acting on nonreducing ends of α-glucans or glucan chains. Due to reversibility of the glucosyl transfer, they mediate both the directed glucan elongation and the directed phosphorolytic degradation. Phosphorolysis is restricted to the terminal interglucose linkage at the nonreducing end (Fig. 7.2b). Terminal glucosyl residues are transferred to orthophosphate yielding glucose 1-phosphate (G1P). Arsenate can replace orthophosphate, but transfer rates are much lower and, unlike G1P, the arsenate ester formed is spontaneously hydrolysed to arsenate and glucose. In the elongating reaction, phosphorylases use the nonreducing chain end as glucosyl acceptor and glucose 1-phosphate as donor. The in vitro determined V_{max} values of elongation are usually higher than those of phosphorolysis. Unless a product of the transfer reactions is immediately removed, α-glucan chains are simultaneously elongated and shortened under a wide range of G1P to orthophosphate ratios. The ratio of both reactions, however, varies depending on the respective G1P/P_i levels. Phosphorylases cannot bypass branchings. Furthermore, maltodextrins with a DP less than four usually cannot further be phosphorolytically (or arsenolytically) degraded. For the plastidial phosphorylase isozyme (Pho1 or, in *Arabidopsis*, PHS1), maltotetraose is an efficient competitive inhibitor of phosphorolysis (Steup and Schächtele 1981).

Pho1 from rice endosperm appears to efficiently elongate small maltodextrins even at high orthophosphate levels as P_i seems to selectively inhibit phosphorolysis (Hwang et al. 2010). The plastidial phosphorylase preferentially uses single-stranded α-glucans or α-glucan chains as substrate. Under in vivo conditions, the enzyme likely acts in both starch synthesising and degrading paths (Satoh et al. 2008; Fettke et al. 2012b; Malinova et al. 2014; see below).

In higher plants, plastidial phosphorylase isozymes (Pho1/PHS1) possess a large insertion (approximately 80 amino acid residues) located between the N- and the C-terminal domain containing a high proportion of charged amino acids (Albrecht et al. 2001).

Cytosolic phosphorylase isozymes (Pho2/PHS2) as well as glycogen phosphorylases do not contain this insertion. Likewise, maltodextrin phosphorylase from *E. coli* (which preferentially acts on oligoglucans as does Pho1/PHS1) lacks the insertion. As opposed to Pho1/PHS1, Pho2/PHS2 exhibits high affinity towards branched polyglucans, such as amylopectin and glycogen, but also to the glucose-containing cytosolic heteroglycans; see below. Non-covalent binding to these glycans occurs even in the absence of P_i or G1P, therefore permitting an easy distinction of the two isozyme types by affinity electrophoresis.

As revealed by carbohydrate microarrays, the cytosolic phosphorylase isozyme (Pho2/PHS2) mediates the glucosyl transfer from G1P to various glycans, such as cytosolic heteroglycans, carrageen, rhamnogalacturan I and II as well as xyloglucans. G1P-dependent labelling pattern observed with recombinant PHS2 was very similar to that obtained with DPE2 in the presence of ^{14}C-maltose. This similarity suggests that in vivo both glucosyl transferases utilise the same glycans (Ruzanski et al. 2013; see below). It does, however, not support the common designation of Pho2/PHS2 as being an isozyme of the α-glucan phosphorylase.

Multiple phosphorylation of the plastidial and the cytosolic phosphorylases is known to occur, but functional implications of the covalent modifications are largely unknown (Walley et al. 2013; see below).

7.3.3.3 Endo-hydrolases (α-Amylases)

The second large group of starch-related hydrolases are α-amylases (GH13) which, unlike β-amylases, cleave internal α-1,4-interglucose bonds and, depending on the structure of the α-glucan substrate, release either linear or branched α-glucans (Fig. 7.2c). When acting on branched substrates, target bonds exist at either site of the α-1,6-bond, provided a minimum distance is given in either direction. Furthermore, α-amylases use the mechanistically more sophisticated retaining (double-replacement) mechanism, and, following hydrolytic cleavage of the target bond, the free carbon atom 1 of the glucan released has α-configuration (Fig. 7.2c). α-Glucans liberated by α-amylases appear to largely lack terminal branchings (Kainuma and French 1970).

Similar to β-amylases, additional activities of endo-hydrolases have been reported (Kim et al. 1999; Qian et al. 2001), but hydrolysis of internal interglucose bonds appears to be the main catalytic activity. Endo-hydrolases from plants act preferentially on single helical and hydrosoluble carbohydrates.

7.3.3.4 Debranching Enzymes (DBEs)

All plant debranching enzymes (GH13) hydrolyse only α-1,6-interglucose bonds following the direct debranching mode and using the double-replacement mechanism. Thus, the reducing end of the α-glucan liberated retains the α-configuration (Fig. 7.2d). Based on sequence similarities and substrate specificities, plant DBEs can be classified into two groups: isoamylases (ISAs) and limited dextrinases (LDs or pullulanases). Pullulan consists of α-1,4-maltotriosyl units linked via α-1,6-interglucose bonds. Under in vitro conditions, LDs (but not by ISAs) are capable of hydrolysing the latter bonds (for details see Zeeman et al. 2010).

In *Arabidopsis*, the ISA type is represented by three genes (designated as *AtISA1* to *AtISA3*), but LD exists as a single gene product. Presumably, both ISA3 and LD act exclusively in the starch-degrading path exerting nonredundant functions (Fig. 7.2d; Delatte et al. 2006). Depending on the botanical source, ISA1 and/or

ISA2 form homomeric or heteromeric complexes apparently functional only in preamylopectin processing (Facon et al. 2013). In rice endosperm, the starch-related FLO6 protein appears to be a scaffolding protein which simultaneously binds to both native starch and ISA1 thereby locating ISA1 to the granule surface (Peng et al. 2014).

7.3.3.5 Disproportionating Enzymes (DPE1 and DPE2)

Some starch-degrading enzymes that, presumably, act selectively on hydrosoluble oligoglucans cleave α-1,4-intersugar bonds (thereby diminishing the DP of the sugar donor) and transfer the carbohydrate moiety to another glycan acting as acceptor (whose DP increases). Formally, the reaction resembles the 'disproportionation' of oxidation states and enzymes mediating this type of carbohydrate transfer are called 'disproportionating' enzymes. DPE1 and DPE2 are located in the plastidial stroma and in the cytosol, respectively. DPE1 acts on maltodextrins and generates neutral sugars to be exported into the cytosol. DPE2 is essential for the cytosolic metabolism of β-maltose.

DPE1 (4-α-glucanotransferase) catalyses readily reversible reactions according to the equation $G_n + G_m \leftrightarrow G_{n-q} + G_{m+q}$ where q (equalling 1, 2, 3) designates the number of glucosyl moieties transferred in a single reaction (Fig. 7.2e). Due to the multiplicity of transfer reactions, DPE1 generates a mixture of linear α-glucans (Kartal et al. 2011).

The cytosolic 'disproportionating enzyme 2' (DPE2) also mediates diversification of α-glucans or glycans but deviates from DPE1in two aspects: first, DPE2 preferentially uses high molecular weight glycans as one of the substrates and, second, it transfers a single glucosyl residue (presumably that containing the nonreducing end; Steichen et al. 2008) from β-maltose as glucosyl donor and cleaves the interglucose bond of the disaccharide (Dumez et al. 2006; Fig. 7.2f). Under in vitro conditions, DPE2 efficiently transfers the glucosyl residue to glycogen (Chia et al. 2004; Fettke et al. 2006) which acts as non-physiological substitute of cytosolic heteroglycans. The latter are common in photoautotrophic and in heterotrophic organs of higher plants (Malinova et al. 2013; for details see Fettke et al. 2012a). Cytosolic heteroglycans (often designated as water-soluble heteroglycan [SHG] subfraction I) are highly branched glycans whose apparent size ranges up to approximately 70 kDa. In glycosidic linkage pattern and monosaccharide composition, cytosolic heteroglycans are similar to apoplastic arabinogalactans, but, unlike the latter, they often do not interact with the synthetic β-glucosyl Yariv reagent. Interestingly, cytosolic heteroglycans are also efficiently used as glucosyl donor or acceptor by another cytoplasmic transferase from plants, Pho2 (or, in *Arabidopsis thaliana*, PHS2; Ruzanski et al. 2013). By contrast, neither the plastidial phosphorylase isozyme, Pho1/PHS1, nor the main muscle glycogen phosphorylase from mammals can utilise cytosolic heteroglycans as substrate (Fettke et al. 2004, 2005a, b).

For the reverse in vitro glucosyl transfer from glycogen, DPE2 uses free D-glucose (yielding maltose) but also several other glucosyl acceptors, such as D-xylose, D-allose, D-mannose and *N*-acetyl-D-glucosamine. As various monosaccharides are used as glucosyl acceptors, DPE2 forms several glucose-containing disaccharides. In this respect, DPE is similar to the prokaryotic MalQ, a transferase essential to the bacterial metabolism of maltose (Dippel and Boos 2005; Fettke et al. 2006; Park et al. 2011; Ruzanski et al. 2013).

7.3.4 Frequently Observed Features of Starch-Degrading Enzymes

In the following section, we discuss some features that are frequently found in starch-related enzymes but also in enzymes acting on cell wall materials. In these cases, many target bonds exist that are thermodynamically similar (Goldberg et al. 1991) and, in principle, can be enzymatically cleaved. A relatively low proportion of the linkages, however, are actually used by the degrading enzymes.

7.3.4.1 Multi-Chain and Single-Chain Attack

Assuming a single starch-degrading enzyme molecule is surrounded by various hydrosoluble α-glucans, the enzyme can cleave a single interglucose bond in one glucan and, subsequently, act on another glucan molecule (Fig. 7.3a). This mode is designated as multi-chain attack as the enzyme apparently randomly selects a target bond and, following a single reaction, interacts with another carbohydrate molecule. On average, this mode of degradation results in a decreasing DP of all substrate molecules. Starch-degrading enzymes can, however, follow another mode of action, designated as single-chain attack or processivity, and repeatedly act on interglucose bonds of the same substrate molecule (Fig. 7.3b). Processive enzymes catalyse essentially the same reaction utilising a series of substrate molecules originating from a single polymeric molecule and, typically, use the series of substrates with essentially the same efficiency. All substrates of a series differ in size but are structurally and chemically very similar. During the repetitive action, the enzymes remain in close vicinity to the substrate and, except the first and the last cycle, do not associate or dissociate. Dissociation of the enzyme–glucan complex terminates a series of catalytic cycles. Depending on the respective processive enzyme and conditions of catalysis, the number of repetitive cycles varies and, therefore, the term 'processive enzyme' covers a wide range of modes of action. If an extended series of catalytic cycles is performed at the same α-glucan chain, intermediate DPs may represent only a minor (and difficult to detect) proportion of substrate molecules and the α-glucan mixture is dominated by two extremes which are close to the starting

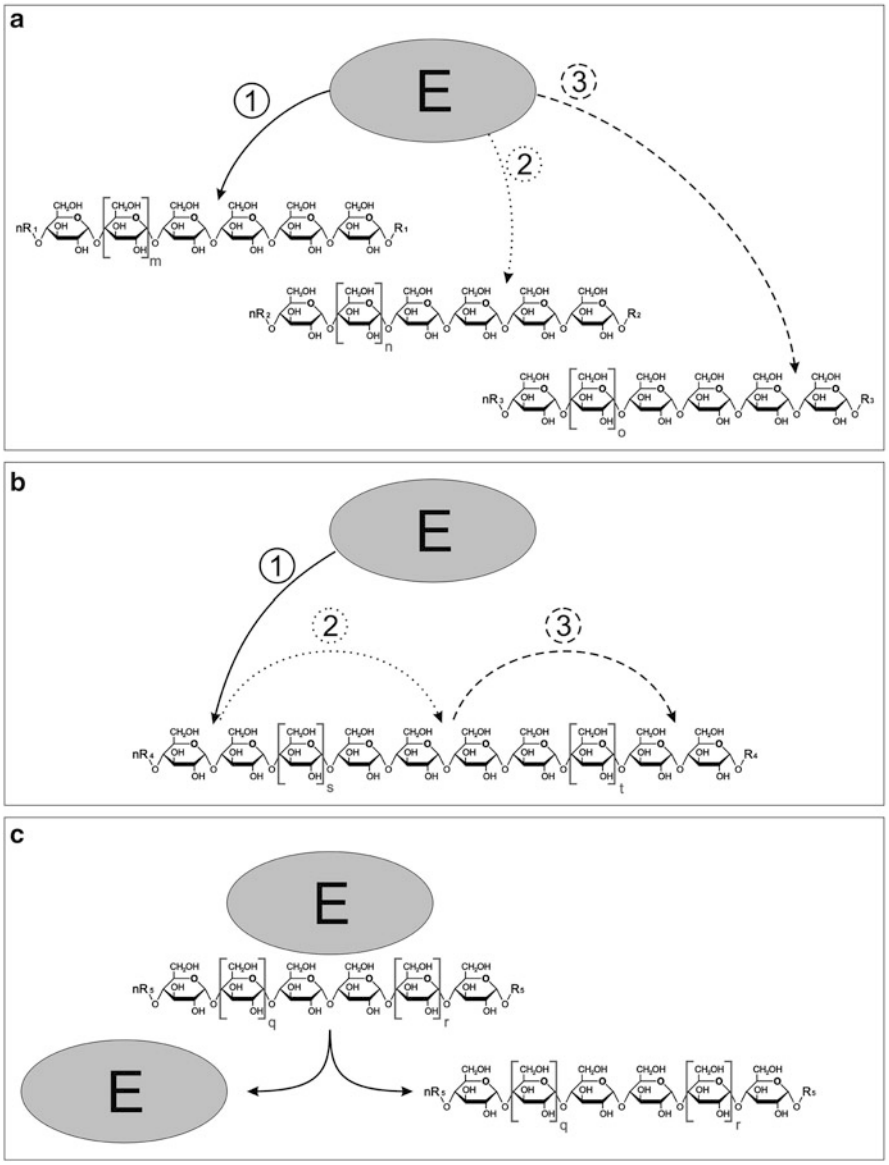

Fig. 7.3 Interaction of starch-degrading enzymes with soluble α-glucans
(**a**) *Multiple attack of a hydrolysing enzyme* (*E*). The enzyme (E) hydrolyses an interglucose bond in one α-glucan molecule molecule (1). Following hydrolysis, it dissociates and interacts with another glucan molecule (2). Finally, it hydrolyses an interglucose bond of the third glucan molecule (3). R_1, R_2, R_3 means a α-glucanyl residue containing the reducing chain end of the α-glucan molecule 1, 2, 3. nR_1, nR_2, nR_3 means a α-glucanyl residue containing the nonreducing end of molecule 1, 2, 3. m, n, o means the number of glucosyl residues in a part (as indicated) of a given α-glucan chain

distribution and near to the final sizes. Depending on the state of degradation, the ratio between both extremes varies.

Several β- and α-amylases from higher plants appear to start catalysis by following a more random approach (i.e. multi-chain attack) and sooner or later largely use the processive mode of action. The precise mode of degradation strongly depends, however, on the biological source of the hydrolase and the experimental conditions, such as temperature and substrate level (Kramhøft et al. 2005; Ishikawa et al. 2007; Nielsen et al. 2012).

Modes of the multi-chain and single-chain attack have, however, been defined using sufficiently diluted hydrosoluble α-glucans. Under these conditions, all interglucose bonds are easily accessible to the enzymes. By contrast, in the hydroinsoluble starch granule, many target bonds are not accessible due to the compact structure of the particle. Degradation of native starch is more complex as it requires additional processes that precede enzymatic hydrolysis of interglucose bonds (see below).

7.3.4.2 Productive and Non-productive Enzyme-Glucan Complexes

Starch-degrading enzymes may also bind to α-glucans resulting in so-called non-productive complexes as they do not lead to catalysis. These complexes are formed by binding of all glucosyl residues of the α-glucan (chain) together with the respective target linkage to subsites of the enzyme that are located at only one side of the catalytic site which, therefore, lack access to interglucose bond to be cleaved (Fig. 7.3c). Formation of non-productive complexes often leads to in a time-dependent decrease of the respective apparent V_{max} values although catalytic activity of the enzyme is fully retained.

7.3.4.3 Non-catalytic Carbohydrate-Binding Sites

Starch-degrading enzymes often posses domains unrelated to catalysis but capable of selectively and non-covalently binding carbohydrate substrate(s). Two types of non-catalytic carbohydrate-binding sites are known: **c**arbohydrate-**b**inding **m**odules

Fig. 7.3 (continued) (**b**) *Single attack of a hydrolysing enzyme* (*E*). The enzyme (E) binds to a α-glucan molecule and, subsequently, hydrolyses sequentially several interglucose bonds before dissociating from the carbohydrate substrate. In this example, three target interglucose bonds (indicated by 1, 2 and 3) are given. R4: α-glucanyl residue of this glucan molecule containing the reducing end. nR4: α-glucanyl residue of the same glucan molecule containing the nonreducing end. (**c**) *Non-productive enzyme-glucan complex and its dissociation*. Due to the mode of binding of a hydrolase (E) to an α-glucan, the catalytic site has no access to an interglucose bond to be hydrolysed. The non-productive complex is retained or dissociates without hydrolysing an interglucose bond. *p* and *r* are the number of glucosyl moieties as indicated. R_5 and nR_5: α-glucanyl residue of the same α-glucan molecule containing the reducing and nonreducing ends, respectively

(CBMs) and **s**econdary **b**inding **s**ites (SBSs; Boraston et al. 2004; Kiessling et al. 2008; Cuyvers et al. 2012). Both types of binding sites support the catalytic action of the respective enzyme by effects such as proximity and targeting. The entire protein–carbohydrate complex is based on multiple interactions between various sites of the protein and those of the bound glycan, but the action of the non-catalytic site(s) may be dominant. Multiple interactions of the entire complex are often designated as avidity or functional affinity (Kiessling et al. 2008). When homomeric or heteromeric protein complexes interact with glycans (see Chap. 8 this volume), multiple binding to the carbohydrate is also often observed.

7.3.4.3.1 Carbohydrate-Binding Modules (CBMs)

Starch-degrading enzymes are often modular proteins. A module is defined as a structural and functional unit of a monomeric protein. In addition to the catalytic module, starch-degrading enzymes frequently possess a single non-catalytic CBM or several CBM copies placed in either the N- or the C-terminal domain. The term CBM covers a contiguous amino acid sequence whose size ranges from 30 to approximately 200 residues. CBMs are often (but not always; Fontes and Gilbert 2010; Atmodjo et al. 2013) directed against the same carbohydrate used by the catalytic module of the respective enzyme. The CBM domain tends to fold into a functional three-dimensional structure even in the absence of the residual sequence of the protein (Luís et al. 2013).

CBMs are often distant from and connected to the catalytic site(s) by a flexible linker sequence (Kiessling et al. 2008; Guillén et al. 2010) which also may participate in carbohydrate binding (Payne et al. 2013). Carbohydrate targets of CBMs are, in principle, distinct monosaccharyl or oligosaccharyl residues (Cantarel et al. 2009). Occasionally, CBMs are found in separate proteins apparently lacking any catalytic domain (for details see Guillén et al. 2010; see also below).

Depending on the physicochemical state, oligoglycans or oligoglycan chains that non-covalently interact with CBMs possess either a low or a significant conformational flexibility. The latter is frequently caused by rotation about glycosidic linkages provided the target carbohydrate is soluble (Kiessling et al. 2008). By contrast, highly ordered and hydroinsoluble glycans possess often little flexibility.

Within the binding sites, distinct aromatic amino acids (such as tryptophan or tyrosine residues) often undergo stacking interactions with a distinct heterocyclic sugar moiety, but other amino acid residues may also contribute to carbohydrate binding (Guillén et al. 2010).

Typically, CBMs tend to favour the action of the respective enzyme by bringing (and retaining) the catalytic domain in close vicinity to the carbohydrate substrate. When acting on highly ordered glycans, binding of CBMs per se may even result in structural alterations (designated as substrate disruption) that locally convert the carbohydrate into a structure favouring subsequent enzymatic catalysis.

7.3.4.3.2 Secondary Bindings Sites (SBSs)

In the families of glycoside hydrolases (GHs) including glycosidases and transglycosidases (Cantarel et al. 2009), non-catalytic carbohydrate binding can also occur by sites that are physically not distant from the catalytic site but are located close to the surface of the structural unit that comprises the active site. These sites are designated as **s**econdary **b**inding **s**ites (SBSs). As opposed to CBMs (which originally were defined as **c**ellulose-**b**inding **m**odules), most SBSs have been discovered in starch-active enzymes (Nielsen et al. 2009; Meekins et al. 2013, 2014), but they also exist in carbohydrate-active enzymes unrelated to starch (Cuyvers et al. 2012). Carbohydrate-active enzymes frequently possess more than a single SBS per polypeptide, and a single monomer may contain both SBSs and CBDs (for details see Cuyvers et al. 2012).

Typically, SBSs are situated on the surface of the module containing the catalytic site and, therefore, are more fixed than CBMs (Cuyvers et al. 2012). Similar to CBMs, aromatic amino acid residues appear to be of special relevance for the selective binding of sugar moieties.

Several functions have been ascribed to SBSs, such as targeting of the enzyme to its substrate, assisting catalysis by substrate loading into the active-site groove, facilitating catalysis by disrupting the structure of target carbohydrates and retaining the enzyme in close contact to the carbohydrate substrate for subsequent reactions. These functions largely overlap those of CBMs. Due to their surface-near location, SBSs may also be involved in the interaction of enzymes with highly ordered carbohydrates (Cuyvers et al. 2012; see below).

7.3.4.4 Starch-Degrading Enzymes Acting on Starch Granules

Any starch-degrading path starts at the surface of the starch particle, but subsequent reactions may either be also restricted to the periphery of the starch particle or may form additional surfaces leading into interior parts of the granule. In any case, the process takes place in a nonhomogeneous system. Understanding of the initial reactions of starch degradation is, however, impeded as detailed structural information on the granule surface is largely lacking. In a formal sense, enzymatic deconstruction of other hydroinsoluble polysaccharides, such as cellulose and chitin, poses similar problems. Microbial deconstructions of cellulose and chitin are, however, extracellular processes, whereas starch is largely degraded within living plant cells. Efficient cellulolysis and chitinolysis by microbial enzymes require a close collaboration of processive and non-processive glycoside hydrolases (Ragauskas et al. 2006; Gilbert 2010; Payne et al. 2012; Shang et al. 2013). It is unknown whether a similar synergistic process is functional in starch degradation.

7.3.4.5 Kinetic Implications for Starch-Degrading Enzymes

Due to features of the enzyme itself, to the mode of enzymatic action or to properties of the carbohydrate substrates, actions of starch-degrading enzymes can often not been described by using the classical concept developed by Michaelis–Menten. For each of the three cases, an example is discussed in more detail.

In the classical theory of Michaelis–Menten (and in some more advanced versions as well), the population of enzyme molecules is assumed to consist either of two states, a catalytically active and a nonactive state. Except at saturating substrate levels, the ratio between both states is determined by the actual substrate concentration and the affinity of the enzyme to the respective substrate. At limiting substrate levels, distinct ratios between the two states of a given enzyme exist that are essentially constant as long as steady state is maintained. Following each catalytic cycle, an enzyme molecule either undergoes a further catalytic action or change from the active state into an inactive state which is caused by the actual lack of substrate for the respective enzyme molecule. To maintain steady state, in this case an enzyme molecule previously catalytically inactive must now participate in catalysis.

If, however, the enzyme itself exhibits heterogeneity in its kinetic properties, the simple approach outlined above cannot be applied. Enzyme heterogeneity can be caused by several processes, such as the reversible formation of protein complexes (that, in some cases, may even include α-glucans) or by covalent modifications of a single enzyme. As an example, the mammalian muscle glycogen synthase possesses at least nine phosphorylation sites selectively used by distinct protein kinases. Some esterification sites significantly alter the kinetic properties of the enzyme, but others affect mainly subcellular location and targeting of the glycogen synthase (for review see Palm et al. 2013).

Plant genomes encode considerably more protein kinases than mammalian genomes (Zulawski et al. 2013). Both phosphorylation sites of starch-degrading enzymes and starch-related protein kinases have not been completely identified. Furthermore, functional implications of covalent modification of starch-degrading enzymes are largely unknown. As a monomeric protein that is independently phosphorylated at n sites exists in up to 2^n phosphorylation states, even a few esterification sites may cause a large kinetic diversity (Salazar and Höfer 2009).

Recent studies have empirically confirmed a large number of phosphorylation sites in plant proteins (Baginsky 2009; Walley et al. 2013; van Wijk et al. 2014). In *Arabidopsis* leaves, several starch-related enzymes and transporters are known to be phosphorylated (Heazlewood et al. 2009; Reiland et al. 2009; see Fig. 7.4).

Starch-related heteromeric protein complexes tend to organise carbohydrate substrate(s) by forming a distinct microenvironment and, therefore, do not act in a homogeneous system. Similarly, processive enzymes often remain in close vicinity to the carbohydrate substrate (for discussion see Nishimo et al. 2004).

Furthermore, starch-degrading enzymes utilising granules as substrate are surface-active enzymes and have no access to compounds inside the dense starch particle irrespective of their chemical similarity or identity. Conventional plots of the reaction velocity versus the entire substrate content of reaction mixtures use virtual substrate levels that, to a large extent, are not relevant to the enzyme. Finally,

due to the large size of native starch, enzyme–substrate complexes are formed only by movement and binding of the enzyme to the surface of starch particles.

7.4 In Vivo Starch Degradation

In living cells, starch degradation consists of both plastidial and cytosolic routes, but autophagy-related starch-degrading processes cannot be excluded (Weidberg et al. 2011). In animals, defects in lysosomal α-glucosidases severely affect glycogen metabolism, and, at least in the long term, lysosomal glycogen degradation or a lysosomal glycogen-related degradative process appears to be essential (glycogen storage disease type II; Roach et al. 2012; Zirin et al. 2013). Autophagy-related glycogen degradation seems also to exist in yeast (see Roach et al. 2012). More than 30 autophagy-related genes (designated as *ATGs*; Mizushima et al. 2011) have been identified in *Arabidopsis thaliana*. Some *AtATGs* are constitutively expressed, but transcript levels are elevated under stress conditions (Liu and Bassham 2012). It is unknown whether in higher plants starch-related autophagy is restricted to stress situations (which in some starch-related mutants may permanently be effective) or also occurs in non-stressed plants. In some autophagy-deficient *Arabidopsis* mutants, transitory starch degradation appears not to be significantly affected (Izumi et al. 2013).

In living cells of higher plants, the widely accepted paths of starch degradation cover several processes that at the level of a single chloroplast usually occur more or less simultaneously rather than strictly sequentially:

- Cleavage of α-1,4-interglucose bonds
- Cleavage of α-1,6-interglucose bonds
- Disproportionating reactions
- Transport of products of the plastidial starch degradation into the cytosol
- Conversion of starch-derived sugars into intermediates of established cytosolic paths of the central carbon metabolism including various biosynthetic routes

7.4.1 Reserve Starch Degradation

Reserve starch metabolism occurs in vegetative storage organs, ranging from potato tubers, roots to more specialised organs like turions of Lemnaceae, as well as in seeds from monocotyledons or dicotelydons. Seeds that essentially retain large quantities of water and their metabolic activities almost unchanged have been designated as recalcitrant, but those that develop desiccation tolerance were named orthodox seeds (Roberts 1973). For the latter, desiccation is essential for the subsequent germination. Dry seeds, however, still contain some water and actually represent a low-hydrated state permitting some metabolic activities (Weitbrecht et al. 2011).

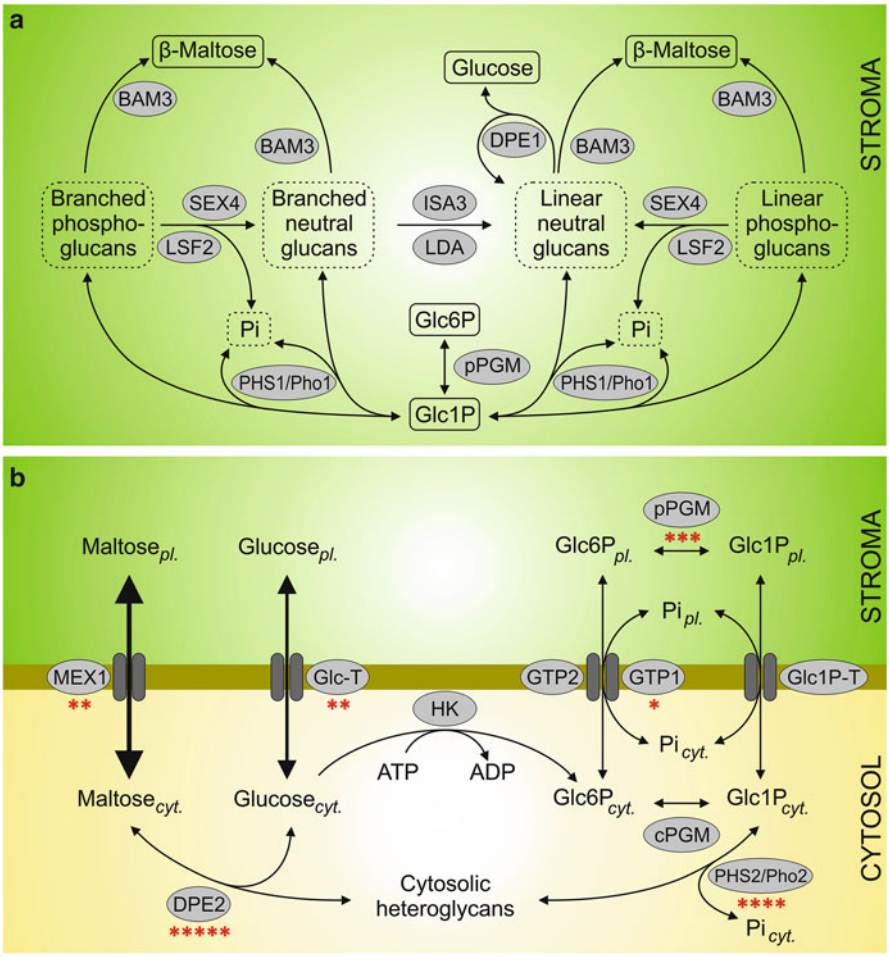

Fig. 7.4 Stromal and cytosolic paths of starch-derived hydrosoluble α-glucans
(**a**) *Plastidial routes*. Hydrolytic enzymes acting on assimilatory starch granules release four groups of α-glucans (branched phosphoglucans, branched neutral glucans, linear neutral glucans and linear phosphoglucans; all marked by *broken lines*). Each group consists of several types of molecules as DP, position of the branching point(s), number and location of monophosphate ester(s) are not defined. In addition, β-amylases (in *Arabidopsis* largely AtBAM3; At4g17090) liberate β-maltose directly from the starch granule surface and the disaccharide released also enters the plastidial β-maltose pool. Phosphorylated α-glucans are converted to neutral oligoglucans by SEX4 (in *Arabidopsis* At3g52180) and/or **L**ike **S**ex **F**our **2** (LSF2; At3g10490). Branched glucans are linearised by isoamylase3 (in *Arabidopsis* AtISA3; At4g09020) and/or limit dextrinase (AtLDA; At5g04360) which both convert side chains into free linear α-glucans. For clarity, actions of α-amylase3 (AMY3; At1g69830) have been omitted. The order of glucan dephosphorylation and debranching is not defined. Depending on DP and structure of the respective α-glucans, they may act as carbohydrate substrate of the plastidial phosphorylase (Pho1/PHS1; At3g29320) yielding glucose 1-phosphate (Glc1P) and/or of BAM3 (At4g17090) forming β-maltose. In addition, linear neutral glucans can undergo disproportionating reactions mediated by DPE1 (At5g64860) which forms α-glucose. Glc1P can be converted to glucose 6-phosphate (Glc6P)

Depending on the botanical source, the relative reserve starch content varies largely. In dry cereal seeds reserve starch can account for approximately 75 % of the grain dry weight, but in roots it is often much lower. The general biochemistry of reserve starch mobilisation appears to be similar, but contributions of distinct enzymes and/or isozymes may significantly vary. Large differences exist in the control of reserve starch degradation and its integration into the entire biology of the respective tissue.

Starch degradation is initiated by various mechanisms, such as carbon or nutrient starvation signals, a given hormone (or a combination of hormones) and/or light. As a common theme, reserve starch degradation appears to be initiated only following a major delay after the period of accumulation. Starch-storing cells may undergo an extended period of desiccation during which cells remain living or die. Desiccation does, however, not occur in other starch-storing organs, such as potato tubers. Thus, reserve starch degradation proceeds in a highly heterogeneous group of biological systems and is integrated into largely differing cellular contexts.

7.4.1.1 Reserve Starch Degradation in Dead Tissue

Typically, germinating cereal seeds degrade starch in dead tissue (Bewley 1997; Sreenivasulu and Wobus 2013). When the dry seeds are subjected to an extended period of time (often designated as after-ripening), dormancy is finally lost and the seeds massively take up water (phase I according to Bewley 1997). This process is driven by the very low matrix potential of the seed and occurs also in dead tissues. During phase I, solutes and metabolites leak into the surrounding medium. Loss of solutes is, however, terminated by rapid reorganisation of cellular membranes

Fig. 7.4 (continued) by the plastidial phosphoglucomutase isozyme (pPGM; At5g51820). The two neutral sugars and the two glucose monophosphates are final products of the plastidial starch-degrading path. Export of β-maltose and/or glucose cannot by fully compensated by other routes (Niittylä et al. 2004; Cho et al. 2011; see text)

(**b**) *Export of starch-derived products into the cytosol and their conversion into glycolytic and/or biosynthetic intermediates*. The neutral disaccharide, β-maltose and free glucose are exported into the cytosol via the transporters of the inner plastidial envelope, MEX1 (At5g17520) and Glc-T (At5g16150), respectively. Glucose 6-phosphate (Glc6P) can be exported into the cytosol in a counter-exchange to an anionic compound via a hexose phosphate transporter (such as At5g54800). (such as At5g54800; GTP1). For GTP1, phosphorylation has been empirically observed as indicated. The *Arabidopsis* genome contains a second GTP encoding gene (At1g61800; GTP2). Expression of this gene is highly variable. So far, no phosphorylation site(s) has/have been empirically confirmed for the gene product. A similar exchange has been shown for the transport of glucose 1-phosphate (Glc1P), but the transporter protein has not been identified. Pi_{cyt} and Pi_{pl}: cytosolic and plastidial orthophosphate pool, respectively. HK: cytosolic hexokinase activity (possibly AtHXK1; At4g29130). As the hexokinase protein has not unequivocally been identified, no phosphorylation sites are given. cPGM and pPGM: the cytosolic (PGM2; At1g70703) and the plastidial (PGM1; At5g51820) phosphoglucomutase isozyme, respectively. Empirically confirmed phosphorylation sites from *Arabidopsis thaliana* are marked by *red asterisks* (Data are taken from PhosphAt; see Sonnewald and Kossmann 2013; van Wijk et al. 2014)

(Bewley 1997). In phase I, protein biosynthesis largely relies on extant mRNAs. Phase II is characterised by a cessating water uptake but also by many intracellular processes that occur during this period, such as translation of newly synthesised mRNAs and of mitochondria. Phase III which actually initiates the postgermination period is characterised by massive mobilisation of storage products, such as starch, cell wall and storage proteins, taking place in the dead endosperm (Tan-Wilson and Wilson 2012). Degradation products are imported by living cells and used for biosynthetic processes and cell divisions (Bewley 1997).

Control of mobilisation of storage products is complex and not yet fully elucidated. It includes sugar and nutrient signalling and the action of antagonistic hormones, especially gibberellic acid (GA; Sreenivasulu et al. 2008; Yamaguchi 2008) and abscisic acid (ABA; Weitbrecht et al. 2011; Sun 2011; Zi et al. 2014), and downstream-acting proteins, such as a unique group of nuclear transcriptional regulators that repress GA responses and inhibit plant growth (DELLA proteins; for review see Claeys et al. 2014) and phytochrome-interacting factors (PIFs; Leivar and Quail 2011; Sun et al. 2012).

α-Amylase isozymes (and many other gene products as well) are massively synthesised in aleurone cells surrounding the starchy endosperm and are secreted into the latter. In germinating barley seeds, two classes of α-amylases (designated as HvAMY1 and HvAMY2) are synthesised, which are both more closely related to the extraplastidial α-amylase AMY1 from *Arabidopsis* rather than to the chloroplastic hydrolase, AMY3. HvAMY2 strongly interacts with native starch, whereas HvAMY1 preferentially hydrolyses linear maltodextrins, suggesting that *in planta* the two classes exert a sequential mode of action (Zeeman et al. 2010). Following the addition of GA to barley and rice aleurone cells, up to 1,300 genes are upregulated, which encode many hydrolases but also other proteins that are functionally diverse (Chen and An 2006; Tsuji et al. 2006). In barley and rice, two MYB transcription factors (designated as MYBS1 and MYBGA) appear to be of crucial importance in integrating signalling paths that are initiated by sugar and/or nutrient starvation and by GA (Hong et al. 2012). MYBGA is a GA-inducible transcription factor that binds to promotor regions of genes encoding α-amylase isozymes (and of other hydrolases as well) and thereby activates gene expression (Tsuji et al. 2006). MYBS1 is a sugar-repressible transcription factor that binds to the same promotors under sugar starvation (Lu et al. 2007).

In principle, the highly complex control of gene expression appears to balance the availability of sugars and nutrient (as formed by hydrolysis of the entire endosperm) and the varying needs of the living heterotrophic cells of the cereal seed but prevent starvation.

β-Amylases are possibly involved in cereal reserve starch degradation, but the exoamylases are deposited in an inactive state during starch granule biosynthesis (Zeeman et al. 2010). Structural features of the inhibition of the β-amylases have been elucidated (Rejek et al. 2011). As in barley and rye mutants that essentially or

completely lack β-amylases, germination appears to proceed largely unaffected and similar to the wild-type (Daussant et al. 1981; Kreis et al. 1987; Kihara et al. 1999), the actual in vivo function of the exoamylases is unclear. Possibly, they mainly act as reserve protein. An α-glucosidase (maltase) is likely to exert a dual function in cereal endosperm as it converts short dextrins to glucose and also acts directly on the starch granule surface (Zeeman et al. 2010).

Extracellular cereal reserve starch degradation apparently lacks cycles of phosphorylation and dephosphorylation of amylopectin which is an important process in turnover of assimilatory starch (see below). The genes of α-glucan phosphorylating and dephosphorylating enzymes are present in cereals (Zeeman et al. 2010), but their contribution to reserve starch metabolism remains unclear. In transgenic barley, varying levels of cereal endosperm starch phosphorylation do affect degradation during germination (Shaik et al. 2014).

During degradation of cereal reserve starch, morphology of the granules usually undergoes large alterations as hydrolysis appears to be initiated at specific sites resulting in pitting and increasing roughness of the entire surface. Hydrolysis proceeds then into interior parts of the particle, whereas other parts of the granule appear to be more resistant to hydrolysis (Shaik et al. 2014). Similar effects are observed during in vitro amylolysis of reserve starch (Blazek and Copeland 2010). Neither kinetic nor structural implications of this mode of degradation are fully understood.

7.4.1.2 Reserve Starch Degradation in Living Tissue

Although highly heterogeneous, both biochemistry and compartmentation of this group appear to be more similar to that of assimilatory starch. For living tissues degrading reserve starch, intact compartmentation is often assumed rather than proven. Starch from potato tubers is highly phosphorylated and glucosyl moieties are esterified during both starch biosynthesis and degradation (for details see Hejazi et al. 2012). Likewise, potato tubers possess both plastidial and cytosolic phosphorylase isozymes as well as cytosolic heteroglycans (see below; Fettke et al. 2008). These glycans and the disproportionating isozyme 2 (DPE2) exist also in roots of *Arabidopsis* (Malinova et al. 2011).

As starch-degrading enzymes and starch-related glycans are similar to those of leaves, reserve starch in living heterotrophic cells appears to be degraded by routes similar to those of photoautotrophic cells. Detailed biochemical analyses are, however, largely lacking. Furthermore, starch-rich heterotrophic tissues may degrade reserve starch not in a synchronised manner. If so, tissue samples consist of cells representing various states of starch metabolism and the metabolic heterogeneity would not favour detailed biochemical analyses.

7.4.2 Transitory Starch Degradation

As opposed to reserve starch, transitory starch is degraded without massive de novo biosynthesis of enzyme cleaving interglucose bonds. Furthermore, it is has not been demonstrated that catalytically inactive β-amylase(s) is included in transitory starch granules as it has been documented for cereal endosperm starch (see above).

Importantly, under a wide range of external conditions (such as length and temperature of the dark period; for leaf starch degradation under elevated night temperatures, see Glaubitz et al. 2014), assimilatory starch turnover during the entire light–dark period remains largely unchanged. As under natural conditions, increasing length of the light period is associated with decreasing length of darkness, an essentially unchanged starch turnover requires that average rates of starch synthesis are diminished and those of degradation are enhanced (Sulpice et al. 2014). In this section, we first consider biochemical processes occurring inside and outside the chloroplasts (Sect. 7.4.2.1) and then discuss regulation of transitory starch degradation (Sect. 7.4.2.2).

The organisation of a typical mesophyll cell certainly affects starch degradation. A single mesophyll cell from *Arabidopsis* leaves contains more than 100 chloroplasts but a single cytosolic compartment. Based on current knowledge, essentially all chloroplasts of a given cell degrade starch. Thus, a metabolic path consisting of both plastidial and cytosolic reactions is likely to include both multiparallel plastidial paths and a reaction sequence in a single compartment, i.e. the cytosol. This type of organisation does not favour any feedback inhibition of starch degradation unless the multiple carbon fluxes that enter the cytosol are integrated.

Within a single chloroplast, the number of starch granules ranges from approximately 5 to 7 starch granules. At the end of the light phase, both the size of the chloroplasts and the volume of the individual starch granules in a given mesophyll cell vary significantly in mature *Arabidopsis* leaves. The number of granules correlates with the volume of the respective chloroplast, but at the end of the dark period, this correlation is not observed (Crumpton-Taylor et al. 2012, 2013; Ingkasuwan et al. 2012; Ragel et al. 2013).

As in mature *Arabidopsis* leaves the number of starch granules per chloroplasts remains largely constant over the entire light–dark cycle, starch is turned over largely (or exclusively) by alterations of starch granule size. By contrast, de novo biosynthesis of granules contributes (if any) little to the light-dependent starch accumulation. Diminished granule volume is a major factor leading to decreasing chloroplast volume during darkness. Presumably, within a single chloroplast degradation is simultaneously initiated in several starch granules (and also at different sites of each starch particle). Imaging of *Arabidopsis* leaf tissue does not indicate a strictly sequential degradation of the granules (Crumpton-Taylor et al. 2012).

As opposed to mature leaves, growing tissues contain dividing chloroplasts and the number of starch granules per organ increases. In *Arabidopsis*, the soluble starch synthase isozyme 4 is likely essential for the de novo biosynthesis of starch granules

under these conditions (Crumpton-Taylor et al. 2013), but it is unknown whether the number of starch granules remains unchanged during darkness. Single cell analyses revealed that starch turnover includes stochasticity which is also inherent to gene expression and partitioning of gene products (for details see Garz et al. 2012).

7.4.2.1 Chloroplast Path of Transitory Starch Degradation

Plastidial degradation of transitory starch includes processes at the starch granule consisting of transition from a highly ordered and less hydrated to a less ordered and more hydrated state as well as those that are distant from the granule and take place in the hydrosoluble phase, i.e. the chloroplast stroma. Formation of a few intermediates that are exported into the cytosol terminates the plastidial path of starch degradation.

7.4.2.1.1 Starch-Phosphorylating Enzymes

For a detailed discussion of starch-phosphorylating enzymes, the reader is referred to Chap. 13. Here only some more general comments are given.

In living plant cells, phase transition at the surface of starch granules often proceeds by covalent starch modifications of very few glucosyl residues (by far less than 1 %) that are phosphorylated at carbon atoms 6, 3, and (at least in some cases) 2. Esterification at C6 and C3 is mediated by two starch-related dikinases (for details see Ritte et al. 2002; Ritte et al. 2004; Hejazi et al. 2012), but the enzyme(s) phosphorylating at C2 is unknown. Starch-related dikinases act in both the A- and B-type allomorph of starches of starch-like particles (Hejazi et al. 2009). Interestingly, the few red algae (such as *Galdieria sulphuraria*) forming glycogen rather than starch lack genes encoding starch-related dikinases (Shimonaga et al. 2008; Schönknecht et al. 2013). Therefore, highly ordered glucans as present in starch strictly correlate with the occurrence of starch-related dikinases.

All three monophosphorylation sites mentioned above are used in mammalian glycogen as well, but none of the phosphorylating enzyme activities have unequivocally been determined. As opposed to starch, glucosyl 6-phosphate residues are not the dominant phosphorylation sites in mammalian glycogen (Tagliabracci et al. 2011; Chikwana et al. 2013; Nitschke et al. 2013; DePaoli-Roach et al. 2015).

Although insignificant in terms of quantity, esterification appears to be sufficient to favour the action of enzymes that hydrolyse interglucose bonds (see below; Edner et al. 2007). Introduction of monophosphate esters into starch also occurs during biosynthesis (Nielsen et al. 1994; Ritte et al. 2004). *Arabidopsis* mutants containing a lower GWD content are compromised in both accumulation and degradation of starch, but the dikinase exerts little control over the total leaf starch content during darkness (Skeffington et al. 2014). GWD-deficient *Arabidopsis* mutants synthesise starch granules that differ from that of the wild-type in morphological and surface-near (bio)chemical features. By contrast, total side chain patterns obtained

for solubilised granules are similar (Mahlow et al. 2014). Thus, mutants lacking functional GWD deviate from the wild-type in both starch-related metabolic paths and some properties of the granule itself.

7.4.2.1.2 Starch-Dephosphorylating Enzymes

Seemingly paradoxical, the normal turnover of transitory starch requires both formation and hydrolysis of monophosphate esters. The directed hydrolytic degradation of α-glucan chains cannot bypass monophosphate esters (Takeda and Hizukuri 1981). Thus, α-1,4-interglucose bonds can be completely hydrolysed only if starch-related monophosphate esters are removed and de-esterification follows the phosphorylation-dependent local alterations at the granule surface.

In this review, we discuss the three putative phosphatases designated as SEX4 [*At3g52180*], **L**ike **S**ex **F**our 1 (LSF1) [*At3g01510*] and **L**ike **S**ex **F**our 2 (LSF2) [*At3g10940*], all of which reside in the plastidial compartment having direct access to both starch and starch-derived α-glucans (Silver et al. 2014). Due to the action of the putative phosphatases, esterification of starch is, to a large extent, transient (Hejazi et al. 2012; Fettke et al. 2012a), and therefore, the intramolecular phosphate patterns as revealed by carbohydrate analyses are determined by both phosphorylating and dephosphorylating activities not necessarily reflecting activity of starch-related dikinases.

The three putative phosphatases are members of the large group of phosphotyrosine phosphatases (PTPs) forming the subgroup of dual-specificity phosphatases (DSPs). The latter have been studied mainly in mammals as some DSPs, if not functional, cause severe diseases. Unlike other protein phosphatases, DSPs are capable of hydrolysing phosphate esters at both serine/threonine and tyrosine residues, and some DSPs act also on nonprotein substrates, such as phospholipids and/or phosphorylated polyglucans (Pulido and Hooft van Huijsduijnen 2008).

SEX4

SEX4 is common in higher plants. The SEX4 gene exhibits a conserved exon/intron structure and its expression is closely related to that of the two starch-related dikinases, GWP and PWD (Ma et al. 2014). The precursor sequence of AtSEX4 contains an N-terminal transit peptide, the DSP domain, and possesses a C-terminal CBM (now classified as CBM48) which is closely related to CBM20 of a starch-related dikinase, PWD (Christiansen et al. 2009). The mature SEX4 protein from *Arabidopsis thaliana* comprises 379 amino acid residues.

Originally, SEX4 was thought to primarily act on phosphoproteins but also being able to bind to starch. Because of its sequence-deduced interaction with SNF1-related protein kinases via a kinase interaction sequence (KIS), SEX4 from *Arabidopsis thaliana* was first named PTPKIS1 (Fordham-Skelton et al. 2002; Kerk et al. 2006). At approximately the same time, this protein (designated as DSP4) was reported to be redox regulated. During illumination, it was found to be associated

with starch granules but to dissociate during night. DSP4-deficient *Arabidopsis* mutants exhibited high leaf starch levels (see below) and enlarged starch granules (Sokolov et al. 2006; see also Silver et al. 2013). It remains, however, unclear how the diel intraplastidial partitioning of DSP4/SEX4 fits proposed in vivo functions.

When chemically mutagenised *Arabidopsis* lines were screened for a starch-excess phenotype, the same locus encoding the so-called SEX4 was independently identified, but the product of the gene identified lacked any known function in starch metabolism. Later studies clearly showed that the protein is capable of dephosphorylating α-polyglucans, such as amylopectins (Gentry et al. 2007; Niittylä et al. 2006). The designation SEX4 is now widely accepted.

When acting as α-glucan phosphatase in vitro, its substrate selectivity is lower than that of the starch-related dikinases. SEX4 hydrolyses both C6 and C3 monophosphates and acts on prephosphorylated starch granules (Kötting et al. 2009). It utilises prephosphorylated maltodextrins in both the insoluble and the soluble state. Dephosphorylation of the latter is almost complete, whereas insoluble maltodextrins retain approximately 50 % of the phosphate esters. This difference, however, is likely due to a structural reorganisation of the insoluble maltodextrins rather than an enzymatic property of SEX4 itself. Unlike crystalline maltodextrins, hydrosoluble neutral α-glucans act as inhibitors of the SEX4 phosphatase activity (Hejazi et al. 2010). These results suggest (but do not prove) that the *in planta* substrate of SEX4 is particulate starch.

SEX4-deficient *Arabidopsis* mutants gradually accumulate more starch as compared to the wild-type leading to elevated starch levels throughout the light–dark cycle. In absolute values, nocturnal leaf starch degradation is slower than in the wild-type. Furthermore, the AtSEX4-deficient mutant accumulates soluble phospho-oligoglucans which are undetectable in wild-type leaves. This phenotypical feature is by far more selective for SEX4 than the starch-excess (see below). The phospho-oligoglucans are likely derived from transitory starch as they are not detectable in essentially starch-free double mutants deficient in both SEX4 and the plastidial phosphoglucomutase (*pgm*). Levels of the soluble phosphoglucans are lowered (but still much higher compared to the wild-type) in double mutants lacking AtSEX4 in an *α-amylase3* (*amy3*) or *isoamylase3* (*iso3*) background. Phospho-oligoglucans remain, however, undetectable when GWD plus SEX4 are nonfunctional (Kötting et al. 2009) confirming that *in planta* AtSEX4 acts downstream of AtGWD. In summary, there is good evidence that SEX4 acts as α-glucan phosphatase, but it is still uncertain whether it also functions as phosphoprotein phosphatase.

Recently, AtSEX4 has been crystallised and the three-dimensional structure has been resolved at high resolution (Vander Kooi et al. 2010; Meekins et al. 2014). Four important results of the structural studies are mentioned. Firstly, the entire SEX4 protein possesses a highly compact structure with extensive interactions between three domains, i.e. the DSP, the CBM and a previously unrecognised C-terminal domain. Secondly, the DSP and the CBM domains directly interact and together form a continuous pocket that runs the length of the protein incorporating both catalytic and glucan binding functions. Thirdly, the C-terminal domain folds into the core of the phosphatase domain and is essential for protein stability (Vander

Kooi et al. 2010). Fourthly, AtSEX4 appears to interact with a phosphorylated α-glucan in two steps: Interaction is initiated by the CBM of AtSEX4 which non-covalently binds both to neutral and phosphorylated α-glucans (or α-glucan chains). Subsequently, DSP (which contributes little to the overall binding of the enzyme to α-glucans) positions the target carbohydrate at the active site in a way that the phosphate ester at C6 preferential is preferentially hydrolysed. In the DSP domain, two amino acid residues were identified which contribute to the preferential action of AtSEX4. Site-directed mutagenesis of these two residues increases hydrolysis of C3 monophosphate esters (Meekins et al. 2014).

Interestingly, SEX4 is common in chlorophytes but absent in prokaryotes and glycogen metabolising eukaryotes. Mammals express a DSP called laforin as, if not functional, it is associated with the Lafora disease (Minassian et al. 1998). This is a recessively inherited form of epilepsy and, probably, one of the most severe rare diseases. Patients suffering Lafora disease accumulate poorly branched but highly phosphorylated glycogen-like intracellular inclusions which are designated as Lafora bodies (Turnbull et al. 2010). Laforin is reported to be highly conserved in vertebrates but is rarely found in invertebrates (Genry and Pace 2009). The three-dimensional crystal structure of laforin has been elaborated only recently (Raththalaga et al. 2015; Sankhala et al. 2015). Structural and functional (dis)similarities of SEX4 and laforin are complex: SEX4 and laforin are certainly not orthologues as they differ in the intramolecular order of the DSP motive and the CBM (Gentry et al. 2009) and, therefore, appear to originate from independent domain fusions. In vitro, both phosphatases dephosphorylate α-glucans, such as amylopectin (Hejazi et al. 2010; Kötting et al. 2009; Worby et al. 2006; Niittylä et al. 2006; Gentry et al. 2007). Under in vivo conditions, laforin and SEX4 share functional similarities as wild-type human laforin largely complements the SEX4-deficient *Arabidopsis* mutant (Niittylä et al. 2006; Gentry et al. 2007). Laforin-deficient mice (that accumulate Lafora bodies) were, however, complemented by a mutated laforin lacking any noticeable phosphatase activity, and no Lafora bodies were observed (Gayarre et al. 2014; but see also Agualdo et al. 2010; Rao et al. 2010). These results appear to argue against the assumption that dephosphorylation of glycogen is crucial in preventing the pathogenic process. True orthologues of laforin (but no SEX4) have been reported for red algae which accumulate starch outside the chloroplast (Deschamps et al. 2008; Collén et al. 2013).

Like Sex Four 1 (LSF1)

Similarly to SEX4, LSF1 possesses a C-terminal CBM and a DSP motive that is oriented towards the N-terminal domain. In both regions, sequence similarity to SEX4 is relatively high. The sequence of LSF1 differs from that of the SEX4 and of LSF2 mainly by the approximately 200 amino acid residues large N-terminal extension whose function is unknown. The extension is also found in LSF1 proteins from other higher plant species. In lower plants, such as green and red algae, LFS1 appears to be absent (Comparat-Moss et al. 2010).

Based on the phenotpye of LSF1-deficient *Arabidopsis* mutants, leaves possess an elevated starch level but, as opposed to *AtSEX4*, no elevated phospho-oligoglucan levels. Double mutants lacking both AtSEX4 and AtLSF1 have a more severe leaf starch-excess phenotype than each parental single knockout mutant (Comparat-Moss et al. 2010). Thus, AtSEX4 and AtLSF1 are likely to exert non-identical starch-related functions. Until now, however, no enzymatic activity of plant-derived or recombinant AtLSF1 has been observed. It has, therefore, been hypothesised that the actual function of the LSF1 protein is non-catalytic, such as mediating the interaction of another protein (or other proteins) with the surface of starch granules (Comparat-Moss et al. 2010), but no target protein of AtLSF1 has been identified so far.

Like Sex Four 2 (LSF2)

Among the three plastidial DSPs in *Arabidopsis*, AtLSF2 is the smallest protein. It lacks any CBM but possesses three secondary binding sites (SBSs) which appear to functionally replace CBMs (Meekins et al. 2013). LSF2 differs from LSF1 in three aspects: Firstly, it is widely distributed in lower and higher plants. Secondly, the protein possesses a phosphatase activity using hydrosoluble phospho-oligoglucans, amylopectin and hydroinsoluble starch particles as substrates, but, unlike SEX4, it selectively hydrolyses starch-related C3 monophosphate esters. Thirdly, AtLSF2-deficient *Arabidopsis* mutants do not possess a starch-excess phenotype but possess elevated starch-related C3 monophosphate levels (Santelia et al. 2011). AtLSF2-deficient mutants do not contain a high level of phospho-oligoglucans. Constitutive double knockout *Arabidopsis* mutants deficient in both AtSEX4 and AtLSF2 have higher leaf starch content than the parental single knockout lines and are more strongly compromised in growth. Despite the massive starch-excess phenotype of the double mutant, leaf starch can be degraded at night with an absolute rate similar to that of the wild-type (Santelia et al. 2011).

Recently, the structure of AtLSF2 has been determined following crystallisation both in the presence and the absence of phosphomaltohexaose (Meekins et al. 2013). Based on this study, AtLFS2 acts on a phosphorylated single glucan chain. The phosphatase possesses an extended active-site channel which binds maltohexaose that selectively is phosphorylated at C3. Five evolutionary conserved aromatic amino acid residues interact with the glucosyl residues and thereby orient the phosphate ester towards the catalytically active site. In a series of mutated AtLSF2 molecules, single aromatic amino acids were replaced by alanine. These replacements severely affected dephosphorylation of the phosphohexaose but had little effect on the hydrolysis of the frequently used non-physiological substrate, *p*-nitrophenyl phosphate. Thus, the aromatic residues close to the active site are involved in binding the phosphorylated carbohydrate substrates. In addition, AtLSF2 possesses two other SBSs that are more distant to the catalytic site and, possibly, mediate the (simultaneous) interaction with other α-glucan chains (Meekins et al. 2013). It is, however, uncertain whether LSF2 exclusively acts on

the granule surface, on the pool of hydrosoluble phosphoglucans or on both types of substrates.

Finally, *Arabidopsis* plants can largely compensate the PWD/LSF2-dependent path of starch degradation. Mutants lacking functional PWD are capable to degrade leaf starch, although at a lower rate, and growth is only slightly reduced (for details see Hejazi et al. 2012). Likewise, mutants deficient in functional AtLSF2 possess a wild-type level of starch (Santelia et al. 2011). As revealed by the LSF2-deficient double mutants, the phenotype, however, severely deviates from the wild-type if an additional metabolic block is introduced (see above). In this case, the capacity of metabolic compensation is strongly diminished.

7.4.2.1.3 Metabolism of Hydrosoluble Starch-Derived Compounds

Neutral and phosphorylated α-glucans released from the starch granule surface (see above) are further metabolised in the stromal space. They undergo a complex net of reactions which ensures metabolic flexibility (but do not favour any efficient feedback inhibition) and in Fig. 7.4a are grouped as branched phosphoglucans, branched neutral glucans, linear neutral glucans and linear phosphoglucans. Each group consists of molecules differing in various features such as DP, the position of the branching point and/or phosphate esters. In addition, β-amylase activity releases β-maltose from the surface of the starch granules which can be directly exported to the cytosol (see below). Depending on DP and structure, the constituents of the four (phospho)oligoglucan groups are further depolymerised by hydrolytic or phosphorolytic enzymes. Furthermore, they can be hydrolysed by the plastidial α-amylase isozyme, AMY3, provided the DP and position of any phosphate ester and/or branching permits endohydrolysis. For the sake of clarity, α-amylolysis is not included in Fig. 7.4a.

Phosphorolysis is likely restricted to the pools of hydrosoluble (phospho-) oligoglucans rather than on particulate starch. At the molecular level, phosphorolysis of linear or branched oligoglucans cannot be separated from the reverse reaction, i.e. the chain elongation, and therefore, the plastidial phosphorylase (Pho1 or, in *Arabidopsis thaliana*, PHS1) diversifies the oligoglucan pools as does DPE1 when acting on the pool of linear dextrins. Finally, two neutral sugars (maltose and glucose) and two monophosphate esters of glucose (glucose 6-phosphate and glucose 1-phosphate) are formed as end products of the plastidial starch degradation (for details see Fig. 7.4a). In terms of quantity, the two neutral sugars are dominant, but the ratio between maltose and glucose is flexible.

7.4.2.1.4 Transport of Starch-Derived Products into the Cytosol

In wild-type plants, most of the starch-derived carbon is exported into the cytosol as maltose. The disaccharide is also the main compound released by darkened isolated chloroplasts (Weise et al. 2004). The maltose transporter, MEX1, has been identified

in higher and lower plants (Niittylä et al. 2004). Leaves from *Arabidopsis* mutants lacking functional AtMEX1 have highly elevated maltose levels, accumulate more starch and are compromised in growth as compared to the wild-type. Furthermore, in these mutants leaf sucrose content decreases during darkness (indicating a decreased nocturnal starch-sucrose conversion) and the gene encoding the plastidial glucose transporter (At5g16150; see below) is more strongly expressed (Cho et al. 2011). Expression of *MEX1* has been reported to be strongly affected by changes in temperature (Purdy et al. 2013).

Several lines of evidence suggest that β-maltose is the metabolically active anomeric form during starch degradation. Firstly, in leaves from *Arabidopsis thaliana* and *Phaseolus vulgaris*, the level of the α-anomer remains equal in the light and in the dark period, but β-maltose is high during darkness and low during illumination. Secondly, *Arabidopsis* mutants that accumulate only tiny amounts of starch possess very low β-maltose levels throughout the light–dark cycle. Thirdly, in wild-type plants the nocturnal β-maltose level is high in chloroplasts but low in the cytosol favouring the export of this anomer during starch degradation, but α-maltose does not form any gradient between both compartments throughout the light–dark cycle (Weise et al. 2005).

The recently identified glucose transporter is highly expressed in leaves (Cho et al. 2011). As opposed to AtMEX1-deficient lines, *Arabidopsis* mutants lacking a functional glucose transporter do not strongly deviate from the wild-type control in leaf starch content and growth suggesting compensation by other routes. Double mutants deficient in both functional maltose and glucose transporter are extremely compromised in growth. Leaves possess less chlorophyll and diminished photosynthetic capacity as compared to the wild-type. Mesophyll chloroplasts are largely deformed and subjected to degradation. Thus, the extremely reduced growth appears to be due to both disturbed starch utilisation and diminished photosynthetic activity. Growth of the double mutant is almost completely restored in the presence of exogenous sugars (Cho et al. 2011) which also prevent chlorophyll degradation.

Both massively retarded growth and chloroplast disintegration have also been reported for an *Arabidopsis* double mutant deficient in both DPE1 and MEX1 (Niittylä et al. 2004). Likewise, in two PHS1-related double mutants, *phs1/dpe2* and *phs1/mex1*, the nocturnal starch degradation is associated with a strongly impaired growth and premature chloroplast disintegration, but none of the single knockout parental lines exhibit this phenotype. Under continuous illumination, neither double mutant exhibits any of these phenotypical features (Malinova et al. 2014). These data strongly suggest that the plastidial phosphorylase isozyme, Pho1/PHS1, mediates distinct reactions during the nocturnal degradation of transitory starch.

During starch degradation, plastidial glucose monophosphate esters are exported predominantly in counter-exchange with orthophosphate. The glucose 6-phosphate/orthophosphate transporter (GTP1) has first been identified in heterotrophic tissues. In addition to orthophosphate, the transporter also utilises phosphoglycerate or triose phosphates but neither fructose 6-phosphate nor glucose 1-phosphate (Kammerer et al. 1998).

When potato tuber discs are incubated with ^{14}C-labelled glucose 1-phosphate, the uptake of label is not affected by external glucose 6-phosphate, and therefore, an additional transporter is postulated to exist. Glucose 1-phosphate is imported at a rate exceeding that of glucose and sucrose. Furthermore, imported glucose 1-phosphate appears to directly act as glucosyl donor for the ^{14}C incorporation into native starch granules (Fettke et al. 2010). By contrast, in chloroplasts isolated from *Arabidopsis* leaves, ^{14}C-glucose 1-phosphate is efficiently taken up but is then almost completely converted to ADP-glucose before the glucosyl moiety is transferred to starch (Fettke et al. 2011).

7.4.2.1.5 Cytosolic Metabolism of Starch-Derived Compounds

A mesophyll cell of higher plants typically contains a large number of chloroplasts considerably varying in size (Crumpton-Taylor et al. 2012) but a single cytosolic compartment. The export of starch-derived compounds into the cytosol links multiparallel processes to a single carbon flux. Feedback inhibitions are difficult to construct unless the cytosol monitors the carbon status of the entire cell by integrating the various fluxes from all chloroplasts. In the cytosol, major starch-derived compounds undergo a complex and highly interconnected process before they enter distinct catabolic or biosynthetic paths including cellular respiration and synthesis of cell wall materials or of sucrose.

An enzyme essential for the cytoplasmic metabolism of maltose is the disproportionating isozyme 2 (DPE2). Transcript levels decrease during dark but increase during illumination. The amount of the DPE2 protein, however, remains essentially unchanged throughout the light–dark cycle (Smith et al. 2004). Post-translational regulations are likely to occur (see Fig. 7.4b). The DPE2 monomer possesses two vicinal copies of a putative CBM20 close to the N-terminus. Truncated forms of AtDPE2 lacking CBM20s retain the disproportionating activity and exhibit a much higher affinity towards maltodextrins, but binding to high molecular weight glucans is largely diminished. Most of the DPE2 sequence is covered by the GH77 domain which, however, is interrupted by a more than 170 amino acid residue large insertion. The two copies of CBM20, the GH77 domain and the large insertion are conserved in plants (and in some non-plant organisms as well). By contrast, DPE1 and the bacterial MalQ (see below) contain an uninterrupted GH77 domain but lack any CBM20 copy (Steichen et al. 2008).

Arabidopsis mutants lacking functional AtDPE2 possess a starch-excess phenotype, reduced growth and up to two orders of magnitude higher maltose levels (Chia et al. 2004). DPE2 selectively acts on β-maltose (Dumez et al. 2006).

In an easily reversible reaction, DPE2 transfers a glucosyl residue from β-maltose to one of the nonreducing ends of a high molecular weight carbohydrate and releases the residual glucosyl moiety as free glucose (Chia et al. 2004). In vitro, glycogen is often used as glucosyl acceptor substituting the in vivo substrate, the cytosolic heteroglycans (often designated as water-soluble heteroglycan subfraction I; see

Fig. 7.2f). They are highly branched and dynamic polyglycans with a relatively wide size distribution (up to 70 kDa). Their monosaccharide pattern consists of arabinose, galactose, glucose, xylose and mannose residues resembling that of apoplastic arabinogalactans. Cytosolic heteroglycans from intact plant organs do, however, not generally interact with the synthetic β-glucosyl Yariv reagent (for review see Fettke et al. 2012a).

During the light–dark cycle, both the glucosyl content and the size distribution of the cytosolic heteroglycans alter (Fettke et al. 2012a, b). Furthermore, the glycans are not used as glucosyl acceptors by the plastidial phosphorylase isozyme (Pho1 or, in *Arabidopsis thaliana*, PHS1) nor by the main mammalian muscle glycogen phosphorylase. By contrast, the cytosolic phosphorylase isozyme (Pho2/PHS2) efficiently utilises the cytosolic heteroglycans both as glucosyl acceptor and donor. To obtain evidence under in vivo conditions, tuber slices from plants that over- or underexpress the cytosolic phosphorylase isozyme were incubated with ^{14}C-labelled glucose 1-phosphate. Incorporation of ^{14}C-labelled glucosyl residues into the cytosolic heteroglycans reflects the level of the Pho2 protein (Fettke et al. 2008). Interestingly, the DPE2-deficient *Arabidopsis* mutant possesses a several times higher level of the cytosolic phosphorylase (PHS2; Chia et al. 2004).

The flux of carbon from starch to the cytosolic heteroglycans was demonstrated using *Arabidopsis* mesophyll protoplasts photosynthetically prelabelled with ^{14}C. Following the transfer to darkness, a transient increase in the labelled glucosyl content of the heteroglycans was observed in wild-type protoplasts but not in those prepared from dpe2-deficient mutants (Malinova et al. 2013).

To some extent, DPE2 can be functionally replaced by MalQ from *E. coli*. In some *Arabidopsis* lines expressing this transferase in a DPE2-deficient background, transitory starch amounts, maltose levels and growth of the entire plants are more close to the wild-type. Likewise, expression of the cytosolic phosphorylase isozyme (AtPHS2) is lower as compared to the DPE2-deficient control. Other *Arabidopsis* lines, however, strongly resemble the phenotype of the genetic background, i.e. DPE2 deficiency. As opposed to DPE2, MalQ has a high affinity towards maltodextrins but is essentially unable to interact with the cytosolic heteroglycans (Ruzanski et al. 2013; Smirnova 2013).

Glucose directly exported from the chloroplasts or released from maltose by the DPE2-mediated glucosyl transfer is phosphorylated by the cytosolic hexokinase activity. Possibly, this activity is largely or exclusively due to a distinct cytosolic isozyme (in *Arabidopsis thaliana* AtHXI1; At4g29130). As the enzyme has not unequivocally been identified (for discussion see Claessen and Rivoal 2007; Häusler et al. 2014), no phosphorylation sites are given in Fig. 7.4b. In any case, glucose exported to the cytosol can be converted to glucose 6-phosphate and join the cytosolic pools of glucose monophosphates that are linked to the plastidial ones by the respective transporters. Thus, several routes lead to the two cytosolic glucose monophosphate pools. Glucose 6-phosphate can enter the glycolytic path but may also be converted to glucose 1-phosphate which is linked to various biosynthetic routes, such as the formation of cell wall materials or sucrose. In addition, it may also act as glucosyl donor for a transfer to the cytosolic heteroglycans (Fig. 7.4b).

7.4.2.2 Regulation of Transitory Starch Degradation

In intact plants, leaf starch is degraded under varying external conditions, such as length of and temperature during the dark period (Graf et al. 2010; Pyl et al. 2012). Irrespective of the actual growth conditions, transitory starch is almost completely mobilised at the end of the night to permit growth to be continued throughout the light and dark phase but preventing carbon starvation. It is obvious that transitory starch-degrading path(s) cannot be regulated by varying the activity of a single starch-related enzyme. Rather a complex and highly flexible regulatory system is required that includes monitoring of the actual availability of carbohydrate(s) and the subsequent balancing of starch mobilisation. Because of the organisation of mesophyll cells, it is likely that regulation of starch degradation acts (at least) on the level of the entire mesophyll cell rather than on that of individual chloroplasts. Importantly, transitory starch appears to be selectively controlled by this postulated regulatory system which prevents carbon starvation. Neither soluble low molecular weight carbohydrates nor hydrosoluble α-glucans, such as phytoglycogen, are continuously metabolised over the entire dark period.

Currently, the cellular control of transitory starch degradation is largely unknown. During recent years, however, two elements have been identified that are likely involved in the complex regulatory system, the circadian clock and trehalose 6-phosphate. Constituents of the circadian clock that control starch metabolism have been recently discussed (Graf et al. 2010; Fettke et al. 2012a).

The other compound presumably involved in the regulation of transitory starch metabolism is trehalose 6-phosphate (Tre6P). Trehalose(phosphate) is a disaccharide composed of two α-D-glucosyl residues linked via a α-1,1-bond and, therefore, lacking any reducing terminus. Typically, higher plants contain sucrose in at least hundred-fold higher molar concentration as compared to trehalose (Carillo et al. 2013). Likewise, illuminated *Arabidopsis* rosettes convert newly fixed carbon approximately four orders of magnitude faster to sucrose than to trehalose (Szecowka et al. 2013) indicating that in plants (as opposed to bacteria, fungi and invertebrates) trehalose has little relevance as carbon store, osmolyte or stress protectant as all these functions require significant amounts of the disaccharide. Despite its low abundance, trehalose-based signals are now considered to effectively control several areas of plant metabolism and development (Paul et al. 2008).

Recently, strong evidence has been provided that Tre6P acts as the actual signal metabolite. By contrast, the neutral disaccharide, trehalose, appears to be an intermediate in the degradation of the metabolic signal, Tre6P (for details see Lunn et al. 2014). Tre6P is synthesised from UDP-glucose and glucose 6-phosphate by trehalose-phosphate synthase (TPS) and dephosphorylated to yield the neutral disaccharide, trehalose, by trehalose-phosphate phosphatase (TPP). Both enzymes are widely distributed in plants. In the *Arabidopsis* genome, 11 and 10 genes putatively encoding TPSs and TPPs, respectively, have been identified (Lunn 2007): Similar isozyme numbers have also been determined in other higher plant species (Henry et al. 2014).

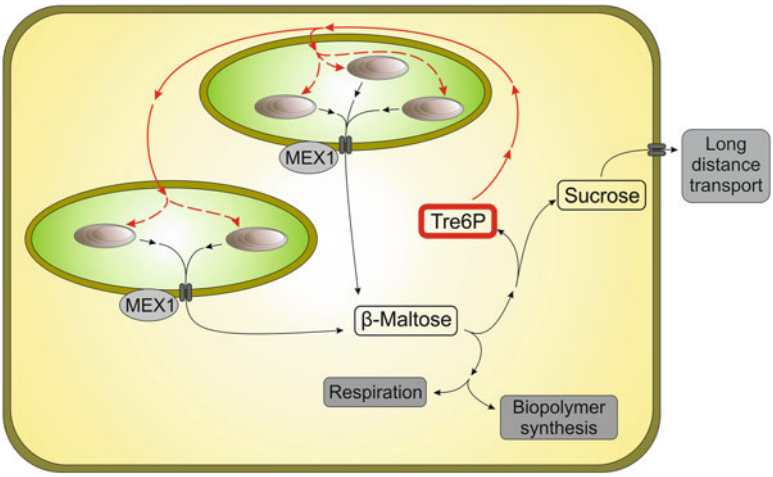

Fig. 7.5 Hypothetical regulation of transitory starch degradation
This scheme integrates some in vivo effects observed by altering Tre6P levels at night on transitory starch degradation into a hypothetical scheme of regulation of starch degradation. Two chloroplasts and the cytosol of a mesophyll cell are given. Only the quantitatively dominant product of starch degradation, β-maltose, is shown which enters the cytosol. Metabolic paths are given in *black*. Hypothetical regulatory processes are marked as closed (cytosolic) or broken (plastidial) *red line*. *MEX1* maltose transporter, *Tre6* trehalose 6-phosphate

For several reasons, Tre6P appears to be the most promising candidate controlling transitory starch degradation (Fig. 7.5). Tre6P and sucrose levels are closely related. Carbon-starved *Arabidopsis* seedlings have very low Tre6P and sucrose levels. Following the application of sucrose, Tre6P concentrations in the seedlings increase in parallel to those of sucrose, but Tre6P levels correlate to a lesser extent if other sugars are added (Lunn et al. 2014; Yadav et al. 2014). In the starch-deficient *Arabidopsis* mutant lacking a functional plastidial phosphoglucomutase (*pgm*), Tre6P levels are lower as compared to the wild-type at the end of the night but increase more strongly during light (Lunn et al. 2014). Using *Arabidopsis* lines that contain an inducible TPS gene, Tre6P contents could be experimentally altered during either the light or the dark period. In the latter case, a two- to threefold increase in Tre6P is associated with rapidly diminished rate of starch degradation and an inhibition of the nocturnal increase in maltose levels (Martins et al. 2013) suggesting that starch degradation is inhibited upstream the release of maltose. As revealed by nonaqueous localisation, Tre6P was recovered predominantly or exclusively in the cytosol. It seems, therefore, likely that Tre6P indirectly controls plastidial starch degradation. Although many steps of the Tre6P-dependent effects mentioned above are unknown, we propose a hypothetical scheme of the potential negative control that is exerted by the cytosol over plastidial starch degradation (Fig. 7.5).

Acknowledgements JS gratefully acknowledges a postdoctoral fellowship from the Deutsche Forschungsgemeinschaft (DFG). MS thanks the Max Planck Institute of Molecular Plant Physiology (Potsdam, Germany) and the University of Guelph (Canada) for providing unlimited access to the library.

References

Aguado C, Sarkar S, Korolchuk VI et al (2010) Laforin, the most common protein mutated in Lafora disease, regulates autophagy. Hum Mol Genet 19:2867–2876

Albrecht T, Koch A, Lode A et al (2001) Plastidic (Pho1-type) phosphorylase isoforms in potato (*Solanum tuberosum* L.) plants: expression analysis and immunochemical characterization. Planta 213:602–613

Asatsuma S, Sawada C, Itoh K et al (2005) Involvement of α-amylase I-1 in starch degradation in rice chloroplasts. Plant Cell Physiol 46:858–869

Atmodjo MA, Hao Z, Mohnen D (2013) Evolving views of pectin biosynthesis. Annu Rev Plant Biol 64:747–779

Baginsky S (2009) Plant proteomics: concepts, applications, and novel strategies for data interpretation. Mass Spectrom Rev 28:93–120

Bailey JM, Whelan WJ (1961) Physical properties of starch I. Relationship between iodine stain and chain length. J Biol Chem 236:969–972

Ball S (2012) Evolution of the starch pathway. In: Tetlow IA (ed) Starch: origins, structure and metabolism, vol 5, Essential reviews in experimental biology. Society for Experimental Biology, London, pp 29–54

Ball S, Morell MK (2003) From bacterial glycogen to starch: understanding the biogenesis of the starch granule. Annu Rev Plant Biol 54:207–233

Ball S, Colleoni C, Cenci U et al (2011) The evolution of glycogen and starch metabolism gives molecular clues to understand the establishment of plastid endosymbiosis. J Exp Bot 62:1775–1801

Bertoft E (2013) On the building block and backbone concepts of amylopectin structure. Cereal Chem 90:294–311

Bewley DJ (1997) Seed germination and dormancy. Plant Cell 9:1055–1066

Bischof S, Umhang M, Eicke S et al (2013) *Cecropia peltata* accumulates starch or soluble glycogen by differentially regulation starch biosynthetic genes. Plant Cell 25:1400–1415

Blazek J, Copeland L (2010) Amylolysis of wheat starches. II. Degradation patterns of native starch granules with varying functional properties. J Cereal Sci 52:295–302

Boraston AB, Bolam DN, Gilbert HJ et al (2004) Carbohydrate-binding modules: fine-tuning polysaccharide recognition. Biochem J 382:769–781

Buléon A, Colonna P, Planchot V et al (1998) Starch granules: structure and biosynthesis. Intern J Biolo Macromol 23:85–112

Buléon A, Cotte M, Putaux J-L et al (2014) Tracking sulfur and phosphorus within single starch granules using synchrotron X-ray microfluorescence mapping. Biochim Biophys Acta 1840:113–119

Bustos R, Fahy B, Hylton CM et al (2004) Starch granule initiation is controlled by heteromultimeric isoamylase in potato tubers. Proc Natl Acad Sci U S A 101:2215–2220

Cantarel BL, Coutinho PM, Rancurel C et al (2009) The carbohydrate-active enzymes database (CAZy): an expert resource for glycogenomics. Nucleic Acids Res 37:D233–D238

Carillo P, Feil R, Gibon Y et al (2013) A fluorometric assay for trehalose in the picomole range. Plant Methods 9:21

Cenci U, Nitschke F, Steup M et al (2014) Transition from glycogen to starch metabolism in archaeplastida. Trends Plant Sci 19:18–28

Chen K, An Y-QC (2006) Transcriptional responses to gibberellin and abscisic acid in barley aleurone. J Integr Plant Biol 48:591–612
Chia T, Thorneycroft D, Chapple A et al (2004) A cytosolic glucosyl transferase is required for conversion of starch to sucrose in *Arabidopsis* leaves at night. Plant J 37:853–863
Chikwana VM, Khanna M, Baskaran S et al (2013) Structural basis for 2′-phosphate incorporation into glycogen by glycogen synthase. Proc Natl Acad Sci U S A 110:20976–20981
Cho M-H, Lim H, Shin DH et al (2011) Role of the plastidic glucose transporter in the export of starch degradation products from the chloroplasts in *Arabidopsis thaliana*. New Phytol 190:101–112
Christiansen C, Hachem NA, Glaring MA et al (2009) A CBM20 low-affinity starch-binding domains from glucan, water dikinase. FEBS Lett 583:1159–1163
Claessen É, Rivoal J (2007) Isoenzymes of plant hexokinase: occurrence, properties and functions. Phytochemistry 68:709–713
Claeys H, De Bodt S, Inzé D (2014) Gibberellins and DELLAs: central nodes in growth regulatory networks. Trends Plant Sci 19:231–239
Collén J, Porcel B, Carré W et al (2013) Genome structure and metabolic features in the red seaweed *Chondrus crispus* shed light on evolution of the Archaeplastida. Proc Natl Acad Sci U S A 110:5247–5252
Comparat-Moss S, Kötting O, Stettler M et al (2010) A putative phosphatase, LSF1, is required for normal starch turnover in *Arabidopsis* leaves. Plant Physiol 152:685–697
Crumpton-Taylor M, Grandison S, Png KMY et al (2012) Control of starch granule number in Arabidopsis chloroplasts. Plant Physiol 158:905–916
Crumpton-Taylor M, Pike M, Lu K-J et al (2013) Starch synthase 4 is essential for coordination of starch granule formation with chloroplast division during Arabidopsis leaf expansion. New Phytol 200:1064–1074
Cuyvers S, Dornez E, Delcour JA et al (2012) Occurrence and functional significance of secondary carbohydrate binding sites in glycoside hydrolases. Crit Rev Biotechnol 32:93–107
Daussant J, Zbaszyniak B, Sadowski J et al (1981) Cereal β-amylase: immunochemical study on two enzyme-deficient inbred lines of rye. Planta 151:176–179
De Schepper V, De Swaef T, Bauweraerts I et al (2013) Phloem transport: a review of mechanisms and controls. J Exp Bot 64:4839–4850
Delatte T, Trevisan M, Parker M et al (2005) Arabidopsis mutants Atisa1 and Atisa2 have identical phenotypes and lack the same multimeric isoamylase, which influences the branch point distribution of amylopectin during starch synthesis. Plant J 41:815–830
Delatte T, Umhang M, Trevisan M et al (2006) Evidence for distinct mechanisms of starch granule breakdown. J Biol Chem 281:12050–12059
Denison FC, Paul A-L, Zupanska AK et al (2011) 14-3-3 proteins in plant physiology. Semin Cell Dev Biol 22:720–727
DePaoli A, Contreras CJ, Segvich DM et al (2015) Glycogen phosphomonoester distribution in mouse models of the progressive myoclonic epilepsy, Lafora disease. J Biol Chem 290:841–850
Deschamps P, Colleoni C, Nakamura Y et al (2008) Metabolic symbiosis and the birth of the plant kingdom. Mol Biol Evol 25:536–548
Dippel R, Boos W (2005) The maltodextrin system of *Escherichia coli*. Metabolism and transport. J Bacteriol 187:8322–8331
Dumez S, Wattebled F, Dauvillee D et al (2006) Mutants of *Arabidopsis* lacking starch branching enzyme II substitute plastidial starch synthesis by cytoplasmic maltose accumulation. Plant Cell 18:2694–2709
Edner C, Li J, Albrecht T, Mahlow S et al (2007) Glucan, water dikinase activity stimulates breakdown of starch granules by plastidial β-amylases. Plant Physiol 145:17–28
Emes MJ, Tetlow IJ (2012) The role of heteromeric protein complexes in starch synthesis. In: Tetlow IJ (ed) Starch: origins, structure and metabolism, Essential reviews in experimental biology. Society for Experimental Biology, London, pp 255–278

Eveland AL, Jackson DP (2012) Sugars, signalling, and plant development. J Exp Bot 63:3367–3377

Facchinelli F, Colleoni C, Ball SG et al (2013) Chlamydia, cyanobion, or host: who was on top in the ménage à trios? Trends Plant Sci 18:673–679

Facon M, Lin Q, Azzaz AM et al (2013) Distinct functional properties if isoamylase-type starch debranching enzymes in monocot and dicot leaves. Plant Physiol 163:1363–1375

Fazedas E, Szabó K, Kandra L et al (2013) Unexpected mode of action of sweet potato β-amylase on maltooligomers. Biochim Biophys Acta 1834:1976–1981

Fettke J, Eckermann N, Poeste S et al (2004) The glycan substrate of the cytosolic (pho2) phosphorylase isozyme from *Pisum sativum* L.: identification, linkage analysis and subcellular localization. Plant J 39:933–946

Fettke J, Eckermann N, Tiessen A et al (2005a) Identification, subcellular localization and biochemical characterization of water-soluble heteroglycans (SHG) in leaves of *Arabidopsis thaliana* L.: distinct SHG reside in the cytosol and in the apoplast. Plant J 43:568–586

Fettke J, Poeste S, Eckermann N et al (2005b) Analysis of cytosolic heteroglycans from leaves of transgenic potato (*Solanum tuberosum* L.) plants that under- or over-express the Pho2 phosphorylase isozyme. Plant Cell Physiol 46:1987–2004

Fettke J, Chia T, Eckermann N et al (2006) A transglucosidase necessary for starch degradation and maltose metabolism in leaves at night acts on cytosolic heteroglycans (SHG). Plant J 46:668–684

Fettke J, Nunes-Nesi A, Alpers J et al (2008) Alterations in cytosolic glucose-phosphate metabolism affect structural features and biochemical properties of starch-related heteroglycans. Plant Physiol 148:1614–1629

Fettke J, Hejazi M, Smirnova J et al (2009) Eukaryotic starch degradation: integration of plastidial and cytosolic pathways. J Exp Bot 60:2907–2922

Fettke J, Albrecht T, Hejazi M et al (2010) Glucose 1-phosphate is efficiently taken up by potato (*Solanum tuberosum*) tuber parenchyma cells and converted to reserve starch granules. New Phytol 185:663–675

Fettke J, Malinova I, Albrecht T et al (2011) Glucose 1-phosphate transport into protoplasts and chloroplasts from leaves of *Arabidopsis*. Plant Physiol 155:1723–1734

Fettke J, Fernie AR, Steup M (2012a) Transitory starch and its degradation in higher plants. In: Tetlow IJ (ed) Starch: origins, structure and metabolism, vol 5, Essential reviews in experimental biology. Society for Experimental Biology, London, pp 311–374

Fettke J, Leifels L, Brust H et al (2012b) Two carbon fluxes to reserve starch in potato (*Solanum tuberosum* L.) tuber cells are closely interconnected but differently modulated by temperature. J Exp Bot 63:3011–3029

Fontes CMGA, Gilbert HJ (2010) Cellulosomes: highly efficient nanomachines designated to deconstruct plant cell wall complex carbohydrates. Annu Rev Biochem 79:655–681

Fordham-Skelton AP, Chilley P, Lumbreras V et al (2002) A novel higher plant protein tyrosine phosphatase interacts with SNF1-related protein kinases via a KIS (kinase interaction sequence) domain. Plant J 29:705–715

Fu F-F, Xue H-W (2010) Coexpression analyses identifies rice starch regulator1, a rice AP2/EREBP family transcription factor, as a novel rice starch biosynthesis regulator. Plant Physiol 154:927–938

Fujita N, Nakamura Y (2012) Distinct and overlapping functions of starch synthase isoforms. In: Tetlow IA (ed) Starch: origin, structure and metabolism, vol 5, Essential reviews in experimental biology. Society for Experimental Biology, London, pp 115–140

Fujita N, Kubo A, Suh DS et al (2003) Antisense inhibition of isoamylase alters the structure of amylopectin and physicochemical properties of starch in rice endosperm. Plant Cell Physiol 44:607–618

Fujita N, Toyosawa Y, Yoshinori U et al (2009) Characterization of pullulanase (PUL)-deficient mutants of rice (*Oryza sativa* L.) and the function of PUL on starch biosynthesis in the developing rice endosperm. J Exp Bot 60:1009–1023

Fulton DC, Stettler M, Mettler T et al (2008) Beta-AMYLASE4, a noncatalytic protein required for starch breakdown, acts upstream of the active beta-amylases in *Arabidopsis* chloroplasts. Plant Cell 20:1040–1058

Garz A, Sandmann M, Rading M et al (2012) Cell-to-cell diversity in a synchronized Chlamydomonas culture as revealed by single cell analyses. Biophys J 103:1078–1086

Gayarre J, Duran-Trío L, Garcia OC et al (2014) The phosphatase activity of laforin is dispensable to rescue EPM2a$^{-/-}$ mice from Lafora disease. Brain 137:806–818

Gentry MS, Dowen RH III, Worby CA et al (2007) The phosphatase laforin crosses evolutionary boundaries and links carbohydrate metabolism to neutral disease. J Cell Biol 178:477–488

Gentry MS, Dixon JE, Worby CA (2009) Lafora disease: insights into neurodegeneration from plant metabolism. Trends Biochem Sci 34:628–639

Gentry MS, Pace RM (2009) Conservation of the glucan phosphatase laforin is linked to rates of molecular evolution and the glucan metabolism of the organism. BMC Evol Biol 9:138

Gentry MS, Romá-Mateo C, Sanz P (2013) Laforin, a protein with many faces: glucan phosphatase, adapter protein, et alii. FEBS J 280:525–537

Gilbert HJ (2010) The biochemistry and structural biology of plant cell wall deconstruction. Plant Physiol 153:444–455

Glaubitz U, Li X, Köhl K et al (2014) Differential physiological responses of different rice (*Oryza sativa*) cultivars to elevated night temperature during vegetative growth. Funct Plant Biol 41:437–448

Goldberg RN, Bell D, Tewari YB et al (1991) Thermodynamics of hydrolysis of oligosaccharides. Biophys Chem 40:69–76

Graf A, Smith AM (2011) Starch and the clock: the dark side of the plant productivity. Trends Plant Sci 16:169–175

Graf A, Schlereth A, Stitt M et al (2010) Circadian control of carbohydrate availability for growth in *Arabidopsis* plants at night. Proc Natl Acad Sci U S A 107:9458–9463

Guillén D, Sánchez S, Rodríguez-Sanoja R (2010) Carbohydrate-binding domains: multiplicity of biological roles. Appl Microbiol Biotechnol 85:1241–1249

Häusler RE, Heinrichs L, Schmitz J et al (2014) How sugars might coordinate chloroplast and nuclear gene expression during acclimation to high light intensities. Mol Plant 7:1121–1137

Heazlewood JL, Durek P, Hummel J et al (2009) PhosPhAt: a database of phosphorylation sites in Arabidopsis thaliana and a plant-specific phosphorylation site predictor. Nucleic Acid Res 36:D1015–D1021

Hehre EJ, Brewer CF, Henghof DS (1979) Scope and mechanism of carbohydrase action. Hydrolytic and nonhydrolytic actions of beta-amylase on alpha- and beta-maltosyl fluoride. J Biol Chem 254:5942–5950

Hehre EJ, Kitabata S, Brewer CF (1986) Catalytic flexibility of glycosidases. The hydration of maltal by β-amylase to form 2-deoxymaltose. J Biol Chem 261:2147–2153

Hejazi M, Fettke J, Haebel S et al (2008) Glucan, water dikinase phosphorylates crystalline maltodextrins and thereby initiates solubilisation. Plant J 55:323–334

Hejazi M, Fettke J, Paris O et al (2009) The two plastidial starch-related dikinases sequentially phosphorylate glucosyl residues at the surface of both the A- and the B-type allomorphs of crystalline maltodextrins but the mode of action differs. Plant Physiol 150:962–976

Hejazi M, Fettke J, Kötting O et al (2010) The laforin-like dual-specificity phosphatase SEX4 from Arabidopsis hydrolyses both C6- and C3-monophosphate esters introduced by starch-related dikinases and thereby affects phase transition of alpha-glucans. Plant Physiol 152:711–722

Hejazi M, Fettke J, Steup M (2012) Starch phosphorylation and dephosphorylation: the consecutive action of starch-related dikinases and phosphatases. In: Tetlow IA (ed) Starch: origins, structure and metabolism, vol 5, Essential reviews in experimental biology. Society for Experimental Biology, London, pp 279–309

Henry C, Bledsoe SW, Siekman A et al (2014) The trehalose pathway in maize: conservation and gene regulation in response to the diurnal cycle and extended darkness. J Exp Bot 65:5959–5973

Hong YF, Ho T-HD, Wu CF et al (2012) Convergent starvation signals and hormone crosstalk in regulating nutrient mobilization upon germination in cereals. Plant Cell 24:2857–2873

Huang X-F, Nazarin-Fironzabadi F, Vincken J-P et al (2014) Expression of an amylosucrase in potato results in larger starch granules with novel properties. Planta 240:409–421

Hussain H, Mant A, Seale R et al (2003) Three isoforms of isoamylase contribute different catalytic properties for the debranching of potato glucans. Plant Cell 15:133–149

Hwang SK, Nishi A, Satoh H et al (2010) Rice endosperm-specific plastidial alpha-phosphorylase is important for synthesis opf short-chain malto-oligosaccharides. Arch Biochem Biophys 495:82–92

Ingkasuwan P, Netrphan S, Prasitwattanaseree S et al (2012) Inferring transcriptional gene regulation network of starch metabolism in Arabidopsis thaliana leaves using graphical Gaussian model. MBC Syst Biol 6:100

Ishikawa K, Nakatani H, Katsuya Y et al (2007) Kinetic and structural analysis of enzyme sliding on a substrate: multiple attack in β-amylase. Biochemistry 46:792–798

Isshiki M, Matsuda Y, Takasaki A et al (2008) *Du3*, a mRNA cap-binding protein gene, regulates amylose content in Japonica rice seeds. Plant Biotechnol 25:483–487

Izumi M, Hidema J, Makino A et al (2013) Autophagy contributes to nighttime energy availability for growth in Arabidopsis. Plant Physiol 161:1682–1693

Jane JL, Kasemsuwaran T, Leas S et al (1994) Anthology of starch granule morphology by scanning electron microscopy. Starch-Starke 46:121–129

Kainuma K, French D (1970) Action of pancreatic alpha-amylase and sweet potato beta-amylase on 6^2 and 6^2 α-glucosylmaltooligosaccharides. FEBS Lett 6:182–186

Kammerer B, Fischer K, Hilpert B et al (1998) Molecular characterization of a carbon transporter in plastids from heterotrophic tissues: the glucose 6-phosphate/phosphate antiporter. Plant Cell 10:105–117

Kartal Ö, Mahlow S, Skupin A et al (2011) Carbohydrate-active enzymes exemplify entropic principles in metabolism. Mol Syst Biol 7:542

Keeling PL, Myers AM (2010) Biochemistry and genetics of starch synthesis. Annu Rev Food Sci 1:271–303

Kerk D, Conley TR, Rodriguez FA et al (2006) A chloroplast-localized dual-specificity protein phosphatase in Arabidopsis contains a phylogenetically dispersed and ancient carbohydrate-binding module, which binds the polysaccharide starch. Plant J 46:400–413

Kiessling LL, Young T, Gruber TD et al (2008) Multivalency in protein-carbohydrate recognition. In: Fraser-Reid B, Tatsuata K, Thiem J (eds) Glycoscience. Springer, Berlin/Heidelberg, pp 2483–2523

Kihara M, Kaneko T, Ito K et al (1999) Geographic variation of β-amylase thermostability among varieties of barley (*Hordeum vulgare*) and β-amylase deficiency. Plant Breed 118:453–455

Kim T-J, Kim M-J, Kim B-C et al (1999) Modes of action of acarbose hydrolysis and transglycosylation catalyzed by a thermo-stable maltogenic amylase, the gene for which was cloned from a Thermus strain. Appl Environ Microbiol 65:1644–1651

Kötting O, Santelia D, Edner C et al (2009) STARCH-EXCESS4 is a laforin-like phosphoglucan phosphatase required for starch degradation in *Arabidopsis thaliana*. Plant Cell 21:334–346

Kötting O, Kossmann J, Zeeman SC et al (2010) Regulation of starch metabolism: the age of enlightenment? Curr Opin Plant Biol 13:321–329

Kramhøft B, Bak-Jensen KS, Mori H et al (2005) Multiple attack, kinetic parameters, and product profiles in amylose hydrolysis by barley α-amylase 1 variants. Biochemistry 44:1824–1832

Kreis M, Williamson M, Buxton B et al (1987) Primary structure and differential expression of β-amylase in normal and mutant barley. Eur J Biochem 169:517–525

Kubo A, Rahman S, Utsumi Y et al (2005) Complementation of *sugary-1* phenotype in rice endosperm with the wheat *isoamylase1* gene supports a direct role for isoamylase1 in amylopectin biosynthesis. Plant Physiol 137:43–56

Kubo A, Colleoni C, Dinges J et al (2010) Functions of heteromeric and homomeric isoamylase-type starch-debranching enzymes in developing maize endosperm. Plant Physiol 153:956–969

Lastdrager J, Hanson J, Smeekens S (2014) Sugar signals and the control of plant growth and development. J Exp Bot 65:799–807
Leivar P, Quail PH (2011) PIFs: pivotal components in a cellular signaling hub. Trends Plant Sci 2011:19–28
Li J, Francisco P, Zhou W, Edner C et al (2009) Catalytically-inactive β-amylase BAM4 required for starch breakdown in Arabidopsis leaves is a starch-binding protein. Arch Biochem Biophys 489:92–98
Liu Y, Bassham DC (2012) Autophagy: pathways for self-eating in plant cells. Annu Rev Plant Biol 63:215–237
Lloyd JR, Kossmann J (2015) Transitory and storage starch metabolism: two sides do the same coin? Curr Opin Biotechnol 32:143–148
Lohmeyer-Vogel EM, Kerk D, Nimick M et al (2008) *Arabidopsis At5g39790* encodes a chloroplast-localized carbohydrate-binding coiled-coil domain-containing putative scaffold protein. BCM Plant Biol 8:120
López CA, de Vries AH, Marrink SJ (2012) Amylose folding under the influence of lipids. Carbohydr Res 364:1–7
Lu CA, Lin CC, Lee KW et al (2007) The SnRK1A protein kinase plays a key role in sugar signaling during germination and seedling growth of rice. Plant Cell 19:2484–2499
Luís AS, Venditto I, Temple MJ et al (2013) Understanding how noncatalytic carbohydrate binding modules can display specificity for xyloglucan. J Biol Chem 288:4799–4809
Lunn JE (2007) Gene families and evolution of trehalose metabolism in plants. Funct Plant Biol 34:550–563
Lunn JE, Delorge I, Figueroa CM et al (2014) Trehalose metabolism in plants. Plant J 79: 544–567
Ma J, Jiang Q-T, Wei L et al (2014) Conserved structure and varied expression reveal key roles of phosphoglucan phosphatase gene starch excess 4 in barley. Planta 240:1179–1190
Mahlow S, Hejazi M, Kuhnert F et al (2014) Phosphorylation of transitory starch by α-glucan, water dikinase during starch turnover affects the surface properties and morphology of starch granules. New Phytol 203:495–507
Malinova I, Steup M, Fettke J (2011) Starch related heteroglycans in roots from *Arabidopsis thaliana*. J Plant Physiol 168:1406–1414
Malinova I, Steup M, Fettke J (2013) Carbon transitions from either Calvin cycle or transitory starch to heteroglycans as revealed by ^{14}C-labeling experiments using protoplasts from Arabidopsis. Physiol Plant 149:25–44
Malinova I, Mahlow S, Alseekh S et al (2014) Double knock-out mutants of Arabidopsis thaliana grown under normal conditions reveal that the plastidial phosphorylase isozyme (PHS1) participates in transitory starch metabolism. Plant Physiol 164:607–621
Martins MCM, Hejazi M, Fettke J et al (2013) Feedback inhibition of starch degradation in Arabidopsis leaves mediated by trehalose 6-phosphate. Plant Physiol 163:1142–1163
Matsushima R, Maekawa M, Kurano M et al (2014) Amyloplast-localized SSG4 protein influences the size of starch grains in rice endosperm. Plant Physiol 164:623–636
Meekins DA, Guo H-F, Husodo S et al (2013) Structure of the *Arabidopsis* glucan phosphatase LIKE SEX FOUR2 reveals a unique mechanism for starch dephosphorylation. Plant Cell 25:2302–2314
Meekins DA, Raththagala M, Husodo S et al (2014) Phosphoglucan-bound structure of starch phosphatase starch excess4 reveals the mechanism for C6 specificity. Proc Natl Acad Sci U S A 111:7272–7277
Meléndez-Hevia E, Waddell TG, Shelton ED (1993) Optimization of molecular design in the evolution of metabolism: the glycogen molecule. Biochem J 295:477–483
Mikami B, Degano M, Hehre EJ et al (1994) Crystal structure of soybean β-amylase reacted with β-maltose and maltal: active site components and their apparent role in catalysis. Biochemistry 33:7779–7787
Minassian BA, Lee JR, Herbick JA et al (1998) Mutations in a gene encoding a novel protein tyrosine phosphatase cause progressive myoclonus epilepsy. Nat Genet 20:171–174

Mizushima N, Yoshimori T, Ohsumi Y (2011) The role of Atg proteins in autophagosome formation. Annu Rev Cell Dev Biol 27:107–132
Moghaddam MRB, Van den Ende W (2012) Sugar and plant immunity. J Exp Bot 63:3989–3998
Nielsen TH, Wischmann B, Enevoldsen K et al (1994) Starch phosphorylation in potato tubers proceeds concurrently with de novo biosynthesis of starch. Plant Physiol 105:111–117
Nielsen MM, Bozonnet S, Seo ES et al (2009) Two secondary carbohydrate binding sites on the surface of barley alpha-amylase I have distinct functions and display synergy in hydrolysis of starch granules. Biochemistry 48:7686–7697
Nielsen JW, Kramhøft B, Boyonnet S et al (2012) Degradation of the starch components amylopectin and amylose by barley α-amylase 1: role of surface binding site 2. Arch Biochem Biophys 528:1–6
Niittylä T, Messerli G, Trevisan M et al (2004) A previously unknown maltose transporter essential for starch degradation in leaves. Science 303:87–89
Niittylä T, Comparat-Moss S, Lue WL et al (2006) Similar protein phosphatases control starch metabolism in plants and glycogen metabolism in mammals. J Biol Chem 281:11815–11818
Nishimo H, Murakawa A, Mori T et al (2004) Kinetic studies of AMP-dependent phosphorolysis of amylopectin catalyzed by phosphorylase b on a 27 MHz microbalance quartz-crystal. J Am Chem Soc 126:14752–14757
Nishiyama Y, Mazeau K, Morin M et al (2010) Molecular and crystal structure of 7-fold V-amylose complexed with 2-propanol. Macromolecules 43:8628–8636
Nitschke F, Wang P, Schmieder P et al (2013) Hyperphosphorylation of glucosyl C6 carbons and altered structure of glycogen in the neurodegenerative epilepsy Lafora disease. Cell Metab 17:756–767
Nougué O, Corbi J, Ball SG et al (2014) Molecular evolution accompanying functional divergence of duplicated genes along the plant starch biosynthesis path. BMC Evol Biol 14(1):103. doi: 10.1186/1471-2148-103
Pal SK, Liput M, Piques M et al (2013) Diurnal changes of polysome loading track sucrose content in the rosette of wild-type Arabidopsis and the starchless *pgm* mutant. Plant Physiol 162:1246–1265
Palm DC, Rohwer JM, Hofmeyr J-HS (2013) Regulation of glycogen synthase from mammalian skeletal muscle – a unifying view of allosteric and covalent regulation. FEBS J 280:2–27
Paparelli E, Parlanti S, Gonzali S et al (2013) Nighttime sugar starvation orchestrates gibberellin biosynthesis and plant growth in Arabidopsis. Plant Cell 25:3760–3769
Park J-T, Shim J-H, Tran P et al (2011) Role of maltose enzymes in glycogen synthesis by *Escherichia coli*. J Bacteriol 193:2517–2526
Paul MJ, Primavesi F, Jhurreea D et al (2008) Trehalose metabolism and signalling. Annu Rev Plant Biol 59:417–441
Payne CM, Baban J, Horn SJ et al (2012) Hallmarks of processivity in glycoside hydrolases from crystallographic and computational studies of the *Serratia marcescens* chitinases. J Biol Chem 287:36322–36330
Payne CM, Resch MG, Chen L et al (2013) Glycosylated linkers in multimodular lignocellulose-degrading enzymes dynamically bind to cellulose. Proc Natl Acad Sci U S A 110:14646–14651
Pederson BA, Turnbull J, Epp JR et al (2013) Inhibiting glycogen synthesis prevents Lafora disease in a mouse model. Ann Neurol 74:297–300
Peng M, Gao M, Båga M et al (2000) Starch-branching enzymes preferentially associated with A-type starch granules in wheat endosperm. Plant Physiol 124:265–272
Peng C, Wang Y, Liu F et al (2014) *FLOURY ENDOSPERM6* encodes a CBM48 domain-containing protein involved in compound granule formation and starch synthesis in rice endosperm. Plant J 77:917–930
Pérez S, Bertoft E (2010) The molecular structure of starch components and their contribution to the architecture of starch granules: a comprehensive review. Starch-Starke 62:389–420
Pfister B, Lu K-J, Eicke S et al (2014) Genetic evidence that chain length and branch point distributions are linked determinants of starch granule formation in Arabidopsis. Plant Physiol 165:1467–1474

Pulido R, Hooft van Huijsduijnen R (2008) Protein tyrosine phosphatases: dual-specificity phosphatases in health and disease. FEBS J 275:848–866

Purdy SJ, Bussell JD, Nunn CP et al (2013) Leaves from the Arabidopsis maltose exporter1 mutant exhibits a metabolic profile with features of cold acclimation in the warm. PLoS ONE 8:e79412

Putaux J-L, Montesanti N, Véronèse G et al (2011) Morphology and structure of A-amylose single crystals. Polymer 52:2198–2205

Pyl E-T, Piques M, Ivakov A et al (2012) Metabolism and growth in *Arabidopsis* depend on the daytime temperature but are temperature-compensated against cool nights. Plant Cell 24:2443–2469

Qian M, Nahoum V, Bumiel J et al (2001) Enzyme-catalyzed condensation reaction in a mammalian α-amylase. High-resolution structural analysis of an enzyme-inhibitor complex. Biochemistry 40:7700–7709

Ragauskas AJ, Williams CK, Davison BH et al (2006) The path for biofuels and biomaterials. Science 311:484–489

Ragel P, Streb S, Feil R et al (2013) Loss of starch granule initiation has a deleterious effect on the growth of Arabidopsis plants due to an accumulation of ADP-glucose. Plant Physiol 163:75–85

Rao SNR, Maity R, Sharma J et al (2010) Sequestration of chaperones and proteasome into Lafora bodies and proteasomal dysfunction induced by Lafora disease-associated mutations. Hum Mol Genet 19:4726–4734

Raththagala M, Brewer MK, Parker MW et al (2015) Structural mechanism of laforin function in glycogen dephosphorylation and Lafora disease. Mol Cell 57:261–272

Regina A, Blazek J, Gilbert E et al (2012) Differential effects of genetically distinct mechanisms of elevating amylose on barley starch characteristics. Carbohydr Polym 89:979–991

Reiland S, Messerli G, Baerenfaller K et al (2009) Large-scale Arabidopsis phosphoproteome profiling reveals novel chloroplast-kinase substrates and phosphorylation networks. Plant Physiol 150:889–903

Reinhold H, Soyk S, Šimková K et al (2011) β-amylase-like proteins function as transcription factors in Arabidopsis, controlling shoot growth and development. Plant Cell 23:1391–1403

Rejek M, Stevenson CE, Southard AM et al (2011) Chemical genetics and cereal starch metabolism: structural basis of the non-covalent and covalent inhibition of barley β-amylase. Mol BioSyst 7:718–730

Ritte G, Lloyd JR, Eckermann N et al (2002) The starch-related R1 protein is an alpha-glucan, water dikinase. Proc Natl Acad Sci U S A 99:7166–7171

Ritte G, Scharf A, Eckermann N et al (2004) Phosphorylation of transitory starch is increased during degradation. Plant Physiol 135:2068–2077

Roach PJ, DePaoli AA, Hurley TD et al (2012) Glycogen and its metabolism: some new developments and old themes. Biochem J 441:763–787

Roberts EH (1973) Predicting the storage life of seeds. Seed Sci Technol 1:499–514

Roblin P, Potocki-Véronèse G, Guieysse D et al (2013) SAXS Conformational tracking of amylose synthesized by amylosucrase. Biomacromolecules 14:232–239

Ruan Y-L (2014) Sucrose metabolism: gateway to diverse carbon use and sugar signaling. Annu Rev Plant Biol 65:26.1–26.35

Ruzanski C, Smirnova J, Rejzek M et al (2013) A bacterial glucanotransferase can replace the complex maltose metabolism required for starch-to-sucrose conversion in leaves at night. J Biol Chem 288:28581–28598

Ryu J-H, Drain J, Kim JH et al (2009) Comparative structural analyses of purified glycogen particles from rat liver, human skeletal muscle and commercial preparations. Int J Biol Macromol 45:478–482

Salazar C, Höfer T (2009) Multiple protein phosphorylation – from molecular mechanisms to kinetic models. FEBS J 276:3177–3198

Sankhala RS, Koksai AC, Ho L et al (2015) Dimeric quarternary structure of human laforin. J Biol Chem 290:4552–4559

Santelia D, Kötting O, Seung D et al (2011) The phosphoglucan phosphatase like SEX Four2 dephosphorylates starch at the C3-position in *Arabidopsis*. Plant Cell 23:4096–4111

Satoh H, Shibahara K, Tokunaga T et al (2008) Mutation of the plastidial alpha-glucan phosphorylase gene in rice affects the synthesis and structure of starch in the endosperm. Plant Cell 20:1833–1849

Scheidig A, Fröhlich A, Schulze S et al (2002) Downregulation of a chloroplast-targeted β-amylase leads to a starch-excess phenotype in leaves. Plant J 30:581–591

Schmitz J, Heinrichs L, Scossa F et al (2014) The essential role of sugar metabolism in the acclimation response of *Arabidopsis thaliana* to high light intensities. J Exp Bot 65:1619–1636

Schönknecht G, Chen W-H, Ternes CM et al (2013) Gene transfer from bacteria and archaea facilitated evolution of an extremophilic eukaryote. Science 339:1207–1210

Shaik SS, Carciofi M, Martens HJ et al (2014) Starch bioengineering affects cereal grain germination and seedling establishment. J Exp Bot 65:2257–2270

Shang BZ, Chang R, Chu J-W (2013) Systems-level modelling with molecular resolution elucidates the rate-limiting mechanisms of cellulose decomposition by cellobiohydrolases. J Biol Chem 288:29081–29089

Shimonaga T, Konishi M, Oyama Y et al (2008) Variation in storage α-glucans of the Porphyridiales (Rhodophyta). Plant Cell Physiol 49:103–116

Silver DM, Silva LP, Issakidis-Bourguet E et al (2013) Insight into the redox regulation of the phosphoglucan phosphatase SEX4 involved in starch degradation. FEBS J 280:538–548

Silver DM, Kötting O, Moorhead GB (2014) Phosphoglucan phosphatase function sheds light on starch degradation. Trends Plant Sci 19:471–478

Sim L, Beeren SR, Findinier J et al (2014) Crystal structure of the Chlamydomonas starch debranching isoamylase ISA1 reveals insights into the mechanism of branch trimming and complex assembly. J Biol Chem 289:22991–23003

Skeffington AW, Graf A, Duxbury Z et al (2014) Glucan, water dikinase exerts little control over starch degradation in Arabidopsis leaves at night. Plant Physiol 165:866–879

Smirnova J (2013) Carbohydrate-active enzymes metabolising maltose: kinetic and structural features. Dissertation, University of Potsdam

Smith SM, Fulton DC, Chia T et al (2004) Diurnal changes in the transcriptome encoding enzymes of starch metabolism provide evidence for both transcriptional and posttranscriptional regulation of starch metabolism in *Arabidopsis* leaves. Plant Physiol 136:2687–2699

Sokolov LN, Dominguez-Solis JR, Allary AL et al (2006) A redox-regulated chloroplast protein phosphatase binds to starch diurnally and functions in its accumulation. Proc Natl Acad Sci USA 103:9732–9737

Sonnewald U, Kossmann J (2013) Starches – from current models to genetic engineering. Plant Biotechnol J 11:223–232

Soyk S, Šimková K, Zürcher E et al (2014) The enzyme-like domain of Arabidopsis nuclear β-amylases is critical for DNA sequence recognition and transcriptional activity. Plant Cell 26:1746–1763

Sparks E, Wachsmann G, Benfey PN (2013) Spatiotemporal signaling in plant development. Nat Rev Genet 14:631–644

Sreenivaculu N, Usadel B, Winter A et al (2008) Barley grain maturation and germination: metabolic pathway and regulatory network commonalities and differences highlighted by new MapMan/PageMan profiling tools. Plant Physiol 146:310–327

Sreenivasulu N, Wobus U (2013) Seed-development programs: a systems biology-based comparison between dicots and monocots. Annu Rev Plant Biol 64:189–217

Steichen JM, Petty RV, Sharkey TD (2008) Domain characterization of a 4-alpha-glucanotransferase essential for maltose metabolism in photosynthetic leaves. J Biol Chem 283:20797–20804

Stettler M, Eicke S, Mettler T et al (2009) Blocking the metabolism of starch breakdown products in *Arabidopsis* leaves triggers chloroplast degradation. Mol Plant 2:1233–1246

Steup M, Schächtele C (1981) Mode of glucan degradation by purified phosphorylase forms from spinach leaves. Planta 153:351–361

Stitt M, Zeeman SC (2012) Starch turnover: pathways, regulation and role in growth. Curr Opin Plant Biol 15:282–292

Stoddard FL (1999) Survey of starch particle-size distribution in wheat and related species. Cereal Chem 67:59–63
Streb S, Delatte T, Umhang M et al (2008) Starch granule biosynthesis in Arabidopsis is abolished by removal of all debranching enzymes but restored by the subsequent removal of an endoamylase. Plant Cell 20:3448–3466
Streb S, Eicke S, Zeeman SC (2012) The simultaneous abolition of three starch hydrolases blocks transient starch breakdown in *Arabidopsis*. J Biol Chem 287:41745–41756
Sullivan MA, Aroney STN, Li S et al (2014) Changes in glycogen structure over feeding cycles sheds new light on blood-glucose control. Biomacromolecules 15:660–665
Sulpice R, Flis A, Ivakov AA, Apelt F et al (2014) *Arabidopsis* coordinates the diurnal regulation of carbon allocation and growth across a wide range of photoperiods. Mol Plant 7:137–155
Sun T-P (2011) The molecular mechanism and evolution of the GA-GID1-DELLA signalling module in plants. Curr Biol 21:R338–R345
Sun X, Jones WT, Rikkerink EHA (2012) GRAS proteins: the versatile roles of intrinsically disordered proteins in plant signalling. Biochem J 442:1–12
Sundberg M, Pfister B, Fulton D et al (2013) The heteromultimeric debranching enzyme involved in starch synthesis in Arabidopsis requires both isoamylase1 and isoamyoase2 subunits for complex stability and activity. PLos ONE 8:e75223
Szecowka M, Heise R, Tohge T et al (2013) Metabolic fluxes of an illuminated *Arabidopsis thaliana* rosette. Plant Cell 25:694–714
Tagliabracci VS, Heiss C, Karthlic C et al (2011) Phosphate incorporation during glycogen biosynthesis and Lafora disease. Cell Metab 13:274–282
Takeda Y, Hizukuri S (1981) Re-examination of the action of sweet-potato beta-amylase on phosphorylated (1 → 4)-α-D-glucan. Carbohydr Res 89:174–178
Tanackovic V, Svenson JT, Jensen S et al (2014) The deposition and characterization of starch in Brachypodium distachyon. J Exp Bot 65:5179–5192
Tan-Wilson AL, Wilson KA (2012) Mobilization of seed protein reserves. Physiol Plant 145:140–153
Tsuji H, Aya K, Ueguchi-Tanaka M et al (2006) GAMYB controls different sets of genes and is differentially regulated by microRNA in aleurone cells and anthers. Plant J 47:427–444
Turgeon R, Wolf S (2009) Phloem transport: cellular pathways and molecular trafficking. Annu Rev Plant Biol 60:207–221
Turnbull J, Wang P, Girard J-M et al (2010) Glycogen hyperphosphorylation underlies lafora body formation. Ann Neurol 68:925–933
van Wijk KJ, Friso G, Walther D, Schulze WX (2014) Meta-analysis of *Arabidopsis thaliana* phospho-proteomics data reveals compartmentalization of phosphorylation motifs. Plant Cell 26:2367–2389
Vander Kooi CW, Taylor AO, Pace RM et al (2010) Structural basis for the glucan phosphatase activity of Starch Excess4. Proc Natl Acad Sci U S A 107:15379–15384
Vilaplana F, Hasjim J, Gilbert RG (2012) Amylose content in starches: towards optimal definition and validating experimental methods. Carbohydr Polym 88:103–111
Vriet C, Welham T, Brachmann A et al (2010) A suite of *Lotus japonicus* starch mutants reveals both conserved and novel features of starch metabolism. Plant Physiol 154:643–655
Walley JW, Shen Z, Sartor R et al (2013) Reconstruction of protein networks from an atlas of maize seed proteotypes. Proc Natl Acad Sci U S A 110:E4808–E4817
Wattebled F, Dong Y, Dumez S et al (2005) Mutants of Arabidopsis lacking a chloroplastic isoamylase accumulate phytoglycogen and an abnormal form of amylopectin. Plant Physiol 138:184–195
Wattebled F, Planchot V, Szydlowski N et al (2008) Further evidence for the mandatory nature of polysaccharide debranching for the aggregation of semicrystalline starch and for overlapping functions of debranching enzymes in Arabidopsis leaves. Plant Physiol 148:1309–1323
Webber BL, Abaloz BA, Woodrow IE (2007) Myrmecophilic food body production in the understorey tree, Ryparosa kurrangii (Archariaceae), a rare Australian rainforest taxon. New Phytol 173:250–263

Weidberg H, Shvets E, Elazar Z (2011) Biogenesis and cargo selectivity of autophagosomes. Annu Rev Biochem 80:125–156

Weise SE, Weber APM, Sharkey TD (2004) Maltose is the major form of carbon exported from the chloroplast at night. Planta 218:474–482

Weise SE, Kim KS, Stewart RP et al (2005) β-Maltose is the metabolically active anomer of maltose during transitory starch degradation. Plant Physiol 137:756–761

Weise SE, Aung K, Jarou ZJ et al (2012) Engineering starch accumulation by manipulation of phosphate metabolism of starch. Plant Biotechnol J 10:545–554

Weitbrecht K, Muller K, Leubner-Metzger G (2011) First off the mark: early seed germination. J Exp Bot 62:3289–3309

Wilson WA, Roach PJ, Montero M et al (2010) Regulation of glycogen metabolism in yeast and bacteria. FEMS Microbiol Rev 34:952–985

Worby CA, Gentry MS, Dixon JE (2006) Laforin, a dual specificity phosphatase that dephosphorylates complex carbohydrates. J Biol Chem 281:30412–30418

Yadav UP, Ivakov A, Feil R et al (2014) The sucrose-trehalose 6-phosphate (Tre6P) nexus: specificity and mechanisms of sucrose signalling by Tre6P. J Exp Bot 65:1051–1068

Yamaguchi S (2008) Gibberellin metabolism and its regulation. Annu Rev Plant Biol 59:225–251

Yin LL, Xue HW (2012) The *MADS29* transcription factor regulates the degradation of the nucellus and the nucellar projection during rice seed development. Plant Cell 24:1049–1065

Yu TS, Zeeman SC, Thorneycroft D et al (2005) α-Amylase is not required for breakdown of transitory starch in Arabidopsis leaves. J Biol Chem 280:9773–9779

Yun M-S, Kawagoe Y (2010) Septum formation in amyloplasts produces compound granules in the endosperm and is regulated by plastid division proteins. Plant Cell Physiol 51:1469–1479

Zeeman SC, Umemoto T, Lue WL et al (1998) A mutant of *Arabidopsis* lacking a chloroplastic isoamylase accumulates both starch and phytoglycogen. Plant Cell 10:1699–1712

Zeeman SC, Kossmann J, Smith AM (2010) Starch: its metabolism, evolution, and biotechnological modification in plants. Annu Rev Plant Biol 61:209–234

Zeng D, Yan M, Wang Y et al (2007) *Du1*, encoding a novel Prp1 protein, regulates starch biosynthesis through affecting the splicing of Wx^b pre-mRNAs in rice (*Oryza sativa* L.). Plant Mol Biol 65:501–509

Zhang Q, Wing R (2013) Genome studies and molecular genetics: understanding the functional genome based on the rice model. Curr Opin Plant Biol 16:129–132

Zhou S-R, Yin L-L, Xue H-W (2013) Functional genomics based understanding of rice endosperm development. Curr Opin Plant Biol 16:236–246

Zi J, Mafu S, Peters RJ (2014) To gibberellins and beyond! Surveying the evolution of (di)terpenoid metabolism. Annu Rev Plant Biol 65:10.1–10.28

Zirin J, Nieuwenhius J, Perrimon N (2013) Role of autophagy in glycogen breakdown and its relevance to chloroquine myopathy. PLoS Biol 11:e1001708

Zulawski M, Braginets R, Schulze WX (2013) PhosPhAt goes kinases – searchable protein kinase target information in the plant phosphorylation site database PhosPhAt. Nucleic Acids Res 41:D1176–D1184

Chapter 8
Protein-Protein Interactions During Starch Biosynthesis

Ian J. Tetlow, Fushan Liu, and Michael J. Emes

Abstract Starch biosynthesis requires the ordered assembly of glucose units into amylose and amylopectin from ADPglucose. Whilst amylose has a relatively simple linear structure, the synthesis of amylopectin requires the formation of regular, repeating clusters of glucan chains. These clusters have a 9 nm periodicity and comprise a crystalline, alpha helical region and an amorphous branched region, a unit which is repeated many times over to give rise to blocklets of amylopectin. Although the individual enzymes of starch biosynthesis have been studied extensively, our knowledge of the mechanisms which give rise to this highly ordered structure is limited. There is an increasing body of literature which has demonstrated that several reactions are regulated post-translationally, including via redox modulation, protein-protein interactions and protein phosphorylation. This chapter summarises our current knowledge of these mechanisms and offers a model of how they serve to coordinate the biosynthesis of amylopectin in particular.

Keywords Amylopectin • Amylose • Protein complexes • Protein phosphorylation • Protein-protein interactions

8.1 Introduction

The architecture of the starch granule is determined primarily by amylopectin (Hizukuri et al. 1989; Yeh et al. 1981). Amylose, which is a largely linear polymer in which glucosyl residues are joined between carbon atoms 1 and 4 of neighbouring moieties, is an important, interspersed component of starch, but is not essential for the formation of a functional starch granule. Amylopectin, on the other hand, is composed of a cluster arrangement of crystalline, densely packed glucosyl residues organised as parallel, linear α-helices joined by α(1–4) bonds, interspersed by more disorganised α(1–6) branches at regular intervals (see Chaps. 1 and 3). Such organisation gives rise to the classic semicrystalline model in which aggregation

I.J. Tetlow (✉) • F. Liu • M.J. Emes
Department of Molecular and Cellular Biology, Summerlee Science Complex, University of Guelph, Guelph, Ontario, N1G 2W1 Canada
e-mail: itetlow@uoguelph.ca

Y. Nakamura (ed.), *Starch*, DOI 10.1007/978-4-431-55495-0_8

of these clusters generates a regular 9 nm repeating unit to define the architecture of a stable, insoluble, glucan polymer the physical disruption of which requires considerable energy (Robin et al. 1974; French 1984; Hizukuri 1986). Depending on the genetic source of the starch, there is variation in granule size and/or morphology, the length of α-helices and the frequency of α(1–6) linkages, but the fundamental features of amylopectin are remarkably conserved, irrespective of origin.

Whereas the synthesis of amylose seems dependent on a single gene encoding granule-bound starch synthase (GBSS), the synthesis of amylopectin requires the coordinated interaction of as many as 10 different enzymes in such a way as to reproducibly generate an insoluble polymer whose characteristics are broadly conserved. This process involves several classes of enzymes including soluble starch synthases (SS), starch branching enzymes (SBE) and debranching enzymes (DBE) all of which are composed of multiple isoforms whose combined activities are in some way coordinated to give rise to an organised, semicrystalline, insoluble glucan polymer. This is remarkably different from the process of glycogen biosynthesis in bacteria and mammals, which requires the action of only a single form of each of glycogen synthase and glycogen branching enzyme and produces a more open glucan polymer, soluble in water, which can be rapidly mobilised by the action of degradative enzymes within minutes (Roach et al. 2012). The hydrosoluble properties of glycogen contrast with the insolubility of the starch granule which contributes to its longer-term storage properties as a calorically rich, dense, osmotically inert assembly of polymers, the complete degradation of which takes place over periods of hours, in the case of diurnal turnover in a leaf, and days in the case of germinating seedlings.

In order to achieve this level of structure and biological functionality, it seems reasonable to suggest that the actions of the soluble enzymes which give rise to the regular, organised, repeating cluster-unit structure of amylopectin are in some way coordinated. This chapter attempts to review our current understanding of the ways in which the enzymes of starch synthesis are regulated and indeed interact genetically, functionally and physically. A better comprehension of how the activities of starch biosynthetic enzymes work cooperatively is leading to the discovery of other factors, including regulatory proteins, which contribute to the control of starch architecture.

8.2 Protein-Protein Interactions in the Pathway of Starch Biosynthesis

8.2.1 Regulation of ADPglucose Biosynthesis

The enzymes involved in the biosynthesis of starch are localised in plastids (Fig. 8.1) and have been covered in detail elsewhere in this book (Chaps. 5, 6 and 11). The first committed step of the pathway is catalysed by ADPglucose pyrophosphorylase

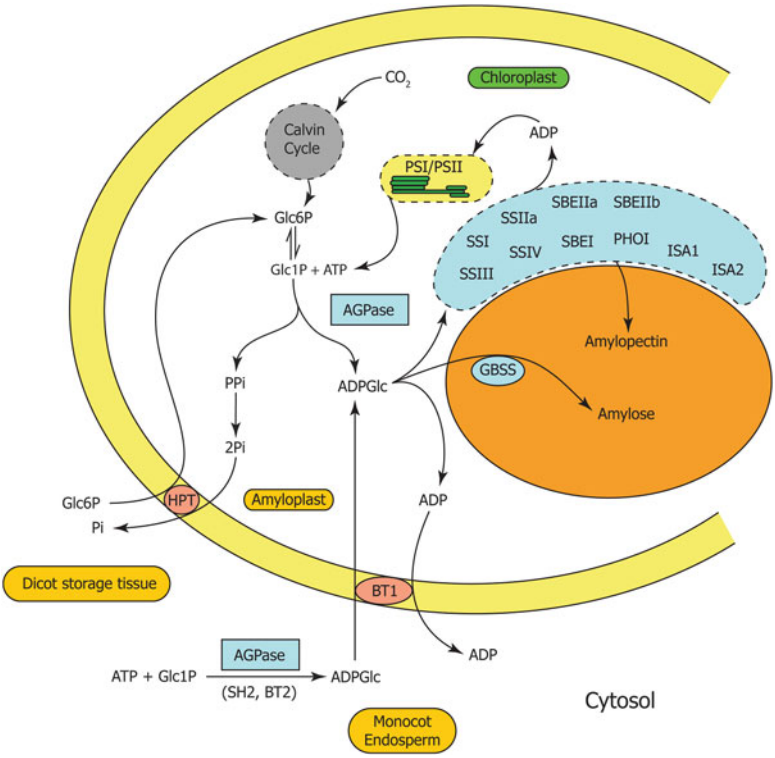

Fig. 8.1 Pathway of starch biosynthesis
The cartoon represents a composite of events which occur in leaves, heterotrophic tissues of dicots and cereal endosperm. AGPase synthesises ADPglucose from G1c1P and ATP. In photosynthetic organelles these are produced as a consequence of photosynthesis. In nongreen tissues of dicotyledonous plants, hexose phosphates and ATP (not shown) are imported from the cytosol. Note that in photosynthetic chloroplasts most of the inorganic orthophosphate (Pi, produced from inorganic pyrophosphate (PPi) in the synthesis of ADPglucose) would be used in photophosphorylation for the synthesis of ATP. In developing cereal endosperm ADPglucose is produced predominantly in the cytosol and imported into the amyloplast via a sugar nucleotide translocator, BT1. Amylose is produced via the action of GBSS. Amylopectin synthesis depends on the coordinated interaction of at least 10 different genes coding for isoforms of soluble starch synthases (SS), starch branching enzymes (SBE), a type of debranching enzyme, isoamylase (ISA) and plastidial starch phosphorylase (PHO1)

(AGPase) which produces the nucleotide sugar, ADPglucose, the soluble substrate for starch biosynthesis. This enzyme is a heterotetramer which consists of two large and two small subunits and is known to be highly regulated in leaves, seeds and tubers of dicots, and to a lesser extent in developing seeds of cereals (Geigenberger et al. 2005; Ghosh and Preiss 1966; Michalska et al. 2009). In leaves AGPase is localised in chloroplasts and regulated according to the availability and utilisation of photosynthate, such that it is strongly activated by 3-phosphoglyceric acid (PGA) and inhibited by orthophosphate (Pi). The PGA/Pi ratio increases during

leaf photosynthesis when sucrose utilisation and export become saturated (Ghosh and Preiss 1966; Preiss 1991), as a consequence of which 25–30 % of the reduced carbohydrate produced in the Calvin cycle is diverted into starch. The enzyme in potato tubers is equally sensitive to this ratio though it is less clear under what conditions such metabolite changes would occur (Hylton and Smith 1992; Ballicora et al. 1995). In developing cereal grain, a second form of the enzyme is found in the cytosol and accounts for the vast majority of the total AGPase activity (Denyer et al. 1996; Sikka et al. 2001), and ADPglucose is imported into amyloplasts via a specialised sugar nucleotide transporter, Brittle 1 (Kirchberger et al. 2007). Wheat endosperm plastidial AGPase is sensitive to PGA and Pi, but the major cytosolic isoform is much less so (Tetlow et al. 2003). An important development in understanding the regulation of this enzyme was the discovery that an intramolecular disulphide bridge can be formed between adjacent small subunits in the heterotetramer of AGPase, leading to inactivation of the enzyme (see Geigenberger 2011, for review). Thus AGPase is also controlled by post-translational modification linked to the redox state of the plastid or cell (Tiessen et al. 2002). This involves interaction of AGPase with thioredoxin (Fu et al. 1998), a 10 kDa protein belonging to a multi-gene family, responsible for redox control of several enzymes and proteins in green and nongreen tissues (for review, see Buchanan and Balmer 2005). When Cys-82 of adjacent small subunits of potato AGPase is oxidised to create a disulphide bond, the enzyme is deactivated (Tiessen et al. 2002). Reduction of the enzyme by reduced thioredoxin (or dithiothreitol in vitro) leads to reactivation. In leaf tissue, the small subunit of AGPase is present as an inactive dimer at night and is activated under reducing conditions during daylight, through photoreduction and transfer of electrons from photosystem I to thioredoxin, via ferredoxin-thioredoxin reductase (Hendriks et al. 2003) or possibly via a novel NADPH-thioredoxin reductase which also is found in amyloplasts (Michalska et al. 2009). The Cys-82 residue is highly conserved in most forms of the small subunit of AGPase with the exception of the cytosolic form found in monocots, which suggests that redox modulation is restricted to the plastidic enzyme. Regulation of AGPase is also linked to the regulation of SNF1-related protein kinase (SnRK). Studies with transgenic *Arabidopsis* indicate a role for trehalose-6-phosphate (T6P) in promoting SnRK redox activation of AGPase in leaves (Kolbe et al. 2005). T6P has emerged as an important signal molecule which correlates closely with sucrose content in photosynthetic and non-photosynthetic tissues (Lunn et al. 2006; Martinez-Barajas et al. 2013) and is thought to regulate SnRK1, though the direct mechanism of action in relation to control of AGPase is unclear, and it may be that T6P and SnRK1 operate through distinct but overlapping pathways (Lunn et al. 2014). Recent proteomic studies have indicated that the large and small subunits of plastidial AGPase may be subject to protein phosphorylation in vivo (Heazlewood et al. 2008; Lohrig et al. 2009), but details of the effect on activity and the protein kinase involved have yet to be determined. Figure 8.2 illustrates the various mechanisms which regulate AGPases in plants, including interactions amongst its subunits and with other proteins.

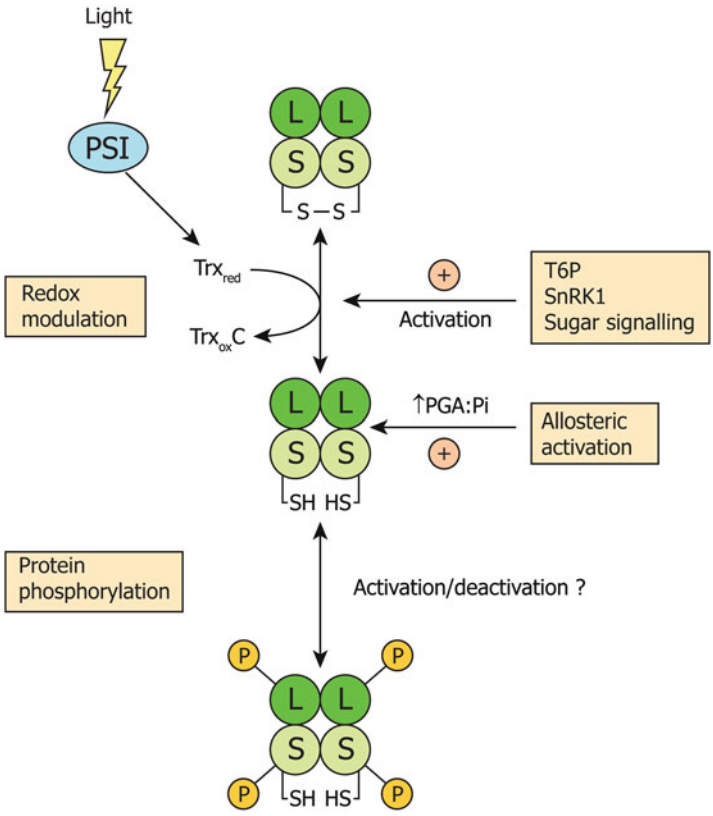

Fig. 8.2 Regulation of AGPase
The plastidial enzyme is a heterotetramer of 2 large (L) and 2 small (S) subunits. Interaction with reduced thioredoxin (Trx) leads to activation by reduction of a disulphide bridge between two small subunits to produce free thiol groups. This process is linked to light activation via photosystem I in chloroplasts and also to sugar-sensing mechanisms involving T6P and SnRK1. These mechanisms also operate in non-photosynthetic plastids such as those found in tubers, where reductant is provided via carbohydrate oxidation through the oxidative pentose phosphate pathway. Both L and S subunits have been found to be phosphorylated in proteomic studies, though the consequences are unclear and it is not known whether this can occur on the reduced or oxidised small subunit (only the reduced subunit is shown). The plastidic enzyme is also subject to fine control by allosteric activation through altered ratios of PGA/Pi. Little is known about the post-translational regulation of the cytosolic isoform of AGPase found in cereal endosperm which lacks the equivalent of Cys-82 found in the plastidic small subunit and is far less sensitive to PGA and Pi

8.2.2 Amylose Biosynthesis

Amylose is composed of long, sparsely branched linear chains, representing a minor component of starch: 6 % of total in *Arabidopsis* leaf starch and up to 25–30 % in storage starches in cereals (Zeeman et al. 2002; French 1984). Amylose

is synthesised by a single enzyme, granule-bound starch synthase (GBSS), and mutants defective in GBSS produce amylose-free *waxy* starches (Shure et al. 1983). Unlike other starch synthases, GBSS is exclusively associated with starch granules and is the most abundant of the granule-associated proteins found in starch granules (Mu-Forster et al. 1996). In sweet potato leaves it was shown that expression of the GBSS gene was under circadian control and also modulated by sucrose levels in the leaf (Wang et al. 2001). Evidence suggests GBSS is also regulated at the post-translational level. A study by Grimaud et al. (2008) showed that maize GBSS is phosphorylated in the starch granule, a finding supported by a recent paper studying rice endosperm GBSS (Liu et al. 2013). Both studies used the staining of the protein with a phospho-specific fluorochrome (Pro-Q Diamond^{TM}) to determine the phosphorylation status. To date no direct evidence for GBSS phosphorylation exists. Liu et al. (2013) also noted that GBSS is able to form oligomers and that oligomerisation of the enzyme is enhanced, in vitro, by addition of ATP and mitogen-activated protein kinase and weakened by phosphatase treatment. In addition, increasing physiological concentrations of ADPglucose promote oligomerisation of GBSS. It is not yet known whether GBSS associates with other proteins in the plastid.

8.2.3 Protein-Protein Interactions Amongst Enzymes of Amylopectin Biosynthesis

8.2.3.1 Biochemical Evidence

The biosynthesis of amylopectin involves the cooperative action of several classes of stromal enzymes inside plastids as shown in Fig. 8.1. The association between SS and SBE activities in a "synthetase-branching enzyme complex" had been suspected for some time (Schiefer et al. 1973) as SS and SBE isoforms of maize readily co-purified (Schiefer et al. 1978). Previous work also showed that purified SS was stimulated by SBE (Hawker et al. 1974; Boyer and Preiss 1979; Pollock and Preiss 1980), probably through an increase in nonreducing ends provided by branching enzyme activity. Studies using recombinant forms of *Arabidopsis* starch synthase isoforms 1–4, combined with either recombinant BE2 or BE3 (both equivalent to SBE class II branching enzymes of cereals), produced polyglucans of varying structure (Brust et al. 2014). Interestingly, when combining recombinant SSI with either form of SBE, the chain length distribution (CLD) pattern, following isoamylase debranching of the glucan product, closely resembled that of wild-type starch extracted from leaves. However, although experiments showed that SSI extracted from *Arabidopsis* leaves appeared to co-migrate electrophoretically with branching enzymes, more exacting electrophoresis demonstrated that the enzymes could be separated from each other, leaving open the question of whether SS and BE interact physically in vivo. Investigations using recombinant enzymes from rice (Nakamura et al. 2014) also suggest that SSI and SBE interact functionally in unprimed

glucan synthesis, and that this is not a simple function of SBE increasing the number of nonreducing ends in the glucan primer with which SBE isoforms can interact.

Several lines of investigation have suggested that enzymes of amylopectin biosynthesis interact directly. Tetlow et al. (2008) and Hennen-Bierwagen et al. (2008) showed that in wheat and maize, respectively, there are heteromeric complexes which involve both SSI and SSII interacting with whichever is the predominant form of SBEII in a given species. In wheat endosperm, protein complexes were detected at the onset of grain filling (Tetlow et al. 2008), as trimers consisting of SSI, SSIIa and either of SBEIIa or SBEIIb, with a molecular weight ca. 260 kDa (Tetlow et al. 2008). In maize the major trimeric complex detected was composed of SSI, SSIIa and SBEIIb (Liu et al. 2009) as the latter is present in large excess of SBEIIa. In maize, very high molecular weight complexes were also found in which SSI, SSIIa, SBEIIa and SBEIIb were associated with SSIII (Hennen-Bierwagen et al. 2008). These large molecular weight complexes (ca. 670 kDa) could be separated by gel permeation chromatography and, as described above, components could be co-precipitated by antibodies raised to other members of the complex. In both wheat and maize endosperms, the SS/SBE protein complexes were stable and, in the case of maize, stabilised by relatively high salt (NaCl) concentrations. Chemical cross-linking showed that the individual enzymes were physically closely associated (Tetlow et al. 2008) and a recombinant form of maize SSI was shown to interact in vitro with SSIIa and SBEIIb, whilst recombinant SBEIIa and SBEIIb interacted with SSI and SSIIa (Hennen-Bierwagen et al. 2008; Liu et al. 2009). Experiments with a chemically cleaveable hetero-bifunctional cross-linker (SULFO-SBED) suggest that, in maize amyloplasts, SSIIa is the central component of a trimeric assembly, positioned between SSI and SBEIIb (Liu et al. 2012b).

Maize SSIII possesses an extended N-terminus referred to as the HD or homology domain, which includes coiled-coil domains thought to be involved in protein-protein interactions, suggesting that this region might be important in providing a scaffold with which other enzymes can interact (Gao et al. 1998). Using a truncated version of SSIII, Hennen-Bierwagen et al. (2009) made an affinity column using the recombinant, expressed sequence of the HD region to investigate these interactions. They demonstrated that SBEIIa and SBEIIb isoforms from an amyloplast preparation could bind to the ligand and subsequently be eluted following a salt wash. However, they could find no evidence for binding of SSIIa or SBEI under the conditions employed. Intriguingly they also found evidence of interaction between the SSIIIHD and pyruvate phosphate dikinase (PPDK), sucrose synthase and the large subunit of AGPase encoded by the *sh2* gene. PPDK is found in both the cytosol and plastids. Products of the *pdk1* gene are found in both subcellular locations, whereas *pdk2* is thought to code selectively for a cytosolic isoform (Sheen 1991). Subsequent reciprocal co-immunoprecipitation studies confirmed the in vitro interaction between PPDK and SSIII. Antibodies to SSIII were also able to co-precipitate the small subunit of AGPase (*bt2* gene) as well as sucrose synthase. The authors proposed a model in which the interaction between inorganic pyrophosphate (PPi) generated by PPDK is channelled to AGPase,

directing ADPglucose away from SS and SBE by favouring the formation of Glc1P (Hennen-Bierwagen et al. 2009). It is not clear how sucrose synthase might fit into this scheme since the evidence favours a cytosolic location of this enzyme and that the particular isoform determined in these studies is membrane bound (Duncan et al. 2006). Whilst the AGPase subunits identified represent the cytosolic enzyme in maize, and therefore would be unlikely candidates to interact with starch synthases, it is possible that, in vivo, the plastidic isoforms are directly involved. We do not know which domains of the AGPase large and small subunits are involved in protein-protein interactions, but there is a good degree of functional and structural similarity between the cytosolic and plastidic sequences (Huang et al. 2014). The cytosolic enzyme accounts for approximately 99 % of the total AGPase activity (Denyer et al. 1996) which may explain why the plastidic isoform was not readily detected in these protein-interaction experiments in vitro.

Recently, Nakamura et al. (2012) provided in vitro evidence for functional interaction between purified rice plastidial starch phosphorylase (PHO1) and recombinant forms of SBEI, SBEIIa or SBEIIb. These were shown to interact synergistically in the formation of branched maltodextrins which the authors hypothesised act as primers for amylopectin biosynthesis. This is an interesting proposition as the role of starch phosphorylase is still not well understood, but is consistent with other observations which show that PHO1 interacts physically with starch branching enzymes (see below). In relation to this, the first such multienzyme complex observed in amyloplasts of developing wheat endosperm (Tetlow et al. 2004) was between SBEIIb, SBEI and starch phosphorylase. The complex could be co-precipitated by antibodies raised to any one of these enzymes, was stimulated by the addition of ATP to amyloplast stromal extract and could be disaggregated by dephosphorylation following treatment with a broad specificity alkaline phosphatase. All three of these enzymes were shown to be phosphorylated (as was the granule-bound form of SSIIa; see later section on protein phosphorylation). Uncomplexed PHO1 is normally found as a tetramer and, in subsequent experiments with maize, it was shown that the monomeric form of the enzyme could interact with either SBEI or SBEIIb, whereas only SBEI interacts with the tetrameric form of PHO1 (Subasinghe et al. 2014). This might suggest that there are multiple variants of enzyme complexes which PHO1 is capable of forming with SBEs.

8.2.3.2 Genetic Evidence

Genetic studies have been consistent with the hypothesis that the enzymes of starch metabolism interact functionally and physically. For example, the *amylose extender* (*ae*$^{-}$) mutation which results in the loss of SBEIIb activity leads to a reduction in the activity of soluble SSI in maize (Boyer and Preiss 1981) and rice (Nishi et al. 2001). Loss of SSIII function in maize (the *dull* mutation) caused a decrease in SBEIIa and SSII activity (Boyer and Preiss 1981; Cao et al. 2000). Mutants of rice in which multiple enzyme steps have been modified also point to such interactions. Using RNAi, Zhang et al. (2011) downregulated the expression of seven different rice SS

genes and also studied the effect of a double knockdown of SSIIa and SSIIIa and determined the consequences of single or double mutations on the physicochemical properties of starch. Effects on chain length distribution were nonadditive in the double-knockdown lines, and the authors suggested that SSIII may regulate SSI in vivo although direct evidence was lacking.

As noted previously (Hennen-Bierwagen et al. 2008) one of the trimeric enzyme complexes which can be detected in the amyloplast stroma of wild-type maize consists of SSI, SSIIa and SBEIIb. Studies of the *ae*$^{-}$ mutant, which affects SBEIIb, have led to considerable insight as to the role of such complexes in vivo. In a null *ae*$^{-}$ mutant (*ae1.1*) in which SBEIIb protein was absent, new multienzyme complexes were detected (Liu et al. 2009). Using a combination of co-immunoprecipitation, gel permeation chromatography and recombinant proteins as affinity ligands, these authors demonstrated the presence of new stromal complexes which involved SSI, SSIIa, SBEI, SBEIIa and PHO1. As the nature of the experiments depends largely on identifying reciprocal, pairwise interactions, it was not possible to determine whether this represents a single multimeric complex (although gel permeation chromatography did not suggest such a "super-complex") or multiple permutations of different heteromeric complexes. Importantly, these changes in the constituents found in enzyme complexes were reflected in granule protein composition such that, in the mutant, SBEI, SBEIIa and PHO1 could now be detected in starch granules in addition to SSI and SSIIa (Grimaud et al. 2008; Liu et al. 2009, 2012a). It was argued that the phenotype of the mutant starch was therefore not solely a result of the loss of SBEIIb but also arose because of the introduction of new functions in such complexes particularly through the presence of SBEI. SBEI has a preference for branching long glucan chains compared with SBEII isoforms (Guan and Preiss 1993) resulting in fewer branch points in the polymer. This contributes to the apparent "high amylose" content of such starches which is actually due to a modification in amylopectin architecture as a result of reduced branching and increased chain length (Ikawa et al. 1978; Klucinec and Thompson 2002). Arguably this could be the case even in the absence of functional, multienzyme complexes. However, Liu et al. (2012a) showed that in a second *ae*$^{-}$ mutant (*ae1.2*), in which an inactive form of SBEIIb was expressed, the outcome of this mutation was different to that observed in the null allele. In this case, the inactive SBEIIb was able to form multienzyme complexes with SSI, SSIIa and SBEI, but not with starch phosphorylase (PHO1). The complement of enzymes seen in complexes was again reflected in the granule proteome, i.e. SBEI was present in the starch granule along with SSI and SSIIa, but not PHO1. What is most significant about this study is that the starches which resulted from two near-isogenic maize lines carrying different *ae*$^{-}$ alleles were markedly different from each other (Table 8.1, derived from Liu et al. (2012a)). There were marked differences in the apparent amylose content and the granule size of the two mutants, as well as between the mutants and the wild-type. There was also a subtle but significant difference in chain length distribution between the null mutant and the mutant containing an inactive SBEIIb (*ae1.2*), the latter showing a relative increase in chain lengths DP 16–20 compared to *ae1.1* (Liu et al. 2012a). Clearly the pleiotropic effects resulting from

Table 8.1 Allelic mutations of maize SBEIIb produce different enzyme complexes which give rise to distinct starch phenotypes

Maize genotype	Granule size (μm)	Grain starch content (as % kernel dry weight)	Apparent amylose content (% total starch)
Wt	8.37 ± 1.33	41.02 ± 0.83	24.9 ± 2.2
ae1.1	6.04 ± 0.56	38.12 ± 1.22	65.6 ± 0.4
ae1.2	4.32 ± 0.94	35.82 ± 0.51	49.3 ± 2.2

SBEIIb is coded for by the *Ae* gene. In wild-type (Wt), a trimeric complex is formed between SSI, SSIIa and SBEIIb. In the null mutant, *ae1.1*, SBEIIb protein is absent leading to protein complexes comprising SSI, SSIIa, SBEI, SBEIIa and PHO1. In a second mutant, *ae1.2*, an inactive form of SBEIIb, is produced. In this case, PHO1 does not interact with any of the other enzymes and results in a starch phenotype which is distinct from the wild-type and *ae1.1*. Since both mutations result in the complete loss of SBEIIb activity, the variation in phenotype must arise as a result of altered protein-protein interactions as well as loss of SBEIIb activity. Data is derived from Liu et al. (2012a)

the ability of the two *ae* alleles to form different protein complexes have a marked effect on the phenotype of the starch observed, even though the primary cause of the mutation, loss of SBEIIb activity, is identical. This adds considerable weight to the argument that it is the heteromeric complexes which are the functionally active components during amylopectin biosynthesis. Similar changes in the starch granule proteome have been observed in rice mutants (Abe et al. 2014) where mutation in SBEIIb led to the appearance of SBEI in granules.

In wheat, barley and rice mutants which lack a functional SSIIa (Yamamori et al. 2000; Morell et al. 2003; Umemoto and Aoki 2005), the granules also become devoid of SSI and SBEII class proteins. The *sugary 2* (*su2)* mutation, which codes for the maize homologue of SSIIa, also results in a marked decrease, if not a complete loss, of SSI and SBEIIb from the granule as well as SSIIa itself (Grimaud et al. 2008). The *su2* mutation produces one of the strongest phenotypes caused by the loss of activity of any single enzyme in starch biosynthesis, resulting in a marked reduction in yield, an altered morphology of granules and a substantial increase in the proportion of short chains DP 7–10 and reduction in DP 12–22 (Zhang et al. 2004). Liu et al. (2012b) examined the formation of protein complexes in a maize mutant of a catalytically inactive *su2* in which a single nucleotide polymorphism gave rise to the substitution of arginine (R) for glycine (G) at residue 522 (a second polymorphism led to an amino acid substitution already present in other fully active SSII homologues), and the protein was present in the same concentration as the wild-type. None of the other enzymes of starch biosynthesis were affected in terms of activity or expression, and SSIIa was still able to form a multienzyme complex with SSI and SBEIIb both of which were fully active when measured in the noncomplexed state. The G522R mutation resulted in SSIIa being unable to bind to starch, as a consequence of which the multienzyme complex of SSI/SSIIa/SBEIIb was not bound to granules even though it could be formed in the soluble amyloplast stroma. Within the heteromeric complex, SSI and SBEIIb retained their individual

affinities for starch, but because they were associated with an inactive SSIIa, the complex itself was unable to bind, leading to the loss of all three proteins from starch granules. Thus it appears that SSIIa is essential for the trafficking of SSI and SBEIIb into starch granules and, as mentioned earlier, appears to be at the core of a trimeric complex between the three enzymes. By contrast, in the case of the *ae*$^{-}$ mutant discussed earlier, in which an inactive form of SBEIIb was translated in vivo, there was no effect on the location of SSI and SSIIa within granules. Importantly, the inactive SBEIIb in the *ae*$^{-}$ mutant was unable to bind starch directly, but was strongly associated with starch granules, reinforcing the conclusion that its presence in the starch granule is a result of being associated with SSIIa (Liu et al. 2012a). Based on these studies in maize and evidence from other mutants, it is proposed that SSI, SSIIa and SBEIIb are primarily responsible for the formation of the branched clusters of glucan chains within the granule (Emes and Tetlow 2012).

Amongst the debranching enzymes (isoamylases, ISAs) which are associated with the biosynthesis of starch, ISA1 and ISA2 have been shown to form a heteromeric complex with each other in which ISA2 acts as a regulatory subunit and ISA1 the catalytic subunit (Hussain et al. 2003; Delatte et al. 2005). Studies of rice endosperm (Utsumi et al. 2011) and maize (Kubo et al. 2010) endosperm ISAs, in which mutations in one or both subunits have been obtained, indicate that ISA1 can exist either as a homo-oligomer or as a hetero-oligomer with ISA2 in these tissues, but the effects of mutation of either one are complex and distinctive depending on the tissue in which they are expressed. For example, overexpression of ISA2 in rice impaired starch synthesis possibly as a result of binding all of the ISA1 in a hetero-oligomer (Utsumi et al. 2011). By contrast, in maize, when all of the ISA1 was associated with ISA2, as a result of a mutation *su1*-P, there was no diminution in starch content even though the homo-oligomer of ISA1 was no longer present, and only the ISA1-ISA2 hetero-oligomer was present (Kubo et al. 2010). Loss of the ISA2 subunit resulted in a decrease in leaf starch content in *Arabidopsis* (Delatte et al. 2005; Wattebled et al. 2008), but had little effect in maize or rice endosperm. Given the previous discussion of how SS interacts with BE, there is, to date, no firm evidence for the direct interaction of DBE with such complexes, although mechanistically, it is clearly important that the debranching of disordered starch needs to be integrated with the branching and elongation process (see Sect. 8.4).

Investigation of maize lines in which both SSIII and the regulatory, non-catalytic subunit of ISA1 were mutated provides some genetic evidence for functional interactions between these enzyme activities (Lin et al. 2012). When the catalytic subunit of ISA1 is lost, as in the *sugary1* (*su1*) mutation of maize, there is a marked reduction in starch, and a soluble, highly branched, glucan polymer, phytoglycogen, accumulates in its place (James et al. 1995). However, loss of ISA2 in cereals does not cause an increase in phytoglycogen as the remaining, catalytically functional, ISA1 homomer is active (Kubo et al. 2010; Utsumi et al. 2011). This contrasts with the situation in dicots such as *Arabidopsis* (Delatte et al. 2005) where mutation in either subunit is detrimental. Likewise, the *du1* mutation in maize SSIII does not, alone, lead to increase in water-soluble glucan polymer (WSP). Analysis of

the phenotypes of two *du1*$^{-}$ maize alleles crossed with *isa2*$^{-}$ surprisingly led to a marked increase in WSP even though the additional loss of ISA2 had negligible effect on the chain length distribution of the residual starch compared to the *du1*$^{-}$ single mutation (Lin et al. 2012). The same results were obtained with either a null allele or a C-terminal truncation of SSIII. This might suggest that their interactive effect is because of the need for one or the other of SSIII or ISA2 to be expressed in order for ISA1 to be functional. Whilst other explanations are possible, one hypothesis which could explain the results is that direct or indirect physical interaction with SSIII is necessary to position ISA1 on the growing amylopectin molecule (Lin et al. 2012).

8.3 Regulation of Protein Complex Formation by Protein Phosphorylation

Studies of developing cereal endosperm have shown that the assembly of individual proteins into multienzyme complexes is dependent on protein phosphorylation (Tetlow et al. 2004, 2008; Hennen-Bierwagen et al. 2008; Lin et al. 2012). Evidence for the role of protein phosphorylation in this process has included the effects on aggregation into higher molecular weight complexes when exogenous ATP was added to amyloplast lysates, or by the application of a non-specific phosphatase which led to their disassembly (e.g. Liu et al. 2009; Lin et al. 2012). Direct evidence about which enzymes are phosphorylated, and the specific sites of phosphorylation, are sparse but increasing. AGPase, GBSS, SSIIa, SBEIIb, SBEIIa, SBEI and PHO1 have all been shown to be phosphorylated by direct biochemical analysis, based either on autoradiography of ^{32}P-labelled proteins, the use of Pro-Q Diamond (which selectively stains proteins in acrylamide gels) or high-throughput phosphoproteomics (e.g. Tetlow et al. 2004; Grimaud et al. 2008; Walley et al. 2013; Subasinghe et al. 2014). Phosphoproteome profiling of *Arabidopsis* chloroplasts identified a phosphopeptide derived from ATSS2 (starch synthase II) (Reiland et al. 2009). However, the sequence of the putative phosphorylation site is near the N-terminus of the protein which is highly variable across species, and candidate serine or threonine residues do not align consistently with the sequences of other species. Phosphopeptides of large and small subunits of AGPase have been identified (Heazlewood et al. 2008; Lohrig et al. 2009; Kötting et al. 2010), though it should be borne in mind that these are from the chloroplastidic enzyme, whereas the major form of AGPase in cereal storage tissues is extra-plastidial (cytosolic). The phosphopeptide of the large AGPase subunit does not appear to be highly conserved across species, whereas the phosphopeptide identified in the small subunit (which contains two potential serine targets) is in a highly conserved region of both cytosolic and plastidial small subunits (IYVLTQN(pS)A(pS)LNR). This raises a question about the location of the protein kinase that would be required to catalyse such a post-translational modification, unless there is both a plastidial

and cytosolic isoform. Likewise, several putative sites of phosphorylation were identified within *Arabidopsis* SSIII (see Kötting et al. 2010, taken from Heazlewood et al. 2008), but there is little conservation across species with the exception of a possible phosphothreonine on residue 1,209 of the *Arabidopsis* enzyme. A recent, extensive, high-throughput proteomic, transcriptomic and phosphoproteomic analysis in developing maize endosperm identified phosphopeptides on several of the starch biosynthetic enzymes including the large and small subunits of AGPase, PHO1, SBEIIb, SBEIIa and SBEI and ISA2, as well as BT1 which is responsible for transporting ADPglucose into amyloplasts (see Table 8.2, derived from Walley et al. 2013, and Makhmoudova et al. 2014). In the case of PHO1, six phosphorylation sites were identified, five of which are closely clustered together in a highly acidic region of the protein. This region sits within a longer polypeptide sequence, L78, which is found in PHO1 of storage tissues and can be removed by an endogenous protease leading to an increase in the catalytic activity in the phosphorolytic direction (Chen et al. 2002). The L78 region of PHO1 represents a large insertion that is typical for PHO1 in plastids of higher plants, but is not observed in the cytosolic isozyme nor in the well-studied glycogen phosphorylase. Surprisingly, five of the phosphorylation sites identified by Walley et al. (2013) within L78 appear to be specific to cereals and not found in dicots such as sweet potato where other phosphorylation sites were identified (Young et al. 2006), whereas the sixth site is conserved amongst all species homologues of PHO1 (Table 8.2). It is tempting to speculate that the hyperphosphorylated acidic region of PHO1 plays a distinctive role in the regulation of starch biosynthesis in the developing seeds of monocots, though any function would be conjecture at this stage.

Mechanistically, it is not clear what phosphorylation does in each case, nor how phosphorylation of individual sites relates to the assembly or disassembly of multienzyme complexes, but the identification of such sites will allow experimental testing of related hypotheses. Similarly, there is little information on the protein kinases and phosphatases which are involved in such regulation. A recent study, which included the co-authors of this chapter, investigated the phosphorylation of maize SBEIIb in detail (Makhmoudova et al. 2014). Using a combination of site-directed mutagenesis of recombinant SBEIIb, mass spectrometry and synthetic peptides as substrates, three serine residues were identified which could be phosphorylated by amyloplast-located, Ca^{2+}-dependent protein kinase activities: Ser^{286}, Ser^{297} and Ser^{649}. Molecular modelling showed that each phosphorylation would likely result in the formation of a salt bridge which would stabilise structure. In the case of Ser^{649} and Ser^{286}, salt bridges were possible between the phosphate residues and either arginine or histidine residues which are close by in terms of both tertiary structure and primary sequence. Interestingly, in the case of phosphorylation of Ser^{297}, a salt bridge could be formed with an arginine residue at a site (R665) which is part of a disorganised loop. This loop, containing the sequence KCRRR, is far removed from Ser^{297} in terms of primary sequence but close in the three-dimensional model. The KCRRR sequence is a predicted interaction domain which is highly conserved in all SBEs, and it is argued that stabilisation of this site could facilitate interaction with other enzymes of starch biosynthesis including SSII.

Table 8.2 Phosphorylation sites identified on enzymes of maize amylopectin biosynthesis

Enzyme	Phosphorylation sites	Relative sequence conservation
SBEIIb	(K)AVMVPEGENDGLAsR(A)	High, cereals
	(R)ADsAQFQSDELEVPDISEETTCGAGVADAQALNR(V)	None
	(F)RHAQPKRPKsLRIYETH(V)	Ser^{286}, high, cereals
	(R)IYETHVGMsSPEPK(I)	Ser^{297}, high, all species
	(R)LPsGKFIPGNNNSYDK(C)	Ser^{649}, moderate, cereal endosperm, T substitutes in some species
SBEIIa	(K)TsSSPTQTTSAVAEASSGVEAEERPELSEVIGVGGTGGTK(I)	Not conserved
PHO1	(R)SVASDRDVQGPVsPAEGLPSVLNSIGSSAIASNIK(H)	High, most species
	(K)tELEEEAEVLsEIEEEKLEsEEVEAEEEssEDELDPFVK(S)	High, cereals
ISA2	(R)WAEMNtR(F)	High, cereals
BT2	(K)AsPPPWNATAAEQPIPK(R)	Not conserved
	(K)IYVLTQFNSAsLNR(H)	High, all species
SH2	(R)VSAIILGGGTGsQLFPLTSTR(A)	High, T substitutes in some species

Phosphopeptide sequences are shown for maize enzymes based on Walley et al. (2013) and Makhmoudova et al. (2014). Ser^{286}, Ser^{297} and Ser^{649} of SBEIIb are phosphorylated by two Ca^{2+}-dependent protein kinases. Dephosphorylation of SBEIIb decreases enzyme activity. Little is known of the significance of the phosphorylation sites identified on other enzymes. The highly acidic phosphopeptide of PHO1, which has 5 phosphorylation sites, is conserved in cereals, but not other species where the same region (termed L78) is phosphorylated on other residues (Chen et al. 2002). A relative indication of the extent to which the identified phospho-amino acids are conserved across species is given

Ser^{297} is highly conserved in all classes of SBE enzymes. It is positioned at the opposite end of the central catalytic β-barrel from Ser^{286}, and therefore these two residues could also affect interaction with glucan substrates. Ser ^{286} is also highly conserved in the SBEII class of enzymes but, notably, is replaced by alanine in SBEI. It had previously been reported that phosphorylation altered the activity of either SBEIIa or SBEIIb from wheat, but not SBEI (Tetlow et al. 2008). This may suggest a role for Ser^{286} in controlling catalysis and activation. Ser^{649} is found in a 12-amino-acid region which is completely absent in the SBEI class of proteins, again suggesting a distinct class of function for this site. Further, Ser^{649} is found in the amino acid sequence of some, but not all, cereal endosperm SBEIIb homologues and in dicot species is substituted by aspartate (D), a phospho-mimic. In a maize ae^{-} mutant in which Ser^{286} and Ser^{297} of the expressed protein are missing, the enzyme becomes hyperphosphorylated (Liu et al. 2012a), presumably at the remaining identified phosphorylation site, Ser^{649}. Importantly, Makhmoudova et al. (2014) separated two amyloplast-located, Ca^{2+}-dependent protein kinases (CDPK) by a combination of chromatographic methods and demonstrated differential specificity for the sites identified. Both CDPKs were able to phosphorylate Ser^{649}, but discriminated between Ser^{286} and Ser^{297}, respectively, again suggesting distinctive roles

for these residues and their regulation. Dreier et al. (1992) showed that SS activity could be stimulated by ATP and that this might involve a calcium-calmodulin-dependent protein kinase, though there was no indication of which isoforms of SS were involved. Whether the same CDPKs are involved in regulating glucan chain elongation and branching remains speculative at this stage. Phosphorylation of wheat SBEIIa and SBEIIb also increases their affinity for glucan polymer (Tetlow et al. 2008) as part of a trimeric complex with SSI and SSII, which may be indicative of more efficient substrate channelling, though it is not known which phosphoserine residues might play a role in this.

Identification of other protein kinases and protein phosphatases which catalyse post-translational modifications of the enzymes of starch synthesis is limited and largely indirect. The sucrose non-fermenting 1 (SNF1) protein kinase was first identified in yeast and regulates a variety of cellular processes in response to nutrient stress (Hardie 2007) including carbohydrate metabolism. Homologues exist in mammalian and plant systems, the SNF1-related protein kinases (SnRKs), which function in a wide range of stress responses and, in plants, are divided into 3 subfamilies (Coello et al. 2011). The SnRK1 subfamily is closely related to mammalian AMP-activated protein kinase (AMPK) and regulates several metabolic enzymes including several involved in carbon and nitrogen metabolism (McBride et al. 2009). SnRK1 enzymes are heterotrimeric complexes consisting of an α catalytic subunit and two regulatory β and γ subunits. In *Arabidopsis* the β subunit AKINβ2 and a γ-type regulatory subunit, AKINβγ, contain glycogen-binding domains. Bioinformatics indicated the possible presence of a chloroplast targeting sequence for both, leading to the proposal that they may be involved in regulation of starch metabolism. Immunolocalisation experiments indicated that AKINβγ is localised within the chloroplast, whereas AKINβ2 is located on the outer membrane of the organelle (Ávila-Castañeda et al. 2014). Both subunits were able to bind starch, and AKINβγ was able to bind an amylose-amylopectin mix, whereas AKINβ2 was not. In *Arabidopsis*, there are two iso-subunits of the catalytic α subunit, AKIN10 and AKIN11. Their localisation is disputed where some reports have suggested they are located in the nucleus and cytosol (Koroleva et al. 2005) and others have proposed a chloroplast localisation (Fragoso et al. 2009). Ávila-Castañeda et al. (2014) found that binding of starch inhibited SnRK1 activity (measured as phosphorylation of the AMARA synthetic peptide) in extracts of *Arabidopsis* leaves, though given that these assays were performed in whole-cell extracts, it is difficult to interpret the significance of these observations.

Large-scale bioinformatics-based surveys of *Arabidopsis* protein kinases and phosphatases identified 45 potential protein kinases and 21 phosphatases which could be localised to the plastid, although analysis of green fluorescent protein (GFP) fusions implied that less than 50 % of these predicted localisations were correct (Schliebner et al. 2008) and that the number of protein kinases in chloroplasts might be as few as 15 (Bayer et al. 2012). Kempa et al. (2007) identified a protein kinase from *Medicago*, MsK4, which possessed sequence similarity to the mammalian glycogen synthase kinase, *GSK3*, and observed that when this was expressed heterologously in *Arabidopsis*, there was an increase in starch

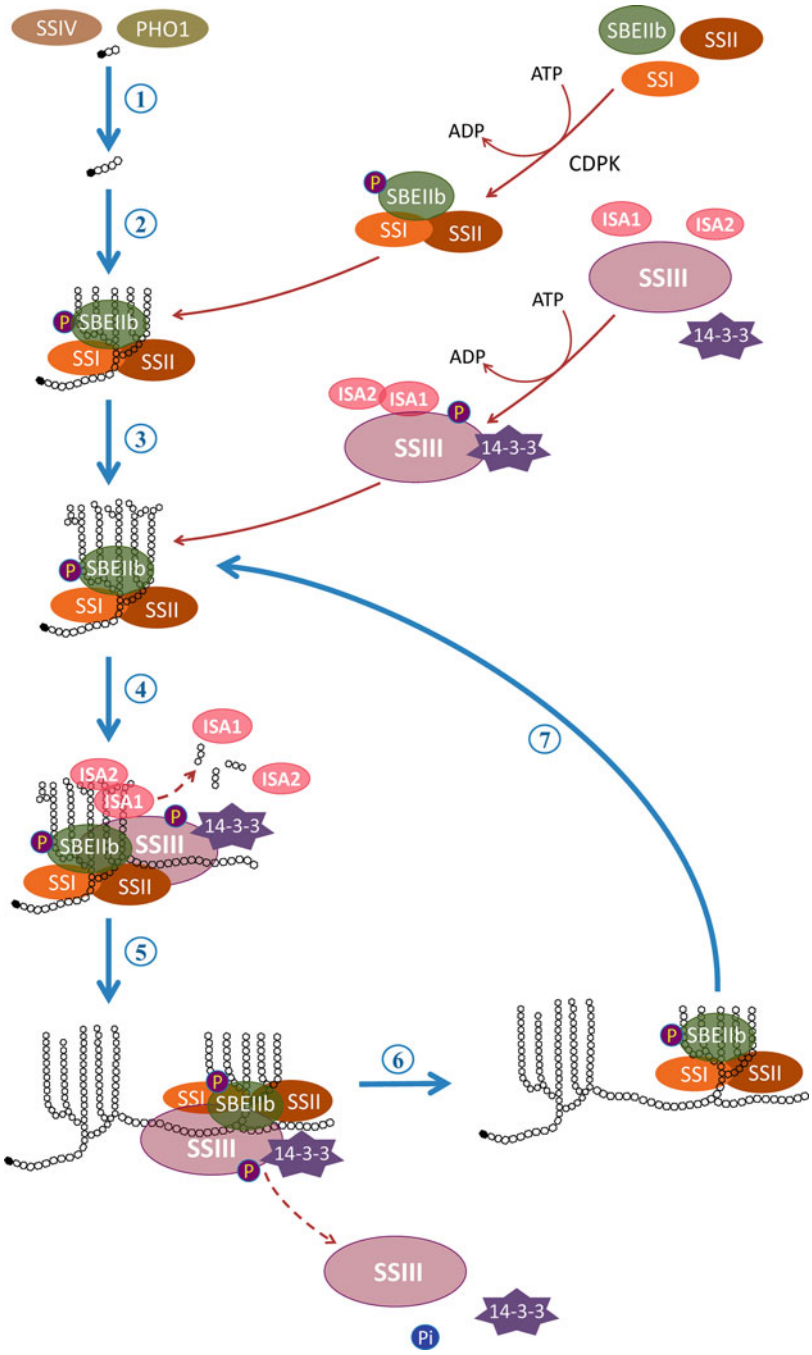
SSIV
PHO1
1
2
SBEIIb
SSII
SSI
ATP
ADP
CDPK
P
SBEIIb
SSI
SSII
ISA1
ISA2
SSIII
14-3-3
ATP
ADP
ISA2
ISA1
P
SSIII
14-3-3
3
P
SBEIIb
SSI
SSII
4
ISA1
ISA2
ISA2
ISA1
P
14-3-3
P
SBEIIb
SSIII
SSI
SSII
5
7
6
P
SBEIIb
SSI
SSII
SSI
SBEIIb
SSII
SSIII
14-3-3
P
SSIII
14-3-3
Pi

content under conditions of salt stress. GSK3-overexpressing plants were also more tolerant of hyperosmotic stress. Of particular note in that study was that this protein was localised to the starch granule (Kempa et al. 2007). However, the nearest *Arabidopsis* homologues of MsK4, AtSK41 and AtDSK1 do not appear to be located in chloroplasts (Bayer et al. 2012). The function and localisation of MsK4 remain uncertain, although *MsK4*-overexpressing *Arabidopsis* contained more maltose which is a product of starch breakdown (Kempa et al. 2007). Chloroplasts contain some 3,000 predicted proteins amongst which 300 proteins have been predicted to be phosphorylated based on a meta-analysis of published and unpublished data (van Wijk et al. 2014), and few plastidic protein kinases and their substrates have been characterised with any certainty (Bayer et al. 2012). The study of starch biosynthesis may offer another route to understand the role of this class of enzymes as well as protein phosphatases which are necessarily involved in their regulation.

Following the phosphorylation of a target protein, a general mechanism for regulating enzymes in eukaryotic systems involves interaction with the 14-3-3 class of proteins (Sehnke and Ferl 2002). 14-3-3 proteins are structurally highly conserved across species, as homo- or heteromeric dimers of 35 kDa subunits. A 14-3-3 isoform was detected in leaf starch of *Arabidopsis* (Sehnke et al. 2001) and subsequently in starch of immature maize pollen (Datta et al. 2002) and barley endosperm (Alexander and Morris 2006). Further, the downregulation of an ε-14-3-3 led to an increase in leaf starch synthesis in *Arabidopsis*, and it was proposed that this might occur through interaction with the SSIIIHD (see earlier) which contains 2 coiled-coil domains and a consensus motif for 14-3-3 binding (Lupas et al. 1991; Sehnke et al. 2001; Hennen-Bierwagen et al. 2009). Using a recombinant barley 14-3-3 protein as an affinity bait, Alexander and Morris (2006) analysed interacting polypeptides from developing barley grains. Amongst many enzymes

Fig. 8.3 Model of protein-protein interactions during the assembly of clusters and the formation of amylopectin

Granule initiation (*1*) requires SSIV and may also involve PHO1. The proposed "functional unit" of cluster assembly is the SSI-SSIIa-SBEII trimer which remains attached to the granule (*2*, *3*), whilst other proteins interact but are released into the soluble phase. ISA is required to remove disordered branching and may do so via ISA2 interaction with SSIII, for which there is genetic evidence (*4*). Given that the regulatory subunit of ISA2 can be phosphorylated on a highly conserved Ser residue, it is suggested that this may offer a mechanism to control its transient association with other enzymes. The long N-terminus of SSIII includes a homology domain (HD) which may provide sites of protein interaction, including for regulatory 14-3-3 protein. It is proposed that SSIII catalyses the extension of the inter-cluster C chains of amylopectin whilst interacting with the SSI-SSIIa-BEII trimer (*5*). The trimer is then "shuttled" by SSIII, after isoamylase dissociates, to begin a new cluster (*6*) and the cycle begins again (*7*). The model is consistent both with the Hizukuri model of amylopectin structure and also that proposed by Bertoft (see Chap. 1) where the C chain forms a helical backbone on which 9 nm clusters can be formed as shown here

which were found to interact with the 14-3-3 protein were SSI, SSII and SBEIIa, again reinforcing the need for further investigation of protein-protein interactions and protein phosphorylation in relation to the regulation of starch synthesis.

8.4 A Model for Protein-Protein Interactions During Amylopectin Synthesis

Drawing together the information described in preceding sections, it is possible to propose a model which attempts to describe the systematic way in which the enzymes of amylopectin biosynthesis work cooperatively (Fig. 8.3). There is ample evidence that starch synthase IV is involved in granule initiation (Roldán et al. 2007; Szydlowski et al. 2009). Interestingly, it has an N-terminus which includes two coiled-coil domains and a putative 14-3-3 binding site (Leterrier et al. 2008). Satoh et al. (2008) provided evidence that PHO1 could be involved in priming granule initiation in rice, and D'Hulst and Merida (2010) speculated that this might involve interaction with SSIV, though there is, as yet, no direct evidence for this. Once initiation has taken place, the model in Fig. 8.3 proposes that the trimeric complex between SSI, SSII and SBEII binds to the glucan via SSII and branches and elongates the polymer, generating the cluster, in effect moving like a "glucan-chaperone". At some point, the complex may not be able to proceed as a result of the formation of disorganised branches which cause steric hindrance. ISA then binds possibly via interaction with SSIIIHD which can also bind to the SSI/SSII/SBE complex (Hennen-Bierwagen et al. 2008; Lin et al. 2012). This interaction could be stimulated by a 14-3-3 protein-dependent mechanism which might also involve phosphorylation of ISA2. After removal of disorganised branches, ISA becomes detached from the complex, and SSIII catalyses the elongation of the inter-cluster C chains before itself becoming detached from SSI/SSII/SBEII complex as a result of dephosphorylation, consistent with experimental evidence (Hennen-Bierwagen et al. 2009). This would leave the trimeric complex positioned to begin the next cluster, eventually becoming entrapped within the granule.

8.5 Future Directions

It is very clear that there remain many unknowns in our understanding of the mechanisms of starch biosynthesis. Whilst the core biosynthetic enzymes have been identified, we are only just beginning to understand how these reactions are coordinated, including via protein-protein interaction. We are just beginning to uncover regulatory proteins involved in post-translational modification, the first example of which are the protein kinases located in amyloplasts which phosphorylate specific serines of SBEIIb (Makhmoudova et al. 2014). Identifying and characterising the

protein kinases and phosphatases involved is a priority if we are to fully comprehend how the highly organised semicrystalline structure of starch is achieved. There will also be a need to understand the timescale over which such regulatory steps operate, which could well be different in developing seed involved in long-term starch storage compared with the more dynamic diurnal turnover of leaf starch.

Acknowledgements The authors gratefully acknowledge the financial support of the Natural Sciences and Engineering Research Council and the Ontario Ministry of Agriculture, Food and Rural Affairs. We thank Mr. Ian Smith for assistance with some of the diagrams.

References

Abe N, Asai H, Yago H et al (2014) Relationships between starch synthase I and branching enzyme isozymes determined using double mutant rice lines. BMC Plant Biol 14:80. doi:10.1186/1471-2229-14-80

Alexander RD, Morris PC (2006) A proteomic analysis of 14-3-3 binding proteins from developing barley grains. Proteomics 6:1886–1896

Ávila-Castañeda A, Gutiérrez-Granados N, Ruiz-Gayosso A et al (2014) Structural and functional basis for starch binding in the SnRK1 subunits AKINβ and AKINβ. Front Plant Sci. doi:10.3389/fpls.2014.00199

Ballicora MA, Laughlin MJ, Fu Y et al (1995) Adenosine 5'-dipho-sphate-glucose pyrophosphorylase from potato tuber. Significance of the N-terminus of the small subunit for catalytic properties and heat stability. Plant Physiol 109:245–251

Bayer RG, Stael S, Rocha AG et al (2012) Chloroplast-localized protein kinases: a step forward towards a complete inventory. J Exp Bot 63:1713–1723

Boyer CD, Preiss J (1979) Properties of citrate-stimulated starch synthesis catalyzed by starch synthase I of developing maize kernels. Plant Physiol 64:1039–1042

Boyer CD, Preiss J (1981) Evidence for independent genetic control of the multiple forms of maize endosperm branching enzymes and starch synthases. Plant Physiol 67:1141–1145

Brust H, Lehmann T, D'Hulst C et al (2014) Analysis of the functional interaction of Arabidopsis starch synthase and branching enzyme isoforms reveals that the cooperative action of SSI and Bes in glucans with polymodal chain length distribution similar to amylopectin. Plos One. doi:10.1371/journal.pone0102364

Buchanan BB, Balmer Y (2005) Redox regulation: a broadening horizon. Annu Rev Plant Biol 56:187–220

Cao H, James MG, Myers AM (2000) Purification and characterization of soluble starch synthases from maize endosperm. Arch Biochem Biophys 373:135–146

Chen H-M, Chang S-C, Wu C-C et al (2002) Regulation of the catalytic behavior of L-form starch phosphorylase from sweet potato roots by proteolysis. Physiol Plant 114:506–515

Coello P, Hey SJ, Halford NG (2011) The sucrose non-fermenting-1-related (SnRK) family of protein kinases: potential for manipulation to improve stress tolerance and increase yield. J Exp Biol 62:883–893

Datta R, Chamusco KC, Choury PS (2002) Starch biosynthesis during pollen maturation is associated with altered patterns of gene expression in maize. Plant Physiol 130:1645–1656

Delatte T, Trevisan M, Parker ML et al (2005) Arabidopsis mutants *Atisa1* and *Atisa2* have identical phenotypes and lack the same multimeric isoamylase, which influences the branch point distribution of amylopectin during starch synthesis. Plant J 41:815–830

Denyer K, Dunlap F, Thorbjørnsen T et al (1996) The major form of ADPglucose pyrophosphorylase in maize endosperm is extraplastidial. Plant Physiol 112:779–783

D'Hulst C, Merida A (2010) The priming of storage glucan synthesis from bacteria to plants: current knowledge and new developments. New Phytol 188:13–21

Dreier W, Preusser E, Griindel M (1992) The regulation of the activity of soluble starch synthase in spinach leaves by a calcium-calmodulin dependent protein kinase. Biochem Physiol Pflanz 188:81–96

Duncan KA, Hardin SC, Huber SC (2006) The three maize sucrose synthase isoforms differ in distribution, localization, and phosphorylation. Plant Cell Physiol 47:959–971

Emes MJ, Tetlow IJ (2012) The role of heteromeric protein complexes in starch synthesis. In: Tetlow IJ (ed) Starch: origins, structure and metabolism, vol 5, SEB essential review series. Society for Experimental Biology, London, pp 255–278

Fragoso S, Espindola L, Paez-Valencia J et al (2009) SnRK1 isoforms AKIN10 and AKIN11 are differentially regulated in Arabidopsis plants under phosphate starvation. Plant Physiol 149:1906–1916

French D (1984) Organization of starch granules. In: Whistler RL, BeMiller JN, Paschall EF (eds) Starch: chemistry and technology. Academic, Orlando, pp 183–237

Fu Y, Ballicora MA, Leykam JF et al (1998) Mechanism of reductive activation of potato tuber ADP-glucose pyrophosphorylase. J Biol Chem 273:25045–25052

Gao M, Wanat J, Stinard PS et al (1998) Characterization of dull1, a maize gene encoding for a noval starch synthase. Plant Cell 10:399–412

Geigenberger P (2011) Regulation of starch biosynthesis in response to a fluctuating environment. Plant Physiol 155:1566–1577

Geigenberger P, Kolbe A, Tiessen A (2005) Redox regulation of carbon storage and partitioning in response to light and sugars. J Exp Bot 56:1469–1479

Ghosh HP, Preiss J (1966) Adenosine diphosphate glucose pyrophosphorylase: a regulatory enzyme in the biosynthesis of starch in spinach leaf chloroplasts. J Biol Chem 241:4491–4504

Grimaud F, Rogniaux H, James MG et al (2008) Proteome and phosphoproteome analysis of starch granule-associated proteins from normal maize and mutants affected in starch biosynthesis. J Exp Bot 59:3395–3406

Guan H-P, Preiss J (1993) Differentiation of the properties of the branching isozymes from maize (*Zea mays*). Plant Physiol 102:1269–1273

Hardie DG (2007) AMP-activated/SNF1 protein kinases: conserved guardians of cellular energy. Nat Rev Mol Cell Biol 8:774–785

Hawker JS, Ozbun H, Ozaki E et al (1974) Interaction of spinach leaf adenosine diphosphate glucose α-1,4-glucan α-4-glucosyl transferase and α-1,4-glucan, α-1,4-glucan-6-glycosyl transferase in synthesis of branched α-glucan. Arch Biochem Biophys 160:530–551

Heazlewood JL, Durek P, Hummel J et al (2008) PhosPhAt: a database of phosphorylation sites in Arabidopsis thaliana and a plant-specific phosphorylation site predictor. Nucleic Acids Res 36:D1015–D1021

Hendriks JHM, Kolbe A, Gibon Y et al (2003) ADP-glucose pyrophosphorylase is activated by posttranslational redox-modification in response to light and to sugars in leaves of Arabidopsis and other plant species. Plant Physiol 133:838–849

Hennen-Bierwagen TA, Liu F, Marsh RS et al (2008) Starch biosynthetic enzymes from developing *Zea mays* endosperm associate in multisubunit complexes. Plant Physiol 146:1892–1908

Hennen-Bierwagen TA, Lin Q, Grimaud F et al (2009) Proteins from multiple metabolic pathways associate with starch biosynthetic enzymes in high molecular weight complexes: a model for regulation of carbon allocation in maize amyloplasts. Plant Physiol 149:1541–1559

Hizukuri S (1986) Polymodal distribution of the chain lengths of amylopectin, and its significance. Carbohydr Res 147:342–347

Hizukuri S, Takeda Y, Maruta N et al (1989) Molecular structures of rice starch. Carbohydr Res 189:227–235

Huang B, Hennen-Bierwagen TA, Myers AM (2014) Functions of multiple genes encoding ADP-glucose pyrophosphorylase subunits in maize endosperm, embryo, and leaf. Plant Physiol 164:596–611

Hussain H, Mant A, Seale R et al (2003) Three forms of isoamylase contribute catalytic properties for the debranching of potato glucans. Plant Cell 15:133–149

Hylton C, Smith AM (1992) The *rb* mutation of peas causes structural and regulatory changes in ADP glucose pyrophosphorylase from developing embryos. Plant Physiol 99:1626–1634

Ikawa Y, Glover DV, Sugimoto Y et al (1978) Amylose percentage and distribution of unit chain-length of maize starches having a specific genetic background. Carbohydr Res 61:211–216

James MG, Robertson DS, Myers AM (1995) Characterization of the maize gene *sugary1*, a determinant of starch composition in kernels. Plant Cell 7:417–429

Kempa S, Rozhon W, Samaj J et al (2007) A plastid-localized glycogen synthase kinase 3 modulates stress tolerance and carbohydrate metabolism. Plant J 49:1076–1090

Kirchberger S, Leroch M, Huynen MA et al (2007) Molecular and biochemical analysis of the plastidic ADP-glucose transporter (ZmBT1) from *Zea mays*. J Biol Chem 282:22481–22491

Klucinec JD, Thompson DB (2002) Structure of amylopectins from *ae*-containing maize starches. Cereal Chem 79:19–23

Kolbe A, Tiessen A, Schluepmann H et al (2005) Trehalose 6-phosphate regulates starch synthesis via posttranslational redox activation of ADP-glucose pyrophosphorylase. Proc Natl Acad Sci U S A 102:11118–11123

Koroleva OA, Tomlinson ML, Leader D et al (2005) High-throughput protein localization in Arabidopsis using Agrobacterium-mediated transient expression of GFP-ORF fusions. Plant J 41:162–174

Kötting O, Kossmann J, Zeeman SC et al (2010) Regulation of starch metabolism: the age of enlightenment? Curr Opin Plant Biol 13:321–329

Kubo A, Colleoni C, Dinges JR et al (2010) Functions of heteromeric and homomeric isoamylase-type starch-debranching enzymes in developing maize endosperm. Plant Physiol 153:956–969

Leterrier M, Holappa L, Broglie K et al (2008) Cloning, characterisation and comparative analysis of astarch synthase IV gene in wheat: functional and evolutionary implications. BMC Plant Biol 8:98

Lin Q, Huang B, Zhang M et al (2012) Functional interactions between starch synthase III and isoamylase-type starch-debranching enzyme in maize endosperm. Plant Physiol 158:679–692

Liu F, Makhmoudova A, Lee EA et al (2009) The *amylose extender* mutant of maize conditions novel protein-protein interactions between starch biosynthetic enzymes in amyloplasts. J Exp Bot 60:4423–4440

Liu D-R, Huang W-X, Cai X-L (2013) Oligomerization of rice granule-bound starch synthase 1 modulates its activity regulation. Plant Sci 210:141–150

Liu F, Ahmed Z, Makhmoudova A et al (2012a) Allelic variants of the *amylose extender* mutation of maize demonstrate phenotypic variation in starch structure resulting from modified protein-protein interactions. J Exp Bot 63:1167–1183

Liu F, Romanova N, Lee EA et al (2012b) Glucan affinity of starch synthase IIa determines binding of starch synthase I and starch-branching enzyme IIb to starch granules. Biochem J 448:373–387

Lohrig K, Muller B, Davydova J et al (2009) Phosphorylation site mapping of soluble proteins: bioinformatical filtering reveals potential plastidic phosphoproteins in Arabidopsis thaliana. Planta 229:1123–1134

Lunn JE, Feil R, Hendriks JHM et al (2006) Sugar-induced increases in trehalose 6-phosphate are correlated with redox activation of ADPglucose pyrophosphorylase and higher rates of starch synthesis in *Arabidopsis thaliana*. Biochem J 397:139–148

Lunn JE, Delorge I, Figueroa CM et al (2014) Trehalose metabolism in plants. Plant J 79:544–567

Lupas A, Van Dyke M, Stock J (1991) Predicting coiled coils from protein sequences. Science 252:1162–1164

Makhmoudova A, Williams D, Brewer D et al (2014) Identification of multiple phosphorylation sites on maize endosperm starch branching enzyme Iib, a key enzyme in amylopectin biosynthesis. J Biol Chem 289:9233–9246

Martinez-Barajas E, Delatte T, Schluepmann H et al (2013) Wheat grain development is characterized by remarkable trehalose 7-phosphate accumulation pregrain filling: tissue distribution and relationship to SNF1-related protein kinase1 activity. Plant Physiol 156:373–381

McBride A, Ghilagaber S, Nikolaev A et al (2009) The glycogen-binding domain on the AMPK beta subunit allows the kinase to act as a glycogen sensor. Cell Metab 9:23–34

Michalska J, Zauber H, Buchanan BB et al (2009) NTRC links built-in thioredoxin to light and sucrose in regulating starch synthesis in chloroplasts and amyloplasts. Proc Natl Acad Sci U S A 106:9908–9913

Morell MK, Kosar-Hashemi B, Cmiel M et al (2003) Barley *sex6* mutants lack starch synthase IIa activity and contain a starch with novel properties. Plant J 34:173–185

Mu-Forster C, Huang R, Powers JR et al (1996) Physical association of starch biosynthetic enzymes with starch granules of maize endosperm. Granule-associated forms of starch synthase I and starch branching enzyme II. Plant Physiol 111:821–829

Nakamura Y, Ono M, Utsumi C et al (2012) Functional interaction between plastidial starch phosphorylase and starch branching enzymes from rice during the synthesis of branched maltodextrins. Plant Cell Physiol 53(5):869–878

Nakamura Y, Aihara S, Crofts N et al (2014) *In vitro* studies of enzymatic properties of starch synthases and interactions between starch synthase I and starch branching enzymes from rice. Plant Sci 224:1–8

Nishi A, Nakamura Y, Tanaka N et al (2001) Biochemical and genetic effects of *amylose-extender* mutation in rice endosperm. Plant Physiol 127:459–472

Pollock C, Preiss J (1980) The citrate-stimulated starch synthase of starchy maize kernels: purification and properties. Arch Biochem Biophys 204:578–588

Preiss J (1991) Biology and molecular biology of starch synthesis and its regulation. In: Miflin BJ (ed) Oxford surveys of cellular and molecular biology, vol 7. Oxford University Press, Oxford, pp 59–114

Reiland S, Messerli G, Baerenfaller K et al (2009) Large-scale Arabidopsis phosphoproteome profiling reveals novel chloroplast kinase substrates and phosphorylation networks. Plant Physiol 150:889–903

Roach PJ, DePaoli-Roach AA, Hurley TD et al (2012) Glycogen and its metabolism: some new developments and old themes. Biochem J 441:763–787

Robin JP, Mercier C, Charbonniere R et al (1974) Lintnerized starches: gel filtration and enzymatic studies of insoluble residues from prolonged acid treatment of potato starch. Cereal Chem 51:389–406

Roldán L, Wattebled F, Lucas MM et al (2007) The phenotype of soluble starch synthase IV defective mutant of Arabidopsis thaliana suggests a novel function of elongation enzymes in the control of starch granule formation. Plant J 49:492–504

Satoh H, Shibahara K, Tokunaga T (2008) Mutation of the plastidial alpha-glucan phosphorylase gene in rice affects the synthesis and structure of starch in the endosperm. Plant Cell 20:1833–1849

Schiefer S, Lee EYC, Whelan WJ (1973) Multiple forms of starch synthase in maize varieties as revealed by disc-gel electrophoresis and activity. Fed Eur Biochem Soc Lett 30:129

Schiefer S, Lee EYC, Whelan WJ (1978) The requirement for a primer in the *in vitro* synthesis of polysaccharide by sweet corn (1 → 4)-α-D-glucan synthase. Carbohydr Res 61:239–252

Schliebner I, Pribil M, Zühlke J et al (2008) A survey of chloroplast protein kinases and phosphatases in Arabidopsis thaliana. Curr Genomics 9:184–190

Sehnke PC, Ferl RJ (2002) 14-3-3 protein: effectors of enzyme function. Annu Plant Rev 7:53–76

Sehnke PC, Chung H-J, Wu K et al (2001) Regulation of starch accumulation by granule-associated plant 14-3-3 proteins. Proc Natl Acad Sci U S A 98:765–770

Sheen J (1991) Molecular mechanisms underlying the differential expression of maize pyruvate, orthophosphate dikinase genes. Plant Cell 3:225–245

Shure M, Wessler S, Fedoroff N (1983) Molecular identification and isolation of the *waxy* locus in maize. Cell 35:225–233

Sikka VK, Choi S, Kavakli IH et al (2001) Subcellular compartmentation and allosteric regulation of the rice endosperm. ADPglucose pyrophosphorylase. Plant J 161:461–468

Subasinghe RM, Liu F, Polack UC et al (2014) Multimeric states of starch phosphorylase determine protein-protein interactions with starch biosynthetic enzymes in amyloplasts. Plant Physiol Biochem 83:168–179

Szydlowski N, Ragel P, Raynaud S (2009) Starch granule initiation in Arabidopsis requires the presence of either class IV or class III starch synthases. Plant Cell 21:2443–2457

Tetlow IJ, Davies EJ, Vardy KA et al (2003) Subcellular localization of ADPglucose pyrophosphorylase in developing wheat endosperm and analysis of a plastidial isoform. J Exp Bot 54:715–725

Tetlow IJ, Wait R, Lu Z et al (2004) Protein phosphorylation in amyloplasts regulates starch branching enzyme activity and protein-protein interactions. Plant Cell 16:694–708

Tetlow IJ, Beisel KG, Cameron S et al (2008) Analysis of protein complexes in amyloplasts reveals functional interactions among starch biosynthetic enzymes. Plant Physiol 146:1878–1891

Tiessen A, Hendriks JHM, Stitt M et al (2002) Starch synthesis in potato tuber is regulated by post-translational redox modification of ADP-glucose pyrophosphorylase. Plant Cell 14:2191–2213

Umemoto T, Aoki N (2005) Single-nucleotide polymorphisms in rice *starch synthase IIa* that alter starch gelatinisation and starch association of the enzyme. Funct Plant Biol 32:763–768

Utsumi Y, Utsumi C, Sawada T et al (2011) Functional diversity of isoamylase oligomers: the ISA1 homo-oligomer is essential for amylopectin biosynthesis in rice endosperm. Plant Physiol 156:61–77

van Wijk KJ, Friso G, Walther D et al (2014) Meta-analysis of *Arabidopsis thaliana* phosphoproteomics data reveals compartmentalization of phosphorylation motifs. Plant Cell 26:2367–2389. http://dx.doi.org/10.1105/tpc.114.125815

Walley JW, Shen Z, Sartor R et al (2013) Reconstruction of protein networks from an atlas of maize seed proteotypes. PNAS 110:E4808–E4817

Wang S-J, Yeh K-W, Tsai C-Y (2001) Regulation of starch granule-bound starch synthase I gene expression by circadian clock and sucrose in the source tissue of sweet potato. Plant Sci 161:635–644

Wattebled F, Planchot V, Dong Y et al (2008) Further evidence for the mandatory nature of polysaccharide debranching for the aggregation of semicrystalline starch and for overlapping functions of debranching enzymes in Arabidopsis leaves. Plant Physiol 148:1309–1323

Yamamori M, Fujita S, Hayakawa K et al (2000) Genetic elimination of a starch granule protein, SGP-1, of wheat generates an altered starch with apparent high amylose. Theor Appl Genet 101:21–29

Yeh JY, Garwood DL, Shannon JC (1981) Characterization of starch from maize endosperm mutants. Starch-Starke 33:222–230

Young G-H, Chen H-M, Lin C-T et al (2006) Site-specific phosphorylation of L-form starch phosphorylase by the protein kinase activity from sweet potato roots. Planta 223:468–478

Zeeman SC, Tiessen A, Pilling E et al (2002) Starch synthesis in *Arabidopsis*; granule synthesis, composition, and structure. Plant Physiol 129:516–529

Zhang X, Colleoni C, Ratushna V et al (2004) Molecular characterization demonstrates that the *Zea mays* gene *sugary2* codes for the starch synthase isoform SSIIa. Plant Mol Biol 54:865–879

Zhang G, Cheng Z, Zhang X et al (2011) Double repression of soluble starch synthase genes *SSIIa* and *SSIIIa* in rice (*Oryza sativa* L.) uncovers interactive effects on the physiochemical properties of starch. Genome 54:448–459

Chapter 9
Initiation Process of Starch Biosynthesis

Yasunori Nakamura

Abstract Plants have developed the metabolic system in which a great amount of starch can be synthesized and store them into granules with semicrystalline structure in the plastid. The fine structure of amylopectin, a major component of starch, is a highly organized distinct structure composed of a unit structure called cluster. Thus, it is highly possible that plants have a specific starch biosynthesis initiation different from that of the well-known glycogen biosynthesis initiation found in animals, fungi, and bacteria. Based on a working hypothesis that the starch biosynthesis initiation has two events, i.e., the initiation of amylopectin synthesis and that of starch granule formation, the possible roles of enzymes which are potentially involved in these events and mechanisms underlying the regulation of amylopectin synthesis from simple sugars and starch granule formation are discussed.

Keywords Amylogenin • Amylopectin • Disproportionating enzyme • Glycogen • Glycogen synthase • Glycogenin • Initiation • Phosphorylase • Starch • Starch branching enzyme • Starch granule • Starch synthase

9.1 Introduction

The starch biosynthesis in plant tissues is a tremendous, remarkable, and specific metabolic process despite its apparently simple and monotonous production process, because starch molecules seem to be produced of repetitive reactions between chain elongation catalyzed by starch synthase (SS) and chain branching catalyzed by starch branching enzyme (BE). First, the rate of starch synthesis is tremendously higher compared with other carbon synthetic processes especially in reserve tissues. Second, considering the structure of amylopectin molecule having the numerous cluster units and starch granules that are highly and specifically

Y. Nakamura (✉)
Faculty of Bioresource Sciences, Akita Prefectural University, Shimoshinjo-Nakano, Akita 010-0195, Japan

Akita Natural Science Laboratory, 25-44 Oiwake-Nishi, Tennoh, Katagami, Akita 010-0101, Japan
e-mail: nakayn@silver.plala.or.jp

Y. Nakamura (ed.), *Starch*, DOI 10.1007/978-4-431-55495-0_9

organized over several dimension levels (see Chaps. 1 and 3), the syntheses of the polysaccharides and the granular structure must need complex phases operating under various metabolic regulations. Third, in spite of the specific structural features, the homogeneous products with uniform structures are reproduced without accumulation of significant amounts of intermediate glucans and/or dextrins under general physiological and environmental conditions.

To achieve such characteristics, it must be impossible for plants to synthesize amylopectin molecules and starch granules only by a one-step metabolic process. Instead, plants must have at least two processes, the initiation process and the amplification (or reproduction) process. However, the conditions of the initiation process must be different between starch and glycogen biosynthesis. In glycogen biosynthesis in animals and fungi, the initiation process has been well defined, and some primary biochemical steps have been characterized at the molecular level (see review by Roach et al. 2012). In contrast, little is known regarding the initial process of the starch biosynthesis and thus at present the content of the process (most of biochemical events) must be conceptual. What are the requisites for the initiation process in starch biosynthesis? The initiation process in starch synthesis must be much more complex than that in glycogen synthesis because in the former glucans are probably produced from the precursor of amylopectin having the cluster structure. Figure 9.1 illustrates a working hypothesis on the initiation process and the amplification process in starch synthesis in higher plants (Nakamura et al. 2009; Jeon et al. 2010; Nakamura 2014). It is hypothesized that in the initiation process, the precursor of amylopectin is synthesized from simple sugars such as glucose, maltose, and maltotriose, possibly via branched dextrins and glucans having an immature cluster structure, while in the amplification process, mature amylopectin structure is synthesized from the precursor by reproducing the clusters. Under physiological conditions especially when starch is vigorously synthesized, the amounts of intermediates involved in the initiation process are considered to be much lower than those of accumulating starch molecules. Thus, the initiation process is usually hidden behind the amplification process, and it is difficult to detect the biochemical events happening at the starch initiation stage, and in fact almost all of the available information has been derived from the results regarding the amplification process.

Transcriptome analysis indicates that genes highly expressed at the very early developmental stage of reserve tissues/organs in which the initiation process is considered to be dominant are different from genes expressed in these tissues during the amplification process where the starch production is at its highest rate which is achieved by the amplification process (Ohdan et al. 2005), suggesting that enzymes involved in the initiation process are different from enzymes responsible for the amplification process, as described below in detail (Sect. 9.3).

In this chapter, the initiation process of starch biosynthesis in reserve tissues/organs is focused upon and discussed from several possible aspects including features of enzymes and glucans potentially involved in this process. It is assumed that the initiation process includes the synthesis of amylopectin prototype which has the cluster structure and can serve as the precursor for the mature amylopectin

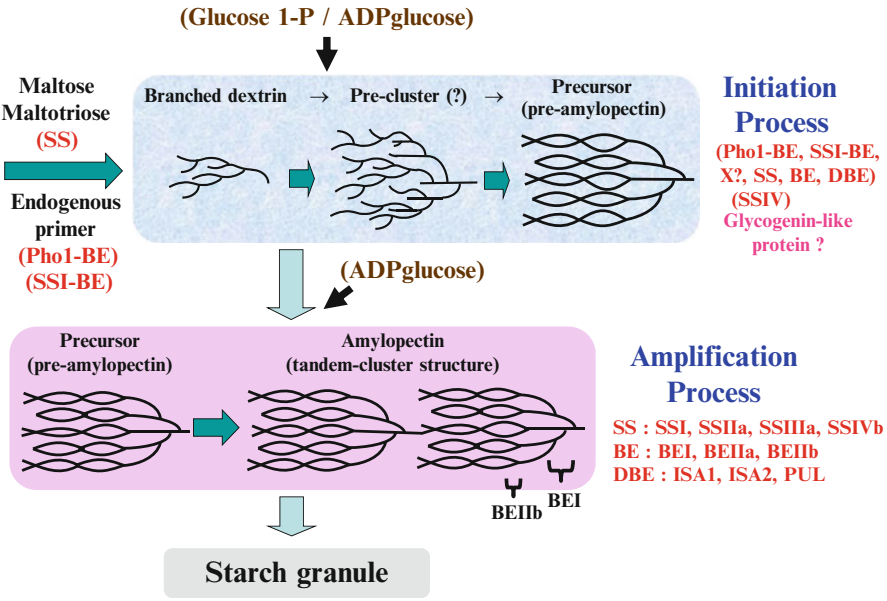

Fig. 9.1 Schematic representation of the initiation process and the amplification process in starch biosynthesis in higher plants

molecules in the subsequent amplification process. The related process in the assimilatory starch synthesis is described in Chap. 6.

9.2 Past and Ongoing Investigations for the Initiation in α-Glucan Biosynthesis

9.2.1 Initiation Process in Glycogen Biosynthesis in Animals, Fungi, and Bacteria

The priming of glycogen synthesis in animals and fungi has been well characterized (see review by Roach et al. 2012). The specialized initiator protein called glycogenin (EC 2.4.1.186) self-glucosylates using a glucose residue of UDPglucose to form a malto-oligosaccharide (MOS) linked by α-1,4 glucosidic bonds (Lomako et al. 1988; Pitcher et al. 1988; Farkas et al. 1991; Cheng et al. 1995) at the highly conserved tyrosine residue (Cao et al. 1993; Mu et al. 1996), which can be subsequently used by glycogen synthase (GS) as primer (Romero et al. 2008). The glycogenin directly interacts with GS to form the majority of glycogen chains. The formation of glycogen molecules is accomplished by concerted and repeated chain-elongation and chain-branching reactions catalyzed by GS and glycogen branching enzyme (BE), respectively.

The glycogen biosynthetic process in bacteria is different from that in animals and fungi because almost all of bacteria have no glycogenin homologues (see review by Wilson et al. 2010). Ugalde et al. (2003) showed that GS from *Agrobacterium tumefaciens* can form MOS by transferring a glucose residue from ADPglucose to an amino acid(s) in the GS protein. Thus, in bacteria the same GS has the capacity for both glycogen initiation and elongation in the absence of added glucan primer.

9.2.2 Investigations for the Initiation Process in Starch Biosynthesis

9.2.2.1 Autoglucosylation: Amylogenin

The expressions of glycogenin-like genes were detected from maize (Rothschild and Tandecarz 1994) and rice (Qi et al. 2005), and the protein was called as amylogenin (Singh et al. 1995). Chatterjee et al. (2005) claimed that knockout of *glycogenin-like protein* gene expression in *Arabidopsis* reduced the amount of starch in the leaf, although they only measured the glucan content by iodine staining method, which is not necessarily the quantitative method. However, a piece of evidences support that this protein is involved in the initiation of cell wall biosynthesis (Delgado et al. 1998; Langeveld et al. 2002; Sandhu et al. 2009). Therefore, at present no definite evidence for an essential role of glycogenin/amylogenin in the initiation process of starch biosynthesis is available.

9.2.2.2 Soluble Starch Synthase IV (SSIV)

There have been several reports indicating the involvement of soluble starch synthase IV (SSIV) in the starch granule initiation in *Arabidopsis* leaves (see Chap. 6 for more details and reviews by D'Hulst and Merida 2010, 2012). Mutation at the *SSIV* locus in *Arabidopsis* reduced the number of starch granules in chloroplasts although SSIV contributed little to the total SS activity in the leaf (Roldán et al. 2007). It is noted, however, that the *ss4* mutants had one or two huge starch granules per chloroplast, suggesting that SSIV is specifically involved in the initial process of starch granule formation, but is not directly involved in the synthesis of starch molecules in the amplification process. Overexpression of *SSIV* gene reportedly enhanced the starch content in *Arabidopsis* leaf and the growth rate (Gámez-Arjona et al. 2011). The *ss4*-related mutations resulted in a wide range of biochemical, physiological, and morphological changes such as starch molecular structure, the contents of sugars, the turnover of starch, the number and morphology of starch granules, the number and size of chloroplasts, and the growth rate and leaf morphology of *Arabidopsis* plant (Roldán et al. 2007; Szydlowsky et al. 2009; Gámez-Arjona et al. 2011; Crumpton-Taylor et al. 2013). Detailed analysis of these phenotypes supports the view that SSIV is directly involved in the starch granule

initiation in *Arabidopsis* leaves (Crumpton-Taylor et al. 2013). Remarkably, the *Arabidopsis* mutants lacking both SSIII and SSIV activities had no detectable starch granules in leaves, while the number of starch granules was apparently not modified in the *ss1/ss2/ss3* triple mutants, but the granule size was strongly reduced (Szydlowsky et al. 2009, 2011). The results indicate that the roles of SSIV and SSIII overlap in the granule initiation process which is indispensable for the starch synthesis, and these roles cannot be substituted by SSI and SSII, or GBSS (see Chap. 6).

However, it is unclear whether the mechanism for the contribution of *SSIV* gene to starch granule formation found in *Arabidopsis* commonly occurs in all the other plant cells. Toyosawa et al. (2015) observed that the single mutation at the *SSIVa* or *SSIVb* locus in rice showed no or little detectable alterations in starch-related phenotypes. However, when both the *SSIVb* and *SSIIIa* genes, the major *SSIV* and *SSIII* genes expressed in developing rice endosperm, were simultaneously defective, the starch granular morphology dramatically changed from the polygonal (wild-type) to the spherical morphology, while the starch content per seed was only slightly reduced (Toyosawa et al. 2015). It is interesting that the spherical starch granules in the *ss3a/ss4b* mutant endosperm were present separately from each other, markedly different from the wild-type polygonal granules packed in a single amyloplast as the compound starch granules (see Chap. 10). The results indicate that SSIIIa and SSIVb have unconventional functions in amyloplast and starch granule developments (see Chap. 13 for details). Thus, at present it is unlikely that SSIVb and SSIIIa play pivotal roles in starch production per se, but they are involved in the determination of starch granule morphology in rice endosperm, although more detailed studies are needed to draw the definitive conclusion.

The SSIII and SSIV are known to share the structural similarity in having a very long N-terminal extension compared with the protein structures of SSI, SSII, and GBSS (Leterrier et al. 2008). Although further studies regarding the contribution of SSIII and SSIV to the starch granule formation are needed, the distinct functional interaction exists between these enzymes (see Chap. 6).

Szydlowsky et al. (2009) found that SSIV could use maltose and maltotriose as glucan primer for glucan synthesis, and the synthetic rate with maltotriose was higher than 90 % of that from amylopectin, suggesting the additional role of SSIV in glucan synthesis, as described below.

9.2.2.3 Plastidial Phosphorylase (Pho1)

The involvement of plastidial phosphorylase (Pho1) in starch biosynthesis has been proposed from in vivo and in vitro studies. A green alga *Chlamydomonas reinhardtii* having plastidial *pho* mutations at the *STA4* locus showed a decreased amount of starch with abnormal shapes of granules and a modified amylopectin structure (Dauvillée et al. 2006). Based on biochemical, molecular, and genetic analyses, they claimed that plastidial Pho is needed for normal starch synthesis in *Chlamydomonas*.

The *pho1* mutation of rice greatly affected the starch phenotype in the endosperm (Satoh et al. 2008). The extent of reduction of starch content in the mutant seeds greatly varied ranging from severely shriveled seed due to no starch accumulation to near normal seed (Fig. 9.2a). The mutant phenotypes were greatly affected by temperatures during growth, and at lower temperature (20 °C) most of seeds became shrunken, while at higher temperature (28–30 °C) the majority of mutant seeds were plump (Fig.9.2b). Despite such drastic reduction of starch amount in seed, the amylopectin fine structure was only slightly altered. Based on these observations, it was proposed that Pho1 is involved in the initiation process of starch biosynthesis, but not in the amplification process in rice endosperm. They also assumed that some unknown factor(s) which can function and/or is(are) expressed only at higher temperatures above 20 °C support(s) the role of Pho1.

Fettke et al. (2010, 2012) have examined a specific incorporation behavior of glucose 1-phosphate (G1P) by potato tuber discs from various transgenic lines and found that the exogenously added G1P was converted to native starch granules in tubers as mediated by Pho1 (Fettke et al. 2010). The rate of incorporation of G1P was much higher than glucose, glucose 6-phosphate (G6P), or sucrose. The amount of carbon incorporated from G1P into starch was abolished only by reduced Pho1 activities, but not inhibited or rather increased by inhibitions of cytosolic and plastidial phosphoglucomutase, cytosolic Pho (Pho2), or cytosolic transglucosidase. The authors also found that incorporations of radioactivity from G1P and sucrose into starch in potato tuber discs differed in amounts in response to temperature during incubation (Fettke et al. 2012). The Pho1-mediated G1P path reached maximal activity at about 20 °C, while the conventional AGPase-mediated sucrose path was markedly activated by higher temperatures above 20 °C. The investigations established that the G1P pathway in which G1P is directly used for starch by Pho1 at least in potato parenchyma cells is regulated by a mechanism different from the primary AGPase pathway for starch biosynthesis.

There have been a lot of pieces of criticisms regarding the involvement of Pho1 in starch biosynthesis. It is often argued that Pho1 is unable to play an important role in starch biosynthesis, considering that actual concentration of Pi is much higher than G1P inside the cellular compartment, despite a good correlation between the activity levels of Pho1 and the rate of starch production in various tissues (Schupp and Ziegler 2004 and References therein). However, in vitro studies showed that rice Pho1 could elongate MOS in the synthetic direction even under physiological conditions of high Pi/G1P concentration ratio (Hwang et al. 2010). Based on the experimental results, Hwang et al. (2010) concluded that Pho1 can play a part in the initiation stage, but not in the amplification process of starch biosynthesis.

Nakamura et al. (2012) found evidence for a close interaction between Pho1 and either BE isozyme from rice in the synthesis of glucans without added primers during the enzymatic reaction (Fig. 9.3). The enhancement of glucan synthesis of Pho1 by BE was not merely due to the increased supply of nonreducing end (acceptor) of glucan substrate, but to a close interaction between both enzymes, which was achieved by activating each of the mutual capacity of the other in terms of increases in catalytic activities and affinities for the glucan (Fig. 9.3b). The glucan

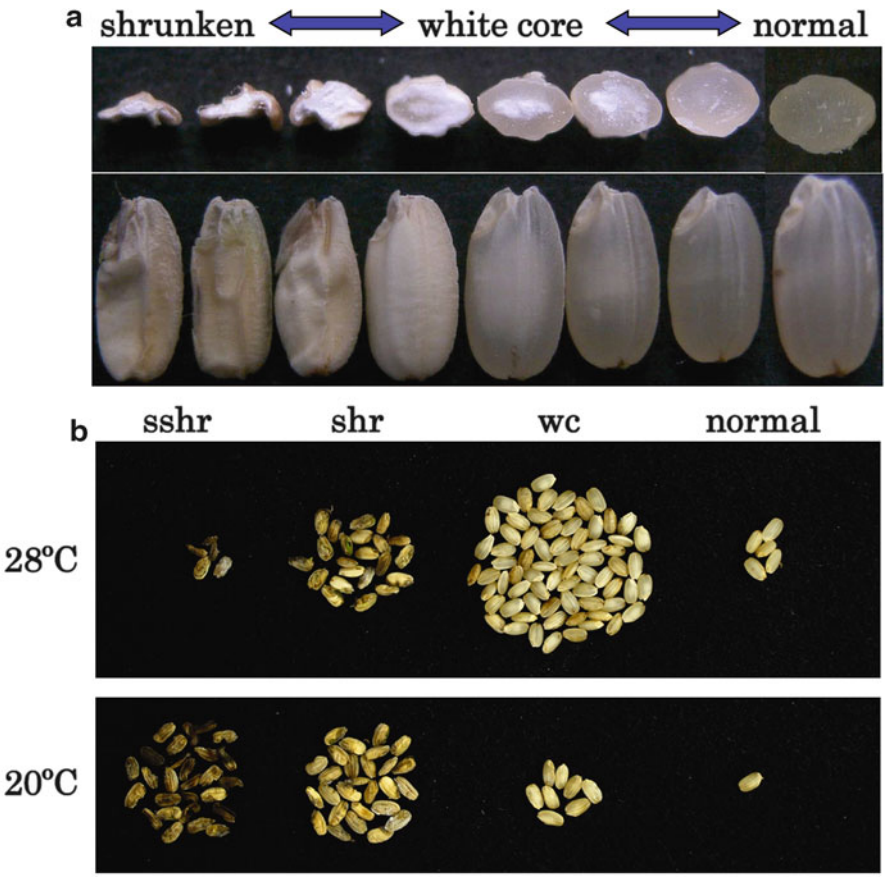

Fig. 9.2 Seed morphology of the rice mutant lines defective in the *plastidial phosphorylase* (*Pho1*) gene. (**a**) Kernels of the homozygous rice *pho1* mutant line ranged from normal to severely shrunken types even when the plant was grown under summer temperature conditions (Satoh et al. 2008). (**b**) Kernels in mature *pho1* mutant seeds of a single panicle were classified into five groups, normal plump, white core (wc), shrunken (shr), severely shrunken (sshr) kernels, and empty seeds (not shown), and these kernels are shown. After flowering, the plants were grown at high (28°) and low (20°) temperatures (Ohdan et al. unpublished)

products were exclusively branched molecules and no linear glucans existed; thus, it is likely that a small amount of endogenous glucan strongly bound to the purified Pho1 preparation from rice endosperm served as primer for the Pho1-BE reaction and all of the products had the branched form.

It is known that Pho1 could easily synthesize very long chains of DP > 100 from MOS (Kitamura et al. 1982), glycogen (Putaux et al. 2006), and amylopectin (Yuguchi et al. 2013) used as primer. The chain preference of Pho1 was similar to GBSS, which elongated glucan chains in a processive manner (Denyer et al. 1999), but was sharply in contrast with that of SS, which could synthesize only short and

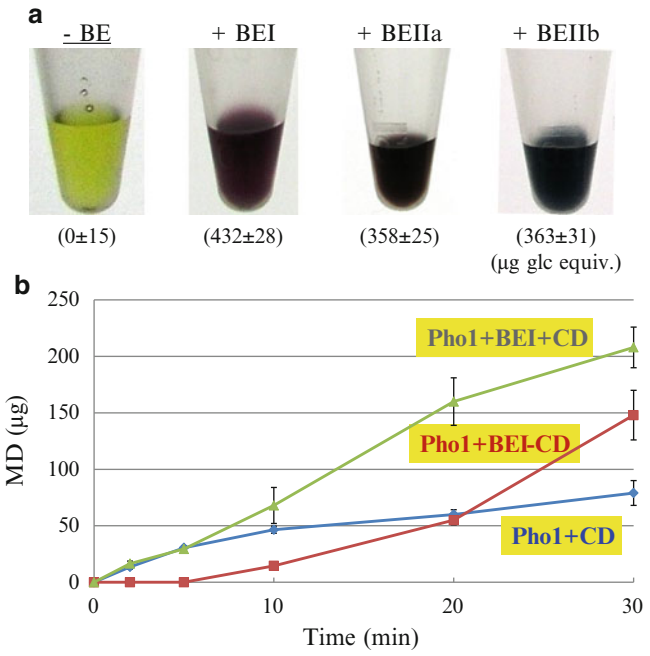

Fig. 9.3 Catalytic interaction between rice plastidial phosphorylase (Pho1) and starch branching enzyme (BE). (**a**) Effects of addition of BE on the in vitro glucan synthesis by Pho1 purified from developing rice endosperm in the absence of added glucan primer, cluster dextrin (CD). (**b**) Effects of concentrations of added glucan primer on the glucan synthesis by Pho1 from rice either in the presence or absence of BE (Data are from Nakamura et al. 2012)

intermediate chains in a distributive manner as long as SS was incubated with the glucan primer added (Denyer et al. 1999; Imparl-Radosevich et al. 2003; Nakamura et al. 2014). For this reason, it is unlikely that Pho1 plays an essential role in the chain elongation of amylopectin molecules because the lengths of amylopectin chains should be strictly restricted to form the cluster structure.

9.2.2.4 Other SS

It is generally believed that the minimum chain length of primer for SS is DP3 (maltotriose) and that SS cannot substantially synthesize glucans in the presence of maltose and glucose (Imparl-Radosevich et al. 2003), although the catalytic activity of SS toward linear MOS and amylose is markedly lower than that toward branched glucan. However, recently, Brust et al. (2013) showed that SSI, SSII, and SSIII from *Arabidopsis* were capable of acting on maltose as glucan acceptor when they were incubated for a prolonged period (22 h), although glucose could not be replaced by maltose (Fig. 9.4). As stated above, *Arabidopsis* SSIV was also able to synthesize

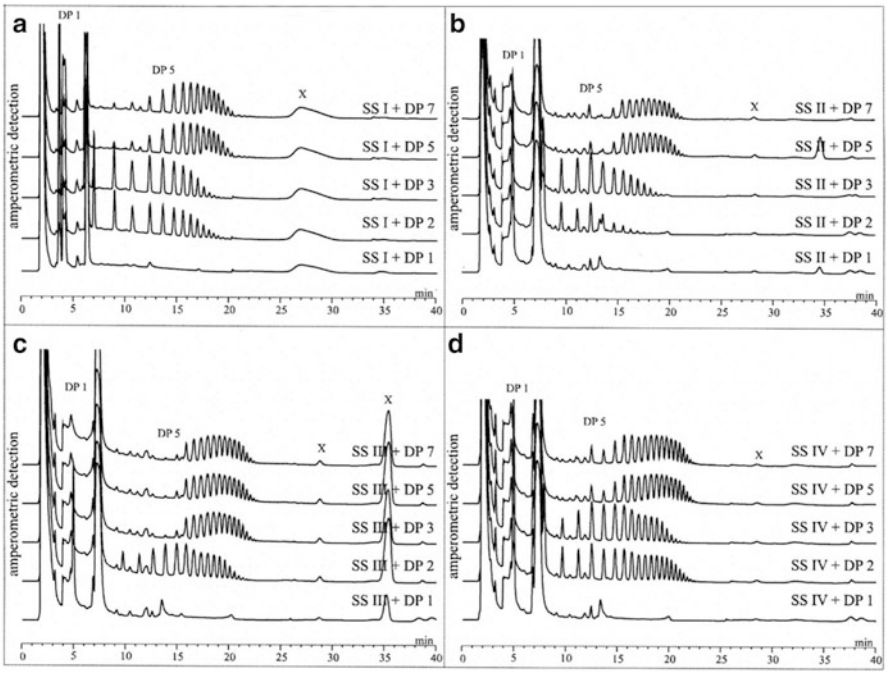

Fig. 9.4 Reactivities of *Arabidopsis* starch synthases (SSI, SSII, SSIII, and SSIV) toward malto-oligosaccharides (MOS) having different chain lengths. The enzymatic action of starch synthases from *Arabidopsis* toward glucose (DP1), maltose (DP2), maltotriose (DP3), maltopentaose (DP5), and maltoheptaose (DP7) at 30 °C for about 22 h in the presence of 3.5 mM ADPglucose and 1.2 mM MOS as primer (Brust et al. 2013)

glucan by using maltotriose and maltose as primer, and this synthesis capacity was much higher than that of SSIII (Szydlowsky et al. 2009).

The results strongly support the view that all the SS isozymes, SSI–SSIV, actually have capacities for the de novo synthesis of MOS having DP≧3 as long as maltose is present in plastids. Since maltose is ubiquitously present in intracellular environments via resulting from the actions of various enzymes such as amylases, Pho, and disproportionating enzyme (DPE) with glucans, this view suggests that plant cells can produce MOS by SS at least to some extent and they do not necessarily need the autoglucosylation process including the specific protein like glycogenin/amylogenin.

Recently, it was found that rice SSI, but not SSIIa and SSIIIa, synthesized glucans in the presence of BE without an addition of exogenous glucan primer (Nakamura et al. 2014) (Fig. 9.5). The role of BE added was not merely to provide SS with the nonreducing end of the glucan, but to enhance the chain-elongation capacity of SS (Fig. 9.5b). In turn, BE was also activated by SSI through its increased affinity for the glucan. Since in addition the branched glucan was also involved in the SSI-BE interacting reaction, the same mechanism might underlie the interactions

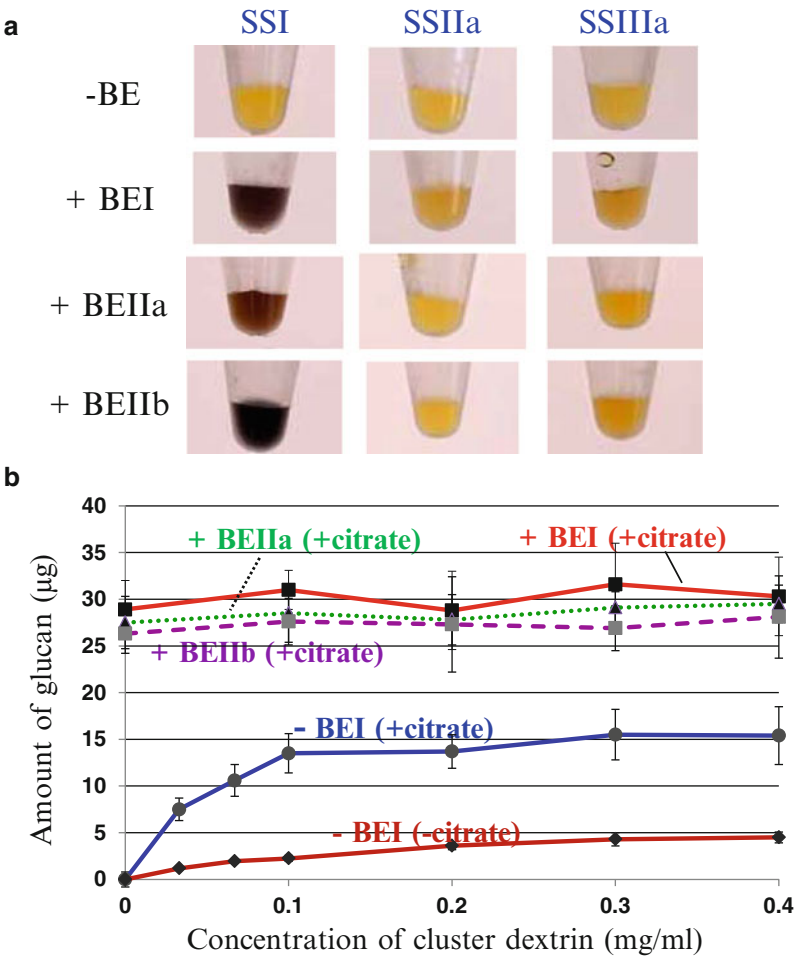

Fig. 9.5 Catalytic interaction between starch synthase (SS) and starch branching enzyme (BE) from rice. (**a**) Effects of addition of BE from rice on the in vitro glucan synthesis by SS from rice in the absence of added glucan primer. The glucans formed were stained with iodine. (**b**) Effects of concentrations of added glucan primer (cluster dextrin) on the glucan synthesis by SS1 from rice either in the presence or absence of BE and/or citrate (Data are from Nakamura et al. 2014)

between both SSI-BE and Pho1-BE. The close interaction between SS-BE in the unprimed synthesis was also reported in *Arabidopsis* enzymes (Brust et al. 2014). At least in rice endosperm, the involvement of branched glucan seemed to be more important for the SSI-BEI interaction than the Pho1-BE interaction because the catalytic activity of SSI was much higher toward branched glucan than to the linear glucan and MOS, whereas Pho1 activity was high toward both branched and linear glucans (see Chap. 5 and review by Fujita and Nakamura 2012). The results suggest

that SSI and BE closely and functionally interact and can efficiently synthesize branched glucans possibly by using an endogenous glucan primer bound to purified SSI preparation.

When SSI from rice was incubated with amylopectin as primer, its elongation was highly specific because the main product during the short incubation period was the DP8 chain formed from acting on very short amylopectin chains of DP6 and 7 (Nakamura et al. 2014). Considering that the maximum chain lengths for the SSI-BEI product were DP10–12, reflecting the chain profile for BEI (see Fig. 5.6d in Chap. 5), these in vitro studies suggest that SSI has dual functions in glucan synthesis, i.e., first, the synthesis of very short chains (DP about 8) of amylopectin in the amplification process and, second, the synthesis of glucan chains longer than the DP8 chains by association with BE in the initiation process of starch biosynthesis.

9.3 Possible Factors Involved in the Initiation of Starch Biosynthesis

Available information suggests that the initiation of starch biosynthesis falls into two categories, i.e., the initiation of formation of starch molecules and that of starch granules, although they must be closely interconnected.

What are features of glucan structures involved in the initiation process of the synthesis of starch differing from the amylopectin synthesis during the amplification process? Practically nothing is known about the glucans and dextrins involved in the initiation process. Preliminary results showed that glucans/dextrins abundant in rice endosperm at the very early developmental stage had some structural features (Nakamura et al. unpublished data). First, the chain-length distribution analysis of the whole glucan chains and the internal segments (chains found in phosphorylase-limit dextrins) indicated that the fine structures of glucans/dextrins possibly involved in the initial stage of glucan synthesis were different from mature amylopectin molecules. In addition, the glucans/dextrins had very short chains of DP2–5, suggesting that that was the results of hydrolysis by amylases, phosphorolysis by Pho1, and/or disproportionation by DPE of outer chains after they were synthesized, whereas mature amylopectin had no or little such short chains, possibly by being protected by such degradation of external chains from actions by these enzymes. Second, the sizes of the glucans/dextrins were much smaller than normal amylopectin. Third, the glucans/dextrins had more hydrophilic properties than starch granules and were not precipitated by a low-speed centrifugation. Fourth, the granular size including the glucans/dextrins was smaller compared with mature starch granules. These results suggest that in the initiation process the intermediate glucans/dextrins with no or immature cluster structure play important roles in amylopectin biosynthesis serving as the precursor of amylopectin-type glucans.

What are candidate enzymes involved in the initiation process? Information from transcriptome analysis of genes encoding starch biosynthetic enzymes of rice plants

is available (Ohdan et al. 2005; Yamakawa et al. 2007, http://ricexpro.dna.affrc.go.jp/Zapping/). Ohdan et al. (2005) classified the four major expression patterns during rice seed development (Fig. 9.6). The first group that includes SSIIIb, BEIIa, and DPE1 was characterized by a high expression level at a very early developmental stage. The second group including SSI, SSIVb, ISA2, and Pho1 showed an intermediate expression level at the initiation seed formation period and rose rapidly to peak at the early developmental stages, and then the level continued to decline in the middle and late developmental stages. The third group composed of SSIIa, SSIIIa, GBSSI, BEI, BEIIb, ISA1, and PUL showed a basal or very low expression level at the initial developmental stage, but rapidly increased to a high level thereafter, and this high level was maintained until seed maturation. The fourth group including SSIIb, SSIIc, SSIVa, GBSSII, and ISA3 was characterized by low expression level at the start and further decreased to a basal level throughout the seed development, whereas some of them were preferentially expressed in leaves. The results suggest that at the early developmental stage of reserve tissue cells, the initiation process of starch synthesis predominantly operates and enzymes involved in the process are vigorously functioning.

The properties of Pho1 match the requirements for the initiation process. Pho1 could synthesize a wide range of chains from short chains to very long chains by using various primers including branched and unbranched glucans (Kitamura et al. 1982; Putaux et al. 2006; Yuguchi et al. 2013), contrasting with SS whose chain preference was distinct depending on each SS type and elongation activity basically decreased with the increase of chain length (Commuri and Keeling 2001; Nakamura et al. 2005; Fujita and Nakamura 2012; Nakamura et al. 2014) (see Sect. 5.3.1.1 in Chap. 5).

SSI might also be potentially involved in the initiation process by closely interacting with BE. It is highly possible that the chain-elongation properties of SSI when the SSI-BE complex synthesized the intermediate glucans/dextrins composed of chains having a wide range of chain lengths (Nakamura et al. unpublished) sharply differed from that when SSI directly reacted to the glucan primer like amylopectin.

What are the advantages of the Pho1-BE and SSI-BE interactions? It should be stressed that both enzyme-enzyme interactions were capable of the glucan synthesis on their own by using the yet unidentified endogenous glucan primers. Thus, their reactions were basically unaffected by surrounding glucans such as mature amylopectin accumulated even at high concentrations, because the Pho1-BE and SSI-BE had much higher affinities for appropriate glucans (Nakamura et al. 2012, 2014) that functioned as primers for the subsequent reactions, compared to other various glucans accumulating in highest amounts in reserve tissues. It is also noted that the minimum chain lengths of branched and linear glucans for BE were DP12 and DP about 48 or larger, respectively (Nakamura et al. 2010; Sawada et al. 2014). This indicates the likely possibility that the contribution of branched dextrins/glucans to the initiation process is much more significant than that of linear MOS/dextrins.

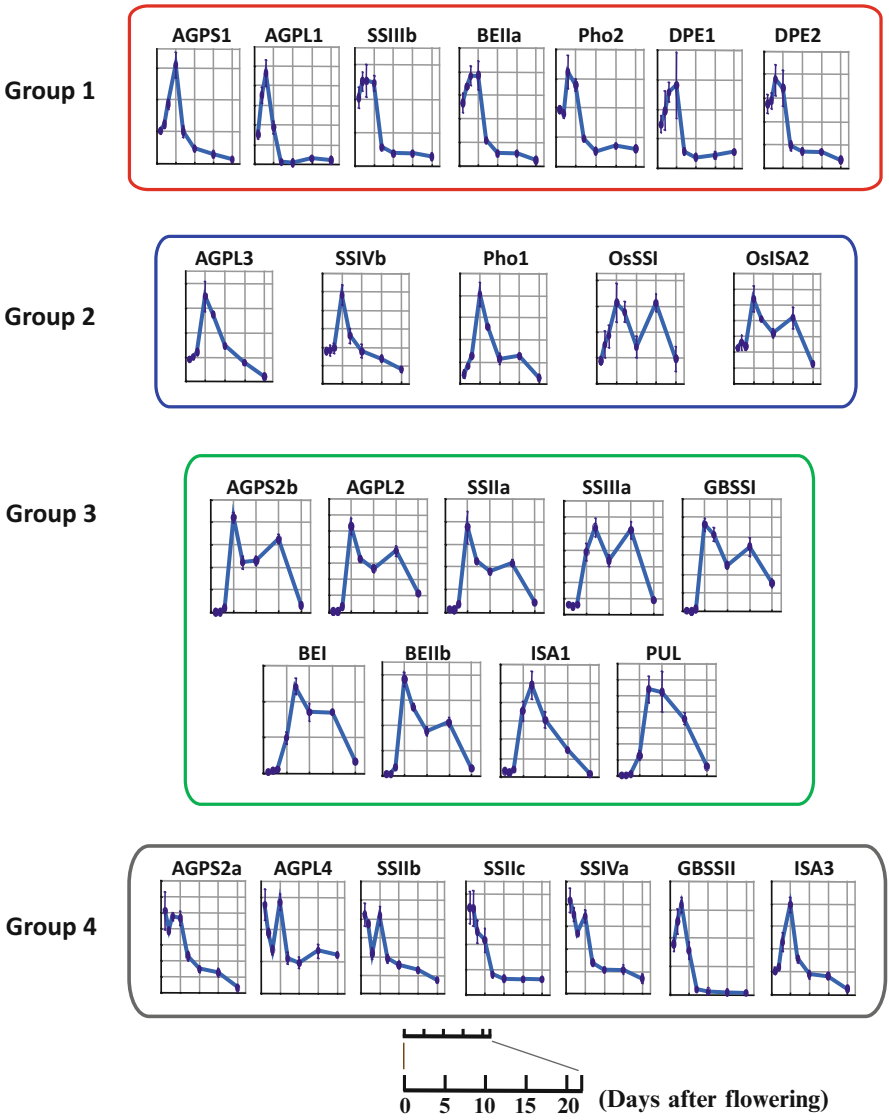

Fig. 9.6 Expression profiles of genes coding for starch synthetic enzymes during development of rice seeds. Genes are classified into 4 groups according to pattern of changes in the transcript levels during development of rice endosperm. The vertical axis shows the amount of the transcript level (see Ohdan et al. 2005 for details)

Plants might have established the specific initiation process in plastids during evolution, which is not found in animals and fungi. Plants must have developed the potential functions of enzymes specifically involved in this process and assigned plastids to perform the highly integrated enzymatic reaction networks by coordi-

nating with other subcellular compartments. SS might have gained the capacity to synthesize MOS from maltose, while Pho1 and SSI in combination with BE have excellent means for the glucan synthesis by using endogenous glucans entrapped with them as primers. Thus, these enzymes have multiple functions in starch biosynthesis: Pho1 would be involved in the initiation process by association with BE, playing a part in the degradation of MOS generated at the amylopectin trimming step by starch debranching enzymes during starch biosynthesis, while SSI could play important roles in the elongation of very short chains of amylopectin (see Sect. 5.3.1.1 in Chap. 5), the synthesis of MOS from maltose and maltotriose (Brust et al. 2013), and the synthesis of branched glucan by forming functional interaction with BE (Nakamura et al. 2014).

Starch granules have distinct size and morphology depending on species, tissues, and developmental stages as well as different genetic backgrounds. Thus, the initiation process for the synthesis of starch granules must be very specific and found in plants. Although several factors are considered to affect directly or indirectly the number, size, and shapes of starch granule structure, the precise mechanism for the initiation of starch granular structure needs to be elucidated.

The specific role of SSIV having some redundancies with SSIII in the starch granule initiation in chloroplasts was revealed by a comprehensive analysis of the *ss4-ss3* mutants of *Arabidopsis* (see Chap. 6 for details). In addition, Yun et al. (2011) proposed that ISA3 was involved not only in starch degradation but also in plastid division in rice endosperm and leaf based on the analysis of rice transformants in which the *ISA3* transcript level was reduced and overexpressed.

Involvement of some enzymes and proteins in plastid division and morphology has also been proposed from the analysis of their localizations in starch granules and inside and outside of plastids by using laser scanning confocal microscopy detecting fluorescence-labeled proteins. Recently, Toyosawa et al. (2015) observed that most of SSIVb proteins were located in the septum-like structure dissecting the inside space of developing rice amyloplast (Yun and Kawagoe 2010), which gave rise to the compound polygonal starch granules in rice endosperm. This sharply contrasts with the observation of Szydlowsky et al. (2009) that SSIV was located in specific regions at the boundaries of starch granules in *Arabidopsis* leaves. Toyosawa et al. (2015) also showed that some SSIIIa proteins were located in the outer envelope and intermembrane spaces of amyloplasts in rice endosperm. These results strongly suggest that SSIVb and SSIIIa have specific secondary functions controlling the division and/or development of amyloplasts in developing rice endosperm, although further concrete evidence is needed.

9.4 Future Perspectives

At present almost nothing is known regarding the molecular mechanism and factors involved in the initiation process of starch biosynthesis and factors involved in this process. No consensus on the consistent definition of the initiation process

has been established. In this chapter, several topics have been described and discussed based on a working hypothesis that the initiation of starch biosynthesis in plant cells is composed of two processes. The first process includes the synthesis from simple carbohydrates such as glucose, maltose, G1P, and ADPglucose to the amylopectin prototype, which is subsequently reproduced at a high rate to form the starch granules in the amplification process. The second is the starch granule initiation process. Since granules including glucans/dextrins synthesized in the initiation process are possibly formed even when they lack the cluster structure, both processes might happen simultaneously at least to some extent and are interrelated. Yet, the possibility that the core region of the granule including cluster-less glucans is used as precursor of the starch granule during the development of the granule packed with mature amylopectin synthesized in the amplification process in its outer starch layer cannot be ruled out. The nature of the initiation process may be different between reserve tissues and leaves and between cereal endosperm and tubers/tuberous roots of potato/sweet potato. In leaves, starch production and consumption are diurnally repeated, and cells may maintain the prototype amylopectin in the very small size of glucans even at the previous night period, which are then used as precursors for amylopectin and starch granules. If this is the case, the true initial process does happen only at the very early leaf developmental stage. On the other hand, developmental and maturing stages of cereal endosperm proceed near synchronously from cell division until the seed desiccation. Thus, the initiation process plays a crucial role in the final production of starch granules in the cereal, and this process might be maintained during the developing stage because amyloplast division and enlargement must be vigorously operating at least until the late developmental stage when amyloplasts are matured. In vegetative tissues such as potato tubers, starch production is accompanied by the process of cell/amyloplast division and expansion, and both the initiation and amplification are not distinctly separated from each other compared with starch synthesis in cereal endosperm. Since these functions are hypothesized based on limited information on characteristics of enzyme actions found in a few plant sources, more detailed analyses of enzymes from various sources must be conducted.

New techniques and approaches required for future studies on starch biosynthesis and described in Chap. 5 are also expected to promote our understanding of the initiation process of starch biosynthesis.

References

Brust H, Orzechowski S, Fettke J et al (2013) Starch synthesizing reactions and paths: *in vitro* and *in vivo* studies. J Appl Glycosci 60:2–20

Brust H, Lehman T, D'Hulst C et al (2014) Analysis of the functional interaction of Arabidopsis starch synthase and branching enzyme isoforms reveals that the cooperative action of SSI and BEs results in glucans with polymodal chain length distribution similar to amylopectin. PLoS One 9:e102364

Cao Y, Skurat AV, DePaoli-Roach AA et al (1993) Initiation of glycogen synthesis. Control of glycogenin by glycogen phosphorylase. J Biol Chem 268:21717–21721

Chatterjee M, Berbezy P, Vyas D et al (2005) Reduced expression of a protein homologous to glycogenin leads to reduction of starch content in *Arabidopsis* leaves. Plant Sci 168:501–509

Cheng C, Mu J, Farkas I et al (1995) Requirement of the self-glucosylating initiator proteins Glg1p and Glgp2 for glycogen accumulation in *Saccharomyces cerevisiae*. Mol Cell Biol 15:6632–6640

Commuri PD, Keeling PL (2001) Chain-length specificities of maize starch synthase I enzyme: studies of glucan affinity and catalytic properties. Plant J 25:475–486

Crumpton-Taylor M, Pike M, Lu K et al (2013) Starch synthase 4 is essential for coordination of starch granule formation with chloroplast division during Arabidopsis leaf expansion. New Phytol 200:1064–1075

Dauvillée D, Chochois V, Steup M et al (2006) Plastidial phosphorylase is required for normal starch synthesis in *Chlamydomonas reinhardtii*. Plant J 48:274–285

Delgado IJ, Wang Z, de Rocher A et al (1998) Cloning and characterization of AtRGP1. Plant Physiol 116:1339–1350

Denyer K, Waite D, Motawia S et al (1999) Granule-bound starch synthase I in isolated starch granules elongates malto-oligosaccharides processively. Biochem J 340:183–191

D'Hulst C, Merida Á (2010) The priming of storage glucan synthesis from bacteria to plants: current knowledge and new developments. New Phytol 188:12–21

D'Hulst C, Merida Á (2012) Once upon a prime: inception of the understanding of starch initiation in plants. In: Tetlow I (ed) Starch: origins, structure and metabolism, vol 5, Essential reviews in experimental biology. The Society for Experimental Biology, London, pp 55–76

Farkas I, Hardy TA, Goebl MG et al (1991) Two glycogen synthase isoforms in Saccharomyces cerevisiae are coded by distinct genes that are differentially controlled. J Biol Chem 266:15602–15607

Fettke J, Albrecht T, Hejazi M et al (2010) Glucose 1-phosphate is efficiently taken up by potato (*Solanum tuberosum*) tuber parenchyma cells and converted to reserve starch granules. New Phytol 185:663–675

Fettke J, Leifels L, Brust H et al (2012) Two carbon fluxes to reserve starch in potato (*Solanum tuberosum* L.) tuber cells are closely interconnected but differently modulated by temperature. J Exp Bot 63:3011–3029

Fujita N, Nakamura Y (2012) Distinct and overlapping functions of starch synthase isoforms. In: Tetlow I (ed) Starch: origins, structure and metabolism, vol 5, Essential reviews in experimental biology. The Society for Experimental Biology, London, pp 115–140

Gámez-Arjona FM, Li J, Raynaud S et al (2011) Enhancing the expression of starch synthase class IV results in increased levels of both transitory and long-term storage starch. Plant Biotechnol J 9:1049–1060

Hwang S, Nishi A, Satoh H et al (2010) Rice endosperm-specific plastidial α-glucan phosphorylase is important for synthesis of short-chain malto-oligosaccharides. Arch Biochem Biophys 495:82–92

Imparl-Radosevich JM, Gameon JR, McKean A et al (2003) Understanding catalytic properties and functions of maize starch synthase isozymes. J Appl Glycosci 50:177–182

Jeon JS, Ryoo N, Hahn TR et al (2010) Starch biosynthesis in cereal endosperm. Plant Physiol Biochem 48:383–392

Kitamura S, Yunokawa H, Mitsuie S et al (1982) Study on polysaccharide by the fluorescence method. II. Micro-Brownian motion and conformational change of amylose in aqueous solution. Polym J 14:93–99

Langeveld SMJ, Vennik M, Kottenhagen M et al (2002) Glucosylation activity and complex formation of two classes of reversibly glycosylated polypeptides. Plant Physiol 129:278–289

Leterrier M, Holappa L, Broglie KE et al (2008) Cloning, characterisation and comparative analysis of a starch synthase IV gene in wheat: functional and evolutionary implications. BMC Plant Biol 8:98

Lomako J, Lomako W, Whelan W (1988) A self-glucosylating protein is the primer for rabbit muscle glycogen biosynthesis. FASEB J 2:3097–3103

Mu J, Cheng C, Roach PJ (1996) Initiation of glycogen synthesis in yeast. J Biol Chem 271:26554–26560

Nakamura Y (2014) Mutagenesis and transformation of starch biosynthesis of rice and the production of novel starches. In: Tomlekova N, Kozgar I, Wani R (eds) Mutagenesis: exploring novel genes and pathways. Wageningen Academic, Wageningen, pp 251–278

Nakamura Y, Francisco PB Jr, Hosaka Y et al (2005) Essential amino acids of starch synthase IIa differentiate amylopectin structure and starch quality between japonica and indica rice varieties. Plant Mol Biol 58:213–227

Nakamura Y, Fujita N, Utsumi Y et al (2009) Revealing the complex system of starch biosynthesis in higher plants using rice mutants and transformants. In: Shu Q (ed) Induced mutations in the genomics era. Food and Agriculture Organization of the United Nations, Rome, pp 165–167

Nakamura Y, Utsumi Y, Sawada T et al (2010) Characterization of the reactions of starch branching enzymes from rice endosperm. Plant Cell Physiol 51:776–794

Nakamura Y, Ono M, Utsumi Y et al (2012) Functional interaction between plastidial starch phosphorylase and starch branching enzymes from rice during the synthesis of branched maltodextrins. Plant Cell Physiol 53:869–878

Nakamura Y, Aihara S, Crofts N et al (2014) *In vitro* studies of enzymatic properties of starch synthases and interactions between starch synthase I and starch branching enzymes from rice. Plant Sci 224:1–8

Ohdan T, Francisco PB Jr, Hosaka Y et al (2005) Expression profiling of genes involved in starch synthesis in sink and source organs of rice. J Exp Bot 56:3229–3244

Pitcher J, Smythe C, Cohen P (1988) Glycogenin is the priming glucosyltransferase required for the initiation of glycogen biogenesis in rabbit skeletal muscle. Eur J Biochem 176:391–395

Putaux JL, Potocki-Véronèse G, Remaud-Simeon M et al (2006) α-D-Glucan-based dendritic nanoparticles prepared by *in vitro* enzymatic chain extension of glycogen. Biomacromolecules 7:1720–1728

Qi Y, Kawano N, Yamauchi Y et al (2005) Identification and cloning of a submergence-induced gene OsGGT (glycogenin glucosyltransferase) from rice (*Oryza sativa* L.) by suppression subtractive hybridization. Planta 221:437–445

Roach PJ, Depaoli-Roach AA, Hurley TD et al (2012) Glycogen and its metabolism: some new developments and old themes. Biochem J 441:763–787

Roldán L, Wattebled F, Lucas MM et al (2007) The phenotype of soluble starch synthase IV defective mutants of *Arabidopsis thaliana* suggests a novel function of elongation enzymes in the control of starch granule formation. Plant J 49:492–504

Romero JM, Issoglio FM, Carrizo ME et al (2008) Evidence for glycogenin autoglucosylation cessation by inaccessibility of the acquired maltosaccharide. Biochem Biophys Res Commun 374:704–708

Rothschild A, Tandecarz JS (1994) UDP-glucose: protein transglucosylase in developing maize endosperm. Plant Sci 97:119–127

Sandhu APS, Randhawa GS, Dhugga KS (2009) Plant cell wall matrix polysaccharide biosynthesis. Mol Plant 2:840–850

Satoh H, Shibahara K, Tokunaga T et al (2008) Mutation of the plastidial α-glucan phosphorylase gene in rice affects the synthesis and structure of starch in the endosperm. Plant Cell 20:1833–1849

Sawada T, Nakamura Y, Ohdan T et al (2014) Diversity of reaction characteristics of glucan branching enzymes and the fine structure of α-glucan from various sources. Arch Biochem Biophys 562:9–21

Schupp N, Ziegler P (2004) The relation of starch phosphorylases to starch metabolism in wheat. Plant Cell Physiol 45:1471–1484

Singh DG, Lomako J, Lomako WM et al (1995) [beta]-Glucosylarginine: a new glucose-protein bond in a self-glucosylating protein from sweet corn. FEBS Lett 376:61–64

Szydlowsky N, Ragel P, Raynaud S et al (2009) Starch granule initiation in *Arabidopsis* requires the presence of either class IV or class III starch synthases. Plant Cell 21:2443–2457

Szydlowsky N, Ragel P, Hennen-Bierwagen TA et al (2011) Integrated functions among multiple starch synthases determine both amylopectin chain length and branch linkage location in *Arabidopsis* leaf starch. J Exp Bot 62:4547–4559

Toyosawa Y, Kawagoe Y, Matsushima R, et al. (2015) Deficiency of starch synthase IIIa and IVb leads to dramatic changes in starch granule morphology in rice endosperm (submitted)

Ugalde JE, Parodi AJ, Ugalde RA (2003) *DE novo* synthesis of bacterial glycogen: *Agrobacterium tumefaciens* glycogen synthase is involved in glucan initiation and elongation. Proc Natl Acad Sci U S A 100:10659–10663

Wilson WA, Roach PJ, Montero M et al (2010) Regulation of glycogen metabolism in yeast and bacteria. FEMS Microbiol Rev 34:952–985

Yamakawa H, Hirose T, Kuroda M et al (2007) Comprehensive expression profiling of rice grain filling-related genes under high temperature using DNA microarray. Plant Physiol 144:258–277

Yuguchi Y, Hashimoto K, Yamamoto K et al (2013) Extension of branched chain of amylopectin by enzymatic reaction and its structural characterization. J Appl Glycosci 60:131–135

Yun M, Kawagoe Y (2010) Septum formation in amyloplasts produces compound granules in the rice endosperm and is regulated by plastid division proteins. Plant Cell Physiol 51:1469–1479

Yun M, Umemoto T, Kawagoe Y (2011) Rice debranching enzyme isoamylase3 facilitates starch metabolism and affects plastid morphogenesis. Plant Cell Physiol 52:1068–1082

Part IV
Biotechnology

Chapter 10
Manipulation of Rice Starch Properties for Application

Naoko Fujita

Abstract Starches that accumulate in the storage organs of green plants are used for industrial applications as well as carbohydrate source for most of organisms. We isolated a lot of rice mutant lines of starch biosynthesis-related enzymes (isozymes) for understanding the starch biosynthesis of green plants. The starches in the endosperm of rice mutant lines were quite different from those of the wild-type. In an attempt to clarify the redundancies and the functional interactions among multiple isozymes, we are trying to isolate many combinations of multiple mutant lines by using genetic procedures. Analyses of several mutant lines show that a deficiency in a specific isozyme is compensated for by other isozymes. The widespread variation in starches should help diversify their application for food and industrial use. It is necessary to analyze the details of starch structure and physicochemistry of these starches and clarify the relationships among these. This chapter summarizes the effects of the deficiencies of starch biosynthetic isozymes on the chain-length distribution of amylopectin, the amylose content, and the gelatinization properties. I also summarize the effects of the deficiency of isozymes on the important agricultural traits, such as fertility of the seeds, starch content, and seed morphology. The possibilities for use of food and industrial purposes and trials for improvement of agricultural traits by backcrossing with elite cultivars are also discussed.

Keywords Amylopectin • Amylose • Endosperm • Isozymes • Mutant • Rice • Starch biosynthesis

10.1 Introduction

10.1.1 Advantages of Rice Endosperm for Studies of Starch

Green plants accumulate starch in their photosynthetic tissues as well as in storage organs. In most cases, storage starches are used as foods and for industrial

N. Fujita (✉)
Department of Biological Production, Akita Prefectural University, Akita City, Akita 010-0195, Japan
e-mail: naokof@akita-pu.ac.jp

Y. Nakamura (ed.), *Starch*, DOI 10.1007/978-4-431-55495-0_10

Table 10.1 The food composition of various crops

Crop	Water (%)	Protein (%)	Lipid (%)	Carbohydrate (%)	Ash (%)
Maize	14.5	8.6	5.0	70.6	1.3
Wheat	12.5	10.6	3.1	72.2	1.6
Rice	15.5	6.8	2.7	73.8	1.2
Kidney bean	16.5	19.9	2.2	57.8	3.6
Azuki bean	15.5	20.3	2.2	58.7	3.3
Sweet potato	66.1	1.2	0.2	31.5	1.0
Potato	79.8	1.6	0.1	17.6	0.9
Banana	75.4	1.1	0.2	22.5	0.8
Apple	84.9	0.2	0.1	14.6	0.2

The data are from The Standard Tables of Food Composition in Japan 2010 edited by the subdivision on resources, the council for Science and Technology Ministry of Education, Culture, Sports, Science and Technology, Japan

applications. One advantage of studying rice starches (among crop starches) is that the carbohydrate (starch) content of rice seeds is the highest among crops (Table 10.1). Therefore, minimal procedures are required for the purification of rice starch. Second, rice (*Oryza sativa* L.) is a model plant for research and is also an important crop species, whereas the model plant *Arabidopsis* is not a crop. Third, the entire DNA sequence of the rice cultivar "Nipponbare" was determined in 2005 (International Rice Genome Sequencing Project 2005). DNA information about rice can be obtained through websites quite easily. Fourth, it is easy to isolate mutant lines in rice compared with mutants in polyploid crops, such as wheat or potato. Moreover, the methods used to produce transgenic rice have been employed for more than 20 years. Thus, the availability of many types of materials harboring different combinations of genes related to starch phenotypes should provide numerous clues during the study of rice starches.

10.1.2 Development of Mutant and Transgenic Lines

To obtain a complete understanding of starch biosynthesis, it is important to know the function of each isozyme related to starch biosynthesis. To understand the function of each isozyme, we are currently performing in vivo analysis using rice mutants and transgenic lines. We usually employ japonica rice cultivars (Nipponbare, Taichung 65, Kinmaze, and so on) as the parent lines for mutant and transgenic rice lines. Most japonica cultivars have an inactive soluble starch synthase (SS)IIa isozyme which elongates amylopectin chains from the degree of polymerization (DP) 6–12 to DP 13–24 due to two point mutations in the *SSIIa* gene. By contrast, most indica rice cultivars have an active SSIIa isozyme (Nakamura et al. 2002, 2005; Umemoto et al. 2002). Granule-bound starch synthase I (GBSSI) is involved in the synthesis of amylose in the endosperm (Tsai 1974). Most japonica rice cultivars

are GBSSI leaky mutants, whereas indica-type cultivars are wild-type (Sano 1984; Wang et al. 1995). The average amylose content of japonica-type cultivars is lower (ca. 20 %) than that of indica cultivars (ca. 25–30 %, Nakamura et al. 2002). The differences in amylose content affect the physicochemical properties of starch (Singh et al. 2006); cooked japonica rice is sticky, which is the Japanese preference. These reports suggest that the single mutant lines derived from japonica rice cultivars may be treated as "triple mutant lines."

Many starch mutant lines were isolated at Kyushu University, Japan, by Prof. Satoh, who treated fertilized embryos of rice flowers with the chemical mutagen N-methyl-N-nitrosourea (MNU) (Satoh and Omura 1979). The biochemical traits and starch properties of lines with specific seed morphologies were analyzed, and the corresponding genes were identified. This strategy is referred to as "forward genetics." Retrotransposon *Tos17* mutant rice stocks with populations greater than 40,000 were also prepared by Dr. Hirochika's group at NIAS, Japan (Hirochika 2001), for use in "reverse genetics" studies. The japonica rice cultivar Nipponbare contains two copies of *Tos17* in its genome, which are duplicated and transported to other positions on the chromosome during culture (as callus). The gene into which *Tos17* inserts cannot be expressed, which results in a mutant phenotype.

In vivo studies can also be performed with transgenic rice lines in which a specific gene is introduced into the wild-type or mutant lines. Since field culture of transgenic plants is limited, we primarily focused on the development of mutant lines. However, we also generated transgenic rice lines for research.

We are currently trying to isolate mutant and transgenic rice lines from japonica rice of genes related to starch biosynthetic enzymes to produce various starches. It appears that some starch synthase (SS), branching enzyme (BE), debranching enzyme (DBE), and phosphorylase (Pho) isozymes have a large impact on the structure of starch (see Figs. 5.4 and 5.7 in Chap. 5). These enzyme classes comprise a total of 20 isozymes in rice (see Fig. 5.3 in Chap. 5), 15 of which [*SSI, SSIIa, SSIIIa, SSIIIb, SSIVa, SSIVb, GBSSI, BEI, BEIIa, BEIIb, Pho1, isoamylase (ISA)1, ISA2, ISA3*, and *pullulanase (PUL)*] were isolated from the corresponding mutant or transgenic lines. Using these lines, the functions of nine isozymes whose starch traits are different from those of the wild-type have been elucidated. By contrast, the functions of isozymes whose traits in the lines are very similar to those of the wild-type are still unknown.

10.1.3 Understanding the Relationships Among Genes (Isozymes) Related to Starch Biosynthesis, Starch Structure, and Physicochemical Properties

The widespread variation in starches should help diversify their application for food and industrial use. Recently, the conversion from plastics derived from petroleum to materials derived from plants, such as bioplastics, has been accelerating. The physicochemical properties of starches are important for their use. The main factor

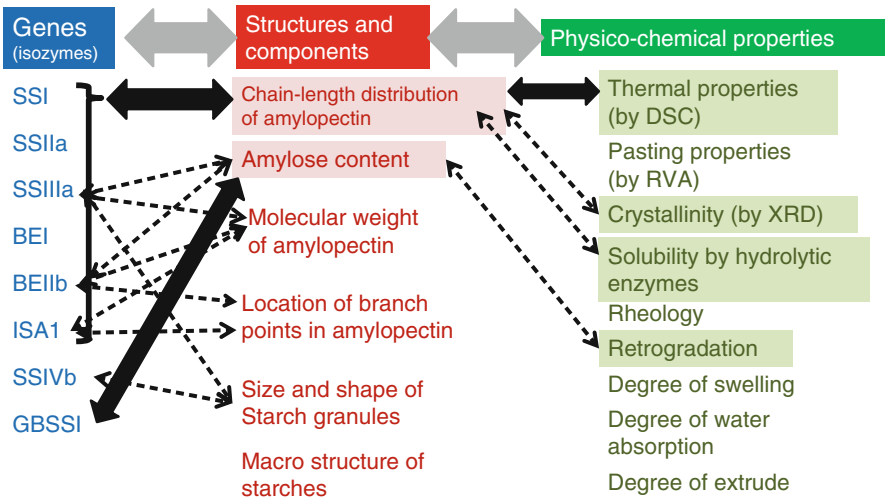

Fig. 10.1 Relationships among genes related to starch biosynthesis, starch structure and components, physicochemical properties, and starch properties for practical applications. The *black arrows* with *arrowheads* on both sides show the more apparent relationships. The *dashed arrows* show the slight apparent relationships

that affects the physicochemical properties of starches includes the starch's structure, as well as the properties of other components (proteins, lipids, and minerals). The structure of starch varies depending on the combination of the deficiencies and strength of enzyme activities related to starch biosynthesis. Therefore, if the relationships among genes (isozymes), starch structure, and physicochemical properties of starches are revealed, it will be possible to regulate starch traits and to design desirable starches for practical applications (Fig. 10.1). Developing mutant and transgenic rice lines harboring different combinations of isozyme deficiencies and analyzing these materials have helped increase our understanding of the relationships among these traits (Fig. 10.1). Although our understanding of these relationships is currently incomplete, the relationship between the chain-length distribution of amylopectin and the gelatinization temperature has been elucidated. The production and analysis of additional starches are needed; the other relationships have not been resolved.

10.1.4 Pleiotropic Effects on Starch Structure and Amylose Content

We noticed through the analyses of several mutant lines that a deficiency in a specific isozyme is compensated for by other isozymes. For example, starch accumulation in the endosperm of *ss1* null mutant lines is similar to that of the wild-type despite the fact that SSI activity, which accounts for more than 60 % of SS activity in

the crude extract of developing rice endosperm, is completely missing in this mutant (Fujita et al. 2006). This observation implies that residual SS isozymes (at least SSIIIa in) elongated α-1,4 chains of endosperm amylopectin instead of SSI. The functions of the residual isozymes are different from those of the deficient isozymes, which results in changes in the starch components and structure. The detailed mechanisms of the effects of these isozymes, known as pleiotropic effects, have not been resolved. It is known that SSIIIa deficiency leads to an increase in the expression levels of *SSI* and *GBSSI* (Fujita et al. 2007). However, the mechanisms underlying this induction of gene expression are currently unknown. The degrees of compensation by the other isozymes in response to deficiencies in specific isozymes are not uniform. Deficiencies in some isozymes that are hardly compensated for by other isozymes are revealed by their strong phenotypes. For example, a deficiency in BEIIb leads to a reduction in starch accumulation of almost one-half and significantly changes the structure of amylopectin (Nishi et al. 2001; Abe et al. 2013). By contrast, a deficiency in BEI does not lead to a reduction in starch accumulation, and the structure of amylopectin is only slightly altered compared to that of the wild-type (Satoh et al. 2003; Abe et al. 2013). These results imply that BEIIb is not easily compensated for by BEI and BEIIb, while BEI is easily compensated for by BEIIa and BEIIb.

10.2 Isozymes Having a Large Impact on the Chain-Length Distribution of Endosperm Amylopectin

Starches consist of two different molecules, i.e., amylose and amylopectin. The biosynthesis of these two molecules is thought to occur separately. BEs are related to the branching of amylopectin molecules. There are 11 SS isozyme genes (*SSI, SSIIa, SSIIb, SSIIc, SSIIIa, SSIIIb, SSIVa, SSIVb, SSV, GBSSI*, and *GBSSII*) in the rice genome. Of these, GBSSI and GBSSII are related to amylose biosynthesis, and residual SSs are thought to be related to amylopectin biosynthesis. This section focuses on isozymes that have a large impact on the chain-length distribution of rice endosperm amylopectin (SSI, SSIIa, SSIIIa, BEI, BEIIb, and ISA1). The isozymes described in this section are also abundantly expressed in developing endosperm. Comparisons between the corresponding mutants and the wild-type have provided many clues about the construction of amylopectin molecules by each isozyme (see Fig. 5.2 in Chap. 5).

10.2.1 SSI

SSI activity accounted for 60–70 % of SS activity in the soluble fraction of developing endosperm in rice (Baba et al. 1993; Fujita et al. 2006) and maize (Cao et al. 2000). Attempts have been made to isolate rice *ss1* mutant lines from retrotrans-

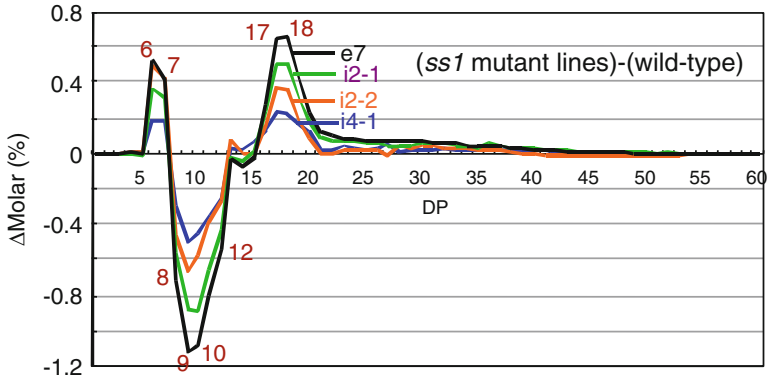

Fig. 10.2 Differences in chain-length distribution patterns of endosperm amylopectin between mature endosperm of the *ss1* mutant lines and the wild-type. e7, i2–1, i2–2, and i4–1 are the names of *ss1* mutant lines. The SSI activity in these lines is 0, 1/6, 1/5, and ¼ that of the wild-type, respectively (Fujita et al. 2006) (Reprinted with permission from Plant Physiology., 140, Fujita et al., Function and characterization of starch synthase I using mutants in rice, 1070–1084, Fig. 5b, © 2006, American Society of Plant Biologists (www.plantohysiol.org))

poson *Tos17* populations using PCR screening. Four mutant lines (i2–1, i2–2, i4, and e7) carrying *Tos17* insertions in different positions of the *SSI* gene (intron 2, intron 4, and exon7, respectively) were isolated, which had 1/6, 1/5, 1/4, and zero SSI activity compared to the wild-type, respectively, as estimated based on the density of SSI activity bands on native-PAGE gels (Fujita et al. 2006). The chain-length distribution of endosperm amylopectin in the *ss1* mutant lines showed specific patterns. However, the extent of this change was not large compared with that of lines such as *isa1* and *be2b*. There was a decrease in the number of chains with a DP value of 8–12 and an increase in the number of chains with DP 6–7 and 16–19; the degree of change was positively correlated with the extent of reduction in SSI activity in the mutant lines (Fig. 10.2). These results strongly suggest that the pattern observed in the mutants was caused by a deficiency in SSI activity (Fujita et al. 2006).

The possible reasons for this pattern of amylopectin chain-length distribution are as follows. The number of DP 6–7 chains that were branched by BEIIb increased in the *ss1* lines because the chains were not elongated to DP 8–12 due to a lack of SSI. In other words, the number of DP 8–12 chains decreased because the DP 6–7 chain precursors were not elongated and most of the available DP 8–12 chains were converted into longer chains by other SS isozymes (probably SSIIIa). By contrast, the increase in the number of DP 16–19 chains could primarily be attributed to the increase in the number of B_1-chains. Chains with DP 16–19 were predicted to have external segments with DP 7 in the B-chains (Fujita et al. 2006). This notion is in agreement with the observed lengths of the A-chains (DP 6–7), which were higher in mutant amylopectin. These results indicate that SSI distinctly generated

DP 8–12 chains from short DP 6–7 chains that emerged from the branch point in the A- or B1-chains of amylopectin. These notions are supported by the results of in vitro analysis of purified rice SSI expressed in *E. coli* (Fujita et al. 2008; Nakamura et al. 2014).

10.2.2 SSIIa

The function of rice SSIIa was revealed based on the differences in chain-length distribution of amylopectin between indica and japonica rice cultivars. Rice cultivars are divided into japonica and indica cultivar groups. The chain-length distribution pattern of starch in japonica rice cultivars (Nipponbare and Kinmaze) was different from that of indica rice cultivars (Kasalath and IR36) (Umemoto et al. 1999, 2002). The number of short chains with DP 6–12 was higher in japonica cultivars than in indica cultivars, while the number of medium chains with DP 13–24 was lower in japonica than in indica (see Fig. 5.4 in Chap. 5). Two of the four single nucleotide polymorphisms (SNPs) in *SSIIa* between indica cultivars (Kasalath and IR36) and japonica cultivars (Nipponbare and Kinmaze) were important for SSIIa activity. The activity of recombinant SSIIa in Nipponbare and Kinmaze was less than 10 % that of wild-type SSIIa from indica cultivars (Nakamura et al. 2005). Transgenic japonica rice (Kinmaze) expressing an introduced indica *SSIIa* gene contained L-amylopectin, with alkaline-resistant starch, rather than japonica-type amylopectin (S-amylopectin) (Nakamura et al. 2005). SSIIa did not affect the number of long chains with DP≥25 (Umemoto et al. 2002), indicating that SSIIa regulates the structure within one cluster of amylopectin (see Fig. 5.4 in Chap. 5). A similar conclusion was obtained through analysis of the transgenic rice line *SSIIa*^{l}*/isa1* (see Sect. 10.6.1; Fujita et al. 2012).

10.2.3 SSIIIa

SSIIIa accounted for the second highest proportion of SS activity in the soluble fraction isolated from developing rice and maize endosperm, followed by SSI (Fujita et al. 2006), as estimated by native-PAGE/SS activity staining. An *ss3a* rice mutant harboring *Tos17* inserted into exon 1 of the *SSIIIa* gene was previously isolated (Fujita et al. 2007). The number of chains with DP 6–9, DP 16–19, and DP≥33 was lower in mutant amylopectin than in the wild-type, while that with DP 10–15 and DP 20–25 was higher (see Fig. 5.4 in Chap. 5). These differences in the range of DP≤20 in the *ss3a* mutants were almost opposite to those of the *SSI*-deficient rice mutant (see Fig. 5.4 in Chap. 5). It should be noted that the number of long chains connecting amylopectin clusters (DP≥33) was only 60 % that of the wild-type, indicating that SSIIIa functions in the elongation of these chains (Fujita et al. 2007; Hanashiro et al. 2011).

10.2.4 BEI

Rice *be1* mutant lines were isolated from mutant rice stocks induced by MNU treatment of fertilized egg cells based on their deficiency in the 83-kDa band, as revealed by SDS-PAGE of endosperm samples (Satoh et al. 2003). The amylopectin from BEI-deficient mutant lines of different backgrounds was characterized by a slight decrease in the number of chains with DP≥37 and short chains with DP 12–21 and an increase in the number of short chains with DP≤10 and DP 24–34. The degree of this difference was not large, but it exhibited a specific pattern (see Fig. 5.7 in Chap. 5). These results suggest that BEI specifically branches long chains (Satoh et al. 2003). The function of BEI is also supported by the results of in vitro analysis of r*Os*BEI (Nakamura et al. 2010).

10.2.5 BEIIb

Cereals such as maize, rice, wheat, and barley have two BEII isozymes (BEIIa and BEIIb; Mizuno et al. 1993). BEIIb-deficient mutants of maize and rice are commonly known as *amylose-extender* (*ae*) mutant lines. The name *amylose-extender* is derived from the high levels of amylose starch in the endosperm (Banks et al. 1974), as starch from *ae* mutant lines is stained blue by iodine, which is characteristic of high amylose starch. However, analysis of the *wx/ae* (amylose-free) double mutant showed that the increased blue staining by iodine was primarily due to the enrichment of the long chains of amylopectin with DP≥14, as well as the significant decrease in short chains with DP<13 in the *ae* mutant (see Fig. 5.7 in Chap. 5; Nishi et al. 2001). These results, along with the results of in vitro analysis of r*Os*BEIIb (Nakamura et al. 2010), suggest that the function of BEIIb is to branch short chains in the crystalline lamellae of amylopectin. BEIIb deficiency has one of the greatest impacts on amylopectin structure in several starch mutant lines (see Fig. 5.7 in Chap. 5).

10.2.6 ISA1

Isoamylase 1 (ISA1)-deficient mutants (*isa1*) are referred to as *sugary-1* mutants in maize (*su1*) and rice (*sug-1*) (James et al. 1995; Nakamura et al. 1996). Many allelic *isa1* mutant lines have been isolated from japonica rice, and the α-glucans (α-glucans accumulated in *isa1* was no longer "starch" due to significant changes in structure; we will therefore refer to these compounds as "α-glucans") in their endosperm have been characterized (Nakamura et al. 1997; Kubo et al. 1999). ISA1 deficiency also had one of the greatest impacts on amylopectin structure. The α-glucans in the regions of the endosperm not stained by iodine were enriched in short chains with DP≤10, i.e., highly branched, water-soluble starches, which was called "phytoglycogen." The α-glucans in the regions of *sug-1* endosperm stained

by iodine were insoluble and similar to wild-type starch, whereas the number of short chains with DP≤12 was higher in the mutant than in wild-type amylopectin (Kubo et al. 1999; Wong et al. 2003).

Numerous reports of *isa1* mutant lines suggest that ISA1 activity is essential for amylopectin crystallinity and the tandem cluster structure of amylopectin, which indicates that ISA1 is involved in the maintenance of the cluster structure of amylopectin. The function of ISA1 is thought to trim improper branches produced by BEs in amylopectin molecules (see Fig. 5.1c in Chap. 5; Nakamura 2002).

10.3 Isozymes Having a Small Impact on the Chain-Length Distribution of Endosperm Amylopectin (SSIIIb, SSIVb, GBSSI, BEIIa, ISA2, ISA3, and PUL)

There are some isozymes whose chain-length distribution patterns of amylopectin in the corresponding mutants were similar to that of the wild-type. Among these, the expression levels of *SSIIIb*, *SSIVb*, *BEIIa*, and *ISA3* were not high in developing rice endosperm. By contrast, *SSIIIb* was highly expressed in leaves (Hirose and Terao 2004; Ohdan et al. 2005). No significant differences in the chain-length distribution of endosperm amylopectin were observed between *ss3b* and the wild-type (Fujita et al. unpublished data). SSIVb was expressed in leaves as well as endosperm at the early stage of development (Hirose and Terao 2004; Ohdan et al. 2005). The chain-length distribution of endosperm amylopectin in *ss4b* was similar to that in the wild-type, although the number of short chains of approximately DP 10 was slightly reduced (Toyosawa et al. submitted). No differences in the chain-length distribution pattern of endosperm amylopectin were observed in *be2a* (Nakamura 2002), and analysis of the corresponding maize mutant yielded similar results (Blauth et al. 2001). BEII isozymes BEIIa and BEIIb both functioned in the branching of short chains, as revealed by in vitro analysis (Nakamura et al. 2010). Therefore, BEIIa deficiency could be adequately compensated for by BEIIb. ISA3 was not expressed in the developing endosperm (Kubo et al. 2010b). The chain-length distribution of endosperm amylopectin in *isa3* was similar to that of the wild-type, although the number of short chains with DP≤19 was slightly reduced (Yun et al. 2011).

The main function of GBSSI (which is strongly expressed in the endosperm) is amylose synthesis. The effect of GBSSI deficiency on the chain-length distribution of amylopectin in rice (Nishi et al. 2001) and diploid wheat (Fujita et al. 2001) was not large. No effects of ISA2 deficiency on the chain-length distribution of amylopectin were observed in rice (Utsumi et al. 2011) or maize (Kubo et al. 2010b), whereas those in potato (Hussain et al. 2003), *Arabidopsis* (Delatte et al. 2005; Wattebled et al. 2005), and *Chlamydomonas* (Dauvillée et al. 2001) were significant, as were those in *isa1*. This result is due to the fact that ISA1 homo-oligomers have more important functions than ISA1–ISA2 hetero-oligomers in rice (Utsumi et al. 2011) and maize (Kubo et al. 2010b). PUL had different substrate specificity from that of ISA (Nakamura 1998).

The role of PUL in trimming improper branches during starch biosynthesis appeared to be much smaller than that of ISA1, although PUL was very highly expressed in developing rice endosperm (Fujita et al. 2009). On the other hand, a slight reduction in the number of short chains with DP≤12 was observed, indicating that PUL may compensate for the function of ISA1 (Fujita et al. 2009).

10.4 Isozymes Having a Large Impact on the Amylose Content of Endosperm Starch

10.4.1 GBSSI

GBSSI has been shown to be an amylose synthase, as starches in the GBSSI-deficient mutants of several crops lacked amylose. Therefore, the expression of *GBSSI* directly affected the amylose content (Fig. 10.3). Typical japonica rice cultivars contained an SNP at the boundary between exon 1 and intron 1 of *GBSSI* compared to indica rice cultivars, which resulted in the inhibition of splicing of intron 1 and the production of incomplete mRNAs (Isshiki et al. 1998). This led to a decrease in the levels of GBSSI and resulted in lower amylose contents (ca. 20 %) compared to indica rice cultivars (ca. 25–30 %; Nakamura et al. 2002; Horibata et al. 2004; Inouchi et al. 2005). In Japan, low amylose mutant rice has been developed as good-tasting rice cultivars. Most of these mutant lines had the additional SNP in the *GBSSI* gene. GBSSI synthesized extra-long chains (ELC) of amylopectin as well as amylose (Takeda et al. 1987). ELC was co-eluted with amylose in the first fraction produced by separation of debranched starch via gel-filtration (Horibata et al. 2004). There are two types of high amylose rice cultivars: high ELC types and high true amylose content types (Horibata et al. 2004). The differences between these two types might be caused by the SNP of *GBSSI* (Hanashiro et al. 2008).

The expression of GBSSI depended on the temperature during development (Hirano and Sano 1998). SNP at the splicing site in the first intron was demonstrated to be associated with different sensitivities to temperature during filling stage

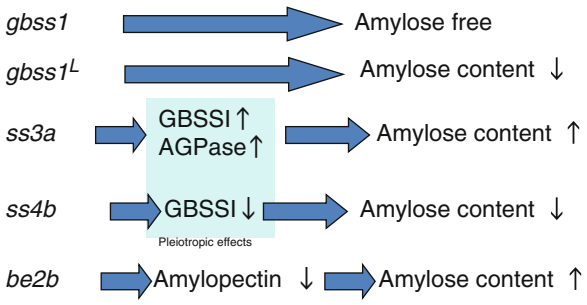

Fig. 10.3 Isozymes have a large impact on the amylose content of endosperm starch and mechanisms. ^{L} of *gbss1*^{L} indicates leaky mutant

(Larkin and Park 1999). A plant with Wx^b locus in japonica rice would accumulate more mature *GBSSI* mRNA at low temperature (18 °C) than at normal (25 °C) or high temperature (32 °C). Therefore, starches in rice seeds that have developed at high temperatures have low amylose contents, whereas starches in rice seeds that have developed at low temperatures have high amylose contents (Zhang et al. 2014).

10.4.2 SSIIIa

SS and BE isozymes (except for GBSS) are involved in amylopectin biosynthesis. However, some isozymes affected the amylose content of rice seeds. The amylose content in SSIIIa-deficient mutant lines was approximately 1.5 times higher than that of the wild-type (Fujita et al. 2007). SSIIIa deficiency led to an increase in GBSSI levels and activity (Fujita et al. 2007; Asai et al. 2014), which appeared to result from transcriptional regulation (Fujita et al. 2007), a mechanism for complementation of the SSIIIa deficiency. ADP-glucose pyrophosphorylase (AGPase) activity was also higher in the *ss3a* mutant than in wild-type endosperm (Fujita et al. 2007, 2011). The high amylose content in this mutant line was likely caused by the increased activities of both GBSSI and AGPase (Fig. 10.3; Fujita et al. 2007). GBSSI had a higher K_m for ADP-glucose than the other SS isozymes (Clarke et al. 1999; Lloyd et al. 1999). The increase in AGPase activity likely resulted in high concentrations of ADP-glucose in amyloplasts, and amylose synthesis by GBSSI was thought to be dominant.

10.4.3 SSIVb

The seed phenotype, size, and chain-length distribution of endosperm amylopectin in the *ss4b* mutant were very similar to those of the wild-type (Toyosawa et al. submitted). However, the amylose content in the *ss4b* lines was lower (11–14 %) than that of the wild-type (Toyosawa et al. submitted). These results could be attributed to the low expression levels of GBSSI (Fig. 10.3), indicating that SSIVb deficiency might lead to the suppression of *GBSSI* (Toyosawa et al. submitted).

10.4.4 BEIIb

The amylose content of the *be2b* rice mutant was approximately 1.5 times higher than that of the wild-type (Nishi et al. 2001; Abe et al. 2014). The main reason for the higher amylose content in *be2b* was the suppression of amylopectin synthesis resulting from the significant reduction in the nonreduced end of amylopectin. BEIIb deficiency also led to a significant decrease in the number of amylopectin short chains, as described above (see Sect. 10.2.5; Nishi et al. 2001), and the dehydration of seeds occurred earlier in a developing endosperm in the mutant

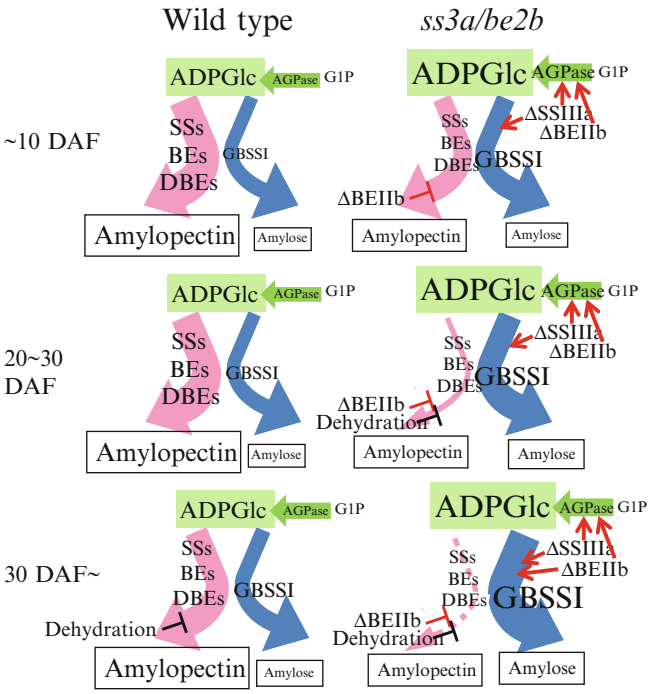

Fig. 10.4 Possible mechanism of the partitioning of carbon into amylopectin and amylose during starch biosynthesis in the wild-type and *ss3a/be2b* mutant rice line. Sizes of the characters correspond to the expression levels of enzymes and the amount of ADP-glucose. Thickness of *curved arrows* indicates the amount of carbon flow into amylopectin and amylose. ΔSSIIIa and ΔBEIIb indicate a deficiency of SSIIIa and BEIIb, respectively. *Red arrows* and *slanted* "T" indicate the enhancement and suppression of enzyme levels, respectively. Note that the flow to ADP-glucose and/or the level of ADP-glucose increases due to a defect in SSIIIa and BEIIb. *ADPase* ADP-glucose pyrophosphorylase, *ADPG* ADP-glucose, *G1P* glucose-1 phosphate, *SSs* starch synthases, *BEs* branching enzymes, *DBEs* debranching enzymes (Asai et al. 2014) (Reprinted with permission from J. Exp. Bot. 65, Asai et al., Deficiencies in both starch synthase (SS) IIIa and branching enzyme IIb lead to a significant increase in amylose in SSIIa inactive japonica rice seeds., 5497–5507, Fig. 7, © 2014, Oxford University Press)

than in the wild-type (Asai et al. 2014). During seed dehydration, amylopectin biosynthesis stopped, while amylose synthesis continued until the late stage of endosperm development (see Fig. 10.4; Asai et al. 2014).

10.5 Combinations of Deficiencies of Isozymes Related to Starch Biosynthesis

Many studies of starch double and/or triple mutants in maize were conducted in the 1980s and 1990s (Shannon and Garwood 1984; Inouchi et al. 1991;

Wang et al. 1993a, b). However, at that time, the genes responsible for the majority of the starch mutant phenotypes had not been identified. Many of the mutant genes have since been identified; this information can be used to elucidate the relationships between starch characteristics and starch biosynthesis genes. A number of single rice mutants exhibited phenotypes similar to those of the wild-type due to complementation by other isozymes, as described at Sect. 10.3. This complementation makes it difficult to characterize the functions of these isozymes. To elucidate the functions of individual isozymes, the overlapping activity of many other isozymes needs to be eliminated through the production of multiple mutant lines. When double, triple, or quadruple mutants were produced in japonica rice (which is already a leaky double mutant of *ss2a* and *gbss1*), sterility and low yield were a concern. However, some of our multiple mutant lines maintained 80–90 % of the seed weight of the wild-type, and large-scale cultivation of these mutants was possible. Leaky mutant lines have been useful for avoiding the sterility that could result especially when key isozyme-deficient mutants were crossed (Fujita et al. 2011; Abe et al. 2014). Some multiple mutant lines possessed unique starch properties that were not solely the additive effects of the mutant parents. Recent work on the multiple rice mutant lines is described below, along with a discussion of the effects of different combinations of the deficiency of multiple isozymes on amylopectin structure, amylose content, seed weight, sterility, and so on.

10.5.1 SSI and SSIIIa

The seed weight and accumulation of starch in the endosperm of both *ss1* and *ss3a* single null mutant lines were similar to those of the wild-type due to compensation by other SS isozymes. In addition to SSI deficiency, SSIIIa, which is the second major SS isozyme, was also eliminated by crossing both mutants (Fujita et al. 2011). In the F_2 populations derived from crosses between null *ss1* and null *ss3a*, developing seeds (more than 50 samples assessed) that lost both SSI and SSIIIa activity were not detected, indicating that the double-recessive developing seeds became sterile. Opaque seeds, whose phenotype differed from that of the parents, were present in the F_2 population, and their genotypes were heterozygotes for *SSI* (*SS1ss1/ss3ass3a*) or *SSIIIa* (*ss1ss1/SS3ass3a*). A double-recessive homozygous mutant line ($ss1^{L}ss1^{L}$/*ss3assd3a*) was successfully obtained by crossing an *ss1 leaky* mutant ($ss1^{L}$) and an *ss3a* mutant (Fujita et al. 2011). These results suggest that a deficiency in either SSI or SSIIIa results in complementation, and either SSI or SSIIIa is necessary for starch biosynthesis in rice endosperm. No other SS isozymes could provide this complementation.

In the *ss1ss1/SS3ass3a* line, the number of amylopectin chains with DP$\leq$10 was significantly reduced, while that with DP 11–20 was significantly higher compared with the wild-type (Fig. 10.5a). The amylopectin of the *SS1ss1/ss3ass3a* line contained fewer long chains of approximately DP 28–60, which was similar to the *ss3a* mutant, although the extent of reduction was more pronounced in the

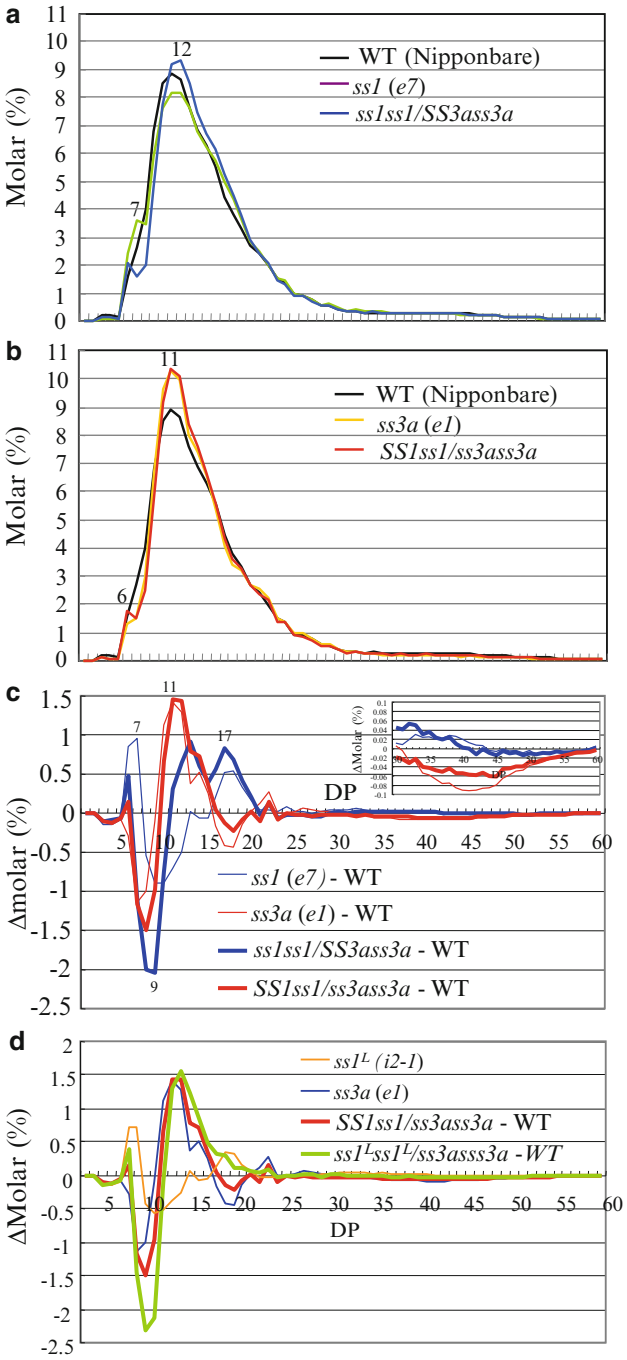
a
Molar (%)
WT (Nipponbare)
ss1 (e7)
ss1ss1/SS3ass3a
b
Molar (%)
WT (Nipponbare)
ss3a (e1)
SS1ss1/ss3ass3a
c
Δmolar (%)
DP
ss1 (e7) - WT
ss3a (e1) - WT
ss1ss1/SS3ass3a - WT
SS1ss1/ss3ass3a - WT
d
ΔMolar (%)
DP
ss1L (i2-1)
ss3a (e1)
SS1ss1/ss3ass3a - WT
ss1Lss1L/ss3asss3a -WT

ss3a mutant (Fig. 10.5c, inset). However, the decrease in the number of short chains with DP≤9 and the increase in that with DP 11–20 were more pronounced than in the *ss3a* mutant (Fig. 10.5c). The pattern in *ss1ss1/SS3ass3a* was quite distinctive compared to that of the *ss1* mutant, whereas the patterns in *SS1ss1/ss3ass3a* and $ss1^{L}ss1^{L}$/*ss3ass3a* were similar to that of the *ss3a* mutant (Fig. 10.5a, b). These phenotypes indicate that the additive reduction in SSIIIa activity affects the fine structure of amylopectin more significantly than that of SSI. Furthermore, the SSIIIa heterozygous mutation is sufficient to alter the fine structure of amylopectin.

SSI deficiency led to a slight increase in amylose content (Abe et al. 2014), although SSIIIa deficiency led to a 1.5-fold increase in amylose content compared to the wild-type (Fujita et al. 2007), as described in Sect. 10.4.2. The reduced SSI activity under SSIIIa deficiency led to a slightly higher amylose content than that observed in the *ss3a* mutant (Fujita et al. 2011; Hayashi et al. 2015).

10.5.2 SSI and BEI

SSI and BEI are indispensable for amylopectin biosynthesis. However, a deficiency in both isozymes did not affect the seed weight or starch accumulation in the endosperm (Abe et al. 2014). Analysis of the chain-length distribution of amylopectin in *ss1/be1* endosperm revealed that the effects of SSI and BEI on amylopectin structure were additive. These observations indicate that the activities of SSI and BEI during amylopectin biosynthesis are independent.

10.5.3 SSI and BEIIb

The complete deficiency of both SSI and BEIIb led to a significant reduction in fertility, and the seeds that were produced could not grow into plantlets

Fig. 10.5 Amylopectin structure of *ss1ss1/SS3ass3a* and *SS1ss1/ss3ass3a*. (**a**) Chain-length distribution patterns of endosperm amylopectin in the mature endosperm of *ss1ss1/SS3ass3a*, the *ss1* mutant (*e7*, *ΔSSI*), and the wild-type parent cultivar Nipponbare. (**b**) Chain-length distribution patterns of endosperm amylopectin in the mature endosperm of *SS1ss1/ss3ass3a*, the *ss3a* mutant (*e1*, *ΔSSIIIa*), and the wild-type parent cultivar Nipponbare. (**c**) Differences in the chain-length distribution patterns of amylopectin in the mature endosperm of *ss1ss1/SS3ass3a* and *SS1ss1/ss3ass3a* and their parent mutant lines. Inset in (**c**) shows a magnified view of the pattern in the range of chains with DP 30–60. (**d**) Differences in the chain-length distribution patterns of amylopectin in the mature endosperm of *ss1ss1/SS3ass3a* and $ss1^{L}ss1^{L}$/*ss3ass3a* and their parent mutant lines. The numbers on the plots are DP values (Fujita et al. 2011) (Reprinted with permission from J. Exp. Bot. 62, Fujita et al., Starch Biosynthesis in Rice Endosperm Requires the Presence of Either Starch Synthase I or IIIa., 4819–4831, Fig. 4 and Fig. 8C, © 2011, Oxford University Press)

(Abe et al. 2014). However, starch accumulation was recovered in the double mutant *ss1*^{L}*/be2b*. The starch accumulation of *ss1*^{L}*/be2b* was higher (69 % of wild-type) than that of the parent *be2b* mutant (56 % of wild-type). The significant decrease in the number of amylopectin chains with DP≤14 in *ss1*^{L}*/be2b* was caused by the deficiency in BEIIb and the additional effect of the reduction in SSI activity (Abe et al. 2014). The amylose content of *ss1*^{L}*/be2b* was the same as that of the wild-type (21.6 %), despite the fact that the amylose content of the parent *be2b* mutant was much higher (29.4 %) than that of the wild-type. The lower SSI activity under BEIIb deficiency may have enhanced amylopectin biosynthesis as a result of a correction of the imbalance between branching by BEs and elongation by SSs found in the single mutant (Abe et al. 2014).

10.5.4 SSI and ISA1

To investigate the function of SSI in the *isa1* background and the relationship between SSI and ISA1, a double mutant *isa1* and *ss1*^{L} (*ss1*^{L}*/isa1*) rice line was generated (Fujita et al. 2013). The *ss1*^{L}*/isa1* seeds were not stained by iodine and accumulate more than 90 % of the soluble α-glucans, indicating that the double mutant lines were much more strongly affected by ISA1-deficiency than by the reduction in SSI activity. The differential plot obtained by subtraction of the chain-length distribution of *isa1* from that of *ss1*^{L}*/isa1* was nearly identical to the corresponding differential plot of *ss1*^{L} vs. wild-type, indicating that the effect of SSI was simply additive for chain-length distribution of the product, regardless of ISA1 activity. This result suggests that SSI elongates the chains of *isa1* phytoglycogens via the addition of only a limited number of Glc residues (2–6 per chain) to A and B_1 chains of phytoglycogen, as well as amylopectin (Fujita et al. 2006). The molar (%) of each fraction (long and short B-chains and A-chains) of the β-limit dextrin of *ss1*^{L}*/isa1* was slightly different from that of *isa1*, suggesting the possibility that SSI activity affected internal chain-length distribution, presumably through its effect on the amount of SSI product, which in turn ultimately serves as a substrate for BEs (Fujita et al. 2013).

10.5.5 SSIIIa and BEIIb

High-amylose starch is useful for producing low-calorie food materials and biodegradable plastics. We generated a double mutant line between *ss3a* (Fujita et al. 2007) and *be2b* (Nishi et al. 2001). The apparent amylose content of *ss3a/be2b* is 46 %, which was the highest starch content measured in non-GM rice (Asai et al. 2014). The number of short chains of amylopectin in *ss3a/be2b* was significantly

reduced, and the starch exhibited B-type crystallinity due to BEIIb deficiency. Long chains with amylopectin DP≥40 were also more abundant in the double mutant than in the wild-type, while they were less abundant compared with those of the *be2b* parent mutant due to the SSIIIa deficiency. In *be2b*, the amylopectin structure was quite different from that of the wild-type, and the starch content in the endosperm was only 60 % of wild-type levels due to the significant decrease in the nonreduced end of amylopectin (Nishi et al. 2001). However, *ss3a/be2b* maintained 80 % of the seed weight of the wild-type, despite the fact that its amylose content and structure were dramatically altered. SSIIIa and BEIIb deficiency led to higher GBSSI and AGPase activities, which partly explained the high amylose content in the double mutant rice endosperm. The apparent amylose content (%) of *ss3a* and *ss3a/be2b* at 10 days after flowering (DAF) was higher than that of the wild-type and *be2b*. At 20 DAF, amylopectin biosynthesis in *be2b* and *ss3a/be2b* was not observed, whereas amylose biosynthesis in these lines was accelerated at 30 DAF (at the start of seed dehydration; Fig. 10.4). These data suggest that the high amylose content in the *ss3a/be2b* double mutant resulted from higher amylose biosynthesis at two stages, until 20 DAF and from 30 DAF to maturity (Fig. 10.4; Asai et al. 2014).

10.5.6 SSIIIa and SSIVb

Wild-type rice endosperm produces characteristic compound-type granules containing dozens of polyhedral starch granules within an amyloplast. On the contrary, some other cereal species such as maize and wheat produce simple-type granules harboring only a single spherical starch granule per amyloplast (Tateoka 1962; Matsushima et al. 2010, 2013; also see Chap. 13). The rice double mutant *ss3a/ss4b* generated spherical granules, while the parental single mutants produced starch granules similar to those of the wild-type (Fig. 10.6; Fujita 2013). The *ss3a/ss4b* amyloplasts contained compound-type starch granules during their early development, indicating that spherical granules separate from each other later in amyloplast development. Analysis of glucan chain-length distribution revealed overlapping roles for SSIIIa and SSIVb in the synthesis of glucan chains with DP≥33. Immunoelectron microscopy of wild-type developing seeds revealed that GBSSI, an enzyme related to starch (amylose) biosynthesis, was localized on starch granules, while the majority of SSIVb was localized between starch granules, which are referred to as septum-like sheets (Yun and Kawagoe 2010), implying the unconventional function of SSIIIa and SSIVb (Toyosawa et al. submitted). The amylose content of *ss3a/ss4b* was slightly higher than that of the *ss3a* parent mutant line, although the amylose content of the *ss4b* mutant parent was lower than that of the wild-type. The combination of SSIIIa and SSIVb deficiency was a typical example of highly different phenotypes between double mutants and their parent lines.

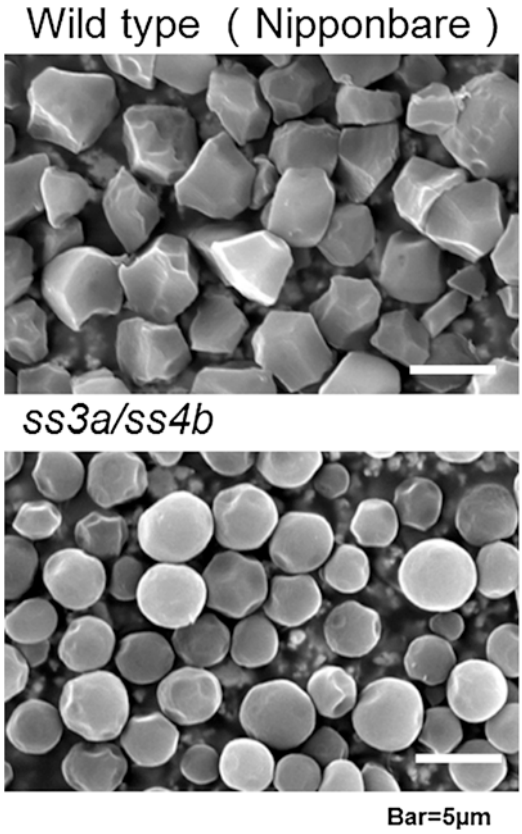

Fig. 10.6 SEM observation of spherical starch granules in the *ss3a/ss4b* double mutant line (Fujita 2013) (Reprinted with permission from Kagaku to seibutsu. 51 (6), Fujita, Denpunhenitaimai no kaiseki to riyou, 400–407, Fig. 3, © 2013, Japan Society for Bioscience, Biotechnology, and Agrochemistry)

10.5.7 ISA1 and PUL

As described in Sect. 10.2.6, ISA1 deficiency had one of the greatest impacts on amylopectin structure. To elucidate the individual contributions of the debranching enzymes ISA1 and PUL, which were mainly expressed in rice endosperm, we generated double mutant of *isa1* and *pul*. There are several allelic *isa1* mutant lines containing different amounts of starch and phytoglycogen, although most ISA1 activity has been eliminated in these lines, which are mainly divided into two types: the severe type, containing nearly 100 % phytoglycogen, and the mild type, containing a starch-filled region in the outer layer of the endosperm. The size of the starch-filled region in the cross section of a seed stained with iodine (starch-filled region) was closely correlated with the level of PUL activity (Nakamura et al. 1997). We previously speculated that when ISA1 is deficient, PUL complementation would prevent the accumulation of phytoglycogen in the endosperm (Kubo et al. 1999). To test this idea, we generated double mutant lines between mild-type *isa1* and a null *pul* mutant (Fujita et al. 2009). If the hypothesis is correct, the phenotype

of the mild-type *isa1* mutant would transform into that of the severe-type *isa1*, which contains phytoglycogen throughout its endosperm cells. The double mutant did not exhibit such a phenotype, although the phytoglycogen content slightly increased in the double mutant lines (Fujita et al. 2009). These results suggest that the compensation of PUL was limited under ISA1 deficiency, and the contribution of PUL to amylopectin trimming was much smaller than that of ISA1 (Fujita et al. 2009).

10.6 Combination of Deficiencies and Overexpression of Isozymes

Analyses of mutant lines have provided information about the function of each isozyme. Transgenic rice lines in which a specific gene is introduced into the wild-type or mutant rice lines are also useful for in vivo studies. It is possible to upregulate or downregulate specific genes in transgenic rice, whereas downregulation occurs in mutants in most cases. In theory, it is possible to introduce any gene from any organism into a host plant, and efficient promoters can be chosen for tissue- or development-specific expression analysis. If a specific gene is introduced into a mutant line, we can elucidate the effects of novel combinations of overexpression and deficiency on the properties of starch.

10.6.1 SSIIa^{I} and ISA1

Our mutant lines are in the japonica rice background; therefore, SSIIa is inactive in these lines. We introduced active SSIIa derived from indica cultivars into the *isa1* mutant (*SSIIa^{I}/isa1*; Fujita et al. 2012), a mutant in the japonica background that accumulates phytoglycogen instead of starch (Nakamura et al. 1996). The host *isa1* mutant endosperm contained only 3.1 % insoluble α-glucan, whereas the endosperm of the high-expressing SSIIa lines (#20) contained more than 60 % insoluble α-glucan. The chains of α-glucan in lines #20 were elongated by DP 3–6 compared to the host phytoglycogen chains (Fig. 10.7). Long chains with approximately DP≥40 were absent in both the *SSIIa^{I}/isa1* lines and the host mutant. In the *SSIIa^{I}/isa1* lines, the inner structure of α-glucans that had their external chains removed by β-amylase is almost the same as that of phytoglycogen. These results suggest that active SSIIa only elongated external chains, not all chains, and elongated α-glucan resulted in insolubility (Fujita et al. 2012). This function of SSIIa is quite different from that of SSI, whose activity affects internal chain-length distribution, as described in Sect. 10.5.4. The crystallinity of insoluble α-glucan in the *SSIIa^{I}/isa1* line (#20) was of the weak B-type, although phytoglycogen showed no crystallinity (Fujita et al. 2012).

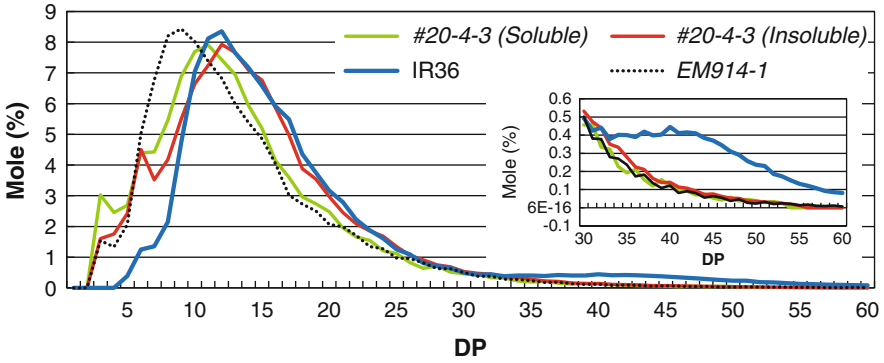

Fig. 10.7 Chain-length distribution patterns of soluble (#20 Soluble) and insoluble (#20 Insoluble) α-glucans in transgenic rice line #20, *isa1* (*EM914*), and the wild-type (IR36). The inset shows a magnified view of the pattern for chains in the range of DP 30–60. The numbers on the plots represent DP values (Fujita et al. 2012) (Reprinted with permission from J. Exp. Bot. 63, Fujita et al., Elongated phytoglycogen chain-length in transgenic rice endosperm expressing active starch synthase IIa affects the altered solubility and crystallinity of the storage α-glucan., 5859–5872, Fig. 4C, © 2012, Oxford University Press)

10.6.2 GBSSI^{I} and SSIIIa

GBSSI expression was significantly lower in japonica cultivars than in indica cultivars, which resulted in the different amylose contents in japonica (ca. 20 %) vs. indica cultivars (ca. 25–30 %; Nakamura et al. 2002; Horibata et al. 2004; Inouchi et al. 2005). To examine the effects of SSIIIa deficiency and strong expression of GBSSI on amylose content and starch structure, a transgenic rice line (WAB; Hanashiro et al. 2008) harboring *GBSSI* derived from indica cultivars (*GBSSI*^{I}) in a *waxy* (*gbss1*) mutant background was crossed with the *ss3a* mutant line (Crofts et al. 2012). The amylose content of WAB and *ss3a* were 25 % and 30 %, respectively, whereas that of the *GBSSI*^{I}*/ss3a* lines was significantly higher (41 %). The amount of GBSSI protein in WAB was ten times higher than that of the wild-type (japonica cultivars). However, the amount of GBSSI protein in *GBSSI*^{I}*/ss3a* did not further increase, although the level of AGPase, which produces a substrate of SS (ADPG), increased compared to that in WAB. The chain-length distribution of amylopectin in *GBSSI*^{I}*/ss3a* was similar to that of *ss3a*. These results suggest that the strong expression of *GBSSI*^{I} derived from indica cultivars in conjunction with SSIIIa deficiency synergistically increased the apparent amylose content in rice endosperm (Crofts et al. 2012). It should be noted that the transgenic line employed in this study, *GBSSI*^{I}*/ss3a*, has inactive SSIIa. We do not yet know the effects of active SSIIa derived from an indica rice line. We are trying to generate the combination *SS2a/ss3a/GBSSI*^{I} and will compare the starch properties among these lines.

10.7 The Effects of Isozyme Deficiencies on Sterility and Starch Accumulation

As described in Sects. 10.2, 10.3, 10.4, 10.5, and 10.6, the respective mutant lines of starch biosynthetic isozymes exhibited unique starches in their endosperm. These mutant starches should be useful for food and industrial applications. On the other hand, some multiple mutant lines exhibited poor agricultural traits, such as low yields, reduced sterility, and so on. The relationships between isozyme deficiency and sterility/starch accumulation in the endosperm of japonica rice mutant lines are summarized below.

10.7.1 The Effects of SSI Deficiency and the Combination of SSI and Other Isozymes

Deficiency of only SSI in the japonica rice background did not affect sterility or starch accumulation (Fujita et al. 2006). Therefore, other SS isozymes must have complemented the function of SSI deficiency in rice endosperm. However, the combination of the deficiency of SSI and other isozymes had a large impact on sterility and starch accumulation. The complete deficiency of both SSI and SSIIIa resulted in sterility (Fujita et al. 2011). By contrast, sterility was dramatically recovered in the presence of residual SSI or SSIIIa activity (Fujita et al. 2011). The complete deficiency of both SSI and BEIIb also led to strong sterility, whereas the combination of *ss1*^{L} and *be2b* also recovered sterility (Abe et al. 2014). The combination of the deficiency of SSI and GBSSI led to a severe reduction in fertility and starch accumulation in the endosperm (Fig. 10.8; Fujita et al. in preparation). The alleles *ss1*^{L} and *gbss1* also recovered starch accumulation (Fig. 10.8; Fujita et al. in preparation). As described above, the residual SSI activity of the *ss1* leaky mutant served as a useful tool for avoiding sterility and reduced starch accumulation. By contrast, the combination of SSI and BEI deficiency did not affect the fertility or starch accumulation in the endosperm (Abe et al. 2014).

10.7.2 The Effects of SSIIIa Deficiency and the Combination of SSIIIa and Other Isozymes

Deficiency of only SSIIIa in the japonica rice background did not affect fertility or seed weight (starch accumulation slightly reduced) (Fujita et al. 2007). The combination of BEI, BEIIa (Fujita et al. in preparation), BEIIb (Asai et al. 2014), SSIVb (Toyosawa et al. submitted), or GBSSI (Fujita et al. in preparation) and SSIIIa deficiency resulted in fertile plants with reduced starch levels, although the

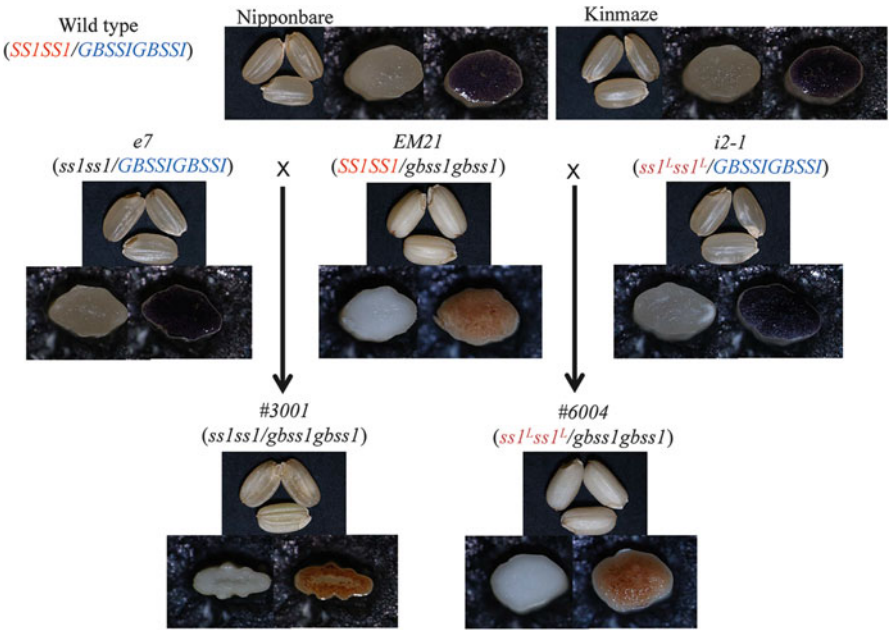

Fig. 10.8 Seed morphology, cross section, and iodine staining of single and double mutant lines

combination of SSI and SSIIIa led to sterility, as described in Sect. 10.5.1. These results indicate that SSIIIa deficiency could be sufficiently complemented by other SS isozymes.

10.7.3 The Effects of BEIIb Deficiency and the Combination of BEIIb and Other Isozymes

Deficiency of only BEIIb (which is strongly expressed in the endosperm) in the japonica background rice significantly affected starch accumulation (Nishi et al. 2001; Abe et al. 2014), indicating that it is difficult for other BEs to compensate for BEIIb deficiency. On the other hand, the seed weights and starch levels of *ss1^L/be2b* (Abe et al. 2014) and *ss3a/be2b* (Asai et al. 2014) were higher than those of the *be2b* parent mutant for a different reason. In *be2b*, the significantly smaller number of nonreduced ends of amylopectin molecules led to a decrease in starch accumulation due to an imbalance between branching by BEs and elongation by SSs. Excess chain elongation may have lead to steric inhibition within the amylopectin cluster structure. In double mutant lines between *be2b* and *ss1^L*, this excessive chain elongation and imbalance may have been encountered due to reduced SSI activity, leading to increased amylopectin accumulation compared

to that in the single mutant. As a result, the same level of amylose was present in *ss1*^{L}*/be2b* and the wild-type (Abe et al. 2014). The larger grain weight of *ss3a/be2b* vs. *be2b* likely resulted from amylose biosynthesis in the endosperm, which occurred until 20 DAF and from 30 DAF to maturity, because higher amylopectin biosynthesis was not observed in *ss3a/be2b*. These two stages of amylose biosynthesis resulted in the extraordinarily high amylose content observed in *ss3a/be2b* (Asai et al. 2014).

10.7.4 The Effects of ISA1 Deficiency and the Combination of ISA1 and Other Isozymes

Many allelic *isa1* mutant lines exhibited widespread variations in phenotype, from severe phenotypes (in which the entire endosperm consisted of 100 % phytoglycogen) to mild phenotypes (in which a small amount of phytoglycogen was present in the central part of the endosperm and starch is present in its periphery) (Nakamura et al. 1997; Wong et al. 2003). These phenotypes are thought to depend on the location of the mutation site in the *ISA1* gene. Many *isa1* mutant lines appeared to be less vigorous and had lower yields than the wild-type, although there were no specific data related to their sterility. The accumulation of phytoglycogen led to the shrunken seed phenotype after seed dehydration and resulted in a severe reduction in seed weight. The phenotypes of *isa1* were maintained in multiple mutants between the other mutant lines (*isa1/pul*, *ss1/isa1*, and so on) (Fujita et al. 2009, 2013).

10.8 The Effects of Isozyme Deficiencies on Seed Morphology and Starch Granule Morphology and Crystallinity, as Revealed by X-Ray Diffraction

Seeds of wild-type rice are translucent due to the presence of densely packed starch granules in the amyloplasts and tightly packed amyloplasts in the endosperm cells. On the other hand, deficiencies of isozymes related to starch biosynthesis sometimes affect starch granule morphology. However, the direct factors that determine seed morphology have not been elucidated. Environmental conditions, such as temperature, during seed development also affected seed morphology (Nagato and Ebara 1965; Tashiro and Wardlaw 1991). The value of rice depended on the appearance of its seeds in Japan (Yamakawa et al. 2007). The milky appearance of rice seeds that occurred at high temperatures was thought to be caused by strong expression of α-amylase (Asatsuma et al. 2006; Hakata et al. 2012).

The shape and size of starch granules were quite different among plant species; however, the factors affecting the morphology of starch granules have not been elucidated.

Rice starches usually exhibit the A-type allomorph in the X-ray diffraction pattern. By contrast, the deficiency of a specific isozyme related to starch biosynthesis could cause a change from A-type to B-type or a reduction in crystallinity. The effects of isozyme deficiencies on seed morphology, starch granule morphology, and starch granule crystallinity (measured by X-ray diffraction peaks) are summarized below.

10.8.1 Isozyme Deficiencies That Affect Seed Morphology in Rice Endosperm

The seeds of both BEIIb- (Nishi et al. 2001; Abe et al. 2014) and GBSSI-deficient mutant lines exhibited opaque morphology. However, the reasons for the opaque appearance of both mutants were quite different. The seeds of double mutant lines *ss3a/be2b* (Asai et al. 2014) and *ss1*^{L}*/be2b* (Abe et al. 2014) also exhibited an opaque phenotype, as did the seeds of the double mutant with *gbss1* as the parent (Fig. 10.8, unpublished data). Seeds that were SSIIIa-deficient exhibited a white core phenotype (Fujita et al. 2007). Most *ss3a/be1* seeds also had a white core, whereas translucent seeds were also observed (Fujita et al. unpublished data). The seed morphology of the single mutant of *ss1* or *be1* was similar to that of the wild-type. On the other hand, the morphology of *ss1/be1* seeds was a mixture of white core and translucent, and the proportion of white core seeds differed depending on the year of harvest (Abe et al. 2014). These results imply that seed morphology is affected by environmental conditions, or perhaps unknown genes that regulate the white core phenotype have continued to be segregated in the double mutant line (Abe et al. 2014). A reduction in SSI activity under SSIIIa deficiency led to opaque seed morphology (Fujita et al. 2011). The opaque or white core seed morphologies described above (except for *gbss1*) were caused by the presence of loosely packed starch granules in the amyloplast, as well as endosperm cells that developed under low levels of starch biosynthesis, although most of the details are still unknown. The starch granules and amyloplasts in *gbss1* were tightly packed in the endosperm cells, as revealed by scanning electron microscopy (SEM) observations (data not shown). Immediately after harvest, *gbss1* seeds (i.e., seeds containing high levels of water) exhibited a translucent phenotype, while after dehydration, the seeds appeared opaque. On the other hand, in the other lines, mutant seeds with an opaque morphology already appeared opaque immediately after harvest. Mature *isa1* seeds exhibited a shrunken morphology due to the accumulation of soluble phytoglycogen and double mutant lines with *isa1* as the parent was also shrunken (Fujita et al. 2009, 2013). By contrast, seeds of the anti-ISA1 transgenic rice line had 6 % ISA activity of the wild-type, which was similar to that of the wild-type (Fujita et al. 2003). The seeds of PUL-deficient mutant lines were also translucent (Fujita et al. 2009).

10.8.2 Isozyme Deficiencies That Affect the Morphology of Starch Granules in Rice Endosperm

Rice starch is of the compound-type; several polygonal sharp-edged starch granules are produced in the amyloplast (Matsushima et al. 2010; also see Chap. 13). SSIIIa deficiency sometimes lead to the production of round-shaped amyloplasts in the endosperm (Fujita et al. 2007). Most starch granules were round when SSI activity was reduced under SSIIIa deficiency (Fujita et al. 2011; Hayashi et al. 2015). The deficiency of both SSIIIa and SSIVb led to the production of completely spherical starch granules in the endosperm (Fig. 10.6; Fujita 2013; Toyosawa et al. submitted). The function of SSIVb in rice endosperm overlapped with that of SSIIIa, i.e., elongation of long chains connecting amylopectin clusters (Toyosawa et al. submitted). The reason for the production of spherical starch granules in *ss3a/ss4b* was not clear. However, detailed microscopic observations and analyses of the starch structure of the double mutant lines suggested the following. One explanation for the production of spherical starch granules is the reduction in the growth of starch granules in the endosperm at the early stage of development. The deficiency in SSIIIa and SSIVb leads to a significant decrease in the number of long chains connecting amylopectin clusters and a reduction in the molecular weight of amylopectin, which results in slower starch accumulation. Polygonal sharp-edged starch granules are present in the wild-type, whose starch biosynthesis is vigorous until they push against neighboring starch granules and amyloplasts. Starch granules tend to be round when the capacity for starch biosynthesis is reduced due to a deficiency in starch biosynthetic isozymes. For example, the starch granules in shriveled seeds of plastidial Pho (Pho1) deficient mutant lines, in which starch biosynthesis is significantly repressed, are partially spherical, whereas polygonal starch granules accumulate in plump seeds of Pho1-deficient mutant lines (Satoh et al. 2008). The second explanation is that the amyloplast membranes are incomplete. The amyloplast envelopes consist of the outer envelope membrane (OEM) and the inner envelope membrane (IEM) which are separated by the intermembrane space (IMS). Confocal microscopic analyses of IEM protein, rice *Brittle 1*, revealed that a septum-like structure (SLS) divides granules in the amyloplast (Yun and Kawagoe 2010). In compound starch granules, the envelopes are thought to function together as a mold that casts growing granules into their characteristic polyhedral sharp-edged starch granules. SSIIIa and SSIVb are thought to be related to the tethering of SLS, IEM, and OEM. Data demonstrating that SSIVb is localized between starch granules and is matched to the SLS support this idea (Toyosawa et al. submitted).

The starch granules in rice deficient in BEIIb and their double mutant lines (*ss1*^{L}*/be2b* and *ss3a/be2b*) comprised mixtures of large and small granules (Abe et al. 2014). Observation of thin sections of these endosperms revealed that large granules comprised aggregates of simple starch granules, although the reason why

these aggregates occurred in response to BEIIb deficiency is currently unclear (Asai et al. 2014). The reduction in ISA1 also had a large impact on starch granule morphology. Soluble phytoglycogen did not produce a granular structure (Wong et al. 2003). By contrast, starch granules of a transgenic rice line whose ISA activity was reduced to 6 % of wild-type levels were smaller than those of the wild-type (Fujita et al. 2003).

10.8.3 Isozyme Deficiencies That Affect the Crystallinity of Starch Granules, as Revealed by X-Ray Diffraction

The crystallinity of starch is thought to depend on its average chain length (Hizukuri 1995). The branch points of B-type starches were only located in amorphous lamella, while those of A-type starches were located in crystalline as well as amorphous lamella (Jane et al. 1997). Rice starch is A-type. On the other hand, the starch of the BEIIb-deficient mutant was B-type (Tanaka et al. 2004), as is potato starch. The branch points in crystalline lamellae produced by BEIIb were absent in the *be2b* mutant lines, resulting in an increase in the average chain length of amylopectin. The endosperm starches in the double mutant lines *ss3a/be2b* (Takahashi et al. in preparation) and *ss1*^{L}*/be2b* (Abe et al. 2013), whose parent was *be2b*, also exhibited B-type crystallinity. The endosperm starches of transgenic rice lines harboring different levels of BEIIb activity (containing *OsBEIIb* genomic DNA in the *be2b* mutant background) showed either A-type or B-type depending on the level of BEIIb activity (Tanaka et al. 2004). Specifically, a transgenic line with partially complemented BEIIb expression (by *OsBEIIb*) exhibited C-type crystallinity (a mixture of A- and B-types), whereas a line with fully complemented BEIIb expression exhibited A-type crystallinity. Interestingly, a line overexpressing BEIIb exhibited no crystallinity due to excess branching of amylopectin molecules via BEIIb (Tanaka et al. 2004). These results suggest that the expression level of BEIIb affects the type and extent of crystallinity of starches. A reduction in ISA1 activity led to a significant reduction in crystallinity (Fujita et al. 2003; Wong et al. 2003). Soluble α-glucans, phytoglycogen, did not exhibit crystallinity.

A reduction in SSI led to a slight decrease in the crystallinity of endosperm starch (Abe et al. 2013), whereas SSIIIa deficiency resulted in a significant decrease in crystallinity due to mainly an increase in the amylose content of endosperm starch (Fujita et al. 2007; Takahashi et al. in preparation). BEI deficiency led to a reduction in crystallinity (86 % of the wild-type), while a deficiency in both BEI and SSI led to a more pronounced reduction in crystallinity (78 % of the wild-type) (Abe et al. 2013).

10.9 Relationship Between Chain-Length Distribution of Amylopectin and Gelatinization Temperature of Starch Granules

As described in Sect. 10.1.3, if the relationships among genes (isozymes), starch structure, and physicochemical properties of starches are revealed, it will be possible to regulate starch traits and to design desirable starches for practical applications (Fig. 10.1). Among these, the relationships between the chain-length distribution of amylopectin and the gelatinization temperature are relatively well understood. Hizukuri (1986) suggested that increasing the number of amylopectin chains with DP≥12–16 would lead to an increase in gelatinization temperature, whereas an increase in the number of amylopectin chains with DP<12 would lead to a decrease in the gelatinization temperature. Based on this theory, we will discuss the relationship between the chain-length distribution and the gelatinization temperature of rice mutant starches (Fig. 10.9). Chains with DP≤24 account for 95 % of amylopectin chains within a single cluster (Bertoft 1991); these chains are thought to mainly affect the gelatinized temperature. Since DP 13 is often the point of inflection observed in the differential patterns between several mutant lines and the wild-type, we propose that the boundary at which chain length upregulates or downregulates the gelatinization temperature is DP 13 (Fig. 10.9). Figure 10.9 shows differential plots of chain-length distribution of amylopectin between mutant lines and the wild-type. An increase in the number of chains with DP<13 and a decrease in those with DP≥13 compared to the wild-type lead to lower gelatinization temperatures compared to the wild-type (blue zones in Fig. 10.9), whereas an increase in the number of chains with DP≥13 and a decrease in those with DP<13 compared to the wild-type lead to higher gelatinization temperatures (red zones in Fig. 10.9). For example, the number of chains with DP<13 and DP≥13 in *be2b* is lower and higher than that of the wild-type, respectively, and both areas are in the red zone, indicating that the gelatinization temperature of *be2b* appears to be significantly higher than that of the wild-type. The gelatinization temperature of *be2b* was apparently 12 °C higher than that of the wild-type (Fig. 10.9). On the other hand, there were fewer chains with DP 6–9 and DP 16–20 and more chains with DP 10–15 and DP 20–24 in *ss3a* compared to the wild-type. These differential plots are detected in both the red and blue zones, with the blue zones slightly dominant, indicating that the gelatinization temperature is slightly lower in *ss3a* than in the wild-type (Fig. 10.9). These results suggest that the chain-length distribution can be used to predict the gelatinization temperature in many cases; however, this rule does not apply in some cases. For example, there were more short chains with DP<9 in *ss1/be1* than in *ss1*, implying that the gelatinization temperature of *ss1/be1* should be lower than that of *ss1*; however, the actual gelatinization temperature was higher in *ss1/be1* than in *ss1* (Abe et al. 2013, 2014). These results suggest that factors other than the chain-length distribution of amylopectin with DP≤24 affect the gelatinization temperature. The degree to which double helices, including

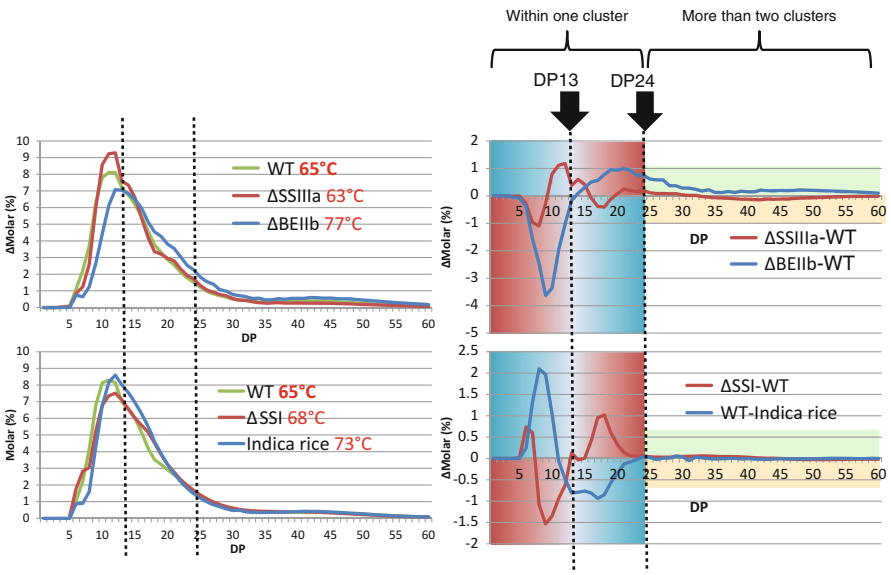

Fig. 10.9 Relationship between chain-length distribution and gelatinization temperature. *Red* values indicate peak gelatinization temperatures of the rice lines

long chains with DP>24, affect the gelatinization temperature remains unknown. Gelatinization is initiated by the absorption of water. Thereafter, the double helices of amylopectin chains must be unwound. The possibility that these steps, including absorption and swelling, affect gelatinization temperature cannot be excluded.

10.10 Possible Practical Applications of Rice Starch Mutant Lines

10.10.1 Low-Calorie Rice

It is generally thought that starch is completely digested to glucose by hydrolase, and glucose is absorbed in the small intestine. However, some starch goes through the small intestine and remains in its high molecular weight form in the large intestine. This starch is referred to as resistant starch. Resistant starch was present in starch that contained an abundance of long chains of amylopectin (Kubo et al. 2010a), as well as high amylose (Jane et al. 2003). Maize *ae* mutants, which contained high levels of amylose starch, have already been used to supply resistant starch materials for food (Jiang et al. 2010). BARLEYmax (*ss2a/ss3a*, Li et al. 2011), developed by CSIRO in Australia, is used in breakfast cereals, porridge, cereal bars, flat bread,

and so on. Some of our mutant rice lines that contain highly resistant starch (Tsuiki et al. in preparation) will be used as low-calorie food materials.

10.10.2 Possible Industrial Uses

Most starches used for industrial purposes (such as paper production) are maize starches due to their low cost. However, it is unknown whether these maize starches are the most suitable starches for these purposes. Rice mutant lines exhibiting unique properties might have the capacity to be used for industrial purposes. For example, high amylose starch from the double mutant rice line *ss3a/be2b* was very easily retrograded and reaches very high levels of hardness after retrogradation (Takahashi et al. in preparation); this material could be used to produce biodegradable plastics.

10.10.3 Improvement of Agricultural Traits by Backcrossing with Elite Cultivars

As described above, mutant rice lines, including double and triple mutant lines, could possibly be used for food and industrial purposes in the future. On the other hand, the low yields and sterility of these lines due to the deficiency of important genes are a concern. It is necessary to improve the agricultural traits of these lines in order to propagate them in the future. We are currently trying to improve the agricultural traits of these mutant lines by crossing them with elite cultivars. For example, the BC_2F_3 (F_3 seeds after 2 times back crossing) seeds produced by crossing our mutant lines (*ss3a* and *ss3a/ss4b*) with Akita63, a high-yielding cultivar grown in our area, were significantly larger than those of the original mutant lines (Fig. 10.10). The starch traits and agricultural traits of novel cultivars with unique starch properties should be examined for their potential applications.

10.11 Conclusion

Some izozymes of starch biosynthetic enzymes affect significantly the starch structure and composition in rice endosperm. The unidentified functions of some rice starch biosynthetic enzymes were accessed by analyzing their double mutants because their functions were masked in single mutants by the activities of isozymes. Biochemical and genetic analyses of multiple mutant lines revealed the following:

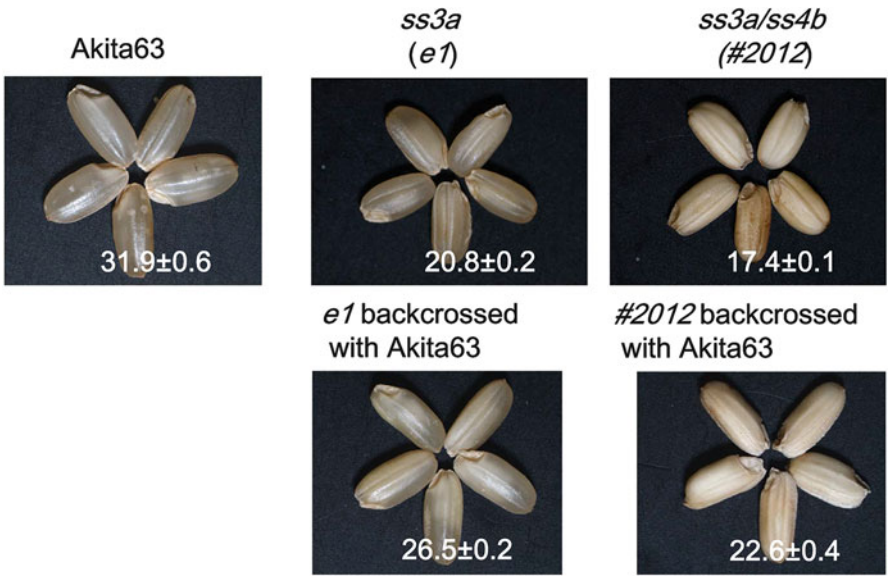

Fig. 10.10 Seed morphology and seed weight (mg) of BC_2F_3 mutant seeds of lines produced by backcrossing with the high-yielding rice cultivar Akita 63. Numbers in the pictures mean the average weights of the kernels (mg per kernel)

1. It was possible to clarify the interrelationship between isozymes of the same class of starch biosynthetic enzyme and determine whether their functions were redundant or independent.
2. The phenotypes of some double mutant lines in the endosperm such as *ss3a/ss4*, which accumulated spherical starch granules, and *ss3a/be2b,* which had an extra-high amylose content, were much more prominent than those of the combined phenotypes of the single mutants.
3. On the other hand, a combination of the deficiencies of indispensable isozymes such as SSI/SSIIIa and SSI/BEIIb led to severe sterility. The use of a leaky mutant as either of the parent lines has been useful for rescuing many mutants from sterility.
4. Some of the multiple mutant lines showing unique starch properties could be used for industrial purposes in the future.
5. The pleiotropic effects of deficiencies in some isozymes resulted in changes in amylose content and amylopectin structure, implying that trans-regulation of expression exists between genes on different chromosomes.

For practical applications of the mutant rice lines, we focused on non-GM mutant lines. Agricultural traits, such as yield, seed weight, resistance to disease, and the timing of flowering, are important for the use of these lines in agricultural applications. The crosses between our mutant lines and elite cultivars improved the agricultural traits of our mutant lines. The genetic background of our mutant

lines was japonica, whose *SSIIa* and *GBSSI* genes are mutated. This is extremely advantageous because many of the mutant lines exhibited distinct phenotypes that were not readily replaced by other plant species. However, we still need to address, in the near future, the effects of the deficiencies of isozymes on the genetic background of indica rice cultivars.

Acknowledgments This work was supported by Science and Technology Research Promotion Program for Agriculture, Forestry, Fisheries, and Food Industry and Akita Prefectural University.

References

Abe N, Nakamura Y, Fujita N (2013) Thermal properties, morphology of starch granules, and crystallinity of endosperm starch in SSI and BE isozyme double mutant lines. J Appl Glycosci 60:171–176

Abe N, Asai H, Yago H et al (2014) Relationships between starch synthase I and branching enzyme isozymes determined using double mutant rice lines. BMC Plant Biol 14(80):1–12

Asai H, Abe N, Matsushima R et al (2014) Deficiencies in both starch synthase (SS) IIIa and branching enzyme IIb lead to a significant increase in amylose in SSIIa inactive japonica rice seeds. J Exp Bot 65:5497–5507

Asatsuma S, Sawada C, Kitajima A et al (2006) α-Amylase affects starch accumulation in rice grains. J Appl Glycosci 53:187–192

Baba T, Nishihara M, Mizuno K et al (1993) Identification, cDNA cloning, and gene expression of soluble starch synthase in rice (*Oryza sativa* L.) immature seeds. Plant Physiol 103:565–573

Banks W, Greenwood CT, Muir DD (1974) Studies on starches of high amylose content: part 17. A review of current concepts. Starch 26:289–300

Bertoft E (1991) Investigation of the fine structure of alpha-dextrins derived from amylopectin and their relation to the structure of *waxy*-maize starch. Carbohydr Res 212:229–244

Blauth SL, Yao Y, Klucinec JD et al (2001) Identification of Mutator insertional mutants of starch-branching enzyme 2a in corn. Plant Physiol 125:1396–1405

Cao H, James MG, Myers AM (2000) Purification and characterization of soluble starch synthases from maize endosperm. Arch Biochem Biophys 373:135–146

Clarke BR, Denyer K, Jenner CF, Smih AM (1999) The relationship between the rate of starch synthesis, the adenosine 5′-diphosphoglucose concentration and the amylose content of starch in developing pea embryos. Planta 209:324–329

Crofts N, Abe K, Aihara S et al (2012) Lack of starch synthase IIIa and high expression of granule-bound starch synthase I synergistically increase the apparent amylose content in rice endosperm. Plant Sci 193–194:62–69

Dauvillée D, Colleoni C, Mouille G et al (2001) Biochemical characterization of wild-type and mutant isoamylases of *Chlamydomonas reinhardtii* supports a function of the multimeric enzyme organization in amylopectin maturation. Plant Physiol 125:1723–1731

Delatte T, Trevisan M, Parker ML, Zeeman SC (2005) Arabidopsis mutants Atisa1 and Atisa2 have identical phenotypes and lack the same multimeric isoamylase, which influences the branch point distribution of amylopectin during starch synthesis. Plant J 41:815–830

Fujita N (2013) Denpunhenitaimai no kaiseki to riyou. Kagaku to Seibutsu. J Soc Biosci Biotechnol Agrochem 51:400–407

Fujita N, Hasegawa H, Taira T (2001) The isolation and characterization of waxy mutant of diploid wheat (*Triticum monococcum* L.). Plant Sci 160:595–602

Fujita N, Kubo A, Suh D-S et al (2003) Antisense inhibition of isoamylase alters the structure of amylopectin and the physicochemical properties of starch in rice endosperm. Plant Cell Physiol 44:607–618

Fujita N, Yoshida M, Asakura N et al (2006) Function and characterization of starch synthase I using mutants in rice. Plant Physiol 140:1070–1084

Fujita N, Yoshida M, Kondo T et al (2007) Characterization of SSIIIa-deficient mutants of rice (*Oryza sativa* L.): the function of SSIIIa and pleiotropic effects by SSIIIa deficiency in the rice endosperm. Plant Physiol 144:2009–2023

Fujita N, Goto S, Yoshida M et al (2008) The function of rice starch synthase I expressed in *E. coli*. J Appl Glycosci 55:167–172

Fujita N, Toyosawa Y, Utsumi Y et al (2009) Characterization of PUL-deficient mutants of rice (*Oryza sativa* L.) and the function of PUL on the starch biosynthesis in the rice endosperm. J Exp Bot 60:1009–1023

Fujita N, Satoh R, Hayashi A et al (2011) Starch biosynthesis in rice endosperm requires the presence of either starch synthase I or IIIa. J Exp Bot 62:4819–4831

Fujita N, Hanashiro I, Suzuki S et al (2012) Elongated phytoglycogen chain-length in transgenic rice endosperm expressing active starch synthase IIa affects the altered solubility and crystallinity of the storage α-glucan. J Exp Bot 63:5859–5872

Fujita N, Hanashiro I, Toyosawa Y, Nakamura Y (2013) Functional study of rice starch synthase I (SSI) by using double mutant with lowered activities of SSI and isoamylase1. J Appl Glycosci 60:45–51

Hakata M, Kuroda M, Miyashita T et al (2012) Suppression of α-amylase genes improves quality of rice grain ripened under high temperature. Plant Biotechnol J 10:1110–1117

Hanashiro I, Itoh K, Kuratomi Y et al (2008) Granule-bound starch synthase I is responsible for biosynthesis of extra-long unit chains of amylopectin in rice. Plant Cell Physiol 49:925–933

Hanashiro I, Higuchi T, Aihara S et al (2011) Structure of starches from rice mutants deficient in the starch synthase isozyme SSI or SSIIIa. Biomacromolecules 12:1621–1628

Hayashi M, Kodama M, Nakamura Y et al (2015) Thermal and pasting properties, morphology of starch granules, and crystallinity of endosperm starch in the rice SSI and SSIIIa double-mutants. J Appl Glycosci (in press)

Hirano HY, Sano Y (1998) Enhancement of *Wx* gene expression and the accumulation of amylose in response to cool temperatures during seed development in rice. Plant Cell Physiol 39:807–812

Hirochika H (2001) Contribution of the *Tos17* retrotransposon to rice functional genomics. Curr Opin Plant Biol 4:118–122

Hirose T, Terao T (2004) A comprehensive expression analysis of the starch synthase gene family in rice (*Oryza sativa* L.). Planta 220:9–16

Hizukuri S (1986) Polymodal distribution of the chain-lengths of amylopectins, and its significance. Carbohydr Res 147:342–347

Hizukuri S (1995) Starch, analytical aspects. In: Eliasson A-E (ed) Carbohydrates in food. Marcel Dekker, New York, pp 347–429

Horibata T, Nakamoto M, Fuwa H, Inouchi N (2004) Structural and physicochemical characteristics of endosperm starches of rice cultivars recently bred in Japan. J Appl Glycosci 51:303–313

Hussain H, Mant A, Seale R et al (2003) Three isoforms of isoamylase contribute different catalytic properties for the debranching of potato glucans. Plant Cell 15:133–149

Inouchi N, Glover DV, Sugimoto Y, Fuwa H (1991) DSC characteristics of gelatinization of starches of single-, double-, and triple-mutants and their normal counterpart in the inbred Oh43 maize (*Zea mays* L.) background. Starch 43:468–472

Inouchi N, Hibiu H, Li T, Horibata T et al (2005) Structure and properties of endosperm starches from cultivated rice of Asia and other countries. J Appl Glycosci 52:239–246

International Rice Genome Sequencing Project (2005) The map-based sequence of the rice genome. Nature 436:793–800

Isshiki M, Morino K, Nakajima M et al (1998) A naturally occurring functional allele of the rice waxy locus has a GT to TT mutation at the 5′ splice site of the first intron. Plant J 15:133–138

James MG, Robertson DS, Myers AM (1995) Characterization of the maize gene sugary1, a determinant of starch composition in kernels. Plant Cell 7:417–429

Jane J-L, Wong K-S, McPherson AE (1997) Branch-structure difference in starches of A- and B-type X-ray patterns revealed by their Naegeli dextrins. Carbohydr Res 300:219–227

Jane JL, Ao Z, Duvick SA et al (2003) Structures of amylopectin and starch granules: how are they synthesized? J Appl Glycosci 50:167–172

Jiang H, Horner HT, Pepper TM et al (2010) Formation of elongated starch granules in high-amylose maize. Carbohydr Polym 80:534–539

Kubo A, Fujita N, Harada K et al (1999) The starch-debranching enzymes isoamylase and pullulanase are both involved in amylopectin biosynthesis in rice endosperm. Plant Physiol 121:399–409

Kubo A, Akdogan G, Nakaya M et al (2010a) Structure, physical, and digestive properties of starch from wx ae double-mutant rice. J Agric Food Chem 58:4463–4469

Kubo A, Colleoni C, Dinges JR et al (2010b) Functions of heteromeric and homomeric isoamylase-type starch-debranching enzymes in developing maize endosperm. Plant Physiol 153:956–969

Larkin PD, Park WD (1999) Transcript accumulation and utilization of alternate and non-consensus splice sites in rice granule-bound starch synthase are temperature-sensitive and controlled by a single-nucleotide polymorphism. Plant Mol Biol 40:719–727

Li Z, Li D, Du X et al (2011) The barley amo1 locus is tightly linked to the starch synthase IIIa gene and negatively regulates expression of granule-bound starch synthetic genes. J Exp Bot 62:5217–5231

Lloyd JR, Springer F, Buleon A, Muller-Rober B, Willmitzer L, Kossmann J (1999) The influence of alterations in ADP-glucose pyrophosphorylase activities on starch structure and composition in potato tubers. Planta 209:230–238

Matsushima R, Maekawa M, Fujita N, Sakamoto W (2010) A rapid, direct observation method to isolate mutants with defects in starch grain morphology in rice. Plant Cell Physiol 51:728–741

Matsushima R, Yamashita J, Kariyama S et al (2013) A phylogenetic re-evaluation of morphological variations of starch grains among Poaceae species. J Appl Glycosci 60:37–44

Mizuno K, Kawasaki T, Shimada H et al (1993) Alteration of the structural properties of starch components by the lack of an isoform of starch branching enzyme in rice seeds. J Biol Chem 268:19084–19091

Nagato K, Ebara M (1965) Effects of high temperature during ripening period on the development and the quality of rice kernels. Jpn J Crop Sci 34:59–66

Nakamura Y (1998) Some properties of starch debranching enzymes and their possible role in amylopectin biosynthesis. Plant Sci 121:1–18

Nakamura Y (2002) Towards a better understanding of the metabolic system for amylopectin biosynthesis in plants: rice endosperm as a model tissue. Plant Cell Physiol 43:718–725

Nakamura Y, Umemoto T, Takahata Y et al (1996) Changes in structure of starch and enzyme activities affected by *sugary* mutant in developing rice endosperm: possible role of starch debranching enzyme (R-enzyme) in amylopectin biosynthesis. Physiol Plant 97:491–498

Nakamura Y, Kubo A, Shimamune T et al (1997) Correlation between activities of starch debranching enzyme and α-polyglucan structure in endosperms of *sugary-1* mutants of rice. Plant J 12:143–153

Nakamura Y, Sakurai A, Inaba Y et al (2002) The fine structure of amylopectin in endosperm from Asian cultivated rice can be largely classified into two classes. Starch 54:117–131

Nakamura Y, Francisco BP Jr, Hosaka Y et al (2005) Essential amino acids of starch synthase IIa differentiate amylopectin structure and starch quality between *japonica* and *indica* rice cultivars. Plant Mol Biol 58:213–227

Nakamura Y, Utsumi Y, Sawada T et al (2010) Characterization of the reactions of starch branching enzymes from rice endosperm. Plant Cell Physiol 51:776–794

Nakamura Y, Aihara S, Crofts N et al (2014) In vitro studies of enzymatic properties of starch synthases and interacting reactions between starch synthase I and starch branching enzymes from rice. Plant Sci 224:1–8

Nishi A, Nakamura Y, Tanaka N, Satoh H (2001) Biochemical and genetic analysis of the effects of *amylose-extender* mutation in rice endosperm. Plant Physiol 127:459–472

Ohdan T, Francisco JPB, Sawada T et al (2005) Expression profiling of genes involved in starch synthesis in sink and source organs of rice. J Exp Bot 56:3229–3244

Sano Y (1984) Differential regulation of *waxy* gene expression in rice endosperm. Theor Appl Genet 68:467–473

Satoh H, Omura T (1979) Induction of mutation by treatment of fertilized egg cell with *N*-methyl-*N*-nitrosourea in rice. J Fac Agric Kyushu Univ 24:165–174

Satoh H, Nishi A, Yamashita K et al (2003) Starch-branching enzyme I-deficient mutation specifically affects the structure and properties of starch in rice endosperm. Plant Physiol 133:1111–1121

Satoh H, Shibahara K, Tokunaga T et al (2008) Plastidic α-glucan phosphorylase mutation dramatically affects the synthesis and structure of starch in rice endosperm. Plant Cell 20:1833–1849

Shannon JC, Garwood DL (1984) Genetics and physiology of starch development. In: Whistler RL, BeMiller JN, Paschal EF (eds) Starch, 2nd edn. Academic, New York, pp 25–86

Singh N, Inouchi N, Nishinari K (2006) Structural, thermal and viscoelastic characteristics of starches separated from normal, sugary and waxy maize. Food Hydrocoll 20:923–935

Takeda Y, Hizukuri S, Juliano BO (1987) Structures of rice amylopectins with low and high affinities for iodine. Carbohydr Res 168:79–88

Tanaka N, Fujita N, Nishi A et al (2004) The structure of starch can be manipulated by changing the expression levels of starch branching enzyme IIb in rice endosperm. Plant Biotechnol J 2:507–516

Tashiro T, Wardlaw IF (1991) The effect of high temperature on kernel dimensions and the type and occurrence of kernel damage in rice. Aust J Agric Res 42:485–496

Tateoka T (1962) Starch grains of endosperm in grass systematics. Bot Mag Tokyo 75:377–383

Tsai CY (1974) The function of waxy locus in starch synthesis in maize endosperm. Biochem Genet 11:83–96

Umemoto T, Nakamura Y, Satoh H, Terashima K (1999) Differences in amylopectin structure between two rice varieties in relation to the effects of temperature during grain-filling. Starch 51:58–62

Umemoto T, Yano M, Satoh H et al (2002) Mapping of a gene responsible for the difference in amylopectin structure between japonica-type and indica-type rice varieties. Theor Appl Genet 104:1–8

Utsumi Y, Utsumi C, Sawada T et al (2011) Functional diversity of isoamylase oligomers: the ISA1 homo-oligomer is essential for amylopectin biosynthesis in rice endosperm. Plant Physiol 156:61–77

Wang YJ, White P, Pollak L, Jane J-L (1993a) Characterization of starch structures of 17 maize endosperm mutant genotype with Oh43 inbred line background. Cereal Chem 70:171–179

Wang YJ, White P, Pollak L, Jane J-L (1993b) Amylopectin and intermediate materials in starches from mutant genotypes of the Oh43 inbred line. Cereal Chem 70:521–525

Wang ZY, Zheng FQ, Shen GZ et al (1995) The amylose content in rice endosperm is related to the post-transcriptional regulation of the waxy gene. Plant J 7:613–622

Wattebled F, Dong Y, Dumez S et al (2005) Mutants of Arabidopsis lacking a chloroplastic isoamylase accumulate phytoglycogen and an abnormal form of amylopectin. Plant Physiol 138:184–195

Wong K-S, Kubo A, Jane J-L et al (2003) Structures and properties of amylopectin and phytoglycogen in the endosperm of *sugary-1* mutants of rice. J Cereal Sci 37:139–149

Yamakawa H, Hirose T, Kuroda M, Yamaguchi T (2007) Comprehensive expression profiling of rice grain filling-related genes under high temperature using DNA microarray. Plant Physiol 144:258–277

Yun MS, Kawagoe Y (2010) Septum formation in amyloplasts produces compound granules in the rice endosperm and is regulated by plastid division proteins. Plant Cell Physiol 51:1469–1479

Yun MS, Umemoto T, Kawagoe Y (2011) Rice debranching enzyme isoamylase3 facilitates starch metabolism and affects plastid morphogenesis. Plant Cell Physiol 52:1068–1082

Zhang H, Duan L, Dai JS et al (2014) Major QTLs reduce the deleterious effects of high temperature on rice amylose content by increasing splicing efficiency of Wx pre-mRNA. Theor Appl Genet 127:273–282

Chapter 11
Increase of Grain Yields by Manipulating Starch Biosynthesis

Bilal Cakir, Aytug Tuncel, Seon-Kap Hwang, and Thomas W. Okita

Abstract Starch is the main carbohydrate storage reserve in many plants. This carbohydrate not only serves as the major caloric source for much of the world's population and as a key feedstock for renewable energy but is also utilized in many food and industrial applications. As the demand for starch as a source of food and energy feedstock will continue to increase in the coming years, increased production of starchy cereals and tuber crops will be needed, a goal that will be moderated by the loss of arable land and unpredictable environmental conditions due to global warming. In this chapter, we provide an update on starch biosynthesis occurring in photoautotrophic and heterotrophic organs, the role of ADPglucose pyrophosphorylase and other enzymes in this process, and the various molecular strategies for increasing starch in cereals. Although extensive efforts have been made, relatively small improvements have been accomplished in enhancing starch content and grain yield, necessitating the employment of new strategies to meet this goal.

Keywords Starch • AGPase • Biotechnological approaches • Crop yields

11.1 Introduction

Starch is the second most abundant biopolymer in the world. It is the main component of the major food crops and, therefore, constitutes the bulk of the daily diet for much of the world's population. The long-term storage properties of major food crops such as tubers and cereal grains enable them to provide a steady supply of calories as well as a significant proportion of other nutrients throughout the nongrowing season. As such, 2,500 million tons of starch-containing crops (Food and Agriculture Organization of the United Nations, http://faostat.fao.org) are harvested annually worldwide and used directly as food. In addition to being the major dietary source of worldwide caloric intake, more than 700 million tons of starch produced annually from roots and tubers are used for non-dietary purposes in industrial and manufacturer applications. For instance, more than 85 billion liters

B. Cakir • A. Tuncel • S.-K. Hwang • T.W. Okita (✉)
Institute of Biological Chemistry, Washington State University, Pullman, WA 99164-6340, USA
e-mail: okita@wsu.edu

Y. Nakamura (ed.), *Starch*, DOI 10.1007/978-4-431-55495-0_11

of automobile fuel, in the form of bio-ethanol, were produced from starch in 2011, and this production continues to increase (Amarasekara 2013). Starch is also used in many manufacturer applications such as an adhesive, thickener, polymer, and an inert material in many household and commercial products.

There have been significant efforts in recent years to generate plants with higher starch content due to the rising demand as a food by the world's growing population and as a feedstock for renewable energy. Such efforts, however, will be constrained by the limited acreage of arable lands and supply of water. Therefore, a better understanding of starch metabolism is essential to improve crop yields under less than ideal agricultural conditions for dietary, bioenergy, and industrial uses. Although starch metabolism has been a subject of intensive research for many years, there are still many questions left to be resolved that will provide new insights and strategies to enhance starch levels in plants.

Starch is synthesized in both photosynthetic and non-photosynthetic cells and plays essential roles during the life cycle of the plant. In leaves, a fraction of photoassimilate is retained in the chloroplasts and stored as transitory starch, a reserve which facilitates normal plant growth and development by providing a continuous supply of carbon and energy during the night. The bulk of fixed carbon, however, is converted into sucrose and exported to heterotrophic tissues and organs to support their growth and development. In storage organs such as cereal grains and tubers, starch is used as long-term storage reserve to support the next plant life cycle. Similar to transient starch in leaves, efficient metabolism of starch in storage organs has a profound effect on plant yields by maximizing the products of CO_2 assimilation.

11.2 The Pathway of Carbon into Starch in Photosynthetic and Heterotrophic Sink Tissues

The pathways leading to starch synthesis in photosynthetic and heterotrophic sink tissues differ. In photoautotrophic leaves, starch biosynthesis is restricted to the chloroplasts, while in heterotrophic sink tissues, the events leading to starch synthesis occur in both the cytoplasm and plastid. In cereals, the majority of the reactions, including synthesis of ADPglucose (ADPglc), take place in the cytosol, whereas production of ADPglc occurs in the amyloplast in non-cereal crops.

11.2.1 Biochemical Events in Leaves

In leaves, the fixed carbon is converted to sugars and amino acids during the day and transported to non-photosynthetic organs. A portion of this carbon is stored within the chloroplasts as transient starch which is broken down at night to provide

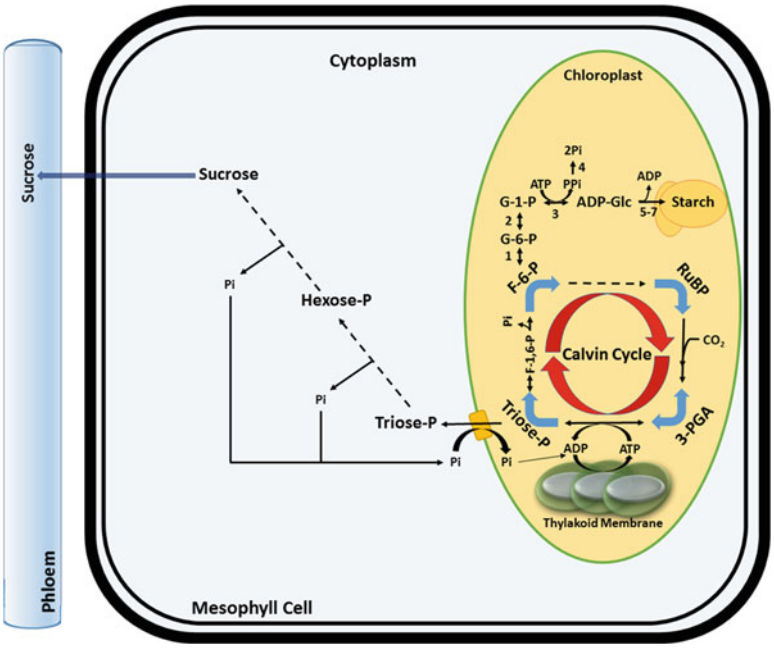

Fig. 11.1 Synthesis of starch in leaves. The fixed carbon in the form of 3-PGA is converted to triose Ps which are used for both the synthesis of starch and sucrose. Sucrose is transported to sink tissues to support plant growth. Starch synthesis is catalyzed by the following enzymes: *1* phosphoglucose isomerase, *2* phosphoglucomutase, *3* AGPase, *4* inorganic pyrophosphorylase, *5* SS, *6* SBE, *7* starch-debranching enzyme

reducing sugars for carbon precursors and energy (Fig. 11.1) (Stitt and Zeeman 2012). Although much of the carbon flux is through the Calvin-Benson-Bassham cycle, some of it is diverted into starch via the action of phosphoglucose isomerase (PGI) which converts fructose 6-phosphate (Fru6P) to glucose 6-phosphate (Glc6P). This hexose-P is then converted by phosphoglucomutase (PGM) into glucose 1-phosphate Glc1P, which together with ATP is used by ADPglucose pyrophosphorylase (AGPase) to generate ADPglc, the sugar nucleotide utilized by starch synthases. Since AGPase catalyzes the first committed step in the starch biosynthetic pathway, it is subjected to several regulatory mechanisms, which are discussed later in this chapter.

Although it is widely accepted that the flow of carbon into starch is dependent on the AGPase reaction and other plastid-localized events, an alternative cytoplasmic-based pathway has been suggested. Sucrose synthase (SuSy) also generates ADPglc by the hydrolysis of sucrose in the presence of ADP. This idea is corroborated by the presence of high amounts of ADPglc in leaves of *Arabidopsis* mutant lines which lack AGPase and PGM and the suggested existence of an ADPglc translocator on the plastid envelope that would support this alternate route to starch synthesis (Shannon et al. 1998). This alternative pathway in leaves involving cytoplasmic and plastidial

events has generated considerable debate in the literature (Baroja-Fernández et al. 2005; Ekkehard Neuhaus et al. 2005) that remains ongoing (Baroja-Fernandez et al. 2012). Suffice to say, irrespective of whether such an alternative pathway to starch synthesis exists, it only, at best, plays a minor role in starch synthesis as evident by the marked reduction in leaf starch in plants harboring a mutation in the AGPase small subunit APS1 gene (Ventriglia et al. 2008).

11.2.2 Biochemical Events in Seeds

Heterotrophic tissues such as developing seeds rely on sucrose produced in source leaves as the major resource to support growth and development. Sucrose is hydrolyzed by SuSy to generate UDPglc and fructose, two products which are eventually converted into Glc6P (Fig. 11.2). The plastid envelope has active Glc6P/Pi and ATP/ADP transporters (Jonik et al. 2012) which provide the carbon and energy for AGPase, respectively, and, in turn, starch biosynthesis.

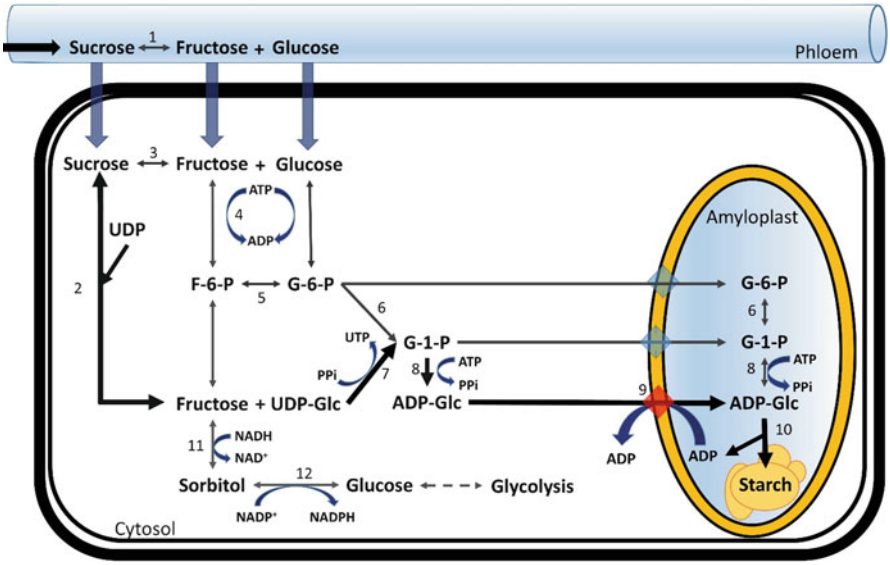

Fig. 11.2 Conversion of sucrose into starch in developing cereal endosperm (Adopted from Tuncel and Okita 2013). Formation of ADPglc and subsequent production of starch in seeds are depicted. Sucrose from leaves is converted into ADPglc in the cytoplasm and then transported into amyloplast. Major reactions of starch synthesis are shown by *bold arrows*. Enzymes shown are (*1*, *3*) invertase, (*2*) sucrose synthase, (*4*) hexokinase, (*5*) phosphoglucose isomerase, (*6*) phosphoglucomutase, (*7*) UGPase, (*8*) AGPase, (*9*) ADPglc transporter, (*10*) starch synthases, (*11*) sorbitol dehydrogenase, (*12*) aldose reductase

Cereal endosperms are unique in containing two different AGPase activities, a major cytoplasmic form and a minor plastidial form (Denyer et al. 1996; Thorbjørnsen et al. 1996; Sikka et al. 2001). Genetic studies (Tsai and Nelson 1966; Morrison et al. 1993; Lee et al. 2007) showed that mutations in the structural genes that code for the cytoplasmic enzyme result in a severe depression in starch accumulation, suggesting that the major site of ADPglc synthesis is cytoplasmic. Expression of an up-regulated bacterial AGPase gene (*glgC*-TM) in the cytoplasm but not in the amyloplast compartment resulted in an enhancement of starch synthesis and accumulation (seed weight) (Sakulsingharoj et al. 2004). Lastly, mutation in the BT1 (*Brittle-1*) sugar nucleotide transporter resulted in a severe reduction in starch levels but exceedingly high increases in ADPglc levels (Sullivan and Kaneko 1995; Shannon et al. 1998). These latter studies provide concrete evidence that the major route of carbon into starch in developing cereal endosperm requires the cytoplasmic AGPase.

Although the exact reason why cereals evolved new AGPase genes to be expressed in the cytoplasm is not exactly known, this subcellular localization provides a more efficient utilization of energy based on its status in maize endosperm (Rolletschek et al. 2005). As the maize endosperm develops, it becomes increasingly micro-aerobic where oxygen levels drop to about 1.4 % of that present in the atmosphere (Rolletschek et al. 2005), and hence, ATP is likely synthesized via glycolysis rather than by respiration. By generating ADPglc in the cytoplasm, high-energy pyrophosphate (PPi) and nucleotide triphosphate products (ATP and UTP) are conserved in this compartment. PPi consumed in the UGPase reaction is regenerated by the AGPase reaction. Conversely, ATP consumed in the AGPase reaction generates an equivalent UTP in the UGPase reaction. Hence, starch synthesis in maize and likely in other cereals recycles considerable energy, especially those contained in PPi. By contrast, in non-endosperm heterotrophic tissues where ADPglc is synthesized in the plastid, the hydrolysis of PPi by inorganic pyrophosphatase drives ADPglc synthesis and recycles Pi in vivo, at the expense of a loss of energy.

Despite extensive biochemical studies, the metabolic fate of fructose and UTP produced by SuSy and UGPase, respectively, has not been completely resolved. The generated UTP could be used by UTP-dependent fructokinase to synthesize Fru6P. However, UTP is more likely to support not only RNA synthesis but also DNA synthesis as there is extensive endoduplication of DNA that occurs during cereal endosperm development. An alternative model of fructose metabolism would be via sorbitol dehydrogenase (SDH) which converts fructose to sorbitol using NADH as a reductant (Fig. 11.2) (Oura et al. 2000), which would recycle NAD^+ to support glycolysis. In turn, sorbitol could then be converted into glucose by an aldose reductase where NADPH is also formed, which can be used for various biosynthetic reactions. The role of SDH in metabolizing fructose is supported by the inverse correlation between enzyme activity and fructose levels (Archbold 1999).

11.3 Structural and Functional Role of AGPase

Both bacteria and plants utilize the action of AGPase for synthesis of α-glucan reserves. Although carrying out the same reaction and subjected to allosteric regulation, the prokaryotic and higher plant AGPases have distinct structures. The prokaryotic enzymes are composed of four identical subunits (α4), while the higher plant enzymes contain a pair of two identical large (L) and two identical small (S) subunits ($\alpha_2\beta_2$) (Preiss 1972; Lin et al. 1988; Okita et al. 1990; Hwang and Okita 2012). Moreover, the genes that code for the higher plant enzymes are more complex and diverse than the prokaryotic genes as they code for multiple L and S subunit forms (Krishnan et al. 1986; Smith-White and Preiss 1992). For instance, *Arabidopsis* and rice have four L subunit genes (*APL1* to *APL4* in *Arabidopsis*, *OsAPL1* to *OsAPL4* in rice) and two S subunit genes (*APS1* and *APS2* in *Arabidopsis*, *OsAPS1* and *OsAPS2* in rice) (Crevillén et al. 2003, 2005; Akihiro et al. 2005; Lee et al. 2007). The *Arabidopsis* APS2 may not be a bona fide AGPase subunit as it does not display any catalytic activity by itself or when co-expressed with any of the four *Arabidopsis* L subunits (Crevillén et al. 2003). The rice AGPase S subunits display a further complexity as the *OsAPS2* gene is subject to alternative mRNA splicing that generates two S subunit isoforms, the leaf-specific OsAPS2a and the endosperm-specific OsAPS2b (Lee et al. 2007). Furthermore, the primary sequences of S subunits are highly conserved between species, whereas L subunits show a lower degree of conservation even within a species (Smith-White and Preiss 1992). Phylogenetic analysis shows that the primary sequences of the S subunits are more conserved than those of the L subunit indicating that amino acid substitutions in the S subunits are more evolutionarily constrained than the L subunits. This phenomenon was explained by the fact that S subunits have fewer gene copies, are less tissue specific, and, hence, have to interact with multiple L subunit isoforms (Georgelis et al. 2008). The L subunit may display more evolutionary flexibility as a means to fine-tune the catalytic and allosteric regulatory properties of the enzyme expressed in different tissues of the plant (Georgelis et al. 2008). The advantages of expressing tissue-specific AGPases with different regulatory and catalytic properties, however, are not readily apparent and would be a fruitful study in the future.

Earlier studies have suggested that the two subunits have different roles in enzyme function. When expressed alone in *Escherichia coli*, the recombinant potato tuber S subunit forms a catalytically active homotetramer with defective allosteric properties (Ballicora et al. 1995; Hwang et al. 2008). The L subunit, on the other hand, does not form an active enzyme without the S subunit. The capacity of the S subunit to form a fully catalytically active, albeit allosterically defective, enzyme suggests that the S subunit is the catalytic subunit and that the L subunit simply modulates the allosteric regulatory properties of the enzyme (Iglesias et al. 1993). This secondary role for the L subunit, however, was discounted by the study of mosaic enzymes composed of primary sequences from maize endosperm and potato

tuber AGPase where both subunits were found to equally contribute to the catalytic activity and allosteric regulatory properties of the enzyme (Cross et al. 2004, 2005). Likewise, detailed kinetic analysis of potato AGPase variants containing different combinations of mutant L and S subunits showed that both subunits contribute equally to the allosteric regulation as the properties are a product of synergy between the two subunit forms (Hwang et al. 2005).

The relative contribution of the L subunit in catalysis of the heterotetrameric enzyme varies considerably depending on the enzyme activity examined. The potato L subunit plays a minor role in catalysis (Ballicora et al. 2005; Hwang et al. 2007). Mutation of catalytic residue D145 of the S subunit resulted in a mutant enzyme ($L^{WT}S^{D145N}$) which displayed more than four orders of magnitude less catalytic activity than wild-type enzyme. By contrast, the comparable mutation (D160N) in the L subunit resulted in a minor reduction (∼40 %) in catalytic activity of the mutant enzyme. Moreover, kinetic studies of the L subunit homotetrameric enzyme showed that it had only 4 % of the catalytic activity of the S subunit homotetramer. Interestingly, the L subunit was not activated by 3-PGA as a homotetramer but activated 30-fold when assembled with the catalytically silenced S subunit (D145N) (Ballicora et al. 2005). This observation indicates that the catalytic activity of the L subunit requires the presence of the S subunit and again supports the contribution of both subunit types in allosteric regulation.

A role for both subunits contributing to catalysis is also evident by mutations in the L subunit that have drastic consequences on catalytic activity and apparent substrate affinities (Hwang et al. 2007). The low catalytic efficiency of the potato L subunit is likely due to mutations at and/or near the catalytic site that occurred during evolution. The potato L subunit is capable of binding ATP (Hwang et al. 2006) and Glc-1-P (Fu et al. 1998b) but is apparently unable to undergo the catalytic cycle efficiently. Ballicora et al. (2005) showed that the L subunit with two amino acid substitutions (K41R and T51K) near the catalytic site, when assembled with catalytically silenced S subunit mutant, resurrected the catalytic activity of the $L^{WT}S^{D145N}$ enzyme nearly 250-fold such that it attained ∼10 % of wild-type enzyme activity (Ballicora et al. 2005).

The low catalytic activity of the potato L subunit is not a conserved property among L subunits from other plant species. For instance, *Arabidopsis* L subunits (APL1 and APL2) exhibited significant catalytic activity when expressed with inactive S subunit (APS1) mutant, whereas heterotetramers containing mutant APS1 and APL3/APL4 were catalytically inactive. Both APL1 and APL2 have Lys residues (K271 and K267) at the corresponding positions of the potato L subunit, which at least partially account for catalytic activity (Hwang et al. 2008; Ventriglia et al. 2008). In addition, the tomato L3 subunit has been demonstrated to have catalytic activity as a monomer (Petreikov et al. 2010). Collectively, both subunits take part in catalysis and allosteric regulation of AGPase although the contribution of the L subunit to catalysis varies depending on the plant species and the isoform examined.

11.4 Allosteric Regulation of AGPase

11.4.1 Leaf Enzymes

In bacteria, cyanobacteria, and higher plants, α-glucans are synthesized during periods of excess sugars and consumed when carbon and energy become limited. Hence, the synthesis of α-glucans needs to be tightly regulated, which is accomplished mainly by controlling the synthesis of ADPglc via AGPase activity. The bacterial AGPase is allosterically activated by metabolic effector molecules that are intermediates of major metabolic pathways, glycolysis or the Entner-Doudoroff, and reflect the "high-energy state" of the cells (Ballicora et al. 2003). The glycolytic intermediate fructose-1,6-bisphosphate (FBP) is an activator of AGPase from *E. coli*, while the enzymes from *Agrobacterium tumefaciens* and *Rhodospirillum rubrum* are activated by Fru6P and pyruvate, respectively (Björn and Govindjee 2009; Ballicora et al. 2003). AGPases from cyanobacteria, green algae, and higher plants are activated by glycerate-3-phosphate (3-PGA) (Heldt et al. 1977; Preiss 1988; Preiss et al. 1989), which is the immediate product of CO_2 fixation. In addition to 3-PGA, AGPases from spinach leaves are also activated by Fru6P, FBP, phosphoenolpyruvate (PEP), and ribose 5-phosphate (Ghosh and Preiss 1966). These other metabolites, however, activate AGPases to a lesser extent, and higher concentrations are required to obtain maximum activation. For example, the most effective activator after 3-PGA is Fru6P, which enhances AGPase activity up to 40 % of the activation level observed for 3-PGA (Ghosh and Preiss 1966). Likewise, AGPase activity is suppressed by specific inhibitors including adenosine 5′-monophosphate (5′AMP) for many of the bacterial AGPases, while inorganic phosphate (Pi) is an inhibitor of the cyanobacterial and plant enzymes.

The regulation of AGPase activities and, in turn, starch synthesis in higher plants is under strict control. In leaves, AGPase is located in chloroplasts, the site of CO_2 fixation (Okita et al. 1979; Morell et al. 1988). During active photosynthesis, 3-PGA is produced and converted into triose phosphates which can reenter the Calvin cycle or be exported to the cytoplasm where it serves as the precursor for sucrose synthesis. An important by-product of the metabolic pathway leading to sucrose synthesis is Pi, which can then be recycled back into the plastid via the Pi translocator to support ATP synthesis. The 3-PGA/Pi ratio in chloroplast allows coordination of starch synthesis in this organelle and sucrose synthesis in cytoplasm according to the energetic state and needs of the cell (Stitt et al. 1987). When sucrose synthesis is not saturated, triose phosphates are exported to the cytoplasm where they are converted into sucrose enabling the by-product Pi to be imported back to the plastid where it can be recycled to generate ATP. Recycling of Pi into chloroplast results in relatively low 3-PGA/Pi ratio, a condition which assures less AGPase activity and, in turn, more carbon flow directed into sucrose synthesis. Hence, the allosteric regulation of AGPase operates in a way to suppress activity of the enzyme so that much of the fixed carbon is diverted for the biosynthesis of sucrose which is exported to support sink organs. However,

when sink tissues are not able to efficiently assimilate the transported carbon, the levels of sucrose and phosphorylated intermediates increase in the cytoplasm while Pi levels correspondingly decrease in the chloroplasts of leaf cells resulting in an increase in the 3-PGA/Pi ratio in the stroma. Therefore, AGPase is activated as a result of the high 3-PGA/Pi ratio enabling triose phosphates to be incorporated into transient starch while generating Pi to support photophosphorylation (Ballicora et al. 2004; Tuncel and Okita 2013). Thus, the allosteric regulation of AGPases in photosynthetic tissues is an essential mechanism enabling starch to serve not only as a transient reserve to support heterotrophic plant growth during the night but also as an important alternative metabolic process to recycle Pi and, thereby, minimize feedback inhibition of photosynthesis. This alternative mechanism to recycle Pi to support photophosphorylation is supported by analysis of transgenic *Arabidopsis* and rice plants which accumulated elevated leaf starch levels by expression of up-regulated AGPases (Gibson et al. 2011). Such plants exhibited increased photosynthetic capacity and, in turn, enhanced growth rates.

11.4.2 Sink Enzymes

One of the most extensively studied AGPases is the potato tuber enzyme. The potato AGPase is activated more than 30-fold by 3-PGA and inhibited by Pi. Fructose 2,6-bisphosphate (Fru2,6BP) and PEP are only partially effective (<30 % of levels obtained with 3-PGA) in activating the enzyme, while Fru6P and Glc6P are very weak activators (Iglesias et al. 1993; Wakuta et al. 2013). Unlike the leaf and stem AGPases, which are activated and inhibited by 3-PGA and Pi, respectively, the enzymes from developing seeds display considerable variation in their dependence on 3-PGA activation. The chickpea enzyme is highly responsive to 3-PGA activation (>30-fold activation) and Pi inhibition (Singh et al. 2003), whereas those from pea embryo (Hylton and Smith 1992) and bean cotyledon (Weber et al. 1995) are only slightly dependent (<30 % activation) on 3-PGA levels for attaining maximum catalytic activity. This variation in 3-PGA response observed for AGPases from developing seeds of dicots is also evident for those from cereal grains. The AGPase from barley endosperm (Doan et al. 1999) exhibits high catalytic activity when assayed in the absence of potential activators and was found to be insensitive to effector molecules. Likewise, the wheat AGPases (Tetlow et al. 2003) are not dependent on 3-PGA for maximum catalytic activity but are allosterically inhibited by Pi, ADP, and FBP. Although they have no impact on the enzyme activity alone, 3-PGA and Fru6P are able to reverse the inhibitory effect of Pi (Gómez-Casati and Iglesias 2002). In contrast, the rice endosperm native AGPase requires 3-PGA for maximal catalytic activity. The major AGPase activity in rice endosperm is stimulated more than 30-fold by 3-PGA, an activation which is reversed by the inhibitor Pi (Tuncel et al. 2014b).

The maize endosperm enzyme, extensively studied in detail by the Hannah laboratory, displays unique properties not seen in other AGPases. Although the enzyme

is activated by 3-PGA, the basal catalytic activity in the absence of 3-PGA is quite substantial resulting in a lower activation (ten-fold or less) than that seen for the leaf and potato tuber enzymes (Boehlein et al. 2005, 2009). It, therefore, shows an intermediate response to 3-PGA activation between that exhibited by the wheat (no 3-PGA response) and rice (high 3-PGA response) endosperm enzymes. Moreover, the enzyme is also appreciably activated by Fru6P and Glc6P, hexose-Ps that serve as poor activators for the leaf and tuber enzymes. In addition to its unique responses to the activators, the maize enzyme also exhibits unusual responses to Pi. In the absence of 3-PGA, the maize enzyme is not inhibited by Pi at low concentrations. In contrast, Pi surprisingly acts as an activator at low concentrations by significantly lowering the K_M values for the substrates ATP and Glc-1-P (Boehlein et al. 2010). Detailed kinetic studies have suggested that 3-PGA and Pi bind to the same or overlapping sites (Boehlein et al. 2013). By contrast, the potato enzyme has separate binding sites for these two effectors. Although the maize enzyme is inhibited by Pi at high concentrations, the K_i is one to two orders of magnitude higher than that of the leaf and tuber enzymes and, moreover, is only inhibited about 50 % compared to the nearly 100 % inhibition seen for the leaf and potato enzymes. Overall, the maize endosperm enzyme is not as sensitive to 3-PGA activation and Pi inhibition as the leaf and tuber enzymes. These unique allosteric regulatory properties suggest that the maize endosperm enzyme is not subject to the same stringent controls required by the leaf and tuber enzymes (Boehlein et al. 2009).

11.4.3 Redox Regulation

The leaf and tuber AGPases are also subject to redox regulation mediated by dimerization of the S subunits. This regulation was first observed in the potato tuber AGPase, where the extent of oxidation of the S subunits to form a 100 kDa dimer correlated with AGPase activity and affinity to ATP (Tiessen et al. 2002; Geigenberger et al. 2005). Incubation of the tuber disks in the presence of the reducing agent, dithiothreitol, or sucrose prevented S subunit dimerization and significant decrease in AGPase activity. Chemical labeling studies showed that activation was due to the reduction of an interchain disulfide bridge formed between Cys12 of the two S subunits (Fu et al. 1998a; Ballicora et al. 2000). Subsequently, Ballicora et al. showed that thioredoxin (Trx) was able to effectively reduce the S subunits (Ballicora et al. 2000). Interestingly, activation is very pronounced (three-fold or more) when the enzyme is reduced with DTT in the absence of 3-PGA. In the presence of 3-PGA, activation (four-fold) is only readily evident at lower activator concentrations (<1 mM), whereas at higher concentrations the difference in catalytic activities between the reduced and oxidized enzyme forms is minimal (Ballicora et al. 2000). Reduction of the S subunits increases the affinity of the enzyme to 3-PGA about 2-fold and affinity to ATP about 1.6-fold.

These studies were extended to the leaf AGPases from pea, potato, and *Arabidopsis* (Hendriks et al. 2003). Light and sugars were shown to modulate the

redox activation of AGPase in leaves. Redox activation of AGPase is similar to the light-dependent activation of enzymes involved in the Calvin-Benson cycle, ATP synthesis, and NADPH export from chloroplast by changing the redox status of the electron transport chain (Scheibe 1991). Photosynthetic electron transport results in the reduction of ferredoxin (Fdx) that can light-activate AGPase activation by two different processes. In one pathway, Fdx can reduce plastidial Trx *f* or Trx *m*, which can then reduce and activate AGPase and, in turn, starch synthesis in response to light. For instance, AGPase from pea leaf was shown to be activated three-fold by either 20 μM Trx *f* or Trx *m*. The second pathway involves the light-dependent activation of NADP-thioredoxin reductase C (NTRC) (Michalska et al. 2009). In the light, photoreduced Fdx activates NTRC by reducing Fdx-NADPH reductase. In turn, NTRC stimulates reductive activation of AGPase and starch synthesis. The knockout *ntrc* mutants of *Arabidopsis* displayed 5-fold decrease in AGPase monomerization in leaves and 2.7-fold decrease in starch levels compared to wild-type plants at the end of the day (Michalska et al. 2009).

In addition to light, sucrose also induces redox activation of AGPase in leaves (Hendriks et al. 2003). Increased sucrose levels elevate trehalose 6-phosphate (Tre6P) by regulating Tre6P synthase (TPS) or Tre6P phosphatase (TPP) (Kolbe et al. 2005), key enzymes that balance Tre6P levels in the cytosol. Overexpression of TPS, which converts Glc6P and UDPglc into Tre6P, in *Arabidopsis* leaves resulted in higher AGPase activation and starch levels compared to wild-type plants. On the other hand, plants overexpressing TPP, which dephosphorylates Tre6P to produce trehalose, had lower AGPase activation and starch levels. Further, intact chloroplasts were isolated from *Arabidopsis* leaves and fed with either 100 μM Tre6P or sucrose. The redox activation of AGPase was observed in chloroplasts fed with Tre6P, but not those fed with sucrose. Thus, it is clear that cytoplasmic synthesized Tre6P regulates starch metabolism by stimulating NTRC- or Trx-dependent redox regulation of AGPase although specific details on the signaling cascade between these players still need to be resolved (Kolbe et al. 2005; Lunn et al. 2006).

The physiological significance of redox regulation of AGPase activity was directly assessed in *Arabidopsis* (Hädrich et al. 2012). The APS1 subunit gene was mutagenized where Cys81 (equivalent to Cys12 of potato tuber enzyme) was replaced with Ser ($APS1_{C81S}$) and then transformed into the *adg1* mutant line lacking the functional APS1 subunit. The expressed mutant $APS1_{C81S}$ was unable to dimerize in the dark indicating that Cys81 was responsible for interchain disulfide linkage between the two S subunits. Despite having significantly lower levels (five- to 10-fold) of AGPase activity, the transgenic *adg1*/$APS1_{C81S}$ lines had higher levels of ADPglc and maltose as well as elevated starch synthesis or elevated starch levels at the end of the dark period than control plants. Hence, redox regulation of AGPase is essential for the diurnal regulation of starch turnover with the loss of regulation impacting starch breakdown. This latter condition would be consistent with the differences in the kinetic properties of the oxidized and reduced AGPase. In the presence of low 3-PGA or low 3-PGA/Pi ratio, the residual catalytic activity of the oxidized enzyme would be significantly smaller than the reduced enzyme. Hence, in the transgenic *adg1*/$APS1_{C81S}$ line, the reduced AGPase would have

higher catalytic activity in the dark allowing more starch synthesis to occur than that for the oxidized enzyme. Hence, the inability to form an oxidized enzyme impedes net starch turnover in the dark resulting in a starch-excess phenotype.

The contribution of redox regulation in controlling AGPase activity was not supported in another study (Li et al. 2012). No significant differences in the levels of reduced APS1 subunits and starch accumulation were evident between the wild-type and *ntrc* mutant lines grown at different light intensities. Therefore, Li and his colleagues (2012) suggested that redox regulation of AGPase via the NTRC pathway does not contribute to the fine regulation of transitory starch synthesis in *Arabidopsis* leaves. However, it should be noted that there were significant differences in the growth conditions (light intensity) of the *Arabidopsis* plants and preparation of protein samples (quenching of samples to prevent oxidation), which likely account for the different conclusions made in these two studies (Hädrich et al. 2012; Li et al. 2012). Likewise, the contribution of thioredoxin *f*/*m* was not discounted. Moreover, the fine down-regulation of AGPase activity in the dark, as suggested by Hädrich and his colleagues, was not evaluated in this study (Li et al. 2012).

11.4.4 Redox Regulation in Sink Organs

The carbon status, *i.e*., the availability of glucose and sucrose in the cell, leads to redox activation of potato tuber AGPase by two different mechanisms (Tiessen et al. 2002, 2003). Firstly, the sucrose-dependent pathway involves SNF-1-like protein kinase (SnRK1), which stimulates the reductive activation of AGPase (Tiessen et al. 2003; McKibbin et al. 2006). In detached potato tubers, AGPase becomes less active and exhibits lower affinity to substrates and less sensitivity to 3-PGA activation, thus decreasing rates of starch synthesis (Tiessen et al. 2002). The differences in kinetic properties between the AGPases of detached and undetached tubers were quite remarkable in that AGPase activity was 10-fold lower in the former case. The AGPase from the detached tubers also exhibited significantly reduced 3-PGA sensitivity at physiological levels, a condition which was reversed by incubation of the detached tubers with sucrose. The components of sucrose signaling that stimulate reductive activation of tuber AGPase have yet to be identified. Secondly, a glucose-dependent pathway for redox activation of AGPase includes hexose phosphorylation by an endogenous hexokinase (Tiessen et al. 2003). When potato disks are incubated in the absence of sugars for 2 h, redox activation of AGPase is decreased due to limited sugar levels. When disks are fed with glucose, reductive activation of AGPase is recovered. Increased glucose supply elevates the $NADPH/NADP^+$ ratio in the cell which, in turn, will alter the plastidial redox modulation. Details on signal transduction between cytosol and the plastid are not fully resolved, but the results suggest that the redox transfer between Trx and its target may be influenced by additional factors.

In contrast to the potato tuber or leaf AGPases, the Cys12 residue is not conserved in S subunits of cereal endosperm AGPases, suggesting that endosperm AGPase

is not regulated by redox status of the cell. Nevertheless, the maize endosperm L subunits and not the S subunits are capable of forming a disulfide bond in the absence of DTT indicating a possible redox regulation of AGPase activity through the L subunit (Linebarger et al. 2005). Direct evidence in support of redox control of the cereal enzymes is seen for the rice endosperm AGPase, which is also subject to redox regulation through Cys residues at the N terminal region of the L subunit (AGPL2) (Tuncel et al. 2014a). Interestingly, the changes in kinetic properties of the native enzyme are more dramatic than the recombinant AGPase when they are reduced. The rice native reduced AGPase exhibits 6-fold higher affinity to 3-PGA and enhanced activity overall 3-PGA levels, whereas the recombinant AGPase only shows 3.4-fold more affinity to 3-PGA in the reduced state and higher activity only at low 3-PGA with no significant differences between the reduced and nonreduced forms at higher 3-PGA levels. Further studies are required to identify the basis for the differences in redox behavior between the native and recombinant enzymes in the presence of 3-PGA.

Lastly, in addition to finely controlling the catalytic activity, redox regulation may also play a role in controlling the enzyme's expression at the protein level. The activities of AGPases from cereal endosperms are significantly affected by heat exposure, an effect which also limits crop productivity. The maize AGPase activity is sensitive to heat and loses much of its activity (∼95 %) when incubated at 57–60 °C for 5 min (Hannah et al. 1980; Greene and Hannah 1998). By contrast, the potato tuber AGPase is much more heat stable, and its activity is still maintained under these conditions (Okita et al. 1990; Hwang et al. 2008). To determine the basis for the differences in heat stability, the conserved QTCL motif which contains the Cys residue responsible for the interchain bond between the pair of potato S subunits was inserted in the maize endosperm S subunit (Linebarger et al. 2005). The mutagenized recombinant maize endosperm enzyme showed a 300-fold increase in the heat stability (Linebarger et al. 2005). A role for general stability is also evident in transgenic *Arabidopsis adg1* plants expressing the $APS1_{C81S}$. Although RNA levels were comparable to that seen in wild-type, net enzyme and $APS1_{C81S}$ subunit levels were significantly reduced. Hence, these results suggest that the AGPase capable of oxidoreduction cycle is more stable than the reduced fixed form.

11.5 Biotechnological Methods to Improve Grain Yields

Multiple approaches have been used to improve grain yields via manipulation of starch metabolism, most of which focused on the manipulation of single genes. Although some progress has been made with these approaches, relatively small improvements have been achieved in terms of starch content and grain yields (Van Camp 2005). In the following sections, the molecular strategies to increase starch levels in cereals and future prospects for enhancing starch yield are discussed.

11.5.1 Manipulation of AGPase Activity

Extensive attempts to increase starch content in cereal seeds have centered on the manipulation of AGPase activity since it catalyzes the first committed and "rate-limiting step" in starch biosynthesis. Indeed, this was first demonstrated in russet Burbank potatoes where expression of an allosteric-insensitive *E. coli glgC* gene elevated starch synthesis and the density of the tubers. Interestingly, a similar study using the potato cultivar Desiree failed to elevate net starch accumulation (Sweetlove et al. 1996). Although a four- to five-fold increase in AGPase activity and increase of carbon flux into starch were observed, elevated starch turnover was also apparent resulting in no net gain in starch (Sweetlove et al. 1996). The basis for the differences seen between these two studies is not clear although the use of different potato cultivars and their corresponding differences in starch content is a likely factor.

In view of the success obtained in elevating starch content in russet Burbank potatoes, considerable effort has exploited AGPase expression as a means to increase starch synthesis in developing cereal endosperm. As discussed in a recent review (Tuncel and Okita 2013), elevated AGPase expression increases the starch content of individual maize and rice grains (Giroux et al. 1996; Sakulsingharoj et al. 2004; Wang et al. 2007). Unexpectedly, expression of AGPase genes under the control of putative endosperm-specific promoters also increased the total number of maize kernels on individual cobs (Hannah et al. 2012) and number of developing grains per rice panicle or wheat head (Smidansky et al. 2002, 2003; Meyer et al. 2004). The increase in grain/seed number indicates that these transgenes are expressed at developmental stages prior to endosperm development. A more recent study also supports this view. AGPase cytosolic large subunit gene (TaLSUI) from wheat was overexpressed under the control of an endosperm-specific promoter in a wheat cultivar (Kang et al. 2013). The transgenic lines exhibited remarkably increased AGPase activity, starch levels, single grain weight, and grain number per spikelet.

11.5.2 Enhancement of Sucrose Synthase (SuSy) Activity

An alternative model for sucrose-starch conversion in cereal species has been proposed for starch biosynthesis where SuSy directly produces ADPglc from sucrose in the cytosol of seeds (Li et al. 2013). The newly synthesized ADPglc is then imported into the amyloplast for starch synthesis. This model also predicts that AGPase has a main role in scavenging glucose units generated by starch breakdown. Therefore, modulation of SuSy activity has been suggested to be a major determinant of the sink strength and crucial for increasing seed yields (Li et al. 2013).

The focus on SuSy originated from the belief that it is the major determinant of starch accumulation in tubers (Baroja-Fernández et al. 2009). Transgenic lines overexpressing SuSy under the CaMV 35S promoter had increased ADPglc and starch levels compared to the wild-type. The SuSy-overexpressing tubers contained 55–85 % higher starch levels per plant than wild-type plants. This approach was extended to maize endosperm where the potato SuSy was expressed under the control of ubiquitin promoter (Li et al. 2013). Transgenic maize lines exhibited increased SuSy activity and ADPglc levels and also had 10–15 % elevated starch levels. Authors argued that sucrose and starch pathways are connected by the action of SuSy, the main provider of ADPglc in the cytoplasm. However, this proposed model fails to account for the dramatic decrease in starch levels in *sh2* and *bt2* maize endosperms (Tsai and Nelson 1966) or significant increases in starch content by overexpression of the Sh2rev6 variant (Hannah et al. 2012). Similar results were also obtained in other cereal species when mutations in AGPase structural genes reduced cytosolic AGPase activity and, in turn, starch accumulation (Lee et al. 2007; Howard et al. 2012). Therefore, SuSy is unlikely to be the major determinant of ADPglc production, in turn, starch accumulation in cereals. A more plausible explanation of elevated starch levels with enhanced SuSy activity is the resulting increases in UDPglc levels and downstream metabolites including ADPglc. SuSy, UGPase, and AGPase catalyze readily reversible reactions, and increase in SuSy would result in elevated UDPglc and downstream metabolites, Glc-1-P, and ADPglc and, in turn, increase starch levels.

11.5.3 Overexpression of ADPglc Transporter (BT1)

Irrespective of the source of ADPglc, this sugar nucleotide must be imported from the cytoplasm into the amyloplast in cereal endosperm. This activity is carried out by BT1, whose gene sequences were first isolated by Sullivan et al. (Sullivan et al. 1991; Sullivan and Kaneko 1995) and found to encode a 39–44 kDa integral membrane protein. BT1 and its orthologs in other cereals belong to the mitochondrial carrier family (MCF) of proteins, a carrier class that has a broad range of substrates (Millar and Heazlewood 2003; Tjaden et al. 2004). Recent studies have demonstrated that BT1 from cereal storage tissues mediates the transport of ADPglc from the cytoplasm into the amyloplast in exchange with AMP or ADP (Emes and Neuhaus 1997; Bowsher et al. 2007; Kirchberger et al. 2007). The role of BT1 in the transport of ADPglc is supported by the analysis of genetic mutants. Maize kernels harboring the *bt1* mutation accumulate 80 % less starch than wild-type kernels (Tobias et al. 1992) but contain 11.5-fold higher levels of ADPglc (Shannon et al. 1996). Similar phenotypic properties were also observed for the barley *lys5* mutants that lack a functional form of the ADPglc transporter (Patron et al. 2004).

The study of transgenic rice plant, CS8, overexpressing the *E. coli glgC*-TM AGPase provides evidence that BT1 transport activity may be a limiting step in

starch biosynthesis (Sakulsingharoj et al. 2004). Transgenic CS8 lines show up to a 15 % increase in seed weight compared to WT plants. However, the extent of the increase in seed weight observed in CS8 lines grown in enriched CO_2 conditions was no different from plants grown under ambient conditions. The photosynthetic rates were significantly increased under elevated CO_2, leading to higher rates of sucrose transport into seeds (Rowland-Bamford et al. 1990; Chen et al. 1994). The inability of developing seeds of CS8 transgenic rice plants to further convert the increases in photoassimilate into starch under elevated CO_2 conditions indicates that starch synthesis is limited by some process other than AGPase. In support of this view, measurement of the carbon metabolites from seeds of CS8 and wild-type lines showed elevated levels of ADPglc in CS8 lines, which were three- to four-fold higher than the increases in seed weight (Nagai et al. 2009). These results suggest that AGPase is no longer a rate-limiting step in the transgenic plant and that maximum carbon flow into starch is constrained by one or more downstream steps, which would include the BT1 transporter and/or major starch synthases (SSs). SSs are present, however, in multiple forms and are unlikely to be limiting starch synthesis during the starch granule maturation phase based on available evidence. Genetic mutants of SSI (Fujita et al. 2006) or SSIII (Fujita et al. 2007) have starch levels comparable to wild-type plants. On the other hand, overexpression of SSIV increases starch content in both *A. thaliana* leaves and potato tubers, suggesting that initiation of starch synthesis is limiting (Gámez-Arjona et al. 2011). Therefore, BT1 and SSIV are likely candidates limiting carbon flow and are prime targets for manipulation to increase starch production in cereals.

11.5.4 Alternative Approaches to Increase Grain Yields

11.5.4.1 Changing the Expression of Starch Biosynthesis Regulators

An alternative strategy to increase starch synthesis is to globally increase the expression of the starch biosynthetic genes. An advantage of this approach is that, in addition to elevating the expression of some known starch biosynthetic genes, other genes yet to be identified that play a role in starch synthesis are also likely to be activated. The rice starch regulator 1 (*RSR1*) gene, which codes for an APETALA2/ethylene-responsive element-binding protein family transcription factor, was identified by genome-wide co-expression analysis. *RSR1* was found to down-regulate the expression of many starch-related genes, including AGPase, SS, granule-bound starch synthase (GBSS), starch-branching enzyme, and starch-debranching enzyme (Fu and Xue 2010). Suppression of *RSR1* gene expression in seeds elevated the expression of starch biosynthetic genes. *Rsr1*-deficient transgenic plants had altered amylose contents, altered formation of starch granule, and increased seed weight. On the other hand, overexpression of *RSR1* resulted in repression of starch synthesis genes, while starch structure and levels in the transgenic plants were comparable to wild-type (Fu and Xue 2010). Therefore, silencing *RSR1* gene seems to be a promising strategy to enhance rice grain yield.

In a recent study, mutation in the *FLO2* gene, which encodes a protein containing a protein-to-protein interaction tetratricopeptide motif, led to reduced grain size and altered starch quality in rice endosperm (She et al. 2010). The *flo2* mutation also decreased the expression of many genes that are involved in starch synthesis such as AGPase, SuSy, SSs, branching enzymes, and α-amylase. As expected, overexpression of *FLO2* resulted in enlarged, heavier grains and increased starch quality. This study proposes that rice grain size and starch quality are regulated by the *FLO2* gene. Further studies are needed to show the importance of *FLO2* orthologs in other grain species.

11.5.4.2 Regulation of Starch Degradation

A novel mechanism for increasing grain yields was described by blocking starch degradation since evidence showed that starch synthesis and breakdown occur concurrently in starch-accumulating organs (Baroja-Fernández et al. 2003). Phosphorylation of starch is critical for degradation of starch granule (Blennow et al. 2002; Smith et al. 2005). Glucan water-dikinase (GWD) and phosphoglucan water-dikinase (PWD) activities phosphorylate starch with the former activity transferring the β-phosphate of ATP to either the C6- or C3-position of amylopectin glucosyl residues (Kötting et al. 2005; Mikkelsen et al. 2006). The negative charges disrupt the ordered structure of amylopectin, thereby facilitating access of degrading enzymes such as α-amylase in cereals (Ritte et al. 2002). A recent study (Ral et al. 2012) showed that down-regulation of GWD by RNAi using a wheat endosperm-specific promoter resulted in significant increases in both wheat grain yields and plant biomass. Similar to the transgenic AGPase studies (Giroux et al. 1996; Wang et al. 2007), down-regulation of GWD under the control of a putative endosperm-specific promoter resulted in unanticipated changes in tissues that are formed well before endosperm development. This study opens up a new perspective on the significance of starch metabolism during the formation of reproductive organs as well as the balance between starch synthesis and breakdown. Collectively, they provide a novel mechanism for increasing grain yields by manipulation of starch metabolism in tissues that support overall plant growth and reproduction.

Sugar sensing and signaling in plants are far from being completely understood. The SnRK1 (for sucrose non-fermenting-1-related kinase-1) was proposed to be involved in regulating expression of many genes that are repressed by glucose and modulating the phosphorylation states of several enzymes (Gancedo 1998). SnRK1 also regulates enzymes that are responsible for starch breakdown in wheat and rice seeds during sugar deprivation (Laurie et al. 2003; Lu et al. 2007). It reduces the expression of α-amylase, and, thus, overexpression of SnRK1 under controlled spatial and temporal patterns could provide an alternative and complementary approach to enhance grain yields.

11.5.4.3 Enhancement of Hexose Levels Within Heterotrophic Cells

Starch production is ultimately dependent on the transport and uptake of sucrose by sink organs from source leaves. In cereals, grain filling is dependent on cell wall invertase. The loss of function of cell wall invertase in developing maize grains resulted in the miniature1 (*mn1*) seed phenotype (Kang et al. 2009), while a similar activity (GIF1) in rice rendered smaller seeds due to slower grain filling (Wang et al. 2008). In maize, expression of the cell wall invertase (*lncw*) occurs at the basal part of the endosperm, while in rice GIF1/OsCIN1 invertase resides on the ovular vascular and lateral stylar vascular traces of the developing grain. The spatial location of the cell wall invertase and pronounced reduction in grain size due to loss of function indicate that the cell wall invertase is required for the efficient unloading of sucrose from vascular tissues. Consistent with this view is the observation that transgenic rice plants overexpressing GIF1 had larger and heavier grains (Wang et al. 2008). Overall, these studies support the manipulation of cell wall invertase and other cellular processes involved in the efficient unloading of sucrose from vascular tissue and subsequent loading into endosperm tissue as potential targets to enhance grain yields.

11.6 Conclusions and Future Prospects

Starch metabolism is an essential process in plants and has a major impact on overall plant productivity and crop yields. The synthesis of starch is a complex and highly regulated process and involves the contribution of enzymes and metabolites in both the cytosol and plastid compartments. Despite several decades of study, the impact of starch metabolism on plant development is far from being understood as illustrated by the unanticipated results in studies attempting to manipulate starch genes during cereal endosperm development. Rather than the expected increase in grain weight due to increase in starch synthesis, unexpected increases in grain number per reproductive organ (wheat head, rice panicle, or maize cob) and number of reproductive organs per plant were evident. These unexpected increases in grain number suggest that the putative endosperm-specific promoters of AGPase are also active in non-endosperm tissue (e.g., the meristematic tissues that give rise to reproductive organs) and/or in ovule during the early stages of fertilization preventing seed abortion by increasing the sink strength of these tissues. Further studies are needed to identify the tissues where these promoters are active and whether enhancement of starch biosynthesis in these tissues stimulates flower development and, in turn, grain yields (Hannah et al. 2012). With such information in hand, a more rational approach can be used to enhance crop yields by the overexpression of single genes such as AGPase or by controlling global regulators that enhance overall expression of starch biosynthetic genes.

Likewise, many gaps in our understanding of starch synthesis still remain to be elucidated. For example, a CBM48 domain-containing protein has been

demonstrated to be essential for starch formation by its interaction with isoamylase and presumably aiding its debranching activity as a chaperone (Peng et al. 2014). As many other starch biosynthetic enzymes lack the ability to bind starch directly, similar carbohydrate-binding domain-containing proteins may be required to facilitate their action.

Moreover, recent studies showing the control of rice endosperm cytosolic AGPase activity by redox regulation (Tuncel et al. 2014a) open new avenues of investigation to identify the sugar signaling pathways which take part in carbon assimilation in developing rice endosperm. Redox activation of endosperm AGPase allows storage organs to adjust carbon storage according to levels of sucrose supplied from leaves. These signaling pathways will be perturbed by the up- or down-regulation of specific genes such as AGPase resulting in significant changes in overall gene expression at the RNA and protein level. Advances in next-generation sequencing, proteomics, and metabolite profiling now enable a more systematic and analytical means to assess these changes, heretofore not possible before. Such an integrated approach will provide a more complete view of starch metabolism, which will likely result in formulating novel approaches to engineer more efficient starch synthesis and, thereby, enhance plant productivity and yields.

References

Akihiro T, Mizuno K, Fujimura T (2005) Gene expression of ADP-glucose pyrophosphorylase and starch contents in rice cultured cells are cooperatively regulated by sucrose and ABA. Plant Cell Physiol 46:937–946. doi:10.1093/pcp/pci101

Amarasekara AS (2013) Handbook of cellulosic ethanol. Wiley, Hoboken

Archbold DD (1999) Carbohydrate availability modifies sorbitol dehydrogenase activity of apple fruit. Physiol Plant 105:391–395. doi:10.1034/j.1399-3054.1999.105301.x

Ballicora MA, Laughlin MJ, Fu Y et al (1995) Adenosine 5′-diphosphate-glucose pyrophosphorylase from potato tuber (significance of the N terminus of the small subunit for catalytic properties and heat stability). Plant Physiol 109:245–251. doi:10.1104/pp.109.1.245

Ballicora MA, Frueauf JB, Fu Y et al (2000) Activation of the potato tuber ADP-glucose pyrophosphorylase by thioredoxin. J Biol Chem 275:1315–1320. doi:10.1074/jbc.275.2.1315

Ballicora MA, Iglesias AA, Preiss J (2003) ADP-glucose pyrophosphorylase, a regulatory enzyme for bacterial glycogen synthesis. Microbiol Mol Biol Rev 67:213–225. doi:10.1128/MMBR.67.2.213-225.2003

Ballicora MA, Iglesias AA, Preiss J (2004) ADP-glucose pyrophosphorylase: a regulatory enzyme for plant starch synthesis. Photosynth Res 79:1–24. doi:10.1023/B:PRES.0000011916.67519.58

Ballicora MA, Dubay JR, Devillers CH et al (2005) Resurrecting the ancestral enzymatic role of a modulatory subunit. J Biol Chem 280:10189–10195. doi:10.1074/jbc.M413540200

Baroja-Fernández E, Muñoz FJ, Saikusa T et al (2003) Sucrose synthase catalyzes the de novo production of ADPglucose linked to starch biosynthesis in heterotrophic tissues of plants. Plant Cell Physiol 44:500–509. doi:10.1093/pcp/pcg062

Baroja-Fernández E, Muñoz FJ, Pozueta-Romero J (2005) Response to Neuhaus et al.: no need to shift the paradigm on the metabolic pathway to transitory starch in leaves. Trends Plant Sci 10:156–158

Baroja-Fernández E, Muñoz FJ, Montero M et al (2009) Enhancing sucrose synthase activity in transgenic potato (*Solanum tuberosum* L.) tubers results in increased levels of starch, ADPglucose and UDPglucose and total yield. Plant Cell Physiol 50:1651–1662. doi:10.1093/pcp/pcp108

Baroja-Fernandez E, Munoz FJ, Li J et al (2012) Sucrose synthase activity in the sus1/sus2/sus3/sus4 *Arabidopsis* mutant is sufficient to support normal cellulose and starch production. Proc Natl Acad Sci U S A 109:321–326. doi:10.1073/pnas.1117099109

Björn L, Govindjee (2009) The evolution of photosynthesis and chloroplasts. Curr Sci 96:1466–1474

Blennow A, Nielsen TH, Baunsgaard L et al (2002) Starch phosphorylation: a new front line in starch research. Trends Plant Sci 7:445–450. doi:10.1016/S1360-1385(02)02332-4

Boehlein SK, Sewell AK, Cross J et al (2005) Purification and characterization of adenosine diphosphate glucose pyrophosphorylase from maize/potato mosaics. Plant Physiol 138:1552–1562. doi:10.1104/pp.105.060699

Boehlein SK, Shaw JR, Stewart JD et al (2009) Characterization of an autonomously activated plant ADP-glucose pyrophosphorylase. Plant Physiol 149:318–326. doi:10.1104/pp.108.126862

Boehlein SK, Shaw JR, Stewart JD et al (2010) Studies of the kinetic mechanism of maize endosperm ADP-glucose pyrophosphorylase uncovered complex regulatory properties. Plant Physiol 152:1056–1064. doi:10.1104/pp.109.149450

Boehlein SK, Shaw JR, McCarty DR et al (2013) The potato tuber, maize endosperm and a chimeric maize-potato ADP-glucose pyrophosphorylase exhibit fundamental differences in Pi inhibition. Arch Biochem Biophys 537:210–216. doi:10.1016/j.abb.2013.07.019

Bowsher CG, Scrase-Field EF, Esposito S et al (2007) Characterization of ADP-glucose transport across the cereal endosperm amyloplast envelope. J Exp Bot 58:1321–1332. doi:10.1093/jxb/erl297

Chen C, Li C, Sung J (1994) Carbohydrate metabolism enzymes in CO2-enriched developing rice grains of cultivars varying in grain size. Physiol Plant 90:79–85. doi:10.1111/j.1399-3054.1994.tb02195.x

Crevillén P, Ballicora MA, Mérida Á et al (2003) The different large subunit isoforms of *Arabidopsis thaliana* ADP-glucose pyrophosphorylase confer distinct kinetic and regulatory properties to the heterotetrameric enzyme. J Biol Chem 278:28508–28515. doi:10.1074/jbc.M304280200

Crevillén P, Ventriglia T, Pinto F et al (2005) Differential pattern of expression and sugar regulation of *Arabidopsis thaliana* ADP-glucose pyrophosphorylase-encoding genes. J Biol Chem 280:8143–8149. doi:10.1074/jbc.M411713200

Cross JM, Clancy M, Shaw JR et al (2004) Both subunits of ADP-glucose pyrophosphorylase are regulatory. Plant Physiol 135:137–144. doi:10.1104/pp.103.036699

Cross JM, Clancy M, Shaw JR et al (2005) A polymorphic motif in the small subunit of ADP-glucose pyrophosphorylase modulates interactions between the small and large subunits. Plant J 41:501–511. doi:10.1111/j.1365-313X.2004.02315.x

Denyer K, Dunlap F, Thorbjornsen T et al (1996) The major form of ADP-glucose pyrophosphorylase in maize endosperm is extra-plastidial. Plant Physiol 112:779–785. doi:10.1104/pp.112.2.779

Doan DN, Rudi H, Olsen O-A (1999) The allosterically unregulated isoform of ADP-glucose pyrophosphorylase from barley endosperm is the most likely source of ADP-glucose incorporated into endosperm starch. Plant Physiol 121:965–975. doi:10.1104/pp.121.3.965

Ekkehard Neuhaus H, Häusler RE, Sonnewald U (2005) No need to shift the paradigm on the metabolic pathway to transitory starch in leaves. Trends Plant Sci 10:154–156

Emes M, Neuhaus H (1997) Metabolism and transport in non-photosynthetic plastids. J Exp Bot 48:1995–2005. doi:10.1093/jxb/48.12.1995

Fu F-F, Xue H-W (2010) Coexpression analysis identifies Rice Starch Regulator1, a rice AP2/EREBP family transcription factor, as a novel rice starch biosynthesis regulator. Plant Physiol 154:927–938. doi:10.1104/pp.110.159517

Fu Y, Ballicora MA, Leykam JF et al (1998a) Mechanism of reductive activation of potato tuber ADP-glucose pyrophosphorylase. J Biol Chem 273:25045–25052. doi:10.1074/jbc.273.39.25045

Fu Y, Ballicora MA, Preiss J (1998b) Mutagenesis of the glucose-1-phosphate-binding site of potato tuber ADP-glucose pyrophosphorylase. Plant Physiol 117:989–996. doi:10.1104/pp.117.3.989

Fujita N, Yoshida M, Asakura N et al (2006) Function and characterization of starch synthase I using mutants in rice. Plant Physiol 140:1070–1084. doi:10.1104/pp.105.071845

Fujita N, Yoshida M, Kondo T et al (2007) Characterization of SSIIIa-deficient mutants of rice: the function of SSIIIa and pleiotropic effects by SSIIIa deficiency in the rice endosperm. Plant Physiol 144:2009–2023. doi:10.1104/pp.107.102533

Gámez-Arjona FM, Li J, Raynaud S et al (2011) Enhancing the expression of starch synthase class IV results in increased levels of both transitory and long-term storage starch. Plant Biotechnol J 9:1049–1060. doi:10.1111/j.1467-7652.2011.00626.x

Gancedo JM (1998) Yeast carbon catabolite repression. Microbiol Mol Biol Rev 62:334–361

Geigenberger P, Kolbe A, Tiessen A (2005) Redox regulation of carbon storage and partitioning in response to light and sugars. J Exp Bot 56:1469–1479. doi:10.1093/jxb/eri178

Georgelis N, Braun EL, Hannah LC (2008) Duplications and functional divergence of ADP-glucose pyrophosphorylase genes in plants. BMC Evol Biol 8:232. doi:10.1186/1471-2148-8-232

Ghosh HP, Preiss J (1966) Adenosine diphosphate glucose pyrophosphorylase a regulatory enzyme in the biosynthesis of starch in spinach leaf chloroplasts. J Biol Chem 241:4491–4504

Gibson K, Park J-S, Nagai Y et al (2011) Exploiting leaf starch synthesis as a transient sink to elevate photosynthesis, plant productivity and yields. Plant Sci (Amst Neth) 181:275–281. doi:10.1016/j.plantsci.2011.06.001

Giroux MJ, Shaw J, Barry G et al (1996) A single mutation that increases maize seed weight. Proc Natl Acad Sci U S A 93:5824–5829

Gómez-Casati DF, Iglesias AA (2002) ADP-glucose pyrophosphorylase from wheat endosperm. Purification and characterization of an enzyme with novel regulatory properties. Planta 214:428–434. doi:10.1007/s004250100634

Greene TW, Hannah LC (1998) Enhanced stability of maize endosperm ADP-glucose pyrophosphorylase is gained through mutants that alter subunit interactions. Proc Natl Acad Sci U S A 95:13342–13347. doi:10.1073/pnas.95.22.13342

Hädrich N, Hendriks JH, Kötting O et al (2012) Mutagenesis of cysteine 81 prevents dimerization of the APS1 subunit of ADP-glucose pyrophosphorylase and alters diurnal starch turnover in *Arabidopsis thaliana* leaves. Plant J 70:231–242. doi:10.1111/j.1365-313X.2011.04860.x

Hannah L, Tuschall D, Mans R (1980) Multiple forms of maize endosperm ADP-glucose pyrophosphorylase and their control by Shrunken-2 and Brittle-2. Genetics 95:961–970

Hannah LC, Futch B, Bing J et al (2012) A shrunken-2 transgene increases maize yield by acting in maternal tissues to increase the frequency of seed development. Plant Cell Online 24:2352–2363. doi:10.1105/tpc.112.100602

Heldt HW, Chon CJ, Maronde D et al (1977) Role of orthophosphate and other factors in the regulation of starch formation in leaves and isolated chloroplasts. Plant Physiol 59:1146–1155. doi:10.1104/pp.59.6.1146

Hendriks JH, Kolbe A, Gibon Y et al (2003) ADP-glucose pyrophosphorylase is activated by posttranslational redox-modification in response to light and to sugars in leaves of Arabidopsis and other plant species. Plant Physiol 133:838–849. doi:10.1104/pp.103.024513

Howard TP, Fahy B, Craggs A et al (2012) Barley mutants with low rates of endosperm starch synthesis have low grain dormancy and high susceptibility to preharvest sprouting. New Phytol 194:158–167. doi:10.1111/j.1469-8137.2011.04040.x

Hwang SK, Okita TW (2012) Understanding structure-function relationship of ADP-glucose pyrophosphorylase by deciphering its mutant forms. In: Tetlow I (ed) Starch: origins, structure and metabolism. The Society for Experimental Biology, London, pp 77–114

Hwang S-K, Salamone PR, Okita TW (2005) Allosteric regulation of the higher plant ADP-glucose pyrophosphorylase is a product of synergy between the two subunits. FEBS Lett 579:983–990. doi:10.1016/j.febslet.2004.12.067

Hwang S-K, Hamada S, Okita TW (2006) ATP binding site in the plant ADP-glucose pyrophosphorylase large subunit. FEBS Lett 580:6741–6748. doi:10.1016/j.febslet.2006.11.029

Hwang S-K, Hamada S, Okita TW (2007) Catalytic implications of the higher plant ADP-glucose pyrophosphorylase large subunit. Phytochemistry 68:464–477

Hwang S-K, Nagai Y, Kim D et al (2008) Direct appraisal of the potato tuber ADP-glucose pyrophosphorylase large subunit in enzyme function by study of a novel mutant form. J Biol Chem 283:6640–6647. doi:10.1074/jbc.M707447200

Hylton C, Smith AM (1992) The rb mutation of peas causes structural and regulatory changes in ADP glucose pyrophosphorylase from developing embryos. Plant Physiol 99:1626–1634. doi:10.1104/pp.99.4.1626

Iglesias AA, Barry GF, Meyer C et al (1993) Expression of the potato tuber adp-glucose pyrophosphorylase in *Escherichia coli*. J Biol Chem 268:1081–1086

Jonik C, Sonnewald U, Hajirezaei MR et al (2012) Simultaneous boosting of source and sink capacities doubles tuber starch yield of potato plants. Plant Biotechnol J 10:1088–1098. doi:10.1111/j.1467-7652.2012.00736.x

Kang B-H, Xiong Y, Williams DS et al (2009) Miniature1-encoded cell wall invertase is essential for assembly and function of wall-in-growth in the maize endosperm transfer cell. Plant Physiol 151:1366–1376. doi:10.1104/pp.109.142331

Kang G, Liu G, Peng X et al (2013) Increasing the starch content and grain weight of common wheat by overexpression of the cytosolic AGPase large subunit gene. Plant Physiol Biochem 73:93–98. doi:10.1016/j.plaphy.2013.09.003

Kirchberger S, Leroch M, Huynen MA et al (2007) Molecular and biochemical analysis of the plastidic ADP-glucose transporter (ZmBT1) from *Zea mays*. J Biol Chem 282:22481–22491. doi:10.1074/jbc.M702484200

Kolbe A, Tiessen A, Schluepmann H et al (2005) Trehalose 6-phosphate regulates starch synthesis via posttranslational redox activation of ADP-glucose pyrophosphorylase. Proc Natl Acad Sci U S A 102:11118–11123. doi:10.1073/pnas.0503410102

Kötting O, Pusch K, Tiessen A et al (2005) Identification of a novel enzyme required for starch metabolism in *Arabidopsis* leaves. The phosphoglucan, water dikinase. Plant Physiol 137:242–252. doi:10.1104/pp.104.055954

Krishnan HB, Reeves CD, Okita TW (1986) ADPglucose pyrophosphorylase is encoded by different mRNA transcripts in leaf and endosperm of cereals. Plant Physiol 81:642–645. doi:10.1104/pp.81.2.642

Laurie S, McKibbin RS, Halford NG (2003) Antisense SNF1-related (SnRK1) protein kinase gene represses transient activity of an α-amylase (α-Amy2) gene promoter in cultured wheat embryos. J Exp Bot 54:739–747. doi:10.1093/jxb/erg085

Lee S-K, Hwang S-K, Han M et al (2007) Identification of the ADP-glucose pyrophosphorylase isoforms essential for starch synthesis in the leaf and seed endosperm of rice (*Oryza sativa* L.). Plant Mol Biol 65:531–546. doi:10.1007/s11103-007-9153-z

Li J, Almagro G, Muñoz FJ et al (2012) Post-translational redox modification of ADP-glucose pyrophosphorylase in response to light is not a major determinant of fine regulation of transitory starch accumulation in *Arabidopsis* leaves. Plant Cell Physiol 53:433–444. doi:10.1093/pcp/pcr193

Li J, Baroja-Fernández E, Bahaji A et al (2013) Enhancing sucrose synthase activity results in increased levels of starch and ADP-glucose in maize (*Zea mays* L.) seed endosperms. Plant Cell Physiol 54:282–294. doi:10.1093/pcp/pcs180

Lin T-P, Caspar T, Somerville C et al (1988) Isolation and characterization of a starchless mutant of *Arabidopsis thaliana* (L.) Heynh lacking ADPglucose pyrophosphorylase activity. Plant Physiol 86:1131–1135. doi:10.1104/pp.86.4.1131

Linebarger CRL, Boehlein SK, Sewell AK et al (2005) Heat stability of maize endosperm ADP-glucose pyrophosphorylase is enhanced by insertion of a cysteine in the N terminus of the small subunit. Plant Physiol 139:1625–1634. doi:10.1104/pp.105.067637

Lu C-A, Lin C-C, Lee K-W et al (2007) The SnRK1A protein kinase plays a key role in sugar signaling during germination and seedling growth of rice. Plant Cell Online 19:2484–2499. doi:10.1105/tpc.105.037887

Lunn J, Feil R, Hendriks J et al (2006) Sugar-induced increases in trehalose 6-phosphate are correlated with redox activation of ADPglucose pyrophosphorylase and higher rates of starch synthesis in *Arabidopsis thaliana*. Biochem J 397:139–148. doi:10.1042/BJ20060083

McKibbin RS, Muttucumaru N, Paul MJ et al (2006) Production of high-starch, low-glucose potatoes through over-expression of the metabolic regulator SnRK1. Plant Biotechnol J 4:409–418. doi:10.1111/j.1467-7652.2006.00190.x

Meyer FD, Smidansky ED, Beecher B et al (2004) The maize Sh2r6hs ADP-glucose pyrophosphorylase (AGP) large subunit confers enhanced AGP properties in transgenic wheat (*Triticum aestivum*). Plant Sci (Amst Neth) 167:899–911. doi:10.1016/j.plantsci.2004.05.031

Michalska J, Zauber H, Buchanan BB et al (2009) NTRC links built-in thioredoxin to light and sucrose in regulating starch synthesis in chloroplasts and amyloplasts. Proc Natl Acad Sci U S A 106:9908–9913. doi:10.1073/pnas.0903559106

Mikkelsen R, Suszkiewicz K, Blennow A (2006) A novel type carbohydrate-binding module identified in α-glucan, water dikinases is specific for regulated plastidial starch metabolism. Biochemistry (Mosc) 45:4674–4682. doi:10.1021/bi051712a

Millar AH, Heazlewood JL (2003) Genomic and proteomic analysis of mitochondrial carrier proteins in *Arabidopsis*. Plant Physiol 131:443–453. doi:10.1104/pp.009985

Morell M, Bloom M, Preiss J (1988) Affinity labeling of the allosteric activator site (s) of spinach leaf ADP-glucose pyrophosphorylase. J Biol Chem 263:633–637

Morrison WR, Tester RF, Snape CE et al (1993) Swelling and gelatinization of cereal starches. IV. Some effects of lipid-complexed. Cereal Chem 70:385–391

Nagai YS, Sakulsingharoj C, Edwards GE et al (2009) Control of starch synthesis in cereals: metabolite analysis of transgenic rice expressing an up-regulated cytoplasmic ADP-glucose pyrophosphorylase in developing seeds. Plant Cell Physiol 50:635–643. doi:10.1093/pcp/pcp021

Okita TW, Greenberg E, Kuhn DN et al (1979) Subcellular localization of the starch degradative and biosynthetic enzymes of spinach leaves. Plant Physiol 64:187–192. doi:10.1104/pp.64.2.187

Okita TW, Nakata PA, Anderson JM et al (1990) The subunit structure of potato tuber ADPglucose pyrophosphorylase. Plant Physiol 93:785–790

Oura Y, Yamada K, Shiratake K et al (2000) Purification and characterization of a NAD＋—dependent sorbitol dehydrogenase from Japanese pear fruit. Phytochemistry 54:567–572. doi:10.1016/S0031-9422(00)00158-8

Patron NJ, Greber B, Fahy BE et al (2004) The lys5 mutations of barley reveal the nature and importance of plastidial ADP-Glc transporters for starch synthesis in cereal endosperm. Plant Physiol 135:2088–2097. doi:10.1104/pp.104.045203

Peng C, Wang Y, Liu F, Ren Y, Zhou K et al (2014) FLOURY ENDOSPERM6 encodes a CBM48 domain-containing protein involved in compound granule formation and starch synthesis in rice endosperm. Plant J 77:917–930. doi:10.1111/tpj.12444

Petreikov M, Eisenstein M, Yeselson Y et al (2010) Characterization of the AGPase large subunit isoforms from tomato indicates that the recombinant L3 subunit is active as a monomer. Biochem J 428:201–212. doi:10.1042/BJ20091777

Preiss J (1972) Regulatory mechanisms in the biosynthesis of plant starch and bacterial glycogen, Piras R, Pontis HG (ed), pp 517–528. Accession number: BIOSIS:PREV197309045963

Preiss J (1988) Biosynthesis of starch and its regulation. In: The biochemistry of plants: carbohydrates. Academic, New York, pp 181–254

Preiss J, Cress D, Hutny J et al (1989) Regulation of starch synthesis – biochemical and genetic studies. Am Chem Soc Symp Ser 389:84–92

Ral JP, Bowerman AF, Li Z et al (2012) Down-regulation of glucan, water-dikinase activity in wheat endosperm increases vegetative biomass and yield. Plant Biotechnol J 10:871–882. doi:10.1111/j.1467-7652.2012.00711.x

Ritte G, Lloyd JR, Eckermann N et al (2002) The starch-related R1 protein is an α-glucan, water dikinase. Proc Natl Acad Sci U S A 99:7166–7171. doi:10.1073/pnas.062053099

Rolletschek H, Koch K, Wobus U et al (2005) Positional cues for the starch/lipid balance in maize kernels and resource partitioning to the embryo. Plant J 42:69–83. doi:10.1111/j.1365-313X.2005.02352.x

Rowland-Bamford AJ, Allen LH, Baker JT et al (1990) Carbon dioxide effects on carbohydrate status and partitioning in rice. J Exp Bot 41:1601–1608

Sakulsingharoj C, Choi SB, Hwang SK et al (2004) Engineering starch biosynthesis for increasing rice seed weight: the role of the cytoplasmic ADP-glucose pyrophosphorylase. Plant Sci (Amst Neth) 167:1323–1333. doi:10.1016/j.plantsci.2004.06.028

Scheibe R (1991) Redox-modulation of chloroplast enzymes a common principle for individual control. Plant Physiol 96:1–3. doi:10.1104/pp.96.1.1

Shannon JC, Pien FM, Liu KC (1996) Nucleotides and nucleotide sugars in developing maize endosperms – synthesis of ADP-glucose in brittle-1. Plant Physiol 110:835–843. doi:10.1104/pp.110.3.835

Shannon JC, Pien F-M, Cao H et al (1998) Brittle-1, an adenylate translocator, facilitates transfer of extraplastidial synthesized ADP-glucose into amyloplasts of maize endosperms. Plant Physiol 117:1235–1252. doi:10.1104/pp.117.4.1235

She K-C, Kusano H, Koizumi K et al (2010) A novel factor FLOURY ENDOSPERM2 is involved in regulation of rice grain size and starch quality. Plant Cell Online 22:3280–3294. doi:10.1105/tpc.109.070821

Sikka VK, Choi S-B, Kavakli IH et al (2001) Subcellular compartmentation and allosteric regulation of the rice endosperm ADPglucose pyrophosphorylase. Plant Sci (Amst Neth) 161:461–468. doi:10.1016/S0168-9452(01)00431-9

Singh S, Slattery CJ, Cho S-B et al (2003) Expression, kinetics and regulatory properties of native and recombinant ADP-glucose pyrophosphorylase isoforms from chickpea. Plant Physiol Biochem 41:399–405. doi:10.1016/S0981-9428(03)00046-9

Smidansky ED, Clancy M, Meyer FD et al (2002) Enhanced ADP-glucose pyrophosphorylase activity in wheat endosperm increases seed yield. Proc Natl Acad Sci U S A 99:1724–1729. doi:10.1073/pnas.022635299

Smidansky ED, Martin JM, Hannah LC et al (2003) Seed yield and plant biomass increases in rice are conferred by deregulation of endosperm ADP-glucose pyrophosphorylase. Planta 216:656–664. doi:10.1007/s00425-002-0897-z

Smith AM, Zeeman SC, Smith SM (2005) Starch degradation. Annu Rev Plant Biol 56:73–98. doi:10.1146/annurev.arplant.56.032604.144257

Smith-White BJ, Preiss J (1992) Comparison of proteins of ADP-glucose pyrophosphorylase from diverse sources. J Mol Evol 34:449–464. doi:10.1007/BF00162999

Stitt M, Zeeman SC (2012) Starch turnover: pathways, regulation and role in growth. Curr Opin Plant Biol 15:282–292. doi:10.1016/j.pbi.2012.03.016

Stitt M, Huber S, Kerr P (1987) Control of photosynthetic sucrose formation. In: The biochemistry of plants: a comprehensive treatise, vol 10. Academic, San Diego

Sullivan TD, Kaneko Y (1995) The maize brittle1 gene encodes amyloplast membrane polypeptides. Planta 196:477–484. doi:10.1007/BF00203647

Sullivan TD, Strelow LI, Illingworth CA et al (1991) Analysis of maize brittle-1 alleles and a defective Suppressor-mutator-induced mutable allele. Plant Cell Online 3:1337–1348. doi:10.1105/tpc.3.12.1337

Sweetlove L, Burrell M, Ap Rees T (1996) Starch metabolism in tubers of transgenic potato (*Solanum tuberosum*) with increased ADPglucose pyrophosphorylase. Biochem J 320:493–498

Tetlow IJ, Davies EJ, Vardy KA et al (2003) Subcellular localization of ADPglucose pyrophosphorylase in developing wheat endosperm and analysis of the properties of a plastidial isoform. J Exp Bot 54:715–725. doi:10.1093/jxb/erg088

Thorbjørnsen T, Villand P, Denyer K et al (1996) Distinct isoforms of ADPglucose pyrophosphorylase occur inside and outside the amyloplasts in barley endosperm. Plant J 10:243–250. doi:10.1046/j.1365-313X.1996.10020243.x

Tiessen A, Hendriks JH, Stitt M et al (2002) Starch synthesis in potato tubers is regulated by post-translational redox modification of ADP-glucose pyrophosphorylase a novel regulatory mechanism linking starch synthesis to the sucrose supply. Plant Cell 14:2191–2213. doi:10.1105/tpc.003640

Tiessen A, Prescha K, Branscheid A et al (2003) Evidence that SNF1-related kinase and hexokinase are involved in separate sugar-signalling pathways modulating post-translational redox activation of ADP-glucose pyrophosphorylase in potato tubers. Plant J 35:490–500. doi:10.1046/j.1365-313X.2003.01823.x

Tjaden J, Haferkamp I, Boxma B et al (2004) A divergent ADP/ATP carrier in the hydrogenosomes of *Trichomonas gallinae* argues for an independent origin of these organelles. Mol Microbiol 51:1439–1446. doi:10.1111/j.1365-2958.2004.03918.x

Tobias RB, Boyer CD, Shannon JC (1992) Alterations in carbohydrate intermediates in the endosperm of starch-deficient maize (*Zea mays* L.). Plant Physiol 99:146–152. doi:10.1104/Pp.99.1.146

Tsai C-Y, Nelson OE (1966) Starch-deficient maize mutant lacking adenosine diphosphate glucose pyrophosphorylase activity. Science 151:341–343. doi:10.1126/science.151.3708.341

Tuncel A, Okita TW (2013) Improving starch yield in cereals by over-expression of ADPglucose pyrophosphorylase: expectations and unanticipated outcomes. Plant Sci 211:52–60

Tuncel A et al (2014a) The role of the large subunit in redox regulation of the rice endosperm ADP-glucose pyrophosphorylase. FEBS J 281(21):4951–4963

Tuncel A et al (2014b) The rice endosperm ADP-glucose pyrophosphorylase large subunit is essential for optimal catalysis and allosteric regulation of the heterotetrameric enzyme. Plant Cell Physiol 55(6):1169–1183

Van Camp W (2005) Yield enhancement genes: seeds for growth. Curr Opin Biotechnol 16:147–153. doi:10.1016/j.copbio.2005.03.002

Ventriglia T, Kuhn ML, Ruiz MT et al (2008) Two Arabidopsis ADP-glucose pyrophosphorylase large subunits (APL1 and APL2) are catalytic. Plant Physiol 148:65–76. doi:10.1104/pp.108.122846

Wakuta S, Shibata Y, Yoshizaki Y et al (2013) Modulation of allosteric regulation by E38K and G101N mutations in the potato tuber ADP-glucose pyrophosphorylase. Biosci Biotechnol Biochem. doi:10.1271/bbb.130276

Wang Z, Chen X, Wang J et al (2007) Increasing maize seed weight by enhancing the cytoplasmic ADP-glucose pyrophosphorylase activity in transgenic maize plants. Plant Cell Tissue Organ Cult 88:83–92. doi:10.1007/s11240-006-9173-4

Wang E, Wang J, Zhu X et al (2008) Control of rice grain-filling and yield by a gene with a potential signature of domestication. Nat Genet 40:1370–1374. doi:10.1038/ng.220

Weber H, Heim U, Borisjuk L et al (1995) Cell-type specific, coordinate expression of two ADP-glucose pyrophosphorylase genes in relation to starch biosynthesis during seed development of *Vicia faba* L. Planta 195:352–361. doi:10.1007/BF00202592

Part V
Modification and Morphology

Chapter 12
Phosphorylation of the Starch Granule

Andreas Blennow

Abstract The presence of starch phosphate monoesters in native starch, especially in tuberous storage starch types, has for many years been known to impart unique and valuable functional assets of importance for food and materials applications. The quest of delineating the incorporation of phosphate groups in storage starch of crops, the general misconception over many years that starch phosphorylation is a "metabolic mistake" or a "side reaction", was disproved when the starch phosphorylator was discovered some 15 years ago. Over the recent years, additional data have evolved to demonstrate that phosphorylation of starch granules in plants is a built-in metabolic feature that is essential for well-functioning starch metabolism. This chapter will embrace the ubiquitous presence of starch phosphorylation in plants and its impact on plant metabolism and starch functionality and very recent studies demonstrating its tremendous impact on crop performance and future prospects for starch bioengineering and polysaccharide innovation.

Keywords Starch phosphorylation • Starch metabolism • Starch modification • Genetic modification

12.1 Starch Phosphorylation: Discovery and Early Work

12.1.1 Discovery of Starch Phosphate Esters

The first indication of the presence of charged substituents in starch was made in 1897 (Coehn 1897) showing that starch displayed an anodic migration behaviour as proven by electrodialysis of different hydrocolloids. Some years after (Fernbach 1904) acid hydrolysis was employed to demonstrate that the anionic nature was due to the presence of phosphate groups in the starch. Using the electrodialysis approach originally applied by Coehn followed by acid hydrolysis, organic phosphate monoesters were shown to be present in the amylopectin fraction

A. Blennow (✉)
Department of Plant and Environmental Sciences, University of Copenhagen, Thorvaldsensvej 40, 1871 Frederiksberg C, Denmark
e-mail: abl@plen.ku.dk

Y. Nakamura (ed.), *Starch*, DOI 10.1007/978-4-431-55495-0_12

(Samec 1914), and later (Takeda and Hizukuri 1982) it was concluded that only trace amounts were present in amylose. Using amylolytic hydrolysis and subsequent chemical analysis of the generated products, some unique resistant maltooligosaccharides could be detected and phosphate found as monoesters bound at the C-6 and the C-3 positions in this polyose material (Posternak 1935). This was later verified using nuclear magnetic resonance, NMR (Bay-Smidt et al. 1994; Blennow et al. 1998a; Hizukuri et al. 1970; Tabata and Hizukuri 1971). Phosphate esterified at the very labile C-2 position of the glucose units has been discussed (Tabata and Hizukuri 1971), but the presence of this phosphoester has not yet been verified. The physical effects, especially paste viscosity, of starch phosphate esters in naturally phosphorylated starch, especially potato starch, were notified somewhat later (Samec and Blinc 1941; Schreiber 1958). These discoveries paved the way for a multitude of potential applications of phosphorylated starch, which will be further detailed in the next sections of this chapter.

12.1.2 The Chemistry of Starch Phosphate Esters

12.1.2.1 The Presence of Phosphate Monoesters in the Amylopectin Chains

Amylopectin is a clustered and semi-crystalline polysaccharide having polymodal chain length distribution (Chaps. 1 and 3; Damager et al. 2010; Pérez and Bertoft 2010). The fact that the presence of phosphate esters mainly is in the amylopectin fraction is seemingly dependent on the biosynthesis and presence of these amylopectin structures. The concentration of phosphate esters in the starch is typically very low and depends on plant origin. For example, cereals normally contain $\leq$1 nmol/mg (Lim et al. 1994), while tubers are highly phosphorylated having up to 33 nmol phosphate/mg starch (Blennow et al. 2000; Hoover 2001; Carciofi et al. 2011; Table 12.1). The highest concentrations are found in tubers, especially those with modified starch having as high as 60 nmol phosphate/mg starch which translates to only 1 out of 200 glucose residues being substituted (Schwall et al. 2000; Blennow et al. 2005b; Wischmann et al. 2005). Yet, the physical and metabolic effects of the phosphate groups are extraordinary. It is now well confirmed that the phosphate groups are monoesterified at both the C-3 and the C-6 positions of the anhydrous pyranosidic glucose residues; C-6 phosphate esters are in majority contributing with approximately 70 % of the total phosphorylation degree (Hizukuri et al. 1970; Tabata and Hizukuri 1971; Bay-Smidt et al. 1994).

12.1.2.2 The Phosphorylated Chains

Phosphorylated chains in the starch granule have some specific features. As compared to non-phosphorylated amylopectin chains, the phosphorylated chains are typically longer, between degree of polymerisation (DP) 10 and 100

Table 12.1 Starch phosphate content (nmol Glc-6-P/mg starch) across plant species and organs demonstrating the tremendous variation

Botanical source	nmol Glc-6-P/mg starch
Potato tuber (*Solanum tuberosum*, cv Dianella)	17.0[a]
Potato tuber (*Solanum tuberosum*, line 87-BDN56)	33.1[b]
Potato tuber (*Solanum tuberosum*, line N-82-ATH-2)	7.8[b]
Potato tuber (*Solanum tuberosum*, line 90-BNT-2)	8.8[b]
Potato tuber (*Solanum tuberosum*, line 663)	13.4[b]
Potato tuber (*Solanum vernei*, line 1642/2)	12.2[b]
Potato leaf (*Solanum tuberosum*, cv Dianella)	4.5[a]
Cassava root (*Manihot esculenta*)	2.5[b]
Arrow root (*Maranta arundinacea*)	4.6[b]
Sorghum grain (*Sorghum bicolor*)	0.9[b]
Rice grain (*Oryza sativa*)	1.0[b]
Barley grain (*Hordeum vulgare*, cv Golden Promise)	0.8 (0.1)[c]
Barley grain (*Hordeum vulgare*, cv Golden Promise StGWD overexpressor)	7.5 (0.7)[c]

Data from Carciofi et al. (2011) and references therein as indicated
Typically, tubers and leaves have high phosphate content, while cereal grain has low content. The barley, StGWD transgenic line expresses the potato starch phosphorylator GWD1. All other starches were commercial and their exact botanical origin not well defined
cv cultivar, *SE* standard error
[a]Blennow et al. (1998a)
[b]Blennow et al. (2000)
[c]Carciofi et al. (2011)

(Blennow et al. 1998a, 2000; Tabata and Hizukuri 1971; Takeda and Hizukuri 1982). Hence, starch types having long chains, typically tuber starches, are highly phosphorylated. Since these starch types typically crystallise as the B-type crystalline polymorph, the crystalline polymorph can be readily predicted from the degree of phosphorylation or vice versa (Blennow et al. 2000). Early work clarified that an amylopectin unit chain can contain one or more phosphate groups (Blennow et al. 1998a); no phosphate groups are esterified on the nonreducing end or closer than nine glucosyl units from an α-1,6 branch point (Takeda and Hizukuri 1982). Dephosphorylated chains as short as 10 glucose units were detected in potato starch supporting these data but do not exclude phosphorylation close to the branch point on the main chain. The structure of phospho-oligosaccharides prepared by hydrolytic degradation of potato starch has provided additional valuable information on the relative positioning of the phosphate esters in the starch. Using a combination of neopullulanase and α-amylases (Kamasaka et al. 1997a), the relative clustering of phosphate groups in the starch chain was determined (Kamasaka et al. 1997b). C-6 or C-3 phosphates can be very closely placed and as close as two glucose residues apart. However, adjacent C-3 and C-6 phosphorylated glucose residues were also found in the hydrolysates indicating the presence of very dense local phosphorylation in the starch granule. In the amylopectin molecule, the α-1,6 branch points are clustered to generate highly branched regions termed clusters.

12.1.2.3 The Phosphorylated Chain Clusters

The so-called cluster model of amylopectin structure in the starch granule suggests that the amorphous lamellae present in the starch granule contain most of the α-1,6-glucosidic linkages and these are constructed of building blocks along the long chains of amylopectin, which collectively form a backbone of the macromolecule (Bertoft and Blennow 2009; Bertoft et al. 2012). The branched clusters are about DP50–DP130 and smaller densely branched building blocks typically being DP5–DP13 but can also be as large as >DP20 (Bertoft et al. 2012). Specifically, the cluster size for a normal potato starch and a transgenic low-phosphate starch with suppressed α-glucan, water dikinase (GWD) activity was DP127 and DP86, respectively (Jensen et al. 2013b). For a high-amylose/high-phosphate potato starch, generated by antisense suppression of starch branching enzyme, the cluster sizes were smaller and contained highly phosphorylated phospho-clusters with low degree of branching as compared to control (Wikman et al. 2011). These data indicate that, even though the effects on cluster size are minor, phosphate monoesters have some effect of the branch clusters in the amylopectin and are depicted in Fig. 12.1.

12.1.2.4 Phosphate Monoester Distribution in the Starch Granule

The starch granule is a complex but highly ordered structural entity with radial, or nearly radial, alternating amorphous and crystalline lamellae repeated with 9 nm spacing packed to form either hexagonal or pseudo-hexagonal crystalline packing of A-type and/or B-type crystalline polymorphs (Chap. 3; Damager et al. 2010; Pérez and Bertoft 2010). A schematic nano-level cross section of the parallel helices is depicted in Fig. 12.1 where the suggested positions of phosphate groups in the C-3 and C-6 position are indicated. From this model it is evident that phosphate groups can be monoesterified in both crystalline and amorphous parts of the granule. The location of phosphoesters in the so-called Naegeli dextrins, representing the crystalline lamella of the starch granule (Blennow et al. 2000; Wikman et al. 2013), confirmed that part of the phosphate groups were indeed located in highly ordered crystalline parts. Such positioning would require a very tight alignment in the crystalline network. As deduced from molecular models (Engelsen et al. 2003), the C-6 phosphate is tightly packed in one of the groves in the double helix. Such tight position was further indicated by its inability to form complex with copper ions as analysed by electron paramagnetic resonance (EPR, Blennow et al. 2006) and the low mobility as demonstrated by NMR (Larsen et al. 2008). As mentioned above, a substantial portion of the phosphate groups (79–84 %) are also found in the amorphous parts of the starch granule (Blennow et al. 2000; Wikman et al. 2013). As deduced from lintnerisation (slow acid hydrolysis of amorphous starch at high acid concentration), the amorphous parts are more enriched in C-6-bound phosphate than C-3-bound phosphate. As indicated, the distribution of phosphate monoesters in the native starch granule is apparently not random at the nm level.

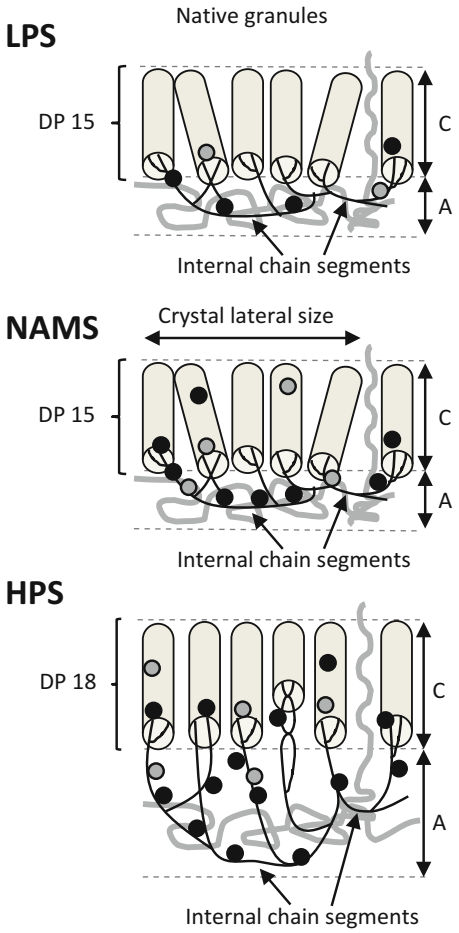

Fig. 12.1 Schematic representation of phosphorylated amylopectin as organised in the potato starch granule being engineered or selected for low (*LPS* low-phosphate starch), intermediate (*NAMS* normal amylopectin starch) and high phosphate (*HPS* high-phosphate starch) content. *Cylinders* represent amylopectin double helices, *black lines* amylopectin chains and *grey lines* amylose chains. The crystalline lamellae (*C*) and the amorphous lamellae (*A*) are enlarged in HPS. C-6-bound phosphate (*black circle symbol*) is enriched in the amorphous lamellae, whereas C-3 (*grey circle symbol*)-bound phosphate is more evenly distributed between crystalline and amorphous lamellae. *DP* degree of polymerisation (Reprinted with permission from Wikman et al. 2013. Copyright (2013) Wiley)

Such lack of phosphate distributional data stems from the inherent difficulty to analyse molecular objects and elements in semi-crystalline matrices like those found in the starch granule. However, at the micrometre scale, previous investigations using chemical surface gelatinisation (Jane and Chen 1993) demonstrated that phosphate concentration was lower in the gelatinised (surface) layers of the starch granules than in the remaining central un-gelatinised parts. This was supported by a particle-induced x-ray emission (PIXE) microscopic study, in which phosphate was found concentrated to the centre of a potato starch granule (Blennow et al. 2005a). However, in more recent studies using confocal laser light scanning microscopy (CLSM) with the phosphate-specific fluorescent phosphoprobe Pro-Q® Diamond, phosphate monoesters were rather found closer to the surface of the granules (Fig. 12.2; Glaring et al. 2006). More precisely, phosphate-related fluorescence was often found at a rim close to the surface or spread out through the starch granule (Fig. 12.2; Glaring et al. 2006). However, variations were found depending on

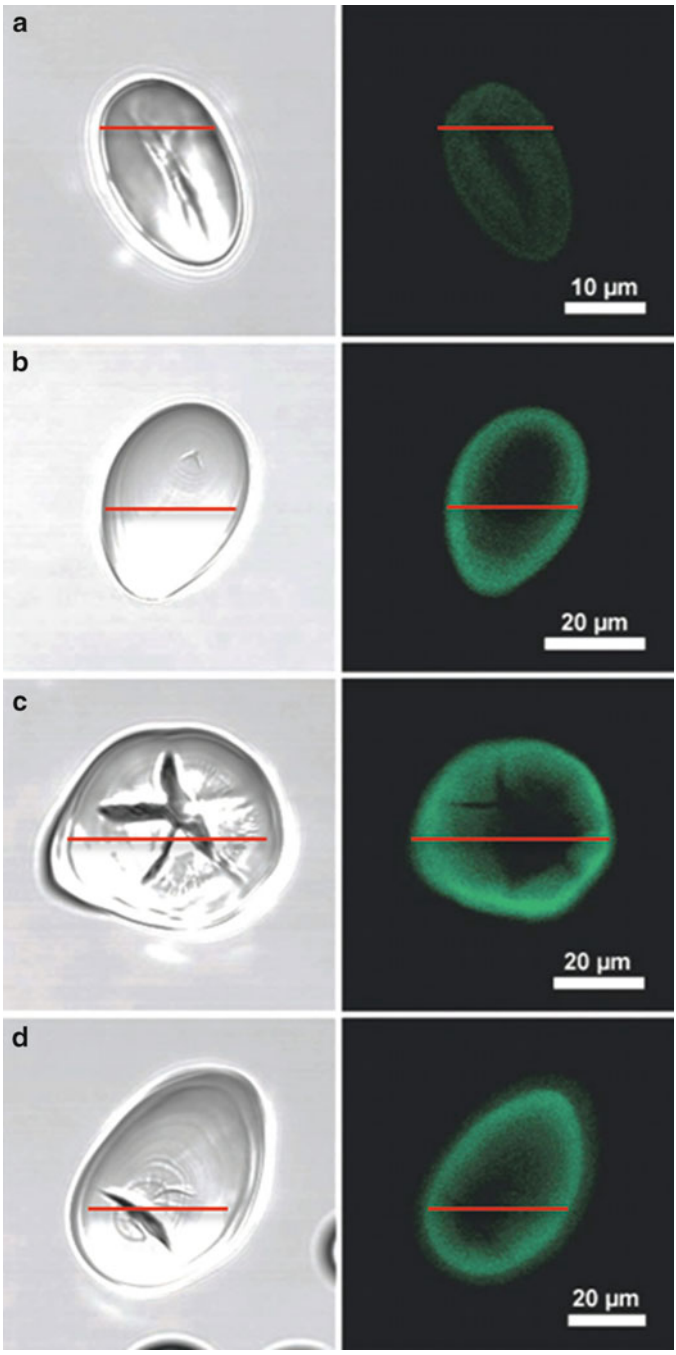
a
10 µm
b
20 µm
c
20 µm
d
20 µm

genotype, and it cannot be excluded that the accessibility of phosphate esters in the granule can affect such fluorescence data preventing a strict interpretation of phosphate distribution.

12.1.2.5 Effects of Phosphate in the Starch Granule

An interesting aspect related to physical and rheological features of starch is that many of these effects are considered to be attributed directly to the glucan configurations like α-1,6 branching structures and amylose content. However, it has recently been proven that many physical properties are directly accredited to the presence of phosphate esters in the starch. For example, their presence in the crystalline lamellae was first indicated by a minor suppression of the crystallinity as judged by differential scanning calorimetry (DSC, Muhrbeck and Eliasson 1991). Subsequent studies using an isogenic potato system (Kozlov et al. 2007) confirmed that the phosphate groups reduce the crystal stability by local amorphisation in the starch granule. The phosphate groups had an effect on the enthalpy of melting (ΔH) of the starch granules, but there was no effect on the melting temperature (Tm) supporting very local disturbance inducted by the phosphate groups. Further recent support for an amorphisation effect induced by phosphate was provided by differently phosphorylated lintners (Wikman et al. 2013). A strong negative correlation was found between melting enthalpy of the lintnerised starch and the phosphate content of the native starch granules, and a negative correlation was found between melting enthalpy and the phosphate content of the remaining lintnerised starch (Wikman et al. 2013). Phosphate groups also seem to affect interactions between branched and linear glucan chains in gelatinised starch. At high (30–40 %) starch paste concentrations, phosphate groups in the amylopectin repel chains between amylopectin and amylose likely resulting in phase separation between these polysaccharides in the paste (Jensen et al. 2013a).

Direct evidence for a phosphate-induced starch solubilising effect with relevance for plant cell metabolism was provided by studying crystallised phosphorylated maltodextrins in vitro (Hejazi et al. 2008). The main starch phosphorylating enzyme α-glucan, water dikinase (GWD) (see Sect. 12.4) efficiently catalysed phosphorylation of crystalline maltodextrins and induced solubilisation of both the neutral and the phosphorylated glucans in these crystalline aggregates (Hejazi et al. 2008).

Fig. 12.2 Wheat and potato starch granules visualised by transmission light (*left*) and the fluorescent phosphoprobe Pro-Q® Diamond (*right*). (**a**) Wheat granule showing the distinct equatorial groove and very low fluorescence. (**b**) Normal potato starch granule with intermediate fluorescence. (**c**) High-amylose potato granule showing internal cracking and high fluorescence. (**d**) High-amylopectin potato granule showing intermediate fluorescence, like the normal granule (**a**). *Red bars* indicate relative size and that phosphate monoesters are found close to the surface of the granules, more precisely at a rim close to the surface or evenly distributed over the starch granule. However, variations are found depending on genotype (Adapted with permission from Glaring et al. 2006. Copyright (2006) American Chemical Society)

Partial dephosphorylation of such A- and B-type crystallised phosphoglucans by the specific *Arabidopsis thaliana* glucan phosphatase AtSEX4 reduced solubilisation of non-phosphorylated chains in these aggregates (Hejazi et al. 2010).

Molecular force field models provided evidence to show that a phosphate ester at the C-6 position can be linked to amylopectin without disturbing its double helical structure. On the other hand, a phosphate ester at the C-3 position imparts molecular strain in the double helical motif thereby preventing optimal crystalline packing (Fig. 12.3; Blennow et al. 2002; Engelsen et al. 2003; Hansen et al. 2008). A general mechanism for phosphate-induced amorphisation and solubilisation based on such models is discussed in Sect. 12.3.

Naturally phosphorylated starch has a significant hydration capacity, and such starch types, especially potato starches, produce clear and very viscous pastes (Muhrbeck and Eliasson 1987; Wiesenborn et al. 1994; Viksø-Nielsen et al. 2001; Jobling 2004) affecting processing (e.g. Jensen et al. 2013b). These effects in relation to starch processing are discussed in more detail in Sect. 12.5.

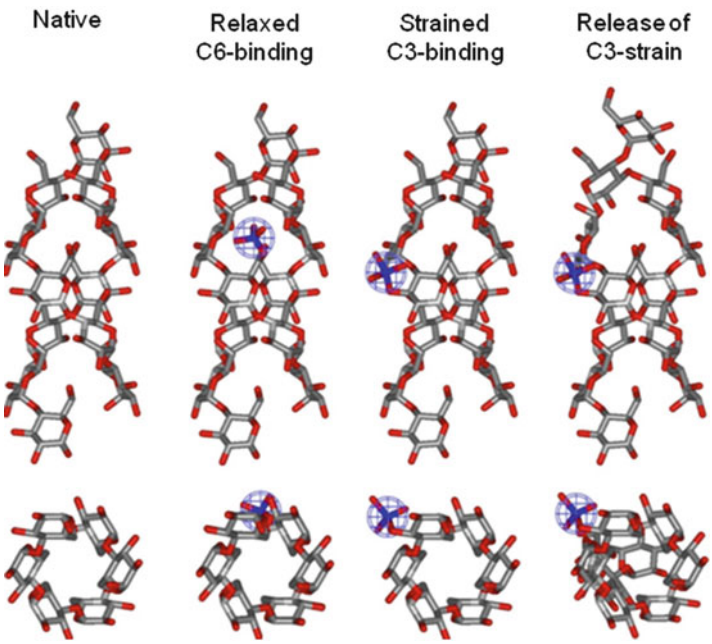

Fig. 12.3 Molecular force field models demonstrating that C-6 phosphorylation does not disturb the double helical structure, while C-3 phosphorylation is more exposed and induces molecular strain in the double helix. This strain can be released by introducing defects in the crystalline structure resulting in local amorphisation of the starch granule (From Blennow and Engelsen 2010. Reprinted with permission from Elsevier Ltd)

12.2 Phosphorylation of the Starch Granule: The Enzymes

Two enzymes are seemingly responsible for the phosphorylation of the starch granule, namely, the α-glucan, water dikinase 1 (GWD1) catalysing the formation of starch phosphate monoesters at the C-6 positions of the glucose units and the α-glucan, water dikinase 3/phosphoglucan, water dikinase GWD3/PWD catalysing phosphorylation at the C-3 positions in the amylopectin. This section will describe the catalysis, specificity and regulation of these two main enzymes. A third dikinase named GWD2 (Glaring et al. 2007) is a homologue of GWD1 but is extra-plastidial, and its function has not yet been elucidated. Generally, GWDs are found throughout the plant kingdom in grasses (Blennow et al. 2013; Tanackovic et al. 2014) and in dicotyledonous plants and algae (Baunsgaard et al. 2005; Glaring et al. 2007) and found in various organs like tubers of potato, sweet potato and yam and cereal endosperm of barley and maize, in fruits like banana and in leaves of *Arabidopsis* and potato (Mikkelsen and Blennow 2005; Ritte et al. 2000a, b) demonstrating their ubiquitous role in plant metabolism.

12.2.1 Discovery of R1/GWD1

α-Glucan, water dikinases (GWDs), responsible for the phosphorylation of starch, belong to a family comprising two classes of phosphotransferases with different substrate specificities and products. GWD was first discovered as a protein termed R1 in potato (*Solanum tuberosum*) by Lorberth et al. (1998). In *Arabidopsis* the enzyme is also known as SEX1 due to the starch excess phenotype found in the leaves (Ritte et al. 2006). The *Arabidopsis* mutant was well known before the discovery of the R1 protein (Yu et al. 2001) due to its starch excess phenotype. The discovery of the potato R1 protein was based on the loss of phosphate esters in potato tuber starch following antisense suppression of this protein (Lorberth et al. 1998). Four years later the activity of the GWD1 (EC 2.7.9.4) was elucidated (Ritte et al. 2002). GWD1 was proven to phosphorylate glucose residues in starch by transferring the β-phosphate of ATP to a glucosyl residue of amylopectin chains, and the γ-phosphate was transferred to water (Ritte et al. 2002). GWD1 was later confirmed to phosphorylate glucose residues exclusively at the C-6 position (Ritte et al. 2006).

Mainly amylopectin, and not amylose, is phosphorylated, which as a consequence explains the apparent substrate recognition requirement of GWD for α-1,6 bonds (Mikkelsen et al. 2004). GWD1 also preferably phosphorylates the long chains (degree of polymerisation, DP30–100) in the amylopectin molecule (Blennow et al. 1998a; Mikkelsen et al. 2004) giving additional evidence for the long phosphorylated chains fond in plants. However, since the catalytic efficiency of the GWD1 is dependent on the chain length of the substrate and that also amylose is being phosphorylated provided that the chains are long enough (Mikkelsen et al. 2004), the requirement of the branch point is possibly an effect of secondary (possibly helical and helical aggregates) structures recognised by the GWD1.

The necessity of such folded or aggregated glucan structures was supported by data (Hejazi et al. 2008) revealing that GWD1 readily phosphorylates crystallised maltodextrins of the B-type starch allomorph having longer side chains as compared to A-type crystalline polymorphs. Interestingly, GWD1 exhibited very low activity on identical soluble maltodextrins (Hejazi et al. 2008). However, both A-type and B-type crystalline polymorphs were efficiently catalysed by the GWD1 (and the GWD3/PWD homologue; see below, Hejazi et al. 2009) further pointing at the importance for preferred phosphorylation of granular structures with well-defined physical arrangements, most possibly directed by the α-1,6 bonds in amylopectin.

As mentioned, a third α-glucan, water dikinase named GWD2 (Glaring et al. 2007) is a homologue of GWD1 but is with a function that has not yet been elucidated. Knockout plants for this gene in *Arabidopsis* show no altered growth or starch and sugar levels, and subcellular localisation studies indicated that this GWD2 is extra-plastidial (starch is mainly synthesised in the plastid) and found expressed in companion cells of the phloem, with expression appearing just before the onset of senescence. Hence, this homologue is seemingly not directly involved in the major routes of transient starch degradation in plants.

12.2.2 Discovery of PWD/GWD3

Some years after the discovery of the GWD1 activity (Ritte et al. 2002), homologues of this protein in *Arabidopsis* were found (Baunsgaard et al. 2005; Kötting et al. 2005; Glaring et al. 2007). Some of these homologues were found to have distinctly different substrate specificities and catalytic activities. One type of these homologues was isolated from *Arabidopsis* and termed GWD3 (EC 2.7.9.5) (Baunsgaard et al. 2005) or phosphoglucan, water dikinase (PWD, Kötting et al. 2005).

The latter name of this enzyme was due to the apparent strict requirement for pre-phosphorylated starch or glucans for its activity (Baunsgaard et al. 2005; Kötting et al. 2005). PWD/GWD3 was demonstrated to strictly phosphorylate pre-phosphorylated starch at the C-3 position of glucose residues in amylopectin chains (Baunsgaard et al. 2005; Kötting et al. 2005; Ritte et al. 2006). The C-3-bound phosphate is a remarkable feature since phosphorylation at this position is rarely seen in nature. The very closely positioned C-3 and C-6 phosphorylated glucose residues found in hydrolysates of potato starch (Kamasaka et al. 1997b) indicate the in vivo action of PWD/GWD3 as well as the requirement for closely situated phosphate groups in the substrate glucan. However, it was later demonstrated that also non-phosphorylated chains could be phosphorylated provided that these were co-crystallised with phosphoglucans (Hejazi et al. 2009). Such differences in substrate specificity between GWD and PWD/GWD3 create metabolic dependence between these two activities in the plant cell that is potentially important for the physiological effect of starch phosphorylation. This is further described in Sect. 12.4.

An interesting feature of the GWDs, and many starch-acting enzymes generally, and of potential importance for their catalytic and physiological function, is the presence of starch-binding domains (SBD) of the type carbohydrate-binding module (CBM) from families 20 and 45 (www.CaZy.org). In GWD1 and GWD2 and also in the plastidial α-amylases, CBM45s are placed at the N-terminus, in tandem repeats (Mikkelsen et al. 2006; Glaring et al. 2007). Conserved tryptophan residues act as putative binding sites. Of specific interest is that CBM45 and CBM20 found in plants have lower affinity (mM) towards starch than typical microbial CBMs (μM) (Blennow and Engelsen 2010; Blennow and Svensson 2010; Glaring et al. 2011). In PWD/GWD3 CBMs from family 20 are found. This CBM family is one of the earliest and best characterised families that occur in several starch-active glycosyl hydrolases. CBM20s are 90–130-amino-acid residue long; some of them are conserved. Two tryptophans are suggested to be involved in glucan interaction. Like the CBM45s in the GWDs, the CBM20s show low affinity in PWD/GWD3 (Christiansen et al. 2009). In contrast to the high affinity of the extracellular CBMs, the low affinity found for these intracellular and plastidial CBMs would ensure dynamic and reversible interactions between the enzymes and starch granule in starch phosphorylation at different light regimes and at stress situations (Blennow and Engelsen 2010; Blennow and Svensson 2010; Glaring et al. 2011). Interestingly, starch granule binding of GWD is dependent on the cellular redox potential which varies on a diurnal basis. It remains to be tested of the CBMs that are involved in such diurnal and redox-dependent partitioning of the GWD. GWD in dark-adapted plants is inactive and attached to granules in its oxidised form. Activity can be reversed by reduction using dithiothreitol (DTT) in vitro, and the active form is expected to be soluble during the light period simultaneously with starch biosynthesis (Mikkelsen et al. 2005).

12.3 Effects on Metabolism

12.3.1 The Importance of Starch Phosphorylation in Plant Primary Metabolism

The transition from glycogen-based metabolism to photosynthesis-driven starch biosynthesis over evolution has imposed some functions that are essential for long-term carbohydrate storage (Ball et al. 1996, 2011). The evolution of starch phosphorylation in plants and algae is interesting since it is directly linked to the necessity of biosynthesis and long-term deposition dense and efficiently molecularly packed polysaccharides in the form of starch granules in the plant and the directly associated physiological problem to rapidly get metabolic access to the immobilised sugars in the starch granule. Even though it has not been possible to precisely trace the evolutionary origin of GWD and PWD/GWD3 (Ball et al. 2011), their function to permit mobilisation of crystalline glucan (starch) is evident. Starch deposited

in virtually all plants is phosphorylated, the only known exception so far being maize storage starch (even though the GWDs are expressed also in this plant, Blennow et al. 2002). I will now describe the current status of the effects of starch phosphorylation on starch degradation and starch biosynthesis with focus on effects related to starch granule structure.

12.3.2 Effects on Starch Degradation

The evolutionary appearance of starch, being in an insoluble and crystalline state in the cell, and the requirement of starch phosphorylation to permit its physical amorphisation, solubilisation and final amylolytic degradation, forms an important biological strategy for the plant to ensure a robust long-term energy storage capacity combined with regulated mobilisation of carbohydrate energy on metabolic demand (Blennow et al. 2002; Blennow and Engelsen 2010). As mentioned above, the knock-down or knockout of the phosphorylating enzymes, GWDs, in the plant leads to starch excess phenotypes in the leaves strongly suggesting that phosphate is required for efficient and complete degradation of the starch. The preferred location of phosphate monoesters in long-chain, B-type polymorphic starch granules (Takeda and Hizukuri 1982; Tabata and Hizukuri 1971; Blennow et al. 1998a) is an interesting feature as such amylopectin crystalline polymorphs are found in tubers and in green photosynthetic tissue of the plant. This indicates there are specific requirements for organising such starches in the plant. A possible explanation is to provide the ability for these starches to be degraded by specific enzymes in the highly hydrated organs as opposed to dry seeds storing starch having considerably less phosphate. B-type crystalline polymorphs are typically more resistant towards amylolytic hydrolysis in vitro (Wickramasinghea et al. 2009; Jane et al. 2003; Planchot et al. 1997) forming a rational explanation for the phosphorylation-dependent amorphisation of only this type of starch.

The partitioning of GWD between the starch granule surface and the stroma of the plastid is very dynamic and dependent on light and the redox potential in the plastid and also on the surface structure of the starch granule. In potato (*Solanum tuberosum*) and pea (*Pisum sativum*) leaf cells, GWD is found bound to starch granule at night where starch degradation takes place (Ritte et al. 2000a, b). Such binding is supposedly dependent both on the enzyme and on the starch granule surface. The importance of the starch granule surface characteristics for GWD interaction was indicated by in vitro binding of GWD showing that GWD was bound more efficiently to dark-adapted granules than to light-treated ones (Ritte et al. 2000a). Moreover, starch extracted from dark-adapted leaves from potato and darkened cells of the unicellular alga *Chlamydomonas reinhardtii* is more efficiently phosphorylated than light-treated cells (Ritte et al. 2004). However, the binding is more dynamic, and after a time period of phosphorylation and starch degradation, affinity decreases (Ritte et al. 2004). Similar effect can be seen in

turion organs of duckweed (*Spirodela polyrhiza*, Reimann et al. 2002). This effect points at a very intense but transient starch phosphorylation just preceding starch degradation. In turions GWD is potentially autophosphorylated, or at least subject to major conformational changes, prior to starch phosphorylation (Reimann et al. 2004). A transposon insertion in the tomato GWD gene caused male gametophytic lethality associated with a reduction in pollen germination (Nashilevitz et al. 2009). Such data have provided clear relationships between starch phosphorylation and starch degradation and physiologic effect thereof, but do not explain the mechanism behind.

As earlier mentioned, the presence of phosphate groups in the starch granule has some intriguing physical effects, and these can be of importance on how the starch granule is metabolised. Based on molecular models, it was speculated that the phosphate groups could provide molecular signals for starch degradation in the plant (Blennow et al. 2002). It was suggested (Blennow et al. 2002) that the phosphate groups themselves, by restructuring of the starch granule, increase the starch granule degradability. The first support for this hypothesis came some years later where data was provided to support that starch phosphate esters can stimulate hydrolytic enzyme activity in vitro verifying that phosphate esters per se can restructure the starch granule to stimulate its degradation (Edner et al. 2007). In vitro β-amylase activity was stimulated by GWD-catalysed starch phosphorylation. Simultaneous β-amylase- and isoamylase-catalysed starch hydrolysis was higher than for the β-amylase alone. This rate was further enhanced in the presence of GWD and ATP (Edner et al. 2007). Interestingly, modelling suggests that phosphoglucans have a stabilising effect on the β-amylase–glucan ligand complex (Dudkiewicz et al. 2008) supporting that starch phosphate esters can direct amylases to phosphorylated spots on starch granules. From these data it is evident that the presence of starch phosphate esters per se can stimulate starch degradation supporting the previously suggested starch amorphisising hypothesis (Blennow et al. 2002).

From a structural point of view, molecular force field models have provided support for how phosphate esters can stimulate starch degradation. As understood from data collected from nuclear magnetic resonance, x-ray diffraction, differential scanning calorimetry and enzyme kinetics and physiological data as described above, and recently supported by molecular modelling, phosphate exerts a stimulating effect on starch degradation (Blennow and Engelsen 2010). Force field models indicate that phosphate esters localised at the C-6 position of the glucose unit in starch do not necessarily disturb the double helical structure in the granule. However, such C-6 phosphorylation can induce hydration and voids in between the helical arrays to distort helix–helix interactions. Such local disturbance in the starch granule can stimulate endo-active hydrolases. Subsequent C-3 phosphorylation catalysed by the PWD/GWD3 can induce helix break (Fig. 12.3) to permit access for exoenzymes such as β-amylases and debranching enzymes such as isoamylase on these unwounded chains (Blennow et al. 2002; Engelsen et al. 2003; Hansen et al. 2008; Blennow and Engelsen 2010).

This hypothesis has gained support from in vitro studies using B-type crystallised maltodextrins as models for the starch granule (Hejazi et al. 2008).

These crystalline aggregates, phosphorylated by GWD1, were readily solubilised. Also chains in these aggregates that were not phosphorylated were efficiently solubilised. Amylolytic enzymes readily attack these solubilised glucans. Further studies demonstrated that both A- and B-type starch crystals were phosphorylated and showed phase transition upon phosphorylation (Hejazi et al. 2010). The hypothesis suggested for these data recommended that phosphorylation by GWD1 at the C-6 position leads to a local structural disturbance to gain access of both non-phosphorylated and phosphorylated glucans to further permit and stimulate C-3 phosphorylation by PWD/GWD3. In conclusion, the two main hypotheses, originally based on molecular models, and followed by physiological and enzymatic data seemingly support each other to form a more robust mechanistic explanation for the stimulation of starch degradation by starch phosphorylation.

Importantly, complete degradation of generated phosphoglucan also requires phosphatases. The phosphatase SEX4 in *Arabidopsis* and in maize has been demonstrated to efficiently dephosphorylate both C-3 and C-6 phosphate esters (Kötting et al. 2009; Hejazi et al. 2010), while an additional phosphatase studied in *Arabidopsis*, LSF2 (LIKE SEX FOUR2), is specific for the C-3 phosphate esters (Santelia et al. 2011). The detailed effects and dynamics of starch degradation dependent on these hydrolytic enzymes are described in Chap. 7 of this book.

12.3.3 Effects on Starch Biosynthesis

As explained in the previous section, there is a clear relationship between starch phosphorylation and starch degradation. Effects on starch biosynthesis are less clear. However, some evidence exists for a role of starch phosphorylation for the formation of a functional and well-structured starch granule. To modulate crystallinity and to prepare the starch granule for dissolution prior to degradation and on physiological demand, most starches are phosphorylated during their biosynthesis (Blennow and Engelsen 2010). Hence, there seems to be a requirement for a biosynthesis-driven pre-phosphorylation. Cooperatively, during starch biosynthesis, branching enzyme, debranching enzyme and GWD act with starch synthases to synthesise proper molecular structures for further growth and crystallisation of the granule permitting efficient molecular packing combined with built-in granule degradability. Starch phosphorylation has not been clearly demonstrated to be an absolutely necessary process in starch biosynthesis. However, some notable effects deserve attention.

Studies on GWD affinity for starch granules and phosphorylating activity have demonstrated that GWD is very dynamic. Its association with starch granules prior to and concurrently with starch degradation seems to be important as described above. However, as deduced from by ^{32}P radiolabelling (Nielsen et al. 1994) and by demonstration of active starch phosphorylation in isolated intact potato amyloplasts fed with sucrose (Wischmann et al. 1999), starch is also phosphorylated during starch biosynthesis, and GWD can have a distinct role also here. GWD activity in leaves has been demonstrated to be dependent on the cellular redox potential, which

in turn is directly linked to the dark–light cycle of the plant cell. In potato, it has been found that GWD isolated from dark-adapted plants is inactive and attached to the starch granules in its oxidised form. Binding and GWD activity can be reversed by reducing the enzyme using dithiothreitol (DTT) in vitro (Mikkelsen et al. 2005). These data suggest that, in its active form during light periods, reduced and soluble GWD phosphorylates starch granules simultaneously with starch biosynthesis (Mikkelsen et al. 2005).

In favour of a role of starch phosphorylation in starch biosynthesis, this seems to be affected by starch phosphorylation as indicated by altered starch deposition in plants with suppressed or overexpressed GWD activity. The deposition of starch in a storage organ such as the potato tuber can be regarded a system virtually devoid of starch degradation. Antisense suppression of GWD1 in potato tubers results in starch granules with altered structure (cracks and fissures) and higher amylose content (Viksø-Nielsen et al. 2001; Glaring et al. 2006) supporting the starch phosphorylation has an important role to form a correct granule structure during starch biosynthesis. Data from the cereal system give further support of this view.

Overexpression of the potato GWD1 gene in the barley endosperm results in grain starch with tenfold increased phosphate content (Carciofi et al. 2011). Interestingly, the starch granules had altered topography showing more porous surfaces and irregular shapes as compared to control (Carciofi et al. 2011). However, the yield of starch in the grain was not significantly affected ruling out significant effects of stimulation of starch degradation in this system. This line also degraded grain starch similarly to the control during germination, but protein and β-glucan degradation was stimulated (Shaik et al. 2014). Hence, it is possible that starch phosphorylation, taking place during biosynthesis in grain filling, can dictate starch granule organisation. RNA interference (RNAi)-mediated downregulation of GWD1 in the wheat endosperm resulted in decreased starch-bound phosphate, an increase in grain size and plant biomass but unaltered starch content (Ral et al. 2012). These data are not readily explained as a direct effect of suppressed stimulation of starch degradation in the grain but rather a more complex metabolic change in grain development potentially affecting also starch biosynthesis.

Very recently, interesting effects of GWD1 suppression were demonstrated possibly relating starch phosphorylation to starch biosynthesis. As for the barley grain data, overexpression of GWD1 did not stimulate starch degradation in leaves of *Arabidopsis*. Moreover, starch degradation was not suppressed until GWD1 was reduced down to 30 % activity (Skeffington et al. 2014). Interestingly, this reduction of GWD1 inhibited starch biosynthesis in the light indicating that starch phosphorylation can stimulate starch biosynthesis as well as starch degradation.

Moreover, starch granules isolated from transgenic *Arabidopsis thaliana* plants with reduced or no GWD activity had glucan chain structures at the granule surface that was suggested to limit the general accessibility to starch-active enzymes, being degradative or biosynthetic (Mahlow et al. 2014). These data support a very general and biophysic effect of starch phosphorylation as previously postulated (Blennow and Engelsen 2010).

In summary, the importance of GWDs in starch degradation is founded on that phosphate groups that decrease the local order within the starch granule and by that facilitate the access of degrading enzymes. However, such effects can also stimulate starch biosynthesis when such transferases are active in the plant. Hence, GWDs play very complex key roles both in the transitory starch metabolism (Ritte et al. 2004; Mikkelsen et al. 2005; Zeeman et al. 2010; Edner et al. 2007) and the cereal endosperm metabolism (Ral et al. 2012; Shaik et al. 2014). Starch phosphorylation affects primary metabolism in the plant as observed both for starch biosynthesis and starch degradation. However, the exact metabolic role of starch phosphorylation remains to be elucidated.

12.4 Starch Phosphate Bioengineering and Implications for Technology

The main volume of produced starch in the world is chemically or physically modified to achieve proper functionality. Raw starches are not suitable for most applications due to high and unstable viscosity and retrogradation following gelatinisation. Modifications typically include improving processability like reduction of viscosity or melting temperature and improving general performance, such as improving film formation or emulsification properties (Mason 2009). Conventional chemical technology includes esterification, etherification or oxidation as well as acid treatment (Chiu and Solarek 2009). For physical modification extrusion cooking, pregelatinisation by heating in aqueous alcohol or alkaline alcohol and heat–moisture treatments are carried out (Haghayegh and Schoenlechner 2011). Just as for natural phosphorylation, such treatments change the crystalline structure of the starch granule.

12.4.1 Clean Phosphorylation of Starch Directly in the Crop

Over the recent years a gradual redirection from conventional chemical modification to more clean technologies such as physical modification and bioengineering by, for instance, enzymatic modification, is emerging. For starch phosphorylation, naturally or chemically phosphorylated, this type of modification yields a tremendous hydration capacity producing clear and highly viscous starch pastes (Muhrbeck and Eliasson 1987; Wiesenborn et al. 1994; Viksø-Nielsen et al. 2001; Thygesen et al. 2003; Jobling 2004). If carried out directly in the crop by transgene biotechnology, modern breeding or mutagenesis, starch functionality can be improved with little or no requirement for postharvest processing having tremendous potential economic and environmental advantages. Engineering the expression of GWD1 or GWD3/PWD is the obvious strategy to alter starch phosphate in the crop. However,

engineering the expression of other enzymes in starch metabolism can also generate changes in starch phosphorylation. Substantial alterations in the phosphate content are obtained by changing the activities of GWD1 or starch branching enzyme (SBE) in the plant. On the contrary, only minor effects are accomplished by antisense suppression of starch synthases (SSs).

The effects of suppression of the GWD1 in potato (Lorberth et al. 1998) or the SEX1 homologue in *Arabidopsis* (Yu et al. 2001), being the original discoveries of the origin of starch phosphorylation, result in starch that is almost totally depleted in phosphate. As mentioned, in the *Arabidopsis* leaf, a starch excess phenotype is observed, and in both *Arabidopsis* and potato, the amylose content is increased (Viksø-Nielsen et al. 2001). The manipulation of the GWD1 has been described in many patents including the overexpression in wheat (Schewe et al. 2002) and corn (Lanahan and Basu 2005) leading to increased viscosity of the starch paste. Moreover, the use of combinations with the overexpression of both starch synthase II and GWDs in rice and corn has been described (Frohberg 2008). The overexpression in *Arabidopsis* the GWD3/PWD also results in increased phosphate content as described in a patent (Frohberg et al. 2012). Recently, overexpression of the potato GWD1 in barley was described resulting in increased phosphorylation (Carciofi et al. 2011) and a more "potato-like" starch. The starch functional effects of such engineering must however be further evaluated since many side effects can be noted. For example, in potato tubers with suppressed GWD1, the amylopectin molecular weight is decreased (Viksø-Nielsen et al. 2001) having adverse effects on starch viscosity.

The engineering of other enzymes in starch biosynthesis also often affects starch phosphorylation since the starch substrate for the GWDs is altered, chaining GWD activity. For example, suppression of SBE in most plants results in significantly increased amylose concentrations and often also in increased lengths of the amylopectin unit chains. An interesting side effect is the dramatic approximately threefold increase in the level of starch phosphate (Schwall et al. 2000; Blennow et al. 2005b). The reason for the latter effect is supposedly that the endogenous GWD1 activity is stimulated by long (DP30–DP100) amylopectin chains (Mikkelsen et al. 2004), which are enriched in these plants. Amylose is possibly not phosphorylated in these plants despite of its long chains. Suppression of the granule-bound starch synthase (GBSS) moderately increases the phosphate concentration as an effect of the removal of amylose, accounting for about 20–30 % of the starch, which is not phosphorylated. Suppression of the soluble starch synthases (SSSs), most of which are responsible for the biosynthesis of amylopectin, also affects the phosphate content. However, such engineering is more unpredictable. When the total SSS activity is repressed, the starch phosphate content is somewhat reduced (Lloyd et al. 1999), whereas suppression of only the SSIII isoform increases the phosphate content by 70 % (Abel et al. 1996), again possibly due to altered amylopectin structure. Different combinations of SSS suppression in the potato tuber result in

very different starch functionalities, for example, freeze–thaw stability, which can be obtained by engineering short starch chains (and low amylose content) combined with a high phosphate content (Jobling et al. 2002).

12.4.2 Technical Use of Bioengineered Phosphorylated Starch

Phosphorylated starches, either naturally selected or bred, transgenics or mutants, are of tremendous value for technical applications. Potato starch, being highly phosphorylated and very clean, is widely used, especially in paper manufacturing. The optimal performance of potato starch in paper manufacturing is potentially an effect of the phosphate esters providing functional groups and high hydration leading to stickiness of the starch paste. However, in a study of potato starches with different phosphate contents and viscosities, it could be concluded that wet-end paper manufacturing performance did not directly correlate with the phosphate level but with a stickiness parameter, possibly related to the presence of phosphate (Blennow et al. 2003). Starch phosphate esters, being natural plasticisers of the starch, can also be potentially exploited for bioplastic purposes. The function of phosphate is however not readily predictable, and recently a water-nondeformable starch film was generated (Gillgren et al. 2011) using the potato tuber starch engineered for low phosphate content by antisense suppression of GWD1. The phosphate levels of this starch are comparable to the levels obtained in the hyperphosphorylated barley starch overexpressing the potato GWD in the grain (Carciofi et al. 2011) suggesting that starch phosphate can be balanced to obtain optimal levels for bioplastic purposes.

Starch phosphate-induced hydration of starch is also of importance for processing due to the noticeable hydration and swelling of phospho-starch. A striking example is a recent enzyme-assisted modification of starch at high starch concentrations to restrict swelling (Jensen et al. 2013b). Phosphorylated starches behaved very different from typical non-phosphorylated starches like maize starch, and it was demonstrated for branching enzyme modification at these high substrate concentrations that phosphorylated starches reacted more like in solution, while non-phosphorylated starch types could be enzymatically cross-linked due to restricted hydration (Jensen et al. 2013b).

The preparation of phospho-maltooligosaccharides (POs) using enzymatic hydrolysis from potato starch has caught special attention for biomedical and food additives (Kamasaka et al. 2003). For example, POs solubilise calcium and iron salts as a direct effect of phosphate–calcium interactions (Kamasaka et al. 1995, 1997b). POs complexed with calcium (POs–Ca) have been demonstrated to exert high absorption in the intestinal tract (To-o et al. 2003) thereby increasing uptake of calcium in the body. Moreover, POs enhance tooth enamel remineralisation (Tanaka et al. 2012) demonstrating potential for use in dental health.

12.5 Future Perspectives

12.5.1 The Future Potential of Starch as a Robust Raw Material

Polysaccharides in general, and starch especially, have tremendous potential for solving future challenges in providing environmentally friendly solutions in the health, technical, food and nonfood sectors. Heading towards more environmentally friendly starch modification, clean, natural starch phosphorylation can potentially partly phase out chemical modification such as phosphorylation as a clean alternative for starch modification. Starch phosphorylation has profound effects on starch biosynthesis and mobilisation in seeds and grain (e.g. Shaik et al. 2014). As an effect, bioengineering phosphorylation in crops also has potential in increasing crop yield as mentioned above (Ral et al. 2012; Weise et al. 2012). Larger volumes and novel, functionalised raw materials are needed to build a robust bioeconomy (Enriques 1998) to take care of expected future major challenges related to climate change and an increasing human population. As such, starch is a multipurpose raw material with tremendous potential to overcome conflicting food, feed and fuel aspects that must be eliminated by increasing crop and starch yield without expanding agricultural area.

12.5.2 The Requirement of Clean, Efficient and Acceptable Production Methods of Modified Starch in Crops

Public concern about transgene (GMO) technology must be taken care of by openly discussing classical and modern breeding procedures including genetic modification, the use of synthetic genes and transgenes or an important upcoming alternatives such as the so-called genome editing (Cermak et al. 2011) which is a collective term for targeting specific genes with mutagenesis or the use of *cisgenes* (Schouten and Jacobsen 2008; Godwin et al. 2009) which uses genes from the plant itself or genes from sexually compatible and genetically closely related species that can intercross. Classical mutagenesis combined with state-of-the art screening will possibly have an important role in the future (Slade et al. 2012).

12.5.3 Cisgenesis for Crop Improvement

In favour of a cisgenic strategy, the European Food Safety Authority (EFSA) recently concluded that an equivalent level of hazard can be associated with cisgenesis as for conventional plant breeding. This assessment can open up possibilities

for case-by-case exemptions of cisgenic plants from the directives that regulate the use of genetically modified crops (Schouten and Jacobsen 2008; EFSA Panel on Genetically Modified Organisms 2012).

12.5.4 Genome Editing

A very new and interesting way forward to improve starch quantity and quality like starch phosphorylation directly in the crop can be represented by novel genome editing technologies. Such techniques are based on the specific recognition of gene sequences in the plant and following mutagenesis in that specific gene. If performed using the so-called transient expression of the foreign genes in these systems, i.e. the gene is not permanently integrated in the plant genome, these techniques can be regarded as a non-GMO approach. To date three main systems are available including zinc-finger domains, TALEN factors and CRISPR. Zinc-fingers are built-in functions in transcription factors and zinc-finger nucleases permitting specific recognition of gene segments and their subsequent cleavage and mutagenesis (Desjarlais and Berg 1992). The so-called TALEN (transcription activator-like effector nuclease) system contains DNA-binding domains linked to artificial restriction enzymes generated by fusing a TAL effector DNA-binding domain to a DNA cleavage domain (Boch et al. 2009; Cermak et al. 2011). An even more recent genome editing technology is the so-called CRISPR (clustered regularly interspaced short palindromic repeats)/Cas9/sgRNA system for targeted gene mutagenesis.

Zinc-finger transcription factors, TALENs and CRISPR technologies (Townsend et al. 2009; Boch et al. 2009; Miller et al. 2011; Sanjana et al. 2012) can become powerful tools for targeting genes in starch biosynthesis and phosphorylation. TALENs and zinc-finger nucleases have proved highly efficient in targeting precise genes and disrupting loci in rice and maize (Shukla et al. 2009; Li et al. 2012), and the CRISPR system was tested in *Arabidopsis*, tobacco, sorghum and rice models for knocking out specific genes (Jiang et al. 2013). Interestingly, problems related to side effects by complete removal of proteins in enzyme complexes by using traditional knockout or knock-down expression are solved by these technologies since they can confer site-directed mutagenesis of catalytically important active amino acid residues without affecting protein biosynthesis.

To this end genome editing has not been documented for starch bioengineering. However, classical mutagenesis strategies are well founded with many examples from the cereal high-amylose system (Blennow et al. 2013). Recently, advanced mutant screening including targeting induced local lesions (TILLING) in genomes of wheat (Slade et al. 2012) and simple sequence repeat (SSR) markers in BEIII in rice (Yang et al. 2012) was accomplished as non-GMO strategies to isolate high-amylose lines. Since BE is involved in the biosynthesis of amylopectin, it should be noted that the so-called high-amylose starch synthesised by BE-deficient plants

actually synthesises modified, long-chain amylopectin, even though such starch types very much resemble natural amylose with respect to molecular size (e.g. Carciofi et al. 2012).

Future non-GMO efforts for more advanced starch functionalisation like phosphorylation await development and establishment.

12.6 Concluding Remarks

Starch phosphorylation plays a fundamental role in plant and crop performance by restructuring the starch granule on metabolic demand. For starch mobilisation, granule physical amorphisation and solubilisation permit starch granule amylolytic degradation. Phosphorylation also unambiguously affects starch biosynthesis, but the effects are less clear, and further research is needed to understand how phosphorylation affects starch deposition in the plant. Starch is a multipurpose raw polysaccharide with invaluable importance for all living organisms and human society. As such, starch has a wide application potential for food, feed and fuel purposes. Most starches must be industrially modified prior to use. Often these processes are expensive and affecting the environment. Phosphorylated starch has unique properties, and upcoming clean starch bioengineering strategies including postharvest enzyme-based and *in planta* (such as genome editing) modulation of starch phosphorylation can provide society with high-value and environmentally friendly modified raw materials to help realising a true bioeconomy.

References

Abel GJW, Springer F, Willmitzer L, Kossmann J (1996) Cloning and functional analysis of a cDNA encoding a novel 139 kDa starch synthase from potato (*Solanum tuberosum* L.). Plant J 10:981–991

Ball S, Guan HP, James M et al (1996) From glycogen to amylopectin: a model for the biogenesis of the plant starch granule. Cell 86:349–352

Ball S, Colleoni C, Cenci U et al (2011) The evolution of glycogen and starch metabolism in eukaryotes gives molecular clues to understand the establishment of plastid endosymbiosis. J Exp Bot 62:1775–1801

Baunsgaard L, Mogensen HL, Mikkelsen R et al (2005) A novel isoform of glucan water dikinase phosphorylates prephosphorylated α-glucans and is involved in starch degradation in Arabidopsis. Plant J 41:595–605

Bay-Smidt AM, Wischmann B, Olsen CE, Nielsen TH (1994) Starch bound phosphate in potato as studied by a simple method for determination of organic phosphate and p-31-nmr. Starch/Stärke 46:167–172

Bertoft E, Blennow A (2009) Chapter 4: Structure of potato starch. In: Singh J, Kaur L (eds) Advances in potato chemistry and technology. Academic Press (imprint of Elsevier), Burlington, pp 83–98

Bertoft E, Koch K, Åman P (2012) Building block organisation of clusters in amylopectin from different structural types. Int J Biol Macromol 50:1212–1223

Blennow A, Engelsen SB (2010) Helix-breaking news: fighting crystalline starch energy deposits in the cell. Trends Plant Sci 15:236–240
Blennow A, Svensson B (2010) Dynamics of starch granule biogenesis – the role of redox regulated enzymes and low affinity CBMs. Biocatal Biotransform 28:3–9
Blennow A, Bay-Smidt AM, Wischmann B et al (1998a) The degree of starch phosphorylation is related to the chain length distribution of the neutral and the phosphorylated chains of amylopectin. Carbohydr Res 307:45–54
Blennow A, Bay-Smidt AM, Olsen CE et al (1998b) Analysis of glucose-3-P in starch using high performance ion exchange chromatography. J Chromatogr 829:385–391
Blennow A, Bay-Smidt AM, Olsen CE et al (2000) The distribution of covalently bound starch-phosphate in native starch granules. Int J Biol Macromol 27:211–218
Blennow A, Engelsen SB, Nielsen TH et al (2002) Starch phosphorylation – a new front line in starch research. Trends Plant Sci 7:445–450
Blennow A, Bay-Smidt A, Leonhardt P et al (2003) Starch paste stickiness is a relevant native starch selection criterion for wet-end paper manufacturing. Starch/Staerke 55:381–389
Blennow A, Sjöland KA, Andersson R et al (2005a) The distribution of elements in the native starch granule as studied by particle-induced X-ray emission and complementary methods. Anal Biochem 347:327–329
Blennow A, Wischmann B, Houborg K et al (2005b) Structure - function relationships of transgenic starches with engineered phosphate substitution and starch branching. Int J Biol Macromol 36:159–168
Blennow A, Houborg K, Andersson R et al (2006) Phosphate positioning and availability in the starch granule matrix as studied by EPR. Biomacromolecules 7:965–974
Blennow A, Jensen SL, Shaik SS et al (2013) Future cereal starch bioengineering – cereal ancestors encounter gene-tech and designer enzymes. Cereal Chem 90:274–287
Boch J, Scholze H, Schornack S et al (2009) Breaking the code of DNA binding specificity of TAL-type III effectors. Science 326:1509–1512
Carciofi M, Shaik SS, Jensen SL et al (2011) Hyperphosphorylation of cereal starch. J Cereal Sci 54:339–346
Carciofi M, Blennow A, Jensen SL et al (2012) Concerted suppression of all starch branching enzyme genes in barley produces amylose-only starch granules. BMC Plant Biol 12(223):1–16
Cermak T, Doyle EL, Christian M et al (2011) Efficient design and assembly of custom TALEN and other TAL effector-based constructs for DNA targeting. Nucleic Acids Res 39:e82
Chiu C-W, Solarek D (2009) Modification of starches. In: BeMiller JN, Whistler RL (eds) Starch: chemistry and technology. Academic, New York, pp 629–655
Christiansen C, Abou Hachem M, Glaring MA et al (2009) A CBM20 low affinity starch binding domain from glucan, water dikinase. FEBS Lett 583:1159–1163
Coehn A (1897) Über elektrische Wanderung von Kolloiden. Z Electrochem 4:63–67
Damager I, Engelsen SB, Blennow A et al (2010) First principles insight into starch-like α-glucans: their synthesis, conformation and hydration. Chem Rev 110:2049–2080
Desjarlais JR, Berg JM (1992) Toward rules relating zinc finger protein sequences and DNA binding site preferences. Proc Natl Acad Sci U S A 89:7345–7349
Dudkiewicz M, Siminska J, Pawlowski K et al (2008) Bioinformatics analysis of oligosaccharide phosphorylation effect on the stabilization of the β-amylase ligand complex. J Carbohydr Chem 27:479–495
Edner C, Li J, Albrecht T, Mahlow S et al (2007) Glucan, water dikinase activity stimulates breakdown of starch granules by plastidial β-amylases. Plant Physiol 145:17–28
EFSA Panel on Genetically Modified Organisms (2012) Scientific opinion addressing the safety assessment of plants developed through cisgenesis and intragenesis. EFSA J 10(2):2561
Engelsen SB, Madsen MAO, Blennow A et al (2003) The phosphorylation site in double helical amylopectin as investigated by a combined approach using chemical synthesis, crystallography and molecular modeling. FEBS Lett 541:137–144
Enriques J (1998) Genomics – genomics and the world's economy. Science 281(5379):925–926

Fernbach A (1904) Quelques observations sur la composition de l'amidon de pommes de terre. C R Acad Sci 138:428–430
Frohberg, C (2008) Genetically modified plants which synthesize a starch having increased swelling power. International patent WO 08/017518
Frohberg C, Kötting O, Ritte G et al (2012) Plants with increased activity of a starch phosphorylating enzyme. US patent application 2012/0017333 A1
Gillgren T, Blennow A, Pettersson AJ, Stading M (2011) Modulating rheo-kinetics of native starch films towards improved wet-strength. Carbohydr Polym 83(2):383–391
Glaring MA, Koch KB, Blennow A (2006) Genotype specific spatial distribution of starch molecules in the starch granule: a combined CLSM and SEM approach. Biomacromolecules 7:2310–2320
Glaring MA, Zygadlo A, Thorneycroft D et al (2007) A cytosolic isoform of α-glucan, water dikinase from Arabidopsis is expressed in the companion cells of the phloem. J Exp Bot 58(14):3949–3960
Glaring MG, Baumann MJ, Hachem MA et al (2011) Characterization of the CBM45 family of low-affinity starch-binding domains involved in plastidial starch metabolism. FEBS J 278:1175–1185
Godwin ID, Williams SB, Pandit PS et al (2009) Multifunctional grains for the future: genetic engineering for enhanced and novel cereal quality. In Vitro Cell Dev Biol Plant 45(4):383–399
Haghayegh G, Schoenlechner R (2011) Physically modified starches: a review. J Food Agric Environ 9:27–29
Hansen PI, Spraul M, Dvortsak P et al (2008) Starch phosphorylation – maltosidic restrains upon 3'- and 6'- phosphorylation investigated by chemical synthesis, molecular dynamics modeling and NMR spectroscopy. Biopolymers 9:179–193
Hejazi M, Fettke J, Haebel S et al (2008) Glucan, water dikinase phosphorylates crystalline maltodextrins and thereby initiates solubilization. Plant J 55:323–334
Hejazi M, Fettke J, Paris O et al (2009) The two plastidial starch-related dikinases sequentially phosphorylate glucosyl residues at the surface of both the A- and B-type allomorphs of crystallized maltodextrins but the mode of action differs. Plant Physiol 150:962–976
Hejazi M, Fettke J, Kötting O et al (2010) The laforin-like dual-specificity SEX4 from Arabidopsis thaliana hydrolyses both C-6 and C-3-phosphate esters introduced by starch-related dikinases and thereby affects phase transition of α-glucans. Plant Physiol 152:711–722
Hizukuri S, Tabata S, Nikuni Z (1970) Studies on starch phosphate. Part 1. Estimation of glucose-6-phosphate residues in starch and the presence of other bound phosphate(s). Starch/Stärke 22:338–343
Hoover R (2001) Composition, molecular structure, and physicochemical properties of tuber and root starches: a review. Carbohydr Polym 45:253–267
Jane J-L, Chen JJ (1993) Internal structure of the potato starch granule revealed by chemical gelatinization. Carbohydr Res 247:279–290
Jane J-L, Ao Z, Duvick SA et al (2003) Structures of amylopectin and starch granules: how are they synthesized? J Appl Glycosci 50:167–172
Jensen SL, Larsen FH, Bandshom O et al (2013a) Stabilization of semi-solid-state starch by branching enzyme-assisted chain-transfer catalysis at extreme substrate concentration. Biochem Eng J 72:1–10
Jensen SJ, Zhu F, Vamadevan V et al (2013b) Structural and physical properties of branching enzyme stabilized starch. Carbohydr Polym 98:1490–1496
Jiang W, Zhou H, Bi H et al (2013) Demonstration of CRISPR/Cas9/sgRNA-mediated targeted gene modification in Arabidopsis, tobacco, sorghum and rice. Nucleic Acids Res 41:e188
Jobling S (2004) Improving starch for food and industrial applications. Curr Opin Plant Biol 7:210–218
Jobling SA, Westcott RJ, Tayal A et al (2002) Production of a freeze-thaw-stable potato starch by antisense inhibition of three starch synthase genes. Nat Biotechnol 20(3):295–929

Kamasaka H, Uchida M, Kusaka K et al (1995) Inhibitory effect of phosphorylated oligosaccharides prepared from potato starch on the formation of calcium phosphate. Biosci Biotechnol Biochem 59:1412–1416

Kamasaka H, To-o K, Kusaka K et al (1997a) Action pattern of neopullulanase on phosphoryl oligosaccharides prepared from potato starch. J Appl Glycosci 44:275–283

Kamasaka H, To-o K, Kusaka K et al (1997b) A way of enhancing the inhibitory effect of phosphoryl oligosaccharides on the formation of a calcium phosphate precipitate using the coupling reaction of cyclomaltodextrin glucanotransferase. J Appl Glycosci 44:285–293

Kamasaka H, Diesuke I, Kentaro M et al (2003) Production and application of phosphoryl oligosaccharides prepared from potato starch. Trends Glycosci Glycotechnol 15:75–89

Kötting O, Pusch K, Tiessen A et al (2005) Identification of a novel enzyme required for starch metabolism in Arabidopsis leaves. The phosphoglucan, water dikinase. Plant Physiol 137:242–252

Kötting O, Santelia D, Edner C et al (2009) STARCH-EXCESS4 is a laforin-like phosphoglucan phosphatase required for starch degradation in Arabidopsis thaliana. Plant Cell 21:334–346

Kozlov SS, Blennow A, Krivandin AV et al (2007) Structural and thermodynamic properties of starches extracted from GBSS- and GWD suppressed potato lines. Int J Biol Macromol 40:449–460

Lanahan MB, Basu SS (2005) Modified starch, uses methods for production thereof. International patent WO 05/002359

Larsen FH, Blennow A, Engelsen SB (2008) Starch granule hydration – A MAS NMR investigation. Food Biophys 3:25–32

Li T, Liu B, Spalding MH et al (2012) High efficiency TALEN-based gene editing produces disease-resistant rice. Nat Biotechnol 30:390–392

Lim S-T, Kasemsuwan T, Jane J-L (1994) Characterization of phosphorus in starch by 31P-nuclear magnetic resonance spectroscopy. Cereal Chem 71(5):488–493

Lloyd JR, Landschütze V, KossmannJ J (1999) Simultaneous antisense inhibition of two starch-synthase isoforms in potato tubers leads to accumulation of grossly modified amylopectin. Biochem J 338:515–521

Lorberth R, Ritte G, Willmitzer L et al (1998) Inhibition of a starch-granule bound protein leads to modified starch and repression of cold sweetening. Nat Biotechnol 16:473–477

Mahlow S, Hejazi M, Kuhnert F et al (2014) Phosphorylation of transitory starch by a-glucan, water dikinase during starch turnover affects the surface properties and morphology of starch granules. New Phytol 203:495–507

Mason WR (2009) Starch use in foods. In: BeMiller JN, Whistler RL (eds) Starch: chemistry and technology. Academic, New York, pp 745–795

Mikkelsen R, Blennow A (2005) Functional domain organization of the potato a-glucan, water dikinase (GWD): evidence for separate site catalysis as revealed by limited proteolysis and deletion mutants. Biochem J 385:355–361

Mikkelsen R, Baunsgaard L, Blennow A (2004) Functional characterization of α-glucan, water dikinase, the starch phosphorylating enzyme. Biochem J 377:525–532

Mikkelsen R, Mutenda K, Mant A et al (2005) α-glucan, water dikinase (GWD): a plastidic enzyme with redox-regulated and coordinated catalytic activity and binding affinity. Proc Natl Acad Sci U S A 102:1785–1790

Mikkelsen R, Suszkiewicz K, Blennow A (2006) A novel type of carbohydrate binding module identified in α-glucan, water dikinases specific for regulated plastidial starch metabolism. Biochemistry 45:4674–4682

Miller JC, Tan SY, Qiao GJ et al (2011) A TALE nuclease architecture for efficient genome editing. Nat Biotechnol 29:143–148

Muhrbeck P, Eliasson A–C (1987) Influence of pH and ionic strength on the viscoelastic properties of starch gels – a comparison of potato and cassava starches. Carbohydr Polym 7:291–300

Muhrbeck P, Eliasson A-C (1991) Influence of the naturally-occurring phosphate-esters on the crystallinity of potato starch. J Sci Food Agric 55:13–18

Nashilevitz S, Melamed-Bessudo C, Aharoni A et al (2009) The legwd mutant uncovers the role of starch phosphorylation in pollen development and germination in tomato. Plant J 57:1–13
Nielsen TH, Wischmann B, Enevoldsen K et al (1994) Starch phosphorylation in potato tubers proceeds concurrently with *de novo* biosynthesis of starch. Plant Physiol 105:111–117
Perez S, Bertoft E (2010) The molecular structures of starch components and their contribution to the architecture of starch granules: a comprehensive review. Starch/Staerke 62:389–420
Planchot V, Colonna P, Buleon A (1997) Enzymatic hydrolysis of a-glucan crystallites. Carbohydr Res 298:319–326
Posternak T (1935) Sur le phosphore des amidons. Helv Chim Acta 18:1351–1369
Ral JP, Bowerman AF, Li Z et al (2012) Downregulation of glucan water-dikinase activity in wheat endosperm increases vegetative biomass and yield. Plant Biotechnol J 10:871–882
Reimann R, Ritte G, Steup M et al (2002) Association of α-amylase and the R1 protein with starch granules precedes the initiation of net starch degradation in turions of Spirodela polyrhiza. Physiol Plant 114:2–12
Reimann R, Hippler M, Machelett B et al (2004) Light induces phosphorylation of glucan water dikinase, which precedes starch degradation in turions of the duckweed *Spirodela polyrhiza*. Plant Physiol 135:121–128
Ritte G, Lorberth R, Steup M (2000a) Reversible binding of the starch related R1 protein to the surface of transitory starch granules. Plant J 21:387–391
Ritte G, Eckermann N, Haebel S et al (2000b) Compartmentation of the starch-related R1 protein in higher plants. Starch/Staerke 52:179–185
Ritte G, Lloyd JR, Eckermann N et al (2002) The starch-related R1 protein is an alpha-glucan, water dikinase. Proc Natl Acad Sci U S A 99:7166–7171
Ritte G, Scharf A, Eckermann N et al (2004) Phosphorylation of transitory starch is increased during degradation. Plant Physiol 135:1–10
Ritte G, Heydenreich M, Mahlow S et al (2006) Phosphorylation of C6- and C3-positions of glucosyl residues in starch is catalysed by distinct dikinases. FEBS Lett 580:4872–4876
Samec M (1914) Studien über Pflanzenkolloide, IV. Die Verschiebungen des Phosphorgehaltes bei der Zustandsänderungen und dem diastatischen Abbau der Stärke. Kolloidchem Beih 4:2–54
Samec M, Blinc M (1941) Die neuere Entwicklung der Kolloidchemie der Stärke. Velag von Theodor Steinkopff, Dresten
Sanjana NE, Cong L, Zhou Y et al (2012) A transcription activator-like effector toolbox for genome engineering. Nat Protoc 7:171–192
Santelia D, Kötting O, Seung D et al (2011) The phosphoglucan phosphatase LIKE SEX FOUR2 dephosphorylates starch at the C3-position in Arabidopsis. Plant Cell 23:4096–4111
Schewe G, Knies P, Amati SF et al (2002) Monocotyledon plant cells and plants which synthesise modified starch. International patent WO 02/34923
Schouten H, Jacobsen E (2008) Cisgenesis and intragenesis, sisters in innovative plant breeding. Trends Plant Sci 13(6):260–261
Schreiber K (1958) Chemie und Biochemie unter besonderer Berücksichtigung qualitätbestimmender Faktoren. In: Schick R, Klinkowski M (eds) Die Kartoffel Ein Handbuch. VED Deutscher Lantvirtschaftverlag, Berlin, pp 193–352
Schwall GP, Safford R, Westcott RJ et al (2000) Production of very-high-amylose potato starch by inhibition of SBE A and B. Nat Biotechnol 18:551–554
Shaik SS, Carciofi M, Martens HJ et al (2014) Starch bioengineering affects cereal grain germination and seedling establishment. J Exp Bot 65(9):2257–2270
Shukla VK, Doyon Y, Miller JC et al (2009) Precise genome modification in the crop species *Zea mays* using zinc-finger nucleases. Nature 459:437–441
Skeffington AW, Graf A, Duxbury Z et al (2014) Glucan, water dikinase exerts little control over starch degradation in Arabidopsis leaves at night. Plant Physiol 165(2):866–879
Slade AJ, McGurie C, Loeffler D et al (2012) Development of high amylose wheat through TILLING. BMC Plant Biol 12:1–17
Tabata S, Hizukuri S (1971) Studies on starch phosphate. Part 2. Isolation of glucose 3-phosphate and maltose phosphate by acid hydrolysis of potato starch. Starch-Starke 23:267–272

Takeda Y, Hizukuri S (1982) Location of phosphate groups in potato amylopectin. Carbohydr Res 102:321–327

Tanackovic V, Svensson JT, Jensen SL, Buléon A, Blennow A (2014) The deposition and characterization of starch in *Brachypodium distachyon*. J Exp Bot 65(18):5179–5192

Tanaka T, Kobayashi T, Kuriki T (2012) Optimization of calcium concentration of saliva with phosphoryl oligosaccharides of calcium (POs-Ca) for enamel remineralization in vitro. Arch Oral Biol 58:174–180

Thygesen LG, Blennow A, Engelsen SB (2003) The effects of amylose and starch phosphate on starch gel retrogradation studied by low-field 1H NMR relaxometry. Starch-Starke 55:241–249

To-o K, Kamasaka H, Nakabou Y (2003) Absorbability of calcium from calcium-bound phosphoryl oligosaccharides in comparison with that from various calcium compounds in the rat ligated jejunum loop. Biosci Biotechnol Biochem 67:1713–1718

Townsend JA, Wright DA, Winfrey RJ et al (2009) High-frequency modification of plant genes using engineered zinc-finger nucleases. Nature 459:442–445

Viksø-Nielsen A, Blennow A, Kristensen KH et al (2001) Structural, physicochemical, and pasting properties of starches from potato plants with repressed r1-gene. Biomacromolecules 3:836–841

Weise SE, Aung K, Jarou ZJ et al (2012) Engineering starch accumulation by manipulation of phosphate metabolism of starch. Plant Biotechnol J 10:545–554

Wickramasinghea HAM, Blennow A, Noda T (2009) Physico-chemical and degradative properties of in-planta re-structured potato starch. Carbohydr Polym 77:118–124

Wiesenborn DP, Orr PH, Casper HH et al (1994) Potato starch paste behavior as related to some physical/chemical properties. J Food Sci 59:644–648

Wikman J, Larsen FH, Motawia MS et al (2011) Phosphate esters in amylopectin clusters of potato tuber starch. Int J Biol Macromol 48:639–649

Wikman J, Blennow A, Buléon A et al (2013) Influence of amylopectin structure and degree of phosphorylation on the molecular composition of potato starch lintners. Biopolymers 101:257–271

Wischmann B, Nielsen TH, Møller BL (1999) In vitro biosynthesis of phosphorylated starch in intact potato amyloplasts. Plant Physiol 119:455–462

Wischmann B, Blennow A, Madsen F et al (2005) Functional characterisation of potato starch modified by specific in planta alteration of the amylopectin branching and phosphate substitution. Food Hydrocoll 19:1016–1024

Yang R, Sun C, Bai J et al (2012) A putative gene *sbe3-rs* for resistant starch mutated from SBE3 for starch branching enzyme in rice (*Oryza sativa* L.). PLoS ONE 7(8):e43026

Yu T-S, Kofler H, Häusler RE et al (2001) SEX1 is a general regulator of starch degradation in plants and not the chloroplast hexose transporter. Plant Cell 13:1907–1918

Zeeman SC, Kossmann J, Smith AM (2010) Starch: its metabolism, evolution, and biotechnological modification in plants. Annu Rev Plant Biol 61:209–234

Chapter 13
Morphological Variations of Starch Grains

Ryo Matsushima

Abstract Starch is synthesized in plant storage organs and forms transparent grains inside cells, which are referred to as starch granules or starch grains (SGs). SGs exhibit different morphologies and sizes depending on the species and are prominent in Poaceae endosperm. Comprehensive observations indicate that SG morphologies can be classified into four types: compound grains, bimodal simple grains, uniform simple grains, and a mixed configuration containing compound and simple grains in the same cells. Phylogenetic evaluation of SG morphological diversity indicates that the compound grain type is the ancestral SG morphology in Poaceae, and the bimodal simple grain type is only observed in specific phylogenetic groups that include barley and wheat. Starch morphology and size are important characteristics for industrial applications. However, the molecular mechanisms that determine SG morphology and size are not completely understood. This review summarizes starch grain morphological characteristics and phylogenetic information about SG morphological diversity. It also discusses methods for cytological observation of SGs and recently identified genes that control SG size.

Keywords Cereal • Diversity • Endosperm • Mutant • Starch grain • Voronoi diagram

13.1 What Is a Starch Grain?

Starch is a biologically important glucose polymer that is synthesized by photosynthetic organisms such as plants and algae (Buléon et al. 1998; Hancock and Tarbet 2000; Nakamura 2002). Starch contains amylose and amylopectin. Amylose is primarily a linear glucose chain, whereas amylopectin is a densely branched glucose chain. Amylopectin is the major component of normal starch, accounting for 65–85 % of total starch weight. Starch is water-insoluble and osmotically inactive, making it a suitable long-term storage form of carbohydrate for seeds and tubers of

R. Matsushima (✉)
Institute of Plant Science and Resources, Okayama University, Kurashiki, Okayama 710-0046, Japan
e-mail: rmatsu@okayama-u.ac.jp

Y. Nakamura (ed.), *Starch*, DOI 10.1007/978-4-431-55495-0_13

many plant species. The higher plant amyloplast, a terminally differentiated plastid, is the site of starch synthesis and storage in organs such as endosperm, potato tubers, and pollen grains from Poaceae (James et al. 2003; Sakamoto et al. 2008). Starch forms transparent grains in amyloplasts, which are referred to as starch granules or starch grains (SGs). High levels of starch accumulate in storage organs, where most of the amyloplast interior is occupied by SGs. SGs are easily visualized using iodine solution and can be clearly observed under a normal light microscope (Matsushima et al. 2010).

13.2 Morphological Variations of Starch Grains

Although starch has a simple glucose polymer composition, SGs exhibit differing morphologies depending on the species (Harz 1880; Tateoka 1954, 1955, 1962; Czaja 1978; Jane et al. 1994; Shapter et al. 2008; Matsushima et al. 2010). SG morphology is classified as either compound or simple (Tateoka 1962; Grass Phylogeny Working Group 2001). For both classes, only one SG is formed in one amyloplast. The difference is that the compound SGs are assembled from several dozen small starch granules, whereas the simple SG is a single particle of one starch granule (Fig. 13.1a). The SG size for simple SGs is equal to that of the starch granules. SGs in Poaceae endosperm have been extensively observed and their morphologies have been comprehensively described (Tateoka 1962; Grass Phylogeny Working Group II 2012). Rice (*Oryza sativa*) endosperm develops compound SGs that are normally 10–20 μm in diameter (Fig. 13.1b, e, h). Each starch granule included in compound SG is a sharp-edged polyhedron with a typical diameter of 3–8 μm. Starch granules are assembled as a compound SG, but they are not fused and are easily separated by conventional purification procedures. Simple SGs are observed in several important crops such as maize (*Zea mays*), sorghum (*Sorghum bicolor*), barley (*Hordeum vulgare*), and wheat (*Triticum aestivum*). Simple SGs are further classified into two subtypes referred to as bimodal and uniform. The bimodal type contains small and large simple SGs that coexist in the same cells. The uniform type contains similar-sized hexagonal, pentagonal, or round simple SGs. Barley and wheat synthesize bimodal simple SGs, whereas maize and sorghum synthesize uniform simple SGs (Fig. 13.1c, f, i, d, g, j). A number of species such as *Miscanthus*, *Perotis*, *Gymnopogon*, and *Thuarea* display a mixed configuration of compound and simple SGs inside the same cell (Tateoka 1962). Phylogenetic considerations about SG morphological diversity in Poaceae will be discussed later. Compound and simple SGs are also observed in tubers. Potato (*Solanum tuberosum*) and Chinese yam (*Dioscorea batatas*) synthesize simple SGs, whereas compound SGs are observed in sweet potato (*Ipomoea batatas*) and eddoe (*Colocasia esculenta*) (Fig. 13.2).

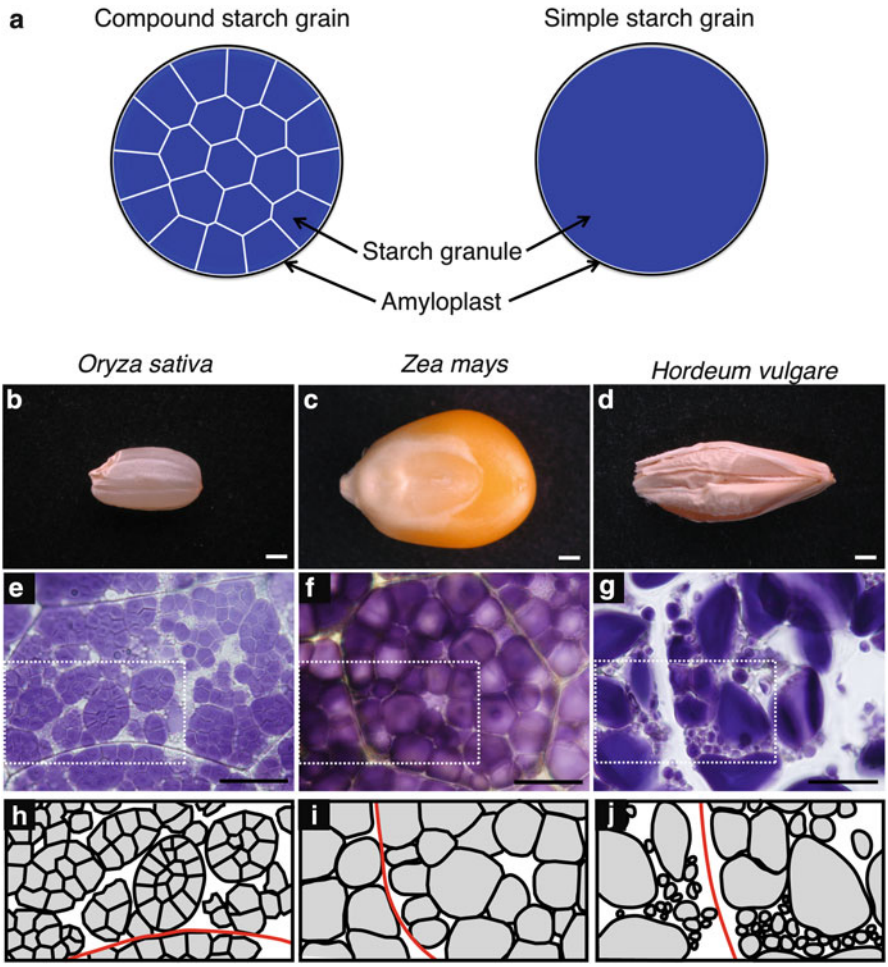

Fig. 13.1 Compound and simple starch grain characteristics. (**a**) Cartoon comparing compound and simple starch grains (SGs). SGs are synthesized and stored in amyloplasts. Compound SG is an assembly of several dozen small starch granules, whereas simple SG is a single particle of one starch granule. (**b**–**d**) Rice (*Oryza sativa*), maize (*Zea mays*), and barley (*Hordeum vulgare*) seeds. Bars = 1 mm. (**e**–**g**) Iodine-stained SGs in endosperm thin sections. Bars = 20 μm. Boxes indicated by white dotted lines are illustrated in **h**–**j**. (**h**–**j**) Illustration of typical SGs of each species. Rice, compound SGs; maize, uniform simple SGs with similar spherical sizes; barley, bimodal simple SGs containing small and large SGs coexisting in the same cell. Red lines indicate cell walls (Modified from Figure 2 in Matsushima et al. 2010)

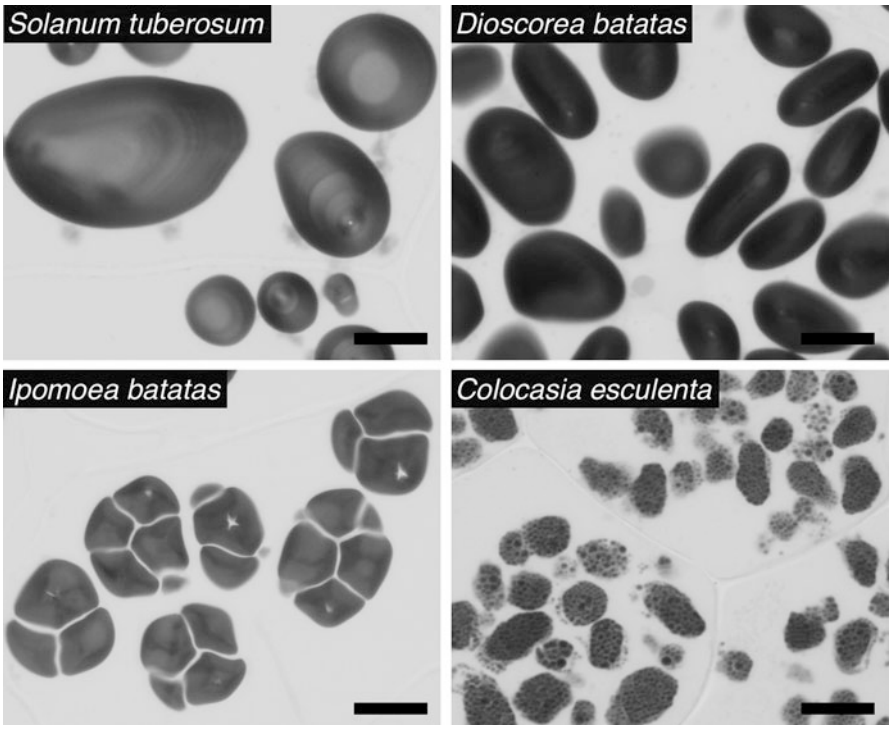

Fig. 13.2 Starch grains in tubers. Potato (*Solanum tuberosum*) and Chinese yam (*Dioscorea batatas*) develop simple SGs, whereas sweet potato (*Ipomoea batatas*) and eddoe (*Colocasia esculenta*) develop compound SGs. Bars = 20 μm

13.3 Phylogenetic Characteristics of Starch Grain Morphologies

Although SG morphological diversity has been observed and described, a detailed examination of the phylogenetic origin is lacking. Recent work extensively reevaluated previous SG observations in Poaceae endosperm for alignment on the newest Poaceae phylogenetic tree (Matsushima et al. 2013) (Fig. 13.3). This work showed that Poaceae early diverging genera, such as *Pharus*, *Anomochloa*, and *Streptochaeta*, synthesize compound SGs, indicating that compound SG is plesiomorphic in Poaceae. Genera with uniform simple SGs are scattered across phylogenetic branches, and this type is most frequent within the tribes Paniceae, Andropogoneae, and Paspaleae. By contrast, bimodal simple SGs were restricted to only five genera, including *Brachypodium*, *Triticum*, *Hordeum*, *Elymus*, and *Bromus*. This indicates that bimodal simple SGs are phylogenetically specific for Poaceae. Currently, there is no information about genetic mechanisms that change SG morphological types. This information will reveal the evolution of SG morphological specification and explain the current phylogenetic profile.

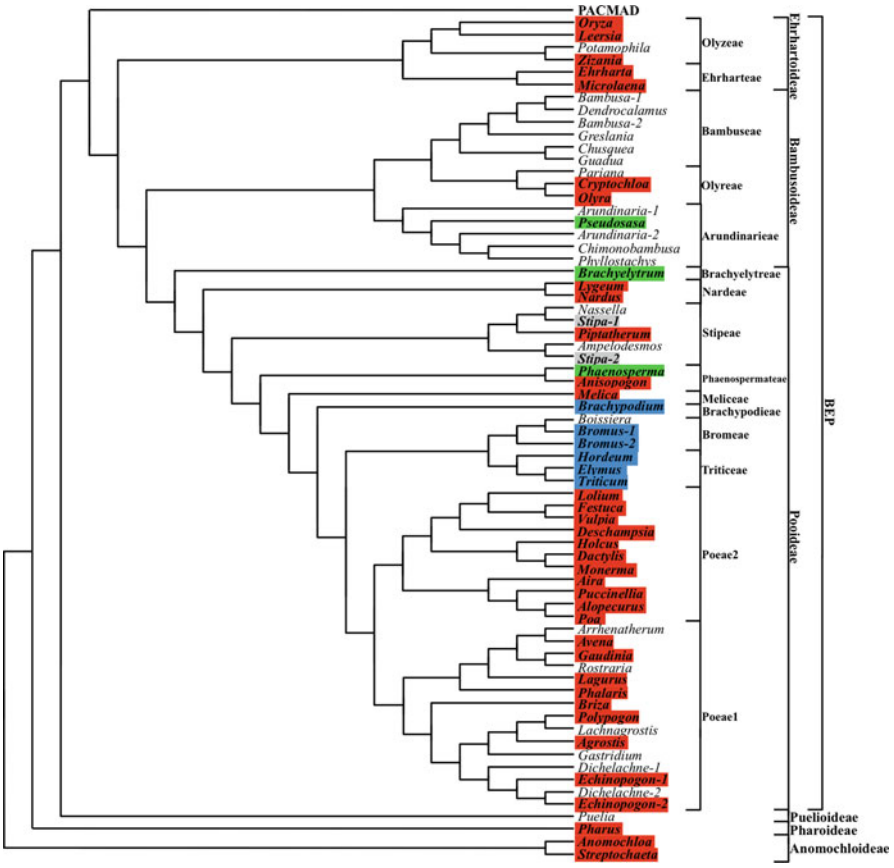

Fig. 13.3 Phylogenetic tree of starch grain morphologies in Poaceae. This tree is based on the Bayesian consensus phylogenetic tree constructed by Grass Phylogeny Working Group II (2012). Genera are color coded for SG morphological type: red, compound SG; blue, bimodal simple SG; green, uniform simple SG; and gray, genera with discrepancies between observations and genera with several SG types reported. For details of PACMAD clade, see supplemental data of Matsushima et al. (2013). BEP, subfamilies Bambusoideae, Ehrhartoideae, and Pooideae; PACMAD, subfamilies Panicoideae, Arundinoideae, Chloridoideae, Micrairoideae, Aristidoideae, and Danthonioideae (Modified from Figure 1 in Matsushima et al. 2013)

13.4 Voronoi Diagram of Compound Starch Grain Interior

Compound SGs are well-ordered structures, in which assembled starch granules are sharp-edged polyhedrons with similar diameters. In thin sections, the starch granule pattern in compound SGs is well fitted to the Voronoi diagram (Fig. 13.4). Voronoi diagrams are a mathematical representation of tessellations developed by Peter Gustav Lejeune Dirichlet (1805–1859) and Georges Voronoï (1868–1908) (Okabe et al. 2000). Given a set of generator points, the Voronoi tessellation

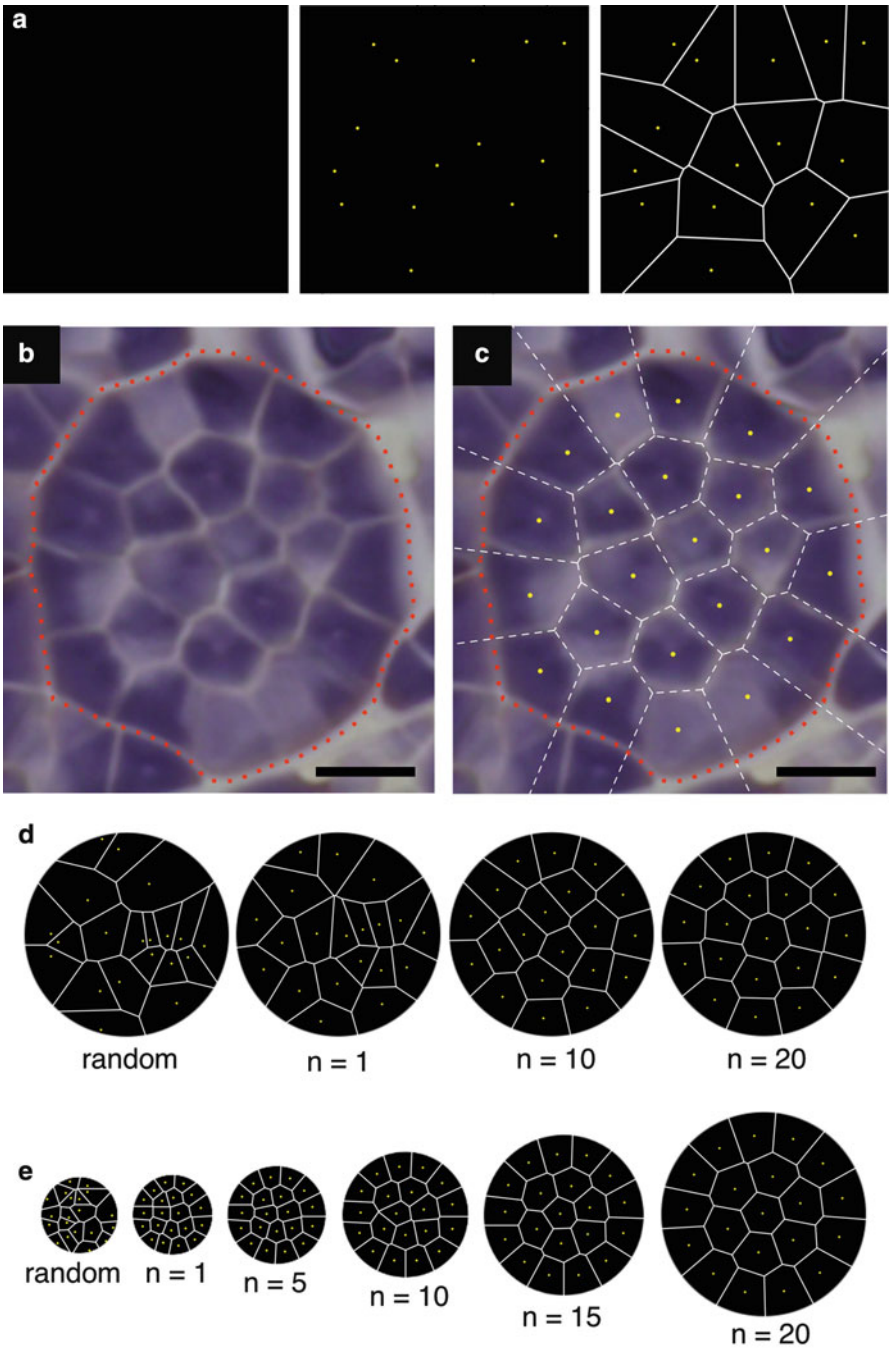
a
b
c
d
random
n = 1
n = 10
n = 20
e
random
n = 1
n = 5
n = 10
n = 15
n = 20

divides space into regions called Voronoi regions (Fig. 13.4a). A Voronoi region should consist of all points that are closer to the generator point in the region than to any other generator points (Okabe et al. 2000; Poupon 2004). To satisfy this condition in two-dimensional planes, the Voronoi region is built by defining the perpendicular bisector between the generator points and selecting the smallest polyhedron formed by these lines. Given the appropriate sets of generator points in thin sections, the area of each starch granule in compound SGs corresponds to Voronoi regions (Fig. 13.4b, c). Agreement between Voronoi diagrams and starch granule shapes indicates two properties about compound SG development. First, during SG synthesis in developing seeds, the enlargement rate of each starch granule is almost equal. Second, the formation of all starch granules starts simultaneously. Otherwise, smaller starch granules than those expected by Voronoi regions would be generated. When the starch granules are observed under polarized light, a characteristic dark cross can be visualized (Pérez and Bertoft 2010). The center of the cross is called hilum, the point around which layers of carbohydrate are deposited (Buléon et al. 1998; D'Hulst and Merida 2010). The hilum is suggested to prime starch synthesis; in this respect, the starch granule hilum may correspond to the generator points in Voronoi regions.

As starch granules enlarge in developing endosperm, they affect the growth of neighboring granules and impose limits on intergranule spacing. This optimizes starch granule packing in amyloplasts and enables formation of densely packed compound SGs. A centroidal Voronoi tessellation has generator points as the centroids (centers of mass) of the corresponding Voronoi regions (Du et al. 1999). When the circle is divided by Voronoi tessellations with randomly located generator points, irregularly sized Voronoi regions are constructed (Fig. 13.4d). However, when the centroids of each Voronoi region are used as the updated generator points, a new Voronoi tessellation can be obtained. The iteration between constructing Voronoi tessellations and calculating centroids can achieve the centroidal Voronoi

Fig. 13.4 Voronoi diagrams of compound starch grains. (**a**) Voronoi tessellation of square (indicated by *black*). Given 15 generator points (*yellow points*), Voronoi tessellation divides the square into 15 Voronoi regions (polygons separated by *white lines*). A Voronoi region consists of all points that are closer to the generator point in the region than to any other generator point. (**b**, **c**) Compound SG (indicated by *red dotted line*) in wild-type rice endosperm (**b**) overlaid with a Voronoi diagram (*white dotted lines*) based on the *yellow* generator points (**c**), which were manually selected. Voronoi diagram was generated by R program using package EBImage, png, and deldir (Team 2013; Pau et al. 2014; Urbanek 2013; Turner 2014). Bars = 5 μm. (**d**) Lloyd method to obtain centroidal Voronoi tessellation for a circle. Voronoi tessellation divides the circle into 20 regions based on 20 generator points that are randomly located in the circle. By iterations ($n = 1$, 10, and 20) of calculating centroids and constructing Voronoi, tessellations converge into a centroidal Voronoi tessellation with well-shaped uniformly sized regions. After 50 iterations, the Voronoi tessellation resembles compound SGs. (**e**) Convergence into the centroidal Voronoi tessellation for an expanding circle. The iteration ($n = 1$, 5, 10, 15, and 20) is 5 % expansion of the circle, calculating centroids, constructing Voronoi tessellations. *Yellow points* indicate generator points of Voronoi tessellation

tessellation with well-shaped, uniformly sized regions: this is the Lloyd method (Du et al. 1999). The centroidal Voronoi tessellation for a circle resembles compound SGs. In developing endosperm, the starch granule enlargement occurs together with amyloplast size expansion. Therefore, centroid position in each starch granule should change depending on the amyloplast size expansion during endosperm development (Fig. 13.4e).

13.5 Observation Methods for Starch Grains

Starch turns violet when stained by iodine solution. Therefore, SGs can be easily observed under a light microscope. Thin sections can be obtained by hand sectioning samples with high water content such as potato tubers, which preserves intact subcellular structures. Staining the sections with iodine solution will label intact SGs inside cells. Thin sections from dry and hard materials such as cereal grains are difficult to prepare by hand sectioning. Cereal grains can be broken into fragments using pliers, and these can be stained with iodine solution to observe SGs. However, crushing by pliers can damage the compound SGs and disperse starch granules.

A rapid and easy method to prepare thin sections for SG analysis from cereal grains was developed recently (Matsushima et al. 2010). Using this method, compound SG morphologies can be observed in an intact state. This method is illustrated in Fig. 13.5. The tip of a 200 μL pipette tip is cut off using scissors (Fig. 13.5a). The cut end is softened by mechanical pinching. A seed can fit into the pinched end for fixation. For rice, barley, and wheat, 200 μL tips are suitable for fixation of seeds. For maize, 1 mL pipette tips are suitable. The seed-embedded tip can be fixed on a block trimmer used for ultramicrotome resin block trimming (Fig. 13.5b) and manipulated under a stereo microscope (Fig. 13.5c) for thin sectioning under magnified observation. The block trimmer can be held by the third and fourth fingers of the nondominant hand, whereas the index finger and thumb of the dominant hand hold a razor blade attached to the seed (Fig. 13.5d). During sectioning, the blade is kept horizontal to the seed. The blade should be supported by the index finger of the nondominant hand to adjust sectioning pressure. The razor cut generates a smooth surface near the top of the seed, which is exposed approximately 1 mm out of the pipette tip (Fig. 13.5e, f). Thin sectioning can be performed with the same hand positions, but holding the blade at an angle of approximately 30° (Fig. 13.5g). The seeds are easily cut using a razor blade, and thin sections can be shaved off the cut end (Fig. 13.5h, i). The razor blade must be sharp for this procedure. The thin section can be picked up by forceps and placed onto a glass slide for iodine staining. This rapid method is easy and suitable for observation of large numbers of samples, such as more than 200 seeds per day. This renders the method an excellent choice for genetic screening of mutants. The embryo remains intact after sectioning if the embryo-containing end is embedded into the tip. Therefore, the sectioned seed can still germinate. There are two disadvantages to the rapid method. It cannot create a large thin section, so a wide-field view at

low magnification cannot be obtained. This method cannot be used to create thin sections from seeds with a floury quality such as floury mutant seeds.

To address the disadvantages of the rapid method, Technovit 7100 resin can be used (Matsushima et al. 2010; Matsushima et al. 2014). Technovit 7100 resin is a low-temperature polymerization resin composed primarily of glycol methacrylate that is available from Heraeus-Kulzer (Germany). In the resin-embedded method, approximately 1 mm cubic blocks of endosperm are subjected to chemical fixation. Samples are subsequently dehydrated through a graded ethanol series and then embedded in Technovit 7100 resin (http://www.bio-protocol.org/e1239). The embedded samples are cut with an ultramicrotome and diamond knife and dried on cover slips. The thin sections are approximately 1 μm thick and can be stained with iodine solution. The resin-embedded method takes approximately 1 week to perform. It is not suitable for large numbers of samples but can produce larger sections than the rapid method and can produce thin sections from floury seeds. The resin-embedded samples are competent for long-term preservation and provide higher-resolution images compared with those of the rapid method.

13.6 Mutants Isolated by Direct Observations of Starch Grains

Molecular mechanisms that determine organelle shape have been studied using genetic approaches and live-cell imaging in *Arabidopsis*. Organelles such as vacuoles, endoplasmic reticulum, Golgi apparatus, mitochondria, and peroxisomes can be visualized by expressing organelle-targeted green fluorescent protein (GFP) in transgenic plants (Mano et al. 2009). This technique enables direct observation of organelles in live plant cells. Live-cell imaging is suitable for genetic screening of mutants showing abnormal organelle morphologies. Molecular characterization of isolated mutants has identified molecular mechanisms involved in determining organelle morphology (Mano et al. 2004; Matsushima et al. 2004; Tamura et al. 2005; Arimura et al. 2008; Nakano et al. 2012).

SGs in mature cereal seeds have not been clearly visualized using live-cell imaging techniques. The rapid method for SG observations in thin sections can be used for genetic screening of mutants. The rapid method utilizes only half of the endosperm and preserves the embryo; therefore, assayed seeds maintain germination competence. The rapid method was successfully employed to isolate five rice mutants with abnormal SG morphology (Fig. 13.6). These mutants were designated *ssg* for *substandard starch grain*. The *ssg1*, *ssg2*, and *ssg3* mutants display higher levels of smaller SGs (<10 μm in diameter) in addition to normal SGs (10–20 μm in diameter). The *ssg4* mutant contains enlarged compound SGs (>30 μm in diameter). The *ssg5* mutant contains SGs that lack characteristic compound structures.

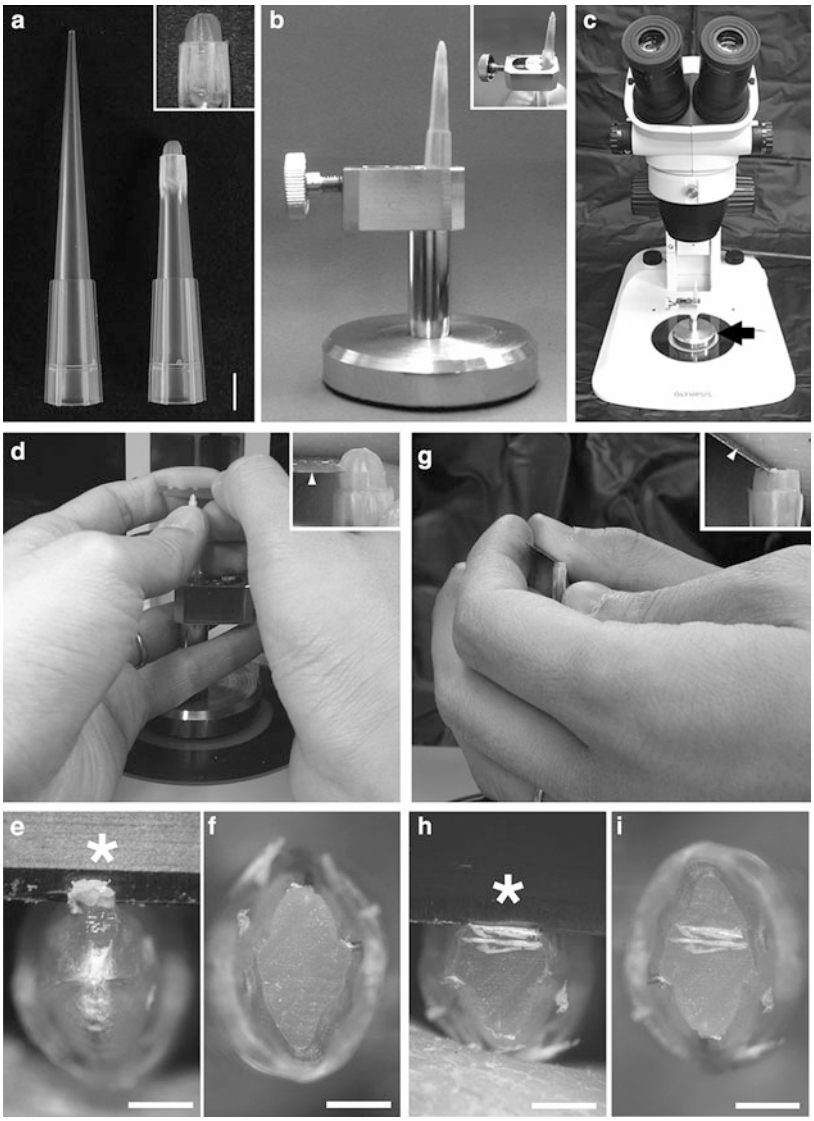

Fig. 13.5 Rapid preparation of rice endosperm thin sections for starch grain observation. (**a**) A rice seed was inserted into a truncated, disposable pipette tip (*right*) (inset, magnified image of the seed). Bar = 5 mm. (**b**) The seed-containing tip was fixed on an ultramicrotome block trimmer (inset, overhead view). (**c**) The block trimmer (indicated by an *arrow*) can be manipulated under a stereo microscope. (**d**) Positions of hands, fingers, razor blade, and the block trimmer equipped with the seed-containing tip for trimming (inset, magnified side view of the captured seed and razor blade, indicated by *arrowhead*). (**e**) Seed images under stereo microscope before trimming (*asterisk* indicates razor blade). Bar = 1 mm. (**f**) Smooth surface after trimming. Bar = 1 mm. (**g**) Side view of hand positions for thin sectioning. Razor blade angle is approximately 30° (inset, *arrowhead*). (**h**, **i**) A thin section can be shaved off using the razor blade (indicated by an *asterisk* in **h**). Bars = 1 mm (Modified from Figure 1 in Matsushima et al. 2010)

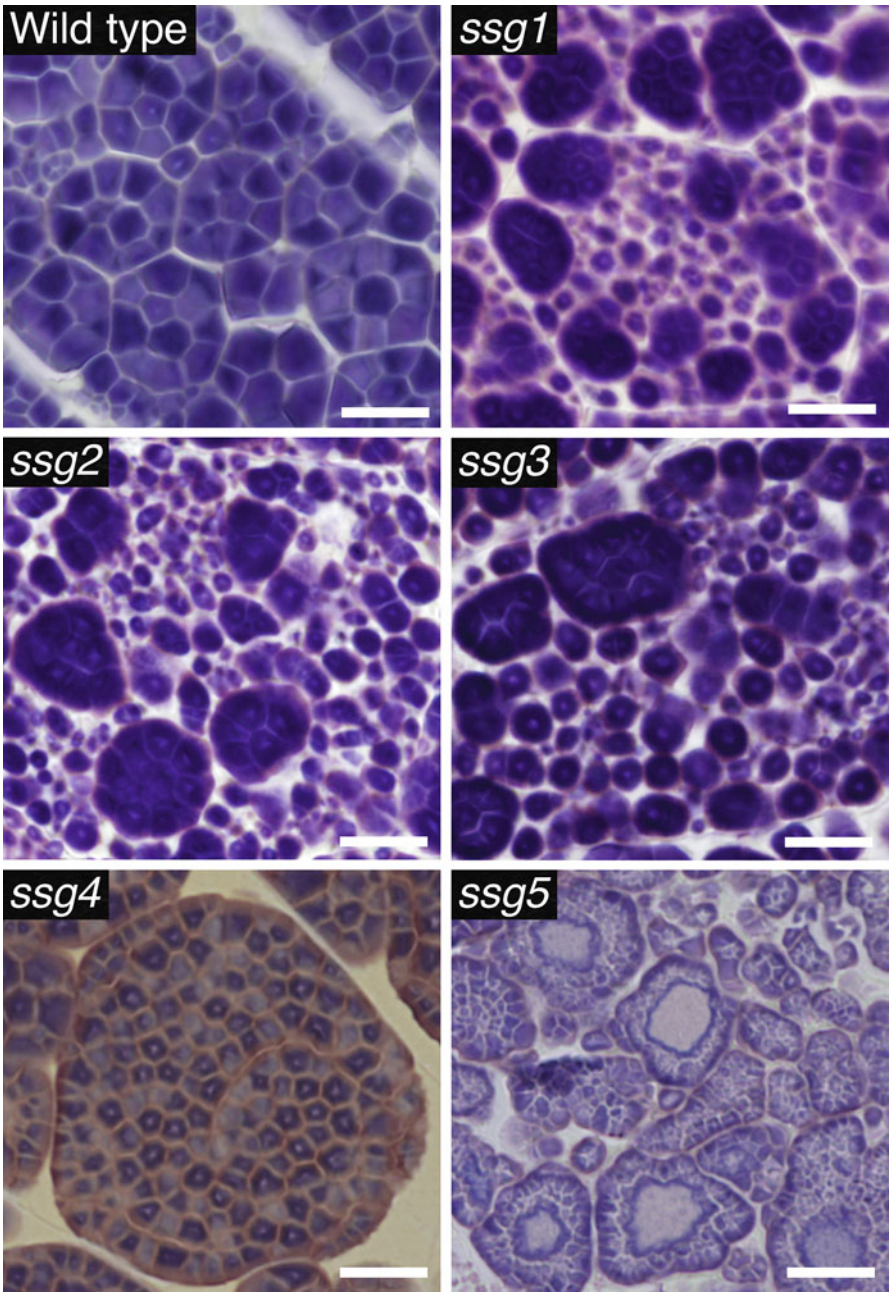

Fig. 13.6 Rice *substandard starch grain* (*ssg*) mutants with abnormal starch grain morphologies. The *ssg1*, *ssg2*, and *ssg3* mutants contain higher levels of smaller SGs. Enlarged compound SGs are detected in *ssg4*. SGs without internal compound structures are observed in s*sg5*. Bars = 10 μm (Modified from Matsushima et al. 2010 and Matsushima et al. 2014)

13.7 Size Variations of Starch Grains

The size of SGs and starch granules is one of the most important starch characteristics for industrial applications (Lindeboom et al. 2004). Small starch granules can replace fat in food applications, because aqueous dispersions of small starch granules show fat mimetic properties (Malinski et al. 2003). Larger starch granules are desirable in maize and cassava because they improve the final yield after wet-milling purification (Gutiérrez et al. 2002). Therefore, engineered size control of SGs and starch granules is a molecular tool that can be used for starch breeding in future biotechnology programs.

SG size in cereal endosperm is diverse and species-specific. *Bromus* species contain intrageneric size variations of SGs, in which even phylogenetic neighbors develop distinctly sized SGs (Matsushima et al. 2013). This indicates that a small number of genes regulate the interspecific SG size variation. As the bimodal simple SGs, barley and wheat SGs contain two discrete size classes of approximately 15–25 μm and <10 μm that coexist in the same cells (Fig. 13.1). The percentage of smaller and larger SGs of bimodal simple SGs varies depending on species. In *Hordeum pusillum*, small SGs are highly abundant compared with other species. In contrast, small SGs are rare in *Elymus caninus* (Matsushima et al. 2013). Genetic factors controlling the numbers of small and large SGs of bimodal SGs have not been identified so far. However, small SGs are known to lack in a few wild wheat species, and a major QTL controlling the small SGs number has been detected (Howard et al. 2011).

13.8 Genetic Factors to Control Starch Grain Size

Four kinds of enzymes have major roles in starch biosynthesis, including ADP-glucose pyrophosphorylase (AGPase), starch synthase (SS), branching enzyme (BE), and debranching enzyme (DBE) (see Chaps. 5 and 6 in this book). These enzymes have multiple isoforms with different substrate specificities and distinct expression patterns. A number of mutants defective in starch biosynthetic enzymes have been isolated in several plant species (Dvonch et al. 1951; Walker and Merritt 1969; Jarvi and Eslick 1975; Satoh and Omura 1981; Yano et al. 1984; Satoh et al. 2003a, b, 2008; Kang et al. 2005; Fujita et al. 2007, 2009). Some of these mutants exhibit distinct sizes of SGs compared to those of the wild-type plants. Mutations in *BEIIb* mutants are designated *amylose extender* (*ae*) (Yano et al. 1985). Rice and maize *ae* endosperm contains smaller SGs (Yano et al. 1985; Li et al. 2007). *ssg1*, *ssg2*, and *ssg3* mutants also contain *BEIIb* mutations (Matsushima et al. 2010).

Mutations in *Arabidopsis SSIV* cause synthesis of one large starch granule per chloroplast in leaves (Roldán et al. 2007). SSIV may be involved in starch granule initiation and priming of amylopectin synthesis (Szydlowski et al. 2009; D'Hulst and Merida 2010). However, the role of SSIV in cereal endosperm is unknown.

Granule-bound starch synthase I (GBSSI) mutants are *waxy* mutants that produce no amylose (Fasahat et al. 2014). In barley and rice, SG size in *waxy* mutants

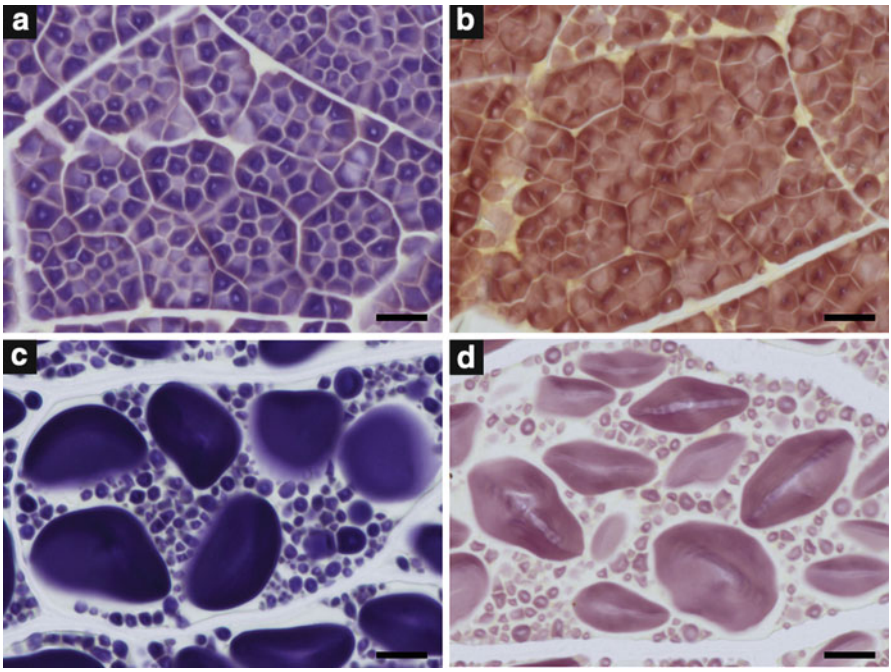

Fig. 13.7 Starch grain morphologies in *waxy* mutants of rice and barley. SGs from non-waxy seeds were stained violet, whereas SGs from *waxy* mutants were stained red. (**a**) Koshihikari variety of rice (non-waxy). (**b**) Odorokimochi variety of rice (waxy). (**c**) Akashinriki variety of barley (non-waxy). (**d**) Tokushima Mochimugi 1 variety of barley (waxy). The barley accessions were provided by the National Bio-Resource Project – barley of the MEXT, Japan. I especially thank Dr. Kazuhiro Sato (Institute of Plant Science and Resources, Okayama University) for providing the seeds. Bars = 10 μm

is comparable to that of wild-type (Fig. 13.7). Therefore, SG size is not directly determined by the amount of amylose.

Most of the amyloplast interior is occupied by SG in storage organs, where the SG is approximately the same size as the amyloplast. Amyloplasts and chloroplasts both develop from proplastids (Sakamoto et al. 2008). The size of chloroplast is controlled by the chloroplast binary fission division machinery, especially by the ring structures that form at the division sites (Miyagishima 2011; TerBush et al. 2013). Proteins involved in the ring structures have been isolated, including FtsZ, MinD, MinE, and ARC5 (DRP5B). *Arabidopsis* mutants that are defective in these proteins have defects in chloroplast division and contain enlarged chloroplasts. Overexpression of FtsZ1 in potato results in partial inhibition of plastid division in tubers (de Pater et al. 2006). The tubers generate fewer but larger amyloplasts and hence larger simple SGs. The diameters of SGs are approximately 1.2–1.7-fold larger in these transgenic potato plants than in wild-type plant. In rice, the *arc5* mutant is the only mutant reported to be defective in chloroplast division (Yun and

Kawagoe 2009). The *arc5* endosperm produces pleomorphic amyloplasts, but not enlarged ones. So, the size of SGs is little affected in rice *arc5* endosperm.

Characterization of the rice *ssg4* mutant identified a novel factor that influences SG size (Matsushima et al. 2014). In *ssg4* endosperm, the cross-sectional areas occupied by SGs are up to 6-fold greater compared with that of wild-type. SSG4 protein is composed of 2,135 amino acids and contains an N-terminal amyloplast-targeted sequence. SSG4 also contains a DUF490 (Domain of unknown function 490) that is conserved from proteobacteria to higher plants. A Gly → Ser amino acid substitution occurs in *ssg4* DUF490. DUF490-containing proteins with lengths greater than 2,000 amino acid residues are predominant in photosynthetic organisms but are minor in proteobacteria. To date, SSG4 homologues of photosynthetic organisms have not been functionally characterized.

The enlargement of SGs does not result in the direct expansion of starch granules in *ssg4*, because SGs in *ssg4* endosperm are the compound SG type. SSG4 homologues in other crops such as barley, maize, and sorghum have a conserved glycine residue at the *ssg4* mutation site (Matsushima et al. 2014). These crops develop simple SGs; therefore, the size of SG is consistent with the size of starch granules. Introduction of the same Gly → Ser mutation into these crops or downregulation of *SSG4* homologues will achieve engineered starch granule enlargement.

13.9 Future Prospects

Cereal mutants with abnormal SG morphologies are not many. Large-scale screening will isolate novel cereal mutants with altered SG morphologies. Such mutants are expected to provide novel physicochemical properties and tastes. The starch of rice *ae* mutant that is allelic with *ssg1*, *ssg2*, and *ssg3* has low amylase digestibility (Kubo et al. 2010). Some saccharides in *ssg4* are elevated compared with those of wild-type (Matsushima et al. 2014). Collecting and identifying mutants with related SG morphologies is important for future breeding programs to improve grain quality. The rapid SG observation method is an effective strategy for isolating such mutants. Using this strategy, commercially desirable mutants such as glutinous rice (*waxy* rice) and sweet corn can be identified in future. These mutants will also provide greater insight into the molecular mechanisms that determine SG morphologies. Ultimately, this will deepen our understanding of interspecific morphological SG variations and evolution of SG morphology.

References

Arimura S, Fujimoto M, Doniwa Y et al (2008) Arabidopsis ELONGATED MITOCHONDRIA1 is required for localization of DYNAMIN-RELATED PROTEIN3A to mitochondrial fission sites. Plant Cell 20:1555–1566

Buléon A, Colonna P, Planchot V, Ball S (1998) Starch granules: structure and biosynthesis. Int J Biol Macromol 23:85–112
Czaja AT (1978) Structure of starch grains and the classification of vascular plant families. Taxon 27:463–470
D'Hulst C, Merida A (2010) The priming of storage glucan synthesis from bacteria to plants: current knowledge and new developments. New Phytol 188:13–21
de Pater S, Caspers M, Kottenhagen M et al (2006) Manipulation of starch granule size distribution in potato tubers by modulation of plastid division. Plant Biotechnol J 4:123–134
Du Q, Faber V, Gunzburger M (1999) Centroidal voronoi tessellations: applications and algorithms. SIAM Rev 41:637–676
Dvonch W, Kramer HH, Whistler RL (1951) Polysaccharides of high-amylose corn. Cereal Chem 28:270–280
Fasahat P, Rahman S, Ratnam W (2014) Genetic controls on starch amylose content in wheat and rice grains. J Genet 93:279–292
Fujita N, Yoshida M, Kondo T et al (2007) Characterization of SSIIIa-deficient mutants of rice: the function of SSIIIa and pleiotropic effects by SSIIIa deficiency in the rice endosperm. Plant Physiol 144:2009–2023
Fujita N, Toyosawa Y, Utsumi Y et al (2009) Characterization of pullulanase (PUL)-deficient mutants of rice (*Oryza sativa* L.) and the function of PUL on starch biosynthesis in the developing rice endosperm. J Exp Bot 60:1009–1023
Grass Phylogeny Working Group (2001) Phylogeny and subfamilial classification of the grasses (Poaceae). Ann Mo Bot Gard 88:373–457
Grass Phylogeny Working Group II (2012) New grass phylogeny resolves deep evolutionary relationships and discovers C4 origins. New Phytol 193:304–312
Gutiérrez OA, Campbell MR, Glover DV (2002) Starch particle volume in single- and double-mutant maize endosperm genotypes involving the soft starch (*h*) gene. Crop Sci 42:355–359
Hancock RD, Tarbet BJ (2000) The other double helix – the fascinating chemistry of starch. J Chem Educ 77:988–992
Harz CO (1880) Beiträge zur systematik der Gramineen. Linnaea 43:1–30
Howard T, Rejab NA, Griffiths S et al (2011) Identification of a major QTL controlling the content of B-type starch granules in Aegilops. J Exp Bot 62:2217–2228
James MG, Denyer K, Myers AM (2003) Starch synthesis in the cereal endosperm. Curr Opin Plant Biol 6:215–222
Jane J-L, Kasemsuwan T, Leas S et al (1994) Anthology of starch granule morphology by scanning electron microscopy. Starch-Starke 46:121–129
Jarvi AJ, Eslick RF (1975) Shrunken endosperm mutants in barley. Crop Sci 15:363–366
Kang HG, Park S, Matsuoka M, An G (2005) White-core endosperm *floury endosperm-4* in rice is generated by knockout mutations in the C_4-type pyruvate orthophosphate dikinase gene (*OsPPDKB*). Plant J 42:901–911
Kubo A, Akdogan G, Nakaya M et al (2010) Structure, physical, and digestive properties of starch from *wx ae* double-mutant rice. J Agric Food Chem 58:4463–4469
Li J-H, Guiltinan MJ, Thompson DB (2007) Mutation of the maize *sbe1a* and *ae* genes alters morphology and physical behavior of *wx*-type endosperm starch granules. Carbohydr Res 342:2619–2627
Lindeboom N, Chang PR, Tyler RT (2004) Analytical, biochemical and physicochemical aspects of starch granule size, with emphasis on small granule starches: A review. Starch-Starke 56:89–99
Malinski E, Daniel JR, Zhang XX, Whistler RL (2003) Isolation of small starch granules and determination of their fat mimic characteristics. Cereal Chem 80:1–4
Mano S, Nakamori C, Kondo M et al (2004) An Arabidopsis dynamin-related protein, DRP3A, controls both peroxisomal and mitochondrial division. Plant J 38:487–498
Mano S, Miwa T, Nishikawa S et al (2009) Seeing is believing: on the use of image databases for visually exploring plant organelle dynamics. Plant Cell Physiol 50:2000–2014

Matsushima R, Fukao Y, Nishimura M, Hara-Nishimura I (2004) NAI1 gene encodes a basic-helix-loop-helix-type putative transcription factor that regulates the formation of an endoplasmic reticulum-derived structure, the ER body. Plant Cell 16:1536–1549

Matsushima R, Maekawa M, Fujita N, Sakamoto W (2010) A rapid, direct observation method to isolate mutants with defects in starch grain morphology in rice. Plant Cell Physiol 51:728–741

Matsushima R, Yamashita J, Kariyama S et al (2013) A phylogenetic re-evaluation of morphological variations of starch grains among Poaceae species. J Appl Glycosci 60:37–44

Matsushima R, Maekawa M, Kusano M et al (2014) Amyloplast-localized SUBSTANDARD STARCH GRAIN4 protein influences the size of starch grains in rice endosperm. Plant Physiol 164:623–636

Miyagishima SY (2011) Mechanism of plastid division: from a bacterium to an organelle. Plant Physiol 155:1533–1544

Nakamura Y (2002) Towards a better understanding of the metabolic system for amylopectin biosynthesis in plants: rice endosperm as a model tissue. Plant Cell Physiol 43:718–725

Nakano RT, Matsushima R, Nagano AJ et al (2012) ERMO3/MVP1/GOLD36 is involved in a cell type-specific mechanism for maintaining ER morphology in Arabidopsis thaliana. PLoS ONE 7:e49103

Okabe A, Boots B, Sugihara K, Chiu SN (2000) Spatial tessellations: concepts and applications of voronoi diagrams, 2nd edn. John Wiley & Sons, New York

Pau G, Oles A, Smith M et al (2014) EBImage: image processing toolbox for R. R package version 4.4.0. http://www.bioconductor.org/packages/release/bioc/html/EBImage.html

Pérez S, Bertoft E (2010) The molecular structures of starch components and their contribution to the architecture of starch granules: a comprehensive review. Starch-Starke 62:389–420

Poupon A (2004) Voronoi and voronoi-related tessellations in studies of protein structure and interaction. Curr Opin Struct Biol 14:233–241

Roldán I, Wattebled F, Lucas MM et al (2007) The phenotype of soluble starch synthase IV defective mutants of *Arabidopsis thaliana* suggests a novel function of elongation enzymes in the control of starch granule formation. Plant J 49:492–504

Sakamoto W, Miyagishima SY, Jarvis P (2008) Chloroplast biogenesis: control of plastid development, protein import, division and inheritance. Arab Book/Am Soc Plant Biol 6:e0110

Satoh H, Omura T (1981) New endosperm mutations induced by chemical mutagenesis in rice, *Oryza sativa* L. Japan J Breed 31:316–326

Satoh H, Nishi A, Fujita N et al (2003a) Isolation and characterization of starch mutants in rice. J Appl Glycosci 50:225–230

Satoh H, Nishi A, Yamashita K et al (2003b) Starch-branching enzyme I-deficient mutation specifically affects the structure and properties of starch in rice endosperm. Plant Physiol 133:1111–1121

Satoh H, Shibahara K, Tokunaga T et al (2008) Mutation of the plastidial α-glucan phosphorylase gene in rice affects the synthesis and structure of starch in the endosperm. Plant Cell 20:1833–1849

Shapter FM, Henry RJ, Lee LS (2008) Endosperm and starch granule morphology in wild cereal relatives. Plant Genet Resour 6:85–97

Szydlowski N, Ragel P, Raynaud S et al (2009) Starch granule initiation in Arabidopsis requires the presence of either class IV or class III starch synthases. Plant Cell 21:2443–2457

Tamura K, Shimada T, Kondo M et al (2005) KATAMARI1/MURUS3 Is a novel golgi membrane protein that is required for endomembrane organization in Arabidopsis. Plant Cell 17:1764–1776

Tateoka T (1954) On the systematic significance of starch grains of seeds in Poaceae. J Japn Bot 29:341–347

Tateoka T (1955) Further studies on starch grains of seeds in Poaceae from the view point of systematics. J Japn Bot 30:199–208

Tateoka T (1962) Starch grains of endosperm in grass systematics. Bot Mag Tokyo 75:377–383

Team RC (2013) R: a language and environment for statistical computing. R Foundation for Statistical Computing, Vienna, Austria. http://www.R-project.org

TerBush AD, Yoshida Y, Osteryoung KW (2013) FtsZ in chloroplast division: structure, function and evolution. Curr Opin Cell Biol 25:461–470

Turner R (2014) deldir: Delaunay triangulation and Dirichlet (Voronoi) Tessellation. R package version 0.1-5. http://cran.r-project.org/web/packages/deldir/index.html

Urbanek S (2013) png: read and write PNG images. R package version 0.1-7. http://cran.r-project.org/web/packages/png/index.html

Walker JT, Merritt NR (1969) Genetic control of abnormal starch granules and high amylose content in a mutant of Glacier barley. Nature 221:482–483

Yano M, Isono Y, Satoh H, Omura T (1984) Genetic analysis of sugary and shrunken mutants of rice, *Oryza sativa* L. Japan J Breed 34:43–49

Yano M, Okuno K, Kawakami J et al (1985) High amylose mutants of rice, *Oryza sativa* L. Theor Appl Genet 69:253–257

Yun MS, Kawagoe Y (2009) Amyloplast division progresses simultaneously at multiple sites in the endosperm of rice. Plant Cell Physiol 50:1617–1626

Index

Y. Nakamura (ed.), *Starch*, DOI 10.1007/978-4-431-55495-0

D